

CLEO: QELS-Fundamental Science

08:00–10:00

FM1A • Quantum Engineering
*Presider: Nicholas Peters; Applied Communication Sciences, USA*FM1A.1 • 08:00 **Tutorial****Quantum Optomechanics**, Markus Aspelmeyer¹; ¹Universitat Wien, Austria. This tutorial provides an introduction to the current state-of-the-art, the challenges and the prospects of achieving quantum optical control over nano-, micro- and macro-mechanical devices, i.e. quantum optomechanics.

Markus Aspelmeyer is Professor of Physics at the University of Vienna, and Speaker of the Vienna Center for Quantum Science and Technology (VCQ). He is regarded as one of the pioneers of the field of cavity optomechanics. His research combines the development of new quantum technologies with fundamental quantum experiments.

08:00–10:00

FM1B • Relativistic Laser-Plasma Interactions
*Presider: Sergei Tochitsky; Univ. of California Los Angeles, USA*FM1B.1 • 08:00 **Invited****High energy ion acceleration and neutron production using relativistic transparency in solids**, Markus Roth¹, Daniel Jung², Katerina Falk², Nevzat Guler², Vincent Bagnoud², Stefan Bedacht¹, Oliver Deppert¹, Matthew J. Devlin², Andrea Favalli², Juan Fernandez², Cort D. Gautier², Matthias Geissel⁴, Robert C. Haight², Chris E. Hamilton², Manuel B. Hegelich², Randall P. Johnson², Annika Kleinschmidt¹, Frank E. Merrill², Alex Ortner¹, Gabriel Schaumann¹, Kurt Schoenberg², Marius Schollmeier⁴, Thomas Shimada², Terry N. Tadducci², Alexandra Tebartz¹, Joshua L. Tybo², Florian Wagner¹, Stephen A. Wender², Carl H. Wilde², Glen A. Wurden²; ¹Inst. for Nuclear Physics, Technische Universität Darmstadt, Germany; ²Los Alamos National Lab, USA; ³Helmholtzzentrum für Schwerionenforschung - GSI, Germany; ⁴Sandia National Lab, USA. Neutrons are unique to diagnose materials and excite nuclear reactions with a large field of applications. For the first time a new ion acceleration mechanism (BOA) has been used to generate intense, directed neutron beams.

FM1B.2 • 08:30

GeV Electrons and High brightness Betatron X-rays from Petawatt-Laser-Driven Plasma Accelerators, Xiaoming Wang¹, Rafal Zgadaj¹, Neil Fazel¹, Zhengyan Li¹, Watson Henderson¹, Yen-Yu Chang¹, Rick Korzekawa¹, S. Yi², V. Khudik¹, X. Zhang¹, Hai-En Tsai¹, Chih-Hao Pai³, H. Quevedo¹, G. Dyer¹, E. Gaul¹, M. Martinez¹, A. Bernstein¹, M. Spinks¹, Michael Donovan¹, Gennady Shvets¹, Todd Ditmire¹, Michael C. Downer¹; ¹Univ. of Texas at Austin, USA; ²Tsinghua Univ., China; ³Los Alamos National Lab, USA. We identify three regimes of correlated GeV-electron/keV-betatron-x-ray generation by a laser-plasma accelerator driven by the Texas Petawatt laser, and relate them to variations in strength of blowout, injection geometry and beam loading.

08:00–10:00

FM1C • Hyperbolic and Epsilon-near-zero Materials
Presider: Philippe Tassin; Chalmers Univ., Sweden

FM1C.1 • 08:00

Wave Propagation in Magnetized Epsilon-Near-Zero Metamaterials, Arthur Davoyan¹, Nader Engheta¹; ¹Univ. of Pennsylvania, USA. In this work we theoretically study light propagation in magnetized epsilon-near-zero (ENZ) metamaterials. We reveal novel regimes of propagation, including optical isolation of circularly polarized waves and back-scattering immune surface wave propagation.

FM1C.2 • 08:15

Nonlocal Response in Transition Metamaterials, Zhaxylyk A. Kudyshev¹, Natalia M. Litchinitser¹; ¹Electrical Engineering, Univ. at Buffalo, USA. We investigate resonant enhancement of light in transition metamaterials under the local and nonlocal response function approximations, and analyze the influence of nonlocality on the field distribution in the near-zero region.

FM1C.3 • 08:30

All Semiconductor Negative-Index Plasmonic Absorbers, Christopher Roberts¹, Stephanie Law², Torin Kilpatrick³, Lan Yu³, Troy Ribaudo², Eric Shaner², Dan Wasserman³, Viktor A. Podolskiy¹; ¹Physics and Applied Physics, Univ. of Massachusetts Lowell, USA; ²Sandia National Labs, USA; ³Electrical and Computer Engineering, Univ. of Illinois Urbana Champaign, USA. We demonstrate all-semiconductor thin-film plasmonic absorbers, where strong absorption in these structures is linked to the excitation of highly-confined negative-index surface plasmon polaritons. We present numerical and analytical descriptions of guided modes of the system.

08:00–10:00

FM1D • PT Symmetry and Related Phenomena
Presider: Matthias Heinrich, Univ. of Central Florida, USA

FM1D.1 • 08:00

Beyond PT-symmetry: SUSY-mediated real spectra in complex refractive index landscapes, Mohammad-Ali Miri¹, Matthias Heinrich¹, Demetrios N. Christodoulides¹; ¹CREOL The College of Optics and Photonics, Univ. of Central Florida, USA. In the presence of gain and loss, supersymmetric transformations facilitate the arbitrary removal of modes from wave-guiding structures. We show how SUSY gives rise to non-PT-symmetric families of complex potentials with entirely real-valued eigenvalue spectra.

FM1D.2 • 08:15

Observation of Gravitational Effects in Nonlocal Nonlinearity, Rivka Bekenstein¹, Ran Schley¹, Maor Mutfafi¹, Carmel Rotschild¹, Ido Dolev², Ady Arie², Mordechai Segev¹; ¹Physics Dept. and Solid State Inst., Technion Israel Inst. of Technology, Israel; ²Dept. of Physical Electronics, Fleischman Faculty of Engineering, Tel Aviv Univ., Israel. We demonstrate optical analogues of gravitational effects such as gravitational lensing, tidal forces and gravitational redshift in the Newton-Schrödinger mainframe, by utilizing long-range interactions between solitons and accelerating beams in nonlocal nonlinear media.

FM1D.3 • 08:30

PT symmetric large area single mode DFB lasers, Hossein Hodaie¹, Mohammad-Ali Miri¹, Matthias Heinrich¹, Demetrios N. Christodoulides¹, Mercedeh Khajavikhan¹; ¹CREOL The College of Optics and Photonics, Univ. of Central Florida, USA. We propose a novel class of large-area single-mode semiconductor lasers in which notions from parity-time symmetry is employed to reliably suppress higher-order modes. The feasibility of our design is investigated in InGaAsP quantum-well arrangements.

CLEO: Science & Innovations

08:00–10:00

SM1E • Atmospheric Sensing

President: Mark Phillips; Pacific Northwest National Lab, USA

SM1E.1 • 08:00 **Tutorial**

Recent developments in measurements of atmospheric trace gases, Steven C. Wofsy¹, Eric Kort², Eric Crosson³, Frank Keutsch⁴; ¹Harvard Univ., USA; ²Dept. of Atmospheric, Oceanic and Space Sciences, Univ. of Michigan, USA; ³Picarro, Inc, USA; ⁴Dept. of Chemistry, Univ. of Wisconsin, USA. Lasers are used to measure extremely low concentrations of reactive species and minute variations greenhouse gases in the atmosphere. Instrument challenges differ sharply, illustrated in case studies for atmospheric glyoxal, methane and others.



Steven Wofsy has a background in chemistry and physics, with interests and experience spanning stratospheric and tropospheric chemistry, from remote clean environments to urban areas, engaging sensor development from the fundamentals to commercialization, field and laboratory applications, and modeling and synthesis.

08:00–10:00

SM1F • Solid State Laser Systems for Secondary Source Generation

President: Thomas Spinka, Lawrence Livermore National Lab., USA

SM1F.1 • 08:00 **Invited**

Cryogenic Composite Disk Laser for Peak and Average Power Scaling, Luis E. Zapata^{1,2}; ¹Research Lab of Electronics, Dept of Electrical Engineering and Computer Science, MIT, USA; ²Center for free electron laser science, Deutsches Elektronen Synchrotron, Germany. We demonstrate high gain producing 60 mJ, 200 ps pulses at 200 Hz from a single 4-mm ASE limited gain-cell. A scaling paradigm utilizing a monolithic array of gain cells is proposed.

SM1F.2 • 08:30

Low temperature active mirror Yb:YAG laser amplifier gain studies, Thierry Goncalves-Novo¹, Samuel Marrazzo¹, Bernard Vincent¹, Jean-Christophe F. Chanteloup¹; ¹Laboratoire Utilisation des Lasers Intenses, Ecole Polytechnique, CNRS, CEA, UPMC, France. Single pass gain of 77mm crystal and ceramic Yb:YAG disks are compared in the 100–200K temperature range. Experiments are performed on a laser amplifier cooled through a static low pressure helium gas cell.

08:00–10:00

SM1G • Optical Signal Processing

President: Takahide Sakamoto; National Inst. of Information & Communication Tech, Japan

SM1G.1 • 08:00

Photonic Generation and Wireless Transmission of W-band Arbitrary Waveforms with High Time-Bandwidth Products, Amir Rashidinejad¹, Yihan Li¹, Jih-Min Wun², Daniel E. Leaird¹, Jin-Wei Shi², Andrew M. Weiner¹; ¹Electrical and Computer Engineering, Purdue Univ., USA; ²Electrical Engineering, National Central Univ., Taiwan. We report photonic radio-frequency arbitrary waveform generation in the W-band, enabled through optical pulse shaping and a near-ballistic uni-traveling-carrier photodiode. Example waveforms spanning 75–110GHz with long time apertures are generated and measured after wireless propagation.

SM1G.2 • 08:15

High Resolution Unambiguous Ranging Based on W-band Photonic RF-Arbitrary Waveform Generation, Yihan Li¹, Amir Rashidinejad¹, Jih-Min Wun², Daniel E. Leaird¹, Jin-Wei Shi², Andrew M. Weiner¹; ¹Electrical and Computer Engineering, Purdue Univ., USA; ²Electrical Engineering, National Central Univ., Taiwan. We demonstrate high resolution W-band ranging based on photonic radio-frequency arbitrary waveform generation. Arbitrarily long unambiguous detection of multiple simultaneous targets is successfully executed using a photonic-assisted time-aperture expansion technique.

SM1G.3 • 08:30

A Novel Intensity Modulator for Photonic ADCs using an Injection-Locked Mode-Locked Laser, Edris Sarailou¹, Abhijeet Ardey¹, Peter J. Delfyett¹; ¹Univ. of Central Florida, CREOL, USA. A novel intensity modulator for pulsed light is proposed and demonstrated here for the first time. This has been realized by introducing an injection-locked AlGaInAs mode-locked laser into one arm of a Mach-Zehnder interferometer.

08:00–10:00

SM1H • Advanced Fabrication Techniques

President: Koji Yamada; NTT Microsystem Integration Labs, Japan

SM1H.1 • 08:00

Arbitrary photonic wave plate operations on-chip: Realizing Hadamard and Pauli-X gates for polarization encoded qubits, René Heilmann¹, Markus Graefe¹, Stefan Nolte¹, Alexander Szameit¹; ¹Inst. of Applied Physics, Germany. We present arbitrary wave plate operations on-chip based on the reorientation of the waveguide's optical axis caused by additional stress fields. A successful implementation of Hadamard and Pauli-X gates for quantum light is shown.

SM1H.2 • 08:15

Mimicking Heterostructure Behavior Within a Single Material at Room Temperature Using Strain, David S. Sukhdeo¹, Donguk Nam¹, Ju-Hyung Kang², Jan Petykiewicz¹, Jae-Hyung Lee¹, Woo Shik Jung¹, Jelena Vuckovic¹, Mark Brongersma², Krishna C. Saraswati¹; ¹Electrical Engineering, Stanford Univ., USA; ²Materials Science and Engineering, Stanford Univ., USA. We present a new platform for mimicking heterostructure behavior within nanowires of a single material by using non-uniform strain. These pseudo-heterostructures have lithographically customizable band profiles and show effective carrier confinement at room temperature.

SM1H.3 • 08:30

Low-Stress Silicon Nitride Platform for Broadband Mid-Infrared Microphotonics, Pao T. Lin¹, Vivek Singh¹, Hao-Yu Greg Lin², Tom Tiwald³, Lionel Kimerling¹, Anuradha Agarwal¹; ¹Microphotonics Center, MIT, USA; ²Center for Nanoscale Systems, Harvard, USA; ³J. A. Woollam Co., Inc., USA. We demonstrate a sophisticated mid-IR microphotonics platform adopting engineered Si-rich and low-stress silicon nitride thin films where transparency up to $\lambda = 8.5 \mu\text{m}$ and loss less than 0.2 dB/cm were achieved.

Technical Digest and Postdeadline Papers Available Online

- Visit www.cleoconference.org
- Select **Download Digest Paper** button
- Use your email address and CLEO Registration ID # to synchronize

Once you have synchronized your conference registration with Optics InfoBase, you can log in directly to Optics InfoBase at any point using the same email address and OSA password.

Access must be established via synchronization within 60 days of the conference start date. Access is provided only to full technical attendees.

Meeting Room
211 B/D

Meeting Room
212 A/C

Meeting Room
212 B/D

Marriott
Salon I & II

CLEO: Science & Innovations

08:00–10:00

SM11 • Parametric Sources

Presider: Peter Schunemann; BAE Systems, USA

SM11.1 • 08:00

Ultra-broadband DFG in CdSiP2 at 6.5 μm with 2.3 cycle transform limit from an Er:Tm:Ho fiber laser, Daniel Sanchez¹, Michael Hemmer¹, Matthias Baudisch¹, Heinar Hoogland², Ronald Holzwarth², Kevin Zawilski³, Peter G. Schunemann³, Jens Biegert^{1,4}; ¹ICFO-Institut de Ciències Fòtoniques, Spain; ²Menlo Systems GmbH, Germany; ³BAE Systems, USA; ⁴ICREA-Institució Catalana de Recerca i Estudis Avançats, Spain. We generate ultra-broadband 6.5 μm pulses with 2.3 cycle transform limit and 85 pJ energy at 100 MHz from a phase-coherent, two-color, two-arm Er:Tm:Ho all-fiber MOPA system in CdSiP2.

SM11.2 • 08:15

Idler-Resonant Femtosecond Optical Parametric Oscillator with High Mid-Infra-Red Beam Quality, Lin Xu¹, David Shepherd¹, David J. Richardson¹, Jonathan H. Price¹; ¹Optoelectronics Research Centre, Univ. of Southampton, UK. We report an idler-resonant femtosecond optical parametric oscillator (OPO) with average output power of 520 mW, repetition-rate of 80 MHz, pulse duration of 90 fs and nearly diffraction-limited beam quality at $\sim 2.4 \mu\text{m}$.

SM11.3 • 08:30

Difference-Frequency Generation of Fs And Ps Mid-IR Pulses in LiInSe2 Based on Yb-Fiber Laser Pump Sources, Marcus Beutler¹, Ingo Rimke¹, Edlef Büttner¹, Valentin Petrov², Ludmila Isaenko³; ¹APE, Germany; ²Max Born Inst., Germany; ³Inst. of Geology & Mineralogy, Russia. Difference-frequency generation between signal and idler of Yb-fiber laser synchronously-pumped femtosecond / picosecond OPOs at 53/80 MHz provides maximum single pulse energies exceeding 1 nJ and continuous tuning from 5 μm to 12 μm .

08:00–10:00

SM1J • UV and Visible LEDs

Presider: Hongping Zhao, Case Western Reserve Univ., USA

SM1J.1 • 08:00

Anisotropic optical polarization of AlGaIn based 275 nm light-emitting diodes due to quantum-size effects, Jonathan J. Wierer¹, Ines Montano¹, Mary Crawford¹, Andy A. Allerman¹; ¹Sandia National Labs, USA. Quantum-size effects strongly influence the valence band and optical polarization of 275nm emitting Al0.44Ga0.56N layers. It's shown experimentally and theoretically that thinner quantum wells and lower carrier densities result in polarization preferential for light extraction.

SM1J.2 • 08:15

Temperature dependence of Sub-220nm Emission from GaN/AlN Quantum Structures by Plasma Assisted Molecular Beam Epitaxy, SM Islam¹, Vladimir Protasenko¹, Huili G. Xing¹, Debdeep Jena¹, Jai Verma¹; ¹Univ. of Notre Dame, USA. GaN/AlN structures are utilized to achieve deep-UV emission. By reducing thickness of GaN QW to 1 ML, 224nm emission is achieved. A further shift to 219nm is gettable as GaN islands are introduced.

SM1J.3 • 08:30


Enhanced Light Extraction Efficiency of Deep-Ultraviolet Light-Emitting Diodes by Al-Coated Selective-Area-Grown GaN stripes, Dong Yeong Kim¹, Jong Won Lee¹, Jeung Jae Oh¹, Sunyong Hwang¹, Junhyuk Park¹, Jong Kyu Kim¹; ¹Materials Science and Engineering, POSTECH, Korea. We present a new type of AlGaIn-based deep ultraviolet light-emitting diodes with Al-coated selective-area-grown n-type GaN stripes to extract strong side emission perpendicular to the [0001] c-axis and to improve the electrical property.

CLEO: QELS-Fundamental Science

08:00–10:00

FM1K • Applications of Localized Surface Plasmons

Presider: Hatice Altug, Boston Univ., USA

FM1K.1 • 08:00 

Coherent Plasmonics: Optimized for Sensing and Energy Transfer, Naomi J. Halas¹; ¹ECE, Rice Univ., USA. Metallic nanostructures give rise to bright and dark plasmon modes, and through their interactions can support a variety of coherent phenomena more typically associated with atomic systems, providing new sensing and energy transfer strategies.

FM1K.2 • 08:30

Surface and Volume Photoemission of Hot Electrons from Plasmonic Nanoantennas, Alexander Uskov^{1,2}, Igor Protsenko¹, Renat Ikhsanov³, Viktoriia Babicheva^{4,5}, Sergei Zhukovskiy⁴, Andrei Lavrinenko⁴, Eoin O'Reilly⁶, Hongxing Xu^{2,7}; ¹P. N. Lebedev Physical Inst. and Advanced Energy Technologies Ltd, Russia; ²Wuhan Univ., China; ³Research Inst. of Scientific Instruments, Russia; ⁴Technical Univ. of Denmark, Denmark; ⁵National Research Univ. for Information Technology, Mechanics, and Optics, Russia; ⁶Tyndall National Inst., Ireland; ⁷Inst. of Physics, Chinese Academy of Sciences, China. We theoretically compare surface- and volume-based photoelectron emission from spherical nanoparticles, obtaining analytical expressions for the emission rate in both mechanisms. We show that the surface mechanism prevails, being unaffected by detrimental hot electron collisions.

CLEO: Applications & Technology


08:00–10:00

AM1L • Advanced Material Processing

Presider: Michael Mielke; Raydiance Inc, USA

AM1L.1 • 08:00 

Innovative Applications of Femtosecond Laser Induced Nanostructure, Yasuhiko Shimotsuma¹, Taiga Asai¹, Masahiro Mori¹, Sho Kubota¹, Tomoaki Sei¹, Kazuki Fujiwara¹, Masaaki Sakakura¹, Kiyotaka Miura¹, Peter G. Kazansky²; ¹Dept. of Material Chemistry, Kyoto Univ., Japan; ²Optoelectronics Research Centre, Univ. of Southampton, UK. The nanostructure induced by the direct-writing of femtosecond-laser pulses can open a new opportunity to develop avant-garde devices such as a 5D optical storage, polarization imaging sensor, thermoelectric conversion elements.

AM1L.2 • 08:30 

Nanotexturing of Glass Surface by Ultrafast Laser Assisted Wet Etching, Rokas Drevinskis¹, Mindaugas Gecevičius¹, Martynas Beresna¹, Yves Bellouard², Peter G. Kazansky¹; ¹Optoelectronics Research Centre, Univ. of Southampton, UK; ²Mechanical Engineering Dept., Eindhoven Univ. of Technology, Netherlands. Surface texturing with 30 nm resolution is demonstrated by KOH wet etching and ultrafast laser nanostructuring of silica. An increase of three times in retardance is achieved leading to the fabrication of dichroic glass-metal patterns.

Monday, 9 June

There is still time to register for a Short Course!

Visit Registration to learn about the courses still available.

View page 17 for complete Short Course Information.

Monday, 9 June

SC270 • High Power Fiber Lasers and Amplifiers
SC301 • Quantum Cascade Lasers: Science, Technology, Applications and Markets
SC376 • Plasmonics
SC402 • Transformational Optics

Tuesday, 10 June

SC271 • Quantum Information-Technologies and Applications
SC352 • Introduction to Ultrafast Pulse Shaping—Principles and Applications
SC362 • Cavity Optomechanics: Fundamentals and Applications of Controlling and Measuring Nano- and Micro-mechanical Oscillators with Laser Light
SC379 • Silicon Photonic Devices and Applications
SC410 • Finite Element Modelling Methods for Photonics and Optics

CLEO: Science & Innovations

CLEO: Applications
& Technology

08:00–10:00


SM1M • Frequency Combs and Novel Light Sources *Presider: Yoshitomo Okawachi; Cornell Univ., USA*SM1M.1 • 08:00  

Ga(In)N Nanowire Light Emitting Diodes and Single Photon Sources, Pallab K. Bhattacharya¹, Saniya Deshpande¹, Shafat Jahangir²; ¹Univ. of Michigan, USA. Abstract: Ga(In)N nanowires and Ga(In)N quantum disks can be grown defect-free on silicon with p- and n-doping to form diodes. We will describe the characteristics of light-emitting diodes and electrically injected single nanowire single photon sources. OCIS codes: (230.3670) Light-emitting diodes; (250.5590) Quantum-well, -wire and -dot devices.

SM1M.2 • 08:30 

Gallium Nitride Nanowire Distributed Feedback Lasers, Jeremy B. Wright^{1,2}, Salvatore Campione^{1,3}, Sheng Liu^{1,3}, Julio Martinez^{3,4}, Huiwen Xu², Ting S. Luk^{1,3}, Qiming Li¹, George T. Wang¹, Brian S. Swartzentruber^{1,3}, Igal Brener^{1,3}; ¹Sandia National Labs, USA; ²Center for High Technology Materials, The Univ. of New Mexico, USA; ³Center for Integrated Nanotechnology, Sandia National Labs, USA; ⁴Dept. of Chemical Engineering, New Mexico State Univ., USA. We have demonstrated single-mode lasing in a single gallium nitride nanowire using distributed feedback by external coupling to a dielectric grating. By adjusting the nanowire grating alignment we achieved a mode suppression ratio of 17dB.

08:00–10:00

SM1N • SDM and Bandgap Fibers*Presider: Siddharth Ramachandran; Boston Univ., USA*SM1N.1 • 08:00 

Emerging Fiber Technology for Space Division Multiplexed Optical Communications, David J. Richardson¹; ¹Optoelectronics Research Centre, Univ. of Southampton, UK. Space Division Multiplexing (SDM) offers the potential for ultrahigh information-flux optical communications at the petabit/s level, as well as reduced costs-per-bit. I review progress to date and discuss some of the technological/commercial challenges and opportunities that lie ahead.




David Richardson is Deputy Director of the Optoelectronics Research Centre at the University of Southampton. His current research interests include amongst others: optical fiber communications, microstructured optical fibers and high-power fiber lasers. He is a Fellow of The Optical Society, the Institute of Engineering and Technology and was made a Fellow of the Royal Academy of Engineering in 2009.

08:00–10:00

SM1O • Pulse Generation and Amplification *Presider: Jeffrey Nicholson; OFS Labs, USA*SM1O.1 • 08:00 

Sub-50fs all-fiber source based on a 100ps passively Q-switched microchip laser, Pascal Dupriez¹, Christophe Pierre¹; ¹Alphanov, France. We demonstrate a fiber-based source producing 50fs pulses at 1055nm starting from fiber amplified 100ps pulses produced by a passively Q-switched microchip laser. Pulse compression is achieved monolithically through succession of spliced microstructured fibers.

SM1O.2 • 08:15 

Spectrally coherent efficient femtosecond Stokes pulse generation from a photonic crystal fiber with two zero dispersion wavelengths (TZDW), Yuhong Yao¹, Wayne Knox¹; ¹Inst. of Optics, Univ. of Rochester, USA. We report the first experimental characterization of spectral coherence of Stokes-side continuum from fiber with two zero dispersion wavelength. We achieve 3-nJ, coherent Stokes pulses localized ~1.28 μm from 300-fs Yb: fiber laser with 32% efficiency.


SM1O.3 • 08:30 

Ultrafast fiber ring lasers with a pair of chirped fiber Bragg gratings, Simon Duval¹, Michel Olivier^{1,2}, Martin Bernier¹, Réal Vallée¹, Michel Piché¹; ¹Centre d'optique, photonique et laser, Université Laval, Canada; ²Département de physique, Cégep Garneau, Canada. The performance of mode-locked fiber ring lasers incorporating two opposite-dispersion chirped fiber Bragg gratings is presented in different dispersion regimes. Pulses of nanojoule energy and duration well below 100 fs are generated.

08:00–10:00

AM1P • Symposium on Advances in Molecular Imaging I *Presider: Yu Chen; Univ. of Maryland at College Park, USA*AM1P.1 • 08:00  

Clinical Translation and Discovery with Near-infrared Fluorescence Lymphatic Imaging, John C. Rasmussen¹, Eva M. Sevcik-Muraca¹; ¹The Brown Foundation Inst. of Molecular Medicine, Univ. of Texas Health Science Center, USA. Near-infrared fluorescence (NIRF) lymphatic imaging enables, for the first time, non-invasive visualization and quantification of human lymphatic architecture and contractile function in health and disease. This contribution reviews NIRF lymphatic imaging and its clinical translation.

AM1P.2 • 08:30 

Clinical translation of near-infrared image-guided surgery: Where do we stand?, Sylvain Gioux¹; ¹Medicine, BIDMC / Harvard Medical School, USA. In this presentation, we will review our translational efforts in image-guided surgery using diffuse NIR light. We will present our latest developments in imaging devices and contrast agents towards clinically-realistic image guidance during surgical interventions.

Visit Registration to Purchase

Access your Favorite Talks or One You Missed!
On-Demand, 24/7

Over 300 high-quality, informative talks representing the full breadth of CLEO's outstanding technical program including:

Tutorials • Contributed • Postdeadline
Symposia • Plenary talks • Invited

CLEO: QELS-Fundamental Science

FM1A • Quantum
Engineering—Continued

FM1A.2 • 09:00

Ultrasensitive measurement of MEMS cantilever displacement below the photon shot noise limit, Benjamin Lawrie¹, Raphael Pooser¹; ¹Quantum Information Science Group, Oak Ridge National Lab, USA. We demonstrate sub-shot-noise microcantilever displacement sensitivity using simple differential measurements with multi-spatial-mode squeezed light, a result that may be critical for ultra-trace sensing and imaging applications.

FM1A.3 • 09:15

Displacement of entanglement back and forth between the micro and macro domains, Natalia Bruno¹, Anthony Martin¹, Nicolas Sangouard¹, Rob Thew¹, Nicolas Gisin¹; ¹Group of Applied Physics, Univ. of Geneva, Switzerland. We report an experimental observation of heralded entanglement involving two components that can be distinguished with detectors resolving only large photon number differences. We demonstrate entanglement in states containing over 500 photons.

FM1B • Relativistic Laser-Plasma
Interactions—Continued

FM1B.3 • 08:45

Ion Acceleration by the 10^{21} W/cm² Intensity High Contrast Laser Pulses Interacting with the Thin Foil Target, Mamiko Nishiuchi¹, Sakaki Hironao¹, Katsuhisa Nishio², Richard Orlandi², Hiroyuki Sako², Tatiana Pikuz^{1,6}, Anatoly Faenov^{1,6}, Timu Esirkepov¹, Alexander Pirozhkov¹, Kenya Matsukawa⁴, Akito Sagisaka¹, Koichi Ogura¹, Masato Kanasaki⁴, Hiromitsu Kiriyama¹, Yuji Fukuda¹, Hiroyuki Koura², Masaki Kando¹, Tomoya Yamauchi⁴, Yukinobu Watanabe⁵, Sergei Bulanov¹, Kiminori Kondo¹, Koichi Imai², Shoji Nagamiya⁷; ¹Kansai Photon Science Inst., Japan Atomic Energy Agency, Japan; ²Advanced Science Research Center, JAEA, Japan; ³J-PARC Center, Japan; ⁴Graduate School of Science Maritime Science, Kobe Univ, Japan; ⁵Interdisciplinary Graduate School of Engineering Sciences, Kyushu Univ., Japan; ⁶Joint Inst. for High Temperature of RAS, RAS, Russia; ⁷RIKEN, Japan. Almost fully stripped aluminum ion acceleration up to 12 MeV/u from the interaction between the ultra-intense short pulse high contrast laser and the micrometer thick foil target is presented.

FM1B.4 • 09:00

Increasing Laser Contrast by Relativistic Self-Guiding and its Application to Laser-Based Proton Acceleration, Yu-hsin Chen¹, David Alessi¹, Derrek Drachenberg¹, Bradley Pollock¹, Félicie Albert¹, Joseph Ralph¹, Constantin L. Haefner¹; ¹Lawrence Livermore National Lab, USA. Laser-produced energetic protons via target normal sheath acceleration are deteriorated by amplified spontaneous emission (ASE). Here we test a new method of reducing ASE and increasing proton energy by relativistic self-guiding in the plasma.

FM1B.5 • 09:15

Generating ultrashort hundreds-of-keV electron bunches using radially polarized laser pulses, Vincent Marceau¹, Charles Varin², Thomas Brabec², Michel Piché¹; ¹Centre d'Optique, Photonique et Laser, Université Laval, Canada; ²Center for Research in Photonics, Univ. of Ottawa, Canada. Particle-in-cell simulations show that quasimonochromatic electron bunches with one-femtosecond initial duration may be produced from direct acceleration in a low-density gas. These bunches could find applications in ultrafast electron diffraction experiments.

FM1C • Hyperbolic and Epsilon-
near-zero Materials—Continued

FM1C.4 • 08:45

Broadband Absorption Engineering of Hyperbolic Metamaterial Patterns, Dengxin Ji¹, Haomin Song¹, Xie Zeng¹, Haifeng Hu¹, Kai Liu¹, Nan Zhang¹, Qiaoqiang Gan¹; ¹Dept. of Electrical Engineering, The State Univ. of New York at Buffalo, USA. We experimentally realize a patterned hyperbolic metamaterial with engineered and freely tunable absorption band from near-IR to mid-IR spectral regions based on multilayered metal/dielectric hyperbolic metamaterial waveguide taper.

FM1C.5 • 09:00

Enhancement of Radiative Emission using a Hyperbolic Metamaterial Nano-antenna, Caner Guclu¹, Ting S. Luk², George T. Wang², Michael B. Sinclair², Filippo Capolino¹; ¹Electrical Engineering and Computer Science, Univ. of California, Irvine, USA; ²Sandia National Labs, USA. A hyperbolic metamaterial resonator is utilized as a nano-antenna for enhancing the radiative emission from a quantum emitter at 660 nm wavelength. Simulated power radiation enhancement up to 100 folds is demonstrated.

FM1C.6 • 09:15

Control of chemical reactions in the vicinity of hyperbolic metamaterials and metallic surfaces, Vanessa Peters¹, Thejaswi U. Tumkur¹, Mikhail A. Noginov¹; ¹Center for Materials Research, Norfolk State Univ., USA. We show that photo-oxidation of organic semiconducting films can be controlled by geometry and composition of metallic and metal/dielectric substrates, in agreement with increase of the chemical reaction rate by the density of photonic states.

FM1D • PT Symmetry and
Related Phenomena—
Continued

FM1D.4 • 08:45

Light Transport in PT Photonic Structures with Hidden Symmetries, Ramy El-Ganainy¹, Mohammad Teimourpour¹, Alexander Eifeld², Demetrios N. Christodoulides³; ¹Physics, Michigan Technological Univ., USA; ²Max Planck Inst. for the Physics of Complex Systems, Germany; ³College of Optics and Photonics-CREOL, Univ. of Central Florida, USA. We introduce a bosonic quantization technique for generating PT photonic structures that possess hidden symmetries. We investigate light transport in these geometries under linear and nonlinear conditions and we demonstrate a host of new effects.

FM1D.5 • 09:00

Scattering off PT-symmetric particles, Mohammad-Ali Miri¹, Mohammad Amin Eftekhar¹, Margarida Facao², Demetrios N. Christodoulides¹; ¹CREOL/College of Optics and Photonics, Univ. of Central Florida, USA; ²Dept. of Physics, Univ. of Aveiro, Portugal. We investigate scattering properties of parity-time-symmetric cylinders. We show that the scattering pattern of such structures changes drastically by changing the angle of incidence. In addition PT particles preferentially deflect light at a certain angle.

FM1D.6 • 09:15

Spontaneous symmetry breaking induced by tachyon condensation in amplifying metal-dielectric multi-layered media, Andrea Marini¹, Truong X. Tran^{1,2}, Samudra Roy^{1,3}, Stefano Longhi⁴, Fabio Biancalana^{1,5}; ¹Max Planck Inst., Germany; ²Physics, Le Quy Don Univ., Viet Nam; ³Physics and Meteorology, Indian Inst. of Technology, India; ⁴Physics, Politecnico di Milano, Italy; ⁵School of Engineering and Physical Sciences, Heriot-Watt Univ., UK. We theoretically investigate an optical analogue of tachyon condensation in amplifying plasmonic arrays. We demonstrate that the vacuum state is unstable and acquires an expectation value with broken chiral symmetry.

CLEO: Science & Innovations

SM1E • Atmospheric Sensing—
Continued

SM1E.2 • 09:00

Isotopic Ratiometry of Nitric Oxide using a Dual-modulation Faraday Rotation Spectrometer, Eric J. Zhang¹, Farhan Nuruzaman², Yin Wang¹, Daniel Sigman², Gerard Wysocki¹; ¹Electrical Engineering, Princeton Univ., USA; ²Geosciences, Princeton Univ., USA. A dual-modulation Faraday rotation spectrometer is employed for isotopic ratiometry of nitric oxide (NO) converted from nitrate/nitrite. Excellent linearity of measured NO to dissolved nitrate is demonstrated. Ratiometry of IAEA-NO-3 standards indicates ~3 % accuracy.

SM1E.3 • 09:15

Compact, Automated Differential Absorption Lidar for Tropospheric Profiling of Water Vapor, David M. Sonnenfroh¹, Kevin Repasky², Amin Nehrir³; ¹Physical Sciences Inc., USA; ²Montana State Univ., USA; ³NASA Langley Research Center, USA. We describe the engineering development of a compact differential absorption lidar, using a diode laser-seeded semiconductor optical amplifier as the transmitter, for profiling water vapor in the lower atmosphere.

SM1F • Solid State Laser
Systems for Secondary Source
Generation—Continued

SM1F.3 • 08:45

Fiber-seeded, 10-ps, 2050-nm, multi-mJ, cryogenic Ho:YLF CPA, Michaël Hemmer¹, Daniel Sanchez¹, Michal Jelínek², Helena Jelínková², Václav Kubeček², Jens Biegert^{1,3}; ¹ICFO - The Inst. of Photonic Sciences, Spain; ²Czech Technical Univ., Czech Republic; ³ICREA - Institutio Catalana de Recerca i Estudis Avancats, Spain. We demonstrate the first picosecond cryogenic Ho:YLF CPA system with Er:Tm:Ho fiber seeder. The system delivers energy-scalable 13-mJ pulses with 10-ps duration at 100 Hz repetition rate.

SM1F.4 • 09:00 **Invited**

1 Joule, 100 Hz Repetition Rate, Picosecond CPA Laser for Driving High Average Power Soft X-Ray Lasers, Brendan A. Reagan¹, Cory Baumgarten¹, Keith Wernsing¹, Herman Bravo¹, Mark Woolston¹, Alden Curtis¹, Federico J. Furch¹, Brad Luther¹, Dinesh Patel¹, Carmen Menoni¹, Jorge J. Rocca¹; ¹Colorado State Univ., USA. A diode-pumped cryogenic Yb:YAG CPA laser that produces 1J, 5ps pulses allowed for the first time the uninterrupted generation of 1.8×10^5 sub-20nm wavelength laser pulses with microjoule energy at 100Hz repetition rate on a table-top.

SM1G • Optical Signal
Processing—Continued

SM1G.4 • 08:45

Experimental Demonstration of Vpi Reduction in EO Modulators using Modulation Instability, David Borlaug¹, Peter DeVore¹, Bahram Jalali¹; ¹Dept. of Electrical Engineering, Univ. of California, Los Angeles, USA. An electrooptic modulator's half-wave voltage is experimentally lowered by 10-fold for intensity modulated waveforms using modulation instability. Results are reported up to 50 GHz.

SM1G.5 • 09:00

Experimental Demonstration of a 2-Stage Continuously Tunable Optical Tapped-Delay-Line in which N+M Pump Lasers Produce N×M Taps, Amirhossein Mohajerin Ariaei¹, Mohammed Chitgarha¹, Morteza Ziyadi¹, Salman Khaleghi¹, Ahmed Almaiman¹, Joseph Touch², Moshe Tur³, Loukas Paraschis⁴, Carsten Langrock⁵, Martin M. Fejer⁵, Alan Willner¹; ¹Electrical Engineering, Univ. of Southern California, USA; ²Information Sciences Inst.-Univ. of Southern California, USA; ³Electrical Engineering, Tel Aviv Univ., Israel; ⁴Cisco Systems, USA; ⁵Edward L. Ginzton Lab-Stanford Univ., USA. We experimentally demonstrate a 2-stage continuously tunable optical tapped-delay-line in which N+M pump lasers produce N×M number of taps. A 3×2-taps optical correlator is implemented to search multiple patterns among 20-Gb/ud QPSK signals using nonlinearities and coherent comb source.

SM1G.6 • 09:15

High-speed ultrawideband compressed sensing of sparse radio frequency signals, Bryan T. Bosworth¹, Mark A. Foster¹; ¹Johns Hopkins Univ., USA. Using chirp processing of ultrafast laser pulses to perform pseudorandom measurements for compressed sensing, we successfully reconstruct multi-tone sparse-frequency microwave signals with an effective sampling rate well beyond the electronic limit.

SM1H • Advanced Fabrication
Techniques—Continued

SM1H.4 • 08:45

Fabrication of Diffractive Optical Elements with Digital Projection Photochemical Etching, Christopher A. Edwards¹, Kaiyuan Wang¹, Benjamin G. Griffin¹, Renjie Zhou¹, Basanta Bhaduri¹, Gabriel Popescu¹, Lynford L. Goddard¹; ¹Dept. of Electrical and Computer Engineering, Univ. of Illinois at Urbana-Champaign, USA. We demonstrate a new fabrication technique called digital projection photochemical etching and apply it to make complicated gray-scale diffractive optical elements, such as a radial sinusoidal grating, in a single processing step.

SM1H.5 • 09:00

Tuning the Visible-to-Infrared Reflectance Spectra of Arrays of Vertical Ge Nanowires, Amit Solanki¹, Hyunsung Park¹, Kenneth B. Crozier¹; ¹School of Engineering and Applied Sciences, Harvard Univ., USA. We experimentally demonstrate that, by varying their diameter, the visible-to-infrared reflectance spectra of arrays of vertical Ge nanowires can be tuned. The results could enable future nanowire-based photodetectors with tailored responsivity spectra.

SM1H.6 • 09:15

On-chip Optical Isolators Based on a Ring Resonator with Bismuth-iron-garnet Overcladding, Kuanping Shang¹, Stanley Cheung¹, Binzhi Li², Ryan P. Scott¹, Yayoi Takamura², S. J. Ben Yoo¹; ¹Electrical Engineering and Computer Science, Univ. of California, Davis, USA; ²Chemical Engineering and Materials Science, Univ. of California, Davis, USA. This paper discusses on-chip optical isolators with bismuth-iron-garnet (BIG) overcladding on a ring resonator for photonic integrated circuit applications. Characterization of BIG prepared by RF magnetron sputtering and pulsed laser deposition methods are also discussed.

CLEO: Science & Innovations

CLEO: QELS-
Fundamental ScienceCLEO: Applications
& TechnologySM11 • Parametric Sources—
Continued

SM11.4 • 08:45

Mid-Infrared ZnGeP₂-Based Source with 0.2 J Pulse Energy, Magnus W. Haakestad¹, Helge Fonnum¹, Espen Lippert¹; ¹Norwegian Defense Research Establishment, Norway. Mid-infrared (3-5 μm) pulses with up to 207 mJ energy at 1 Hz repetition rate are produced using nonlinear conversion in a ZnGeP₂-based master oscillator-power amplifier, pumped by a cryogenic Ho:YLF oscillator.

SM11.5 • 09:00

Multiwatt-level Continuous-Wave Midwave Infrared Generation using Difference Frequency Mixing in Periodically Poled Lithium Niobate, Shekhar Guha¹, Jacob O. Barnes², Leonel P. Gonzalez³; ¹US Air Force Research Lab, USA; ²UES, Inc., USA. More than 2 Watts of continuous-wave external power at 3400 nm was obtained by difference frequency mixing of 1064.6 nm and 1549.8 nm fiber lasers in a periodically poled lithium niobate crystal at 50 C.

SM11.6 • 09:15

Tunable mid-infrared (6.3-7.8 μm) optical vortex laser, Micheal Tomoki Horikawa¹, Kenji Furuki¹, Yu Tokizane¹, Katsuhiko Miyamoto¹, Takashige Omatsu^{1,2}; ¹Chiba Univ., Japan; ²CREST, Japan. We demonstrate a tunable mid-infrared (6.3-7.8-μm) vortex laser formed of a 1-μm vortex pumped optical parametric oscillator and a difference frequency generator. Maximum output energy of 160-μJ was obtained at a wavelength of 6.5-μm.

SM11J • UV and Visible LEDs—
Continued

SM11J.4 • 08:45

Excellent Color Rendering Index Quantum Dots White Light-Emitting Diode with Distributed Bragg Reflector Structure, Kuo-Ju Chen¹, Bing-Cheng Lin¹, Hau-Vei Han¹, Chien-Chung Lin², Chia-Yu Lee¹, Shih-Hsuan Chien¹, Kuan-Yu Wang², Sheng-Huan Chiu¹, Teng-Ming Chen³, Min-Hsiung Shih^{1,4}, Hao-chung Kuo¹; ¹Dept. of Photonic, Inst. of Electro-Optical Engineering, National Chiao Tung Univ., Taiwan; ²Inst. of Photonic System, Taiwan; ³Dept. of Applied Chemistry, Inst. of Molecular Science, National Chiao Tung Univ., Taiwan; ⁴Research Center for Applied Sciences, Academia Sinica, Taiwan. This study demonstrated the high CRI and excellent uniformity colloidal quantum dot white-light-emitting diodes with the DBR structure at different correlated color temperature from 2500 K to 4500K.

SM11J.5 • 09:00 **Invited**

Auger recombination in light-emitting materials, Emmanouil Kiopakis^{1,2}, Qimin Yan^{2,3}, Chris G. Van de Walle²; ¹Materials Science and Engineering, Univ. of Michigan, USA; ²Materials Dept., Univ. of California, USA; ³The Molecular Foundry, Lawrence Berkeley National Lab, USA. First-principles calculations show that phonon-assisted Auger recombination and its interplay with the polarization fields in polar nitride LEDs play an important role in the efficiency-droop and green-gap problems of these devices.

FM1K • Applications of
Localized Surface Plasmons—
Continued

FM1K.3 • 08:45

Metal single-nanowire plasmonic sensors, Fuxing Gu¹, Heping Zeng^{1,2}; ¹School of Optical-Electrical and Computer Engineering, Univer. of Shanghai for Science and Tech, China; ²State Key Lab of Precision Spectroscopy, East China Normal Univ., China. Metal nanowires including Pd nanoparticle-coated Au nanowires, polyacrylamide film-supported Ag nanowires, and single-crystal Pd nanowires are used for hydrogen and humidity plasmonic sensing, with higher sensitivity and faster response than those in conventional photonic nanowires.

FM1K.4 • 09:00

Titanium nitride nanoparticles for therapeutic applications, Urcan Guler¹, Alexander Kildishev¹, Alexandra Boltasseva^{1,2}, Vladimir M. Shalaev¹; ¹School of Electrical & Computer Engineering and Birk Nanotechnology Center, Purdue Univ., USA; ²Dept. of Photonics Engineering, Technical Univ. of Denmark, Denmark. Titanium nitride nanoparticles exhibit plasmonic resonances in the biological transparency window where high absorption efficiencies can be obtained with small dimensions. Both lithographic and colloidal samples are examined from the perspective of nanoparticle thermal therapy.

FM1K.5 • 09:15

Bidirectional Wavelength Multiplexing with an Optical Fano Nanoantenna, Rui Guo¹, Manuel Decker¹, Isabelle Staude¹, Dragomir N. Neshev¹, Yuri S. Kivshar¹; ¹Nonlinear Physics Centre, Australian National Univ., Australia. We introduce the novel concept of a single-element Fano nanoantenna allowing for strong directional scattering of light in opposite directions depending on wavelength. Our design opens the way for novel bi-directional wavelength multiplexers.

AM1L • Advanced Material
Processing—ContinuedAM1L.3 • 08:45 **▶**

Femtosecond laser processing for mobile display manufacturing, Eric Mottay¹, Clemens Hoenninger¹, Laurie Wipliez², Jiyeon Choi³, Sung-Hak Cho³; ¹Amplitude Systemes, France; ²Alphanov, France; ³Korean Inst. of Machinery and Materials, Korea. The development of new display technologies, such as organic LEDs and flexible displays, put stringent requirements in term of manufacturing processes. We report on new results aiming at improving processing quality and yield.

AM1L.4 • 09:00 **▶**

Fiber Laser Annealing of Ti CP1 and Al6060 aimed at improving formability in Hydroforming Technology, Stefano Zarini¹, Ehsan Moasted¹, Barbara Previtali¹, Maurizio Vedani¹; ¹Dept. of Mechanical Engineering, Politecnico di Milano, Italy. This paper presents the feasibility study of laser annealing of two materials: Ti CP1 and Al6060. Effectiveness of the method is proved firstly on planar samples and then applied on a real industrial component.

AM1L.5 • 09:15 **▶**

Modeling of Powder Absorption in Additive Manufacturing, Charles Boley¹, Saad Khairallah¹, Alexander M. Rubenchik¹; ¹Lawrence Livermore National Lab, USA. We have investigated optical absorption by a powder of metal spheres, via ray-trace calculations. The absorptivity significantly exceeds that for normal incidence, because of multiple scattering. The effect of beam size is also discussed.



Join the conversation. Use #CLEO14.
Follow us @cleoconf on Twitter.

CLEO: Science & Innovations

CLEO: Applications
& TechnologySM1M • Frequency Combs
and Novel Light Sources—
ContinuedSM1M.3 • 08:45 

Spectral Coherence in Microresonator Combs, Victor Torres-Company¹, Enrique Silvestre², David Castello-Lurbe²; ¹Dept. of Microtechnology and Nanoscience, Chalmers Univ. of Technology, Sweden; ²Departament d'Optica, Universitat Valencia, Spain. We provide a quantitative analysis of the coherence in microresonator frequency combs. We show how to achieve coherent transform-limited pulses on-chip without actively manipulating the pump setting conditions in the course of comb formation.

SM1M.4 • 09:00 

Switchable Optical Frequency Comb in Aluminum Nitride Microring Resonator, Hojoong Jung¹, King Y. Fong¹, Chi Xiong¹, Xufeng Zhang¹, Hong Tang¹; ¹Yale Univ., USA. Aluminum nitride is a promising nonlinear optical material with its strong Kerr and Pockels effects. Here we report optical frequency comb generation from aluminum nitride microring resonators and electrical switching of the comb.

SM1M.5 • 09:15 

Tailoring of a Broader and Flatter Frequency Comb using a Microring Resonator with a Low-Index Slot, Changjing Bao¹, Lin Zhang², Yan Yan¹, Hao Huang¹, Guodong Xie¹, Anu Agarwal², Lionel Kimerling², Jurgen Michel², Alan Willner¹; ¹Dept. of Electrical Engineering, Univ. of Southern California, USA; ²Dept. of Material Science and Engineering, MIT, USA. A dispersion-flattened microresonator based on slot waveguide exhibits great performance improvement of Kerr frequency combs by engineering the 2nd-order dispersion amount and anomalous-dispersion bandwidth with all-order dispersion taken into account.

SM1N • SDM and Bandgap
Fibers—Continued

SM1N.2 • 09:00

37-cell hollow-core-fiber designs with improved single-modedness, John M. Fini¹, Brian Mangan¹, Linli Meng¹, Eric M. Monberg¹, Jeffrey W. Nicholson¹, Robert S. Windeler¹; ¹OFS Labs, USA. Simulations show that the PRISM strategy for suppression of higher-order modes can be applied broadly, to cores larger than 19-cell and core thicknesses larger than half the lattice web thickness.

SM1N.3 • 09:15


Ultra low-loss hypocycloid-core kagome hollow-core photonic crystal fiber for the green spectral-range applications, Benoît Debord¹, Meshaal Alharbi¹, Aurélien Benoît¹, Madhoussoudhana Dontabactouy¹, Jean-Marc Blondy¹, Frédéric Gérôme¹, Fetah Benabid¹; ¹GPPMM group, Xlim Research Inst., UMR CNRS 7252, France. We report on the development of hypocycloidal-core kagome HC-PCF operating efficiently in the 450nm-650nm visible spectral range. Transmission loss as low as 70dB/km is achieved. Strong Raman comb generation and laser beam delivery are demonstrated.

SM1O • Pulse Generation and
Amplification—ContinuedSM1O.4 • 08:45 

Tunable Broadband Source of Femtosecond Pulses in the 2 μm Region, Andrew Klose¹, Daniel Maser^{1,2}, Gabriel Ycas^{1,2}, Scott A. Diddams¹; ¹NIST, USA; ²Physics, Univ. of Colorado, USA. A polarization maintaining Er: fiber-based source of femtosecond pulses was constructed using a 250 MHz mode-locked oscillator, fiber amplifier, and highly nonlinear fiber. The system generated 35 fs pulses with power variation of 1.3% on a timescale of days.

SM1O.5 • 09:00 

FCPA System at 2.08 μm and 7 MHz in All-PM Design Delivering Pulses at 10 nJ and 390 fs Pulse Duration, Heinar Hoogland¹, Steffen Wittek¹, Wolfgang Hänsel¹, Ronald Holzwarth^{1,2}; ¹Menlo Systems GmbH, Germany; ²Max-Planck-Inst. of Quantum Optics, Germany. We report on an all-PM fiber oscillator-CPA system at 2.08 μm running at 7 MHz pulse repetition rate with 10 nJ pulse energy and 390 fs pulse duration behind external compression.

SM1O.6 • 09:15 

Visible short pulse generation in waterproof fluoro-aluminate glass fibers using graphene thin film, Takafumi Suzuki^{1,2}, Ricardo Arturo Ochante Muray¹, Moto-ichiro Murakami¹, Takashi Hirayama^{1,2}, Minoru Yoshida², Osamu Ishii³, Masaaki Yamazaki³, Hiroyuki Shiraga¹, Yasushi Fujimoto¹; ¹Osaka Univ., Japan; ²Kinki Univ., Japan; ³Sumita Optical Glass, Inc., Japan. We have successfully generated a Q-switched short pulse in a Pr-doped waterproof fluoro-aluminate glass fiber using a single layer graphene as a saturable absorber. The laser pulse duration was observed to be 17.6 ns.

AM1P • Symposium on
Advances in Molecular Imaging
I—ContinuedAM1P.3 • 09:00  

In Vivo Molecular Imaging using Cerenkov Luminescence, Simon Cherry¹; ¹Univ. of California Davis, USA. Many radionuclides, upon decay, produce visible light via the Cerenkov effect. This allows radiotracers to be imaged using sensitive optical technologies providing opportunities for in vivo optical molecular imaging using Cerenkov luminescence.



For Conference News & Insights
Visit blog.cleoconference.org

CLEO: QELS-Fundamental Science

FM1A • Quantum
Engineering—Continued

FM1A.4 • 09:30

Parametric Interaction between Two Single Photons, Thiago B. Guerreiro¹, Anthony Martin¹, Bruno Sanguinetti¹, Nicolas Sangouard¹, Jason Pelc², Carsten Langrock², Martin M. Fejer², Hugo Zbinden¹, Rob Thew¹, Nicolas Gisin¹; ¹Group of Applied Physics, Univ. of Geneva, Switzerland; ²E. L. Ginzton Lab, Stanford Univ., USA. We report the experimental demonstration of an interaction between two independent single photons. The interacting photons are generated via parametric downconversion in distinct sources. An efficient waveguide is employed to realise the first single photon demonstration of sum frequency generation.

FM1A.5 • 09:45

On-chip generation and analysis of maximal path-frequency entanglement, Raffaele Santagati¹, Joshua W. Silverstone¹, Damien Bonneau¹, Michael J. Strain², Marc Sorel², Jeremy L. O'Brien¹, Mark G. Thompson¹; ¹H. H. Wills Physics Lab, Univ. of Bristol, UK; ²School of Engineering, Univ. of Glasgow, UK. We present a silicon-on-insulator quantum photonic device able to generate and analyze two maximally entangled qubits. Quantum interference between resonant four-wave mixing sources, phase-stable frequency-selection, and quantum state tomography are shown.

FM1B • Relativistic Laser-Plasma
Interactions—Continued

FM1B.6 • 09:30

Two-dimensional Supercontinuum Spectral Interferometry for Measurement of Laser-induced Plasmas, Jared K. Wahlstrand¹, Sina Zahedpour¹, Howard Milchberg¹; ¹Univ. of Maryland at College Park, USA. The plasma-induced phase shift of a probe is measured in 2D spatially with $\sim 3 \mu\text{m}$ resolution and temporally with ~ 5 fs resolution. From this ionization rates for the noble gases are found for a 40 fs, 800 nm pulse, for intensities up to nearly full depletion of the neutral population.

FM1B.7 • 09:45

Electron Injection into a Capillary Laser Wakefield Accelerator, Mark Wiggins¹, Ranaul Islam¹, Gregory Vieux¹, Gregor Welsh¹, Salima Abuazoum¹, Enrico Brunetti¹, Silvia Cipiccia¹, Bernhard Ersfeld¹, David Grant¹, Cristian Ciocarlan¹, Dino Jaroszynski¹; ¹Univ. of Strathclyde, UK. The role played by self-focusing of a high-intensity femtosecond laser in the entrance plume of a gas-filled capillary discharge waveguide is investigated for laser-plasma wakefield acceleration of electrons.

FM1C • Hyperbolic and Epsilon-
near-zero Materials—Continued

FM1C.7 • 09:30

Mie resonance based transition metamaterial, Liu Xiaoming¹, Sun Jingbo², Litchinitser Natasha M², Zhou Ji¹; ¹Tsinghua Univ., China; ²The State Univ. of New York at Buffalo, USA. We design a Mie resonance based transition metamaterial whose effective permeability gradually changed from positive to negative values. We demonstrate anomalous field enhancement near the zero permeability point under oblique incidence of the microwave radiation.

FM1C.8 • 09:45

Visible-Frequency Unidirectional Transmission Device incorporating a Hyperbolic Metamaterial, Ting Xu¹, Henri J. Lezec¹; ¹NIST, USA. We propose and experimentally demonstrate that unidirectional transmission of visible light can be provided by a reciprocal and passive planar device of wavelength-scale-thickness, incorporating subwavelength-pitch gratings and a hyperbolic metamaterial.

FM1D • PT Symmetry and
Related Phenomena—
Continued

FM1D.7 • 09:30

Stimulated Brillouin Scattering, hybrid acoustic modes and nonreciprocal mode-conversion in nanophotonic waveguides, Chris G. Poulton¹, Iman Aryanfar², Christian Wolff¹, Alvaro Casas-Bedoya², Michael J. Steel³, Benjamin J. Eggleton²; ¹CUDOS, School of Mathematical Sciences, Univ. of Technology Sydney, Australia; ²CUDOS, IPOS, School of Physics, Univ. of Sydney, Australia; ³CUDOS, School of Physics, Macquarie Univ., Australia. We theoretically investigate non-reciprocal mode-conversion arising from Stimulated Brillouin Scattering (SBS) in sub-micron nanophotonic waveguides. We find that hybrid acoustic modes can be efficiently generated via radiation pressure, leading to enhancement of SBS-based mode conversion.

FM1D.8 • 09:45

Using Nonlinear Optical Networks for Optimization: Primer of the Ant Colony Algorithm, Wenchao Hu¹, Kan Wu¹, Ping Perry Shum¹, Nikolay I. Zheludev^{1,2}, Cesare Soci¹; ¹Centre for Disruptive Photonic Technologies, Nanyang Technological Univ., Singapore; ²Optoelectronics Research Centre, Univ. of Southampton, UK. Using nonlinear Erbium doped optical fiber network we have implemented an optimization algorithm for the famous problem of finding the shortest path on the map for the ant colony to travel to the foraging area.

10:00–10:30 Coffee Break, Concourse Level

NOTES

CLEO: Science & Innovations

SM1E • Atmospheric Sensing—Continued

SM1E.4 • 09:30

QCL Based Absorption Sensor for Simultaneous Trace-Gas Detection of CH₄ and N₂O, Wei Ren¹, Wenzhe Jiang¹, Frank K. Tittel¹; ¹Dept. of Electrical and Computer Engineering, Rice Univ., USA. A quantum cascade laser (QCL) absorption sensor system operating at 7.83 μm was developed for simultaneous dual-species monitoring of CH₄ and N₂O using a novel compact multipass gas absorption cell with a sampling volume of 225 mL.

SM1E.5 • 09:45

Widely tunable Distributed Bragg Quantum Cascade laser for gas sensing applications, Abdou Diba¹, Ihor Sydoryk¹, Barry Gross¹, Fred Moshary¹, Feng Xie², Zah Chung-En²; ¹Electrical Engineering, City College of New York, USA; ²Science and Technology, Corning Incorporated, USA. We report continuous mode-hop free tuning of a sample-grating distributed Bragg reflector (SG-DBR) quantum cascade laser (QCL) operating at 4.55 μm wavelength observing N₂O features in this range by controlling all three sections of laser namely: front DBR, back DBR and the phase.

SM1F • Solid State Laser Systems for Secondary Source Generation—Continued

SM1F.5 • 09:30

Table-top hard x-ray source driven by sub-100 fs mid-infrared pulses, Jannick Weisshaupt¹, Vincent Juvé¹, Shian Ku¹, Marcel Holtz¹, Michael Woerner¹, Thomas Elsaesser¹, Skirmantas Alisauskas², Audrius Puglys², Andrius Baltuska²; ¹Max-Born-Institut Berlin, Germany; ²Photonics Inst., Austria. Powerful 90 fs pulses at a midinfrared wavelength of λ=3.9 μm drive a femtosecond hard x-ray source (Cu Kα: hbarω=8.05 keV). Up to 10¹⁸ X-ray photons/pulse are generated which is twice as many as with 800 nm drivers of a 100 times higher peak intensity.

SM1F.6 • 09:45

Compact 10 TW laser to generate multifilament arrays, Benjamin Webb¹, Joshua Bradford¹, Khan Lim¹, Nathan Bodnar¹, Andreas Vaupel¹, Erik McKee¹, Matthieu Baudelet¹, Magali M. Durand¹, Lawrence Shah¹, Martin Richardson¹; ¹College of Optics, Univ. of Central Florida, USA. The design and construction of a compact 10 TW Ti:sapphire CPA system for the generation of filament arrays is presented. The design and implementation challenges are discussed, in particular the optimization of beam quality.

SM1G • Optical Signal Processing—Continued

SM1G.7 • 09:30

Large-bandwidth compressive sampling based on multi-channel random optical pulses with nonuniform time delays, Yunhua Liang¹, Minghua Chen¹, Hongwei Chen¹, Shizhong Xie¹; ¹Tsinghua Univ., China. In this paper, a four-channel photonic-assisted compressive sampling system with large bandwidth is demonstrated, where sparse spectrum in the 2-19 GHz range with 50-kHz resolution is recovered from samples of compressed spectrums with 360-MHz bandwidth.

SM1G.8 • 09:45

Recirculating Frequency Shifting Based Photonic-assisted Broadband Instantaneous Radio-frequency Measurement, Cheng Lei¹, Minghua Chen¹, Hongwei Chen¹, Sigang Yang¹, Shizhong Xie¹; ¹Tsinghua Univ., China. By trapping the RF signal within the RFS loop and measuring the frequency components slice by slice, the proposed method provides a promising candidate for broadband instantaneous radio-frequency measurement with simple structure and commercial devices.

SM1H • Advanced Fabrication Techniques—Continued

SM1H.7 • 09:30

Polycrystalline Anatase Micro-Ring Resonators at Telecommunication Wavelengths, Orad Reshef¹, Katia Shtyrkova², Michael G. Moebius¹, Christopher Evans¹, Sarah Griesse-Nascimento¹, Erich Ippen², Eric Mazur¹; ¹School of Engineering and Applied Sciences, Harvard Univ., USA; ²Dept. of Electrical Engineering and Computer Science, MIT, USA. We fabricate and characterize integrated polycrystalline anatase TiO₂ micro-ring resonators at around λ = 1550 nm. We obtain quality factors of 1.5×10⁴ and calculate a propagation loss of 8.0 ± 1.3 dB/cm.

SM1H.8 • 09:45

Simple Microfluidic Integration of 3D Optical Sensors Based on Solvent Immersion Lithography, Andreas E. Vasdekis¹, Michael J. Wilkins¹, Jay W. Grate¹, Allan E. Konopka¹, Sotiris S. Xantheas¹, Tsun-Mei Chang²; ¹Pacific Northwest National Labs, USA; ²Chemistry, Univ. of Wisconsin-Parkside, USA. We will present Solvent Immersion Lithography (SIL) for microsystem prototyping in less than one minute. Our focus will primarily be on 3D optical sensor integration for biological applications in microfluidics and chemical microreactors.

10:00–10:30 Coffee Break, Concourse Level

NOTES

Blank lined area for taking notes.

CLEO: Science & Innovations

CLEO: QELS-
Fundamental Science

CLEO: Applications
& Technology

SM11 • Parametric Sources—
Continued

SM11.7 • 09:30

Influence of Pump Pulse Duration on Doubly Resonant Optical Parametric Oscillators Build-up Time, Guillaume Aoust¹, Myriam Raybaut¹, Jean-Michel Melkonian¹, Guillaume Canat¹, Jean-Baptiste Dherbecourt¹, Antoine Godard¹, Michel Lefebvre¹; ¹ONERA-The French Aerospace Lab, France. A single-frequency doubly resonant optical parametric oscillator is pumped by a master oscillator-fiber power amplifier whose pulse duration is varied for 40 ns to 10 μs, enabling to optimize the pumping parameters.

SM11.8 • 09:45

Autoresonant Harmonic Generation in Nonuniform Crystals, Oded Yaakobi¹, Anna Mazhorova¹, Matteo Clerici^{1,2}, Gabriel Dupras¹, Daniele Modotto³, François Vidal¹, Roberto Morandotti¹; ¹INRS-EMT, Univ. of Quebec, Canada; ²School of Engineering and Physical Sciences, Heriot-Watt Univ., UK; ³Dipartimento di Ingegneria dell'Informazione, Università di Brescia, Italy. An experiment of second harmonic generation in a nonuniform crystal is presented, and interpreted in terms of an autoresonant wave-mixing theory. A good agreement is found between numerical simulations, analytical solutions and experimental data.

SM11J • UV and Visible LEDs—
Continued

SM11J.6 • 09:30

Utilizing Two-Dimensional Photonic Crystals to Investigate the Correlation between the Air Duty Cycle and the Light Extraction Efficiency of InGaN-Based Light-Emitting Diodes, Ming-Lun Lee¹, Yao-Hong You¹, Cheng-Ju Hsieh¹, Vin-Cent Su¹, Chun Nien¹, Po-Hsun Chen¹, Hung-Chou Lin¹, Han-Bo Yang¹, Yen-Pu Chen¹, Shen-Han Tsai¹, Chieh-Hsiung Kuan¹; ¹Graduate Inst. of Electronics Engineering, National Taiwan Univ., Taiwan. By incorporating two dimensional photonic crystals into the surface of InGaN-based LEDs, the strong correlation between the air duty cycle and the light extraction efficiency of LEDs was demonstrated by optical and electrical measurement results.

SM11J.7 • 09:45

Electrically Driven Light Emission from an Atomic Monolayer Crystal, Andreas Pospischil¹, Marco M. Furchi¹, Thomas Mueller¹; ¹Inst. of Photonics, Vienna Univ. of Technology, Austria. We report electrically driven light emission from a two-dimensional monolayer of tungsten diselenide (WSe₂). Our device is operated as a lateral p-n junction diode, formed by electrostatic doping.

FM1K • Applications of
Localized Surface Plasmons—
Continued

FM1K.6 • 09:30

Plasmonic quasi-dark mode excitation, Daniel E. Gomez^{1,2}, Ranjith Rajasekharan³, Zhi Qin Teo³, Timothy James^{2,3}, Timothy J. Davis^{1,2}, Ann Roberts³; ¹Division of Materials Science and Engineering, CSIRO, Australia; ²Melbourne Centre for Nanofabrication, Australian National Fabrication Facility, Australia; ³School of Physics, Univ. of Melbourne, Australia. Progress in the excitation of 'dark-modes' in plasmonic structures is reported. The interaction of vector beams possessing a spatially inhomogeneous polarization profile with plasmonic nanostructures provides an avenue to probe these resonances.

FM1K.7 • 09:45

Experimental Demonstration of Q-factor Control in Plasmonic Meta-Surfaces Exhibiting Double-Continuum Fano Resonances, Nihal Arju¹, Alexander B. Khanikaev^{1,2}, Purtseladze Purtseladze¹, Kaya Tatar¹, Chih-Hui Wu^{1,3}, Hossein S. Mousavi¹, Gennady Shvets¹; ¹Univ. of Texas at Austin, USA; ²City Univ. of New York, Queens College, USA; ³Univ. of California, Berkeley, USA. Fano resonant metamaterials (FRAMM) with varying degree of symmetry breaking were designed, tested, and simulated. Field enhancement of different FRAMM designs were simulated. This will help design FRAMMs suitable for a specific requirement.

AM1L • Advanced Material
Processing—Continued

AM1L.6 • 09:30

Ultra-Short Pulse Lasers as Versatile Tools in the Fabrication of Medical Micro Implants, Nils-Agne Feth¹, Martin Strobel¹; ¹Admedes Schuessler GmbH, Germany. We give an overview of the application of ultra-short pulse (USP) lasers in the fabrication of miniaturized medical implants and devices like stents. Furthermore, we estimate the economic requirements to be fulfilled by USP lasers.

Invited

10:00–10:30 Coffee Break, Concourse Level

NOTES

CLEO: Science & Innovations

CLEO: Applications
& Technology

SM1M • Frequency Combs
and Novel Light Sources—
Continued

SM1M.6 • 09:30 **Modifying the Coherence Properties of Microresonator Combs with Feedback Loop Filtering**, Yufeng Jiang¹, Xin Zhao¹, Jian Wang², Ben Niu², Pei-Hsun Wang², Minghao Qi², Zheng Zheng¹; ¹*School of Electronic and Information Engineering, Beihang Univ., China*; ²*School of Electrical and Computer Engineering & Birck Nanotechnology Center, Purdue Univ., USA*. The coherence properties of a frequency comb generated by a SiN microring resonator is shown to be changed by the feedback through a self tracking, narrowband single longitudinal mode filter in an active fiber loop.

SM1M.7 • 09:45 **Analysis and experiments on harmonic mode locking in an optical microcavity**, Takumi Kato¹, Ryo Suzuki¹, Tomoya Kobatake¹, Takasumi Tanabe¹; ¹*Keio Univ., Japan*. We investigated harmonic mode locking in a microcavity with split-step Fourier method and demonstrated it experimentally. Harmonic mode locking in an ultra-small cavity allows us to obtain ultra-high repetition rate pulse trains.

SM1N • SDM and Bandgap
Fibers—Continued

SM1N.4 • 09:30 **Doppler-Assisted Tomography of Photonic Crystal Fiber Structure by Side-Scattering**, Alessio Stefani¹, Michael H. Frosz¹, Tijmen G. Euser¹, Gordon K. L. Wong¹, Philip St.J. Russell^{1,2}; ¹*Max Planck Inst. for the Science of Light, Germany*; ²*Dept. of Physics, Univ. of Erlangen-Nuremberg, Germany*. Using a non-destructive side-scattering technique, the internal structure of a microstructured fibre is determined. The rotating fiber is illuminated by a laser beam and an inverse Radon transform is applied to the frequency-modulated scattered signal.

SM1N.5 • 09:45 **Chalcogenide negative curvature hollow-core photonic crystal fibers with low loss and low power ratio in the glass**, Chengli Wei¹, Robinson Kuis², Francois Chenard², Jonathan Hu¹; ¹*Baylor Univ., USA*; ²*IRflex Corporation, USA*. We study the chalcogenide negative curvature hollow-core PCFs. The leakage loss and power ratio in the glass decrease as the number of tubes increases or the ratio of tube wall thickness to diameter decreases.

SM1O • Pulse Generation and
Amplification—Continued

SM1O.7 • 09:30 **Widely Tunable Normal Dispersion Fiber Optical Parametric Oscillator**, Khanh Q. Kieu¹, Nam Nguyen¹, Roopa Gowda¹, Takefumi Ota^{2,1}, Shinichiro Uno^{2,1}, Nasser Peyghambarian¹; ¹*Univ. of Arizona, USA*; ²*Canon USA Inc., Canon, USA*. We demonstrate a very wide tuning range normal dispersion fiber optical parametric oscillator (FOPO) using a femtosecond, fixed wavelength fiber laser as the pump source. We believe that the proposed laser design will be useful for developing widely tunable fiber laser sources.

SM1O.8 • 09:45 **Passive Waveform Amplification by Self-Imaging**, Reza Maram¹, James Van Howe^{1,2}, Ming Li^{1,3}, José Azaña¹; ¹*INRS-Energie Matériaux et Telecom, Canada*; ²*Dept. of Physics and Astronomy, Augustana College, USA*; ³*Inst. of Semiconductors, Chinese Academy of Sciences, China*. We show experimentally undistorted, intensity amplification of optical pulse waveforms with gain from 2 to ~20 without using active gain by recycling energy already stored in the input repetitive signal.

AM1P • Symposium on
Advances in Molecular Imaging
I—Continued

AM1P.4 • 09:30 **3D Optoacoustic Tomography: From Molecular Targets in Mouse Models to Functional Imaging of Breast Cancer**, Alexander A. Oraevsky¹; ¹*TomoWave Labs, Inc, USA*. A review of our recent works advancing three-dimensional optoacoustic tomography systems and their applications in preclinical imaging using small animal models and clinical application in diagnostic imaging of breast cancer is presented.

10:00–10:30 Coffee Break, Concourse Level

NOTES

Blank lined area for taking notes.

CLEO: QELS-Fundamental Science

10:30–12:30

FM2A • Quantum Logic and Interference*Presider: Julio Barreiro; Univ. of California San Diego, USA*

FM2A.1 • 10:30

Network of femtosecond degenerate OPOs for solving NP-Hard Ising problems, Alireza Marandi^{1,2}, Kenta Takata², Zhe Wang¹, Robert L. Byer¹, Yoshihisa Yamamoto^{1,2}; ¹Stanford Univ., USA; ²National Inst. of Informatics, Japan. We report implementation of a configurable network of four degenerate optical parametric oscillators as an Ising spin system using time-multiplexed femtosecond pulses. This coherent Ising machine solves an instance of NP-hard MAXCUT problem without error.

FM2A.2 • 10:45

Solving The Ising Problem Using Degenerate Optical Parametric Oscillators, Zhe Wang¹, Alireza Marandi^{1,2}, Kai Wen¹, Robert L. Byer¹, Yoshihisa Yamamoto^{1,2}; ¹Stanford Univ., USA; ²National Inst. of Informatics, Japan. A degenerate optical parametric oscillator network is proposed to solve the NP-hard problem of finding a ground state of the Ising Hamiltonian.

FM2A.3 • 11:00

An integrated programmable quantum photonic processor for linear optics, Jacob C. Mower¹, Nicholas C. Harris¹, Greg Steinbrecher¹, Yoav Lahini², Dirk Englund¹; ¹EECS, MIT, USA; ²Physics, MIT, USA. We introduce a reconfigurable silicon quantum photonic network for implementing general linear optics transformations in the spatial mode basis. This network enables implementation of a range of quantum algorithms; we discuss the phase estimation algorithm.

10:30–12:30

FM2B • New Trends in Attoscience*Presider: Eiji Takahashi; RIKEN, Japan*

FM2B.1 • 10:30

Photoionization Time Delay Measurement close to a Fano Resonance Using Tunable Attosecond Pulses, Marija Kotur¹, Diego Guenet¹, David Kroon¹, Esben Witting-Larsen¹, Miguel Miranda¹, Maite Louisy¹, Samuel Bengtsson¹, Stefanos Carlström¹, Johan Mauritsson¹, J. Marcus Dahlström², Sophie Canton³, Mathieu Gisselbrecht¹, Cord L. Arnold¹, Anne L'Huillier¹; ¹Dept. of Physics, Lund Univ., Sweden; ²Dept. of Physics, Stockholm Univ., Sweden; ³Dept. of Synchrotron Radiation Instrumentation, Lund Univ., Sweden. We investigate the influence of a Fano resonance on the delays for electron emission in two-photon, near-resonant ionization of argon. The delays were measured using an interferometric method that employed an attosecond pulse train.

FM2B.2 • 10:45

Temporal characterization of emitted field from autoionization state stimulated by isolated attosecond pulse, Hiroki Mashiko¹, Tomohiko Yamaguchi^{1,2}, Katsuya Oguri¹, Akira Suda², Hideki Gotoh¹; ¹Quantum Optical Physics Research Group, NTT Basic Research Labs, Japan; ²Physics, Tokyo Univ. of Science, Japan. We characterized field emission from autoionization transition in atomic neon stimulated by isolated attosecond field. The spectrum of the emitted field broadens approximately 1 eV bandwidth, which corresponds to shorter than 2.5 fs-duration

FM2B.3 • 11:00

Attosecond Transient Absorption in Molecular Hydrogen, Yan Cheng¹, Michael Chini¹, Xiaowei Wang^{1,2}, Yi Wu¹, Zenghu Chang¹; ¹CREOL and Dept. of Physics, Univ. of Central Florida, USA; ²Dept. of Physics, National Univ. of Defense Technology, China. Isolated attosecond pulses are used to probe laser-perturbed hydrogen molecules using attosecond absorption spectroscopy. We observe dynamic features in the delay-dependent absorption on both the electronic and nuclear timescales for the first time.

10:30–12:30

FM2C • Optics in Random Media I*Presider: Qiaoqiang Gan, State Univ. of New York at Buffalo, USA*

FM2C.1 • 10:30

3D Optical Invisibility Cloak in the Diffusive-Light Limit, Robert Schittny¹, Muamer Kadic^{1,2}, Martin Wegener^{1,2}; ¹Inst. of Applied Physics, Karlsruhe Inst. of Technology, Germany; ²Inst. of Nanotechnology, Karlsruhe Inst. of Technology, Germany. We design, fabricate, and characterize three-dimensional macroscopic free-space omnidirectional polarization-independent visible-wavelength broad-bandwidth invisibility cloaks in the diffusive limit of light propagation. The simple core-shell geometries are inspired by near-field optics.

FM2C.2 • 10:45

Metamaterial Broadband Angular Selectivity, Yichen Shen¹, Ivan Celanovic¹, Marin Soljacic¹, John Joannopoulos¹; ¹MIT, USA. We present a method that achieves light selection based purely on the angle of propagation, by tailoring the overlap of the bandgaps of multiple one-dimensional photonic crystals, each contains metamaterial and with a different periodicity.

FM2C.3 • 11:00

Long Range Correlations of Light Intensity inside Photonic Nanostructures, Raktim Sarma¹, Alexey G. Yamilov², Boris Shapiro³, Hui Cao¹; ¹Yale Univ., USA; ²Missouri Univ. of Science & Technology, USA; ³Physics, Technion-Israel Inst. of Technology, Israel. We measured directly long range spatial intensity correlations inside quasi-two dimensional disordered photonic waveguides. Enhancement of long-range correlations is observed in narrower waveguides due to localization effects, enabling manipulation of intensity correlations inside random media.

10:30–12:30

FM2D • Graphene and Novel Phenomena*Presider: Zhigang Chen, San Francisco State Univ., USA*FM2D.1 • 10:30 **Invited**

Optical Phenomena in Graphene/Boron Nitride Heterostructures, Feng Wang^{1,4}, Zhiwen Shi¹, Chenhao Jin¹, Wei Yang², Hans A. Bechtel³, Michael C. Martin³, Guangyu Zhang²; ¹Univ. of California Berkeley, USA; ²Chinese Academy of Sciences, China; ³Advanced Light Source Division, Lawrence Berkeley National Lab, USA; ⁴Materials Science Division, Lawrence Berkeley National Lab, USA. Electrons in graphene are described by massless Dirac Fermions with unusual electrical and optical properties. The Moire superlattice in graphene/boron nitride heterostructure strongly modifies the electronic structure, and leads to unusual changes in infrared absorption.

FM2D.2 • 11:00

Direct observation of "pseudospin"-mediated vortex generation in photonic graphene, Daohong Song¹, Liqin Tang¹, Yi Zhu^{2,3}, Mark Ablowitz³, Vassilis Paltoglou⁴, Nikolaos K. Efremidis⁴, Jingjun Xu¹, Zhigang Chen^{1,5}; ¹Nankai Univ., China; ²Tsinghua Univ., China; ³Univ. of Colorado, USA; ⁴Univ. of Crete, Greece; ⁵San Francisco State Univ., USA. We observe vortex generation by selective excitation of two honeycomb sublattices at the vicinity of Dirac points. Such vortices arise from graphene "pseudospin", suggesting that "pseudospin" could be observable and possess real angular momentum.



For Conference News & Insights
Visit blog.cleoconference.org

CLEO: Science & Innovations

10:30–12:30

SM2E • Spectroscopic Chemical Detection*Presider: Gerard Wysocki; Princeton Univ., USA*SM2E.1 • 10:30 **Invited**

Solvent-driven Ionic Processes in Water: Surface Adsorption and Cation-Cation Pairing, Studied by X-ray Absorption and UV-SHG Spectroscopy, Richard James Saykally¹; ¹Univ. of California Berkeley, USA. Seemingly unlikely processes that ostensibly conflict with fundamental electrostatics can occur in polar liquid media, and underlie important natural phenomena. We have recently examined the above phenomena by state of the art experiments and theory.

SM2E.2 • 11:00

Ultra-Sensitive Mid-Infrared Photoexpansion Nanospectroscopy with Background Suppression, Feng Lu¹, Mingzhou Jin¹, Mikhail A. Belkin¹; ¹Electrical and Computer Engineering, Univ. of Texas at Austin, USA. The ultimate sensitivity of mid-infrared photoexpansion nanospectroscopy is limited by the background signal from photoexpansion of the sample substrate and the probe tip. Here we demonstrate suppression of this signal using a second mid-infrared laser.

10:30–12:30

SM2F • Advanced Solid State Laser Architectures*Presider: Dennis Harris; MIT Lincoln Lab, USA*

SM2F.1 • 10:30

Intracavity Coherent Beam Combining of Solid-State Gain Elements using Active Phase Control, Juan Montoya¹, Steve Augst¹, Jan Kinsky¹, Kevin Creedon¹, Antonio Sanchez-Rubio¹, Tso Yee Fan¹; ¹Massachusetts Inst of Tech Lincoln Lab, USA. Here we report on intracavity coherent beam combining (iCBC) of nine solid-state gain elements resulting in 27 W of combined power with a combining efficiency of 87% and a beam quality of $M^2 = 1.7$.

SM2F.2 • 10:45

Simple Non-PM Fiber Based Beam Combination Architecture, Andrew Benedick¹, Michael Riley¹, Shawn Redmond¹, Tso Yee Fan¹; ¹MIT Lincoln Lab, USA. Efficient combination of an array of lasers requires alignment of their polarization states. We demonstrate a simple architecture for polarization control by coherently combining eight passive non-PM fibers resulting in a PER of 19 dB.

SM2F.3 • 11:00

Theory and Experimental Verification of Kramers-Kronig Self-Phasing in Coherently Combined Fiber Lasers, James R. Leger¹, Hung-Sheng Chiang¹, Johan Nilsson², Jayanta K. Sahu²; ¹Univ. of Minnesota Twin Cities, USA; ²Optoelectronics Research Centre, Univ. of Southampton, UK. The recently observed self-phasing of coherently coupled fibers due to Kramers-Kronig effects is theoretically described using a simple model. Direct measurements of the Kramers-Kronig effect and Henry's alpha parameter are reported.

10:30–12:30

SM2G • Silicon Photonic Modulators*Presider: Joyce Poon; Univ. of Toronto, Canada*

SM2G.1 • 10:30

Enhanced modulation performance by cascaded uncoupled dual-ring, Tingyi Gu^{1,2}, Chee Wei Wong², Youngkai Chen¹, Po Dong¹; ¹Bell Labs, Alcatel-Lucent, USA; ²Columbia Univ., USA. We demonstrate enhanced modulation speed by using serial uncoupled microring modulators. By reducing photon lifetime, the extinction ratio of eye diagram increases from 5.9 dB to 7.1 dB, by driving two rings at 20 Gbps.

SM2G.2 • 10:45

Low-Voltage 25 Gbps Modulators Based On Si Photonic Crystal Slow Light Waveguides, Yosuke Terada¹, Toshihiko Baba¹; ¹Yokohama National Univ., Japan. 25 Gbps operation was obtained with extinction ratios of 2 - 4 dB for $V_{pp} = 1.00 - 1.75$ V in MZI modulator consisting of 200- μ m photonic crystal slow light waveguide phase shifters.

SM2G.3 • 11:00

Monolithic Travelling-Wave Mach-Zehnder Transmitter with High-Swing Stacked CMOS Driver, Douglas M. Gill¹, Jonathan E. Proesel², Chi Xiong¹, Jessie Rosenberg¹, Marwan Khater¹, Tymon Barwicz¹, Solomon Assefa¹, Steven M. Shank³, Carol Reinholm³, Edward Kiewra¹, John J. Ellis-Monaghan³, Swetha Kamalapurkar¹, William M. Green¹, Yurii Vlasov¹; ¹Electronic/Photonic Integrated Systems Research and Applications Development, IBM T.J. Watson Research Center, USA; ²Analog & Mixed-Signal Circuit Design, IBM T.J. Watson Research Center, USA; ³Microelectronics Division, IBM Systems & Technology Group, USA. We present a 20 Gb/s monolithically integrated transmitter with stacked CMOS driver and periodic-loaded PN-junction Mach-Zehnder modulator (MZM) fabricated in IBM's sub-100nm technology node. Transmitter extinction ratios of 10 dB at 20 Gb/s are demonstrated.

10:30–12:30

SM2H • Novel Approaches for Detection, Sensing and Characterization*Presider: Ofer Levi; Univ. of Toronto, Canada*

SM2H.1 • 10:30

Direct observation of electromagnetic near field in silicon nanophotonics devices using Scanning Thermal Microscopy (SThM) technique, Meir Y. Grajower¹, Liron Stern¹, Borid Desiatov¹, Ilya Goykhman¹, Uriel Levy¹; ¹Dept. of Applied Physics, Hebrew Univ. of Jerusalem, Israel. We observe directly for the first time optical near field in silicon nanophotonics devices with nanoscale resolution using near field scanning thermal microscopy and demonstrated its advantage over the NSOM technique.

SM2H.2 • 10:45

Silicon Wire Refractive Index Characterization using Microring Resonator Effective Length from Interferograms, Shih-Hsiang Hsu¹, Yung-Chia Yang¹, Yu-Hou Su¹; ¹National Taiwan Univ of Science & Tech, Taiwan. The optical low-coherence interferometry built with an optical ruler was proposed to demonstrate silicon-wire transverse-magnetic polarized indices of refraction and birefringence as 2.02 and 0.64, respectively, from the microring resonator effective length using various interferograms.

SM2H.3 • 11:00 **Invited**

Nano-focused ultrafast spectroscopy and imaging reaching the single quantum level, Markus B. Raschke¹; ¹Univ. of Colorado at Boulder, USA. The near-field tip-antenna enhanced signal transduction with femtosecond laser pulses allows for spatio-spectral and spatio-temporal imaging and quantum coherent control with the perspective to reach the single electronic or vibrational quantum level.

CLEO: Science & Innovations

10:30–12:30

SM2I • Mode-locked OPOs

Presider: Yen-Hung Chen;
National Central Univ., Taiwan

SM2I.1 • 10:30

FM Mode-Locked Optical Parametric Oscillator: Pulse Formation and Spectral Characteristics, Kavita Devi¹, Suddapalli Chaitanya Kumar¹, Majid Ebrahim-Zadeh^{1,2}; ¹ICFO -The Inst. of Photonic Sciences, Spain; ²Institucio Catalana de Recerca i Estudis Avancats (ICREA), Spain. We report pulse formation and spectral characteristics of a FM mode-locked OPO in the mid-IR. The singly-resonant OPO based on MgO:PPLN, pumped by a cw Yb-fiber laser at 1064 nm, generates 236ps pulses at 80MHz.

SM2I.2 • 10:45

Dynamics and Design Trade-Offs in CW-Pumped Singly-Resonant Optical Parametric Oscillator Based Combs, Christopher R. Phillips¹, Ville Ulvila², Lauri Halonen², Markku Vainio^{2,3}; ¹ETH Zurich, Switzerland; ²Univ. of Helsinki, Finland; ³Centre for Metrology and Accreditation, Finland. We analyze frequency comb generation in CW-pumped singly-resonant optical parametric oscillators using cascaded second-order nonlinearities. We explain experimental results, trade-offs and current limits on performance, and examine scaling towards broader bandwidths in the future.

SM2I.3 • 11:00 **Invited**

Asynchronous Mid-Infrared Optical Parametric Oscillator Frequency Combs and Applications in Spectroscopy, Zhaowei Zhang¹, Tom Gardiner², Derryck T. Reid¹; ¹Heriot-Watt Univ., UK; ²National Physical Lab, UK. Principles of asynchronous optical parametric oscillator frequency combs are introduced and their performance in dual-comb mid-infrared molecular spectroscopy is presented, including a specific demonstration of methane absorption spectroscopy with a resolution of 0.2 cm⁻¹.

10:30–12:30

SM2J • Nanostructured LEDs and Photovoltaics

Presider: Jonathan Wierer; Sandia National Labs, USA

SM2J.1 • 10:30

Selective-Area Growth of III-Nitride Core-Shell Nanowalls for Light-Emitting and Laser Diodes, Ashwin Rishinaramangalam¹, Michael Fairchild¹, Saadat Ul Masabih¹, Darryl Shima¹, Ganesh Balakrishnan¹, Daniel Feezell¹; ¹Electrical and Computer Engineering, Univ. of New Mexico, USA. We demonstrate selective-area growth of patterned III-nitride core-shell nanowalls with nonpolar InGaN quantum well shells over large areas. Transmission electron microscopy and photoluminescence are utilized to examine the growth morphology and emission characteristics.

SM2J.2 • 10:45

Red to Near-Infrared Emission from InGaN/GaN Quantum-Disks-in-Nanowires LED, Tien Khee Ng¹, Chao Zhao^{1,2}, Chao Shen¹, Shafat Jahangir³, Bilal Janjua¹, Ahmed B. Slimane¹, Chun H. Kang¹, Ahad A. Syed², Jingqi Li², Ahmed Y. Alyamani⁴, Munir M. El-Desouki⁴, Pallab K. Bhattacharya³, Boon S. Ooi¹; ¹Photonics Lab, King Abdullah Univ. of Science and Tech, Saudi Arabia; ²Advanced Nanofabrication and Imaging Core Lab, King Abdullah Univ. of Science and Tech, Saudi Arabia; ³Dept. of Electrical Engineering and Computer Science, Univ. of Michigan, USA; ⁴National Center for Nanotechnology, King Abdulaziz City for Science and Tech, Saudi Arabia. The InGaN/GaN quantum-disks-in-nanowire light-emitting diode (LED) with emission centered at ~830nm, the longest emission wavelength ever reported in the InGaN/GaN system, and spectral linewidth of 290nm, has been fabricated with p-side-down on a Cu substrate.

SM2J.3 • 11:00

InGaN Quantum Dots for High Efficiency Blue and Green Light Emitters, Arthur J. Fischer¹, Xiaoyin Xiao¹, Jeffrey Y. Tsao¹, Daniel D. Koleske¹, Ping Lu¹, Jeremy B. Wright¹, Sheng Liu¹, George T. Wang¹; ¹Sandia National Labs, USA. InGaN quantum dots at high densities (~10¹¹ dots/cm²) are demonstrated using metalorganic chemical vapor deposition combined with post growth processing of InGaN materials. Optical and structural studies are performed to characterize InGaN quantum dots.

CLEO: QELS-Fundamental Science

10:30–12:30

FM2K • Plasmonic Nanoantennas

Presider: Uriel Levy, Hebrew Univ. of Jerusalem, Israel

FM2K.1 • 10:30

All-Semiconductor Plasmonic Nano-Antennas, Stephanie Law¹, Lan Yu¹, Aaron Rosenberg¹, Dan Wasserman¹; ¹Electrical and Computer Engineering, Univ. of Illinois, USA. We demonstrate a new type of infrared plasmonic antenna for long-wavelength nano-scale enhanced sensing. The plasmonic materials utilized are epitaxially-grown semiconductor engineered metals, which results in high-quality, low-loss infrared plasmonic metals with tunable optical properties.

FM2K.2 • 10:45

Meta-Coaxial Nanoantenna, Alexei Smolyaninov¹, Lin Pang¹, Lindsay Freeman¹, Yeshaiahu Fainman¹; ¹Dept. of Electrical and Computer Engineering, Univ. of California San Diego, USA. Novel meta-coaxial nano-antennas are studied numerically, fabricated and experimentally characterized. These antennas provide local field enhancements of 200-800, super-localized fields with spatial FWHM of ~1nm, and wide spectral ranges with FWHM bandwidths greater than 900nm.

FM2K.3 • 11:00

Interacting dark resonances with metallic nano-antennas, Michael Mrejen¹, Pankaj K. Jha¹, Jeongmin Kim¹, Chihhui Wu¹, Yuan Wang¹, Xiaobo Yin¹, Xiang Zhang^{1,2}; ¹NSF Nano-scale Science and Engineering Center (NSEC), Univ. of California, Berkeley, USA; ²Materials Science Division, Lawrence Berkeley National Lab, USA. We theoretically investigate interacting dark resonances in a plasmonic meta-molecule comprising a bright nano-antenna coupled to cascaded dark elements. This structure enables efficient energy transfer and exhibits sub-natural spectral response analogous to the atomic counterpart.

CLEO: Applications & Technology

10:30–12:30

AM2L • Innovative Laser Sources Detectors and Beam Delivery

Presider: Eric Mottay; Amplitude Systemes, France

AM2L.1 • 10:30

15 mW of CW emission at 193 nm using the crystal KBBF, Matthias Scholz¹, Dmitrijs Opalevs¹, Jürgen Stuhler¹, Patrick Leisching¹, Wilhelm Kaenders¹, Guiling Wang², Xiaoyang Wang², Rukang Li², Chuangtian Chen²; ¹Research and Development, TOP-TICA Photonics AG, Germany; ²Key Lab of Functional Crystals and Laser Technology, Beijing Center for Crystal Growth and Development, China. We report on a narrow-band continuous-wave laser source in the deep-ultraviolet with an output power of > 15 mW at 193 nm. We see applications of this laser source in semiconductor metrology and high-resolution spectroscopy.

AM2L.2 • 10:45 **Invited**

Yb-doped LMA Fiber Fabricated by Chelate Deposition System for High Power Laser Applications, Tengfei Shi^{1,2}, Zhou Zhiguang^{1,2}, Xiao Xusheng^{1,2}, Zhang Aidong^{1,2}, Lin Aoxiang^{1,2}; ¹Chinese Academy of Sciences (CAS), China; ²State Key Lab of Transient Optics and Photonics, Xi'an Inst. of Optics and Precision Mechanics (XIOPM), China. We report Yb-doped LMA fiber fabricated by chelate doping system (CDS). All-fiber laser output ($\eta=54.2\%$ at 1080 nm) is 700W. CDS is found effective to fabricate homogeneous preform for high power fiber laser development.

AM2L.3 • 11:00


Withdrawn

CLEO: Science & Innovations

10:30–12:30

SM2M • Novel Platforms for Silicon Photonics 

Presider: Chi Xiong, IBM TJ Watson Research Center, USA

SM2M.1 • 10:30  **Tutorial** 
Organic Electro-optic Materials and Devices: Molecular Engineering Driving Device Performance and Technology Innovation, Robert A. Norwood¹; ¹Univ. of Arizona, USA. Electro-optic polymers have developed dramatically, with commercially available materials exhibiting EO coefficients > 250pm/V with excellent stability. This has resulted in low voltage (< 1V), ultrahigh bandwidth EO modulators and integration with silicon photonics is emerging.



Robert A. Norwood received a B.S. in physics and mathematics from MIT and the Ph.D. in physics from the University of Pennsylvania. After several leadership positions in industry, he became a Professor in the College of Optical Sciences at the University of Arizona, where he performs research on a broad range of organic photonic materials and devices. He has more 100 refereed publications, 7 book chapters, 30 issued US patents, and has delivered more than 60 invited talks. He is a Fellow of The Optical Society and SPIE.

10:30–12:30

SM2N • Modes in Fibers

Presider: John Fini; OFS Labs, USA

SM2N.1 • 10:30
Optical Activity Enhanced by Orbital Angular Momentum Resonances in Helically Twisted PCF, Gordon K. Wong¹, Xiaoming Xi¹, Thomas Weiss^{1,3}, Philip St.J. Russell^{1,2}; ¹Max Planck Inst. for the Science of Light, Germany; ²Dept. of Physics, Univ. of Erlangen-Nuremberg, Germany; ³4th Physics Inst. and Research Center SCOPE, Univ. of Stuttgart, Germany. We demonstrate that twisted solid-core PCF develops strongly enhanced optical activity and circular dichroism in the vicinity of orbital angular momentum resonances in the cladding. It may be used as a circular polarizer.

SM2N.2 • 10:45
OAM Stability in Fiber due to Angular Momentum Conservation, Patrick Gregg¹, Poul Kristensen², Siddharth Ramachandran¹; ¹Boston Univ., USA; ²OFS-Fitel, Denmark. We demonstrate that degenerate, higher order ($|L|>1$) OAM modes resist polcon-like perturbations, with coupling efficiencies at least 10dB less than that of SMF. We attribute this stability to the large angular momenta of these modes.



SM2N.3 • 11:00  **Invited**
The Photonic Lantern, Timothy A. Birks¹, Itandehui Gris-Sánchez¹, Stephanos Yeroslatsitis¹; ¹Univ. of Bath, UK. Photonic lanterns are made by adiabatically merging several single-mode cores into one multimode core. They provide low-loss interfaces between single-mode and multimode systems where the precise optical mapping between cores and modes is unimportant.


CLEO: Applications
& Technology

10:30–12:30


AM2O • Endoscopy & Minimally Invasive Optical Imaging 

Presider: Yu Chen; Univ. of Maryland at College Park, USA



AM2O.1 • 10:30  **Invited** 
Mueller Polarimetric Endoscopy, Ji Qi¹, Mohan Singh¹, Neil Clancy¹, Daniel S. Elson¹; ¹Imperial College London, UK. Mueller polarimetric imaging is a promising technique which is able to provide additional polarisation contrast for surgical imaging. In this work, improved 3×3 and 4×4 Mueller matrix endoscopic systems were constructed and tested with tissue samples.

AM2O.2 • 11:00 
Multiphoton GRIN Endoscope for Evaluation of Human Prostatic Tissue Ex Vivo, David Huland¹, Manu Jain², Dimitre Ouzounov¹, Brian D. Robinson³, Ashutosh Tewari², Chris Xu¹; ¹School of Applied and Engineering Physics, Cornell Univ., USA; ²Dept. of Urology of Weill Medical College of Cornell Univ., New York-Presbyterian Hospital, USA; ³Dept. of Surgical Pathology of Weill Medical College of Cornell Univ., New York-Presbyterian Hospital, USA. We characterize the diagnostic performance of a multiphoton GRIN endoscope using human prostate samples obtained from radical prostatectomy surgery. Ex vivo images of benign and tumor areas and images of peri-prostatic tissue are shown.

10:30–12:30

AM2P • Symposium on Advances in Molecular Imaging II 

Presider: John Rasmussen; Univ. of Texas Health Science Center, USA

AM2P.1 • 10:30  **Invited** 
NIR fluorescent contrast agents for detection of inflammation of lungs in vivo, Haiying Zhou¹, Shawn He¹, Sean Gunsten², Steven Brody², Walter Akers¹, Mikhail Berezin¹, Jeff Thompson³; ¹Radiology, Washington Univ. School of Medicine, USA; ²Medicine, Washington Univ. School of Medicine, USA; ³Harvard Univ., USA. Inflammatory responses to lung injuries are mediated through enhanced production of reactive oxygen species (ROS). We describe the use of activatable NIR fluorescent agents with high sensitivity to ROS to image the lung during conditions of high inflammation.

AM2P.2 • 11:00  **Invited** 
Emerging Trends with Molecularly Targeted Optobeacons for Photoacoustic Tomographic Imaging, Dipanjan Pan¹; ¹Univ. of Illinois at Urbana-Champaign, USA. In this talk we will discuss the potential of photoacoustic imaging in combination with molecularly targeted contrast agents to detect early, sprouting angiogenic expression and the opportunities for improved recognition of cancer metastases.

CLEO: QELS-Fundamental Science

FM2A • Quantum Logic and Interference—Continued

FM2A.4 • 11:15

All-Optical Continuously Tunable Delay of Single Photons, Stéphane Clemmen¹, Alessandro Farsi¹, Alexander L. Gaeta¹, ¹*School of Applied and Engineering Physics, Cornell Univ., USA*. We report the first demonstration of all-optical continuously tunable delay imparted on single photons using a frequency conversion-dispersion technique. Delays tunable over 23 times the photon duration are demonstrated with on/off efficiency of 20-55%.

FM2A.5 • 11:30 **Invited**

Quantum Information Processing with Photons, Yuao Chen¹; ¹*Shanghai Branch, National Lab for Physical Sciences at Microscale and Dept. of Modern Physics, Univ. of Science and Technology of China, China*. In this talk I shall present a brief overview on some recent exciting experimental progress towards scalable quantum information processing (QIP), e.g., quantum communication, quantum computation and quantum simulation, via manipulation of photonic qubits.

FM2B • New Trends in Attoscience—Continued

FM2B.4 • 11:15

Following Attosecond Photoemission from Solids Using Interferometry, Lukas Gallmann^{1,2}, Matteo Lucchini¹, Luca Castiglioni³, Reto Locher¹, Michael Greif³, Jürg Osterwalder³, Matthias Hengsberger³, Ursula Keller¹; ¹*Dept. of Physics, ETH Zurich, Switzerland*; ²*Inst. of Applied Physics, Univ. of Bern, Switzerland*; ³*Dept. of Physics, Univ. of Zurich, Switzerland*. Implementing RABBIT on solids for the first time, we record energy-resolved absolute photoemission delays from noble metal surfaces. The structure of the observed delays in Ag(111) and Au(111) is inconsistent with previously promoted models.

FM2B.5 • 11:30

Coherent VUV Emission from Field-Controlled Bound States, Michael Chini¹, Xiaowei Wang^{1,2}, Yan Cheng¹, He Wang³, Yi Wu¹, Eric Cunningham¹, Peng-Cheng Li^{4,5}, John Heslar⁴, Dmitry Telnov⁶, Shih-I Chu^{4,7}, Zenghu Chang¹; ¹*Univ. of Central Florida, USA*; ²*National Univ. of Defense Technology, China*; ³*Lawrence Berkeley National Lab, USA*; ⁴*National Taiwan Univ., Taiwan*; ⁵*North-west Normal Univ., China*; ⁶*St. Petersburg State Univ., Russia*; ⁷*Univ. of Kansas, USA*. We demonstrate a dramatic enhancement of the below-threshold harmonics in the vicinity of atomic resonances. The dependence on the driving laser carrier-envelope phase suggests a nonperturbative mechanism. Phase matching promises scalability to microJoule pulse energies.

FM2B.6 • 11:45

Combining Attosecond Science with Coincidence Momentum Spectroscopy, Robert Boge¹, Mazyar Sabbar¹, Sebastian Heuser¹, Claudio Cirelli¹, Lukas Gallmann^{1,2}, Ursula Keller¹; ¹*Physics Dept., ETH, Switzerland*; ²*Inst. of Applied Physics, Universität Bern, Switzerland*. We combine an attosecond beam line with a 3D momentum imaging spectrometer to achieve coincidence pump probe experiments with unprecedented attosecond time-resolution. Besides technical details, first coincidence and pump-probe experiments are presented.

FM2C • Optics in Random Media I—Continued

FM2C.4 • 11:15

Optical resonances in topological defect structures, Seng Fatt Liew¹, Yaron Bromberg¹, Hui Cao¹; ¹*Applied Physics, Yale Univ., USA*. We study numerically optical resonances in 2D topological defect structures with wavelength-scale anisotropic scattering units. Both spatially extended and localized modes exhibit vortex-like energy flow due to breaking of chiral symmetry of the underlying structure.

FM2C.5 • 11:30 **Invited**

Densities of states, dynamics and intensity profiles of transmission eigenchannels of opaque media, Azriel Z. Genack¹, Matthieu Davy^{1,2}, Zhou Shi¹, Jing Wang¹, Jongchul Park¹; ¹*CUNY Queens College, USA*; ²*Univ. of Rennes 1, France*. We determine the frequency derivative of the composite phase of transmission eigenchannels and relate this to their contribution to the density of states, their dwell time and their intensity profile within the random medium.

FM2D • Graphene and Novel Phenomena—Continued

FM2D.3 • 11:15

Optical Second-Harmonic Generation Induced by Electric Current in Epitaxial Graphene on Vicinal SiC(0001), Yong An¹, J. E. Rowe², Daniel B. Dougherty², Ji Ung Lee¹, Alain C. Diebold¹; ¹*State Univ. of New York, USA*; ²*North Carolina State Univ., USA*. We find that surface second-harmonic generation (SHG) from epitaxial graphene on a vicinal SiC(0001) substrate is enhanced ~25% by direct electric current in graphene and that the enhanced SHG varies strongly with the measurement location.

FM2D.4 • 11:30

Observation of the Imbert-Fedorov effect via weak value amplification, Gaurav Jayaswal¹, Giampaolo Mistura¹, Michele Merano¹; ¹*Dipartimento di Fisica e Astronomia "G. Galilei", UNIV. OF PADOVA, Italy*. We report the first experimental observation of the Imbert-Fedorov shift via weak value amplification.

FM2D.5 • 11:45

Observation of band gaps in amorphous photonic structures with different temperatures in the near infrared, serdar kocaman¹, James F. McMillan¹, Di Wang¹, Mikael Rechtsman², Chee Wei Wong¹; ¹*Optical Nanostructures Lab, Columbia Univ., USA*; ²*Physics Dept. and Solid State Inst., Technion, Israel*. We examine numerically and experimentally photonic band-gaps in liquid-like two dimensional photonic materials. Subwavelength dielectric rods and holes are randomly placed with Monte Carlo simulations, fabricated on silicon-on-insulator chips, and measured in near infrared wavelengths.



CLEO: Science & Innovations

SM2E • Spectroscopic Chemical
Detection—Continued

SM2E.3 • 11:15

Mid-IR Photothermal Spectroscopy with an Integrated Fiber Probe Laser, Michelle Y. Sander^{1,5}, Hui Liu^{1,5}, Alket Mertiri^{2,5}, Atcha Totachawattana^{1,5}, Shyamsunder Erramilli^{3,4}; ¹Electrical and Computer Engineering, Boston Univ., USA; ²Division of Materials Science and Engineering, Boston Univ., USA; ³Physics Dept., Boston Univ., USA; ⁴Dept. of Biomedical Engineering, Boston Univ., USA; ⁵Photonics Center, Boston Univ., USA. We present the first compact, all-fiber probe laser system for mid-IR photothermal spectroscopy. Images of the vibrational CH bands of a liquid crystal sample with high contrast are demonstrated.

SM2E.4 • 11:30

Multi-Color Laser Spectroscopy with a Dual-Wavelength Quantum Cascade Laser, Jana Jägerová¹, Pierre Jouy², Béla Tuzson¹, Herbert Looser³, Andreas Hugi², Markus Mangold¹, Patrik Soltic¹, Lukas Emmenegger¹, Jérôme Faist²; ¹Lab for Air Pollution/Environmental Technology, EMPA, Switzerland; ²Inst. for Quantum Electronics, ETHZ, Switzerland; ³Inst. for Aerosol and Sensor Technology, FHNW, Switzerland. A new concept of multi-color spectroscopy based on a dual-wavelength QCL is presented. The latter emits at two distinct wavelengths (5.26 and 6.25 μm), featuring simultaneous detection of two different gas species without any beam combining optics.

SM2E.5 • 11:45

Intracavity Quartz-Enhanced Photoacoustic Sensor for Mid-Infrared Trace-Gas Detection, Simone Borri^{1,3}, Iacopo Galli^{1,3}, Davide Mazzotti^{1,3}, Vincenzo Spagnolo^{2,4}, Paolo De Natale^{1,3}, Gaetano Scamarcio^{2,4}, Giovanni Giusfredi^{1,3}, Pietro Patimisco^{2,4}; ¹CNR - INO, Italy; ²CNR - IFN, Italy; ³LENS, Italy; ⁴Università di Bari, Italy. Quartz-enhanced photoacoustic spectroscopy (QEPAS) and cavity-enhanced spectroscopy are merged in a novel gas sensor. Thanks to the intracavity power build up, sensitivity is increased by more than a factor 100 with respect to standard QEPAS.

SM2F • Advanced Solid State
Laser Architectures—Continued

SM2F.4 • 11:15

Power-scaling continuous-wave solid-state Raman lasers using intracavity adaptive optics, Ran Li¹, Mike Griffith², Leslie Laycock², Walter Lubeigt¹; ¹Univ. of Strathclyde, UK; ²BAE Systems Advanced Technology Centre, UK. Initial investigations to alleviate thermal lensing, a fundamental limitation in Raman lasers performance, are reported. An adaptive-optics feedback loop was incorporated into a Nd:YVO₄ self-Raman laser demonstrating a 40% Raman output power increase

SM2F.5 • 11:30

High-efficiency continuous-wave index-antiguided planar waveguide laser with large mode area, Yuanye Liu¹, Tsing-Hua Her¹, Lee Casperson²; ¹Physics and Optical Science, Univ. of North Carolina Charlotte, USA; ²Dept. of Electrical and Computer Engineering, Univ. of North Carolina at Charlotte, USA. We demonstrate robust continuous-wave lasing in planar index-antiguided waveguides with a 220- μm Nd:YAG active layer. A pump-limited output of 1.5 W with a slope efficiency of 30% with respect to absorbed pump power is achieved.

SM2F.6 • 11:45

Diode-pumped Tm:KYW 1.9- μm Microchip Laser with 71% Slope Efficiency and 1 W cw Output Power, Maxim S. Gaponenko¹, Nikolay Kuleshov², Thomas Südmeyer¹; ¹Laboratoire Temps-Fréquence, Université de Neuchâtel, Switzerland; ²Belarusian National Technical Univ., Belarus. We report on a diode-pumped Tm:KYW microchip laser generating 1 W TEM₀₀ continuous-wave output power with 71% slope efficiency relative to the absorbed pump power and 42% overall optical efficiency to the incident pump power.

SM2G • Silicon Photonic
Modulators—Continued

SM2G.4 • 11:15

Ultralow Power Consumption of 1.5nW Over Wide Optical Spectrum Range in Silicon Organic Hybrid Modulator, Xingyu Zhang¹, Amir Hosseini², Jongdong Luo³, Alex Jen³, Ray Chen¹; ¹Dept. of Electrical and Computer Engineering, Univ. of Texas at Austin, USA; ²Omega Optics, Inc., USA; ³Dept. of Materials Science and Engineering, Univ. of Washington, USA. We demonstrate an ultralow-power, low-dispersion and compact silicon-organic-hybrid photonic crystal waveguide modulator. RF power consumption of 1.5nW, effective in-device r₃₃ of 1190pm/V and $V_{\pi} \times L$ of $0.291 \pm 0.006 \text{V} \times \text{mm}$ over 8nm optical bandwidth are demonstrated.

SM2G.5 • 11:30

A Lumped Michelson Interferometric Modulator in Silicon, David Patel¹, Venkat Veerasubramanian¹, Samir Ghosh¹, Alireza Samani¹, Qiuhan Zhong¹, David Plant¹; ¹Electrical and Computer Engineering, McGill Univ., Canada. We demonstrate the operation of a low V_{π} , lumped, and compact Michelson modulator fabricated in SOI. The modulator operates up to 25 Gbps with measured error free operation up to 12.5 Gbps.

SM2G.6 • 11:45 Invited

16QAM Silicon-Organic Hybrid (SOH) Modulator Operating with 0.6 V_{π} and 19 fJ/bit at 112 Gbit/s, Matthias Lauer¹, Robert Palmer¹, Sebastian Koeber^{1,2}, Philipp C. Schindler¹, Dietmar Korn¹, Thorsten Wahlbrink³, Jens Bolten³, Michael Waldow³, Delwin L. Elder⁴, Larry R. Dalton⁴, Juerg Leuthold^{1,5}, Wolfgang Freude^{1,2}, Christian G. Koos^{1,2}; ¹Inst. of Photonics and Quantum Electronics, Karlsruhe Inst. of Tech, Germany; ²Inst. of Microstructure Tech, Karlsruhe Inst. of Tech, Germany; ³AMO GmbH, Germany; ⁴Dept. of Chemistry, Univ. of Washington, USA; ⁵Electromagnetic Fields Lab, Swiss Federal Inst. of Tech (ETH), Switzerland. We demonstrate a silicon-based 16QAM modulator with a record-low drive voltage of 0.6 V_{π} and an energy consumption of 19fJ/bit. The device employs silicon slot waveguides with electro-optic organic cladding and enables data transmission at 112Gbit/s.

SM2H • Novel Approaches
for Detection, Sensing and
Characterization—Continued

SM2H.4 • 11:30

A New Type of "Black Silicon" Materials with High Infrared Absorption and Annealing-Insensitivity, Yan Peng¹, Yiming Zhu¹; ¹Shanghai Key Lab of Modern Optical System, Univ. of Shanghai for Science and Technology, China. A new type of "black silicon" materials with high optical absorbance and annealing-insensitivity is designed and fabricated by femtosecond laser pulses. These results have important implications for the fabrication of highly efficient optoelectronic devices.

SM2H.5 • 11:45

Extended Infrared Absorption to 2.2 μm with $\text{Ge}_{1-x}\text{Sn}_x$ Photodetectors Grown on Silicon, Benjamin Conley¹, Liang Huang¹, Sayed A. Ghetmiri¹, Aboozar Mosleh¹, Wei Du¹, Greg Sun², Richard Soref², John Tolle³, Hameed A. Naseem¹, Shui-Qing Yu¹; ¹Electrical Engineering, Univ. of Arkansas, USA; ²Dept. of Physics, Univ. of Massachusetts, USA; ³ASM America Inc., USA. Thin film $\text{Ge}_{1-x}\text{Sn}_x$ photodetectors fabricated on Si using a CMOS compatible process had responsivities at 1.55 μm of 6.59, 1.49, 2.63, and 0.84 mA/W for 0.9, 2.57, 3.2, and 7.0 % Sn. Spectral response for a $\text{Ge}_{0.93}\text{Sn}_{0.07}$ photodetector had extended infrared response out to 2.2 μm .

CLEO: Science & Innovations

SM2I • Mode-locked OPOs—
Continued

SM2I.4 • 11:30

2.09- μ m degenerate femtosecond OPO with over 60% conversion efficiency and 0.6-W output, Kirk A. Ingold¹, Alireza Marandi¹, Charles Rudy^{1,2}, Robert L. Byer¹; ¹Stanford Univ., USA; ²IPG Photonics Silicon Valley Technology Center, USA. We report a broad frequency comb centered at 2.09 μ m produced by a degenerate OPO. We achieve 0.6W of 94-fs transform limited pulses at 250MHz and a conversion efficiency of 64%.

SM2I.5 • 11:45

Few-Cycle, Broadband, Mid-Infrared Parametric Oscillator Pumped by a 20-fs Ti:sapphire Laser, Suddapalli Chaitanya Kumar¹, Adolfo Esteban-Martin¹, Takuro Ideguchi², Ming Yan^{2,3}, Simon Holzner², Theodor W. Hänsch^{2,3}, Nathalie Picqué^{2,4}, Majid Ebrahim-Zadeh^{1,5}; ¹ICFO -The Inst. of Photonic Sciences, Spain; ²Max-Planck Institut für Quantenoptik, Hans-Kopfermann-Strasse, Germany; ³Ludwig-Maximilians-Universität München, Fakultät für Physik, Schellingstr, Germany; ⁴Institut des Sciences Moléculaires d'Orsay, CNRS, Bâtiment 350, Université Paris-Sud, France; ⁵Instituto Catalana de Recerca i Estudis Avançats (ICREA), Spain. We report a broadband mid-IR femtosecond OPO tunable across 2179-3732 nm, pumped by 20-fs pulses at 790 nm, generating idler pulses of 4.3 optical cycles (33 fs) at 2282 nm, with high stability and beam-quality.

SM2J • Nanostructured LEDs
and Photovoltaics—Continued

SM2J.4 • 11:15

Investigation of Purcell Factor and Light Extraction Efficiency in Ag-Coated GaN/InGaN Core-Shell Nanowires, Mohsen Nami¹, Jeremy Wright¹, Daniel Feezell¹; ¹Electrical and Computer Engineering, Univ. of New Mexico, USA. We calculate the Purcell factor and light extraction efficiency in Ag-coated GaN/InGaN core-shell nanowires using a model that includes the structural features necessary for electrical injection. The nanowires exhibit maximum Purcell factors of ~60 and maximum light extraction efficiencies of ~12%.

SM2J.5 • 11:30 

Nanowire-based LEDs and Photovoltaics, Lars Samuelson^{1,2}; ¹Solid State Physics/the Nanometer Structure Consortium, Lund Univ., Sweden; ²Glo AB & Sol Voltaics AB, Sweden. I will describe principles and advantages of the growth of semiconductor nanowires, specifically for fabrication of light-emitting diodes for display and solid state lighting applications as well as for the realization of nanowire array solar cells.

CLEO: QELS-
Fundamental ScienceFM2K • Plasmonic
Nanoantennas—Continued

FM2K.4 • 11:15

Circuit Theory of Optical Antenna Shedding Light on Fundamental Limit of Rate Enhancement, Michael Eggleston¹, Kevin Messer¹, Eli Yablonoitch¹, Ming Wu¹; ¹Electrical Engineering and Computer Science, Univ. of California Berkeley, USA. A circuit model of a single-element linear optical antenna is presented. It agrees well with FDTD simulations and predicts spreading resistance will ultimately limit the maximum rate enhancement an efficient antenna can achieve to ~10,000.

FM2K.5 • 11:30

Spectral interferometric microscopy reveals absorption by individual optical nano-antennas from extinction phase, Sylvain D. Gennaro¹, Yannick Sonnefraud¹, Niels Verellen², Pol Van Dorpe³, Victor Moshchalkov², Stefan Maier¹, Rupert F. Oulton¹; ¹Physics, Imperial College London, UK; ²INPAC, Belgium; ³IMEC, Belgium. We demonstrate a method to extract absorption and scattering from phase and intensity measurements of extinction from a single optical nano-antenna by developing a novel spectrally resolved interferometer integrated within a confocal microscope.

FM2K.6 • 11:45

Multi-Photon Photoluminescence Spectral Behavior of Single Gold Nanorods, Vanessa Knittel¹, Marco Fischer¹, Alfred Leitenstorfer¹, Daniele Brida¹; ¹Univ. of Konstanz, Germany. The spectral shape and nonlinear order of optical emission from single gold nanorods is investigated. The results highlight the complex absorption cascade in the out-of-equilibrium electronic distribution after few-cycle excitation by near-infrared pulses.

CLEO: Applications
& TechnologyAM2L • Innovative Laser
Sources Detectors and Beam
Delivery—Continued

AM2L.4 • 11:15

Optics-free kagome fiber-aided laser micro-machining, Benoît Debord¹, Meshaal Alharbi¹, Clemens Hoenninger³, Eric Motay³, Frédéric Gêrôme^{1,2}, Fetah Benabid^{1,2}; ¹GPPMM Group, Xlim Research Inst., CNRS UMR 7252, France; ²GLOphotonics S.A.S, France; ³Amplitude Systèmes, France. We report on focus-optics free laser micro-processing of several materials using up to milli-joule energy-level fs-pulses directly delivered by 10m-long hypocycloid-core kagome HC-PCFs. The ablation rate and depth were studied showing high-precision drilling.

AM2L.5 • 11:30 

Ultrafast Beam Modulation and Delivery for Printing and Embossing Applications, Guido Hennig¹, Baldermann Thomas¹, Christian Nussbaum¹, Beat Neuenschwander², Stephan Bruening³; ¹Daetwyler Graphics AG, Switzerland; ²Berner Fachhochschule, Switzerland; ³Schepers GmbH, Germany. Optimized ps laser processing improves direct laser engraving of embossing rollers and high power fiber laser combined with ultrafast modulation and scanning techniques enable for digital print applications based on laser induced forward transfer (LIFT).

Technical Digest and Postdeadline Papers
Available Online

- Visit www.cleoconference.org
- Select **Download Digest Paper** button
- Use your email address and CLEO Registration ID # to synchronize

Once you have synchronized your conference registration with Optics InfoBase, you can log in directly to Optics InfoBase at any point using the same email address and OSA password.

Access must be established via synchronization within 60 days of the conference start date. Access is provided only to full technical attendees.

CLEO: Science & Innovations

SM2M • Novel Platforms for
Silicon Photonics—Continued

SM2M.2 • 11:30

Dispersion engineering of silicon microdisk resonators by thermal oxidation, Wei C. Jiang¹, Nicholas Usechak², Qiang Lin^{1,3}; ¹*Inst. of Optics, Univ. of Rochester, USA*; ²*Air Force Research Lab, USA*; ³*Electrical and Computer Engineering, Univ. of Rochester, USA*. We demonstrate a convenient approach for precise dispersion engineering of silicon microdisk resonators via thermal oxidation. This technique potentially enables efficient correlated photon-pair generation for quantum photonics.

SM2M.3 • 11:45

Multilayer Platform for Low-Power/Passive Configurable Photonic Device, Majid Soudagar¹, Amir H. Hosseinnia¹, Ali A. Eftekhar¹, Ali Adibi¹; ¹*ECE, Georgia Inst. of Technology, USA*. We demonstrate the possibility of forming ultra-compact, field-configurable, and low-power resonance-based passive integrated photonic structures based on charge accumulation in a high-quality multilayer material platform comprising Si/SiO₂/Si layers prepared through direct bonding of SOI wafers.

SM2N • Modes in Fibers—
Continued

SM2N.4 • 11:30

Characterization of Optical Fibers Supporting OAM States using Fiber Bragg Gratings, lixian wang^{1,2}, Bora Ung¹, Pravin Vaity¹, Leslie Rusch¹, Younès Messaddeq¹, Sophie LaRochelle¹; ¹*Centre d'Optique, Photonique et Laser (COPL), Université Laval, Canada*; ²*Inst. of Semiconductor, Chinese Academy of Sciences, China*. The reflectogram of a fiber grating is used to characterize vector modes of an optical fiber supporting orbital angular momentum states. All modes, with a minimal effective index separation around 10e-4, are successfully measured.

SM2N.5 • 11:45

Selective Excitation of Pure Higher Order Modes in Hollow-Core PCF via Side-Coupling, Barbara M. Trabold¹, David Novoa¹, Amir Abdolvand¹, Philip St.J. Russell¹; ¹*Max Planck Inst. for the Science of Light, Germany*. Side-coupling enables the selective excitation of individual higher order modes in hollow-core PCF, permitting the complex near-field modal patterns to be cleanly observed at any wavelength. Modal phase indices and losses can be accurately measured.

CLEO: Applications
& TechnologyAM2O • Endoscopy & Minimally
Invasive Optical Imaging—
Continued

AM2O.3 • 11:15

Real-time Epidural Anesthesia Guidance Using Optical Coherence Tomography Needle Probe, Qinggong Tang¹, Chia-Pin Liang¹, Kyle Wu², Anthony Sandler², Yu Chen¹; ¹*Bioengineering, Univ. of Maryland-College Park, USA*; ²*Sheikh Zayed Inst. for Pediatric Surgical Innovation, Children's National Medical Center, USA*. Epidural anesthesia is one of the most widely used anesthesia methods. We developed a small hand-held OCT forward-imaging needle device for real-time epidural anesthesia surgery guidance and demonstrated its feasibility through ex vivo experiments.

AM2O.4 • 11:30 **Invited**

Methods for enhancing visualization of subsurface tissue structures in real time, Stavros G. Demos¹; ¹*Lawrence Livermore National Lab, USA*. Methods and prototype instrumentation suitable for near surface imaging in tissues are presented. These methods are designed to address two main applications: a) vein imaging to assist cannulation and venipuncture of near surface veins; b) noncontact biometric identification using distinguishing traits in the human hand.

AM2P • Symposium on
Advances in Molecular
Imaging II—Continued

AM2P.3 • 11:30

Approximating the Concentration of Lipids on the Surface of Virus-Like Particles through Plasmon Coupling, Amin Feizpour¹, Bjorn M. Reinhard¹; ¹*Chemistry Dept., Boston Univ., USA*. The superior optical properties of gold nanoparticles were used to estimate the concentration of two crucial lipids on virus surface. This is a novel high-throughput and rapid surface characterization approach for viruses in low-concentration samples.

AM2P.4 • 11:45

A Depth Perturbation Method for Determining Depth of Fluorophore in Tissue, Tuo Zhou¹, Takehiro Ando¹, Hongen Liao², Etsuko Kobayashi¹, Ichiro Sakuma¹; ¹*Univ. of Tokyo, Japan*; ²*Tsinghua Univ., China*. Estimating bio-distribution of fluorophore in tissue is challenging. In this paper, we demonstrated that our depth perturbation method can accurately determine depth of fluorophore located in tissue as deep as 5.8 mm by phantom experiments.

Download the CLEO Mobile App

Search for CLEO:2014
in the app stores or
scan the QR code



CLEO: QELS-Fundamental Science

FM2A • Quantum Logic and Interference—Continued

FM2A.6 • 12:00

Quantum Noise in Large-Scale Photonic Circuits, Charles M. Santori¹, Jason S. Pelc¹, Raymond G. Beausoleil¹, Nikolas Tezak², Ryan Hamerly², Hideo Mabuchi²; ¹Hewlett-Packard Labs, USA; ²Edward L. Ginzton Lab, Stanford Univ., USA. We describe a simulation approach for studying quantum-mechanical noise in large-scale nonlinear optical circuits. We apply this model to predict the behavior of a 4-bit counter circuit containing several hundred optical components.

FM2A.7 • 12:15

Verifying Quantum Complexity in Linear Optical Experiments, Jacques Carolan¹, Jasmine Meinecke¹, Pete Shadbolt¹, Nicholas J. Russell¹, Nur Ismail², Kerstin Worhoff², Terry Rudolph³, Mark Thompson¹, Jeremy L. O'Brien¹, Jonathan Matthews¹, Anthony Laing¹; ¹Centre for Quantum Photonics, Univ. of Bristol, UK; ²Integrated Optical Microsystems Group, Univ. of Twente, Netherlands; ³Inst. for Mathematical Sciences, Imperial College London, UK. We develop techniques to verify the computational complexity of a class of analogue quantum computers known as boson samplers. We demonstrate these techniques with up to 5 photons in two different types of integrated linear optical circuit, observing Hilbert spaces of up to 50,000 dimensions.

FM2B • New Trends in Attoscience—Continued

FM2B.7 • 12:00

Ultrafast Relaxation and Photodissociation Dynamics of 1,3-Butadiene Studied by Probing Molecular Orbitals, Ayumu Makida¹, Takehisa Fujiwara¹, Yu Harabuchi², Tetsuya Taketsugu², Taro Sekikawa¹; ¹Applied Physics, Hokkaido Univ., Japan; ²Chemistry, Hokkaido Univ., Japan. Femtosecond relaxation and picosecond photodissociation dynamics of 1,3-butadiene were investigated by time-resolved photoelectron spectroscopy with high harmonics pulses, probing the deeper molecular orbitals which are sensitive to the molecular structure.

FM2B.8 • 12:15

THz streaking of attosecond pulse trains, Fernando Ardana-Lamas^{1,2}, Andrey Stepanov¹, Christian Erny^{1,2}, Ishkhan .gorgisya^{1,2}, Pavle Juranic¹, Christoph P. Hauri^{1,2}; ¹Paul Scherrer Inst., Switzerland; ²École polytechnique fédérale de Lausanne, Switzerland. We present the first streaking of an attosecond pulse train using an intense THz field. Streaking with THz enables temporal characterization of the full pulse train in a single shot measurement.

FM2C • Optics in Random Media I—Continued

FM2C.6 • 12:00

Transmission channels for light in absorbing random media, Seng Fatt Liew¹, Sebastian Popoff¹, Allard P. Mosk², Willem L. Vos², Hui Cao¹; ¹Applied Physics, Yale Univ., USA; ²Complex Photonic Systems, MESA+ Inst. for Nanotechnology, Univ. of Twente, Netherlands. We study numerically the effects of optical absorption on highly transmitting channels in strongly scattering media. We observe that they are robust against weak absorption. Surprisingly, in case of strong absorption diffusive transport becomes ballistic-like.

FM2C.7 • 12:15

Momentum-resolved Electron Energy Loss Spectroscopy (q-EELS) for Quantum Plasmonics and Metamaterials, Prashant Shekhar¹, Vaibhav Gaiind³, Marek Malac^{2,1}, Ray Egerton^{2,1}, Zubin Jacob¹; ¹Univ. of Alberta, Canada; ²National Inst. of Nanotechnology, Canada; ³KLA Tencore, USA. We report on experimental and theoretical results on EELS from 12nm single-crystal gold films. Our results show that momentum resolution of the electrons gives insight into signatures of non-locality and quantum nature of the excitations.

FM2D • Graphene and Novel Phenomena—Continued

FM2D.6 • 12:00

Terahertz Induced Transparency in Single-Layer Graphene, Michael Paul¹, Byoungwak Lee¹, Jenna Wardini¹, Zack Thompson¹, Andrew Stickel¹, Ali Mousavian¹, Ethan Minot¹, Yun-Shik Lee¹; ¹Physics, Oregon State Univ., USA. We demonstrate THz-induced transparency in two types of single-layer CVD graphene samples utilizing high-field THz pulses. The nonlinear THz transmission depends on the local conductivity of the samples and dynamically varies in the time domain.

FM2D.7 • 12:15

Graphene coated ZnO nanowire optical waveguides, Bigeng Chen¹, Limin Tong¹; ¹Dept. of Optical Engineering, State Key Lab of Modern Optical Instrumentation, China. Using a tape-assist-transfer method and micromanipulation, we have fabricated graphene coated ZnO nanowire (GZN) optical waveguides. The GZNs exhibit significant saturable absorption (differential transmission of 15% at 1064nm), which can be employed for optical modulation.

12:30–13:30 Lunch Break (on your own)

NOTES

CLEO: Science & Innovations

SM2E • Spectroscopic Chemical
Detection—Continued

SM2E.6 • 12:00
Phase Locked System for Dual Comb Molecular Spectroscopy at 2-6 μ m Based on Tm-fiber Laser, Viktor O. Smolski¹, Kevin F. Lee², Christian Mohr², Jie Jiang², Ingmar Hartl³, Martin Fermann², Konstantin L. Vodopyanov¹; ¹CREOL, Univ. of Central Florida, USA; ²IMRA America, inc, USA; ³Deutsches Elektronen-Synchrotron (DESY), Germany. We demonstrate phase-coherent, frequency-stabilized dual-comb system at 2 μ m, extendable to mid-IR via phase-coherent frequency conversion in a doubly-resonant GaAs OPO. Results of dual-comb molecular spectroscopy with ~1M spectral points taken in ~1ms will be presented.

SM2E.7 • 12:15
Tunable Diode Laser Absorption Spectrometer for Detection of Hydrogen Fluoride Gas at Ambient Pressure, Ian M. Craig¹, Matthew S. Taubman¹, Bruce E. Bernacki¹, Robert D. Stahl¹, John T. Schiffer¹, Tanya L. Myers¹, Bret D. Cannon¹, Mark C. Phillips¹; ¹Pacific Northwest National Lab, USA. We present a tunable diode laser absorption spectrometer (TDLAS) sensor for hydrogen fluoride (HF) detection at ambient pressure operating around the fundamental R(1) transition at 2.476 μ m. We achieve 38 ppt sensitivity for 1-s integration time.

SM2F • Advanced Solid State
Laser Architectures—Continued

SM2F.7 • 12:00
Generation of 300 ps laser pulse with 1.2 J energy at 532 nm by stimulated Brillouin scattering in water, Chengyong Feng¹, Xiaozhen Xu¹, Jean-Claude M. Diels¹; ¹Univ. of New Mexico, USA. We experimentally demonstrate SBS pulse compression in water from 10 ns, 2.3 J to 300 ps, 1.2 J. To our best knowledge, this is the highest compressible energy that has been achieved at 532 nm.

SM2F.8 • 12:15
A Linear Phase-Conjugation Imaging System, Seung-Wan Bahk¹, Jake Bromage¹, Jonathan D. Zuegel¹; ¹Univ. of Rochester, USA. An imaging system based on phase conjugation is demonstrated for application in long-working-distance imaging. A liquid crystal device is adaptively controlled using a near-field feedback to achieve the conjugation of the incident phase.

SM2G • Silicon Photonic
Modulators—Continued

SM2G.7 • 12:15
A Silicon Photonic Chip-Scale AWGR Switch for High Performance Computing Systems, Runxiang Yu¹, Stanley Cheung¹, Roberto Proietti¹, Yuliang Li¹, Katsunari Okamoto², S. J. Ben Yoo¹; ¹Univ. of California Davis, USA; ²AiDi Corporation, Japan. This paper demonstrates a silicon-photonic AWGR-based optical switch for HPC systems. Simulations show high throughput and low latency even at high input load. A fabricated silicon-photonic AWGR switch with 32 Tx/Rx pairs showed error-free performance.

SM2H • Novel Approaches
for Detection, Sensing and
Characterization—Continued

SM2H.6 • 12:00
Ultra-broad Bandwidth Ultrasound Detector Using Imprinted Polymer Microring Resonator, Cheng Zhang¹, Tao Ling¹, Sung-Liang Chen¹, L. Jay Guo¹; ¹Electrical Engineering and Computer Science, Univ. of Michigan, USA. A novel ultra-broad bandwidth ultrasound detector is demonstrated using imprinted polymer microring, with flat frequency response up to ~350 MHz at -3dB. A record high sub-3 μ m axial resolution in ultrasound/photoacoustic imaging applications is demonstrated.

SM2H.7 • 12:15
Modeling and Optimization of Magnesium-thermally-formed Porous Silicon in Silicon-on-insulator Microresonator Sensors, Zhixuan Xia¹, Ali A. Eftekhar¹, Qing Li¹, Ali Adibi¹, Stan C. Davis², Ari S. Gordin², Kenneth H. Sandhage²; ¹School of Electrical and Computer Engineering, Georgia Inst. of Technology, USA; ²School of Materials Science and Engineering, Georgia Inst. of Technology, USA. We develop a model for silicon-on-insulator microresonators with magnesium-thermally-formed porous silicon cladding possessing three-dimensional interconnected pores. Investigation of waveguide design and geometrical parameters indicates an optimized areal mass sensitivity of ~ 0.2 pm/(pg/mm²).

12:30–13:30 Lunch Break (on your own)

NOTES

Handwritten notes area with horizontal lines.

CLEO: QELS-Fundamental Science

13:30–15:30

FM3A • Quantum Detection
Presider: Sae Woo Nam; NIST, USA

FM3A.1 • 13:30

An Improved Method for Photon-Number Discrimination for Transition-Edge Sensors, Boris L. Glebov¹, Jingyun Fan¹, Alan L. Migdall¹, Adriana Lita¹, Sae Woo Nam¹, Thomas Gerrits¹; ¹NIST, USA. Proposed discrimination of photon numbers is based on sum-squared error between detector response curve and a calibration suite of response templates. Templates for higher numbers are extrapolated from fits describing incremental differences between low-number templates.

FM3A.2 • 13:45

GHz gated single-photon detection based on harmonic spectral balancing techniques, Yan Liang¹, Haibin Du¹, Heping Zeng^{1,2}; ¹State Key Lab of Precision Spectroscopy, East China Normal Univ., China; ²Shanghai Key Lab of Modern Optical System, Engineering Research Center of Optical Instrument and System, Ministry of Education, School of Optical-Electrical and Computer Engineering, Univ. of Shanghai for Science and Technology, China. We demonstrated GHz-gated InGaAs/InP single-photon detection with ultrashort pulses using harmonic spectral differencing, attaining avalanche signals by subtracting spike noise from mimic signals composed of sinusoidal waves of multi-frequencies and reducing the error counts robustly.

FM3A.3 • 14:00

Asymmetric Multi-Quantum Well Infrared Photodetector with a Bound State in the Continuum, Germano Maioli Penello¹, Arvind Pawan Ravikumar¹, Deborah L. Sivco¹, Claire F. Gmachl¹; ¹Electrical Engineering, Princeton Univ., USA. By carefully designing a multi-quantum well infrared photodetector (QWIP) heterostructure, we present an asymmetric QWIP with a localized state in the continuum. A narrow photocurrent spectrum confirms the electron confinement above the barrier.

13:30–15:30

FM3B • Quantum Fluids and Gases in Solids
*Presider: Junichiro Kono; Rice Univ., USA*FM3B.1 • 13:30 **Tutorial**

Quantum fluids of light, Cristiano Ciuti¹; ¹Université Paris Diderot, France. This tutorial reviews recent advances in the fundamental understanding and active control of quantum fluids of light in nonlinear optical media. Perspectives in the direction of strongly correlated photon systems are outlined.



Cristiano Ciuti graduated from Scuola Normale Superiore, Pisa in 1997 and received his PhD at EPFL, Lausanne in 2001. After a postdoc at the University of California, San Diego, in 2003 he became a lecturer at Ecole Normale Supérieure, Paris. Since 2006 he has been a professor at Université Paris Diderot.

13:30–15:30

FM3C • Optics in Random Media II
*Presider: Azriel Genack; CUNY Queens College, USA*FM3C.1 • 13:30 **Invited**

Coherent Control of Total Transmission of Light through Disordered Media, Sebastian Popoff¹, Seng Fatt Liew¹, Arthur Goetschy¹, A. Douglas Stone¹, Hui Cao^{1,2}; ¹Applied Physics, Yale Univ., USA; ²Physics, Yale Univ., USA. We used wavefront shaping to enhance/suppress the transmission of coherent light through open highly scattering media. The total transmission was varied by one order of magnitude as a result of mesoscopic correlations of coherent transport.

FM3C.2 • 14:00

Enhanced evanescent transport and Goos-Hanchen localization in a disordered dielectric multilayer, Hanan Herzig Sheinfux¹, Mordechai Segev¹; ¹Technion Israel Inst. of Technology, Israel. We show that disorder in dielectric structures made of multiple layers of deep subwavelength thickness can induce extremely short-ranged localization. Additionally the disorder can convert evanescent waves into bulk localized modes, enhancing transport dramatically (*10,000).

13:30–15:30

FM3D • Nonconventional Beams and Applications
Presider: Dragomir Neshev; Australian National Univ., Australia

FM3D.1 • 13:30

Diffraction-resisting Vortex Bessel beams with arbitrary trajectories, Ioannis D. Chremmos^{1,2}, Juanying Zhao³, Demetrios N. Christodoulides⁴, Zhigang Chen^{3,5}, Nikolaos K. Efremidis¹; ¹Dept. of Mathematics and Applied Mathematics, Univ. of Crete, Greece; ²Max Planck Inst. for the Science of Light, Germany; ³Dept. of Physics and Astronomy, San Francisco State Univ., USA; ⁴CREOL/College of Optics, Univ. of Central Florida, USA; ⁵Teda Applied Physics Inst., Nankai Univ., China. We theoretically show that it is possible to generate diffraction-resisting higher order Bessel beams with vortex profiles that follow arbitrary trajectories. Our theoretical results are supported by numerical simulations and agree well with experimental observations.

FM3D.2 • 13:45

Temporal tweezing of light, Jae K. Jang¹, Miro J. Erkintalo¹, Stuart G. Murdoch¹, Stephane Coen¹; ¹Univ. of Auckland, New Zealand. We experimentally demonstrate temporal tweezing of picosecond optical pulses, extending the concept of optical tweezers to the time-domain. By adjusting the phase profile of the driving beam, we can trap and manipulate temporal cavity solitons.

FM3D.3 • 14:00

Spiral Phase Matching, Thomas Roger¹, Julius Heitz¹, Joseph Lowney², Ewan M. Wright², Daniele Faccio¹; ¹Inst. of Photonics and Quantum Sciences, Heriot-Watt Univ., UK; ²College of Optical Sciences, Univ. of Arizona, USA. We study the nonlinear interaction between two non-collinear light beams that carry orbital angular momentum (OAM). Theory and experiments highlight the presence of new phase matching conditions in the presence of OAM.

CLEO: Science & Innovations

13:30–15:15

SM3E • Nano-, Micro-, and Waveguide-sensing

Presider: Yosuke Tanaka;
Tokyo Univ of Agriculture and
Technology, Japan

SM3E.1 • 13:30

Mid-infrared Noninvasive in vivo Glucose Detection in Healthy Human Subjects, Sabir Liakat¹, Kevin A. Bors¹, Laura Xu¹, Callie M. Woods¹, Jessica Doyle^{2,1}, Claire F. Gmachl¹; ¹Princeton Univ., USA; ²Hunterdon Regional Central High School, USA. A novel hollow-core fiber based mid-infrared noninvasive in vivo sensor, capable of clinically accurate predictions of glucose concentrations ranging from 80 - 160 mg/dL in healthy humans, is presented.

SM3E.2 • 13:45

Improved Signal Processing for Distributed Sensing Network based on Chirped Laser Dispersion Spectroscopy, Genevieve Plant¹, Yue Tian^{1,2}, Ting Wang², Gerard Wysocki¹; ¹Princeton Univ., USA; ²NEC Labs America, USA. Centralized detection in a network of Chirped Laser Dispersion Spectroscopy (CLaDS) sensors requires efficient signal processing. The optimization of CLaDS processing and development of a custom digital signal processing unit in place of restricting conventional bench-top instruments is discussed.

SM3E.3 • 14:00

A novel method to acquire ring-down interferograms using a double-looped mach-zehnder interferometer, Jin Hwan Kim¹, Won Sik Kwon¹, Hyub Lee¹, Kyung-Soo Kim¹, Soohyun Kim¹; ¹Division of Mechanical Engineering, Korea Advanced Inst. of Science and Technology, Korea. We present a novel, simple and cost-effective method to acquire ring-down interferograms based on a double-looped mach-zehnder interferometer requiring only a few millimeters of scanning range. Internal loss characterization of two loops is demonstrated.

13:30–15:30

SM3F • Advanced Laser Materials

Presider: Martin Richardson, Univ.
of Central Florida, CREOL, USA

SM3F.1 • 13:30

The role played on the Yb:LuAG laser performance by high doping levels and high ion excitation density, Angela Pirri¹, Guido Tocci², Martin Nikl³, Vladimir Babin³, Matteo Vannini²; ¹Istituto di Fisica Applicata "Nello Carrara", IFAC, National Research Council, CNR, Italy; ²Istituto Nazionale di Ottica, INO, National Research Council, CNR, Italy; ³Inst. of Physics, Academy of Sciences, Czech Republic. We present the laser performance achieved by 15 at.% Yb:LuAG crystal. Experimental evidences of a non-linear loss mechanism which occurs at high ion excitation density is observed and characterized.

SM3F.2 • 13:45

Spectroscopic Properties and Laser Operation of Sm,Mg:SrAl₂O₉, Daniel-Timo Marzahl¹, Fabian Reichert¹, Benedikt Stumpf¹, Philip W. Metz¹, Christian Kraenkel^{1,2}, Günter Huber^{1,2}; ¹Inst. of Laser-Physics, Germany; ²The Hamburg Centre for Ultrafast Imaging, Germany. We realized the first visible Sm³⁺-doped oxide laser. In Sm(6.7at.%)SrAl₂O₉, 28mW of self-pulsed average output power at 703.0nm were achieved with 8% slope efficiency under 2w-OPSL-pumping at 479.6nm. Furthermore, detailed spectroscopic investigations were performed.

SM3F.3 • 14:00

anti-B18H22: A brand-new laser material, Luis Cerdán¹, Jakub Braborec², Inmaculada Garcia-Moreno¹, Angel Costela¹, Michael G. S. Londesborough²; ¹Inst. of Physical Chemistry (CSIC), Spain; ²Inst. of Inorganic Chemistry (AS-CR), Czech Republic. The first laser borane, anti-B18H22, exhibits blue laser emission at 406nm with an efficiency of 9.5% and a photostability superior to that of commercial laser dyes, providing a new solution to an old problem.

13:30–15:30

SM3G • Micro-Resonators

Presider: Hideki Yagi; Sumitomo
Electric Industries Ltd, Japan

SM3G.1 • 13:30 **Invited**

Breaking the Conventional Limitations of Microrings, Joyce K. Poon¹, Wesley D. Sacher¹, Jared C. Mikkelsen¹, Solomon Assefa², Douglas M. Gill², Tymon Barwicz², Huapu Pan², Steven M. Shank³, Yurii Vlasov², William M. Green²; ¹Electrical and Computer Engineering, Univ. of Toronto, Canada; ²IBM T. J. Watson Research Center, USA; ³Microelectronics Division, IBM Systems Technology Group, USA. We demonstrate microring resonators with full tunability, modulation bandwidths exceeding the linewidth limit, and improved tolerance to wafer-scale variations. Novel device architectures and designs enable microrings to become more practical for integrated photonics.

SM3G.2 • 14:00

Wideband-Tunable Optical Resonators on Double-Layer SOI Platforms using Electrostatic Actuation, Razi Dehghannasiri¹, Ali Asghar Eftekhari¹, Majid Sodagar¹, Ali Adibi¹; ¹School of Electrical and Computer Engineering, Georgia Inst. of Technology, USA. We present mechanically-tunable microdisk resonators using electrostatic actuation in double-layer-SOI material platform. The possibility of achieving resonance wavelength shifts as-high-as 5.5 nm/volt and 1.35 nm/nm over a wavelength tuning range of 35 nm is demonstrated.

13:30–15:30

SM3H • 2D and Other Novel Materials

Presider: Jacob Khurgin; Johns
Hopkins Univ., USA

SM3H.1 • 13:30

Adaptive Photonic Meta-surfaces Exploiting Interfacial Phase Change in Elemental Gallium, Robin F. Waters¹, Kevin F. MacDonald¹, Peter A. Hobson², Nikolay I. Zheludev^{1,3}; ¹Optoelectronics Research Centre & Centre for Photonic Metamaterials, Univ. of Southampton, UK; ²QinetiQ Ltd., UK; ³Centre for Disruptive Photonic Technologies, Nanyang Technological Univ., Singapore. Surface-driven metallization in a nanoscale layer of elemental gallium forming the backplane of a photonic metamaterial absorber provides a mechanism for reversible all-optical and thermo-optical tuning of resonant response.

SM3H.2 • 13:45

Extracting the complex optical conductivity of true two-dimensional layers by ellipsometry, You-Chia Chang^{1,2}, Chang-Hua Liu³, Zhaohui Zhong³, Theodore Norris^{1,3}; ¹Center for Ultrafast Optical Science, Univ. of Michigan, USA; ²Applied Physics Program, Univ. of Michigan, USA; ³Dept. of Electrical Engineering and Computer Science, Univ. of Michigan, USA. A simple and robust technique to extract the complex optical conductivity of truly two-dimensional materials is developed. Applying the method to chemical-vapor-deposited graphene, we extract the complex conductivity, including Fermi level and scattering time.

SM3H.3 • 14:00

Graphene Stacks as the Darkest Material, Kevin J. Webb¹, Sunny Chugh¹, Mengren Man¹, Zhihong Chen¹; ¹Purdue Univ., USA. We present the fabrication and characterization of a graphene stack that can function as the darkest material and serve as the basis for a new class of sensitive, high-speed photodetectors.

Meeting Room
211 B/D

Meeting Room
212 A/C

Meeting Room
212 B/D

Marriott
Salon I & II

CLEO: Science & Innovations

13:30–15:30
**SM3I • Few-Cycle-Pulse
Nonlinear Optical Technologies**
President: Jeffrey Moses; MIT, USA

SM3I.1 • 13:30 **Invited**
**Sources and Diagnostics for Attosecond
Science**, Cord L. Arnold¹, Christoph Heyl¹,
Samuel Bengtsson¹, Johan Mauritsson¹,
Per Johnsson¹, Anne L'Huillier¹; ¹Dept. of
Physics, Lund Univ., Sweden. We present a
novel scheme to generate trains of angularly
separated single attosecond pulses by driv-
ing high-order harmonic generation with
two identical, but temporally delayed, laser
pulses, which are noncollinearly overlapped
in the generation medium.

SM3I.2 • 14:00
**High Gain Frequency domain Optical
Parametric Amplifier (FOPA) preserves ps
Pulse Contrast**, Philippe Lassonde¹, Maxime
Boivin¹, Ladan Arissian², Légaré Légaré¹,
Bruno E. Schmidt^{1,3}; ¹Institut National de
la Recherche Sci., Canada; ²Electrical and
Computer Engineering, Univ. of New Mexico,
USA; ³few-cycle Inc., Canada. 800nm, nJ level
pulses are amplified >2.000 times in a single
2mm BBO crystal, pumped by picosecond
400nm pulses. Experiments evidence that
the picosecond pulse contrast within the
pump window remains unchanged upon
amplification.

13:30–15:30
SM3J • Spatial Multiplexing
*President: David Caplan; MIT
Lincoln Lab, USA*

SM3J.1 • 13:30
**Experimental Demonstration of an Apo-
dized Aperture for Receiving a Data-Car-
rying Orbital-Angular-Momentum Beam**,
Nisar Ahmed¹, Guodong Xie¹, Yongxiang
Ren¹, Long Li¹, Hao Huang¹, Yan Yan¹, Alan
Willner¹; ¹Univ. of Southern California, USA.
We experimentally demonstrate an apodized
aperture for receiving OAM beams carrying
50-Gbaud QPSK channels. The performance
in terms of power in desired mode and leak-
age to neighboring modes is compared with
a hard aperture.

SM3J.2 • 13:45
**Experimental Comparison of Single and
Double Partial Receiver Apertures for
Recovering Signals Transmitted using
Orbital-Angular-Momentum**, Guodong Xie¹,
Yongxiang Ren¹, Hao Huang¹, Nisar Ahmed¹,
Long Li¹, Yan Yan¹, Martin P. Lavery², Miles
Padgett², Moshe Tur³, Samuel Dolinar⁴, Alan
Willner¹; ¹Dept. of Electrical Engineering,
Univ. of Southern California, USA; ²School
of Physics and Astronomy, Univ. of Glasgow,
UK; ³School of Electrical Engineering, Tel Aviv
Univ., Israel; ⁴Jet Propulsion Lab, California
Inst. of Technology, USA. We compared
power spreading of a partially captured
orbital-angular-momentum (OAM) beam by
using single and double apertures. Double
apertures could help reducing crosstalk from
OAM l to OAM $l+m$ by ~ 10 dB, where l is an
integer and m is an odd number.

SM3J.3 • 14:00
**Evaluation of channel capacity of the OAM-
based FSO links with a precise assessment
of turbulence impact**, Ming Li^{1,2}, Milorad
Cvijetic¹, Yuzuru Takashima¹, Zhongyuan Yu²;
¹College of Optical Sciences, Univ. of Arizona,
USA; ²State Key Lab of Information Photonics
and Optical Communications, Beijing Univ.
of Posts and Telecommunications, China.
The channel capacity of FSO links based on
modulation of inconsecutive OAM-modes
is evaluated by using modified Von Karman
model. The results show significant reduces
in crosstalk with channel capacity converging
to an ideal case.

CLEO: QELS- Fundamental Science

13:30–15:30
**FM3K • Plasmonic Biochemical
Sensors and Systems**
*President: Hatice Altug; Boston
Univ., USA*

FM3K.1 • 13:30 **Invited**
**Plasmonic Biosensors and Their Analytical
Applications**, Jiri Homola¹; ¹Inst. of Photonics
and Electronics, Czech Republic. Advances
in the field of optical biosensors based on
surface plasmons are reviewed and examples
of applications of plasmonic biosensors for
detection of chemical and biological sub-
stances are given.

FM3K.2 • 14:00
**Hand-Held Plasmonic Biosensor for High-
Throughput Sensing for Point-of-Care
Applications**, Arif E. Cetin^{1,2}, Ahmet F.
Coskun^{3,4}, Betty C. Galarreta¹, Min Huang¹,
David Herman³, Aydogan Ozcan^{3,5}, Hatice Altug^{2,1};
¹Electrical and Computer Engineering,
Boston Univ., USA; ²Bioengineering Dept.,
EPFL, Switzerland; ³Electrical Engineer-
ing, UCLA, USA; ⁴Chemistry and Chemical
Engineering, California Inst. of Technology,
USA; ⁵California NanoSystems Inst., UCLA,
USA. We introduce a hand-held biosensor
based on large-area plasmonic microarrays
coupled with a lens-free computational imag-
ing system for high-throughput biosensing.
Our light-weight device, 60 g and 7.5 cm, is
highly suitable for point-of-care applications
for field-settings.

CLEO: Applications & Technology

13:30–15:30
**AM3L • Symposium on Enabling
Photonics Technologies for
Miniaturization I** **▶**
*President: Saulius Juodkazis;
Swinburne Univ. of Technology,
Australia*

AM3L.1 • 13:30 **Invited** **▶**
**Mapping (slow) Light at the Nanoscale -
Don't Forget the Magnetic Field**, L. (Kobus)
Kuipers¹; ¹FOM Inst. AMOLF, Netherlands.
We present local investigations of the
spectral evolution of ultrashort slow pulses
as they propagate. We also show that na-
noscale electrical and magnetic fields can
be detected simultaneously.

AM3L.2 • 14:00 **Invited** **▶**
**Management of the photon orbital angular
momentum at small scale**, Etienne Brasse-
let¹; ¹Univ. of Bordeaux, CNRS, France. The
elaboration of photonic devices enabling
the control of the optical orbital angular
momentum at small spatial scales remains
a contemporary challenge that needs to be
addressed. We will discuss recent progresses
in that direction.

CLEO: Science & Innovations

13:30–15:30

SM3M • Nanophotonic Structures for Quantum Optics ▶

Presider: Kartik Srinivasan; NIST, USA

SM3M.1 • 13:30 **Invited** ▶

Nonlinear optics and quantum networks based on single atoms coupled to a photonic crystal cavity, Mikhail Lukin¹, Jeff Thompson¹, Tobias Tiecke¹, Vladan Vuletic¹, Nathalie de Leon¹, Lee Liu¹; ¹Harvard Univ., USA. We present an experimental demonstration of an optical switch operating in the quantum regime, consisting of a single trapped atom near a nanoscale photonic crystal cavity.

SM3M.2 • 14:00 ▶

Composite Photonic Crystal Cavity on a Nanofiber, Mark Sadgrove¹, Ramachandrarao Yalla¹, Kali P. Nayak¹, Kohzo Hakuta¹; ¹Center for Photonic Innovations, Univ. of Electro-communications, Japan. We realize a photonic crystal cavity by mounting an optical nanofiber on a nanostructured grating which includes a designed defect. The device has a Q-factor of ~1000 and excellent coupling to the nanofiber fundamental mode.

13:30–15:30

SM3N • Gas-Filled Hollow Fibers

Presider: Poul Kristensen; OFS Fitel Denmark I/S, Denmark

SM3N.1 • 13:30 **Invited**

Tunable sources from the visible to vacuum-UV based on gas-filled hollow-core photonic crystal fibers, John C. Travers¹, Ka Fai Mak¹, Alexey Ermolov¹, Francesco Tani¹, Philipp Hoelzer¹, Nicolas Joly^{2,3}, Philip St.J. Russell^{1,2}; ¹Russell Division, Max Planck Inst. for the Science of Light, Germany; ²Dept. of Physics, Univ. of Erlangen-Nuremberg, Germany. High-energy, single-mode, coherent, ultrafast pulses of light - tunable from the vacuum-UV to the visible spectral region - can be generated in gas-filled hollow-core photonic-crystal fibers through a simple experimental scheme.

SM3N.2 • 14:00

Generation of Raman comb over two octaves with picosecond pulse laser in hydrogen-filled Kagome HC-PCF, Aurélien Benoit^{1,2}, Benoit Beaudou³, Meeshal Alharbi¹, Benoit Debord¹, Frederic Gerome^{1,3}, François Salin², Fetah Benabid^{1,3}; ¹GPPMM Group, Xlim Research Inst. UMR CNRS/Univ. of Limoges n°7252, France; ²Eolite Systems, France; ³Glophotronics, France. We report on 33 W picosecond pulse laser pumped Raman comb generation with fifty spectral lines over two frequency octaves from the visible to the near infrared range obtained in hydrogen-filled hypocycloid-core Kagome HC-PCF.

13:30–15:30

SM3O • Symposium on Large-Scale Silicon Photonic Integration I ▶

Presider: Xuezhe Zheng, Oracle Corp., USA

SM3O.1 • 13:30 **Invited** ▶

Ge-on-Si Integrated Photonics, Jifeng Liu¹; ¹Thayer School of Engineering, Dartmouth College, USA. We present the latest progress in epitaxial Ge-on-Si lasers, electroabsorption modulators, and photodetectors for integrated photonics. We also discuss an emerging monolithic 3D photonic integration scheme based on high crystallinity GeSn directly grown on SiO₂.

SM3O.2 • 14:00 **Invited**

Heterogeneous Integration on Silicon, Alexander Fang¹, Brian R. Koch¹, Erik J. Norberg¹, Jonathon Roth¹, Byungchae Kim¹, Anand Ramaswamy¹, John Hutchinson¹, Jae-Hyuk Shin¹, Gregory Fish¹; ¹Aurion, Inc., USA. Aurion's heterogeneous integration process enables high performance active components such as lasers, modulators, and photodetectors to be elegantly integrated on a silicon photonics platform with high performance passive components.

13:30–15:30

SM3P • Bioimaging I ▶

Presider: Audrey Ellerbee; Stanford Univ., USA

SM3P.1 • 13:30 ▶

Three-Dimensional Cell Culture on Microscaffolds with Spatially Resolved Surface Chemistry, Benjamin Richter¹, Thomas Pauloehr², Johannes Kaschke³, Joachim Fischer³, Alexandra M. Greiner¹, Martin Wegener³, Guillaume Delaittre⁴, Christopher Barner-Kowollik⁴, Martin Bastmeyer¹; ¹Cell- and Neurobiology, Karlsruhe Inst. of Technology, Germany; ²Preparative Macromolecular Chemistry, Karlsruhe Inst. of Technology, Germany; ³Inst. of Applied Physics, Karlsruhe Inst. of Technology, Germany; ⁴Inst. for Toxicology and Genetics, Karlsruhe Inst. of Technology, Germany. To spatially control protein-binding and cell-attachment in three dimensions (3D) we employ a two-photon-triggered cycloaddition of functional (e.g. biotinylated) dienophiles on the surface of 3D microscaffolds, which have been silanized with photoactivatable diens (photoenol).

SM3P.2 • 13:45

Microfluidic Flow Cytometer for Multiparameter Screening of Fluorophore Photophysics, Kevin M. Dean¹, Lloyd M. Davis², Jennifer L. Lubbeck³, Premashis Manna³, Amy E. Palmer¹, Ralph Jimenez²; ¹BioFrontiers Inst., Univ. of Colorado at Boulder, USA; ²Dept. of Physics and Center for Laser Applications, Univ. of Tennessee Space Inst., USA; ³JILA, NIST and Univ. of Colorado, USA. We present a microfluidic cytometer that sorts mammalian or yeast cells by laser force deflection following real-time multibeam, multiparameter fluorescence measurements, including photobleaching, lifetime and expression level, of the intrinsic fluorophores within each cell.

SM3P.3 • 14:00 ▶

Hyperspectral Stimulated Raman Microscopy with Fiber-based, Rapidly Wavelength Swept cw-Lasers, Sebastian Karpf¹, Matthias Eibl¹, Thomas Klein¹, Wolfgang Wieser¹, Robert Huber^{2,1}; ¹LMU Munich, Germany; ²BMO Luebeck, Germany. A hyperspectral stimulated Raman microscopy system using rapidly wavelength swept lasers is presented. Imaging of biological samples with shot noise limited detection is demonstrated with the fiber based setup.

CLEO: QELS-Fundamental Science

FM3A • Quantum Detection—
Continued

FM3A.4 • 14:15

A New Picture of Inhomogeneities in Nanowire Superconducting Single Photon Detectors, Rosalinda Gaudio¹, Koen op 't Hoog¹, Zili Zhou¹, Dondu Sahin¹, Andrea Fiore¹; ¹COBRA Research Inst., Netherlands. We introduced, characterized and modeled a simple nanodetector to investigate the efficiency and yield limitations of NbN superconducting single photon detectors. These crucial issues are related to the detectors strongly inhomogeneous nature at the nanoscale.

FM3A.5 • 14:30

Experimental realization of a photon-number-resolving homodyne detector, Duan Huang¹, Erhu Han¹, Weiqi Liu¹, Dakai Lin¹, Chao Wang¹, Peng Huang¹, Guihua Zeng¹; ¹State Key Lab of Advanced Optical Communication Systems and Networks, Dept. of Electronic Engineering Shanghai Jiao Tong Univ., State Key Lab of Advanced Optical Communication Systems and Networks, Shanghai Jiaotong Univ., China. We demonstrate a photon-number-resolving homodyne detector based on InGaAs PIN photodiodes with active phase compensation. Our detector preserves the capability of detecting single photon and allows 20 photons to be precisely discriminated.

FM3A.6 • 14:45

QPSK Receiver outperforming the Standard Quantum Limit for any Signal Power, Christian R. Müller^{1,2}, Gerd Leuchs^{1,2}, Christoph Marquardt^{1,2}; ¹Max Planck Inst. for the Science of Light, Germany; ²Dept. of Physics, Univ. of Erlangen-Nuremberg, Germany. We present a quantum receiver for the discrimination of quadrature phase-shift keyed signals that approaches the Helstrom bound for any signal power. The discrimination is performed via adaptive displacements prior to a single photon detector.

FM3B • Quantum Fluids and
Gases in Solids—Continued

FM3B.2 • 14:30

Quantum Electron-Hole Droplets in GaAs Quantum Wells, Andrew E. Hunter^{1,2}, Hebin Li¹, Steven T. Cundiff^{1,2}, Martin Mootz², Mackillo Kira³, Stephan W. Koch³; ¹JILA, Univ. of Colorado, USA; ²Physics, Univ. of Colorado, Boulder, USA; ³Physics, Philipps-Univ. Marburg, Germany. We present evidence from transient-absorption spectra for quantum electron-hole droplets in GaAs quantum wells. Quantum droplets have a two-particle correlation function characteristic of a liquid, but, unlike macroscopic droplets, have quantized binding energy.

FM3B.3 • 14:45

Build-up dynamics of degenerate exciton luminescence at sub-K temperature in a trap in cuprous oxide, Hirotsuke Suzuki¹, Yusuke Morita¹, Kosuke Yoshioka¹, Makoto Kuwata-Gonokami^{1,2}; ¹Physics, The Univ. of Tokyo, Japan; ²Photon Science Center, The Univ. of Tokyo, Japan. We demonstrate time- and space- resolved luminescence measurements of quantum degenerate paraexcitons in cuprous oxide. We report dynamics of ultracold excitons such as the drift in a trap potential, cooling process, and lifetime of excitons.

FM3C • Optics in Random
Media II—Continued

FM3C.3 • 14:15

Photon transport and localization in optical superlattices, PIN-CHUN HSIEH¹, Chung-Jen Chung², James F. McMillan¹, Ming Lu³, Nicolae Panoiu⁴, Chee Wei Wong¹; ¹Mechanical Engineering, Columbia Univ., USA; ²Center for Micor/Nano Science and Technology, National Cheng Kung Univ., Taiwan; ³Center for Functional Nanomaterials, Brookhaven National Lab, USA; ⁴Dept. of Electronic and Electrical Engineering, Univ. College London, UK. Here we examine the photon transport and collimation in optical superlattices, involving transverse guided resonances and disorder-induced localization. With increasing structural disorder, we observe the crossover from cascaded guided resonances into transverse localization modes.

FM3C.4 • 14:30

Effective temperature of optically-controlled active media, Colin Constant¹, Sergey Sukhov¹, Aristide Dogariu¹; ¹Univ. of Central Florida, CREOL, USA. The interaction between light and matter allows for selective excitation into nonequilibrium states. Using spatially and temporally-varying potentials in active colloidal systems we demonstrate control of diffusion and effective temperatures for particles at thermodynamic equilibrium.

FM3C.5 • 14:45

Active control of the emission of a 2D optofluidic random laser, nicolas bachelard¹, Xavier Noblin¹, Patrick Sebbah¹; ¹Institut Langevin, CNRS, France; ²LPMC, CNRS, France. We present an optofluidic 2D random laser where multiple scattering replaces the optical cavity. Spatial emission, which is isotropic for uniform transverse optical pumping, is forced in any given direction by iteratively shaping the optical pump profile.

FM3D • Nonconventional
Beams and Applications—
Continued

FM3D.4 • 14:15

Non-Paraxial Acceleration and Rotation in Curved Surfaces, Rivka Bekenstein¹, Yonatan Sharabi¹, Jonathan Nemirovsky¹, Ido Kaminer¹, Tal Carmon¹, Mordechai Segev¹; ¹Physics Dept., Technion, Israel. We present non-paraxial shape-preserving accelerating electromagnetic wavepackets propagating in micro-sized curved surfaces, revealing exotic trajectories and polarization rotation dynamics caused by the interplay of interference effects and the curvature of space.

FM3D.5 • 14:30

Dynamics of Microparticles Trapped in a Perfect Vortex Beam, Mingzhou Chen¹, Michael Mazilu¹, Yoshihiko Arita¹, Ewan M. Wright^{2,1}, Kishan Dholakia^{1,2}; ¹Univ. of St Andrews, UK; ²The Univ. of Arizona, USA. We trap and rotate particles using a perfect vortex beam with integer or fractional topological charges. A linear relationship is observed between the rotation speed and orbital angular momentum content of the beam.

FM3D.6 • 14:45

Cherenkov Radiation From Electron Vortex Beams, Ido Kaminer^{1,2}, Maor Mutzafi², Gal Harari², Hanan Herzig Sheinfux², Jonathan Nemirovsky², Mordechai Segev²; ¹Dept. of Physics, MIT, USA; ²Physics Dept. and Solid State Inst., Technion Israel Inst. of Technology, Israel. We find the Cherenkov radiation emitted by vortex electrons, and show that a properly designed photonic waveguide can increase the angular momentum of the electrons. We calculate the selection rules in a relativistic quantum formalism.



Join the conversation. Use #CLEO14.
Follow us @cleoconf on Twitter.

CLEO: Science & Innovations

SM3E • Nano-, Micro-, and Waveguide-sensing—Continued

SM3E.4 • 14:15

A Novel Nanoslotted Quadrabeam Photonic Crystal Cavity Sensor with High Sensitivity and High Q-factor, Daquan Yang^{1,2}, Shota Kita², Cheng Wang², Qimin Quan², Marko Loncar², Huiping Tian¹, Yuefeng Ji¹; ¹State Key Lab of Information Photonics and Optical Communications, Beijing Univ. of Posts and Telecommunications, China; ²School of Engineering and Applied Sciences, Harvard Univ., USA. We experimentally demonstrate a sensor based on a novel nanoslotted quadrabeam photonic-crystal cavity (NQPC). The NQPC possesses both high-sensitivity and high-Q factor. We achieved sensitivity of 451nm/RIU and Q-factor >7000 in water at telecom-wavelength range.

SM3E.5 • 14:30

Nanobeam Photonic Crystal Cavity Based Multifunctional Gas-Phase Chemical Sensor, Yu Chen¹, William S. Fegadolli², Axel Scherer^{2,3}, Mo Li¹; ¹Univ. of Minnesota Twin Cities, USA; ²Physics, California Inst. of Technology, USA; ³Electrical Engineering, California Inst. of Technology, USA. By applying chemical functionalization to a nanobeam photonic crystal cavity, an ultrasensitive gas-phase chemical sensor was demonstrated. Its nonlinear thermo-optical bi-stability is utilized to realize a novel threshold detector for cumulative chemical exposure.

SM3E.6 • 14:45

Polymeric Whispering Gallery Mode Resonators for Biosensing Applications, Sarah Wiegeler¹, Torsten Beck¹, Tobias Grossmann¹, Raphael Schmagel¹, Jan Fischer¹, Martin Mai¹, Tobias Wienhold², Uwe Bog², Christian Friedmann³, Timo Mappes^{2,4}, Heinz Kalt¹; ¹Inst. of Applied Physics, Karlsruhe Inst. of Technology, Germany; ²Inst. of Microstructure Technology, Karlsruhe Inst. of Technology, Germany; ³Inst. of Functional Interfaces, Karlsruhe Inst. of Technology, Germany; ⁴Carl Zeiss AG, Corporate Research and Technology, Germany. We report on polymeric high-Q microresonators and a method for spatially selective functionalization. Furthermore we present coupled resonators exhibiting a higher bulk refractive index sensitivity than single resonators making them promising candidates for high-sensitivity sensing.

SM3F • Advanced Laser Materials—Continued

SM3F.4 • 14:15

Updating of temperature coefficients of refractive index in Nd:GdVO₄ and Nd:YVO₄, Yoichi Sato¹, Takunori Taira¹; ¹Inst. for Molecular Science, Japan. Experimental errors in the interferometric evaluation for temperature coefficient of refractive index (dn/dT) were studied. We updated dn/dT of Nd:vanadates with the reduction of experimental errors from 7.8% to 1.5% compared to our previous report.

SM3F.5 • 14:30

High-Power, Continuous-Wave Cr:Colquiriite Lasers Pumped by Multi-Mode Diodes, Umit Demirbas¹, Ilyes Baali¹, Durmus Alp Emre Acar¹, Alfred Leitenstorfer²; ¹Laser Technology Lab, Antalya International Univ., Turkey; ²Dept. of Physics and Center for Applied Photonics, Univ. of Konstanz, Germany. We report multi-mode diode pumped, continuous-wave Cr:Colquiriite lasers with up to 2.54-W of near infrared (800-850 nm) and 0.9-W of blue (400 nm) output power, with optical-to-optical conversion efficiencies as high as 33%.

SM3F.6 • 14:45

Efficient diode-pumped Tm,Ho:KLuW laser, Xavier Mateos^{1,2}, Fabrizio Di Trapani^{2,3}, Valentin Petrov³, Uwe Griebner³, Magdalena Aguiló¹, Diaz Francesc¹; ¹Universitat Rovira i Virgili, Spain; ²Università di Pavia, Italy; ³Max-Born Inst., Germany. Output powers exceeding 1 W are achieved with a diode-pumped Tm,Ho:KLu(WO₄)₂ laser at 2078 nm at slope efficiency of ~30% with respect to the absorbed power. Continuous tuning is possible over ~180 nm.

SM3G • Micro-Resonators—Continued

SM3G.3 • 14:15

Demonstration of compact high-Q silicon microring resonators suspended in air, Wei C. Jiang¹, Jidong Zhang², Qiang Lin^{1,2}; ¹Inst. of Optics, Univ. of Rochester, USA; ²Electrical and Computer Engineering, Univ. of Rochester, USA. We demonstrate compact silicon microring resonators suspended in air with ultra-high optical quality, achieving an intrinsic quality factor of 9.2×10^5 in the telecom band for the resonator with a radius of 9 μm .

SM3G.4 • 14:30

A Multi-Channel Thermally Reconfigurable SiN Spectral Shaper, Jian Wang¹, Yi Xuan¹, Andrew J. Metcalf¹, Pei-Hsun Wang¹, Xiaoxiao Xue¹, Daniel E. Leaird¹, Andrew M. Weiner¹, Minghao Qi¹; ¹Purdue Univ., USA. We demonstrate a 4-channel SiN spectral shaper capable of 2π -phase tuning and 30dB-amplitude control in each frequency channel. The phase tuning efficiency of $410\text{mW}/2\pi$ is measured using both optical intensity autocorrelation and RF beat notes.

SM3G.5 • 14:45

On-chip Electrical Modulation of Phase Shift between Optical Vortices with Opposite Topological Charge, Huanlu Li¹, Michael Strain^{3,4}, Laura Meriggi¹, Lifeng Chen¹, Jiangbo Zhu¹, Kenan Cicek¹, Xinlun Cai^{1,2}, Jianwei Wang², Marc Sorel¹, Mark Thompson², Siyuan Yu¹; ¹Electrical and Electronics Engineering, Univ. of Bristol, UK; ²Centre for Quantum Photonics, Univ. of Bristol, UK; ³Inst. of Photonics, Univ. of Strathclyde, UK; ⁴School of Engineering, Univ. of Glasgow, UK. On-chip electrical modulation of relative phase between pairs of optical vortices with opposite signs has been demonstrated, enabling useful functions in lab-on-chip, communications and sensing applications.

SM3H • 2D and Other Novel Materials—Continued

SM3H.4 • 14:15

Q factor variation in graphene-loaded silicon ring resonators, Rai Kou^{1,2}, Tai Tsuchizawa^{1,2}, Kaori Warabi³, Tsuyoshi Yamamoto², Hiroki Hibino⁴, Hirochika Nakajima³, Koji Yamada^{1,2}; ¹NTT Nanophotonics Center, Japan; ²NTT Basic Research Labs, Japan; ³Graduate School of Advanced Science and Engineering, Waseda Univ., Japan; ⁴NTT Microsystem Integration Labs, Japan. A drastic Q factor variation from 7900 to 1200 is observed in a silicon ring resonator loaded by micrometer-scale graphene with various lengths. The significant decay of the Q factor agrees with a numerical analysis.

SM3H.5 • 14:30

Probing Electron-Phonon Interactions at the Saddle Point in Graphene, Adam T. Roberts^{1,2}, Rolf Binder¹, Nai H. Kwong¹, Dheeraj Golla¹, Daniel Cormode¹, Brian J. LeRoy¹, Henry O. Everitt², Arvinder Sandhu¹; ¹Univ. of Arizona, USA; ²US Army, USA. High frequency differential transmission spectroscopy of graphene, probing near the M-point, is performed and analyzed theoretically. Electron-phonon coupling is identified as the chief mechanism for renormalization with an effective acoustic deformation potential of approximately 5eV.

SM3H.6 • 14:45

Q-switched Fiber Laser with MoS₂ Saturable Absorber, Robert I. Woodward¹, Edmund J. Kelleher¹, T. H. Runcorn¹, Sergei V. Popov¹, Felice Torrisi², R. C. Howe², Tawfique Hasan²; ¹Femtosecond Optics Group, Imperial College London, UK; ²Cambridge Graphene Centre, Univ. of Cambridge, UK. A MoS₂-based saturable absorber is fabricated using wet chemistry techniques. We use it to passively Q-switch a fiber laser at 1068 nm.



CLEO: Science & Innovations

SM3I • Few-Cycle-
Pulse Nonlinear Optical
Technologies—Continued

SM3I.3 • 14:15

Generation and optical parametric amplification of near-IR, few-cycle light pulses, Alexander Kessel¹, Christoph Skrobo^{1,2}, Sandro Klingebiel¹, Christoph Wandt¹, Izhar Ahmad¹, Sergei A. Trushin¹, Zsuzsanna Major^{1,2}, Ferenc Krausz^{1,2}, Stefan Karsch^{1,2}; ¹Max-Planck-Institut für Quantenoptik, Germany; ²Physics, Ludwig-Maximilians-Universität München, Germany. We present different schemes for the generation of few-cycle multi-mJ light pulses in the range of 700-1400 nm together with the amplification of these pulses to several mJ in two ps-pumped optical parametric amplification stages.

SM3I.4 • 14:30

Generation of 17- μ J mid-infrared ultrafast laser pulses by SiC crystal based noncollinear optical parametric amplifier, Haitao Fan¹, Chunhua Xu¹, Zhaohua Wang¹, Gang Wang¹, Xiaolong Chen¹, Zhiyi Wei¹; ¹Inst. of Physics, CAS, China. A femtosecond OPA system for mid-infrared ultrafast laser is established. Pulse energy of 17- μ J is obtained from SiC crystal at central wavelength of 3.75- μ m, which proves SiC an ideal nonlinear crystal for mid-infrared pulse generation.

SM3I.5 • 14:45

Tunable and Near-Fourier-limited Few-Cycle Mid-IR Pulses via an Adiabatically Chirped Difference Frequency Grating, Peter Kroger¹, Haim Suchowski², Gregory J. Stein¹, Franz Kärtner³, Jeffrey Moses¹; ¹Dept. of Electrical Engineering and Computer Science and Research Lab of Electronics, MIT, USA; ²NSF Nanoscale Science and Engineering Center, Univ. of California, USA; ³Center for Free-Electron Laser Science, DESY and Physics Dept. Univ. of Hamburg, Germany. A μ J-level source of few-cycle, mid-IR pulses tunable over 2-4 microns is demonstrated based on adiabatic difference frequency generation. This opens up the possibility for single-cycle mid-IR pulses controllable by a near-IR phase shaper.

SM3J • Spatial Multiplexing—
Continued

SM3J.4 • 14:15

Method for Bi-directional Conversion between Fundamental Gaussian Beams and Spatially Polarized Beams using a Spatial Light Modulator, Zhe Zhao¹, Yongxiong Ren¹, Hao Huang¹, Guodong Xie¹, Yan Yan¹, Nisar Ahmed¹, Changjing Bao¹, Long Li¹, Yinwen Cao¹, Alan Willner¹; ¹Dept. of Electrical Engineering, Univ. of Southern California, USA. We describe a method for bi-directional conversion between fundamental Gaussian beams and spatially polarized beams using a spatial light modulator with angular sliced phase pattern.

SM3J.5 • 14:30

Power-Controllable Multicasting of a Single Gaussian Mode to Multiple Orbital Angular Momentum (OAM) Modes, Shuhui Li¹, Jun Liu¹, Chao Li², Chengcheng Gui¹, Long Zhu¹, Qi Yang², Jian Wang¹; ¹Wuhan National Lab for Optoelectronics, China; ²State Key Lab of Optical Comm. Technologies and Networks, China. We experimentally demonstrate power-controllable multicasting of OFDM 64-QAM signal from single Gaussian mode to multiple OAM modes using a single phase-only spatial light modulator assisted by a feedback control. The precision of power control is less than 1 dB.

SM3J.6 • 14:45

Experimental Demonstration of Orbital-Angular-Momentum Demultiplexing using an Optical FFT in the Spatial Domain, Hao Huang¹, Guodong Xie¹, Nisar Ahmed¹, Yongxiong Ren¹, Yan Yan¹, Martin P. Lavery², Miles Padgett², Samuel Dolinar³, Alan Willner¹; ¹Univ. of Southern California, USA; ²Glasgow Univ, UK; ³Jet Propulsion Lab, USA. We demonstrate orbital angular momentum modes separation using a geometrical transform-based mode sorter combined with a spatial Fast Fourier Transform. The observed crosstalk between the adjacent modes is <-11.8 dB. A lower crosstalk of <-18.6 dB is anticipated by simulation results.

CLEO: QELS-
Fundamental ScienceFM3K • Plasmonic Biochemical
Sensors and Systems—
Continued

FM3K.3 • 14:15

On-chip Plasmonic Interferometer Array for Portable Multiplexed Biosensing System, Xie Zeng¹, Yongkang Gao², Dengxin Ji¹, Nan Zhang¹, Haomin Song¹, Qiaoqiang Gan¹, Filbert Bartoli²; ¹Dept. of Electrical Engineering, The State Univ. of New York at Buffalo, USA; ²Electrical and Computer Engineering Dept., Lehigh Univ., USA. We report a multiplexed intensity-modulated sensing platform using a plasmonic interferometer array with the resolution of 1.6×10^5 RIU. This sensing mechanism is then integrated with a smartphone imaging system to demonstrate a portable biosensing device.

FM3K.4 • 14:30

Colorimetric Sensors using Plasmonics Grating on a Metallic Mirror, Mohammadreza Khorasaninejad¹, Mohsen Raeis-Zadeh Mohsen Raeis-Zadeh², Navid Abedzadeh^{1,2}, Hadi Amarloo², Safieddin Safavi-Naeini², Simarjeet S. Saini²; ¹School of Engineering and Applied Sciences, Harvard Univ., USA; ²Electrical and Computer Engineering, Univ. of Waterloo, Canada. We experimentally demonstrate a low-cost colorimetric sensor in which the change in surrounding refractive index is measured using simple image processing. This sensor consists of two-dimensional gold nanopatch grating on a highly reflective mirror.

FM3K.5 • 14:45

Ultra-Sensitive Refractive Index Sensor Utilizing Plasmonic Resonance Splitting, Yuval Yifat¹, Michal Eitan¹, Zeev Iluz¹, Jacob Scheuer¹; ¹Dept. of Physical Electronics, Tel-Aviv Univ., Israel. We demonstrate experimentally an ultra-sensitive RI sensor based on plasmonic slot nano-antenna arrays utilizing a novel resonance splitting phenomenon observed at small incidence angles. Sensitivities exceeding 1000nm/RIU and high FOM exceeding 50 are demonstrated.

CLEO: Applications
& TechnologyAM3L • Symposium on Enabling
Photonics Technologies for
Miniaturization I—Continued

AM3L.3 • 14:30  
Recent advances in ultrafast laser nanostructuring: S-waveplate and eternal data storage, Peter G. Kazansky¹, Jingyu Zhang¹, Mindaugas Gecevičius¹, Martynas Beresna¹; ¹Univ. of Southampton, UK. Ultrashort light pulses create self-assembled sub-wavelength structures in the bulk of silica glass. Recent progress in applications of this phenomenon ranging from polarization and vortex converters to 5D optical data storage is reviewed.




For Conference News & Insights
Visit blog.cleoconference.org

CLEO: Science & Innovations

SM3M • Nanophotonic
Structures for Quantum
Optics—ContinuedSM3M.3 • 14:15 

Coupling of quantum dots with a photon cage, Rémy Artinian¹, Aziz Benamrouche¹, Cherif Belacel^{1,2}, Alice Berthelot², Pedro Rojo-Romeo¹, Romain Peretti¹, Bastian Gonzalez-Alcevedo¹, Guillaume Beaudin³, Vincent Aimez², Jean Louis Leclercq¹, Xavier Letartre¹, Segolene Callard¹; ¹INL Lyon, France; ²ILM Lyon, France; ³3IT, Canada. We report on the investigation of the coupling between the high-Q mode of a tri-dimensional hollow silicon-based micro-resonator and PbS quantum dots in the near-infrared range, using near-field scanning optical microscopy and far-field spectroscopy.

SM3M.4 • 14:30 

Cavity Quantum Electrodynamics in Quantum Dot-Photonic Crystal Nanocavity Coupled System with Large g/k, Satoshi Iwamoto¹, Yasutomo Ota¹, Hiroyuki Takagi¹, Daisaku Takamiya¹, Yasuhiko Arakawa¹; ¹Inst. of Industrial Science and Inst. for Nano Quantum Information Electronics, Univ. of Tokyo, Japan. We report experimental progresses in cavity quantum electrodynamics using H1 and H0-type photonic crystal nanoacivities embedding single quantum dots. Strong coupling and enhanced optical Stark effect in these systems with large g/k will be discussed.

SM3N • Gas-Filled Hollow
Fibers—Continued

SM3N.3 • 14:15

CW Hollow Core Optically Pumped Fiber Gas Laser, Vasudevan A. Nampoothiri¹, Wolfgang Rudolph¹, Benoît Debord², M. M. Alharbi², Frédéric Gérôme², Fetah Benabid²; ¹Physics and Astronomy, Univ. of New Mexico, USA; ²Xlim Research Inst., Université de Limoges, France. CW lasing in the 1280-1340 nm region is demonstrated from molecular iodine gas contained in a hollow-core kagome structured photonic crystal fiber when optically pumped at 532 nm.

SM3N.4 • 14:30

Highly efficient wavelength conversion in CF4-filled hollow-core photonic bandgap fibers, Lior Ben Yehud^{1,2}, Amiel Ishaaya¹; ¹Electrical and Computer Engineering, Ben-Gurion Univ. of the Negev, Israel; ²Electro-optics Unit, Ben-Gurion Univ. of the Negev, Israel. We investigate Raman wavelength conversion in CF4-filled hollow-core photonic bandgap fibers. We obtain a record of more than 35% conversion efficiency in a 35cm-long, weakly pressurized, fiber at a peak power of only 2.6kW.

SM3N.5 • 14:45


Dual strong picoseconds laser emissions at 1.8 and 2 μm, Aurélien Benoit^{1,2}, Benoit Beaudou³, Meeshal Alharbi¹, Benoît Debord¹, Frederic Gerome^{1,3}, François Salin², Fetah Benabid^{1,3}; ¹GPPMM group, Xlim Research Inst., CNRS UMR 7252, France; ²Eolite Systems, France; ³Glophotronics, France. We report on generation of two strong ps-laser emissions at 1.8 μm and 2 μm through hydrogen-filled Kagome HC-PCF. Each line exhibits tens of kW of peak power and operates in a single mode fashion.

SM3O • Symposium on
Large-Scale Silicon Photonic
Integration I—ContinuedSM3O.3 • 14:30 

Silicon-Organic Hybrid - A Compact and Energy Efficient CMOS Compatible Active Silicon Photonic Solution, Juerg Leuthold¹; ¹ETH Zurich, Switzerland. Organic materials combined with silicon waveguides offer a path to highly efficient electro-optical devices. Modulators based on this technology have already shown frequency responses up to 100 GHz, switching with as little as 0.6 fJ/bit, and operation up to 160 Gbit/s.

SM3P • Bioimaging I—
ContinuedSM3P.4 • 14:15 

Microwave assisted nanosecond CARS multiplex system, Dominique Pagnoux¹, Farid El Bassri^{1,2}, Christophe Louot¹, Vincent Couderc¹; ¹Xlim Institut, Limoges Univ., CNRS, France; ²CILAS, France. Experimental measurements on microwave assisted Multiplex Coherent Anti-Stokes Raman Spectroscopy (M-CARS) in liquids are presented. Nanosecond electric field applied on samples allows M-CARS signal enhancement and offers potentialities to remove non resonant background.

SM3P.5 • 14:30 

Fluorescence Lifetime Imaging for Biomedicine, Paul M. French¹; ¹Physics, Imperial College London, UK. I will review our development and application of fluorescence lifetime imaging implemented in microscopy, tomography and endoscopy to provide molecular readouts across the scales from super-resolved microscopy through imaging of disease models to clinical applications.

Visit Registration to Purchase

Access your Favorite Talks or One You Missed!
On-Demand, 24/7

Over 300 high-quality, informative talks representing the full breadth of CLEO's outstanding technical program including:

Tutorials • Contributed • Postdeadline
Symposia • Plenary talks • Invited

CLEO: QELS-Fundamental Science

FM3A • Quantum Detection—
Continued

FM3A.7 • 15:00

High-efficiency superconducting nanowire single photon detectors based on amorphous $\text{Mo}_0.75\text{Ge}_0.25$, Varun Verma¹, Adriana Lita¹, Michael R. Vissers¹, Francesco Marsili¹, David P. Pappas¹, Richard P. Mirin¹, Sae Woo Nam¹; ¹NIST, USA. We measure a saturation of the internal quantum efficiency of superconducting nanowire single-photon detectors based on a $\text{Mo}_0.75\text{Ge}_0.25$ alloy with peak system detection efficiency of 30%.

FM3A.8 • 15:15

Scalable single-photon detection on a photonic chip, Faraz Najafi¹, Jacob C. Mower¹, Nicholas C. Harris¹, Francesco Bellei¹, Andrew Dane¹, Catherine Lee¹, Solomon Assefa², Karl K. Berggren¹, Dirk Englund¹; ¹Dept. of Electrical Engineering and Computer Science, MIT, USA; ²IBM TJ Watson Research Center, USA. We developed a scalable method for integrating sub-70-ps-timing-jitter superconducting nanowire single-photon detectors with photonic integrated circuits. We assembled a photonic chip with four integrated detectors and performed the first on-chip $g^{(2)}(t)$ -measurements of an entangled-photon source.

FM3B • Quantum Fluids and
Gases in Solids—Continued

FM3B.4 • 15:00

Mid-infrared absorption imaging of trapped paraexcitons in cuprous oxide, Kosuke Yoshioka¹, Makoto Kuwata-Gonokami^{1,2}; ¹Dept. of Physics, Univ. of Tokyo, Japan; ²Photon Science Center, Univ. of Tokyo, Japan. Absorption imaging of trapped dark excitons in a bulk semiconductor is realized. 1s-2p transition in the mid-infrared is used to detect 1s paraexcitons. This technique is crucial to observe the Bose-Einstein condensate of excitons directly.

FM3B.5 • 15:15

Spin Currents and Polarization Textures in Optically Created Indirect Excitons, Yuliya Y. Kuznetsova¹, Eric V. Calman¹, Jason Leonard¹, Leonid Butov¹, Kenneth Campman², Arthur Gossard²; ¹Dept. of Physics, Univ. of California at San Diego, USA; ²Materials Dept., Univ. of California at Santa Barbara, USA. We report the observation of spin currents and spin polarization textures in optically generated indirect excitons. The textures are observed in linear and circular polarizations and are controlled by magnetic fields.

FM3C • Optics in Random
Media II—Continued

FM3C.6 • 15:00

Optical Anderson localized modes switched electronically, Shayan Mookherjee¹, Junrong Ong¹, Xianshu Luo², Guo-Qiang Lo²; ¹Electrical and Computer Engineering, Univ. of California San Diego, USA; ²Inst. of Microelectronics, A*STAR, Singapore. Electronic on-off switching control over optical Anderson localized modes is demonstrated for the first time, using a lithographically-fabricated CMOS-compatible silicon photonic waveguide infiltrated by about 100 sub-micron-scale p-n junction diodes.

FM3C.7 • 15:15

Coherent Backscattering in Multimode Optical Fibers, Yaron Bromberg¹, Sebastien Popoff¹, Brandon Redding¹, Hui Cao¹; ¹Applied Physics, Yale Univ., USA. We investigate experimentally two counter-propagating beams that travel through multimode fibers with strong mode coupling. The interferences between waves going through time-reversed paths can enhance, and surprisingly sometimes suppress, coherent backscattering to the input mode.

FM3D • Nonconventional
Beams and Applications—
Continued

FM3D.7 • 15:00

Non-Linear Shape Preserving Electron-Beams, Maor Mutzafi¹, Ido Kaminer¹, Gal Harari¹, Mordechai Segev¹; ¹Physics, Technion, Israel. We show that shaping the initial wavefunction of a multi-electron system can lead to electron beams displaying shape-preserving propagation in spite of the inherent repulsion among electrons. This idea suggests applications in microscopy and lithography.

FM3D.8 • 15:15

Nonparaxial Bessel-like beams following curved trajectories, Nikolaos K. Efremidis^{1,2}, Ioannis D. Chremmos^{1,2}; ¹Mathematics and Applied Mathematics, Univ. of Crete, Greece; ²Max Planck Inst. for the Science of Light, Germany. We introduce a new class of nonparaxial optical beams with a Bessel-like profile that are capable to laterally shift along fairly arbitrary trajectories during propagation in free space. Numerical simulations confirm our theoretical predictions.

15:30–16:00 Coffee Break, Concourse Level

NOTES

CLEO: Science & Innovations

SM3M • Nanophotonic Structures for Quantum Optics—Continued

SM3M.5 • 15:00  Experimentally controlling the quantum spectrum generated by a silicon nanophotonic chip, Ranjeet Kumar¹, Junrong Ong¹, Marc Savanier¹, John Recchio¹, Shayan Mookherjee¹; ¹Univ. of California San Diego, USA. To demonstrate control over the quantum spectrum of light, we tune the joint spectral intensity of photon pairs generated at telecommunications wavelengths using a low-power diode-pumped compact CMOS-compatible silicon chip at room temperature.

SM3M.6 • 15:15 1-to-32 H-tree Optical Distribution on Adhesively Bonded Silicon Nanomembrane, Yang Zhang¹, Xiaochuan Xu¹, David Kwong¹, John Covey¹, Amir Hosseini², Ray Chen¹; ¹Electrical and Computer Engineering, The Univ. of Texas at Austin, USA; ²Omega Optics, Inc, USA. We developed an adhesive bonding process to integrate silicon nanomembranes onto silicon chips. A grating-coupled 1-to-32 H-tree optical distribution is experimentally demonstrated with an excess loss of 2.2 dB and a uniformity of 0.72 dB.

SM3N • Gas-Filled Hollow Fibers—Continued


SM3N.6 • 15:00 Generation of three-octave-spanning transient Raman frequency comb in hydrogen-filled hollow-core PCF, Francesco Tani¹, Federico Belli¹, Amir Abdolvand¹, John C. Travers¹, Philip St.J. Russell^{1,2}; ¹Division III, Max-Planck-Inst Physik des Lichts, Germany; ²Dept. of Physics, Univ. of Erlangen-Nuremberg, Germany. A noise-seeded transient Raman frequency comb spanning three octaves from 180 to 2400 nm is generated by pumping a hydrogen-filled hollow-core photonic crystal with 300 fs pulses of energy 26 μJ and wavelength 800 nm.


SM3N.7 • 15:15 Single-mode hollow-core fiber for portable acetylene sub-Doppler frequency reference, Chenchen Wang¹, Shun Wu¹, Brian Mangan², Linli Meng², John M. Fini², Robert S. Windeler², Eric M. Monberg², Anthony Desantolo², Kazunori Mukasa², Jeffrey W. Nicholson², David DiGiovanni², Brian R. Washburn¹, Kristan L. Corwin¹; ¹Kansas State Univ., USA; ²OFS Labs, USA. A newly-developed, single-mode hollow-core fiber is employed for saturated absorption spectroscopy in a molecular gas. Lack of surface modes, ease of angle splicing, and single-modedness make it promising for portable frequency references.

SM3O • Symposium on Large-Scale Silicon Photonic Integration I—Continued

SM3O.4 • 15:00  CMOS Integrated Silicon Photonics - Does it Make Sense?, Wilfried Haensch¹, Douglas M. Gill¹, Jason S. Orcutt¹; ¹IBM, USA. CMOS integrated Silicon Photonics offers a compact solution for a fully functional optical engine. The interdependence of optical and electrical components is discussed and arguments for a co-optimization of these components are given

SM3P • Bioimaging I—Continued

SM3P.6 • 15:00  Optical Thermophoresis for the Manipulation and Detection of Biomolecules, Li-Hsien Yu¹, Yih-Fan Chen^{2,1}; ¹Dept. of Biomedical Engineering, National Cheng Kung Univ., Taiwan; ²Inst. of Biophotonics, National Yang-Ming Univ., Taiwan. We use thermophoresis to accumulate and quantify biomolecules under a laser-induced temperature gradient. As biomolecules accumulate at the heated region, the concentration of the molecules can be determined based on the level of accumulation.

SM3P.7 • 15:15  THG microscopy imaging of blood using sub-50fs Yb fiber laser, Ilyas Saytashev¹, Bai Nie², Marcos Dantus^{1,2}; ¹Dept. of Chemistry, Michigan State Univ., USA; ²Dept. of Physics and Astronomy, Michigan State Univ., USA. We report on multimodal imaging of blood using sub-50 fs pulses centered at 1060 nm wavelength. We find that red blood cells appear dark on SHG images while on THG images of blood provide bright signal and good contrast.

15:30–16:00 Coffee Break, Concourse Level

NOTES

Blank lined area for notes.

CLEO: QELS-Fundamental Science

16:00–18:00

FM4A • Quantum Key Distribution

President: Paul Toliver; Applied Communication Sciences, USA

FM4A.1 • 16:00

Experimental demonstration of the coexistence of continuous-variable quantum key distribution with an intense DWDM classical channel, Rupesh Kumar¹, Hao Qin¹, Romain Alléaume¹; ¹Telecom ParisTech, France. We have experimentally performed continuous variable quantum key distribution over up to 50 km, in coexistence with a dense-wavelength-multiplexed channel of several dBms. This opens new perspectives for QKD integration over existing optical network architectures.

FM4A.2 • 16:15

Continuous-Variable Measurement-Device-Independent Quantum Key Distribution with Imperfect Detectors, Zhengyu Li¹, Xiang Peng¹, Hong Guo¹; ¹Peking Univ., China. We show that the performance of continuous-variable measurement-device-independent quantum key distribution will decline dramatically when considering detector's imperfections. However, it can be improved by using phase sensitive optical amplifiers.

FM4A.3 • 16:30

High-dimensional time-energy entanglement-based quantum key distribution using dispersive optics, Catherine Lee^{1,2}, Zheshe Zhang¹, Jacob C. Mower¹, Greg Steinbrecher¹, Hongchao Zhou¹, Ligong Wang¹, Robert Horansky³, Varun B. Verma³, Michael Allman³, Adriana Lita³, Richard P. Mirin³, Francesco Marsili², Andrew D. Beyer⁴, Matthew Shaw⁴, Sae Woo Nam³, Gregory Wornell¹, Franco Wong¹, Jeffrey H. Shapiro¹, Dirk Englund¹; ¹MIT, USA; ²Dept. of Physics, Columbia Univ., USA; ³National Inst. of Standards and Technology, USA; ⁴NASA Jet Propulsion Lab, USA. We implement a high-dimensional quantum key distribution protocol secure against collective attacks. We transform between conjugate measurement bases using group velocity dispersion. We obtain > 3 secure bits per photon coincidence.

16:00–18:00

FM4B • Dynamics in Strongly Correlated Materials

President: Matthias Hoffmann; SLAC National Accelerator Lab, USA

FM4B.1 • 16:00

Femtosecond Magneto-optics of FePt nanocrystals for Heat Assisted Magnetic Recording, Jean-Yves Bigot¹, Mircea Vomir¹, Jiwan Kim¹, Oleksandr Mosendz², Shikha Jain², Dieter Weller²; ¹Université de Strasbourg, CNRS, France; ²HGST a Western Digital Company, USA. We report about the magnetization dynamics in L1₀ FePt discs, designed for Heat Assisted Magnetic Recording. We also determine the different nonlinear behaviors of the coercive field and saturation magnetization with increasing laser pulse energy.

FM4B.2 • 16:15

Ultrafast Exchange-Coupling Strengthening in FeNi/FePt Film Induced by Femtosecond Laser, Zhifeng Chen¹, Shufa Li², Bingzhi Zhang¹, Feipeng Pi¹; ¹School of Physics and Electronic Engineering, Guangzhou Univ., China; ²State-Key Lab of Optoelectronic Materials and Technologies, Sun Yat-Sen Univ., China. We study laser-induced evolution of exchange coupling in FeNi/L1₀-FePt film using pump-probe polar Kerr spectroscopy. Ultrafast coupling-strengthening with significant reduction of hard coercivity is observed. The mechanism is discussed.

FM4B.3 • 16:30

Terahertz Cherenkov Radiation from Ultrafast Magnetization in Terbium Gallium Garnet, Sergei Gorelov¹, Eugene Mashkovich¹, Maxim Tsarev¹, Michael Bakunov¹; ¹Univ. of Nizhny Novgorod, Russia. Terahertz Cherenkov radiation from a moving pulse of ultrafast magnetization optically induced in terbium gallium garnet is experimentally observed and analyzed for the characterization of the ultrafast inverse Faraday effect.

16:00–18:00

FM4C • Novel Optics I

President: Xiang Zhang; Univ. of California Berkeley, USA

FM4C.1 • 16:00

Gate-controlled Electromagnetically Induced Transparency Analogue in Graphene Metamaterials, Teun-Teun Kim¹; ¹School of Physics and Astronomy, Univ. of Birmingham, UK. We show an electric control of metamaterial-induced transparency through active tuning of the dark mode. By hybridizing gated graphene with diatomic metamaterials, the transparency window switching is obtained at a frequency of 0.85 THz.

FM4C.2 • 16:15

Tunable Pulse-Shaping with Gated Graphene Nanoribbons, Ludmila J. Prokopenko¹, Naresh K. Emani¹, Alexandra Boltasseva^{1,2}, Alexander Kildishev¹; ¹Birk Nanotechnology Center, Purdue Univ., USA; ²Dept. of Photonics Engineering, Technical Univ. of Denmark, Denmark. We propose a pulse-shaper made of gated graphene nanoribbons. Simulations demonstrate tunable control over the shapes of transmitted and reflected pulses using the gating bias. Initial fabrication and characterization of graphene elements is also discussed.

FM4C.3 • 16:30

Lorentz Force Metamaterial with Giant Optical Magnetolectric Response, João A. Valente¹, Jun-Yu Ou¹, Eric Plum¹, Ian J. Youngs², Nikolay I. Zheludev^{1,3}; ¹Optoelectronics Research Centre, Univ. of Southampton, UK; ²Physical Sciences Dept., DSTL, UK; ³Centre for Disruptive Photonic Technologies, Nanyang Technological Univ., Singapore. We demonstrate the first reconfigurable photonic metamaterial controlled by electrical currents and magnetic fields, providing first practically useful solutions for sub-megahertz and high contrast modulation of metamaterial optical properties.

16:00–18:00

FM4D • Accelerating Beams

President: Roberto Morandotti; INRS-Energie Mat & Tele Site Varennes, Canada

FM4D.1 • 16:00 **Tutorial**

Self Accelerating Beams of Photons and Electrons, Ady Arie¹; ¹Tel-Aviv Univ., Israel. The properties of optical, electron and plasmon beams that preserve their shape, while propagating along curved trajectories in free-space or on a surface are discussed. Methods to generate these beams and potential applications are presented.



Ady Arie is a Professor of Electrical Engineering and the Head of the School of Electrical Engineering at Tel-Aviv University, Israel. He is a Fellow of The Optical Society and a topical editor of Optics Letters. His current research is in the areas of nonlinear optics, plasmonics and electron microscopy.



Join the conversation. Use #CLEO14.
Follow us @cleoconf on Twitter.

CLEO: Science & Innovations

16:00–18:00

SM4E • Remote and Stand-off Optical Detection

Presider: David Sonnenfroh;
Physical Sciences Inc., USA

SM4E.1 • 16:00

Active Coherent Laser Spectrometer (ACLaS) for Standoff Detection of Chemicals, Neil Macleod¹, Damien Weidmann¹; ¹Space Science and Technology Dept., Rutherford Appleton Lab, UK. An active spectrometer has been developed based on diffuse backscattering by solid targets combined with coherent detection and mid-infrared quantum cascade lasers. High selectivity and sensitivity have been shown at standoff distances of 40 m.

SM4E.2 • 16:15

Stand-Off Spectroscopy and Chemical Sensing using a Femtosecond Optical Parametric Oscillator, Zhaowei Zhang¹, Rhea J. Clewes², Christopher R. Howle², Derryck T. Reid¹; ¹Scottish Universities Physics Alliance (SUPA), Inst. of Photonics and Quantum Sciences, Heriot-Watt Univ., UK; ²Defence Science and Technology Lab, UK. Fourier-transform spectroscopy using a femtosecond optical parametric oscillator is demonstrated. Specifically, this system is used to detect a thiodiglycol droplet from concrete and aluminum surfaces and atmospheric water vapor at a 2-m stand-off distance.

SM4E.3 • 16:30

Remote Spectroscopy at Kilometer-Scale Distances via Random Raman Lasing, Brett H. Hokr¹, Joel N. Bixler¹, Vladislav V. Yakovlev¹, Marlan O. Scully^{1,2}; ¹Texas A&M Univ., USA; ²Princeton Univ., USA. The single-shot remote identification of chemicals at kilometer-scale distances is experimentally demonstrated utilizing random Raman lasing.

16:00–18:00

SM4F • Diode Pumped Mode-locked Oscillators and Amplifiers

Presider: Todd Clatterback;
Raytheon SAS, USA

SM4F.1 • 16:00

Diode-pumped 73-fs Kerr-lens mode-locked Yb:YCa4O(BO3)3 laser, Ziyi Gao¹, Jiangfeng Zhu¹, Wenlong Tian¹, Junli Wang¹, Xiaodong Zeng¹, Zhaohua Wang², Zhiguo Zhang², Zhiyi Wei², Huaijin Zhang³; ¹School of Physics and Optoelectronic Engineering, Xidian Univ., China; ²Beijing National Lab for Condensed Matter Physics, Inst. of Physics, Chinese Academy of Sciences, China; ³State Key Lab of Crystal Material and Inst. for Crystal Material, Shandong Univ., China. Pulses as short as 73-fs were generated from a Kerr-lens mode-locked Yb:YCa4O(BO3)3 laser at 1043 nm. To the best of our knowledge, this is the first demonstration of a Kerr-lens mode-locked Yb:YCa4O(BO3)3 laser.

SM4F.2 • 16:15

A Mode-Locked Ti:Sapphire Laser Pumped Directly with a Green Diode Laser, Shota Sawai¹, Aruto Hosaka¹, Kenichi Hirose¹, Fumihiko Kannari¹; ¹Keio Univ., Japan. We report a mode-locked Ti:Sapphire laser pumped directly with a 1-W InGaN diode laser emitting at 518 nm. Pulse durations as short as 62 fs and average output powers of up to 23.5 mW are obtained.

SM4F.3 • 16:30

$\chi^{(2)}$ -Lens Mode-Locking of a High Average Power Nd:YVO₄ Laser, Veselin Aleksandrov¹, Teodora Grigорова¹, Hristo Iliev², Anton Trifonov¹, Ivan C. Buchvarov¹; ¹Sofia Univ. St. Kliment Ohridski, Bulgaria; ²Binovation Ltd., Bulgaria. We report 20 W, 6 ps, 170 MHz, passive mode-locking of a Nd:YVO₄ laser using $\chi^{(2)}$ -lens formation in a LBO frequency doubling crystal. The laser is pumped at 808 nm with optical efficiency of 38%.

16:00–18:00

SM4G • Integrated Photonic Devices and Circuits

Presider: Dominic Siriani, MIT
Lincoln Lab, USA

SM4G.1 • 16:00

Cascaded Performance of a Monolithic MZI-SOA Hybrid Switch, Qixiang Cheng¹, Adrian Wonfor¹, Jinlong Wei¹, Richard V. Pentyl¹, Ian H. White¹; ¹Engineering Dept., Univ. of Cambridge, UK. We demonstrate for the first time the feasibility of a 32×32 MZI-SOA hybrid switch by means of a recirculating loop. A power penalty of less than 2.9dB at a data rate of 10Gb/s is obtained.

SM4G.2 • 16:15

50-dB Extinction-Ratio in 2×2 Silicon Optical Switch with Variable Splitter, Keijiro Suzuki¹, Guangwei Cong¹, Ken Tanizawa¹, Sang-Hun Kim¹, Shu Namiki¹, Hitoshi Kawashima¹; ¹AIST, Japan. We demonstrate that record-high extinction-ratio of 50 dB is achievable in a 2×2 Si optical switch by making use of a variable splitter. The proposed switch will enable such high extinction-ratio even in volume production.

SM4G.3 • 16:30

Faraday Polarisation Rotation in Semiconductor Waveguides Incorporating Periodic Garnet Claddings, Cui Zhang¹, Barry Holmes¹, David C. Hutchings¹, Prabesh Dulal², Andrew D. Block², Sang-Yeob Sung², Bethanie Stadler²; ¹School of Engineering, Univ. of Glasgow, UK; ²Univ. of Minnesota, USA. Nonreciprocal polarisation mode conversion is demonstrated in semiconductor waveguides with an alternating periodic upper cladding incorporating a segmented magneto-optic iron garnet fabricated with a novel lift-off process and crystallised by rapid thermal annealing

16:00–18:00

SM4H • Light Emitting Materials and Devices

Presider: Uriel Levy; Hebrew Univ.
of Jerusalem, Israel

SM4H.1 • 16:00 **Tutorial**

Light Emission from Silicon Photonic Crystals, Thomas F. Krauss¹; ¹Univ. of York, UK. We review some of the most promising methods for generating light in the silicon photonics context; nonlinear effects, defects, dopants and germanium alloying have all shown promise and can be enhanced using photonic crystals.



Thomas Krauss is Professor of Photonics at the University of York. His work on fundamental and applied concepts in photonic crystals has been pivotal for transforming photonic crystals from a scientific curiosity to the essential building block in photonics that they are today.

Technical Digest and Postdeadline Papers Available Online

- Visit www.cleoconference.org
- Select **Download Digest Paper** button
- Use your email address and CLEO Registration ID # to synchronize

Once you have synchronized your conference registration with Optics InfoBase, you can log in directly to Optics InfoBase at any point using the same email address and OSA password.

Access must be established via synchronization within 60 days of the conference start date. Access is provided only to full technical attendees.

Meeting Room
211 B/D

CLEO: Science & Innovations

16:00–18:00

SM4I • Advanced QPM Devices

Presider: Antoine Godard;
ONERA - the French Aerospace
Lab, France

SM4I.1 • 16:00

Complex-Transfer-Function Analysis of Optical-Frequency Converters, Derek Chang^{1,2}, Carsten Langrock¹, Corey Bennett², Martin M. Fejer¹; ¹Stanford Univ., USA; ²Lawrence Livermore National Lab, USA. We measure the complex transfer function (CTF) of aperiodically poled lithium niobate waveguide devices and investigate the sources of CTF distortions, which are related to variations in the spatial distribution of the nonlinear coefficient and phase-mismatch profile.

SM4I.2 • 16:15

Polarization-entangled photons from domain-engineered, periodically poled LiNbO₃, Paulina S. Kuo¹, Jason Pelc², Oliver Slattery¹, Lijun Ma¹, Xiao Tang¹; ¹Information Technology Lab, NIST, USA; ²Hewlett-Packard Labs, USA. Using a domain-engineered, periodically poled LiNbO₃ grating, we investigate polarization-entangled photon-pair generation near 1550 nm wavelength using type-II spontaneous parametric down-conversion.

SM4I.3 • 16:30

Single-photon-compatible spectral broadening and shaping via nonlinear mixing and phase modulation, Imad Agha^{1,2}, Serkan Ates^{2,3}, Luca Sapienza^{2,3}, Kartik Srinivasan²; ¹Physics and Electro-Optics Graduate Program, Univ. of Dayton, USA; ²Center for Nanoscale Science and Technology, National Inst. of Standards and Technology, USA; ³Maryland Nanocenter, Univ. of Maryland, USA. We experimentally demonstrate spectral broadening and shaping of weak mono-exponentially decaying pulses via nonlinear mixing and phase modulation. This method is compatible with single photons wavepackets generated by quantum emitters.

Meeting Room
212 A/C

16:00–18:00

SM4J • Free Space Laser Communications

Presider: Michael Dennis; JHU
Applied Physics Lab, USA

SM4J.1 • 16:00 **Invited**

Overview and On-orbit Performance of the Lunar Laser Communication Demonstration Uplink, Mark L. Stevens¹, David O. Caplan¹, Robert T. Schuelein¹, John J. Carney¹, Robert E. Lafon^{2,1}, Bryan S. Robinson¹, Don M. Boroson¹, Laura E. Elgin¹, Steven Constantine¹, Joseph A. Greco¹; ¹Massachusetts Inst of Tech Lincoln Lab, USA; ²NASA, Goddard Space Flight Center, USA. We present an implementation overview and demonstrated error-free coded performance over the 400,000-km link between an Earth-based laser communication terminal and the LADEE satellite orbiting the moon at 9.72-Mbps and 19.44-Mbps uplink rates.

SM4J.2 • 16:30

A Receiver for the Lunar Laser Communication Demonstration Using the Optical Communications Telescope Lab, Matthew Shaw¹, Kevin Birnbaum¹, Michael Cheng¹, Meera Srinivasan¹, Kevin Quirk¹, Joseph Kovalik¹, Abhijit Biswas¹, Andrew D. Beyer¹, Francesco Marsili¹, Varun Verma², Richard P. Mirin², Sae Woo Nam², Jeffrey A. Stern¹, William H. Farr¹; ¹Jet Propulsion Lab, USA; ²National Inst. of Standards and Technology, USA. We discuss the implementation of a receiver for the Lunar Laser Communication Demonstration based on a 12-pixel array of WSi SNSPDs. The receiver was used to close a communication link from lunar orbit at 39 and 79 Mbps.

Meeting Room
212 B/D

CLEO: QELS-
Fundamental Science

16:00–18:00

FM4K • Localized Plasmon Enhanced Sensing: SERS, SEIRA

Presider: Jiri Homola; Inst. of
Photonics and Electronics, Czech
Republic

FM4K.1 • 16:00 **Invited**

Plasmonics: Quantum on the Angstrom Scale, as Observed by Surface-enhanced Raman Scattering, Wenqi Zhu¹, Kenneth B. Crozier¹; ¹School of Engineering and Applied Sciences, Harvard Univ., USA. We fabricate plasmonic dimers consisting of two metallic nanostructures spaced by a few angstroms using lithographic methods, and show that quantum mechanical tunneling across the gaps limits the enhancement in surface-enhanced Raman scattering.

FM4K.2 • 16:30

Ultra-sensitive time-resolved infrared spectroscopy of biomolecule interactions with plasmonic nanoantennas, Ronen Adato¹, Haticé Altug^{2,1}; ¹Boston Univ., USA; ²Ecole Polytechnique Federale de Lausanne (EPFL), Switzerland. We demonstrate a plasmonically enhanced infrared spectroscopy technology that enables in-situ and real-time measurements of protein and nano particle interactions at ultra-high sensitivity by overcoming fundamental water absorption limitations.

Marriott
Salon I & II

CLEO: Applications
& Technology

16:00–18:00

AM4L • Symposium on Enabling Photonics Technologies for Miniaturization II

Presider: Yves Bellouard;
Eindhoven Univ. of Technology,
Netherlands

AM4L.1 • 16:00 **Invited**

Fabrication of subwavelength optics using glass imprint process, Junji Nishii¹; ¹Hokkaido Univ., Japan. Glass imprint process was developed for the fabrication of micro- and nano-structures on the surface of glasses. Application of DC voltage to the mold was effective to suppress the imprint temperature and pressure.

AM4L.2 • 16:30 **Invited**

Micro-Optics Technology Supply Chain as Key-enabler for Applied Research and Industrial Innovation, Hugo Thienpont¹, Jürgen Van Erps¹; ¹Brussels Photonics Team, Vrije Universiteit Brussel, Belgium. We present our polymer micro-optics technology supply chain and its key constituents. We show how it is a key-enabler for frontier applied research and demonstrate how it paves the way towards efficient technology take-up and effective industrial innovation.

CLEO: Science & Innovations

16:00–18:00

SM4M • Photonic Crystals ▶

Presider: Paul Barclay, Univ. of Calgary, Canada

SM4M.1 • 16:00 ▶

Buried-Heterostructure L3 Nanocavity All-Optical Memory with 2.3-nW Power Consumption, Eiichi Kuramochi^{1,2}, Kengo Nozaki^{1,2}, Akihiko Shinya^{1,2}, Hideaki Taniyama^{1,2}, Koji Takeda^{1,3}, Tomonari Sato^{1,3}, Shinji Matsuo^{1,3}, Masaya Notomi^{1,2}; ¹NTT Nanophotonics Center, NTT Corporation, Japan; ²NTT Basic Research Labs, NTT Corporation, Japan; ³NTT Photonics Labs, NTT Corporation, Japan. A tuned L3 design with an enhanced Q factor and a small mode volume enabled 2.3-nW bias power for a buried-heterostructure InGaAsP/InP nanocavity optical memory that was 1/10 of the previous record (30 nW).

SM4M.2 • 16:15 ▶

L3 Photonic Crystal Nanocavities with Measured Q-factor Exceeding One Million, Yiming Lai¹, Stefano Pirota², Giulia Urbinati², Dario Gerace², Matteo Galli², Momchil Minkov³, Vincenzo Savona³, Antonio Badolati¹; ¹Physics and Astronomy, Univ. of Rochester, USA; ²Physics, Università di Pavia, Italy; ³Lab of Theoretical Physics of Nanosystems, Ecole Polytechnique Federale de Lausanne EPFL, Switzerland. We experimentally demonstrate ultra-high quality factors ($Q = 1.45 \times 10^6$) in evolutionary optimized 2D L3 photonic crystal nanocavities fabricated in Si slabs. Together with ultra-small effective mode volumes $\sim 0.96(N/n)^3$, such a nanocavity offers a new platform in future integrated nanophotonics.

SM4M.3 • 16:30 **Invited** ▶

High-Q Optical Nanocavities in Bulk Single-crystal Diamond, Michael Burek¹, Yiwen Chu², Madelaine Liddy³, Parth Patel³, Jake Rochman³, Mikhail Lukin², Marko Loncar¹; ¹School of Engineering and Applied Sciences, Harvard Univ., USA; ²Dept. of Physics, Harvard Univ., USA; ³Univ. of Waterloo, Canada. Optical nanocavities (racetrack resonators and photonic crystal cavities) are fabricated in bulk single-crystal diamond via angled-etching. Devices operating in the telecom band exhibited Q-factors exceeding 10^5 , while devices in the visible yielded Q-factors approaching 10^4 .

16:00–18:00

SM4N • Nonlinear Optical Effects in Fibers

Presider: Axel Schulzgen; Univ. of Central Florida, USA

SM4N.1 • 16:00

Visible Light Stimulated Brillouin Scattering in Small-Core Photonic Crystal Fibers, Robert I. Woodward¹, Edmund J. Kelleher¹, Sergei V. Popov¹, James R. Taylor¹; ¹Femtosecond Optics Group, Imperial College London, UK. A reduced stimulated Brillouin scattering threshold power in small-core PCFs is achieved using visible wavelength excitation. We explain this in the context of acousto-optic interactions at length-scales relative to the fiber geometry.

SM4N.2 • 16:15

Operation of regenerative sources based on alternating SPM and SSFS, Thibault North¹, Alaa Al-kadry¹, Martin Rochette¹; ¹Electrical and Computer Engineering, McGill Univ., Canada. We report on the operation of regenerative sources based on self-phase modulation (SPM) and soliton self-frequency shift (SSFS). Such stochastic sources generate a wide continuum spreading over 450 nm.

SM4N.3 • 16:30

Thulium Assisted Parametric Conversion from Near to Short Wave Infrared, Adrien Billat¹, Steevy Cordette¹, Yu-Pei Tseng¹, Camille-Sophie Brès¹; ¹Photonic Systems Lab, EPFL, Switzerland. We report an all-fiber continuous wave source, tunable between 1935–1980nm, based on parametric conversion combined with thulium amplification. More than 150mW of power and 30dB optical signal-to-noise ratio is obtained over the entire range.

16:00–18:00

SM4O • Symposium on Large-Scale Silicon Photonic Integration II ▶

Presider: Christian Malouin; Juniper Networks Inc., USA

SM4O.1 • 16:00 **Invited** ▶

Highly Integrated Silicon Photonic Integrated Circuits for Telecommunications, Christopher R. Doerr¹; ¹Acacia Communications, Inc., USA. We discuss silicon photonic integrated circuits for telecommunications that integrate many elements. We include transmitters, receivers, transceivers, and add-drop filters. Advanced modulation formats and coherent systems are especially investigated.

16:00–18:00

SM4P • Bioimaging II: Thermal, Spectral and Nanoparticles ▶

Presider: Chulmin Joo; Yonsei Univ., Korea

SM4P.1 • 16:00 ▶

Subdiffraction-Limited Quantum Imaging of a Living Cell, Michael Taylor¹, Jiri Janousek², Vincent Daria², Joachim Knittel¹, Boris Hage², Hans Bachor², Warwick P. Bowen¹; ¹Univ. of Queensland, Australia; ²Australian National Univ., Australia. Spatial variations in the thermal motion of a nanoparticle are mapped with quantum enhanced precision over an extended region of a cell. This enables both subdiffraction-limited quantum metrology and quantum enhanced spatial resolution in biology.

SM4P.2 • 16:15 ▶

3-D Imaging of Malaria-infected Human Red Blood Cells Using Optical Diffraction Tomography, Kyoohyun Kim¹, HyeOk Yoon^{1,2}, YongKeun Park¹; ¹Dept. of Physics, KAIST, Korea; ²Dept. of Applied Physics, Stanford Univ., USA. We measure 3-D refractive index distributions of malaria-infected red blood cells (RBCs) using optical diffraction tomography. Optical diffraction tomography reveals high resolution details of morphological changes in RBCs during the intraerythrocytic cycles of malaria parasites.

SM4P.3 • 16:30 ▶

in vivo Photothermal Optical Coherence Tomography of Targeted Mouse Brain Tumors using Gold Nanostars, Jung Heo¹, Eunji Jang², Seungjoo Haam², Seung Jae Oh³, Yong-Min Huh³, Jin-Suck Suh³, Eunheon Chung⁴, Chulmin Joo¹; ¹Mechanical Engineering, Yonsei Univ., Korea; ²Chemical and Biomolecular Engineering, Yonsei Univ., Korea; ³YUHS-KRIBB Medical Convergence Research Inst., Korea; ⁴Medical System Engineering & Mechatronics, GIST, Korea. We present structural and molecular-contrast imaging of mouse brain tumors using photothermal optical coherence tomography (PT-OCT) in vivo. Based on strong PT response of gold nanostars, we demonstrate clear visualization of brain cancer margins.

SM4O.2 • 16:30 **Invited** ▶

Silicon photonics transmitters and receivers for 4x25 Gb/s interconnects, Mehdi Asghari¹, Dazeng Feng¹, Jonathan Luff¹, Shashank Jatar¹, Roshanak Shafiiha¹, Pegah Seddighian¹, Saeed Fatholouloumi¹, Bhavin Bijlani¹, Daniel C. Lee¹, Zhi Li¹, Joe Zhou¹, Jacob Levy¹, Wei Qian¹, Hong Liang¹, Yann Malinge¹, Chris Keller¹; ¹Mellanox, USA. In this talk, we will review the latest progress of the highly integrated Silicon photonics devices for 4x25 Gb/s active optical cables and transceivers. This includes hybrid lasers, WDM multiplexers, electro-absorption modulators, and germanium detectors.

CLEO: QELS-Fundamental Science

FM4A • Quantum Key
Distribution—Continued

FM4A.4 • 16:45

Squeezed-State Measurement-Device-Independent Quantum Key Distribution, Yi-Chen Zhang¹, Song Yu¹, Wanyi Gu¹; ¹Beijing Univ. of Posts and Telecommunications, China. We report a squeezed-state measurement-device-independent quantum key distribution protocol, which could greatly increase the maximum transmission distance and enhance the robustness to channel noise than the coherent-state based protocol.

FM4A.5 • 17:00

Nonlocal Interferometry Using Macroscopic States and State Discrimination, Brian T. Kirby¹, James D. Franson¹; ¹Univ. of Maryland Baltimore County, USA. A nonlocal interferometer that can violate Bell's inequality using macroscopic phase-entangled coherent states is described. An operating range of 400 km in optical fiber can be achieved using state discrimination techniques.

FM4A.6 • 17:15

Direct Counterfactual Communication with Single Photons, Yuan Cao^{1,2}, Yu-Huai Li^{1,2}, Zhu Cao³, Juan Yin^{1,2}, Yuao Chen^{1,2}, Xiongfang Ma³, Cheng-Zhi Peng^{1,2}, Jian-Wei Pan^{1,2}; ¹Shanghai Branch, Hefei National Lab for Physical Sciences at Microscale and Dept. of Modern Physics, Univ. of Science and Technology of China, China; ²Synergetic Innovation Center of Quantum Information & Quantum Physics, Univ. of Science and Technology of China, China; ³Center for Quantum Information, Inst. for Interdisciplinary Information Sciences, Tsinghua Univ., China. Using a single photon source, we experimentally demonstrate counterfactual communication and successfully transfer a monochrome bitmap from one location to another by employing a nested version of the quantum Zeno effect.

FM4B • Dynamics in Strongly
Correlated Materials—
Continued

FM4B.4 • 16:45

Probing Giant Magnetoresistance with THz Spectroscopy, Zuanming Jin¹, Alexander Tkach², Frederick Casper², Victor Spetter³, Hubert Grimm³, Mathias Kläui², Mischa Bonn¹, Dmitry Turchinovich^{1,4}; ¹Max Planck Inst. for Polymer Research, Germany; ²Institut für Physik, Johannes Gutenberg-Universität Mainz, Germany; ³Sensitec GmbH, Germany; ⁴DTU Fotonik, Technical Univ. of Denmark, Denmark. We observe a giant magnetoresistance effect in CoFe/Cu-based multistack using THz time-domain spectroscopy. The magnetic field-dependent dc conductivity, electron scattering time, as well as spin-asymmetry parameter of the structure are successfully determined.

FM4B.5 • 17:00

Ultrafast optical manipulation of interfacial magnetoelectric coupling, Yu-Miin Sheu¹, Stuart A. Trugman¹, Li Yan¹, Quanxi Jia¹, Antoinette Taylor¹, Rohit P. Prasadkumar¹; ¹Los Alamos National Lab, USA. We demonstrate a new paradigm for all-optical detection and control of interfacial magnetoelectric coupling on ultrafast timescales, achieved by using time-resolved second harmonic generation (SHG) in a ferroelectric/ferromagnet oxide heterostructure.

FM4B.6 • 17:15

Studying Correlated Electron Systems with a New Tunable (<25 eV) Tabletop XUV Source, Arthur K. Mills¹, Sergey Zhdanovich¹, Elia Rampi¹, Riccardo Comin¹, Giorgio Levy^{1,2}, Andrea Damascelli^{1,2}, David J. Jones¹; ¹Physics and Astronomy, Univ. of British Columbia, Canada; ²Quantum Materials Inst., Univ. of British Columbia, Canada. We characterize a new table-top, tunable XUV source spanning 8 to 25 eV based on a femtosecond enhancement cavity. This source is designed to investigate correlated electron systems with angle and time resolved photoemission spectroscopy.

FM4C • Novel Optics I—
Continued

FM4C.4 • 16:45

Quasi-PT Symmetry in Waveguide Optical Directional Couplers, Marco Ornigotti¹, Alexander Szameit¹, Toni Eichelkraut¹; ¹Institut für Angewandte Physik, Friedrich-Schiller Universität, Germany. A comparison between light dynamics in PT-symmetric and passive optical coupler is presented. We show that, apart from an overall damping factor, the dynamics in the passive coupler fully reproduce the PT-symmetric ones.

FM4C.5 • 17:00

High-temperature plasmonic thermal emitter for thermo-photovoltaics, Jingjing Liu¹, Urcan Guler¹, Wei Li^{1,2}, Alexander Kildishev¹, Alexandra Boltasseva^{1,3}, Vladimir M. Shalaev¹; ¹Purdue Univ., USA; ²Wuhan Univ. of Technology, China; ³Technical Univ. of Denmark, Denmark. We use titanium nitride (TiN) to demonstrate an ultra-thin plasmonic thermal emitter operating at high temperatures (830 K). The spectrally selective emitter exhibits a large emittance at around 2.5 μm and below, and suppresses emission at longer wavelengths.

FM4C.6 • 17:15

Tunable hyperbolic metamaterials using metal-insulator transition in VO₂, Harish Krishnamoorthy^{1,2}, You Zhou³, Shriram Ramanathan³, Evgenii Narimanov⁴, Vinod M. Menon^{1,2}; ¹Physics, CUNY Queens College, USA; ²Physics, Graduate Center of CUNY, USA; ³School of Engineering and Applied Science, Harvard Univ., USA; ⁴Electrical and Computer Engineering, Purdue Univ., USA. We present a tunable hyperbolic metamaterial by exploiting the metal-insulator phase transition in vanadium oxide and demonstrate the transition of its in-plane dielectric constant from positive to negative value by temperature control.

FM4D • Accelerating Beams—
Continued

FM4D.2 • 17:00

Incoherent Nonparaxial Accelerating Beams, Yaakov Lumer¹, Ran Schley¹, Ido Kamirer¹, Elad Greenfield¹, Mordechai Segev¹; ¹Technion Israel Inst. of Technology, Israel. Accelerating beams completely rely on interference: coherent superposition of waves. In spite of that fundamental feature, we demonstrate, experimentally and theoretically, partially-spatially-incoherent nonparaxial accelerating beams.

FM4D.3 • 17:15

Radially Self-Accelerating Beams, Christian Vetter¹, Toni Eichelkraut¹, Marco Ornigotti¹, Alexander Szameit¹; ¹Inst. of Applied Physics, Friedrich-Schiller-Universität, Germany. We report on optical non-paraxial beams that exhibit a self-accelerating behavior in radial direction. Hence, the intensity profile evolves on a spiraling trajectory. The beam parameters have been optimized for high contrast and rotation rate.



CLEO: Science & Innovations

SM4E • Remote and Stand-off Optical Detection—Continued**SM4E.4 • 16:45**

Towards remote magnetic anomaly detection using Radar REMPI, Arthur Dogariu¹, Tat Loon Chng¹, Richard Miles¹; ¹Princeton Univ., USA. We demonstrate remote trace detection of Xe in air using microwave scattering off plasma induced by resonant laser ionization. For the purpose of magnetic detection we propose using isotopic Xe rotationally polarized via double resonant three photon pumping.

SM4E.5 • 17:00

Electrical, parametric down-conversion methodology for high-speed, low-noise, and narrow-bandwidth photodetection, Andreas Hangauer¹, Gerard Wysocki¹; ¹Electrical Engineering Dept., Princeton Univ., USA. We investigate methods to modulate the photodiode responsivity for high-speed photodetection, i.e., parametric down-conversion. Electrical modulation is preferred over optical modulation and gives near optimum efficiency of ~20%. Applications are near- and mid-infrared spectroscopy methods.

SM4E.6 • 17:15

Sensitivity in Synthetic Aperture Ladar Imaging, Jason Dahl¹, Zeb W. Barber¹; ¹The Spectrum Lab, Montana State Univ., USA. Synthetic Aperture Ladar (SAL) imaging experiments show that cross-range compression, including image based phase error correction, can be performed at very low return light levels. This includes images where the precompression shot-noise-limited signal-to-noise ratio is much less than unity.

SM4F • Diode Pumped Mode-locked Oscillators and Amplifiers—Continued**SM4F.4 • 16:45**

Mode-locked Nd³⁺,Y³⁺:SrF₂ laser with 181 fs pulse duration, Long Wei^{1,2}, Wenlong Tian^{1,2}, Jiaying Liu¹, Zheng Zhu¹, Hainian Han¹, Zhiyi Wei¹, Liangbi Su², Jun Xu²; ¹Inst. of Physics, Chinese Academy of Sciences, China; ²Xidian Univ., China; ³Key Lab of Transparent and Opto-functional Inorganic Materials, Shanghai Inst. of Ceramics, CAS, China. We demonstrate a mode-locked Nd³⁺,Y³⁺:SrF₂ laser for the first time. Pumped with 1.5W continuous Ti:sapphire laser, average output power of 280mW was obtained with pulse duration of 181fs at central wavelength of 1057 nm.

SM4F.5 • 17:00

Generation of 61fs pulse from a diode-pumped Yb:LYSO laser with SESAM for mode-locking, Wenlong Tian^{1,2}, Zhaohua Wang¹, Zhiyi Wei¹, Jiangfeng Zhu², Lihe Zheng³, Jun Xu³; ¹Beijing National Lab for Condensed Matter Physics, Inst. of Physics, Chinese Academy of Sciences, China; ²School of Physics and Optoelectronic Engineering, Xidian Univ., China; ³Key Lab of Transparent and Opto-functional Inorganic Materials, Shanghai Inst. of Ceramics, China. We report a diode-pumped Yb:LYSO laser with a SESAM for mode-locking. Pulse with duration as short as 61 fs was obtained at repetition rate of 113 MHz. The average output power was 40 mW.

SM4F.6 • 17:15

Gigahertz diode-pumped Yb:CALGO laser with 60-fs pulses and an average output power of 3.5 W, Alexander Klenner¹, Matthias Golling¹, Ursula Keller¹; ¹Eidgenössische Technische Hochschule Zurich, Switzerland. We present a SESAM modelocked diode-pumped Yb:CaGdAlO₄ laser with a 1.8 GHz repetition-rate, a 3.5 W average output power and a 60-fs pulse duration, which results in a record high peak power of 28.9 kW.

SM4G • Integrated Photonic Devices and Circuits—Continued**SM4G.4 • 16:45**

Reconfigurable Thermo-Optic Polymer Switch Based True-Time-Delay Network Utilizing Imprinting and Inkjet Printing, Zeyu Pan¹, Harish Subbaraman², Xiaohui Lin¹, Qiaochu Li³, Cheng Zhang³, Tao Ling³, L. Jay Guo³, Ray Chen¹; ¹Dept. of Electrical and Computer Engineering, The Univ. of Texas at Austin, USA; ²Omega Optics, Inc, USA; ³Dept. of Electrical Engineering & Computer Science, The Univ. of Michigan, USA. Reconfigurable true-time-delay lines, comprising of 2x2 thermo-optic polymer switches and rib waveguides are fabricated utilizing a combination of roll-to-roll (R2R) compatible UV imprinting and ink-jet printing, which promises high throughput and low cost photonic devices.

SM4G.5 • 17:00

Integrated Al₂O₃:Er³⁺ DFB Laser for Temperature Control Free Operation with Silicon Nitride Ring Filter, Purnawirman Purnawirman¹, Ehsan S. Hosseini¹, Michele Moresco¹, Zhan Su¹, Erman Timurdogan¹, Anna Baldycheva¹, Jie Sun¹, Michael R. Watts¹, Thomas Adam², Gerald Leake², Douglas Coolbaugh²; ¹MIT, USA; ²CNSE, Univ. of Albany, USA. We demonstrate almost synchronized temperature dependent wavelength shift of Al₂O₃:Er³⁺ DFB laser (2.57 GHz/oC) and Si₃N₄ ring filter (2.47 GHz/oC), which makes it possible for on-chip transceiver operation without temperature control.

SM4G.6 • 17:15

Wavelength-Tracking Tunable Photodetector, Stephen Adair Gerke¹, Weijian Yang¹, Connie J. Chang-Hasnain¹; ¹U.C. Berkeley, USA. We report on a 1550 nm tunable high-speed photodetector configured to exhibit self-wavelength-tracking behavior. This enables a low-cost WDM system showing resilience to wavelength drift.

SM4H • Light Emitting Materials and Devices—Continued**SM4H.2 • 17:00**

Spontaneous emission control of InGaN/GaN pyramidal structure by localized surface plasmonic modes, Su-Hyun Gong¹, Je-Hyung Kim¹, Yong-Ho Ko¹, Yong-Hoon Cho¹; ¹KAIST, Korea. To improve poor emissions from quantum wires and dots in GaN pyramidal structure, we introduced silver film on pyramid structure. Due to the pyramidal geometry, we could successfully control the spontaneous emission of these structures.

SM4H.3 • 17:15

Tensile-strained, Heavily N-doped Germanium-On-Insulator for Light Emitting Devices on Silicon, Xuejun Xu¹, Keisuke Nishida¹, Kentarou Sawano¹, Takuya Maruizumi¹, Yasuhiro Shiraki¹; ¹Tokyo City Univ., Japan. Strong direct gap light emission is obtained from germanium-on-insulator (GOI) with tensile strain of 0.16% and ultra-high n-type doping concentration up to 1.0×10²⁰ cm⁻³. Microdisk resonators are also fabricated on GOI and show modulated emission spectra.

Thank you for
attending CLEO: 2014.

Look for your
post-conference survey
via email and let us
know your thoughts on
the program.

CLEO: Science & Innovations

SM4I • Advanced QPM
Devices—Continued

SM4I.4 • 16:45

Double-Prism Domain PPLN as Simultaneously a Laser Q-Switch and an Optical Parametric Down Converter in a Nd:YVO₄ Laser, Yen-Hung Chen¹, Wei-Kun Chang¹, Hung-Ping Chung¹, Jin-feng Huang¹, Shang-Sheng Huang¹, Jui-Wen Chang¹; ¹Dept. of Optics and Photonics, National Central Univ., Taiwan. We report a tunable pulsed optical parametric oscillator using a double-prism domain PPLN as simultaneously an electro-optic Q-switch and a parametric generator in a Nd:YVO₄ laser. >2.3-kW peak-power eye-safe light was obtained with this system.

SM4I.5 • 17:00

Thermal Management in High-Power Continuous-Wave Second Harmonic Generation, Suddapalli Chaitanya Kumar¹, Saeed Ghavami Sabouri², A. Khorsandi², Majid Ebrahim-Zadeh^{1,3}; ¹ICFO -The Inst. of Photonic Sciences, Spain; ²Univ. of Isfahan, Islamic Republic of Iran; ³Institutio Catalana de Recerca i Estudis Avancats (ICREA), Spain. We report a systematic study of thermal effects in high-power single-pass SHG in the presence of absorption, and propose an optimum heating configuration for the crystal to minimize thermal lensing at various fundamental power levels.

SM4I.6 • 17:15

Monolithic Fan-out PPMgSLT device for cascaded 355nm generation, Junji Hirohashi¹, Tetsuo Taniuchi², Satoshi Makio¹, Koichi Imai¹, Masami Hatori¹, Hiroshi Motegi¹, Yasuhiro Tomihari¹, Masayuki Hoshi¹, Yasunori Furukawa¹; ¹Oxide Corporation, Japan; ²FRIS, Tohoku Univ., Japan. Monolithic Fan-out PPMgSLT device is demonstrated to generate third harmonic generation from 1064nm laser. By integrating single and fan-out QPM structures into one device, 100mW of third harmonic was obtained without any critical tunings.

SM4J • Free Space Laser
Communications—Continued

SM4J.3 • 16:45

Simulating Atmospheric Turbulence Using a Spatial Light Modulator based on Fourier Transform, Xu Tong¹; ¹BUPT, China. We present an atmospheric turbulence simulator based on a spatial light modulator, using phase screens generated by Fourier Transform method. The effects of different atmospheric turbulence on laser beam are successfully demonstrated.

SM4J.4 • 17:00

A Multimode Fiber-coupled Photon-counting Optical Receiver for the Lunar Laser Communication Demonstration, Matthew E. Grein¹, Oleg Shatrovov¹, Daniel Murphy¹, Bryan S. Robinson¹, Don M. Boroson¹; ¹Massachusetts Inst of Tech Lincoln Lab, USA. We designed and successfully demonstrated a multimode fiber-coupled photon-counting optical receiver at 1550 nm for the Lunar Laser Communications Demonstration that achieves low coupling loss through atmospheric turbulence without requiring adaptive optics.

SM4J.5 • 17:15

A fiber-coupled photon-counting optical receiver based on NbN superconducting nanowires for the Lunar Laser Communication Demonstration, Matthew E. Grein¹, Matthew Willis¹, Andrew Kerman¹, Eric Dauler¹, Barry Romkey¹, Danna Rosenberg¹, Jung Yoon¹, Richard Molnar¹, Bryan S. Robinson¹, Daniel Murphy¹, Don M. Boroson¹; ¹Massachusetts Inst of Tech Lincoln Lab, USA. We have designed and demonstrated a multimode fiber-coupled optical receiver based on NbN superconducting nanowires for the Lunar Laser Communications Demonstration and achieved error-free operation at 622 Mb/s over the ~400,000 km link.

CLEO: QELS-
Fundamental ScienceFM4K • Localized Plasmon
Enhanced Sensing: SERS,
SEIRA—Continued

FM4K.3 • 16:45

Optimizing the Surface Enhanced Raman Signal for Accurate Identification of DNA Base Pairs, Lindsay Freeman¹, Lin Pang¹, Yeshaiahu Fainman¹; ¹Univ. of California, San Diego, USA. DNA sequencing currently lacks optical based techniques such as Raman spectroscopy. We have identified previous issues that prevented sequencing with Raman measurements and proposed a solution for base pair identification via surface enhanced Raman spectroscopy.

FM4K.4 • 17:00

10¹⁰ Electromagnetic SERS enhancement in a nanosphere-plane junction under radially polarized focused excitation, Jing Long¹, Hui Yi¹, Hongquan Li¹, Xiaolong He¹, Tian Yang¹; ¹UM-SJTU Joint Inst., Shanghai Jiao Tong Univ., China. A monolayer of MGITC molecules in a gold nanosphere-plane junction is excited by focusing a radially polarized laser beam. A record electromagnetic enhancement factor of 10¹⁰ for deterministic SERS experiments has been obtained.

FM4K.5 • 17:15

3D plasmonic nanostructures as building blocks for ultrasensitive Raman spectroscopy, Andrea Toma¹, Manohar Chirumamilla¹, Anisha Gopalakrishnan¹, Gobind Das¹, Remo Proietti Zaccaria¹, Roman Krahn¹, Eliana Rondanina¹, Marco Leoncini¹, Carlo Liberale¹, Francesco De Angelis¹, Enzo Mario Di Fabrizio^{2,3}; ¹Italian Inst. of Technology, Italy; ²PSE and BESE divisions, King Abdullah Univ. of Science and Technology, Saudi Arabia; ³Dipartimento di Medicina Sperimentale e Clinica, Università Magna Graecia di Catanzaro, Italy. The fabrication of complex 3D plasmonic nanostructures opens new scenarios towards the realization of high electric field confinement and enhancement. We exploit the unique properties of these nanostructures for performing Raman spectroscopy in the single/few molecules detection limit.

CLEO: Applications
& TechnologyAM4L • Symposium on Enabling
Photonics Technologies for
Miniaturization II—Continued

AM4L.3 • 17:00




Optically driven microfluidic devices produced by two-photon microfabrication, Shoji Maruo¹; ¹Yokohama National Univ., Japan. Optically driven microfluidic devices such as micropumps have been developed by two-photon microfabrication. We also developed metalized micromachines driven by an ultralow power laser beam by the combination of two-photon microfabrication and electroless plating.

CLEO: Science & Innovations

SM4M • Photonic Crystals—
ContinuedSM4M.4 • 17:00 

Photonic Crystal Cavities in Cubic Silicon Carbide, Marina Radulaski¹, Sonia Buckley¹, Linda Zhang¹, Armand Rundquist¹, Thomas Babinec¹, J. Provine², Kassem AlAssaad³, Gabriel Ferro³, Jelena Vuckovic¹; ¹E. L. Ginzton Lab, Stanford Univ., USA; ²Dept. of Electrical Engineering, Stanford Univ., USA; ³Laboratoire des Multimateriaux et Interfaces, Universite de Lyon, France. We present high quality factor ($Q \sim 1,000$) photonic crystal cavities in cubic silicon carbide (3C-SiC) films grown directly on silicon. We show results in shifted-L3 and nanobeam cavity geometries for applications in nonlinear and quantum photonics.

SM4M.5 • 17:15 

Fabrication and optimization for waveguides in sub-micron scale hyperuniform disordered photonic bandgap materials, Sam Tsitrin¹, Marian Florescu², Milan Milošević³, Geev Nahal¹, Ruth A. Mullen³, Paul Steinvurzel⁴, Sal Torquato⁴, Paul Chaikin⁵, Weining Man¹; ¹San Francisco State Univ., USA; ²Advanced Technology Inst., Univ. of Surrey, UK; ³Etaphase, Inc., USA; ⁴Princeton Univ., USA; ⁵New York Univ., USA. We report experimental and simulation results for low-loss wave-guiding in Si-based hyperuniform disordered photonic bandgap materials at infrared wavelengths. These results pave the way for deploying disordered photonic solids in integrated photonic circuits.

SM4N • Nonlinear Optical
Effects in Fibers—Continued

SM4N.4 • 16:45

Four-Wave Mixing and Bragg Scattering in Resonant Seed Modulation Instability in Optical Fiber, Duc Minh NGUYEN^{1,2}, Yang Di^{3,4}, Cesare Soci², Xuan Quyen Dinh^{1,5}, Ming Tang⁴, Ping Perry Shum^{1,3}; ¹CINTRA CNRS/NTU/THALES, UMI 3288, Nanyang Technological Univ., Singapore; ²Centre for Disruptive Photonic Technologies, Nanyang Technological Univ., Singapore; ³OPTIMUS, Photonics Centre of Excellence, Nanyang Technological Univ., Singapore; ⁴NGIA, Huazhong Univ. of Science and Technology, China; ⁵R&T Centre, Thales Solutions Asia Pte. Ltd., Singapore. We interpret physically the dynamics of resonant seed modulation instability of quasi-continuous picosecond pulses in terms of cascaded four-wave mixing and Bragg scattering. We also report a critical condition to excite the resonant seeding effect.

SM4N.5 • 17:00

Experimental Observation Tunable Second-harmonic Generation in a Chalcogenide-tellurite Hybrid Optical Fiber, Tonglei Cheng¹, Weiqing Gao¹, Hiroyasu Kawashima¹, Dinghuan Deng¹, Meisong Liao¹, Morio Matsumoto², Takashi Misumi², Takenobu Suzuki¹, Yasutake Ohishi¹; ¹ofmlab, Japan; ²Furukawa Denshi Co., Ltd., Japan. When the chalcogenide-tellurite hybrid optical fiber is pumped by an optical parametric oscillator with the pump wavelength from 1700 to 3000 nm, widely tunable second-harmonic generation (SHG) from 850 nm to 1502 nm is obtained.

SM4N.6 • 17:15


Improvement of Optical Signal-to-Noise Ratio of a High-Power Pump by Stimulated Brillouin Scattering in an Optical Fiber, Michel E. Marhic¹, Noran A. Cholan²; ¹Swansea Univ., UK; ²Universiti Putra Malaysia, Malaysia. We propose and demonstrate improvement of optical signal-to-noise ratio of a high-power pump by saturated stimulated Brillouin amplification of a backward seed in a fiber. A 27-dB improvement was obtained for a 1-W pump.

SM4O • Symposium on
Large-Scale Silicon Photonic
Integration II—ContinuedSM4O.3 • 17:00  


A WDM CMOS Photonic Platform for Chip-to-Chip Optical Interconnects, Xuezheng Zheng¹, Ashok V. Krishnamoorthy¹; ¹Oracle Corporation, USA. Optical interconnects play a continually-increasing role in the interconnect hierarchy of high-speed digital systems. We present our vision for photonically-interconnected many-chip modules and progress toward an ultra-dense, low-power silicon photonic technology that supports this vision.

SM4P • Bioimaging II: Thermal,
Spectral and Nanoparticles—
ContinuedSM4P.4 • 16:45 

Ultrahigh-resolution optical coherence tomography using supercontinuum source in 1.9 μm wavelength region, Hiroyuki Kawagoe¹, Norihiko Nishizawa¹; ¹Electrical Engineering and Computer Science, Nagoya Univ., Japan. Ultrahigh-resolution OCT in 1.9 μm wavelength region was demonstrated using fiber laser supercontinuum. The wavelength dependence of imaging was investigated, and the decrement in attenuation coefficient in longer-wavelength was confirmed for tooth sample.

SM4P.5 • 17:00 

Deep tissue imaging using Nd-doped upconverting nanoparticles, Haichun Liu¹, Can T Xu¹, Hugo Söderlund¹, Monirehalsadat Mousavi¹, Stefan Andersson-Engels¹; ¹Physics, Lund Univ., Sweden. Deep tissue excitation of upconverting nanoparticles is limited for biomedical applications by water absorption. By modifying the nanoparticles to shift the excitation wavelength, we demonstrate better depth sensitivity.

SM4P.6 • 17:15 

Detection of Single Nanoparticles Using Photonic Crystal Enhanced Microscopy, Yue Zhuo¹, Huan Hu², Weili Chen², Meng Lu², Limei Tian³, Hojeong Yu², Kenneth D. Long¹, Edmond Chow⁴, William P. King^{5,6}, Srikanth Singamaneni³, Brian T. Cunningham^{1,2}; ¹Bioengineering, Univ. of Illinois at Urbana-Champaign, USA; ²Electrical and Computer Engineering, Univ. of Illinois at Urbana-Champaign, USA; ³Mechanical Engineering and Materials Science, Washington Univ. in St. Louis, USA; ⁴Micro and Nanotechnology Lab, Univ. of Illinois at Urbana-Champaign, USA; ⁵Mechanical Science and Engineering, Univ. of Illinois at Urbana-Champaign, USA; ⁶Materials Science and Engineering, Univ. of Illinois at Urbana-Champaign, USA. We demonstrate a label-free biosensor imaging approach that utilizes a photonic-crystal surface to detect attachment of individual nanoparticles down to $65 \times 30 \times 30 \text{ nm}^3$. Matching nanoparticle plasmon resonant-frequency to the photonic-crystal resonance substantially increases sensitivity of the approach.

CLEO: QELS-Fundamental Science

FM4A • Quantum Key
Distribution—Continued

FM4A.7 • 17:30

Experimental heralded amplification of time-bin qubits, Natalia Bruno¹, Anthony Martin¹, Nicolas Sangouard¹, Hugo Zbinden¹, Nicolas Gisin¹, Rob Thew¹; ¹Group of Applied Physics, Switzerland. We present an experimental realisation of heralded amplification of time-bin qubits for quantum communication, based on a source of separable photons at telecom wavelengths, with Hong-Ou-Mandel visibility > 90% without any filtering and high coupling efficiency.

FM4A.8 • 17:45

Mapping Qubit Protocols to Coherent-State Protocols in Quantum Communication, Juan Miguel Arrazola¹, Norbert Lutkenhaus¹; ¹Physics, Inst. for Quantum Computing, Univ. of Waterloo, Canada. We introduce a general mapping for encoding quantum communication protocols involving pure states of multiple qubits, into another set of protocols that employ coherent states of light, linear optics transformations and measurements with single-photon threshold detectors.

FM4B • Dynamics in Strongly
Correlated Materials—
Continued

FM4B.7 • 17:30

Hotspot Dynamics in Current Carrying WSi Superconducting Nanowires, Francesco Marsili¹, Martin J. Stevens², Alexander Kozorezov³, Varun B. Verma², Colin Lambert², Jeffrey A. Stern¹, Robert Horansky², Shellee D. Dyer², Matthew D. Shaw¹, Richard P. Mirin², Sae Woo Nam²; ¹Instrument Electronics and Sensors, Jet Propulsion Lab, USA; ²National Inst. of Standards and Technology, USA; ³Dept. of Physics, Lancaster Univ., UK. We measured the temporal dynamics of optically excited hotspots in current carrying WSi superconducting nanowires as a function of bias current, temperature and excitation wavelength, observing an unexpected effect: hotspot relaxation depends strongly on bias current.

FM4B.8 • 17:45

Current-Controlled Optical Modulation in Thin VO₂ Wires, Arash Joushaghani¹, Junho Jeong¹, Suzanne Paradis², David Alain², J. Stewart Aitchison¹, Joyce K. Poon¹; ¹Electrical and Computer Engineering, Univ. of Toronto, Canada; ²Defence Research and Development Canada - Valcartier, Canada. We imaged VO₂ wires with IR light and monitored the optical properties at the metal-insulator phase transition. Depending on the geometry of the wires, the phase transition either had an electrical or thermal character.

FM4C • Novel Optics I—
Continued

FM4C.7 • 17:30

Plasmonic Properties and Photoinduced Reflectance of Topological Insulator, Zilong Wang^{1,2}, Jun Yin², Giorgio Adamo¹, Azat Sulaez², Lan Wang², Nikolay I. Zheludev^{1,3}, Cesare Soci^{1,2}; ¹Centre for Disruptive Photonic Technologies, Nanyang Technological Univ., Singapore; ²School of Physical and Mathematical Sciences, Nanyang Technological Univ., Singapore; ³Optoelectronics Research Centre, Univ. of Southampton, UK. We report on linear and nonlinear infrared and plasmonic properties of chalcogenide crystal of the Bi-Sb-Te-Se family that was recently identified as a prospective platform for switchable broadband plasmonic devices.

FM4C.8 • 17:45

Titanium Nitride as a Refractory Plasmonic Material for High Temperature Applications, Urcan Guler¹, Wei Li^{1,2}, Alexandra Boltasseva^{1,3}, Alexander Kildishev¹, Vladimir M. Shalaev¹; ¹School of Electrical & Computer Engineering and Birk Nanotechnology Center, Purdue Univ., USA; ²State Key Lab of Advanced Technology for Materials Synthesis and Processing, Wuhan Univ. of Technology, China; ³Dept. of Photonics Engineering, Technical Univ. of Denmark, Denmark. The use of titanium nitride as a plasmonic material for high temperature applications such as solar/thermophotovoltaics is studied numerically and experimentally. Performance of titanium nitride is compared with widely used materials in each field.

FM4D • Accelerating Beams—
Continued

FM4D.4 • 17:30

Electromagnetic Fields Produced by Self-Accelerating Shape-Preserving Electrons in Free-Space, Ido Kaminer^{1,2}, Jonathan Nemirovsky², Mikael Rechtsman², Rivka Bekenstein², Mordechai Segev²; ¹Dept. of Physics, MIT, USA; ²Physics Dept. and Solid State Inst., Technion, Israel. A recent experiment confirmed the 35 years old prediction of Airy-shaped electron beams that accelerate in the absence of any potential. Yet their most intriguing property remained unclear: will such electrons emit radiation in free-space?

FM4D.5 • 17:45

Dynamical Two-Dimensional Accelerating Beams and Enhancement of Their Peak Intensities, domenico bongiovanni¹, Yi Hu^{1,2}, Raúl Amaury Robles³, Gregorio Mendoza Gonzalez², Erwin Marti-Panameño³, Chen Zhigang^{2,4}, Roberto Morandotti¹; ¹INRS-EMT, INRS, Canada; ²The MOE Key Lab of Weak-Light Nonlinear Photonics, TEDA Applied Physics Inst. and School of Physics, Nankai Univ., China; ³Benemérita Universidad Autónoma de Puebla, Mexico; ⁴Dept. of Physics & Astronomy, San Francisco State Univ., USA. We analytically study the propagation dynamics of two-dimensional accelerating beams in a generalized way and propose an optimized method to enhance their peak intensities. Our theoretical analysis is confirmed by experimental results.

18:30–20:30 Special Symposium in Memory of James P. Gordon, Grand Ballroom 

The James P. Gordon Memorial Speakership

- Fundraising Campaign will honor the legacy of Dr. Gordon's impact in Quantum Optics and Quantum Information.
- Endowment will fund a speakership at CLEO.
- Presentations will be archived and shared online.


Make a donation at the OSA booth or
www.osa.org/Gordon

OSA
Foundation

CLEO: Science & Innovations

SM4M • Photonic Crystals—
Continued

SM4M.6 • 17:30  **Holographic Design of Light in the Volume of Photonic Crystals**, Jonathan Nemirovsky¹, Ido Kaminer¹, Rivka Bekenstein¹, Mordechai Segev¹; ¹Technion, Israel. We develop holographic methods to generate arbitrarily-shaped light intensity distributions inside photonic crystals slabs, through shaping the electromagnetic field launched at the facets of the crystal. The technique can be generalized to any photonic structure.

SM4M.7 • 17:45  **2D-material Based Nano-photonics**, Arka Majumdar^{1,2}, Sanfeng Wu², Sonia Buckley³, Aaron M. Jones², Jason S. Ross⁴, Nirmal J. Ghimire^{5,6}, Jiaqiang Yan^{6,7}, David J. Mundros², Wang Yao⁸, Fariba Hatami⁹, Jelena Vuckovic³, Xiadong Xu^{2,4}; ¹Electrical Engineering, Univ. of Washington, USA; ²Physics, Univ. of Washington, USA; ³E L Ginzton Lab, Stanford Univ., USA; ⁴Dept. of Material Science and Engineering, Univ. of Washington, USA; ⁵Dept. of Physics and Astronomy, Univ. of Tennessee, USA; ⁶Materials Science and Technology Division, Oak Ridge National Lab, USA; ⁷Dept. of Materials Science and Engineering, Univ. of Tennessee, USA; ⁸Dept. of Physics and Center of Theoretical and Computational Physics, Univ. of Hong Kong, China; ⁹Dept. of Physics, Humboldt Univ., Germany. We demonstrate a nanophotonic platform based on 2D materials coupled to photonic crystal cavities. We show strong enhancement (~60 times) of light emission due to the photonic crystal.

SM4N • Nonlinear Optical
Effects in Fibers—Continued


SM4N.7 • 17:30
Relative intensity noise of Raman solitons: which one is more noisy?, Wei Liu¹, Gengji Zhou¹, Jinkang Lim², Hung-Wen Chen², Franz Kärtner^{1,2}, Guoqing Chang^{1,2}; ¹Center for Free-Electron Laser Science, DESY, Germany; ²Research Lab of Electronics, MIT, USA. We experimentally study the relative intensity noise of Raman solitons and find that earlier ejected Raman soliton exhibits lower noise. We also observe the bound soliton pair existing in a large range of excitation power.


SM4N.8 • 17:45
Experimental Demonstration of Soliton Cascade in Higher-Order-Mode Fibers, Kriti Charan¹, Martin Pedersen², Ke Wang³, Lars Grüner-Nielsen⁴, Dan Jakobsen⁴, Chris Xu¹; ¹Cornell Univ., USA; ²NKT Photonics, Denmark; ³Shenzhen Univ., China; ⁴OFS Fitel, Denmark. Concatenation of two different higher-order-mode fibers (HOMFs) was used to extend the soliton wavelength shift beyond the mode-crossing wavelengths of the fibers. A 3.5 nJ, 55 fs soliton was obtained at 1170 nm.


SM4O • Symposium on
Large-Scale Silicon Photonic
Integration II—Continued

SM4O.4 • 17:30  **Very Large Scale Silicon Photonics Integration**, Michael R. Watts¹, Erman Timurdogan¹, Jie Sun¹, Ehsan S. Hosseini¹, Cheryl Sorace-Agaskar¹, Ami Yaacobi¹, Zhan Su¹, Michele Moresco¹, Purnawirman Purnawirman¹, Jonathan Bradley¹, Gerald Leake², Thomas Adam², Douglas Coolbaugh²; ¹Research Lab of Electronics, MIT, USA; ²College of Nanoscale Science and Engineering, SUNY, USA. We present on the demonstration of a number of critical device technologies including record low power modulators, tunable filters, and integrated lasers, along with the world's largest silicon photonic circuit, integrated on a 300mm platform.

SM4P • Bioimaging II: Thermal,
Spectral and Nanoparticles—
Continued

SM4P.7 • 17:30  **Mid-IR Laser Tissue Ablation with Little Collateral Damage Using a Laser Tunable in the Water Absorption Peak**, Danail V. Chuchumishev^{1,2}, Elizabeth Nagel¹, Alexandra Nierlich¹, Stanislav Philipov³, Tsvetin Genadiev³, Torsten Fiebig¹, Ivan C. Buchvarov^{1,2}, Claus-Peter Richter^{1,4}; ¹Department of Otolaryngology, Northwestern Univ., USA; ²Dept. of Physics, Sofia Univ., Bulgaria; ³Dept. of Medicine, Sofia Univ., Bulgaria; ⁴Dept. of Biomedical Engineering, Northwestern Univ., USA. An experimental study of tissue ablation across the water absorption peak is presented. A novel all-solid-state table-top mid-IR laser has been used for observation of wavelength-dependent effects on the ablation of hard and soft tissue.

SM4P.8 • 17:45  **Nanoscale precision subcellular chemical identification using quantitative IR nano-image analysis based on multiple-IR laser illumination**, Eamonn Kennedy¹, Rasoul Al-Majmaie^{1,2}, Dominic Zerulla¹, Mohamed Al-Rubeai², James H. Rice¹; ¹School of Physics, Univ. College Dublin, Ireland; ²School of Chemical and Bioprocess Engineering, Univ. College Dublin, Ireland; ³Inst. of laser for postgraduate studies, Univ. of Baghdad, Iraq. Recent advances in infrared (IR) nano-imaging as a non-invasive and robust method for chemically detecting subcellular features and intracellular exogenous agents without the use of labels at nanoscale resolutions are discussed.

18:30–20:30 Special Symposium in Memory of James P. Gordon, Grand Ballroom 

NOTES

Blank lined area for notes.

CLEO: QELS-Fundamental Science

08:00–10:00 Plenary and Awards Session I, *Grand Ballroom* ▶10:00–17:00 Exhibition Open, *Exhibit Halls 1 & 2*10:00–11:00 Coffee Break (10:00-10:30) and Unopposed Exhibit Only Time, *Exhibit Halls 1 & 2*10:30–12:30 Market Focus Session I:
Emerging Mid-Infrared Market Opportunities: Air Quality Monitoring Related to Energy Extraction, *Exhibit Hall Theater*

11:00–13:00
FTu1A • Symposium on
Quantum Repeaters I
Presider: Jungsang Kim; Duke Univ., USA

FTu1A.1 • 11:00 **Invited**
Ultrafast Quantum Repeaters for Long Distance Quantum Communication, Liang-Xing Jiang¹; ¹*School of Metallurgical Science and Engineering, Central South Univ., China*. We investigate and optimize three generations of quantum repeater protocols for long distance quantum communication, which can overcome the major challenges of photon loss and operational imperfections.

11:00–13:00
FTu1B • Dynamics in
Semiconductor Quantum Wells
Presider: Robert Kaindl; Lawrence Berkeley National Lab, USA

FTu1B.1 • 11:00
Multidimensional coherent optical photocurrent spectroscopy of a semiconductor quantum well, Travis Autry^{1,2}, Gael Nardin¹, Kevin Silverman³, Steven T. Cundiff^{1,2}; ¹*JILA, Univ. of Colorado, USA*; ²*Physics, Univ. of Colorado, USA*; ³*National Inst. of Standards and Technology, USA*. We present a new technique for Multi-Dimensional Coherent spectroscopy of nano-structures. We measure the Four-Wave Mixing (FWM) amplitude and phase via photocurrent detection. The measurement is suitable for any nano-structures that can be electrically contacted.

FTu1B.2 • 11:15
Superradiant Decay of Coherent Cyclotron Resonance in Ultrahigh-Mobility Two-Dimensional Electron Gases, Qi Zhang¹, Takashi Arikawa¹, Michael A. Zudov², John L. Reno³, Wei Pan³, John D. Watson⁴, Michael J. Manfra⁴, Junichiro Kono¹; ¹*Electrical and computer engineering, Rice Univ., USA*; ²*Physics, Univ. of Minnesota, USA*; ³*Sandia National Labs, USA*; ⁴*Physics, Purdue Univ., USA*. We study the coherent dynamics of cyclotron resonance in ultrahigh-mobility two-dimensional electron gases via time-domain terahertz magneto-spectroscopy. We show that superradiant damping is the dominant decoherence mechanism at low temperatures.

11:00–13:00
FTu1C • Novel Optics II
Presider: Jean-Jacques Greffet; Institut d'Optique, France

FTu1C.1 • 11:00 **Invited**
Planar Superconducting Toroidal Metamaterial: A Source for Oscillating Vector-Potential?, Vassili Savinov¹, Kaveh Delfanzari¹, Vassili A. Fedotov¹, Nikolay I. Zheludev^{1,2}; ¹*Optoelectronics Research Centre and Centre for Photonic Metamaterials, Univ. of Southampton, UK*; ²*Centre for Disruptive Photonic Technologies, Nanyang Technological Univ., Singapore*. We demonstrate the first superconducting metamaterial that can exhibit a profound toroidal dipolar resonance. Quantum behaviour of the superconductor and toroidal excitation of the metamaterial are both necessary prerequisites for observing the time-dependent Aharonov-Bohm effect.

11:00–13:00
FTu1D • Strong-Field Physics
Presider: Tenio Popmintchev; JILA, Univ. of Colorado at Boulder, USA

FTu1D.1 • 11:00 **Tutorial**
Approaching the Atomic Unit of Time with Isolated Attosecond Pulses, Zenghu Chang¹; ¹*Univ. of Central Florida, CREOL, USA*. Isolated attosecond pulses are powerful tools for studying electron dynamics in atoms, molecules and condensed matter. The shortest pulses achieved so far are 67 as. Challenges and approaches for further shortening such pulses are introduced.



Zenghu Chang is a Distinguished Professor of Physics and Optics at the University of Central Florida, where he directs the Institute for the Frontier of Attosecond Science and Technology. He is a fellow of The Optical Society and the APS. Chang is the author of the book "Fundamentals of Attosecond Optics."

CLEO: Science & Innovations

08:00–10:00 Plenary and Awards Session I, *Grand Ballroom* ▶10:00–17:00 Exhibition Open, *Exhibit Halls 1 & 2*10:00–11:00 Coffee Break (10:00-10:30) and Unopposed Exhibit Only Time, *Exhibit Halls 1 & 2*10:30–12:30 Market Focus Session I:
Emerging Mid-Infrared Market Opportunities: Air Quality Monitoring Related to Energy Extraction, *Exhibit Hall Theater*11:00–13:00
STu1E • Applications of fs
LasersPresident: Andy Kung; National
Tsing Hua Univ., Taiwan

STu1E.1 • 11:00 Tutorial
Femtosecond Laser Processing of Materials, Eric Mazur¹; ¹Harvard Univ., USA. We review recent work involving the interaction of femtosecond laser pulses with materials. We discuss the fundamental processes involved and applications, classifying the work into the interaction with transparent materials and with absorbing materials.



Eric Mazur is the Balkanski Professor of Physics and Applied Physics at Harvard University and Dean of Applied Physics. He is a prominent physicist known for his contributions in nanophotonics, an internationally recognized educational innovator, a sought-after lecturer, and successful entrepreneur. Mazur received the Esther Hoffman Beller award from The Optical Society and the Millikan Medal from the American Association of Physics Teachers.

11:00–13:00
STu1F • Manipulation &
Detection of THz RadiationPresident: Daniel Mittleman; Rice
Univ., USA

STu1F.1 • 11:00
Terahertz Field Induced Second Harmonic Coherent Detection Scheme based on a Biased Nonlinear Micro-slit, Anna V. Mazhorova¹, Sze Ping Ho^{1,2}, Matteo Clerici^{1,3}, Marco Peccianti⁴, Alessia Pasquazi⁴, Luca Razzari¹, Jalil Ali², Roberto Morandotti¹; ¹Energy Materials Telecommunications Research Centre, Institut National de la Recherche Scientifique, Canada; ²Nanophotonics Research Alliance, Universiti Teknologi Malaysia, Malaysia; ³School of Engineering and Physical Sciences, Heriot-Watt Univ., UK; ⁴Dept of Physics and Astronomy, Univ. of Sussex, UK. We demonstrated coherent Terahertz characterization based on Terahertz Field Induced Second Harmonic effect in a Silica samples, operated with 10-100 V sources. Our sample is an infinitely long 30 μm slit written in gold. Our results pave the way to a novel approach towards broadband THz detection.

STu1F.2 • 11:15
Active modulation of terahertz wave front, Yan Zhang¹; ¹Capital Normal Univ., China. A novel method is proposed to dynamically modulate the THz wave front with photo-generated carriers. Some special wave fronts are generated using this method. This new method is structure free, high resolution, and broadband.

11:00–13:00
STu1G • Integrated
Components for Optical
CommunicationsPresident: Leif Johansson;
Freedom Photonics, LLC, USA

STu1G.1 • 11:00
Ultra-Low Voltage Wide Bandwidth Electro-optic Modulators, Selim Dogru¹, Nadir Dagli¹; ¹Univ. of California Santa Barbara, USA. Wide bandwidth, ultra-low voltage modulators based on substrate removal technology and loaded line traveling wave electrodes are presented. Drive voltage product is 0.06 V-cm and 2 mm long devices have electrical-to-electrical bandwidths exceeding 80 GHz.

STu1G.2 • 11:15
Error-Free Optical Data Generation Using Quantum Dot Electro-Optic Modulator with Semiconductor Optical Amplifier in Ultra-Broad Optical Frequency Bandwidth, Naokatsu Yamamoto¹, Kouichi Akahane¹, Toshimasa Umezawa¹, Tetsuya Kawanishi¹; ¹National Inst. of Information and Communications Technology, Japan. Error-free Gbps-order high-speed optical data signal generation in a > 5.5-THz ultra-broad optical frequency bandwidth of the O-band was successfully demonstrated using a newly developed quantum dot electro-optic modulator integrated with a semiconductor optical amplifier.

11:00–13:00
STu1H • Plasmonic Devices
President: Zhaowei Liu; Univ. of
California San Diego, USA

STu1H.1 • 11:00
AFM-Based Pick-and-Place Handling of Individual Nanoparticles inside an SEM for the Fabrication of Plasmonic Nano-Patterns, Uwe Mick^{1,2}, Peter Banzer^{1,2}, Silke Christiansen^{1,3}, Gerd Leuchs^{1,2}; ¹Max Planck Inst. for the Science of Light, Germany; ²Inst. of Optics, Information and Photonics, Friedrich-Alexander-Univ. Erlangen-Nuremberg, Germany; ³Inst. for Nanoarchitectures for Energy Conversion, Helmholtz Zentrum Berlin, Germany. Integrating AFM technology into an SEM enables the interactive assembling of individual nanoparticles by in-situ pick-and-place handling. We present a hardware setup and introduce examples for the nanofabrication of plasmonic patterns.

STu1H.2 • 11:15
High Excitation Efficiency of Channel Plasmon Polaritons in Tailored, UV-Lithography-Defined V-Grooves, Cameron L. Smith¹, Anil H. Thilsted¹, Cesar E. Garcia-Ortiz², Ilya P. Radko², Rodolphe Marie¹, Claus Jeppesen³, Christoph Vannahme¹, Sergey I. Bozhevolnyi², Anders Kristensen¹; ¹Dept of Micro- and Nanotechnology, Technical Univ. of Denmark, Denmark; ²Inst. of Technology and Innovation, Univ. of Southern Denmark, Denmark; ³Dept of Photonics Engineering, Technical Univ. of Denmark, Denmark. We demonstrate >50% conversion of light to V-groove channel plasmon-polaritons (CPPs) via compact waveguide-termination mirrors. Devices are fabricated using UV-lithography and crystallographic silicon etching. The V-shape is tailored by thermal oxidation to support confined CPPs.

Meeting Room
211 B/D

Meeting Room
212 A/C

Meeting Room
212 B/D

Marriott
Salon I & II

CLEO: Science & Innovations

CLEO: QELS-
Fundamental Science

CLEO: Science &
Innovations

08:00–10:00 Plenary and Awards Session I, *Grand Ballroom* ▶

10:00–17:00 Exhibition Open, *Exhibit Halls 1 & 2*

10:00–11:00 Coffee Break (10:00-10:30) and Unopposed Exhibit Only Time, *Exhibit Halls 1 & 2*

10:30–12:30 Market Focus Session I:
Emerging Mid-Infrared Market Opportunities: Air Quality Monitoring Related to Energy Extraction, *Exhibit Hall Theater*

11:00–13:00

STu1I • Nonlinear Optical
Materials

Presider: Valentin Petrov; Max
Born Inst., Germany

11:00–13:00

STu1J • Short Reach
Communications

Presider: Ivan Djordjevic; Univ. of
Arizona, USA

11:00–13:00

FTu1K • Near-field Imaging
with Photons, Plasmons and
Electrons

Presider: Rashid Zia; Brown Univ.,
USA

11:00–13:00

STu1L • Mid-infrared Fiber
Lasers ▶

Presider: Shibin Jiang; AdValue
Photonics, Inc., USA

STu1I.1 • 11:00

Optical nonlinearity in silicon at mid-infrared wavelengths, Ting Wang¹, Nalla Venkatram^{2,3}, Wei Ji², Dawn Tan¹; ¹Engineering Product Development, Singapore Univ. of Technology and Design, Singapore; ²Dept of Physics, National Univ. of Singapore, Singapore; ³Centre for Disruptive Photonic Technologies, Nanyang Technological Univ., Singapore. We report the wavelength dependency of third-order nonlinearity and multiphoton absorption of silicon in the spectral range from 1.6 μm to 6 μm , including the nonlinear figure of merit.

STu1J.1 • 11:00

Millimeter-wave Radio-over-Fiber Access Architecture for Implementing Real-time Cloud Computing Service, Feng Lu¹, Jing Wang¹, Lin Cheng¹, Mu Xu¹, Ming Zhu¹, Gee-Kung Chang¹; ¹School of Electrical and Computer Engineering, Georgia Inst. of Technology, USA. A cloud computing access network architecture based on millimeter-wave radio-over-fiber technologies has been proposed and demonstrated. Real-time communication between centralized computing resources and mobile wireless users are provided by bidirectional millimeter-wave over fiber links.

FTu1K.1 • 11:00

Sub-diffraction Imaging via Surface Plasmon Decompression, Alessandro Salandrino¹, Hu Cang², Yuan Wang¹, Xiang Zhang^{1,3}; ¹NSF Nanoscale Science and Engineering Center (NSEC), Univ. of California Berkeley, USA; ²Waitt Advanced Biophotonics Center, Salk Inst. for Biological Studies, USA; ³Materials Sciences Division, Lawrence Berkeley National Lab, USA. We theoretically propose a novel scheme for sub-diffraction imaging based on a process of adiabatic decompression of the local wavelength of a surface plasmon polariton supported by two adjoining curved metal surfaces.

STu1L.1 • 11:00 **Invited** ▶

Robust Multimaterial Tellurium-based Chalcogenide Glass Infrared Fibers, Guangming Tao¹, Soroush Shabahang¹, He Ren^{2,1}, Farnood Khalilzadeh-Rezaie³, Robert E. Peale³, Zhiyong Yang⁴, Xunsi Wang^{5,1}, Ayman F. Abouraddy¹; ¹CREOL, The College of Optics & Photonics, Univ. of Central Florida, USA; ²School of Physics and Electronic Engineering, Jiangsu Normal Univ., China; ³Dept of Physics, Univ. of Central Florida, USA; ⁴Laser Physics Centre, Research School of Physics and Engineering, The Australian National Univ., Australia; ⁵Lab of Infrared Material and Devices, Ningbo Univ., China. We demonstrate the scalable production of the first robust tellurium-based chalcogenide glass fibers provided with a built-in polymer jacket and transmit mid-wave and long-wave infrared light across the 3 - 12 micron window.

STu1I.2 • 11:15

Synchronously coupled fiber lasers and sum frequency generation using graphene composites, MENG ZHANG¹, Edmund J. Kelleher¹, T. H. Runcorn¹, Daniel Popa², Felice Torrisi², Andrea C. Ferrari², Sergei V. Popov¹, James R. Taylor¹; ¹Dept of Physics, Imperial College London, UK; ²Cambridge Graphene Centre, Univ. of Cambridge, UK. Graphene mode-locked and self-synchronized fiber lasers are used for sum-frequency mixing in a graphene-polymer composite.

STu1J.2 • 11:15

Energy-efficient, digitally-driven "fat pipe" silicon photonic circuit switch in the UCSD MORDIA data-center network, Ryan Aguinaldo¹, Alex Forencich¹, Christopher DeRose², Anthony L. Lentine², Douglas C. Trotter², Andrew Starbuck², Yeshaiahu Fainman¹, George Porter¹, George Papen¹, Shayan Mookherjee¹; ¹Univ. of California San Diego, USA; ²Applied Microphotonic Systems, Sandia National Lab, USA. Using a compact (0.03 mm²) silicon photonic thermo-optic switch with five cascaded thermo-optic phase-shifters, we demonstrate low insertion loss, low power, microsecond-scale cross-bar switching of twenty wavelength channels, each carrying 10 Gbit/second data concurrently.

FTu1K.2 • 11:15

Sub-diffraction limited imaging with a spatially dispersive slab, Avner Yanai¹, Uriel Levy¹; ¹Hebrew Univ. of Jerusalem, Israel. We obtain sub-diffraction limited imaging at $\omega > \omega_p$ using a flat silver slab. Unlike Superlenses, the formation of subdiffraction imaging is attributed to high-k longitudinal modes that are supported by the non-local response of the media.

CLEO: Science & Innovations

CLEO: Applications
& Technology08:00–10:00 Plenary and Awards Session I, *Grand Ballroom* ▶10:00–17:00 Exhibition Open, *Exhibit Halls 1 & 2*10:00–11:00 Coffee Break (10:00-10:30) and Unopposed Exhibit Only Time, *Exhibit Halls 1 & 2*10:30–12:30 Market Focus Session I:
Emerging Mid-Infrared Market Opportunities: Air Quality Monitoring Related to Energy Extraction, *Exhibit Hall Theater*11:00–13:00
STu1M • Applied Plasmonics ▶
*Presider: Jon Schuller; Univ. of California Santa Barbara, USA*STu1M.1 • 11:00 ▶
Low-Loss Plasmonic Titanium Nitride Strip Waveguides, Nathaniel Kinsey¹, Marcello Ferrera¹, Gururaj Naik¹, Alexander Kildishev¹, Vladimir M. Shalaev¹, Alexandra Boltasseva¹; ¹ECE, *Purdue Univ., USA*. In this work we report low-loss insulator-metal-insulator plasmonic interconnects using the CMOS-compatible material titanium nitride. The mode profile shows the characteristic exponential decay of the plasmonic regime, with propagation losses as low as 0.79 dB/mm.STu1M.2 • 11:15 ▶
Plasmonic Photomixers for Increased Terahertz Radiation Powers at 1550 nm Optical Pump Wavelength, Christopher W. Berry¹, Mohammed R. Hashemi^{1,2}, Sascha Preu³, Hong Lu⁴, Arthur Gossard⁴, Mona Jarrahi^{1,2}; ¹Electrical Engineering and Computer Science, *Univ. of Michigan Ann Arbor, USA*; ²Electrical Engineering, *Univ. of California Los Angeles, USA*; ³Inst. for Microwave Engineering and Photonics, *Technical Univ. Darmstadt, Germany*; ⁴Materials Dept, *Univ. of California Santa Barbara, USA*. We experimentally demonstrate an order of magnitude higher radiated power from a 1550 nm photomixer with plasmonic contact electrodes in comparison with an analogous photomixer without plasmonic contact electrodes in the 0.25-2.5 THz frequency range.11:00–13:00
STu1N • Mode-locked Fiber Lasers
*Presider: Ingmar Hartl; DESY, Germany*STu1N.1 • 11:00
Soliton mode-locked fiber laser using a modulator-based saturable absorber, Ruixin Wang¹, Yitang Dai¹, Ziping Zhang¹, Hao Chen¹, Haijie Yu¹, Feifei Yin¹, Kun Xu¹, Jianqiang Li¹, Jintong Lin¹; ¹Beijing Univ of Posts & Telecom, *China*. We demonstrate a novel saturable absorber based on a dual-drive modulator with a feed-forward path for soliton pulse shaping. The fundamentally mode-locked laser produces 16.7-MHz repetition rate pulse train with 1.4-ps pulse width.STu1N.2 • 11:15
Pulse dynamics in a mode-locked fiber laser and its quantum limited comb linewidth, Chengying Bao^{1,2}, Andrew Funk², Changxi Yang¹, Steven T. Cundiff²; ¹Tsinghua Univ., *China*; ²JILA, *Univ. of Colorado & National Inst. of Standards and Technology, USA*. We fully characterized the pulse dynamics in a mode-locked Er fiber laser experimentally by measuring its response to gain modulation. The measurement allows us to evaluate quantum-limited comb linewidth and phase noise spectrum.11:00–13:00
STu1O • High Average Power Lasers for Industrial Applications ▶
*Presider: Constantin Haefner; Lawrence Livermore National Lab, USA*STu1O.1 • 11:00 Tutorial ▶
Laser Additive Manufacturing LAM - Fundamentals of Selective Laser Melting SLM and Laser Material Deposition LMD, Reinhart Poprawe¹, Ingomar Kelbassa², Yves-Christian Hagedorn¹; ¹Fraunhofer Institut, *Germany*; ²RWTH-Aachen Univ., *Germany*. With Additive Manufacturing AM, parts can be manufactured for design instead of being designed for manufacture. This tutorial introduces the two laser based AM processes, Selective Laser Melting SLM and Laser Material Deposition LMD.11:00–13:00
ATu1P • Applications of Optical Microscopy and Imaging ▶
*Presider: Yu Chen; Univ. of Maryland at College Park, USA*ATu1P.1 • 11:00 Invited ▶
Increasing the Diagnostic Yield and Accuracy of Bronchial Biopsy for the Assessment of Lung Cancer, Melissa J. Suter¹, Lida P. Hariri¹, Alyssa J. Miller¹, David C. Adams¹, Michael Lanuti¹, Mari Mino-Kenudson¹; ¹Harvard Medical School, *Mass General Hos, USA*. Low-risk bronchoscopy techniques for retrieving biopsy samples for the diagnosis of lung cancer are hampered by low diagnostic yields, and trans-thoracic and surgical approaches carry higher intrinsic risk of complications. We are investigating the use of optical coherence tomography to increase the diagnostic yield and accuracy of bronchial biopsy.

CLEO: QELS-Fundamental Science

FTu1A • Symposium on
Quantum Repeaters I—
Continued

FTu1A.2 • 11:30

Memory-based Quantum Repeaters with NV Centers, Kae Nemoto¹, Simon Devitt¹, Michael Trupke², Ashley Stephens¹, Mark Everitt¹, Kathrin Buczak², Tobias Noebauer², Jorg Schmiedmayer², William Munro^{3,1}; ¹National Inst. of Informatics, Japan; ²Vienna Center for Quantum Science and Technology, Tu-Wien, Austria; ³NTT BRL, Japan. We present a simple design of a quantum repeater design build from single NV- centers embedded in an optical cavity. We compare different quantum networks from a simple linear chain to a fully fault-tolerant quantum internet.

FTu1A.3 • 11:45

Trapped Ion Implementation of Memory-Assisted Extended Quantum Key Distribution, Kai Hudek¹, Geert Vrijsen¹, Louis Isabella¹, Dan Gaultney¹, Jungsang Kim¹, Liang Jiang³, Norbert Lutkenhaus²; ¹Electrical and Computer Engineering, Duke Univ., USA; ²Inst. for Quantum Computing, Univ. of Waterloo, Canada; ³Applied Physics, Yale Univ., USA. We discuss a practical scheme to implement memory-assisted measurement-device-independent quantum key distribution protocol using trapped ion systems with the potential to extend the range of conventional QKD by a factor of 2.

FTu1A.4 • 12:00 **Invited**

Quantum Repeater Approach based on Diamond Spin Qubit, Hideo Kosaka^{1,2}; ¹Research Inst. of Electrical Communication, Tohoku Univ., Japan; ²Graduate School of Engineering, Yokohama National Univ., Japan. Challenges for building a quantum repeater system using a nitrogen vacancy center in diamond are overviewed and our approach for quantum repeater network with NV-based entanglement detection for entanglement swapping will be presented.

FTu1B • Dynamics in
Semiconductor Quantum
Wells—Continued

FTu1B.3 • 11:30

Spatiotemporal coherence of GaN excitons excited by an optical vortex with multiple orbital angular momentum, Kyohhei Shigematsu¹, Keisaku Yamane^{1,2}, Ryuji Morita^{1,2}, Yasunori Toda^{1,2}; ¹Hokkaido Univ., Japan; ²JST CREST, Japan. The spatiotemporal coherence of excitons is investigated by degenerate four-wave-mixing using optical vortices with multiple orbital angular momentum (OAM). The OAM-resolved signal indicates that the topological phase with large OAM is robust against spatial decoherence.

FTu1B.4 • 11:45

Electroluminescence from a GaAs/AlGaAs Heterostructure at High Electric Fields: Evidence for Real- & k-Space Transfer, Weilu Gao¹, Xuan Wang¹, Rui Chen², Gottfried Strasser³, Jonathan Bird^{2,4}, Junichiro Kono^{1,5}; ¹ECE, Rice Univ., USA; ²EE, Univ. of Buffalo, the State Univ. of New York, USA; ³Center for Micro and Nanostructures and Inst. for Solid State Electronics, Vienna Univ. of Technology, Austria; ⁴Graduate School of Advanced Integration Science, Chiba Univ., Japan; ⁵Physics and Astronomy, Rice Univ., USA. We study impact-ionization-induced electroluminescence (EL) from a GaAs/AlGaAs heterostructure under high bias. In addition to k-space transfer (the Gunn effect), EL spectra indicate real-space (GaAs-to-AlGaAs) transfer. Microscopy shows strong EL near the anode.

FTu1B.5 • 12:00

Optically Controlled Excitonic Transistor, Peristera Andreakou^{1,2}, Sergey Poltavtsev^{1,3}, Jason Leonard¹, Eric V. Calman¹, Mikas Remelka¹, Yuliya Y. Kuznetsova¹, Leonid Butov¹, Joe Wilkes⁴, Micah Hanson⁵, Arthur Gossard⁵, Matthew Hasling¹; ¹Dept of Physics, Univ. of California at San Diego, USA; ²Laboratoire Charles Coulomb, Universite Montpellier, France; ³Spin Optics Lab, St. Petersburg State Univ., Russia; ⁴Dept of Physics and Astronomy, Cardiff Univ., UK; ⁵Materials Dept, Univ. of California at Santa Barbara, USA. We present experimental proof of principle for all-optical excitonic routers and all-optical excitonic transistors with a high ratio between the excitonic signal at the optical drain and the excitonic signal due to the optical gate.

FTu1C • Novel Optics II—
Continued

FTu1C.2 • 11:30

Is There a Metamaterial Route to High Temperature Superconductivity?, Igor Smolyaninov¹, Vera Smolyaninova²; ¹Univ. of Maryland, USA; ²Towson Univ., USA. We argue that the metamaterial approach to dielectric response engineering may considerably increase the critical superconducting temperature of a composite superconductor-dielectric metamaterial.

FTu1C.3 • 11:45

Mid-infrared Plasmonic Inductors, Víctor Torres¹, Rubén Ortuño¹, Pablo Rodríguez-Ulibarri¹, Amadeu Griol², Alejandro Martínez², Miguel Navarro-Cia³, Miguel Beruete¹, Mario Sorolla¹; ¹Universidad Pública de Navarra, Spain; ²Universitat Politècnica de València, Spain; ³Imperial College London, UK. Expanding ideas from microwaves, we demonstrate experimentally a terahertz inductor by using meander-lines in a canonical extraordinary transmission (ET) hole array leading to a strong resonance's redshift and an unprecedented enlargement of the operation bandwidth.

FTu1C.4 • 12:00

Ultrafast and ultra-Low Power All-Optical Tunable Plasmon-Induced-Transparency in Gold/Graphene Trimers, Cuicui Lu¹, Xiaoyong Hu¹, Hong Yang¹, Qihuang Gong¹; ¹Physics Dept, Peking Univ., China. We proposed a novel meta-structure of gold/graphene trimers and realized ultrafast and ultra-low power all-optical tunable plasmon-induced transparency around 1150 nm. The nonlinear susceptibility of graphene/ITO film was up to 2.90×10^{-5} esu.

FTu1D • Strong-Field Physics—
Continued

FTu1D.2 • 12:00

Experimental Observation of Light Induced Conical Intersections in a Diatomic Molecule, Adi Natan^{1,2}, Matthew R. Ware^{1,2}, Philip H. Bucksbaum^{1,2}; ¹Stanford PULSE Inst., SLAC National Accelerator Lab, USA; ²Physics, Stanford Univ., USA. We observe quantum interferences in the angular distributions of H₂⁺ photodissociation arising from the geometric singularity induced by strong laser fields. This is the first experimental observation of light induced conical intersections in diatomic molecules.

There is still time to
register for a Short
Course!

Visit Registration to
learn about the courses
still available.

Tuesday, 10 June

- SC271 • Quantum Information-Technologies and Applications
- SC352 • Introduction to Ultrafast Pulse Shaping—Principles and Applications
- SC362 • Cavity Optomechanics: Fundamentals and Applications of Controlling and Measuring Nano- and Micro-mechanical Oscillators with Laser Light
- SC379 • Silicon Photonic Devices and Applications
- SC410 • Finite Element Modelling Methods for Photonics and Optics

View page 17 for complete Short Course Information.

CLEO: Science & Innovations

STu1E • Applications of fs
Lasers—Continued

STu1E.2 • 12:00

Graphene Supercapacitor as a Voltage Controlled Saturable Absorber for Femtosecond Pulse Generation, Isinsu Baylam^{1,2}, Melissa N. Cizmecian^{1,2}, Sarper Ozharar³, Emre O. Polat⁴, Coskun Kocabas⁴, Alphan Sennaroglu^{1,2}; ¹Physics and Electrical-Electronics, Koc Univ., Turkey; ²Surface Science and Technology Center, Koc Univ., Turkey; ³College of Arts and Sciences, Bahcesehir Univ., Turkey; ⁴Physics, Bilkent Univ., Turkey. For the first time to our knowledge, we employed a graphene supercapacitor as a voltage controlled saturable absorber at bias voltages of 0.5-1V to generate 84-fs pulses from a solid-state laser near 1255 nm.

STu1F • Manipulation &
Detection of THz Radiation—
Continued

STu1F.3 • 11:30 **Invited**
Silicon-based Sources and Detectors for Terahertz Applications, Ullrich Pfeiffer¹, Janusz Grzyb¹, Richard Al Hadi¹; ¹IHCT, Bergische Universität Wuppertal, Germany. Today's terahertz instrumentation lacks cost-effective sources and detectors compatible with standard microelectronics to drive down the system cost. This paper presents recent developments based on silicon process technologies and discusses the challenges in implementing source and detectors. It presents a 530GHz source array with up to 1mW radiated power, a 1024-pixel CMOS camera, and a heterodyne 830GHz imaging chip-sets.

STu1F.4 • 12:00

Real-Time Absolute Frequency Measurement of CW-THz Wave Based on Dual THz Combs, Kenta Hayashi¹, Hajime Inaba^{2,3}, Kaoru Minoshima^{2,4}, Takeshi Yasui^{1,3}; ¹The Univ. of Tokushima, Japan; ²National Inst. of Advanced Industrial Science and Technology, Japan; ³ERATO Intelligent Optical Synthesizer Project, Japan; ⁴The Univ. of Electro-Communications, Japan. We demonstrated a frequency measurement of CW-THz wave referring to dual THz frequency comb in real time. The absolute frequency of the CW-THz wave is measured with an accuracy of 3.5×10^{-11} 10ms each.

STu1G • Integrated
Components for Optical
Communications—Continued

STu1G.3 • 11:30 **Invited**
InP-Based 100 Gb/s Coherent Receiver Technologies, Hideki Yagi¹, Yoshihiro Yoneda¹, Masaru Takechi¹, Hajime Shoji¹; ¹Sumitomo Electric Industries Ltd, Japan. We review and discuss InP-based monolithic integration technologies and their application to compact 100 Gb/s coherent receivers.

STu1G.4 • 12:00

A silicon photonic channelized spectrum monitor for UCSD's multi-wavelength ring network, Ryan Aguinaldo¹, Peter O. Weigel¹, Hannah R. Grant¹, Christopher DeRose², Anthony L. Lentine², Andrew T. Pomerene², Andrew Starbuck², Andre Tkacenko³, Shayan Mookherjee¹; ¹Univ. of California San Diego, USA; ²Applied Microphotonic Systems, Sandia National Lab, USA; ³Signal Processing Research Group, NASA Jet Propulsion Lab, USA. A compact silicon photonic channelized optical spectrum monitor is designed and realized, which can replace a large rack-mounted OSA's channel power monitoring functionality, and the signal processing algorithm underlying its operation is described.

STu1H • Plasmonic Devices—
Continued

STu1H.3 • 11:30 **Invited**
Semiconductor Plasmonic Devices for Interconnects, Meir Orenstein¹; ¹Technion Israel Inst. of Technology, Israel. Plasmonic assisted nanodetectors and LEDs may be the only solution for power efficient onchip optical communications - the holy grail of integrated photonics. Localized plasmons in novel detectors and fast LEDs will be described in detail.

STu1H.4 • 12:00

Optically Readable Resistive Random Access Memory in Silicon Plasmonics Platform, Alexandros Emboras¹, Boris Desiatov¹, Ilya Goykhan¹, Noa Mazurski¹, Liron Stern¹, Joseph Shappir¹, Uriel Levy¹; ¹Hebrew Univ. of Jerusalem, Israel. We experimentally demonstrate resistive random access memory device integrated with a silicon plasmonic waveguide, and relying on the formation of nanoscale metallic needles. The measured electrical and optical response show distinct bistability with well-defined hysteresis.



For Conference News & Insights
Visit blog.cleoconference.org

CLEO: Science & Innovations

STu11 • Nonlinear Optical
Materials—Continued

STu11.3 • 11:30 **Invited**
Room-temperature Bonding and its Applications to Solid-state Lasers and Wavelength-conversion Devices, Ichiro Shoji¹; ¹Chuo Univ., Japan. We develop composite solid-state lasers and nonlinear wavelength-conversion devices by room-temperature bonding. The room-temperature-bonding technique has a potential of realizing new high-power and highly efficient laser devices over a wide wavelength range.

STu11.4 • 12:00
> 0.5 MW Peak Power, kHz Repetition Rate at 266 nm Using [100]-Cut Nd:YAG Microchip Laser, Rakesh Bhandari¹, Takunori Taira¹; ¹Inst. for Molecular Science, Japan. We report the use of [100]-cut YAG/Nd:YAG composite in a microchip laser to reduce depolarization at high average power. Consequently, we achieve FHG giving > 0.5 MW peak power, 1 kHz at 266 nm.

STu1J • Short Reach
Communications—Continued

STu1J.3 • 11:30
A Carrier Centralized Hybrid Long Reach PON with DDO-OFDM Downstream and Nyquist-WDM Upstream, You-Wei Chen¹, Jih-Heng Yan¹, Kuo-Ping Huang², Kai-Ming Feng^{1,2}; ¹Inst. of Photonics Technologies, National Tsing Hua Univ., Taiwan; ²Inst. of Communications Engineering, National Tsing Hua Univ., Taiwan. A carrier centralized bi-directional 150/60 Gbps hybrid DDO-OFDM/Nyquist-WDM Long Reach PON is experimentally demonstrated. Uniform performance, high spectral efficiency, asynchronous upstream manipulation, and 1:1024 splitting ratio are achieved.

STu1J.4 • 11:45
Colorless Self-Seeded Fiber Cavity Laser Transmitter for WDM-PON, Simon Arega Gebrewold¹, Lucia Marazzi², Paola Parolari², Marco Brunero², Romain Brenot³, David Hillerkuss¹, Christian Hafner¹, Juerg Leuthold¹; ¹ETH Zurich, Switzerland; ²Politecnico di Milano, Italy; ³III-V Labs, France. Colorless, self-seeded km-long fiber cavity RSOA lasers embedded in an access network are investigated for the optimum operation conditions. Theoretical predictions on the proper configuration and the impact of dispersion are supported by experiments.

STu1J.5 • 12:00
Mitigating Rayleigh Backscattering Noise in WDM-PON by Using Cascaded SOAs and Microwave Photonic Filter, Hanlin Feng^{1,2}, Jia Ge², Shilin Xiao¹, Mable Fok²; ¹The State Key Lab of Advanced Optical Communication Systems and Networks, Shanghai Jiao Tong Univ., China; ²College of Engineering, Univ. of Georgia, Georgia. We present a Rayleigh backscattering noise mitigation scheme for 10-Gb/s loop-back WDM-PON with cascaded SOAs. OSNR is reduced to 16.5 dB and BER is improved by 6 dB with the incorporation of microwave photonic filter.

CLEO: QELS-
Fundamental ScienceFTu1K • Near-field Imaging
with Photons, Plasmons and
Electrons—Continued

FTu1K.3 • 11:30
Direct Reconstruction of Transversally Spinning Electric Fields in Tightly Focused Vector Beams, Martin Neugebauer^{1,2}, Thomas Bauer^{1,2}, Gerd Leuchs^{1,2}, Peter Banzer^{1,2}; ¹Max Planck Inst. for the Science of Light, Germany; ²Inst. of Optics, Information and Photonics, Univ. Erlangen-Nuremberg, Germany. We demonstrate a simple measurement technique for the direct reconstruction of local transversally spinning electric fields in tightly focused vector beams. Our scheme is based on an easy-to-implement difference measurement of intensities in k-space.

FTu1K.4 • 11:45
Fluorescent Scanning Near-Field Probe Maps the Radiative and Non-Radiative Local Density of Optical States at the Nanometer Scale, Valentina KRACHMAL-NICOFF¹, Da Cao¹, Alexandre Cazé¹, Michele Calabrese¹, Romain Pierrat¹, Nathalie Bardou², Stéphane Collin², Rémi Carminati¹, Yannick De Wilde¹; ¹Institut Langevin - ESPCI CNRS, France; ²Laboratoire de Photonique et Nanostructures (LPN-CNRS), France. We present a novel approach for mapping the radiative and non-radiative local density of states in the near-field of a nanostructure by using a fluorescent near-field probe. Experiments are in quantitative agreement with numerical simulations.

FTu1K.5 • 12:00
Apertureless Optical Near-Field Imaging of Localized Modes of Silicon Nanodisks, Terefe G. Habteyes¹, Isabelle Staude², Katie E. Chong², Jason Dominguez³, Manuel Decker², Andrey Miroshnichenko², Yuri S. Kivshar², Igal Brener²; ¹Dept of Chemistry and Chemical Biology, and Center for High Technology Materials, Univ. of New Mexico, USA; ²Nonlinear Physics Centre, Australian National Univ., Australia; ³Center for Integrated Nanotechnologies, Sandia National Lab, USA. We measure near-field distributions of Mie-type optical modes of silicon nanodisks using apertureless near-field optical microscopy. Excellent agreement with numerical predictions is obtained, further enabling multipole analysis of the observed modes.

CLEO: Science &
InnovationsSTu1L • Mid-infrared Fiber
Lasers—Continued

STu1L.2 • 11:30
Wavelength-Swept Tm-doped Fiber Lasers, Masaki Tokurakawa^{1,3}, Jae M. Daniel¹, Chi Shing Cheung², Haida Liang², W. A. Clarkson¹; ¹Optoelectronics Research Centre, Univ. of Southampton, UK; ²Nottingham Trent Univ., School of Science & Technology, UK; ³Inst. of Laser Science, Univ. of Electro-Communications, Japan. Wavelength-swept operation of cladding-pumped and core-pumped thulium-doped fiber lasers using a novel intracavity rotating disk wavelength-scanning arrangement is reported. Scanning ranges from 1905-2049nm (for cladding pumping) and 1768-1956nm (for core pumping) were obtained.

STu1L.3 • 11:45 **▶**
3.4 W Ho³⁺, Pr³⁺ Co-Doped Fluoride Fibre Laser, Stephanie Crawford¹, Darren D. Hudson¹, Stuart Jackson¹; ¹School of Physics, Univ. of Sydney, Australia. A maximum output power of 3.4 W, generated at 20.9% efficiency, was obtained from a Ho³⁺, Pr³⁺-co-doped ZBLAN fibre laser pumped at 1150 nm by a Raman fibre laser and pumped by a tunable Yb³⁺ fibre laser.

STu1L.4 • 12:00 **▶**
Mid-infrared passively mode-locked fiber ring laser, Tomonori Hu¹, Darren D. Hudson¹, Stuart Jackson¹; ¹Centre for Ultrahigh bandwidth Devices for Optical Systems (CUDOS), Univ. of Sydney, Australia. Stable and self-starting passively mode-locked pulses of 6 ps, 465 W peak power, are produced from a holmium-praseodymium co-doped ring fiber laser at 2.9 μm, with a repetition rate of 24.8 MHz.

Visit Registration to Purchase



Access your Favorite Talks or One You Missed! On-Demand, 24/7

Over 300 high-quality, informative talks representing the full breadth of CLEO's outstanding technical program including:

Tutorials • Contributed • Postdeadline
Symposia • Plenary talks • Invited


CLEO: Science & Innovations

CLEO: Applications
& TechnologySTu1M • Applied Plasmonics—
ContinuedSTu1M.3 • 11:30 

Enhanced Spontaneous Emission Rate of InP using an Optical Antenna, Kevin Messer¹, Michael Eggleston¹, Ming Wu¹, Eli Yablonovitch¹; ¹EECS, Univ. of California - Berkeley, USA. Experimental evidence of enhanced spontaneous emission from InP coupled to an optical antenna is presented. Photoluminescence measurements show a 120x increase in light emission from antenna-coupled devices over bare InP emitters.

STu1M.4 • 11:45 

Electrically-driven surface plasmonic nano-circuits, Min-Kyo Seo^{1,2}, Kevin C. Huang^{2,3}, Tomas Sarmiento³, Yijie Huo³, James S. Harris³, Mark Brongersma²; ¹Physics, KAIST, Republic of Korea; ²Geballe Lab for Advanced Materials, Stanford Univ., USA; ³Electrical Engineering, Stanford Univ., USA. We realized electrically-driven sub- λ surface plasmonic nano-circuits integrating gap-plasmon emitting nano-LEDs and slot-waveguides with a cross-section of $\sim 0.016\lambda^2$. Gap plasmons are efficiently extracted by the Purcell effect and routed to slot-waveguides, T-splitters, and directional couplers.

STu1M.5 • 12:00 

Compact Broadband 50:50 Hybrid Plasmonic Coupler for Silicon Photonics, Jan Niklas Caspers¹, Mo Mojahedi¹; ¹The Edward S. Rogers Sr. Dept of Electrical and Computer Engineering, Univ. of Toronto, Canada. A compact hybrid plasmonic 50:50 directional coupler for the next generation of silicon photonics integrated circuit was fabricated and measured. Our device has a small footprint of only 21.2 μm by 1.1 μm , a bandwidth of more than 100 nm around 1.55 μm and an insertion loss of less than 1dB.

STu1N • Mode-locked Fiber
Lasers—Continued

STu1N.3 • 11:30

Development of Femtosecond Thulium-Doped ZBLAN Fiber Laser Oscillators, Yutaka Nomura¹, Masatoshi Nishio², Sakae Kawato^{2,3}, Takao Fuji¹; ¹Inst. for Molecular Science, Japan; ²Graduate School of Engineering, Univ. of Fukui, Japan; ³Research and Education Program for Life Science, Univ. of Fukui, Japan. We demonstrate a mode-locked fiber laser system using thulium-doped ZBLAN fibers. Very low dispersion of ZBLAN glass fibers enabled generation of pulses with the duration of 45 fs at 1900 nm.

STu1N.4 • 11:45

300 GHz Bound Pulse Generation in a Filter-Assisted Harmonic Mode-Locked Er-doped Fiber Laser with 20 GHz Phase Modulation, Sheng-Min Wang¹, Siao-Shan Jyu¹, Yinchieh Lai¹; ¹Dept of Photonic and Inst. of Electro-Optical Engineering, National Chiao Tung Univ., Taiwan. By inserting a section of PM fiber for birefringence interference filtering with 100 GHz spacing, stable 300GHz bound pulses have been successfully generated in a harmonic mode-locked Er-doped fiber laser with 20GHz phase modulation frequency.

STu1N.5 • 12:00

Low-temperature PECVD grown carbon-rich silicon carbide saturable absorber for sub-picosecond passively mode-locked fiber lasers, Chih-Hsien Cheng¹, Gong-Ru Lin¹; ¹Graduate Inst. of Photonics and Optoelectronics and Dept of Electrical Engineering, National Taiwan Univ., Taiwan. The low-temperature PECVD grown carbon-rich silicon carbide film with thickness of 200 nm is employed to passively mode-lock the fiber laser with pulsewidth of 510 fs and linewidth of 5.46 nm.

STu1O • High Average
Power Lasers for Industrial
Applications—Continued

YSTu1O.2 • 12:00

1.3 kW average output power Yb:YAG thin-disk multipass amplifier for multi-mJ picosecond laser pulses, Jan-Philipp Negel¹, Andreas Voss¹, Marwan Abdou Ahmed¹, Dominik Bauer², Dirk Sutter², Alexander Killi², Thomas Graf¹; ¹Institut fuer Strahlwerkzeuge (IFSW), Univ. of Stuttgart, Germany; ²TRUMPF Laser GmbH+Co. KG, Germany. An Yb:YAG thin-disk multipass amplifier delivering sub-8 ps laser pulses with an average output power of 1.3 kW at a repetition rate of 300 kHz, corresponding to a pulse energy of 4.4 mJ is presented.

ATu1P • Applications of Optical
Microscopy and Imaging—
ContinuedATu1P.2 • 11:30 

Hand-held RCM/OCT Probe for Assessing Skin Burns, Ernest Chang¹, Ankit Patel¹, William Fox², Milind Rajadhyaksha³, Mircea Mujat¹, Daniel Ferguson¹, Nicusor Iftimia¹; ¹Physical Sciences Inc., USA; ²Lucid, Inc, USA; ³Memorial Sloan Kettering Cancer Center, USA. We report a hand-held probe combining high-resolution reflectance confocal microscopy (RCM) and optical coherence tomography (OCT) within the same optical path. Probe development and preliminary testing is being discussed.

ATu1P.3 • 11:45  

In vivo Imaging of Nanoparticle Delivery and Tumor Microvasculature with Multimodal Optical Coherence Tomography, Melissa Skala¹; ¹Biomedical Engineering, Vanderbilt Univ., USA. Photothermal OCT is used to monitor gold nanoparticle delivery in tumors with co-registered speckle variance OCT of vascular morphology. This work demonstrates multimodal OCT as a tool to optimize in vivo drug delivery platforms.

Technical Digest and Postdeadline Papers Available Online

- Visit www.cleoconference.org
- Select **Download Digest Paper** button
- Use your email address and CLEO Registration ID # to synchronize

Once you have synchronized your conference registration with Optics InfoBase, you can log in directly to Optics InfoBase at any point using the same email address and OSA password.

Access must be established via synchronization within 60 days of the conference start date. Access is provided only to full technical attendees.

CLEO: QELS-Fundamental Science

FTu1A • Symposium on
Quantum Repeaters I—
Continued

FTu1A.5 • 12:30

Long range quantum key distribution using frequency multiplexing in broadband solid state memories, Hari Krovi¹, Zachary Dutton¹, Saikat Guha¹, Chris Fuchs¹, Wolfgang Tittel², Christoph Simon², Joshua A. Slater², Khabat Heshami², Morgan P. Hedges², Gregory S. Kanter³, Yu-Ping Huang³, Charles Thiel⁴, ¹Raytheon BBN Technologies, USA; ²Univ. of Calgary, Canada; ³Northwestern Univ., USA; ⁴Montana State Univ., USA. We present simulations of rates for a quantum key distribution scheme using a frequency multiplexed repeater architecture with broadband solid-state quantum memories. We find that key can be generated over 1000 km with eight elementary links.

FTu1A.6 • 12:45

Quantum Repeater for Spectrally Entangled Photons, Warren P. Grice¹, Raphael Pooser¹, Brian P. Williams², ¹Oak Ridge National Lab, USA; ²Univ. of Tennessee, USA. We describe a quantum repeater architecture for spectrally entangled photons based on sum frequency. The repeater, which does not require a conventional quantum memory, includes a novel scheme for re-using unconverted photons.

FTu1B • Dynamics in
Semiconductor Quantum
Wells—Continued

FTu1B.6 • 12:15

Observation and manipulation of dipole-forbidden exciton transitions in semiconductors, Lukas Schneebeli¹, Christoph N. Boettge¹, Benjamin Breddermann¹, Mackillo Kira¹, Stephan W. Koch¹, William D. Rice^{2,3}, Junichiro Kono^{2,3}, Sabine Zybell^{4,5}, Stephan Winnerl⁴, Jayeeta Bhattacharyya⁴, Faina Esser^{4,5}, Harald Schneider⁴, Manfred Helm^{4,5}, Benjamin Ewers¹, Alexej Chernikov¹, Martin Koch¹, Sangam Chatterjee¹, Galina Khitrova⁶, Hyatt Gibbs⁶, Aaron M. Andrews⁷, Gottfried Strasser⁷, ¹Dept of Physics and Material Sciences Center, Philipps-Univ., Germany; ²Dept of Electrical and Computer Engineering, Rice Univ., USA; ³Dept of Physics and Astronomy, Rice Univ., USA; ⁴Helmholtz-Zentrum Dresden-Rossendorf, Germany; ⁵Technische Universitaet Dresden, Germany; ⁶College of Optical Science, Univ. of Arizona, USA; ⁷Inst. of Solid State Electronics, Technische Universitaet Wien, Austria. We discuss recent experimental and theoretical results that report on the observation of dipole-forbidden intra-exciton transitions in semiconductors via terahertz excitation. Additional manipulation capabilities are gained through the application of a magnetic field.

FTu1B.7 • 12:30

Indirect Excitons in High Magnetic Fields, Yuliya Y. Kuznetsova¹, Eric V. Calman¹, Leonid Butov¹, Kenneth Campman², Arthur Gossard², ¹Dept of Physics, Univ. of California at San Diego, USA; ²Materials Dept, Univ. of California at Santa Barbara, USA. Transport, relaxation, and correlation effects are observed for indirect excitons in high magnetic fields.

FTu1B.8 • 12:45

Terahertz Time-Domain Magnetospectroscopy Using a Table-Top Repetitive Pulsed Magnet, Gary T. Noe II¹, Qi Zhang¹, Joseph Lee¹, Eiji Kato², Hiroyuki Nojiri³, Gary Woods¹, Junichiro Kono¹, ¹Electrical and Computer Engineering, Rice Univ., USA; ²Advantest America, Inc., USA; ³Inst. for Materials Research, Tohoku Univ., Japan. We have observed coherent cyclotron resonance oscillations from a two-dimensional electron gas by combining a rapid scanning terahertz time-domain spectrometer with a table-top mini-coil pulsed magnet.

FTu1C • Novel Optics II—
Continued

FTu1C.5 • 12:15

UV & Visible Plasmonic Metamaterials Made of Topological Insulator, Jun-Yu Ou¹, Jin-Kyu So¹, Giorgio Adamo², Azat Sulae³, Lan Wang³, Nikolay I. Zheludev^{1,2}; ¹Optoelectronics Research Centre & Centre for Photonic Metamaterials, Univ. of Southampton, UK; ²Centre for Disruptive Photonic Technologies, Nanyang Technological Univ., Singapore; ³School of Physical and Mathematical Sciences, Nanyang Technological Univ., Singapore. Plasmonic resonances are observed in metamaterials made of a topological insulator, Bi_{1.5}Sb_{0.5}Te_{1.8}Se_{1.2}, at the UV and visible frequencies due to the material's interband transition and nontrivial surface conducting state.

FTu1C.6 • 12:30

Electrically Tunable Mid-Infrared Metamaterials Based on Strong Light-Matter Coupling, Alexander Benz^{1,2}, Ines Montano², John F. Klem², Igal Brener^{1,2}; ¹Center for Integrated Nanotechnologies (CINT), Sandia National Labs, USA; ²Sandia National Labs, USA. We present an actively tunable mid-infrared metamaterial operating in the strong light-matter coupling regime. We can tune the upper polariton branch continuously over 8% of the center frequency by applying 5 V.

FTu1C.7 • 12:45

Dielectric meta-atoms coupled by non-resonant metallic antennas: high-quality resonances, Aditya Jain¹, Philippe Tassin^{2,1}, Thomas Koschny¹, Costas Soukoulis^{1,3}; ¹Ames Lab-U.S. DOE and Dept of Physics, Iowa State Univ., USA; ²Dept of Applied Physics, Chalmers Univ., Sweden; ³Inst. of Electronic Structure and Lasers, FORTH, Greece. We demonstrate a new class of metamaterials with dielectric meta-atoms coupled to the incident waves by nonresonant metallic antennas. The storage of energy in the dielectric enables high-quality resonances in negative-permittivity and negative-permeability sheet metamaterials.

FTu1D • Strong-Field Physics—
Continued

FTu1D.3 • 12:15

Two Color Interferences and Quantum Phase Shifts in Above Threshold Ionization, Lucas Zipp^{1,2}, Adi Natan^{1,2}, Philip H. Bucksbaum^{1,2}; ¹Pulse Inst., Stanford/SLAC, USA; ²Physics, Stanford, USA. The two color ($\omega+2\omega$) above threshold ionization spectrum of argon is measured at different intensity ratios and relative optical phase. We observe quantum phase shifts between interfering ionization pathways, indicating electron dispersion in strong-field ionization.

FTu1D.4 • 12:30

Extraction of Elastic Scattering Cross Sections from Half-Cycle Cutoffs in Photoelectron Spectra, Henning Geiseler¹, Nobuhisa Ishii¹, Keisuke Kaneshima¹, Kenta Kitano¹, Teruto Kanai¹, Jiro Itatani¹; ¹Inst. for Solid State Physics, Univ. of Tokyo, Japan. We observe half-cycle cutoffs in above-threshold ionization spectra using carrier-envelope phase-stabilized, sub-two-cycle infrared pulses. The waveform-dependent photoelectron spectra allow the retrieval of a resonance-like structure in the cross section for elastic backscattering from Xe⁺.

FTu1D.5 • 12:45

Carrier-envelope phase sensitive strong-field photoemission from plasmonic nanoparticles, William Putnam¹, Richard Hobbs¹, Yujia Yang¹, Karl K. Berggren¹, Franz Kärtner^{1,2}; ¹Electrical Engineering and Computer Science and Research Lab of Electronics, MIT, USA; ²Center for Free-Electron Laser Science, DESY and Univ. of Hamburg, Germany. Strong-field photoemission from plasmonic nanoparticles is demonstrated on the surface of a chip under ambient conditions. The photoemission shows a carrier-envelope phase-sensitive component with a 27 dB signal-to-noise ratio at a 0.78 Hz resolution bandwidth.

13:00–14:00 Lunch and Unopposed Exhibit Only Time, Exhibit Halls 1 & 2 (concessions available)

14:00–16:00 Market Focus Session II:
The Solid-State Lighting Revolution: How LEDs are Transforming the \$75 Billion Lighting Market, Exhibit Hall Theater

CLEO: Science & Innovations

STu1E • Applications of fs Lasers—Continued

STu1E.3 • 12:15

Nanometer-Scale Structuring of Gold Thin-Films and Graphene by Femtosecond Laser Bessel Beams, Ramazan Sahin¹, Ergun Simsek², Selcuk Akturk¹; ¹Dept of Physics, Istanbul Technical Univ., Turkey; ²Dept of Electrical and Computer Engineering, George Washington Univ., USA. We report nanometer-size patterning of various thin films by femtosecond pulsed Bessel beams. Nanoslit arrays fabricated on gold films exhibit excitation of surface plasmon polaritons. We extend the approach to single-atomic-layer systems such as graphene.

STu1E.4 • 12:30

Efficient Femtosecond Mid-infrared Pulse Generation by Dispersive Wave Radiation in Bulk Lithium Niobate Crystal, Binbin Zhou¹, Hairun Guo¹, Morten Bache¹; ¹Danmarks Tekniske Universitet, Denmark. We experimentally demonstrate efficient mid-infrared pulse generation by dispersive wave radiation in bulk lithium niobate crystal. Femtosecond Mid-IR pulses centering from 2.8-2.92 μm are generated using the single pump wavelengths from 1.25-1.45 μm .

STu1E.5 • 12:45

All-optical ultrafast control of SOI waveguide elements employing localized absorption, Roman Bruck¹, Otto L. Muskens¹; ¹Faculty of Physical Sciences and Engineering, Univ. of Southampton, UK. An on-chip technique for all-optical ultrafast control of silicon photonic elements was demonstrated by controlling transmission of SOI multimode interference-devices. Localized absorption by free carriers generated by ultraviolet pump pulses was used for achieving control.

STu1F • Manipulation & Detection of THz Radiation—Continued

STu1F.5 • 12:15

Measured THz pulse propagation between buildings, Eom-Bae Moon¹, Tae In Jeon¹, Daniel R. Grischkowsky²; ¹Electrical and Electronics Engineering, Korea Maritime and Ocean Univ., Republic of Korea; ²Electrical and Computer Engineering, Oklahoma State University, USA. We measured atmospheric propagation of broad-band THz ps pulses between two buildings separated by 79.3 m, using a mode-locked laser as an optical clock. Measurements with a precision of ± 0.1 ps were made in different weather conditions.

STu1F.6 • 12:30

Spectrally resolved measurements of the terahertz beam profile generated from a two-color air plasma, Pernille K. Pedersen¹, Maksim Zalkovskij¹, Andrew C. Strikwerda¹, Peter U. Jepsen¹; ¹DTU Fotonik, Technical Univ. of Denmark, Denmark. Using a THz camera and THz bandpass filters, we measure the frequency-resolved beam profile emitted from a two-color air plasma. We observe a frequency-independent emission angle from the plasma.

STu1F.7 • 12:45

Concentration of broadband terahertz radiation using a periodic array of conically tapered apertures, Shuchang Liu¹, Z. Vally Vardeny², Ajay Nahata¹; ¹Dept of Electrical and Computer Engineering, Univ. of Utah, USA; ²Dept of Physics and Astronomy, Univ. of Utah, USA. We describe the optical concentration properties of periodic arrays of conically tapered metallic apertures. We also discuss possible future transmission enhancement that utilize cascaded structures by tilting the apertures towards the array center.

STu1G • Integrated Components for Optical Communications—Continued

STu1G.5 • 12:15

Polarization-Diversified, Multichannel Orbital Angular Momentum (OAM) Coherent Communication Link Demonstration using 2D-3D Hybrid Integrated Devices for Free-Space OAM Multiplexing and Demultiplexing, Binbin Guan¹, Chuan Qin¹, Ryan P. Scott¹, Nicolas K. Fontaine², Tiejun Su¹, Roberto Proietti¹, S. J. Ben Yoo¹; ¹Univ. of California Davis, USA; ²Bell Labs, Alcatel-Lucent, USA. We present dual-polarization QPSK link transmission performance below the FEC limit with simultaneous transmission of three OAM states carrying 14 \times 10 GbD WDM channels using silica 2D-3D hybrid integrated devices for OAM state multiplexing/demultiplexing capacity of 1.68 Tb/s.

STu1G.6 • 12:30

Latch-to-Latch CMOS-Driven Optical Link at 28 Gb/s, Benjamin G. Lee¹, Seongwon Kim¹, Yoon Ho Daniel Lee^{2,1}, Jonathan E. Proesel¹, Christian W. Baks¹, Alexander V. Rylakov¹, Clint L. Schow¹; ¹IBM TJ Watson Research Center, USA; ²School of Electrical and Computer Engineering, Cornell Univ., USA. We demonstrate a 3.4-pJ/bit CMOS-driven VCSEL link incorporating latched half-rate inputs and outputs operating error-free at 28 Gb/s over a few meters of multimode fiber.

STu1G.7 • 12:45

25 Gb/s Data Transmission over a 1.4 m Long Multimode Polymer Spiral Waveguide, Nikos Bamiedakis¹, Richard V. Penty¹, Ian H. White¹, Petter Westbergh², Anders Larsson²; ¹Engineering Dept, Univ. of Cambridge, UK; ²Dept of Microtechnology and Nanoscience, Chalmers Univ. of Technology, Sweden. Data transmission studies of a 1.4m long multimode polymer spiral waveguide using an 850nm VCSEL are presented. Error-free 25 Gb/s data transmission is demonstrated over that waveguide length, achieving a record bandwidth-length product of 21GHz \times m.

STu1H • Plasmonic Devices—Continued

STu1H.5 • 12:15

Plasmonic Heating and Temperature-Sensing in the Terahertz Regime - Thermometry and Imaging, Rafik Naccache¹, Anna Mazhorova¹, Matteo Clerici^{1,2}, Luca Razzari¹, Firenze Vetrone¹, Roberto Morandotti¹; ¹Institut National de la Recherche Scientifique - Centre EMT, Canada; ²School of Engineering and Physical Sciences, Heriot-Watt Univ., UK. Resonant near-infrared excitation induces localized heating of colloidal gold nanorod dispersions. We show that detection and imaging are possible using Terahertz (THz) waves, which possess absorption and refractive indices sensitive to water temperature change.

STu1H.6 • 12:30

Giant Kerr Rotation Enhancement in Magneto-plasmonic Metamaterials, Evangelos Atmatzakis¹, Nikitas Papisimakis¹, Vassili A. Fedotov¹, Nikolay I. Zheludev^{1,2}; ¹Optoelectronics Research Centre, Univ. of Southampton, UK; ²Centre for Disruptive Photonic Technologies, Nanyang Technological Univ., Singapore. We report for the first time an order of magnitude enhancement of Kerr rotation in hybrid plasmonic/ferromagnetic metamaterial resonators. Our results pave the way towards magnetically controlled metamaterials and integrated magneto-plasmonics.

STu1H.7 • 12:45

Optical Exceptional Points at Nano and Macro Scales, Liang Feng^{1,2}, Xiang Zhang²; ¹Electrical Engineering, The State Univ. of New York at Buffalo, USA; ²UC Berkeley, USA. Here, we exploit implementation of optical losses to develop innovative optical phenomena and devices, for example, mimicking exceptional points and their unique transport characteristics in optics at both nano and macro scales.

13:00–14:00 Lunch and Unopposed Exhibit Only Time, Exhibit Halls 1 & 2 (concessions available)

14:00–16:00 Market Focus Session II:
The Solid-State Lighting Revolution: How LEDs are Transforming the \$75 Billion Lighting Market, Exhibit Hall Theater

CLEO: Science & Innovations

STu1I • Nonlinear Optical
Materials—Continued

STu1I.5 • 12:15

Fabrication of large-aperture PPMgLN device using X-axis Czochnralski-grown crystal, Hideki Ishizuki¹, Takunori Taira¹; ¹*Inst. for Molecular Science, Japan*. New PPMgLN arrangement fabricated from X-axis Czochnralski-grown crystal was proposed to improve a laser-beam distortion problem after passing the PPMgLN device. Availability of periodic poling in the new arrangement could be confirmed in 5-mm-thick MgLN.

STu1I.6 • 12:30

Growth of device quality orientation-patterned gallium phosphide (OPGaP) by improved hydride vapour phase epitaxy, Peter G. Schunemann¹, Lee Mohnkern¹, Alice Vera¹, Xiaoping S. Yang¹, Angie C. Lin², James S. Harris², Vladimir Tassev³, Michael R. Snure³; ¹*BAE Systems Inc, USA*; ²*Stanford Univ., USA*; ³*Sensors Directorate (AFRL/RDHD), Air Force Research Lab, USA*. Substantial increases in substrate temperature, super-saturation, and V/III ratio have dramatically improved vertical domain propagation during hydride vapour phase epitaxy of orientation-patterned gallium phosphide, leading to device-quality quasi-phases-matched layer thicknesses exceeding 400 μm .

STu1I.7 • 12:45

Mid-Infrared Difference-Frequency Generation in Suspended GaAs Waveguides, Todd H. Stievater¹, Rita Mahon¹, Doewon Park¹, William Rabinovich¹, Marcel Pruessner¹, Jacob Khurgin², Christopher J. K. Richardson²; ¹*US Naval Research Lab, USA*; ²*Lab for Physical Sciences, USA*; ³*Johns Hopkins Univ., USA*. We experimentally demonstrate mid-infrared difference frequency generation in suspended 181-nm thick GaAs waveguides. The extreme form-birefringence in the nanoslab waveguide enables phase-matching between the CW signal (1550 nm), pump (1025 nm), and idler (3000 nm).

STu1J • Short Reach
Communications—Continued

STu1J.6 • 12:15

Avalanche Photodiode (APD)-based PAM-16 4 Gb/s LED-POF Link, Xin Li¹, Nikos Bamiedakis¹, Jinlong Wei¹, Richard V. Pentyl¹, Ian H. White¹; ¹*Engineering Dept, Univ. of Cambridge, UK*. The use of an APD-based receiver in a PAM-16 4 Gb/s LED-POF link is shown to provide 10 dB greater link power budget over a PIN photodiode link. Error-free transmission is achieved over 25m SI-POF.

STu1J.7 • 12:30

Experimental Demonstration of a High-Dimension Quasi-Passive Reconfigurable (QPAR) Node, Yingying Bi¹, Jing Jin¹, Ahmad Dhaini¹, Leonid G. Kazovsky¹; ¹*Electrical Engineering, Stanford Univ., USA*. Quasi-Passive Reconfigurable (QPAR) devices can provide flexible power/wavelength distribution in next generation optical access networks. We experimentally demonstrate and analyze a high-dimension QPAR with one wavelength, four power levels and four output ports.

STu1J.8 • 12:45

Optical SSB Modulation Scheme Based on Phase-Modulator and Vertical-Cavity-Surface-Emitting Laser, Ching-Hung Chang¹, Jui-Hsuan Chang¹; ¹*Electrical Engineering, National Chiayi Univ., Taiwan*. A novel optical single sideband (OSSB) modulation scheme is proposed based on a phase-modulator (PM) and a tunable optical band pass filter (TOBPF) composed by a vertical-cavity surface-emitting laser (VCSEL) and an optical circulator (OC).

CLEO: QELS-
Fundamental ScienceFTu1K • Near-field Imaging
with Photons, Plasmons and
Electrons—Continued

FTu1K.6 • 12:15

Evidence of random Surface Plasmon modes in fractal metal films, Arthur Losquin¹, Sophie Camelio², David Rossouw³, Mondher Besbes⁴, Frédéric Pailloux², David Babonneau², Gianluigi A. Botton³, Jean-Jacques Greffet⁴, Odile Stéphan¹, Mathieu Kociak¹; ¹*Laboratoire de Physique des Solides, Université Paris-Sud, CNRS, France*; ²*Institut P, Université de Poitiers, CNRS, France*; ³*Dept of Materials Science and Engineering, McMaster Univ., Canada*; ⁴*Laboratoire Charles Fabry, Institut d'Optique, Université Paris-Sud, CNRS, France*. The extraordinary character of Surface Plasmon modes of disordered metallic systems has been predicted theoretically. We here demonstrate through Electron Energy Loss Spectroscopy that percolating fractal metal films sustain numerous strongly confined Surface Plasmon modes.

FTu1K.7 • 12:30

Electron energy-loss spectroscopy of surface plasmon modes in silver nanowires: reconciling experiment and theory, Xiuli Zhou¹, Andrew Herzing², Anton Hörl³, Andreas Trügler³, Ulrich Hohenester³, Theodore Norris¹; ¹*Center for Ultrafast Optical Science, Univ. of Michigan, USA*; ²*Material Measurement Laboratory, National Inst. of Standards and Technology, USA*; ³*Institut für Physik, Karl-Franzens-Univ. Graz, Austria*. Spectral shifts due to the excitation of higher-order modes occurred when an electric beam is directed near the silver nanowires. Three different theoretical approaches predict the main features of the observed spectra very well.

FTu1K.8 • 12:45

Spatially resolved characterization of gas-metallic nanoparticle interaction by energy loss spectroscopy in an environmental transmission electron microscope, John Kohoutek^{1,2}, Pin Ann Lin^{1,2}, Jonathan Winterstein¹, Henri J. Lezec¹, Renu Sharma¹; ¹*CNST, NIST, USA*; ²*IREAP, Univ. of Maryland, USA*. We use an environmental transmission electron microscope to identify gas adsorption sites for various concentrations of hydrogen and carbon monoxide on Au nanoparticles by collecting electron energy-loss spectra. Experimental results are consistent with simulation.

CLEO: Science &
InnovationsSTu1L • Mid-infrared Fiber
Lasers—Continued

STu1L.5 • 12:15

Graphene enabled 3 μm pulsed fiber lasers, Xiushan Zhu¹, Fengqiu Wang², Gongwen Zhu¹, Chen Wei¹, Yuanda Liu², Yongbing Xu², Kaushik Balakrishnan¹, Robert A. Norwood¹, Nasser Peyghambarian¹; ¹*Univ. of Arizona, USA*; ²*Nanjing Univ., China*. Graphene has emerged as innovative and effective saturable absorber for mid-infrared lasers. Pulsed erbium- and holmium-doped ZBLAN fiber lasers in the 3 μm region based on graphene saturable absorbers are reported.

STu1L.6 • 12:30

Superluminescent Fiber Laser Source in the Mid-Infrared via Dual-Pumping, Darren D. Hudson¹, Nikolas Iwanus¹, Tomonori Hu¹, Stuart Jackson¹; ¹*Univ. of Sydney, Australia*. By dual pumping the upper and lower laser level of the 516 \rightarrow 517 transition (2.9 μm) of Ho³⁺ we demonstrate a power-scalable fiber laser that can be modulated between continuous wave lasing and superluminescence.

STu1L.7 • 12:45


Mid-infrared Er:ZBLAN fiber lasers at 3.5 μm using dual wavelength pumping, Ori Henderson-Sapir¹, David J. Ottaway¹, Jesper Munch¹; ¹*Dept of Physics and Inst. for Photonics and Advanced Sensing (IPAS), Univ. of Adelaide, Australia*. An erbium doped ZBLAN glass fiber laser operating at 3.5 μm with an output power of 260mW at room temperature is reported. Substantial efficiency improvement is achieved by employing a novel dual wavelength pumping scheme.


13:00–14:00 Lunch and Unopposed Exhibit Only Time, Exhibit Halls 1 & 2 (concessions available)

14:00–16:00 Market Focus Session II:
The Solid-State Lighting Revolution: How LEDs are Transforming the \$75 Billion Lighting Market, Exhibit Hall Theater

CLEO: Science & Innovations

CLEO: Applications
& TechnologySTu1M • Applied Plasmonics—
Continued

STu1M.6 • 12:15  **Ultrathin Nanostructured Metals for Highly Transmissive Plasmonic Subtractive Color Filters**, Beibei Zeng¹, Yongkang Gao¹, Filbert Bartoli¹, ¹*Lehigh Univ., USA*. We present a systematic investigation of the counter-intuitive phenomenon of Extraordinary Low Transmission through ultrathin nanostructured metals, and present results on novel plasmonic subtractive color filters, exhibiting both record-high transmission efficiency and spatial resolution.

STu1M.7 • 12:30  **Plasmonic sub-wavelength phase-gradient meta-surfaces for real time dispersive imaging**, Yuewang Huang¹, Qiancheng Zhao¹, Salih K. Kalyoncu¹, Rasul Torun¹, Yumeng Lu¹, Filippo Capolino¹, Ozdal Boyraz¹, ¹*Univ. of California Irvine, USA*. We have designed and fabricated a sub-wavelength plasmonic deflector based on phase-gradient meta-surfaces for dispersion imaging at 1.55 μ m. We demonstrate dispersive imaging with <300 μ m resolution and 75.6% power efficiency by incorporating the fabricated plasmonic deflectors.

STu1M.8 • 12:45  **Strong Purcell enhancement of Er atoms embedded in a gold nano-trench**, Jung-Hwan Song¹, Hoon Jang¹, Yong-Hee Lee¹, ¹*Physics, Korea Advanced Inst. of Science and Technology, Republic of Korea*. We demonstrate large enhancement of spontaneous emission ($F_p > 70$) from Er atoms embedded in gold nano-trench structures. This is confirmed by clear correlation between increased decay rate and enhanced photoluminescence as a function of resonant wavelength.


STu1N • Mode-locked Fiber
Lasers—Continued


STu1N.6 • 12:15
A 380 fs, 40 GHz Mode-Locked Erbium Fiber Laser with an MQW Nonlinear PM/AM Modulator Using the Pockels Effect and the QCSE, Masataka Nakazawa¹, Masato Yoshida¹, Ken Tsuzuki², ¹*Tohoku Univ., Japan*; ²*NTT Photonics Labs, Japan*. We have successfully generated a 380 fs pulse train at 40 GHz from an actively mode-locked erbium fiber laser with an InGaAlAs/InAlAs MQW nonlinear PM/AM modulator using the Pockels effect and the quantum confined Stark effect.


STu1N.7 • 12:30
Cladding-pumped mode-locked fiber laser with a chirped fiber Bragg grating, Yi-Jing You¹, Alexey Zaytsev², Chih-Hsuan Lin¹, Ci-Ling Pan^{1,2}, ¹*Inst. of Photonics Technologies, National Tsing Hua Univ., Taiwan*; ²*Dept of Physics, National Tsing Hua Univ., Taiwan*. A mode-locked cladding-pumped Yb-doped fiber laser using a saturable Bragg reflector and a chirped fiber Bragg grating at 1064 nm wavelength can generate 170 mW of average power and 34 nJ of pulse energy.

STu1N.8 • 12:45
Sub-50 fs compressed pulses from a graphene-mode locked fiber laser, David Purdie¹, Daniel Popa¹, Valentin J. Wittwer¹, Zhe Jiang¹, Felice Torrisi¹, Andrea C. Ferrari¹, ¹*Cambridge Graphene Centre, Univ. of Cambridge, UK*. We demonstrate a graphene mode-locked fiber laser system generating 42 fs pulses with 53 mW output power, ideal for high temporal resolution applications.

STu1O • High Average
Power Lasers for Industrial
Applications—Continued

STu1O.3 • 12:15  **130 MW peak power femtosecond laser pulses in a Kerr lens mode-locked thin-disk ring oscillator**, Abdolreza Amani Eilanlou¹, Yasuo Nabekawa¹, Makoto Kuwata-Gonokami^{2,3}, Katsumi Midorikawa^{1,2}, ¹*Center for Advanced Photonics, RIKEN, Japan*; ²*Photon Science Center, The Univ. of Tokyo, Japan*; ³*Graduate School of Science, The Univ. of Tokyo, Japan*. We report generation of 860 W average power, 440 fs pulses in a 15.2 MHz thin-disk ring oscillator by placing a Kerr lens mode-locking setup in a low-pressure chamber.

STu1O.4 • 12:30  **High efficiency laser-diode-pumped continuous-wave Yb:YAG laser at room temperature**, Masatoshi Nishio¹, Sakae Kawato^{1,2}, AKIYUKI MARUKO¹, Naoya Shimojo¹, Hiroaki Okunishi¹, Kento Kato¹, Keisuke Kyomoto¹, Takeshi Yoshida¹, ¹*Fukui Univ., Japan*; ²*Univ. of Fukui, Japan*. A high-efficiency continuous-wave laser-diode-pumped Yb:YAG laser has been realized at room temperature by high intensity pumping. The slope efficiency and optical-to-optical conversion efficiency were 77% and 72% for the absorbed pump power, respectively.

STu1O.5 • 12:45  **Pulse Energy Scaling of Modelocked Oscillators: Moving from 80 μ J to >100 μ J from SESAM-modelocked Thin Disk Lasers**, Clara J. Saraceno^{1,2}, Florian Emaury¹, Cinia Schriber¹, Martin Hoffmann², Matthias Golling¹, Thomas Südmeyer², Ursula Keller¹, ¹*Dept of Physics, ETH Zurich, Switzerland*; ²*Dept of Physics - Time and frequency Lab, Univ. of Neuchâtel, Switzerland*. An Yb:YAG SESAM-modelocked thin-disk laser delivering 1.07ps pulses with record-high pulse energy of 80 μ J at 242W of average power is presented. Improved SESAM designs and nonlinearity limits are explored towards multi-100 μ J modelocked oscillators

ATu1P • Applications of Optical
Microscopy and Imaging—
Continued

ATu1P.4 • 12:15  **Visible light optical coherence tomography to quantify retinal blood oxygenation**, Ji Yi¹, Wenzhong Liu¹, Hao F. Zhang¹, ¹*Northwestern Univ., USA*. We presented the method of using visible-light optical coherence tomography (vis-OCT) for retinal oximetry. We demonstrated for the first time in vivo OCT measurement of the arterial and venous oxygenation in retinal circulation.

ATu1P.5 • 12:30  **Invited** **Searching for Biomarkers of Glaucoma using Adaptive Optics Scanning Ophthalmoscopy**, Alfredo Dubra¹, ¹*Medical College of Wisconsin, USA*. This presentation will review the latest linear microscopy techniques applied to imaging the living retina, as well as the normal and pathological retinal structures that can now be visualized non-invasively.

13:00–14:00 Lunch and Unopposed Exhibit Only Time, Exhibit Halls 1 & 2 (concessions available)

14:00–16:00 Market Focus Session II:
The Solid-State Lighting Revolution: How LEDs are Transforming the \$75 Billion Lighting Market, Exhibit Hall Theater

CLEO: QELS-Fundamental Science

14:00–16:00

FTu2A • Symposium on Quantum Repeaters II

Presider: Wolfgang Tittel; Inst. of Quantum Information, Univ. of Calgary, USA

FTu2A.1 • 14:00 **Invited**

Toward a quantum network based on semiconductor quantum dots, Olivier Gazdano¹, Anna Kamila Nowak¹, Valérie Giesz¹, Vivien Loo¹, Christophe Arnold¹, Simone L. Portalupi¹, Justin Demory¹, Marcelo P. Almeida², Andrew G. White², Claudio Dal Savio³, Pierre-François Braun³, Khaled Karrai³, Isabelle Sagnes¹, A. Lemaître¹, Loïc Lanco^{1,4}, Pascale Senellart¹; ¹CNRS-Laboratoire de Photonique et Nanost, France; ²Centre for Quantum Computer and Communication Technology, School of Mathematics and Physics, Univ. of Queensland, Australia; ³Attocube systems AG, attocube, Germany; ⁴Département de Physique, Université Paris Diderot, France. Recent advances in quantum dot based quantum technology are presented: scalable fabrication of bright sources of single photons or entangled photon pairs, optical non-linearities at the few photon scales and first implementations of quantum gates.

FTu2A.2 • 14:30

Quantum dot spin-photon interface and teleportation from a photon to a spin, Weibo Gao¹, Parisa Fallahi¹, Emre Togan¹, Javier Miguel-Sanchez¹, Atac Imamoglu¹; ¹Inst. of Quantum Electronics, ETH Zurich, CH-8093, Switzerland. Particularly in the frame of quantum information, my talk will focus on the optical manipulation of a quantum dot spin; the creation of entanglement between a flying photon and a semiconductor quantum dot spin; and the photon-to-spin teleportation experiment.

14:00–16:00

FTu2B • Optical Properties of Low-Dimensional Materials

Presider: Steven T. Cundiff, Univ. of Colorado at Boulder JILA, USA

FTu2B.1 • 14:00

Cavity Optomechanics with Suspended Carbon Nanotubes, Mian Zhang¹, Arthur Barnard², Paul L. McEuen^{2,3}, Michal Lipson^{1,3}; ¹Electrical and Computer Engineering, Cornell Univ., USA; ²Lab of Atomic and Solid State Physics, Cornell Univ., USA; ³Kavli Inst. at Cornell, Cornell Univ., USA; ⁴Instituto de Física Gleb Wataghin, Universidade Estadual de Campinas, Brazil. We demonstrate large optomechanical coupling between a carbon nanotube and an optical microresonator. We measured a dominantly dissipative optomechanical coupling coefficient of $g_c = 1$ MHz/nm

FTu2B.2 • 14:15

Observation of rapid carrier relaxation in graphene oxide probed by ultrafast terahertz spectroscopy, Jaeseok Kim¹, Juyeong Oh², Chihun In¹, Yun-Shik Lee³, Theodore B. Norris⁴, Seong Chan Jun², Hyunyoung Choi¹; ¹School of Electrical and Electronic Engineering, Yonsei Univ., Republic of Korea; ²Dept of Mechanical Engineering, Yonsei Univ., Republic of Korea; ³Dept of Physics, Oregon State Univ., USA; ⁴Dept of Electrical Engineering and Computer Science, Univ. of Michigan, Ann Arbor, USA. We investigate the carrier relaxation dynamics in graphene oxide (GO) using ultrafast optical-pump terahertz-probe spectroscopy. Unlike graphene, we observe the dynamics of GO show rapid percolation behaviors related to the multi-particle Auger scattering.

FTu2B.3 • 14:30

Characterization of Fast Temporal Photoresponse in a Broadband Graphene Photodetector, Ryan J. Suess¹, Xinghan Cai², Mohamad M. Jadidi¹, Andrei B. Sushkov², Gregory S. Jenkins², Jun Yan^{2,3}, Luke O. Nukit¹, Rachel L. Myers-Ward², D Kurt Gaskill¹, Thomas E. Murphy¹, H Dennis Drew², Michael S. Fuhrer^{2,4}; ¹Inst. for Research in Electronics & Applied Physics, Univ. of Maryland, USA; ²Dept of Physics, Center for Nanophysics & Advanced Materials, Univ. of Maryland, USA; ³Dept of Physics, Univ. of Massachusetts, USA; ⁴Texas A&M Univ., USA; ⁵U.S. Naval Research Lab, USA; ⁶School of Physics, Monash Univ., Australia. The temporal response of a broadband, monolayer graphene photodetector based on the photothermoelectric effect is characterized. Pulse-coincidence and impulse response measurements indicate fast photodetection on the timescale of 10 ps.

14:00–16:00

FTu2C • Novel Anisotropic Structures

Presider: Jingbo Sun, State University of New York at Buffalo, USA

FTu2C.1 • 14:00

Photonic Hyper-Crystals, Evgenii E. Narimanov¹; ¹Purdue Univ., USA. We introduce a new "universality class" of artificial optical media - photonic hyper-crystals. These hyperbolic metamaterials with periodic spatial variation of dielectric permittivity on subwavelength scale, combine the features of optical metamaterials and photonic crystals.

FTu2C.2 • 14:15

Self-Assembled Tunable Photonic Hyper-Crystals, Vera Smolyaninova¹, Bradley Yost¹, David Lahneman¹, Evgenii Narimanov², Igor Smolyaninov³; ¹Towson Univ., USA; ²Birck Nanotechnology Centre, Purdue Univ., USA; ³ECE, Univ. of Maryland, USA. We demonstrate a novel artificial optical material, a "photonic hyper-crystal", which combines properties of hyperbolic metamaterials and photonic crystals. It is based on cobalt nanoparticle ferrofluid subjected to magnetic field.

FTu2C.3 • 14:30

Multi-Periodic Photonic Hyper-Crystals: Volume Plasmon Polaritons and the Purcell Effect, Viktoriia Babicheva^{1,2}, Ivan Iorsh², Alexey Orlov², Pavel A. Belov², Andrei Lavrinenko¹, Andrei Andryieuski¹, Sergei Zhukovsky^{1,2}; ¹Technical Univ. of Denmark, Denmark; ²National Research Univ. for Information Technology, Mechanics, and Optics, Russia. We theoretically demonstrate superior degree of control over volume plasmon polariton propagation and the Purcell effect in multi-period (4-layer unit cell) plasmonic multilayers, which can be viewed as multiscale hyperbolic metamaterials or multi-periodic photonic hyper-crystals.

14:00–16:00

FTu2D • Novel XUV/X-Ray Sources

Presider: Oliver Muecke; Deutsches Elektronen Synchrotron, Germany

FTu2D.1 • 14:00 **Invited**

Lightwave control of plasma mirrors, Rodrigo B. Lopez-Martens¹; ¹Laboratoire d'Optique Appliquée, ENSTA ParisTech, Ecole Polytechnique, CNRS UMR 7639, France. We show how tailored few-cycle lightwaves with near relativistic intensity (~1018W/cm²) can be used to control the attosecond electron dynamics of plasma mirrors and produce beam manifolds of fully synchronized attosecond EUV light pulses.

FTu2D.2 • 14:30

High Harmonic Generation of Fiber Laser Systems with more than 100 μW Average Power per Harmonic, Steffen Hädrich^{1,2}, Jan Rothhardt^{1,2}, Arno Klenke^{1,2}, Manuel Krebs¹, Armin Hoffmann¹, Oleg Pronin³, Vladimir Pervak³, Jens Limpert^{1,2}, Andreas Tünnermann^{1,4}; ¹Inst. of Applied Physics, Germany; ²Helmholtz-Institut Jena, Germany; ³Ludwig-Maximilian-Universität München, Germany; ⁴Fraunhofer Inst. of Applied Optics and Precision Engineering, Germany. Sub-30 fs pulses at 600 kHz (82 W) repetition rate are utilized for HHG. More than 30 μW average power are obtained for harmonics between H21-H33 and the strongest harmonic is H25 with 143 μW.

CLEO: Science & Innovations

14:00–16:00

STu2E • fs - Oscillators

Presider: Clara Saraceno, ETH Zurich, Switzerland

STu2E.1 • 14:00

37 fs - 1.5 W Kerr-lens mode-locked Yb:CALGO laser oscillator, Pierre Sevilano¹, Romain Dubrasquet^{1,2}, Frederic Druon³, Patrick Georges³, Dominique Descamps¹, Eric Cormier¹; ¹CELIA, France; ²Azur light System, France; ³Laboratoire Charles Fabry, France. Kerr-lens mode-locking (KLM) in Yb:CALGO has been demonstrated by means of a high-brightness optical pumping with an Yb: fiber laser. Stable 37 fs pulses are produced with an average power of 1.5 W.

STu2E.2 • 14:15

62 fs Pulse Generation from a SESAM Modelocked Yb:CALGO Thin Disk Laser, Andreas Diebold¹, Florian Emaury¹, Cinia Schriber¹, Matthias Golling¹, Clara J. Saraceno^{1,2}, Thomas Südmeyer², Ursula Keller¹; ¹Inst. of Quantum Electronics, ETH Zurich, Switzerland; ²Laboratoire Temps-Fréquence, Université de Neuchâtel, Switzerland. We present the shortest pulses of any modelocked thin disk laser (TDL): a SESAM modelocked Yb:CALGO TDL generates 62 fs pulse duration at 5.1 W average power and we present new noise characterization.

STu2E.3 • 14:30

Soliton Modelocking via Cascaded Quadratic Nonlinearities in a SESAM-modelocked Yb:CALGO Laser, Aline Sophie Mayer¹, Christopher R. Phillips¹, Alexander Klenner¹, Ursula Keller¹; ¹ETH Zurich, Switzerland. We present soliton modelocking based on cascading of quadratic nonlinearities using an LBO crystal in a SESAM-modelocked Yb:CaGdAlO₄ laser cavity, enabling pulse formation in the positive GDD-regime, reaching 114-fs pulses at 1.1-W average output power.

14:00–16:00

STu2F • THz Metamaterials and Plasmonics

Presider: Marco Rahm; Technische Universität Kaiserslautern, Germany

STu2F.1 • 14:00

Metamaterial Composite with an Ultra-Broadband Usable Range of over 25 Terahertz, Andrew C. Strikwerda¹, Maksim Zalkovskij¹, Alexander Krabbe¹, Dennis Lund Lorenzen¹, Andrei Lavrinenko¹, Peter U. Jepsen¹; ¹Dept of Photonics Engineering, Technical Univ. of Denmark, Denmark. Using a metamaterial composite, we demonstrate a bandpass filter that has only a single transmission mode from 0 to >25 THz. This usable bandwidth matches, or exceeds, that of currently used THz sources.

STu2F.2 • 14:15

Orbit Angular Momentum Multiplexing in 0.1-THz Free-space Communication via 3D Printed Spiral Phase Plates, Xuli Wei¹; ¹Wuhan National Lab for Optoelectronics, China. We present a proof of concept demonstration of THz free-space communication employing orbital angular momentum (OAM) multiplexing. Two different OAM modes are multiplexed and de-multiplexed in experiment via 3D printed spiral phase plates.

STu2F.3 • 14:30

Wavevector selective surface, Vassili A. Fedotov¹, Jan Wallauer², Markus Walther², Nikitas Papisimakis¹, Nikolay I. Zheludev^{1,3}, Evangelos Atmatzakis¹; ¹Optoelectronics Research Centre and Centre for Photonic Metamaterials, Univ. of Southampton, UK; ²Dept of Molecular and Optical Physics, Univ. of Freiburg, Germany; ³Centre for Disruptive Photonics Technologies, Nanyang Technological Univ., Singapore. Frequency selective surfaces are very well known and have been investigated in detail. Here we for the first time introduce the concept of a wavevector selective surface and demonstrate it experimentally.

14:00–16:00

STu2G • RF Photonics

Presider: Willie Ng; Univ. of Southern California, USA

STu2G.1 • 14:00

Master-Slave Locking of Optomechanical Oscillators Over A Long Distance, Shreyas Y. Shah¹, Mian Zhang¹, Michal Lipson^{1,2}; ¹School of Electrical and Computer Engineering, Cornell Univ., USA; ²Kavli Inst. at Cornell, Cornell Univ., USA. We show that two independent mechanical oscillators, placed ~3.2km apart, and separated in frequency by ~80kHz, can be locked in a master-slave configuration, using light. This scheme can be generalised for an arbitrary network configuration.

STu2G.2 • 14:15

Widely Tunable Dual-loop Optoelectronic Oscillator, Xiaopeng Xie¹, Tao Sun¹, Huanfa Peng¹, Cheng Zhang¹, Peng Guo¹, Lixin Zhu¹, Weiwei Hu¹, Zhangyuan Chen¹; ¹Peking Univ., China. We demonstrate a record widely tunable dual-loop optoelectronic oscillator with tunable band from 3.39 to 57.50 GHz. The single-side band phase noise is below -120 dBc/Hz at 10 kHz offset for all the measurement frequency points.

STu2G.3 • 14:30

On-chip Quasi-THz Bandwidth Microwave Photonic Phase Shifter based on a Waveguide Bragg Grating on Silicon, Maurizio Burla¹, Luis Romero Cortés¹, Ming Li², Xu Wang³, Lukas Chrostowski³, José Azaña¹; ¹Ultrafast Optical Processing group, Institut National de la Recherche Scientifique, Canada; ²Inst. of Semiconductors, Chinese Academy of Sciences, China; ³Dept of Electrical and Computer Engineering, Univ. of British Columbia, Canada. We experimentally demonstrate a continuously-tunable quasi-THz RF-photonics phase shifter based on a dual-phase-shifted waveguide Bragg grating on silicon. Phase shifts up to ~90° are demonstrated over the 16-20 GHz band, constrained only by instrumentation limitations.

14:00–16:00

STu2H • Controlling Light in Resonators and Photonic Crystals

Presider: Avi Zadok; Bar-Ilan Univ., Israel

STu2H.1 • 14:00

Optical Preparation of Stable Supercooled VO₂ Nanocrystals: A Route Towards Reconfigurable Photonic Devices for Telecom Wavelengths, Thorben Jostmeier¹, Johannes Zimmer², Helmut Karl³, Hubert J. Krenner², Markus Betz¹; ¹Experimentelle Physik 2, TU Dortmund Univ., Germany; ²Lehrstuhl für Experimentalphysik I and Augsburg Centre for Innovative Technologies (ACIT), Universität Augsburg, Germany; ³Lehrstuhl für Experimentalphysik IV, Universität Augsburg, Germany. Single-domain VO₂ nanocrystals in a fused silica matrix exhibit an extremely large thermally and/or optically induced hysteresis around room temperature. We demonstrate optical imprinting of persistent diffraction gratings and repetitive (>10⁴) cycling through the phase transition.

STu2H.2 • 14:15

Helium-Ion-Induced Radiation Damage in LiNbO₃ Thin Film Electro-Optic Modulators, Hsu-Cheng Huang¹, Jerry I. Dadap¹, Richard M. Osgood¹, Girish Malladi², Has-saram Bakhrut²; ¹Columbia Univ., USA; ²SUNY at Albany, USA. We study He⁺-induced radiation damage in 10-µm-thick LiNbO₃-thin-film modulators. Results show induced-strain, scattering from interstitials, and the degree of overlap between guided modes with damaged region result in degradation of device extinction ratio and V_{πL}.

STu2H.3 • 14:30

Scalable High-Frequency Silicon Carbide Optomechanical Microresonators, Xiyuan Lu¹, Jonathan Yiho Lee¹, Philip X.-L. Feng², Qiang Lin¹; ¹Univ. of Rochester, USA; ²Case Western Reserve Univ., USA. We demonstrate silicon carbide optomechanical microresonators with mechanical frequency up to 1.7GHz, mechanical quality above 5500 and optomechanical coupling around 100GHz/nm. The frequency can match the zero-field splitting of the defect spin in silicon carbide.

Meeting Room
211 B/D

CLEO: Science & Innovations

14:00–16:00
STu2I • All Optical and Quantum Signal Processing
Presider: Paulina Kuo; National Inst. of Standards and Technology, USA

STu2I.1 • 14:00 **Invited**
New Applications and Devices for Quantum Frequency Conversion, Kartik Srinivasan¹, Imad Agha^{1,2}, Serkan Ates^{1,2}, Marcelo I. Davanco¹, Yuxiang Liu^{1,2}; ¹Center for Nanoscale Science and Technology, NIST, USA; ²Maryland Nanocenter, Univ. of Maryland, USA. We review recent experiments demonstrating quantum frequency conversion (QFC) of single photon states of light and discuss perspectives for combining QFC with temporal wavepacket shaping. Progress in developing nanophotonic geometries for QFC is also presented.

STu2I.2 • 14:30
Effects of Raman scattering in quantum state-preserving frequency conversion, Søren M. Friis¹, Lasse Mejling¹, Mario A. Usuga¹, Anders T. Pedersen¹, Colin J. McKinstry², Karsten Rottwitt¹; ¹DTU Fotonik, Technical Univ. of Denmark, Denmark; ²Bell Labs, Alcatel-Lucent, USA. We analyse frequency conversion by Bragg scattering numerically including Raman scattering. The frequency configuration that performs the best under influence of Raman noise results in 95% conversion over a 3.25 THz bandwidth with a 2.5-dB noise figure.

Meeting Room
212 A/C

14:00–16:00
STu2J • Phase Sensitive Amplification and Optical Regeneration
Presider: Michael Vasilyev; Univ. of Texas at Arlington, USA

STu2J.1 • 14:00 **Invited**
Signal Regeneration Techniques for Advanced Modulation Formats, Francesca Parmigiani¹, Kyle R. Bottrill¹, Graham Hesketh¹, Peter Horak¹, Periklis Petropoulos¹, David J. Richardson¹; ¹Univ. of Southampton, UK. We review recent results on all-optical regeneration of phase encoded signals based on phase sensitive amplification achieved by avoiding phase-to-amplitude conversion in order to facilitate the regeneration of amplitude/phase encoded (QAM) signals.

STu2J.2 • 14:30
Multilevel amplitude regeneration of 256-symbol constellation, Mariia Sorokina¹; ¹Aston Univ., UK. We propose a novel scheme for multilevel (9 and more) amplitude regeneration based on nonlinear optical loop mirror and demonstrate its efficiency and cascadedability on 256-symbol constellation.

Meeting Room
212 B/D

CLEO: QELS-Fundamental Science

14:00–16:00
FTu2K • Plasmonic Waveguides, Lenses and Circuits
Presider: Henri Lezec; NIST, USA

FTu2K.1 • 14:00
Suspended MIM Optical Waveguides with Optical Nano-Antennas, Brian E. Edwards¹, Nader Engheta¹; ¹Electrical and Systems Engineering, Univ. of Pennsylvania, USA. In this work we experimentally demonstrate suspended gold-air-gold (MIM) plasmonic waveguides operating at the NIR wavelengths. The waveguide interfaces with the far field using optical nano-antennas with main beams normal to the structure.

FTu2K.2 • 14:15
Plasmonic antennas nanocoupler for telecom range: simulation, fabrication and near-field characterization, Andrei Andryieuski¹, Vladimir A. Zenin², Radu Malureanu¹, Valentyn S. Volkov², Sergey I. Bozhevolnyi², Andrei Lavrinenko²; ¹DTU Fotonik, Technical Univ. of Denmark, Denmark; ²Inst. of Technology and Innovation, Univ. of Southern Denmark, Denmark. We report simulation, fabrication and amplitude-phase near-field characterization in telecom range of the compact and efficient plasmonic antenna coupler to slot waveguide. Near-field data allowed measuring propagation losses and effective mode index that agree well with simulation results.

FTu2K.3 • 14:30
Linearly Dichroic Plasmonic Lens and Hetero-Chiral Structures, Grisha Spektor¹, Asaf David¹, Bergin Gjonaj¹, Lior Gal¹, Meir Orenstein¹; ¹Electrical Engineering, Technion, Israel. We present an experimental study of plasmonic Hetero-Chiral structures, comprised of constituents with opposite chirality. We show selective focusing of orthogonal polarization states, standing plasmonic 'vortex fields' and more.

Marriott
Salon I & II

CLEO: Applications & Technology

14:00–16:00
ATu2L • Symposium on Laser Processing for Consumer Electronics I **▶**
Presider: Eric Mottay; Amplitude Systemes, France

ATu2L.1 • 14:00 **Invited** **▶**
Ultrafast laser processing and metrology, Keiji Nomaru¹, Hiroshi Morikazu¹, Kunimitsu Takahashi¹; ¹Laser Engineering, DISCO Corporation, Japan. Precisely controlled blind vias were formed in multilayer substrates by an ultrafast laser. A LIBS detector integrated into the laser processing machine realizes the full potential of the ultrafast laser.

ATu2L.2 • 14:30 **Invited** **▶**
Opaque Film Metrology using PULSE Technology, Manjusha Mehendale¹; ¹Rudolph Technologies, USA. PULSE Technology™ involves generation and detection of acoustic waves in opaque layers using ultrafast laser pulses. Its application in advanced semiconductor and packaging industry for single and multi-layer thin film metrology is presented above

Download the
CLEO
Mobile App

Search for CLEO:2014
in the app stores or
scan the QR code




CLEO: Science & Innovations

CLEO: Applications
& Technology

14:00–16:00

STu2M • Novel Concepts in
Nanophotonics *Presider: Thomas Mueller, Vienna
Univ of Tech., Austria*STu2M.1 • 14:00  

Photonic Topological Insulators, Mordechai Segev¹, Yonatan Plotnik¹, Mikael Rechtsman¹, Yaakov Lumer¹, Miguel A. Bandres¹, Julia M. Zeuner², Alexander Szameit²; ¹Technion Israel Inst. of Technology, Israel; ²Inst. of Applied Physics, Abbe Center of Photonics, Friedrich-Schiller-Universität Jena, Germany. We review the recent progress on the first experimental demonstration of photonic topological insulators, along with a variety of new ideas associated with it.

STu2M.2 • 14:30 

Topological Edge States in Silicon Photonics, Sunil Mittal¹, Jingyun Fan¹, Alan L. Migdall¹, Jacob Taylor¹, Mohammad Hafezi¹; ¹Joint Quantum Inst., Univ. of Maryland, College Park / National Inst. of Standards and Technology, Gaithersburg, USA. We demonstrate the robustness of topological edge states in a photonic system of coupled microring resonators. Using direct imaging and transmission analysis, we show that the edge states are robust to lattice disorders.

14:00–16:00

STu2N • High Power Pulsed
Fiber Lasers*Presider: Akira Shirakawa; Univ. of
Electro-Communications, Japan*

STu2N.1 • 14:00

300W monolithic actively Q-switched fiber laser at 1064 nm, Wei Shi^{1,2}, Qiang Fang^{2,3}, Xueping Tian³, Jingli Fan³; ¹Tianjin Univ., China; ²Tianjin Inst. of Modern Laser & Optics Technology, China; ³Shandong HFB Photonics Co. Ltd., China. We report a high power monolithic nanosecond pulsed fiber laser at 1064nm in MOPA configuration. More than 300W average power was achieved for 475 ns pulses at repetition rate of 100 kHz.


STu2N.2 • 14:15

700kW peak power monolithic nanosecond pulsed fiber laser, Wei Shi^{1,2}, Qiang Fang^{2,3}, Jingli Fan³; ¹Tianjin Univ., China; ²Tianjin Inst. of Modern Laser & Optics Technology, China; ³Shandong HFB Photonics Co. Ltd., China. We report a high peak power monolithic nanosecond pulsed fiber laser in MOPA configuration. The system can produce ~ 709 kW peak power for 3.3 ns fiber laser pulses at 10 kHz repetition rate.

STu2N.3 • 14:30

High Power Er-doped Yb-free Double-Clad Fiber Amplifiers, Leonid V. Kotov^{1,2}, Mikhail E. Likhachev¹, Mikhail M. Bubnov¹, Denis S. Lipatov³, Mikhail V. Yashkov³, Aleksei N. Guryanov³, Sébastien Février⁴, Jérôme Lhermite⁵, Eric Cormier⁵; ¹Fiber Optics Research Center RAS, Russia; ²Moscow Inst. of Physics and Technology, Russia; ³Inst. of Chemistry of High Purity Substances RAS, Russia; ⁴XLIM, UMR 7252 CNRS - Univ. of Limoges, France; ⁵CeLIA, Université Bordeaux 1, CNRS UMR 5107, France. We present simple and efficient laser schemes based on newly developed Er-doped fibers cladding pumped at 976 nm. 103 W CW-power amplifier with 37 % conversion efficiency and 1.5 mJ-pulse energy nanosecond laser were demonstrated.

14:00–16:00


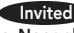
STu2O • Symposium on
Microcavity Exciton-Polaritons,
Devices and Applications I *Presider: Vinod Menon; CUNY
Queens College, USA*STu2O.1 • 14:00  

Persistent Current of a Microcavity Polariton Condensate in a Ring Geometry, David W. Snoke¹, Gangqiang Liu¹, Andrew Daley², Loren N. Pfeiffer³, Kenneth W. West³; ¹Univ. of Pittsburgh, USA; ²Strathclyde Univ., UK; ³Princeton Univ., USA. We have created microcavity polaritons with a lifetime of about 200 ps, which allows them to condense in the ground state of a ring trap. Optical measurements show they have quantized vorticity.


STu2O.2 • 14:30 

Stimulated polariton emission from ZnO nanoparticles based microcavity, Xiaozhe Liu^{1,2}, Kannatassen Appavoo³, Matthew Sfeir³, Stéphane Kéna-Cohen⁴, Vinod M. Menon^{1,2}; ¹Dept. of Physics, Graduate School and Univ. Center of the City Univ. of New York, USA; ²Dept. of Physics, Queens College of the City Univ. of New York, USA; ³Center for Functional Nanomaterials, Brookhaven National Lab, USA; ⁴Dept. of Engineering Physics, École Polytechnique de Montréal, Canada. We demonstrate stimulated polariton emission at room temperature in a dielectric microcavity embedded with ZnO nanoparticles. The polariton lifetime is also shown to decrease drastically above the stimulated emission threshold.

14:00–16:00

ATu2P • Symposium on Novel
Light Sources and Photonic
Devices in Optical Imaging I *Presider: Benjamin Vakoc;
Harvard Medical School, USA*ATu2P.1 • 14:00 

Advancements in Nanophotonic-Based Optical Coherence Tomography, Nicholas Sherwood¹, Kyle J. Preston¹, Arthur Nitkowski¹, Nitin Kalra¹, Arsen R. Hajian², Bradley S. Schmidt²; ¹Tornado Spectral Systems, USA; ²Tornado Spectral Systems, Canada. In 2013, TSS introduced the OCTANE-860, the first chip-based nanophotonic spectrometer for Spectral-Domain OCT. Challenges and benefits have been identified during development and a new strategy for optimizing performance will be discussed.

ATu2P.2 • 14:30 

Next Generation Swept-sources for OCT and Other Applications, Brian Goldberg¹; ¹AXSUN Technologies Inc, USA. We report on recent progress in the design and understanding of next-generation swept sources and systems for optical coherence tomography and discuss methods for tailoring lasers for specific swept source OCT applications.

CLEO: QELS-Fundamental Science

FTu2A • Symposium on
Quantum Repeaters II—
Continued

FTu2A.3 • 14:45

Spectrally multiplexed solid-state memories for quantum repeaters, wolfgang tittel¹, Neil Sinclair¹, Erhan Saglamyurek¹, Hassan Mallazahdeh¹, Joshua A. Slater¹, Mathew George², Raimund Ricken², Morgan P. Hedges¹, Daniel Oblak¹, Wolfgang Sohler²; ¹Physics and Astronomy, Univ. of Calgary, Canada; ²Physics, Univ. of Paderborn, Germany. We present experimental work that demonstrates frequency-multiplexed quantum state storage in solid-state quantum memories with readout on demand.

FTu2A.4 • 15:00

Quantum teleportation from a telecom-wavelength photon to a solid-state quantum memory, Felix Bussières¹, Christoph Clausen¹, Alexey Tiranov¹, Boris A. Korzh¹, Varun B. Verma², Sae Woo Nam², Francesco Marsili³, Alban Ferrier⁴, Philippe Goldner¹, Harald Herrmann⁵, Christine Silberhorn⁵, Mikael Afzelius¹, Nicolas Gisin¹; ¹Group of Applied Physics, Univ. of Geneva, Switzerland; ²National Inst. of Standards and Technology, USA; ³Jet Propulsion Lab, California Inst. of Technology, USA; ⁴Chimie ParisTech, CNRS-UMR 7574, UPMC Univ Paris 06, France; ⁵Applied Physics / Integrated Optics Group, Univ. of Paderborn, Germany. We demonstrate quantum teleportation of the polarization state of a telecom-wavelength photon onto the state of a solid-state quantum memory. The fidelity exceeds the classical bound with transmission over 25 km of optical fibre.

FTu2A.5 • 15:15

Heralded single photon storage in a room-temperature, broadband quantum memory, Patrick Michelberger¹, Joshua Nunn¹, Theresa F. Champion¹, Michael R. Sprague¹, Krzysztof Kaczmarek¹, Dylan Saunders¹, William S. Kolthammer¹, Xian-Min Jin¹, Duncan England², Ian A. Walmsley¹; ¹Physics Dept, Univ. of Oxford, UK; ²National Research Council of Canada, Canada. We demonstrate storage of heralded single photons in a room-temperature quantum memory, a key step towards scalable quantum networks. We evaluate the photon statistics of the stored photons and discuss limitations from four-wave mixing noise.

FTu2B • Optical Properties of
Low-Dimensional Materials—
ContinuedFTu2B.4 • 14:45 **Invited**

Optoelectronics of 2D-Semiconductors, Xiadong Xu¹; ¹Univ. of Washington, USA. Newly discovered 2D semiconductors offer a platform to investigate valley excitons at the two dimensional limit. Here, we present optoelectronic control of valley exciton polarization and coherence, and their device applications in monolayer limit.

FTu2B.5 • 15:15

Ultrafast optical microscopy of single monolayer molybdenum disulfide flakes, Minah Seo^{1,2}, Hisato Yamaguchi², Aditya Mohite², Stephane Boubanga-Tombet², Antoinette Taylor², Rohit P. Prasankumar²; ¹Korea Inst. of Science and Technology, Republic of Korea; ²Los Alamos National Lab, USA. We use ultrafast optical microscopy to investigate carrier dynamics in single flakes of atomically thin molybdenum disulfide. By tuning the probe wavelength through the bandgap, we reveal the influence of layer thickness on carrier dynamics.

FTu2C • Novel Anisotropic
Structures—Continued

FTu2C.4 • 14:45

Manipulating Microwave Signals Using Plasma-Based Metamaterial Structures in Air, Scott Will¹, Zhaxylyk A. Kudyshv¹, Natalia M. Litchinitser¹; ¹Electrical Engineering, Univ. at Buffalo, USA. In this work, we theoretically and numerically demonstrate several new plasma filament-based structures used for increasing the angular and range resolution of microwave radar systems, and show that they can survive in adverse environments.

FTu2C.5 • 15:00

Coherent Control of Birefringence and Optical Activity, Seyedmohammad A. Mousavi¹, Eric Plum¹, Jinhui Shi^{1,2}, Nikolay I. Zheludev^{1,3}; ¹Optoelectronics Research Centre, Univ. of Southampton, UK; ²College of Science, Harbin Engineering Univ., China; ³Centre for Disruptive Photonic Technologies, Nanyang Technological Univ., Singapore. Control of polarization of light with light is demonstrated in thin slabs of linear material promising ultrafast all-optical data processing at arbitrarily low intensities. In proof-of-principle experiments we access any polarization azimuth and any ellipticity.

FTu2C.6 • 15:15

Polarization-Dependent One-way Surface Wave Propagation, Fereshteh Abbasi¹, Arthur Davoyan¹, Alexander Schuchinsky², Nader Engheta¹; ¹Dept of Electrical and Systems Engineering, Univ. of Pennsylvania, USA; ²The Inst. of Electronics, Communications and Information Technology, Queen's Univ., Ireland. We numerically study nonreciprocal regimes of surface plasmon-polariton at the interface between two gyrotropic media. We predict existence of isolated unidirectional TE and TM surface modes guided by the interface between gyroelectric and gyromagnetic media.

FTu2D • Novel XUV/X-Ray
Sources—Continued

FTu2D.3 • 14:45

Power-Scalable and Efficient Geometric XUV Output Coupling for Cavity-Enhanced High-Harmonic Generation, Simon Holzberger^{1,2}, Maximilian Högner^{1,2}, Johannes Weitenberg³, Dominik Esser⁴, Tino Eidam⁵, Jens Limpert⁵, Andreas Tünnermann⁵, Ernst Fill^{1,2}, Ferenc Krausz^{1,2}, Vladislav S. Yakovlev^{1,2}, Ioachim Pupeza^{1,2}; ¹Max-Planck-Institute of Quantum Optics, Germany; ²Ludwig-Maximilians-Universität München, Germany; ³Lehrstuhl für Lasertechnik, RWTH Aachen Univ., Germany; ⁴Fraunhofer-Institut für Lasertechnik, Germany; ⁵Inst. of Applied Physics, Friedrich Schiller Univ. Jena, Germany. We demonstrate cavity-enhanced HHG with a tailored transverse mode simultaneously allowing for efficient conversion to the XUV and for unparalleled output coupling efficiencies. Due to its purely geometric nature, this method is power scalable.

FTu2D.4 • 15:00

Femtosecond Time-and-Angle-Resolved EUV Photoemission Spectroscopy with Mid-IR Pumping, Cephise M. Cacho¹, Jesse C. Petersen^{2,3}, Isabella Gierz², Haiyun Liu³, Stefan Kaiser³, Richard Chapman¹, Edmond Turcu¹, Andrea Cavalleri^{2,3}, Emma Springate¹; ¹Central Laser Facility, STFC Rutherford Appleton Lab, UK; ²Clarendon Lab, Univ. of Oxford, UK; ³Max Planck Inst. for the Structure and Dynamics of Matter, Germany. Time- and angle-resolved photoemission spectroscopy directly enables observation of electron dynamics in condensed matter. Using EUV high harmonic probe extends the observation window in energy and momentum. Tunable mid-infrared pumping allows control of excitation mechanisms.

FTu2D.5 • 15:15

Ultra-High Energy Density Relativistic Plasmas and X-ray Generation by Ultrafast Laser Irradiation of Nanowire Arrays, Michael Purvis¹, Jorge Rocca¹, Reed Hollinger¹, Clayton Bargsten¹, Vyacheslav Shlyaptsev¹, Brad Luther¹, Alexander Pukhov², Carmen S. Menoni¹, Yong Wang¹, Liang Yin¹, Amy Prieto¹, Amanda Townsend¹, David Keiss¹; ¹Electrical and Computer Engineering, Colorado State Univ., USA; ²Institut für Theoretische Physik, Heinrich-Heine-Universität, Germany. We demonstrate that trapping of femtosecond laser pulses of relativistic intensity deep within nanowire arrays volumetrically heats matter into a new ultra-hot plasma regime with electron densities nearly 100 times critical and multi-keV temperatures.

CLEO: Science & Innovations

STu2E • fs - Oscillators—
Continued

STu2E.4 • 14:45

Dual-Gain SESAM Modelocked Thin Disk Laser Combining the Emission Spectra of Yb:Lu2O3 and Yb:Sc2O3 Laser Crystals, Cinia Schriber¹, Florian Emaury¹, Kolja Beil², Matthias Golling¹, Clara J. Saraceno^{1,4}, Christian Kraenkel^{2,3}, Thomas Südmeyer⁴, Ursula Keller¹; ¹Inst. of Quantum Electronics, ETH Zurich, Switzerland; ²Inst. of Laser Physics, Univ. of Hamburg, Germany; ³Hamburg Centre for Ultrafast Imaging, Germany; ⁴Laboratoire Temps-Frequence, Univ. of Neuchâtel, Switzerland. We present the first dual-gain SESAM-modelocked thin-disk laser. Using Yb-doped sesquioxide crystals with 8 nm shifted emission peaks, we achieve large overall bandwidth from crystals with excellent thermo-mechanical properties and generate 138-fs pulses in proof-of-principle experiments.

STu2E.5 • 15:00

Mode-locking of a diode-pumped Yb:CLNGG laser using single-walled carbon nanotube saturable absorber, Yuangeng Zhang^{1,2}, Valentin Petrov¹, Uwe Griebner¹, Xingyu Zhang², Sun Y. Choi³, Ji Yoon Gwak³, Fabian Rotermund³, Xavier Mateos⁴, Haohai Yu⁵, Huaijin Zhang⁶, Junhai Liu⁴; ¹Max-Born-Inst. for Nonlinear Optics and Ultrafast Spectroscopy, Germany; ²School of Information Science and Engineering, and Shandong Provincial Key Lab of Laser Technology and Application, Shandong Univ., China; ³Dept of Physics & Division of Energy Systems Research, Ajou Univ., Republic of Korea; ⁴Física i Cristallografia de Materials, Universitat Rovira i Virgili, Spain; ⁵State Key Lab of Crystal Materials, Shandong Univ., China; ⁶College of Physics, Qingdao Univ., China. A diode-pumped Yb:CLNGG laser is mode-locked with a single-walled carbon nanotube saturable absorber achieving pulse durations as short as 90 fs at ~1049 nm and maximum average output power of 90 mW at 83 MHz.

STu2E.6 • 15:15

Kerr-Lens Mode-Locked Femtosecond mid-IR Laser Oscillations in Polycrystalline Cr²⁺:ZnSe and Cr²⁺:ZnS, Sergey Vasilyev¹, Mike Mirov¹, Valentin Gapontsev²; ¹IPG Photonics Corp., Mid-IR Lasers, USA; ²IPG Photonics Corp., USA. We demonstrate Kerr-lens mode-locked polycrystalline Cr²⁺:ZnSe and Cr²⁺:ZnS lasers with pulse duration of 125 fs, 160 MHz pulse repetition rate and output power of 60 mW (Cr²⁺:ZnSe) and 30 mW (Cr²⁺:ZnS).

STu2F • THz Metamaterials and
Plasmonics—Continued

STu2F.4 • 14:45

Highly Anisotropic THz Plasmonic Filter created using a K-Space Design Methodology, Andrew Paulsen¹, Ajay Nahata¹; ¹Electrical and Computer Engineering, Univ. of Utah, USA. We demonstrate a versatile method to filter design in the THz region based on k-space. Using this methodology we show an anisotropic filter where transmittance is varied by 80 percent with rotation in polarization angle.

STu2F.5 • 15:00

Reconfigurable pressure-sensitive terahertz metamaterials using liquid metals, Jinqi Wang¹, Shuchang Liu¹, Sivaraman Guruswamy², Ajay Nahata¹; ¹Electrical and Computer Engineering, Univ. of Utah, USA; ²Metallurgical Engineering, Univ. of Utah, USA. We demonstrate a liquid metal-based reconfigurable terahertz metamaterial device that is not only pressure driven, but also exhibits pressure memory. The discrete response is obtained by injecting eutectic gallium indium into a microfluidic structure.

STu2F.6 • 15:15

Terahertz Optical Modulator Based on Metamaterial Split-ring Resonators and Graphene, Riccardo Degl'Innocenti¹, David S. Jessop¹, Yash D. Shah¹, Juraj Sibik², Axel Zeitler², Piran R. Kidambi³, Stephan Hofmann³, Harvey E. Beere¹, David A. Ritchie¹; ¹Physics, Univ. of Cambridge, UK; ²Chemical Engineering and Biotechnology, Univ. of Cambridge, UK; ³Engineering, Univ. of Cambridge, UK. We realized an optical modulator working at terahertz frequencies, based on the interplay between split-ring resonators and graphene. A modulation depth of about 18% was achieved with a bias voltage as low as 0.5 V.

STu2G • RF Photonics—
Continued

STu2G.4 • 14:45

Free Space Millimeter Wave-Coupled Electro-Optic High Speed Phase Modulator Based on Nonlinear Optical Polymer In-Plane Waveguide Structure, Dong Hun Park^{1,2}, Vincent R. Pagán^{1,2}, Thomas E. Murphy², Jongdong Luo³, Alex Jen³, Warren N. Herman¹; ¹Lab for Physical Sciences, USA; ²Electrical and Computer Engineering, Univ. of Maryland, USA; ³Materials Science and Engineering, Univ. of Washington, USA. We report antenna-coupled electro-optic phase modulators operating at Ka-band based on in-plane polymeric waveguides using the nonlinear guest-host polymer SEO125. Design, simulation, fabrication, and experimental results are discussed.

STu2G.5 • 15:00

A 1 Gbps 105.4 GHz Link with a Directly Modulated Photonic Integrated Dual Laser Source, Zhen Yang¹, Martyn J. Fice², Katarzyna Balakier², Adrian Wonfor¹, Cyril C. Renaud², Guillermo Carpintero³, Gaël Kervella⁴, Frederic Van Dijk⁴, Alwyn J. Seeds², Richard V. Penty¹, Ian H. White¹; ¹Electrical Division, Dept of Engineering, Univ. of Cambridge, UK; ²Dept of Electronic and Electrical Engineering, Univ. College London, UK; ³Universidad Carlos III de Madrid, Spain; ⁴III-V Lab, a joint lab of Thales Research and Technology, Alcatel-Lucent Bell Labs France, and CEA Leti, France. A 1 Gbps 105.4 GHz wireless link is demonstrated by directly modulating a photonic integrated dual-laser source. A 50 m link is predicted to achieve error free operation using FEC.

STu2G.6 • 15:15

High Performance Analog Photonic Link Based on Modified Uni-traveling-carrier Photodiode, Xiaojun Xie¹, Qiugui Zhou¹, Kejia Li¹, Andreas Beling¹, Joe C. Campbell¹; ¹Dept of Electrical and Computer Engineering, University of Virginia, USA. An analog fiber optic link that employs a high performance photodiode has achieved high gain of 26.4 dB and 26 dB and low noise figure of 6.1 dB and 6.7 dB at 1 GHz and 10 GHz, respectively.

STu2H • Controlling Light
in Resonators and Photonic
Crystals—Continued

STu2H.4 • 14:45

Mechanically Flexible Photonic-Crystal Cavities on Strained-Germanium Nanomembranes, Cicek Boztug¹, Jose Sanchez-Perez², Jian Yin¹, Max G. Lagally², Roberto Paiella¹; ¹Electrical and Computer Engineering, Boston Univ., USA; ²Materials Science and Engineering, Univ. of Wisconsin - Madison, USA. Photonic-crystal cavities compatible with the highly subwavelength thicknesses and flexibility requirements of mechanically-stressed Ge nanomembranes are developed and used to demonstrate a strong (20×) strain-induced light-emission efficiency enhancement.

STu2H.5 • 15:00

Semiconductor Nanowire Induced Photonic-Crystal Nanocavity with Selectable Resonant Wavelength, Atsushi Yokoo^{1,2}, Masato Takiguchi^{1,2}, Danang Birowosuto^{1,2}, Guoqiang Zhang², Kouta Tatenos², Eiichi Kuramochi^{1,2}, Hideaki Taniyama^{1,2}, Masaya Notomi^{1,2}; ¹NTT Nanophotonics Center, Japan; ²NTT Basic Research Labs, Japan. A photonic-crystal nanocavity is induced by a III/V nanowire in a line defect in a Si photonic crystal with several serially-connected lattice constants. The resonant wavelength changes by moving the nanowire along the line defect.

STu2H.6 • 15:15

Guided Resonance Manipulation and Degeneracy Removal by Elliptical Nano-Holes in Photonic Crystal Slabs, Raanan Gad^{1,2}, Costa Nicholaou^{1,2}, Soroosh Ahmadi^{1,2}, Ofer Levi^{1,2}; ¹Electrical and Computer Engineering, Univ. of Toronto, Canada; ²Inst. of Biomaterials and Biomedical Engineering, Univ. of Toronto, Canada. We demonstrate a method to manipulate the modes and retain high quality factors of 2D photonic crystal slabs with relatively large nano-features over a wide aspect ratio range through structural symmetry breaking within the unit cell by elliptical nano-holes.

CLEO: Science & Innovations

CLEO: QELS-
Fundamental ScienceCLEO: Applications
& TechnologySTu2I • All Optical and
Quantum Signal Processing—
Continued

STu2I.3 • 14:45

Coherent detection of phase modulated ultrashort optical pulses using time-to-space conversion at $1.55\mu\text{m}$, Dror Shayovitz¹, Harald Herrmann², Wolfgang Sohler², Raimund Ricken², Christine Silberhorn², Dan M. Marom¹; ¹Hebrew Univ. of Jerusalem, Israel; ²The Univ. of Paderborn, Germany. Phase information is preserved and faithfully recovered in a time-to-space conversion process of ultrashort optical pulses for the first time. Spatial interference between the pulse image and a coherent reference is used for phase detection.

STu2I.4 • 15:00

Novel Polarisation-assisted Phase Sensitive Optical Signal Processor Requiring Low Nonlinear Phase Shifts, Francesca Parmigiani¹, Graham Hesketh¹, Radan Slavik¹, Peter Horak¹, Periklis Petropoulos¹, David J. Richardson¹; ¹Univ. of Southampton, UK. We demonstrate a new scheme to achieve binary step-like phase response and high phase-sensitive extinction ratio at low powers. Phase-sensitive operation is achieved by polarisation filtering phase-locked signal/idler in a degenerate dual-pump vector parametric amplifier.

STu2I.5 • 15:15

Efficient Wavelength Multicasting through Four-Wave Mixing with a Comb Source, Hong-Fu Ting¹, Ke-Yao Wang¹, Jasper Stroud¹, Amy C. Foster¹, Mark A. Foster¹; ¹Johns Hopkins Univ., USA. We utilize a coherent optical comb generator to accomplish source-efficient wavelength multicasting via four-wave mixing in both a highly-nonlinear fiber and a silicon nanowaveguide. We demonstrate 23 multicast channels with error-free operation at 10-Gb/s.

STu2J • Phase Sensitive
Amplification and Optical
Regeneration—Continued

STu2J.3 • 14:45

Experimental Demonstration of Optical Regeneration of DP-BPSK/QPSK Using Polarization-Diversity PSA, Morteza Ziyadi¹, Amirhossein Mohajerin-Ariaei¹, Jeng-yuan Yang², Youichi Akasaka², Mohammed Chitgarha¹, Salman Khaleghi¹, Ahmed Almaiman¹, Amin Abouzaid³, Joseph Touch³, Motoyoshi Sekiya²; ¹Univ. of Southern California, USA; ²Fujitsu Labs of America, USA; ³Information Science Inst., Univ. of Southern California, USA. We experimentally investigate a polarization-diversity phase-sensitive amplifier (PSA) for phase regeneration of 25-Gbaud DP-BPSK and DP-QPSK signals and show effective reduction on phase noise in both polarizations. BER measurements and reduced phase noise are achieved for both polarizations.

STu2J.4 • 15:00 **Tutorial**

Phase-sensitive Amplification in Communications and Signal Processing, Zhi Tong^{1,2}, Stojan Radic¹; ¹Univ. of California San Diego, USA; ²Infinera Corp, USA. Recent progress in low-noise optical amplification and signal processing has raised prospects of practical devices operating below the conventional quantum limit. We review basic principles, practical implementation, and performance of such devices.



Zhi Tong received his B.S. and Ph.D. degrees, both in electrical engineering, from Beijing Jiaotong University, Beijing, China, in 1999 and 2004, respectively. Since 2008, he worked at Chalmers University of Technology and University of California San Diego, focusing on parametric effects and nonlinear optics. In 2013, he joined Infinera Corporation.

FTu2K • Plasmonic Waveguides,
Lenses and Circuits—Continued

FTu2K.4 • 14:45

Self-accelerating plasmonic beams having arbitrary caustic trajectories, Itai Epstein¹, Ady Arie¹; ¹Tel Aviv Univ., Israel. We demonstrate, numerically and experimentally, the generation of self-accelerating surface plasmon beams along arbitrary caustic curvatures by two-dimensional plasmonic phase masks. We examine both paraxial and non-paraxial curvatures accelerating along polynomial and exponential trajectories.

FTu2K.5 • 15:00

Plasmonic Super-oscillations and Sub-Diffraction Focusing, Guanghui Yuan¹, Edward T. Rogers², Tapashree Roy², Luping Du³, Zexiang Shen¹, Nikolay I. Zheludev^{1,2}; ¹Centre for Disruptive Photonic Technologies, Nanyang Technological Univ., Singapore; ²Optoelectronics Research Centre and Centre for Photonic Metamaterials, Univ. of Southampton, UK; ³School of Electrical and Electronic Engineering, Nanyang Technological Univ., Singapore. We demonstrate experimental focusing of surface plasmon polaritons beyond the plasmon diffraction limit using a super-oscillatory plasmonic antenna at the wavelength of 785nm, achieving a hot-spot as small as 300nm.

FTu2K.6 • 15:15

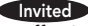

Optical Signal Processing using Nano-scale Plasmonic Circuits, Fatima Eftekhari¹, Daniel E. Gomez^{1,2}, Ann Roberts³, Timothy J. Davis^{1,2}; ¹Melbourne Centre for Nanofabrication, Australian National Fabrication Facility, Australia; ²Materials Science and Engineering, Commonwealth Sci and Indus Res Org, Australia; ³The Univ. of Melbourne, Australia. We present a plasmonic circuit architecture for performing linear mathematical operations on optical signals. We demonstrate experimentally how one such nano-scale circuit performs a difference operation giving a measure of subwavelength optical phase differences.


ATu2L • Symposium on Laser
Processing for Consumer
Electronics I—ContinuedATu2L.3 • 15:00 **Invited**

Laser Micronanostructuring for High-Performance Organic Optoelectronic Devices, Hong-Bo Sun¹, ¹Jilin University, China. We report series of work on multi-beam interference ablation of organic materials, by which problems like extract efficiency and view angle in OLED were solved. The devices are promising for high-efficiency and long-life time display.

CLEO: Science & Innovations

CLEO: Applications
& TechnologySTu2M • Novel Concepts in
Nanophotonics—Continued

STu2M.3 • 14:45  
Observation of an effective magnetic field for light, Lawrence D. Tzuang¹, Kejie Fang², Paulo A. Nussenzeig^{1,3}, Shanhui Fan², Michal Lipson^{1,4}; ¹*School of Electrical and Computer Engineering, Cornell Univ., USA*; ²*Dept of Electrical Engineering, Stanford Univ., USA*; ³*Instituto de Física, Universidade de São Paulo, Brazil*; ⁴*Kavli Inst. at Cornell for Nanoscale Science, Cornell Univ., USA*. We observe an effective magnetic field for photons using an on-chip silicon-based Ramsey-type interferometer. This interferometer generates a direction-dependent phase which corresponds to a magnetic field of 0.2 Gauss in an Aharonov-Bohm configuration for electrons.

STu2M.4 • 15:15 
Voltage Controlled Polarization Rotation from Berry's Phase in Silicon Optical Microring Resonators, Qiang Xu¹, Li Chen¹, Michael Wood¹, Ronald M. Reano¹; ¹*Ohio State Univ., USA*. We present an on-chip electrically tunable polarization rotator in silicon utilizing topological phase. Optical polarization is dynamically tuned between TE and TM modes with 9 dB polarization extinction ratio and 1.4 dB conversion loss.


STu2N • High Power Pulsed
Fiber Lasers—Continued

STu2N.4 • 14:45
High Pulse-energy Generation in a Monolithic Yb-doped All-fiber Dual-cavity Oscillator with Fiber-based Passive Q-switcher, Dongchen Jin¹, Yijian Jiang¹, Ruoyu Sun¹, Huihui Li¹, Jiang Liu¹, Pu Wang¹; ¹*BJUT, China*. A novel high pulse-energy Yb-doped all-fiber dual-cavity laser with large core-diameter fiber-based passive Q-switcher is reported. The monolithic fiber oscillator generates pulses with peak power of 3.4 kW and single pulse energy of 484 μ J.

STu2N.5 • 15:00
1 mJ narrow-linewidth master oscillator fiber amplifier system continuously tunable from 1010 nm to 1086 nm, Jérôme Lhermite¹, Romain Royon¹, Eric Cormier¹; ¹*Centre Lasers Intenses et Applications, France*. We report on a narrow-linewidth master oscillator fiber amplifier system continuously tunable from 1010nm to 1086nm, delivering ns pulses with 1mJ energy over the entire band. Tunable second-harmonic generation in the visible is also presented.


STu2N.6 • 15:15
High Energy Diode-Seeded Nanosecond 2 μ m Fiber MOPA Systems Incorporating Active Pulse Shaping, Zhihong Li¹, Alexander M. Heidt¹, Peh S. Teh¹, Martin Berendt¹, Jayanta K. Sahu¹, Richard Phelan², Brian Kelly², Shaif-ul Alam¹, David J. Richardson¹; ¹*Univ. of Southampton, UK*; ²*Eblana Photonics Ltd, Ireland*. We present the first demonstration of nanosecond-pulsed fiber MOPA systems seeded by semiconductor laser diodes at 2 μ m incorporating arbitrary pulse shaping capabilities, achieving up to 1.0 mJ (12.5 kHz, 100 ns) pulse energy.

STu2O • Symposium on
Microcavity Exciton-Polaritons,
Devices and Applications I—
Continued

STu2O.3 • 14:45 
A study of the formation of dark-solitons in semiconductor microcavities, Pasquale Cilibrizzi¹, Hamid Ohadi¹, Tomas Ostatnicky², Alexis Askitopoulos¹, Wolfgang Langbein³, Pavlos Lagoudakis¹; ¹*School of Physics and Astronomy, Univ. of Southampton, UK*; ²*Faculty of Mathematics and Physics, Charles Univ. in Prague, Czech Republic*; ³*School of Physics and Astronomy, Cardiff Univ., UK*. We demonstrate that the previously reported experimental signatures of dark-solitons and half-solitons in polariton condensates are observed for negligible nonlinearity and are therefore not sufficient to identify such solitons. A Maxwell equation model is shown to reproduce the observations.

STu2O.4 • 15:00  
Single-mode Polariton Laser in a Designable Microcavity, Bo Zhang¹, Zhaorong Wang¹, Seonghoon Kim¹, Sebastian Brodbeck², Christian Schneider², Martin Kamp², Sven Hoeffling², Hui Deng¹; ¹*Univ. of Michigan, USA*; ²*Univ. of Wuerzburg, Germany*. We demonstrate strong coupling and a coherent polariton laser in a microcavity consisting of a sub-wavelength grating in the top mirror. The designable grating mirror allows 3D confinement, polarization selectivity, and dispersion engineering by design.

ATu2P • Symposium on Novel
Light Sources and Photonic
Devices in Optical Imaging I—
Continued

ATu2P.3 • 15:00 
A 15-MHz wavelength-stepped laser based on intracavity pulse stretching and compression for optical coherence tomography, Serhat Tozburun^{1,2}, Meena Siddiqui³, Benjamin J. Vakoc^{1,2}; ¹*Harvard Medical School, USA*; ²*Wellman Center for Photomedicine, Massachusetts General Hospital, USA*; ³*Harvard-MIT Division of Health Sciences and Technology, USA*. We introduce a wavelength-stepped laser that uses dispersive fibers in combination with a lithium-niobate modulator and a fixed Fabry-Perot etalon to achieve wavelength selection for optical-domain subsampled OCT. A 15 MHz A-scan rate is demonstrated.

ATu2P.4 • 15:15 
Silicon Photonic Optical Coherence Tomography System, Simon Schneider¹, Matthias Lauermann¹, Claudius Weimann¹, Wolfgang Freude^{1,2}, Christian G. Koos^{1,2}; ¹*Inst. of Photonics and Quantum Electronics (IPQ), Karlsruhe Inst. of Technology (KIT), Germany*; ²*Inst. of Microstructure Technology (IMT), Karlsruhe Inst. of Technology (KIT), Germany*. A swept-source optical coherence tomography system is realized as a silicon photonic integrated circuit comprising passive components and germanium photo detector. Experiments show uniform sensitivity over 5 mm scanning range, enabling simple imaging demonstrations.



CLEO: QELS-Fundamental Science

FTu2A • Symposium on
Quantum Repeaters II—
Continued

FTu2A.6 • 15:30

Double-heralded single-photon absorption by a single atom, Jose M. Brito¹, Stephan Kucera¹, Pascal Eich¹, Christoph Kurz¹, Michael Schug¹, Philipp Müller¹, Jan Huwer¹, Jürgen Eschner¹; ¹Saarland Univ., Germany. We present a single-photon to single-atom interface, where a heralded single photon generated by Spontaneous Parametric Conversion is absorbed by a single trapped ion, subsequently generating a single Raman-scattered photon that heralds the absorption event.

FTu2A.7 • 15:45

Progress and prospects for high efficiency and gigacount per second detectors for quantum repeaters using superconducting nanowire detectors, Varun Verma¹, Michael S. Allman¹, Robert Horansky¹, Francesco Marsili², Jeffrey A. Stern², Andrew D. Beyer², Matthew D. Shaw², Sae Woo Nam¹, Richard P. Mirin¹; ¹NIST, USA; ²Jet Propulsion Lab, USA. We describe our work on superconducting nanowire detector arrays and how they may be adapted to meet the requirements for implementing a quantum repeater.

FTu2B • Optical Properties of
Low-Dimensional Materials—
Continued

FTu2B.6 • 15:30

Excitons in Atomically Thin Transition-Metal Dichalcogenides, Alexey Chernikov¹, Timothy C. Berkelbach², Heather M. Hill¹, Albert Rigosi¹, Yilei Li¹, Özgür B. Aslan¹, David R. Reichman², Mark S. Hybertsen³, Tony F. Heinz¹; ¹Depts of Physics and Electrical Engineering, Columbia Univ., USA; ²Dept of Chemistry, Columbia Univ., USA; ³Center for Functional Nanomaterials, Brookhaven National Lab, USA. Excitons are studied experimentally and theoretically in atomically thin WS₂ layers. We find a binding energy of 0.32eV as well as non-hydrogenic behavior of the exciton states due to the non-uniformity of the dielectric environment.

FTu2B.7 • 15:45

Coherent Electronic Coupling in Transition Metal Dichalcogenide Monolayer, Akshay Singh¹, Galan Moody¹, Sanfeng Wu², Yanwen Wu^{1,3}, Nirmal J. Ghimire^{4,5}, Jiaqiang Yan^{5,6}, David Mandrus^{4,5}, Xiadong Xu^{2,7}, Xiaoqin Li¹; ¹Physics, Univ. of Texas at Austin, USA; ²Physics, Univ. of Washington, USA; ³Physics and Astronomy, Univ. of South Carolina, USA; ⁴Physics and Astronomy, Univ. of Tennessee, USA; ⁵Materials Science and Technology, Oak Ridge National Lab, USA; ⁶Materials Science and Engineering, Univ. of Tennessee, USA; ⁷Materials Science and Engineering, Univ. of Washington, USA. We present two-color pump-probe spectra of excitons and trions in monolayer MoSe₂. Isolated spectral cross-peaks reveal coherent exciton-trion coupling due to many-body interactions. Density matrix calculations suggest the formation of a correlated exciton-trion state.

FTu2C • Novel Anisotropic
Structures—Continued

FTu2C.7 • 15:30

Circular Polarization Converters Based on Pairs of Oppositely-Handed Gold Helices, Johannes Kaschke¹, Leonard W. Blume¹, Michael Thiel², Wu Lin³, Zhenyu Yang³, Martin Wegener¹; ¹Inst. of Applied Physics, Karlsruhe Inst. of Technology, Germany; ²Nanoscribe GmbH, Germany; ³School of Optical and Electronic Information, Huazhong Univ. of Science and Technology, China. We introduce a helix-based metamaterial, a circular polarization converter, composed of pairs of oppositely-handed helices on a square array. We compare our theoretical findings to measurements on samples made by laser lithography and electroplating.

FTu2C.8 • 15:45

How to Guide Light Around Sharp Corners: Topologically Protected Surface Waves without Magnetic Field, Tzuhsuan Ma¹, Alexander B. Khanikaev², Hossein S. Mousavi², Gennady Shvets¹; ¹Physics, Univ. of Texas at Austin, USA; ²Electrical Engineering, Univ. of Texas at Austin, USA; ³Physics, Queens College of The City Univ. of New York, Flushing, USA. We propose a new design of bi-anisotropic meta-waveguide exhibiting topologically protected edge mode which can be guided around sharp corners without external magnetic field. The geometry is very simple and easy to be experimentally implemented.

FTu2D • Novel XUV/X-Ray
Sources—Continued

FTu2D.6 • 15:30

Sparsity-based Ankylography: Recovering 3D structures from a single-shot 2D scattered intensity, Maor Mutzafi¹, Yoav Shechtman¹, Oren Cohen¹, Yonina C. Eldar², Mordechai Segev¹; ¹Physics, Technion, Israel; ²Electrical Engineering, Technion, Israel. We present an algorithmic paradigm for deciphering the 3D structure of a molecule from the far-field intensity of scattered x-ray photons before the molecule disintegrates. Our approach enables surpassing current limits on recoverable information capacity.

FTu2D.7 • 15:45

Microscopic Verification of Terahertz Generation Mechanism in Two-Color Laser-Produced Plasma, Yong Sing You¹, Ki-Yong Kim¹, Dongwen Zhang^{1,2}; ¹Inst. for Research in Electronics and Applied Physics, Univ. of Maryland, USA; ²Dept of Physics, National Univ. of Defense Technology, China. Terahertz radiation from two-color laser-produced plasma is studied with simultaneous measurements of absolute two-color phases, near-field plasma currents, and far-field THz radiation. This verifies the microscopic mechanism of terahertz radiation generation at various laser intensities.

16:00–16:30 Coffee Break (16:00-16:30) and Unopposed Exhibit Only Time, Exhibit Halls 1 & 2

NOTES

CLEO: Science & Innovations

**STu2E • fs - Oscillators—
Continued**

STu2E.7 • 15:30

Ceramic Cr:ZnS Laser Mode-Locked by Graphene, Nikolai Tolstik¹, Evgeni Sorokin², Irina T. Sorokina¹; ¹Norwegian Univ. of Science and Technology, Norway; ²Inst. for Photonics, Technical Univ. of Vienna, Austria. We report a high-power graphene mode-locked ceramic Cr:ZnS-laser, producing 3.9 nJ, 140 fs pulses with 45 nm spectral bandwidth at 270 MHz repetition rate, at output power for the first time exceeding 1 W level.

STu2E.8 • 15:45

Gain-Matched Output Couplers (GMOCs) for Efficient and Robust Kerr-Lens Mode-Locking of Cr:LiSAF lasers, Can Cihan¹, Ersen Beyatli¹, Ferda Canbaz¹, Li-Jin Chen², Bernd Sumpf³, Götz Erbert³, Alfred Leitenstorfer⁴, Franz Kärtner^{2,5}, Alphan Sennaroglu¹, Umit Demirbas⁶; ¹Laser Research Lab, Koç Univ., Turkey; ²Research Lab of Electronics, MIT, USA; ³Ferdinand-Braun-Institut, Leibniz Institut für Höchstfrequenztechnik, Germany; ⁴Dept of Physics and Center for Applied Photonics, Univ. of Konstanz, Germany; ⁵Center for Free-Electron Laser Science, DESY and Dept of Physics, Univ. of Hamburg, Germany; ⁶Laser Technology Lab, Antalya International Univ., Turkey. We report efficient and robust Kerr-lens mode-locking of single-mode and tapered diode-pumped Cr:LiSAF lasers by using gain-matched output couplers. Sub-15-fs pulses were generated with peak powers above 60-kW and optical-to-optical conversion efficiencies up to 21%.

**STu2F • THz Metamaterials and
Plasmonics—Continued**

STu2F.7 • 15:30

Symmetric and asymmetric T-shaped plasmonic waveguides, Shashank Pandey¹, Barun Gupta¹, Ajay Nahata¹; ¹Univ. of Utah, USA. We fabricate, experimentally characterize and numerically validate the origin of modes on periodically spaced T-shaped structure for Terahertz input. Effect of parameters such as height, periodicity, asymmetry and symmetry of 'T' structure is explained.

STu2F.8 • 15:45

Terahertz Plasmonic Structures Based on a Spatially Varying Conductivity, Barun Gupta¹, Shashank Pandey¹, Ajay Nahata¹; ¹Univ. of Utah, USA. We demonstrate a new technique for fabricating terahertz plasmonic structures that incorporates a spatial variation into the conductivity of the metallic layer using inkjet printing of a conductive and resistive ink simultaneously.

**STu2G • RF Photonics—
Continued**

STu2G.7 • 15:30

Bandwidth Tunable, High Suppression RF Photonic Filter with Improved Insertion Loss, Mattia Pagani¹, David Marpaung¹, Blair Morrison¹, Benjamin J. Eggleton¹; ¹Univ. of Sydney, Australia. We demonstrate a scheme for minimising the insertion loss of an RF photonic filter, by exploiting the phase response of stimulated Brillouin scattering. We achieve a filter with high suppression, tunable bandwidth and low loss.

STu2G.8 • 15:45

All-optical single-side-band GHz to THz microwave sources via SOA gain engineering, Fangxin Li¹, Amr S. Helmy¹; ¹ECE, Univ. of Toronto, Canada. We propose and demonstrate low noise broadly tunable single side-band microwaves using cascaded semiconductor optical amplifiers using no RF bias. Microwaves between 40GHz and 875GHz with a linewidth ~22 KHz are demonstrated.

**STu2H • Controlling Light
in Resonators and Photonic
Crystals—Continued**

STu2H.7 • 15:30

Transport in millimeter scale disordered photonic crystals, PIN-CHUN HSIEH¹, Chung-Jen Chung², James F. McMillan¹, Ming Lu³, Nicolae Panoiu⁴, Chee Wei Wong¹; ¹Mechanical Engineering, Columbia Univ., USA; ²Center for Micro/Nano Science and Technology, National Cheng Kung Univ., Taiwan; ³Center for Functional Nanomaterials, Brookhaven National Lab, USA; ⁴Dept of Electronic and Electrical Engineering, Univ. College London, UK. We examine the influence of disorder over millimeter lengthscales, in the transport of photons. Super-collimation is achieved for varying controlled degrees of disorder in large-scale measurements, supported by physical theory and simulations.

STu2H.8 • 15:45

Artificial Selection for Structural Color on Butterfly Wings and Comparison to Natural Evolution, Seng Fatt Liew¹, Bethany R. Wasik², David Lilien¹, April J. Dinwiddie², Heeso Noh¹, Antonia Monteiro², Hui Cao¹; ¹Applied Physics, Yale Univ., USA; ²Ecology and Evolutionary Biology, Yale Univ., USA. We evolved violet structural color from brown-colored butterflies over six generations of artificial selection. The mechanism of color generation was identified and found to mimic the natural evolution of violet/blue color in closely related species.

16:00–16:30 Coffee Break (16:00-16:30) and Unopposed Exhibit Only Time, Exhibit Halls 1 & 2

NOTES

Meeting Room
211 B/D

Meeting Room
212 A/C

Meeting Room
212 B/D

Marriott
Salon I & II

CLEO: Science & Innovations

**CLEO: QELS-
Fundamental Science**

**CLEO: Applications
& Technology**

**STu2I • All Optical and
Quantum Signal Processing—
Continued**

**STu2J • Phase Sensitive
Amplification and Optical
Regeneration—Continued**

**FTu2K • Plasmonic Waveguides,
Lenses and Circuits—Continued**

**ATu2L • Symposium on Laser
Processing for Consumer
Electronics I—Continued**

STu2I.6 • 15:30
Photonic RF-Channelized Receiver based on Wideband Parametric Mixers and Coherent Detection, Andreas O. Wiberg¹, Daniel J. Esman¹, Lan Liu¹, Evgeny Myslivets¹, Nikola Alic¹, Stojan Radic¹; ¹Univ. of California San Diego, USA. We present a photonic RF-channelized receiver based on parametric multicasting and LO generation. Using frequency locking and coherent detection, contiguous channelization of 12 sub-channels is achieved covering 24-30GHz. System analysis and characterizations are presented.

STu2I.7 • 15:45
Multi-Channel Amplification in a 20-dB Gain Hybrid Optical Parametric Amplifier, Gordon K. P. Lei¹, Michel E. Marhic¹; ¹College of Engineering, Swansea Univ., UK. We demonstrate amplification of multiple 40 Gb/s channels in a hybrid fiber optical parametric amplifier. Experimental results show that the proposed amplifier has negligible power penalties compared with traditional parametric amplifier, and reduced inter-channel crosstalk.

FTu2K.7 • 15:30
Near-field Interference in Optics and RF, Pavel Ginzburg¹, Polina V. Kapitanova², Francisco José Rodríguez-Fortuño³, Daniel O'Connor¹, Dmitry S. Filonov², Pavel M. Voroshilov², Alexander N. Poddubny², Gregory A. Wurtz¹, Pavel A. Belov², Yuri S. Kivshar⁴, Anatoly V. Zayats¹; ¹Physics, King's College London, UK; ²National Research Univ. of Information Technologies, Mechanics and Optics (ITMO), Russia; ³Nanophotonics Technology Center, Universitat Politècnica de València, Spain; ⁴Nonlinear Physics Center, Research School of Physics and Engineering, Australian National Univ., Australia. Interference, one of the major physical phenomena, relies on coherent superposition of waves, undertaking different phase lag. Considering vectorial near-fields structure, the fundamental concept was reconsidered, reformulated, and demonstrated at optical and radio frequencies.

FTu2K.8 • 15:45
Subwavelength multilayer dielectrics: ultra-sensitive transmission and breakdown of effective-medium, Hanan Herzig Sheinfux¹, Ido Kaminer¹, Yonatan Plotnik¹, Guy Bartal¹, Mordechai Segev¹; ¹Technion Israel Inst. of Technology, Israel. We show that a structure of alternating dielectric layers with deep subwavelength thicknesses exhibits novel transmission effects that depend on the order of the layers and on nanometer scale variations of the layer widths.

ATu2L.4 • 15:30 **Invited**
Laser Direct Ablation for Patterning Printed Wiring Boards Using Ultrafast Lasers and High Speed Beam Delivery Architectures, Hisashi Matsumoto¹, Mark Unrath¹, Jan Kleinert¹, Haibin Zhang¹; ¹Electro Scientific Industries, Inc., USA. A vector scanning based system that incorporates Acousto-Optic Deflectors in addition to galvanometers and linear stages enables in conjunction with an ultrafast laser high accuracy, high bandwidth random beam positioning and precise material removal. see above.

16:00–16:30 Coffee Break (16:00-16:30) and Unopposed Exhibit Only Time, Exhibit Halls 1 & 2

NOTES


Blank lined area for notes.


Tuesday, 10 June

CLEO: Science & Innovations

**CLEO: Applications
& Technology**

STu2M • Novel Concepts in Nanophotonics—Continued

STu2M.5 • 15:30  **Tunable Liquid Crystal-loaded Metasurfaces for IR and THz Applications**, Oleksandr Buchnev¹, Jan Wallauer², Markus Walther², Nina Podoljak¹, Malgosia Kaczmarek³, Nikolay I. Zheludev^{1,4}, Vassili A. Fedotov¹; ¹Optoelectronics Research Centre and EPSRC Centre for Photonic Metamaterials, Univ. of Southampton, UK; ²Dept of Molecular and Optical Physics, Univ. of Freiburg, Germany; ³Physics and Astronomy, Univ. of Southampton, UK; ⁴Centre for Disruptive Photonic Technologies, Nanyang Technological Univ., Singapore. We experimentally demonstrate a family of compact and efficient IR and THz electro-optical modulators based on active planar metamaterials (metasurfaces) hybridised with liquid crystals.

STu2M.6 • 15:45  **Shape Optimization of Nanophotonic Devices Using the Adjoint Method**, Christopher Lalau-Keraly¹, Samarth Bhargava¹, Vidya Ganapati¹, Eli Yablonovitch¹; ¹UC Berkeley, USA. We use an adjoint method integrated with a classical Maxwell solver to optimize several nanophotonic devices, providing an adaptable and efficient tool for photonics design.


STu2N • High Power Pulsed Fiber Lasers—Continued

STu2N.7 • 15:30 **Effect of seed linewidth on few-moded fiber amplifiers**, Jae M. Daniel¹, Nikita Simakov^{1,2}, Peter C. Shardlow¹, W. A. Clarkson¹; ¹Optoelectronics Research Centre, Univ. of Southampton, UK; ²Cyber and Electronic Warfare Division, Defence Science and Technology Organisation, Australia. Suppression of detrimental modal interference effects within a cladding-pumped multimode thulium fiber amplifier is achieved using variable bandwidth seed source. The amplifier produced pulse energies of 1.1mJ and peak powers over 20kW at 1956nm.


STu2N.8 • 15:45 **16µJ-Pulse-Energy, Picosecond, Narrow-linewidth Master Oscillator Power Amplifier Using Direct Amplification**, Ho-Yin Chan¹, Lin Xu¹, James Bateman¹, Shaif-ul Alam¹, David J. Richardson¹, David Shepherd¹; ¹Optoelectronics Research Centre, Univ. of Southampton, UK. We present a gain-switched-diode-seeded 1034.5-nm master oscillator power amplifier, employing direct amplification through standard commercial Yb3+-doped fibres to generate 15.6µJ-pulse-energy, 126kW-peak-power, picosecond pulses with 3dB spectral bandwidth of 0.87nm.

STu2O • Symposium on Microcavity Exciton-Polaritons, Devices and Applications I—Continued

STu2O.5 • 15:30  **Influence of interactions with non-condensed particles on the coherence of a 1D polariton condensate**, Johannes Schmutzler¹, Tomasz Kazimierzuk¹, Ömer Bayraktar¹, Marc Assmann¹, Sebastian Brodbeck², Martin Kamp², Christian Schneider², Sven Höfling³, Manfred Bayer¹; ¹TU Dortmund Univ., Germany; ²Würzburg Univ., Germany; ³Univ. of St Andrews, UK. We study interactions between background carriers and a polariton condensate. Second order correlation measurements and Young's double-slit experiment demonstrate a detrimental effect on the coherence of a polariton condensate mediated by background carriers.

STu2O.6 • 15:45  **Engineering Dispersion Relation of Photons in Vertical Cavity using High-Contrast Gratings**, Zhaorong Wang¹, Hui Deng¹; ¹U of Michigan, USA. We show the dispersion relation of high-contrast grating based vertical cavity can be altered by orders of magnitude by engineering the angular phase response. The results may benefit Purcell enhancement and strong coupling using the cavity.

ATu2P • Symposium on Novel Light Sources and Photonic Devices in Optical Imaging I—Continued

ATu2P.5 • 15:30  **Micro-fluid Channel Based on Ultralow-loss Silicon Crossing Waveguide for Various Sensing**, Zheng Wang^{1,2}, Swapnajt Chakravarty³, Harish Subbaraman³, Xiaochuan Xu³, Donglei Fan^{1,4}, Alan X. Wang⁵, Ray Chen^{1,2}; ¹Materials Science and Engineering Program, Texas Materials Inst., The Univ. of Texas at Austin, USA; ²Dept of Electrical and Computer Engineering, The Univ. of Texas at Austin, USA; ³Omega Optics, Inc., USA; ⁴Dept of Mechanical Engineering, The Univ. of Texas at Austin, USA; ⁵School of Electrical Engineering and Computer Science, Oregon State Univ., USA. We experimentally demonstrate a new type of micro-fluid channel design with crossing optical waveguides that not only block any gaps in the microfluidic channels in one fabrication step but also enable nearly lossless optical propagation in the primary waveguides on a chip

ATu2P.6 • 15:45  **Femtosecond laser stimulated nanosystems for neuroscience applications**, Takashi Nakano¹, Catherine Chin², David Myint³, Eng Tan³, Peter J. Hale², John Reynolds⁴, Jeff Wickens¹, Keshav M. Dani²; ¹Neurobiology Research Unit, Okinawa Inst. of Sci and Tech, Japan; ²Femtosecond Spectroscopy Unit, Okinawa Inst. of Sci and Tech, Japan; ³Dept of Chemistry, Univ. of Otago, New Zealand; ⁴Dept of Anatomy and the Brain Health Research Centre, School of Medical Sciences, Univ. of Otago, New Zealand. The development of fast and robust chemical delivery systems is important step for nanomedicine. We demonstrate on-demand, sub-second, controlled release of a euromodulator by applying femtosecond laser pulse trains to robust, liposome structures

16:00–16:30 Coffee Break (16:00-16:30) and Unopposed Exhibit Only Time, Exhibit Halls 1 & 2

NOTES

Large empty rectangular box for taking notes during the session.

Tuesday, 10 June

CLEO: QELS-Fundamental Science

16:30–18:30

FTu3A • Quantum Repeater Technologies*Presider: Kae Nemoto; National Inst. of Informatics, Japan*FTu3A.1 • 16:30 **Invited**

Atoms, Ions and Photons for Quantum Tasks: Strengths and Weaknesses, Julio T. Barreiro¹; ¹Univ. of California, San Diego, USA. I will describe applications employing ions, photons and neutral atoms for quantum science. This will lead to an insider's comparison of single- and many-particle aspects of the production (ease and time), lifetime, manipulation and measurement of these quantum systems.

16:30–18:30

FTu3B • Advances in High-Harmonic Generation*Presider: François Légaré; INRS-Energie Mat & Tele Site Varennes, Canada*

FTu3B.1 • 16:30

Magnetic Circular Dichroism Probed with Bright High-order Harmonics, Ofer Kfir¹, Patrik Grychtol², Emrah Turgut², Ronny Knut^{2,3}, Dmitriy Zusin², Dimitar Popmintchev², Tenio Popmintchev², Hans Nembach³, Justin M. Shaw⁴, Avner Fleischer^{1,4}, Henry Kapteyn², Margaret Murnane², Oren Cohen¹; ¹Solid State Inst. and Physics Dept, Technion - Israel Inst. of Technology, Israel; ²Dept of Physics and JILA, Univ. of Colorado and NIST, USA; ³Electromagnetics Division, National Inst. of Standards and Technology, USA; ⁴Dept of Physics and Optical Engineering, Ort Braude College, Israel. We demonstrate the first bright circularly-polarized high-order harmonics. Using this new tabletop light source, we demonstrate magnetic circular dichroism measurements at the M-shell absorption edges of Cobalt.

FTu3B.2 • 16:45

High flux coherent supercontinuum soft X-ray source driven by a single-stage 10 mJ, kHz, Ti:sapphire laser amplifier, Chengyuan Ding¹, Wei Xiong¹, Tingting Fan¹, Daniel Hickstein¹, Tenio Popmintchev¹, Xiaoshi Zhang², Mike Walls², Margaret Murnane¹, Henry Kapteyn¹; ¹Physics, JILA, Univ. of Colorado at Boulder, USA; ²Kapteyn-Murnane Labs, USA. We demonstrate the highest flux tabletop coherent soft X-ray source to date, using high harmonics driven by a single-stage Ti:sapphire-pumped OPA at 1.3 μ m. The spectrum extends to 200eV, with a flux of >106 photons/pulse/1% bandwidth.

FTu3B.3 • 17:00

High flux table-top ultrafast soft X-ray source generated by high harmonic generation, Nicolas Thiré¹; ¹INRS-EMT / ALLS, Canada. Intense, few-cycle infrared laser pulses centered at 1.8 μ m wavelength, coupled to a new gas cell design, are employed to drive high harmonic generation with high flux down to the soft X-ray regime.

16:30–18:30

FTu3C • Quantum Meta Optics*Presider: Liang Feng, Univ. of California Berkeley, USA*

FTu3C.1 • 16:30

Stimulated emission of SPPs on top of hyperbolic metamaterials, John K. Kitur¹, Thejaswi Tumkur¹, Lei Gu¹, Mikhail A. Noginov¹; ¹Norfolk State Univ., USA. We show that the stimulated emission of surface plasmon polaritons on top of lamellar metal/dielectric metamaterial has much lower threshold than on top of silver.

FTu3C.2 • 16:45

Classical and Quantum Opto-mechanics with Plasmonics and Metamaterials, Pavel Ginzburg¹, Alexey V. Krasavin¹, Alexander S. Shalin², Pavel A. Belov², Yuri S. Kivshar^{3,2}, Anatoly V. Zayats¹; ¹Physics, King's College London, UK; ²National Research Univ. of Information Technologies, Mechanics and Optics (ITMO), Russia; ³Nonlinear Physics Center, Research School of Physics and Engineering, Australian National Univ., Australia. Opto-mechanical phenomena on nano-scale change balance between macroscopic forces and introduce novel quantum effects. Manipulation and control over nano-objects dynamics with plasmonics and metamaterials emphasizing radiation reaction recoil and all-optical modulation will be discussed.

FTu3C.3 • 17:00 **Invited**

Thermal emission control with surface waves, Jean-Jacques Greffet¹, Daniele Costantini¹, Giovanni Bruccoli¹, Henri Benisty¹, Francois Marquier¹; ¹Institut d'Optique, France. Cheap infra red (IR) sources are incandescent sources such hot membranes. In this paper, we show how it is possible to overcome their limitations (omnidirectional, broadband, low efficiency, slow modulation rate) by taking advantage of surface waves.

16:30–18:30

FTu3D • Filamentation and the THz Generation*Presider: Stephane Barland; Universite de Nice Sophia Antipolis, USA*

FTu3D.1 • 16:30

Enhancing the Gain by Quantum Coherence in Terahertz Quantum Cascade Lasers, Elodie Strupiechonski^{2,1}, Romain Blanchard¹, Patrice Genevet^{3,1}, Yongrui Wang³, Alexey Belyanin³, Lianhe Li⁴, Edmund Linfield⁴, A. G. Davies⁴, Federico Capasso¹, Marlan O. Scully^{3,2}; ¹School of Engineering and Applied Sciences, Harvard Univ., USA; ²Baylor Univ., USA; ³Texas A&M Univ., USA; ⁴School of Electronic and Electrical Engineering, Univ. of Leeds, UK. We present an experimental study of a GaAs/Al₂₅Ga₇₅As terahertz quantum cascade laser in which a mid-infrared radiation serves as a coherent drive for enhancing terahertz gain.

FTu3D.2 • 16:45

Terahertz-Field-Induced Second Harmonic Generation Through Pockels Effect in Gallium Phosphide Crystal, Emmanuel Abraham^{1,2}, Marion Cornet^{1,2}, Amine Ould Hamouda^{1,2}, Jérôme Degert^{1,2}, Eric Freysz^{1,2}; ¹Bordeaux Univ., France; ²LOMA UMR 5798, CNRS, France. We report the second harmonic generation of a near-infrared pulse in a Gallium Phosphide crystal through the Pockels effect induced by an intense terahertz pulse. This demonstrates cascading second-order nonlinear phenomena in the terahertz range.

FTu3D.3 • 17:00

Terahertz wave guiding by femtosecond laser filament in air, Jiayu Zhao¹, Yizhu Zhang², Zhi Wang¹, Wei Chu³, Bin Zeng³, Ya Cheng³, Zhizhan Xu³, Weiwei Liu¹; ¹Inst. of Modern Optics, Nankai Univ., China; ²Shanghai Advanced Research Inst., Chinese Academy of Sciences, China; ³Shanghai Inst. of Optics and Fine Mechanics, Chinese Academy of Sciences, China. Superluminal propagation of THz pulse has been observed by investigating THz waveform emitted from different length of filaments. Numerical simulation has implied that a THz waveguide-like photonic structure may be formed, leading to this phenomenon.

FTu3A.2 • 17:00

Frequency Conversion of Narrowband Single Photons from a SPDC Pair Source, Andreas Lenhard¹, Stephan Kucera¹, Jose Brito¹, Jürgen Eschner¹, Christoph Becher¹; ¹Fachrichtung 7.2, Universität des Saarlandes, Germany. We report on frequency down conversion of single photons from a photon pair source resonant with an atomic transition of Calcium ions. The temporal correlation between the photon pair is preserved in the conversion process.

CLEO: Science & Innovations

16:30–18:30

STu3E • Pulse Characterization and Ultrafast Imaging

Presider: Jared Wahlstrand; Univ. of Maryland, USA

STu3E.1 • 16:30

Characterization techniques for aligning spatio-temporal focused ultrafast pulses, Amanda K. Meier¹, Michael Greco¹, Charles G. Durfee¹; ¹Dept of Physics, Colorado School of Mines, USA. To optimize intensity-localization in spatio-temporally focused ultrafast beams we demonstrate spectral interferometric and spectrally-resolved knife edge scan methods to characterize lateral and angular spatial chirp. A novel dispersion scan yields the focused-pulse spectral phase.

STu3E.2 • 16:45

Angle-multiplexed spatial-spectral interferometry for simultaneous measurement of spectral phase and polarization state, Ming-wei Lin¹, Abdurahim Rakhman¹, Igor Jovanovic¹; ¹Pennsylvania State Univ., USA. An angle-multiplexed spatial-spectral interferometry between an arbitrary polarized signal pulse and two orthogonal linearly polarized reference pulses is demonstrated to characterize the polarization state and relative spectral phase of a radially polarized laser pulse.

STu3E.3 • 17:00

Anamorphic temporal imaging using a warped time lens, Mohammad H. Asghari¹, Bahram Jalali¹; ¹Univ. of California, Los Angeles, USA. Anamorphic temporal imaging concept incorporating a warped time lens is introduced. The system is placed in front of spectrometer to enhance its spectral resolution and update rate and minimizes the volume of the generated data.

16:30–18:30

STu3F • Technologies for High Intensity

Presider: Federico Canova; Amplitude Technologies, France

STu3F.1 • 16:30 **Invited**

High Repetition Rate kJ-class Nanosecond to Femtosecond Lasers, Todd Ditmire^{1,2}; ¹Dept. of Physics, Univ. of Texas at Austin, USA; ²National Energetics, USA. Using novel liquid cooled slab laser amplifier technology we have developed laser systems capable of amplifying nanosecond laser pulses to energy of ~1 kJ at repetition rate up to 0.1 Hz.

STu3F.2 • 17:00

Generation of 0.61 PW, 33.8fs Pulse by CPA and OPCPA Hybrid Laser System, Xiaoyan Liang¹, Lianghong Yu¹, Lu Xu¹, Yuxi Chu¹, Zhanggui Hu², Yi Xu¹, Cheng Wang¹, Xiaoming Lu¹, Yuxin Leng¹, Ruxin Li¹, Zhizhan Xu¹; ¹Shanghai Inst. of Optics and Fine Mechanics, China; ²Key Lab of Functional Crystals and Laser Technology, Technical Inst. of Physics and Chemistry, China. We reported a hybrid chirped pulse amplification (CPA) and optical parametric chirped pulse amplification (OPCPA) laser system with peak power of 0.61PW. The conversion efficiency of LBO-OPCPA reached 25.38% with output energy of 28.68 J. The compressed pulse width of hybrid laser was 33.8fs.

16:30–18:30

STu3G • Photodetectors

Presider: Michael Grzesik, MIT Lincoln Lab, USA

STu3G.1 • 16:30

Zn⁺ Implanted Silicon Waveguide Photodiodes for On-Chip Mid-Infrared Detection, Richard R. Grote¹, Brian Souhan¹, Noam Ophir², Jeffrey Driscoll¹, Hassaram Bakhr³, Keren Bergman², William M. Green⁴, Richard M. Osgood¹; ¹Microelectronics Sciences Labs, Columbia Univ., USA; ²Dept of Electrical Engineering, Columbia Univ., USA; ³College of Nanoscale Science and Engineering, State Univ. of New York at Albany, USA; ⁴T. J. Watson Research Center, IBM, USA. We present the first experimental demonstration of Zn⁺ implanted Si waveguide photodiodes for 2.2–2.4 μm operation. Preliminary responsivities > 65 mA/W are measured, suggesting suitability for on-chip sensing and communications applications in the mid-infrared.

STu3G.2 • 16:45

Rapid melt grown Germanium p-i-n photodiode wrapped around a Silicon waveguide, Ryan Going¹, Tae Joon Seok¹, Ming Wu¹; ¹Univ. of California, Berkeley, USA. We report on a compact germanium photodiode design where single crystal germanium wraps around a single mode silicon waveguide. A 32 μm long, 626 aF, p-i-n device has 0.8 A/W responsivity at 1550 nm.

STu3G.3 • 17:00

The Monolithic Heterogeneous Integration of GaAs PIN Photodiode and Si CMOS-based Transimpedance Amplifier, Eiji Kume¹, Hiroyuki Ishii¹, Taro Itatani¹, Sadanori Yamanaka², Tomoyuki Takada², Masahiko Hata², Takenori Osada², Takayuki Inoue², Yoshinori Matsumoto³; ¹National Inst. of Advanced Industry, Japan; ²Sumitomo Chemical Co., LTD, Japan; ³Keio Univ., Japan. This article describes a GaAs PIN photodiode was directly grown on a Si substrate in which CMOS-based transimpedance amplifier (TIA) was fabricated using general Si CMOS process. This monolithic integration device was successfully demonstrated.

16:30–18:30

STu3H • Quantum & Nonlinear Materials & Devices

Presider: Amy Foster; Johns Hopkins Univ., USA

STu3H.1 • 16:30

Recent Advancements of Strained Silicon as an Optically Nonlinear Material, Matthew W. Puckett¹, Joseph S. Smalley¹, Yeshaiah Fainman¹; ¹Electrical and Computer Engineering, Univ. of California, San Diego, USA. We present several improvements to the understanding of strained silicon's second-order optical nonlinearity. In addition to incorporating the material into electro-optic modulators and wave-mixers, we analyze the nature of the optical nonlinearity on the nanoscale.

STu3H.2 • 16:45

Three-photon absorption in hydrogenated amorphous silicon at 1.55μm for all-optical processing, Xin Gai¹, Duk-Yong Choi¹, Barry Luther-Davies¹; ¹Laser Physics Centre of ANU, Australia. Three-photon absorption (3PA) has been observed as the dominant mechanism for nonlinear absorption in wide-bandgap hydrogenated amorphous silicon (a-Si:H) at 1.55μm.

STu3H.3 • 17:00

CW backward second harmonic generation with 720 nm-period domains in a QPM adhered-ridge waveguide, Masaki Shimizu^{1,2}, Takuya Utsugida^{1,2}, Satoshi Horikawa^{1,2}, Kazufumi Fujii¹, Sunao Kurimura^{1,2}, Hirochika Nakajima²; ¹National Inst. for Materials Science (NIMS), Japan; ²Waseda Univ., Japan. Ultrafine domain structure (720 nm period) achieved first CW backward SHG in Mg:LiNbO₃-based adhered-ridge waveguide.

CLEO: Science & Innovations

16:30–18:30

STu3I • Novel Applications of Nonlinear Optics

Presider: Valdas Pasiskevicius;
Royal Inst. of Technology
(JORCEP), Sweden

STu3I.1 • 16:30

Self-Phase Modulation Compensation in a Regenerative Amplifier Using Cascaded Second-Order Nonlinearities, Christophe Dorrer¹, Rick Roides¹, Jake Bromage¹, Jonathan D. Zueggel¹; ¹Univ. of Rochester, USA. Cascaded nonlinearities are theoretically and experimentally investigated for intracavity nonlinearity compensation in a Nd:YLF regenerative amplifier. Spectral broadening is significantly reduced, in agreement with simulations, allowing for efficient amplification in a Nd:YLF power amplifier.

STu3I.2 • 16:45

Generation of Flat, Rectangular Frequency Combs with Tunable Bandwidth and Frequency Spacing, Stefan Preussler¹, Norman Wenzel¹, Thomas Schneider¹; ¹Hochschule für Telekommunikation Leipzig, Germany. A method to produce flat, rectangular shaped frequency combs with tunable bandwidth and spacing is shown. It is based on the selection of lines from a mode-locked laser and a following modulation with cascaded modulators.

STu3I.3 • 17:00

A technique to measure the correlation of optical frequencies using four-wave mixing, Aravind Anthur¹, Regan Watts², Tam Huynh², Deepa Venkitesh¹, Liam Barry²; ¹Indian Inst. of Technology, Madras, India; ²Dublin City Univ., Ireland. We propose a novel technique to measure the correlation between two optical frequencies using a FWM scheme. To verify, we measure the evolution of de-correlation as a function of the path length difference between them.

16:30–18:30

STu3J • DSP and Coding

Presider: Christian Malouin;
Juniper Networks Inc., USA

STu3J.1 • 16:30

Efficient FIR Filter Configuration to Joint IQ Imbalance and Carrier-Phase Recovery in 16-QAM Coherent Receivers, Md Ibrahim Khalil¹, Arshad M. Chowdhury^{1,2}, Gee-Kung Chang²; ¹Dept of Electrical Engineering and Computer Science, North South Univ., Bangladesh; ²School of Electrical and computer Engineering, Georgia Inst. of Technology, USA. We propose an efficient configuration of FIR-filter for joint quadrature-imbalance (IQ) compensation and carrier-phase-recovery 16-QAM optical coherent receivers. Through computer simulation we demonstrate proposed scheme can mitigate wide-range of phase-noise and IQ-mismatch of optical front-end.

STu3J.2 • 16:45

Pilot-tone-Aided Two-stage Carrier Phase Recovery in dual-carrier Nyquist m-QAM Transmission System, Jiachuan Lin¹, Zhao-min Zhang¹, Lixia Xi¹, Xiaoguang Zhang¹; ¹BUPT, China. We propose an optically generated pilot tone aided carrier phase recovery scheme in dual-carrier Nyquist-mQAM systems. Both side channels can be compensated using one pilot, providing a high linewidth tolerance with small complexity.

STu3J.3 • 17:00

Fast Convergence Single-Stage Adaptive Frequency Domain Equalizer in Few Mode Fiber Transmission Systems, Xuan He¹, Yi Weng¹, Zhongqi Pan¹; ¹Dept of Electrical and Computer Engineering, Univ. of Louisiana at Lafayette, USA. We propose a fast convergence single-stage adaptive frequency domain algorithm for simultaneously compensating CD&DMGD in few-mode fiber system. The proposed algorithm can increase the convergence speed by 51% with 8% complexity increase.

CLEO: QELS-Fundamental Science

16:30–18:30

FTu3K • Active Plasmonic and Nanophotonic Modulators

Presider: Mikhail Belkin, Univ. of Texas at Austin, USA

FTu3K.1 • 16:30

Coherent Modulation of Light with Graphene, Thomas Roger¹, Julius Heitz¹, Niclas Westerberg¹, Genevieve Gariepy¹, Eliot Bolduc¹, John Jeffers², Jonathan Leach¹, Daniele Faccio¹; ¹Inst. of Photonics and Quantum Sciences, Heriot-Watt Univ., UK; ²Dept of Physics and Applied Physics, Univ. of Strathclyde, UK. Recent advances in light matter interaction have demonstrated the possibility to coherently absorb and modulate light with sub-wavelength, partially absorbing thin films. We demonstrate an ON-OFF ratio of 90% using graphene as a broadband modulator.

FTu3K.2 • 16:45

Ultrafast voltage-tunable plasmonic metamaterials based on intersubband polaritons, Jongwon Lee¹, Seungyong Jung¹, Pai-Yen Chen¹, Feng Lu¹, Frederic Demmerle², Gerhard Boehm², Markus Amann², Andrea Alu¹, Mikhail A. Belkin¹; ¹Univ. of Texas at Austin, USA; ²Walter Schottky Institut, Germany. We report ultra-fast voltage-tunable optical response from metamaterials based coupling of plasmonic resonances in metallic nanostructures with intersubband polaritons. Over 310nm of spectral peak tuning around 7 μ m with 10ns response time was experimentally demonstrated.

FTu3K.3 • 17:00



CMOS Compatible Ultra-Compact Modulator, Viktoriia Babicheva^{1,3}, Nathaniel Kinsey², Gururaj Naik², Marcello Ferrera^{2,4}, Andrei Lavrinenko¹, Vladimir M. Shalaev^{2,5}, Alexandra Boltasseva^{2,1}; ¹Technical Univ. of Denmark, Denmark; ²Purdue Univ., USA; ³National Research Univ. for Information Technology, Mechanics, and Optics, Russia; ⁴Heriot-Watt Univ., UK; ⁵The Russian Quantum Center, Russia. A planar layout for an ultra-compact plasmonic modulator is proposed and numerically investigated. Our device utilizes potentially CMOS compatible materials and can achieve 3-dB modulation in just 65nm and insertion loss <1dB at telecommunication wavelengths.

CLEO: Applications & Technology

16:30–18:00

ATu3L • Symposium on Laser Processing for Consumer Electronics II

Presider: Michael Mielke;
Raydiance Inc, USA

ATu3L.1 • 16:30  

Laser Cutting of Flexible Glass, Xinghua Li¹, Sean Garner¹; ¹Corning Incorporated, USA. In this invited talk, we review our cutting research on flexible glass substrates using both laser ablation and laser crack propagation methods. The methods are evaluated in terms of cut edge quality, speed and path to manufacturing.

ATu3L.2 • 17:00  


High Throughput Laser Processing with Ultra-Short Pulses by High Speed Line-Scanning in Synchronized Mode, Beat Neuenschwander¹, B. Jäggi¹, M. Zimmermann¹, L. Penning², R. de Loor²; ¹Inst. of Applied Laser, Bern Univ. of Applied Sciences, Switzerland; ²Next Scan Technology, Netherlands. Keeping the high efficiency and machining quality with today high average power ultrafast lasers demands new and fast beam deflecting systems. We will report on our latest results obtained with a fast polygon line scanner synchronized with a picosecond and femtosecond laser.

CLEO: Science & Innovations

CLEO: Applications
& Technology

16:30–18:30
STu3M • Microresonators 
Presider: Michael Watts, MIT, USA

STu3M.1 • 16:30 
Microgrooved Bottle Microresonators, Mohd Narizee Mohd Nasir¹, Ming Ding¹, Ganapathy Senthil Murugan¹, Michalis N. Zervas¹; ¹Optoelectronics Research Centre, Univ. of Southampton, UK. Spectral cleaning in bottle microresonators is presented by inscribing periodic surface microgrooves. Cleaning down to single strong WGM family is demonstrated, with Qs > 10E5 (similar to original microresonator).

STu3M.2 • 16:45 
Fifth Power Scaling of Quality Factor in Silicon Photonic Degenerate Band Edge Resonators, Justin Burr¹, Michael Wood¹, Ronald M. Reano¹; ¹Ohio State Univ., USA. We observe experimentally a transition of quality factor scaling from third power to fifth power of the number of periods in periodic silicon optical waveguides designed to exhibit a degenerate band edge.

STu3M.3 • 17:00 
High-Q Free-standing Silicon Nitride Micordisk Vertically Coupled with On-chip Waveguide, Weiqiang Xie¹, Dries Van Thourhout¹; ¹Photonics Research Group, Belgium. We designed and fabricated silicon nitride micordisk-waveguide vertical coupling devices processed at a low temperature of 270°. We experimentally demonstrate an intrinsic quality factor of 7.2x104 in the disk with only 15µm radius operating near 1310nm.


16:30–18:30
STu3N • Fiber Measurement and Devices
Presider: Mike Messerly, Lawrence Livermore National Lab., USA

STu3N.1 • 16:30 
Broadband and Ultrahigh Resolution Optical Spectroscopy using a Tapered Fiber, Noel Wan^{1,2}, Fan Meng^{1,3}, Ren-Jye Shiue¹, Edward Chen¹, Tim Schroeder¹, Dirk Englund¹; ¹Electrical Engineering and Computer Science, MIT, USA; ²Physics, Columbia Univ., USA; ³State Key Lab of Information Photonics and Optical Communications, Beijing Univ. of Posts and Telecommunications, China. We introduce a new integrated-optics spectroscopy scheme based on multimode interference, achieving ultra-high resolving powers ($Q > 10^5$) with linewidths down to 10 pm at 1500 nm, and a broad spectroscopy range from 500 nm to 1600 nm within a monolithic, millimeter-scale device.


STu3N.2 • 17:00
Spatially and temporally resolved imaging of modal content in photonic-bandgap fiber, Joel A. Carpenter¹, Benjamin J. Eggleston¹, Jochen Schroeder¹; ¹Univ. of Sydney, Australia. The principles of spatially and spectrally resolved imaging are extended to include spectral phase information which yields a measurement which is resolved both spatially and temporally.

16:30–18:30
STu3O • Symposium on Microcavity Exciton-Polaritons, Devices and Applications II 
Presider: Stephane Kena-Cohen; Imperial College London, UK

STu3O.1 • 16:30 
Polariton Lattices for Quantum Simulation, Alberto Amo¹; ¹Laboratoire de Photonique et Nanostructures, CNRS, France. Coupled micropillars etched in semiconductor microcavities are an excellent platform to engineer the properties of exciton-polaritons. These microstructures can be used to simulate various solid-state hamiltonians using photons in a non-linear environment.

STu3O.2 • 17:00 
Control of Turing Patterns in a Coherent Quantum Fluid, Y. C. Tse¹, P. Lewandowski², V. Ardizzone³, Nai H. Kwong^{1,4}, M. H. Luk^{1,4}, A. Lücke², M. Abbarchi^{3,5}, J. Bloch⁵, E. Baudin³, E. Galopin⁵, A. Lemaître⁵, C. Y. Tsang¹, K. P. Chan¹, P. T. Leung¹, Ph. Roussignol³, Rolf Binder⁴, J. Tignon³, S. Schumacher²; ¹Chinese Univ. of Hong Kong, China; ²Univ. of Paderborn, Germany; ³CNRS, France; ⁴Univ. of Arizona, USA; ⁵CNRS, France. A generalization of Turing patterns, originally developed for chemical reactions, to patterns in quantum fluids can be realized with microcavity polaritons. Theoretical concepts of formation and control, together with experimental observations, will be presented.

16:30–18:30
ATu3P • Symposium on Novel Light Sources and Photonic Devices in Optical Imaging II 
Presider: Benjamin Vakoc; Harvard Medical School, USA

ATu3P.1 • 16:30 
Laser sources for deep tissue multiphoton imaging, Chris Xu¹; ¹Applied and Engineering Physics, Cornell Univ., USA. Deep tissue multiphoton microscopy (MPM) using solitons generated from optical fibers are reviewed. The main characteristics of the excitation source for deep tissue MPM, such as wavelength, pulse energy, and repetition rate, are discussed.

ATu3P.2 • 17:00 
Multiphoton imaging and manipulation of biological systems, Jeffrey A. Squier¹, Erica Block¹, Michael Greco¹, Michael Young¹, Charles G. Durfee¹, Jens Thomas³, Jeff Field², Randy Bartels²; ¹Colorado School of Mines, USA; ²Colorado State Univ., USA; ³Friedrich-Schiller Univ., Germany. Through the development of simultaneous spatial and temporal focusing, platforms that can ablate tissue with excellent axial precision, and perform high-speed multiphoton imaging are converging. Recent developments in these platforms are presented.

Thank you for attending CLEO: 2014.

Look for your post-conference survey via email and let us know your thoughts on the program.

Tuesday, 10 June

CLEO: QELS-Fundamental Science

FTu3A • Quantum Repeater
Technologies—Continued

FTu3A.3 • 17:15

Long-lived dark states in a superconductor diamond hybrid quantum system, William Munro^{1,3}, Xiaobo Zhu¹, Yuichiro Matsuzaki¹, Robert Amsuss^{1,4}, Kosuke Kakuyanagi¹, Takaaki Shimo-Oka², Norikazu Mizuochi², Kae Nemoto³, Kouichi Semba³, Shiro Saito¹; ¹NTT Basic Research Labs, Japan; ²Univ. of Osaka, Graduate school of Engineering Science, Japan; ³National Inst. for Informatics, Japan; ⁴Vienna Center for Quantum Science and Technology, Atominstytut, TU Wien, Austria. We have observed a sharp resonance in the spectrum of flux qubit NV- diamond hybrid quantum system where its measured line-width is much narrower than that of both the flux-qubit and spin ensemble. This resonance is evidence of a collective & long-lived dark state.

FTu3A.4 • 17:30

Demonstration of a NV spin qubit interacting with a cavity mode in the Purcell regime, Luozhou Li^{1,2}, Tim Schroeder¹, Edward Chen¹, Michael Walsh¹, Igal Bayn^{1,2}, Ophir Gaathon¹, Matthew Trusheim¹, Ming Lu³, Jacob C. Mower¹, Hassaram Bakhr⁴, Matthew Markham⁵, Daniel Twitchen⁵, Dirk Englund¹; ¹Electrical Engineering and Computer Science, MIT, USA; ²Electrical Engineering, Columbia Univ., USA; ³Center for Functional Nanomaterials, Brookhaven National Lab, USA; ⁴College of Nanoscale Science and Engineering, Univ. at Albany-State Univ. of New York, USA; ⁵Element Six Ltd, UK. We demonstrate an over-80-fold enhancement of an NV's zero-phonon line emission inside cavity in the Purcell regime within a high-purity, electronic-grade diamond substrate. This system is a promising building block for quantum networks.

FTu3A.5 • 17:45

Hybrid Quantum Nanophotonic Devices for Coupling to Rare-Earth Ions, Evan Miyazono¹, Alex Hartz¹, Tian Zhong¹, Andrei Faraon¹; ¹Applied Physics, California Inst. of Technology, USA. Gallium arsenide photonic crystal resonators are designed and fabricated for evanescent coupling to localized ensembles of rare-earth ions in crystalline hosts. These devices will enable nano-scale on-chip optical quantum memories.

FTu3B • Advances in High-Harmonic Generation—Continued

FTu3B.4 • 17:15

Half-cycle Cutoffs up to the Oxygen K-edge: Signatures of Isolated Attosecond Pulses Across the Water Window, Francisco Silva¹, Stephan M. Teichmann¹, Seth L. Cousin¹, Michael Hemmer¹, Jens Biegert^{1,2}; ¹ICFO - Institut de Ciències Fotòniques, Spain; ²ICREA - Institució Catalana de Recerca i Estudis Avançats, Spain. We produce CEP-dependent X-ray continua up to the oxygen edge (543 eV) through high harmonic generation driven by sub-2-cycle 1.85 μm pulses at 1kHz, supporting isolated attosecond pulses of 45 as in the water window.

FTu3B.5 • 17:30

Generation of Bright Isolated Attosecond Soft X-Ray Pulses Driven by Multi-Cycle Mid-Infrared Lasers, Christopher A. Mancuso¹, Ming-Chang Chen^{1,2}, Carlos Hernandez-Garcia^{1,3}, Franklin Dollar¹, Benjamin Galloway¹, Dimitar Popmintchev¹, Benjamin Langdon⁴, Amelie Auger⁴, P. C. Huang², Barry C. Walker⁵, Luis Plaja³, Agnieszka Jaron-Becker¹, Andreas Becker¹, Margaret Murnane¹, Henry Kapteyn¹, Tenio Popmintchev¹; ¹Physics, JILA and Univ. of Colorado at Boulder, USA; ²Inst. of Photonics Technologies, National Tsing Hua Univ., Taiwan; ³Grupo de Investigación en Óptica Extrema, Universidad de Salamanca, Spain; ⁴Kapteyn-Murnane Labs Inc., USA; ⁵Physics, Univ. of Delaware, USA. By driving the high harmonic generation process with multi-cycle mid-infrared laser pulses, we demonstrate bright isolated, attosecond soft X-ray pulses for the first time.

FTu3B.6 • 17:45

Dispersion-free monochromator for selecting a single high-order harmonic beam, Eiji J. Takahashi¹, Masatoshi Hatayama², Satoshi Ichimaru², Katsumi Midorikawa¹; ¹Extreme Photonics Research Group, RIKEN Center for Advanced Photonics, Japan; ²NTT Advanced Technology Corporation, Japan. We propose a method to monochromatize high-order harmonics to isolate a single beam of harmonic radiation comprising femtosecond pulses. This novel method uses a multilayer-mirror approach, and has broadband tunability and high reflectivity in the soft-xray region.

FTu3C • Quantum Meta Optics—Continued

FTu3C.4 • 17:30

Probing Epsilon Near Zero-related Enhancements in Silver, Rabia Hussain¹, Mikhail A. Noginov¹, Maxim Durach², Natalia Noginova¹; ¹Norfolk State Univ., USA; ²Georgia Southern Univ., USA. We probe effects of field enhancements in silver-dielectric layers using a highly luminescent organic system with Eu^{3+} . Significant enhancement in the excitation spectra is observed at the spectral range corresponding to epsilon-near zero for silver.

FTu3C.5 • 17:45

Shaping Emission Spectra of Quantum Dots by All-dielectric Metasurfaces, Dragomir N. Neshev¹, Isabelle Staude¹, Nche T. Fofang², Sheng Liu², Jason Dominguez², Manuel Decker¹, Andrey Miroshnichenko¹, Vyacheslav V. Khaidkov³, Ting S. Luk², Igal Brener², Yuri S. Kivshar¹; ¹Australian National Univ., Australia; ²Sandia National Lab, USA; ³National Academy of Sciences of Ukraine, Ukraine. Silicon nanodisks support electric and magnetic resonances, which can be tuned independently via the nanodisk geometry. We utilize such engineered resonances and demonstrate dielectric metasurfaces for efficient shaping of the emission spectra of quantum dots.

FTu3D • Filamentation and the THz Generation—Continued

FTu3D.4 • 17:15

Optical heating of femtosecond laser filaments for long-range guidance of electrical discharges in air, Maik Scheller¹, Norman Born², Jerome V. Moloney¹, Pavel G. Polynkin¹; ¹Optical Sciences, Univ. of Arizona, USA; ²Philipps-Universität Marburg, Germany. We experimentally demonstrate that through conditioning dilute plasma in femtosecond laser filaments in air by an energetic nanosecond laser pulse, we reduce the breakdown voltage along the filament by up to the factor of 40.

FTu3D.5 • 17:30

Study of the interaction between multiple filaments in air, Guillaume Point¹, Yohann Brelet¹, Aurélien Houard¹, Vytautas Jukna², Carles Milian², Jérôme Carbonnel¹, Arnaud Couairon², André Mysyrowicz¹; ¹Laboratoire d'Optique Appliquée, France; ²Centre de Physique Théorique, France. Interaction between a large number of conventional infrared filaments in air leads to the emergence over meter long distance of plasma channels one order of magnitude denser than standard filaments. Simulations reproduce well these features.

FTu3D.6 • 17:45

Helical Filaments, Nicholas Barbieri¹, Zahra Hosseinimakarem², Khan Lim¹, Magali Durand¹, Benjamin Webb¹, Joshua Bradford¹, Erik McKee¹, Nathan Bodnar¹, Lawrence Shah¹, Matthieu Baudelet¹, Eric Johnson², Martin Richardson¹; ¹Univ. of Central Florida, USA; ²Clemson, USA. We demonstrate the use of non-diffracting beams to control and organize multiple filamentation in air. Here, a pair of laser filaments which twist about the optical axis during propagation is obtained using a Bessel beam superposition.



Join the conversation. Use #CLEO14.
Follow us @cleoconf on Twitter.

CLEO: Science & Innovations

STu3E • Pulse Characterization
and Ultrafast Imaging—
Continued

STu3E.4 • 17:15

Spatiotemporal Characterization of Ultrashort Laser Pulses Using Time-Domain Spatially Resolved Interferometry, Miguel Miranda¹, Marija Kotur¹, Cord L. Arnold¹, Anne L'Huillier¹; ¹Atomic Physics, Lund Univ., Sweden. We present a technique for characterizing ultrashort pulses in the spatiotemporal domain with high spatial resolution, based on a spatially-resolved Fourier-transform spectrometer. Spatiotemporal characterization of a pulse with pulse-front tilt is presented.

STu3E.5 • 17:30

THG of ZnO nanorods for efficient third order interferometric FROG, Susanta K. Das¹, Frank Güell², Ciarán Gray³, Prasanta K. Das⁴, Ruediger Grunwald¹, Enda McGlynn³, Gunter Steinmeyer¹; ¹Max Born Inst. for Nonlinear Optics and Short-Pulse Spectroscopy, Germany; ²Departament d'Electrònica, Universitat de Barcelona, Spain; ³School of Physical Sciences, National Centre for Plasma Science and Technology, Dublin City Univ., Ireland; ⁴School of Applied Sciences, KIIT Univ., India. Efficient third harmonic generation was found in ZnO nanorod layers grown by phase transport and low temperature chemical bath deposition method. Interferometric frequency-resolved optical gating of few cycle fs pulses was demonstrated.

STu3E.6 • 17:45

Observing the Conditional Decoherence of a Mixed State of Light, Marc Assmann¹, Mackillo Kira², Steven T. Cundiff¹; ¹JILA, Univ. of Colorado & National Inst. of Standards and Technology, USA; ²Dept of Physics, Philipps-Univ. Marburg, Germany. We demonstrate a method to capture the temporal evolution of a light field using continuous-variable conditional two-time Wigner functions. Reference beams with fixed phase relationship to the signal are not required.

STu3F • Technologies for High
Intensity—Continued

STu3F.3 • 17:15

A White-Light-Seeded Front End for Ultra-Intense Optical Parametric Chirped-Pulse Amplification, Jake Bromage¹, Rick Roides¹, Seung-Wan Bahk¹, Chad Mileham¹, Leva E. McIntire¹, Christophe Dorrer¹, Jonathan D. Zuegel¹; ¹Lab for Laser Energetics, Univ. of Rochester, USA. Ultra-intense optical parametric chirped-pulse amplification (OPCPA) requires a high-performance front end at 910 nm. Progress on developing a white-light-seeded chain of noncollinear optical parametric amplifiers (NOPAs) and a cylindrical Offner stretcher is presented.

STu3F.4 • 17:30

High-contrast, CEP-controlled double-CPA laser, Aurelie Jullien¹, Aurelien Ricci¹, Frederik Bohle¹, Jean-Philippe Rousseau¹, Stephanie Gabrielle², Nicolas Forget², Pierre Tournois², Rodrigo B. Lopez-Martens¹; ¹Laboratoire d'Optique Appliquée, France; ²Fastlite, France. We present the first CEP stable double-CPA laser system, producing 8 mJ, 22 fs pulses and featuring high temporal contrast (10^{11}) for performing relativistic intensity laser-plasma interactions at 1 kHz repetition rate.

STu3F.5 • 17:45

Spectral and Temporal Properties of Optical Signals with Multiple Sinusoidal Phase Modulations, Christophe Dorrer¹; ¹Univ. of Rochester, USA. High-energy laser systems use optical signals with multiple sinusoidal phase modulations for on-target smoothing and stimulated Brillouin scattering suppression. The spectrum and temporal frequency-modulation-to-amplitude-modulation conversion of these signals are analytically studied.

STu3G • Photodetectors—
Continued

STu3G.4 • 17:15

High Detectivity Short Wavelength II-VI Quantum Cascade Detector, Arvind Pawan Ravikumar¹, Thor A. Garcia², Joel De Jesus³, Maria C. Tamargo², Claire F. Gmachl¹; ¹Dept of Electrical Engineering, Princeton Univ., USA; ²Dept of Chemistry, The City College of New York of CUNY, USA; ³Dept of Physics, The City College of New York of CUNY, USA. We demonstrate the first II-VI based short-wave ($\lambda \leq 4 \mu\text{m}$) Quantum Cascade Detector. Peak responsivity and background limited detectivity of 0.1 mA/W and $2.5 \times 10^{10} \text{ cm}^2/\text{Hz/W}$, respectively, were measured at 80 K.

STu3G.5 • 17:30 **Tutorial**

Single Photon Imagers, Edoardo Charbon¹; ¹Technische Universiteit Delft, Netherlands. Photon counting has become a key technology in imaging science for biomedicine, physics, and engineering. This tutorial will review the first 10 years of CMOS single-photon imager history and give a perspective for the future.



Edoardo Charbon received the Ph.D. in EECS from Univ. of California Berkeley in 1995. He was with Cadence and Canesta until 2002, when he joined EPFL's faculty. Since 2008 he has been Chair of VLSI design at Delft University of Technology. Charbon has published over 250 articles in journals and proceedings and two books; in addition he holds 14 patents and is the co-recipient of the European Photonics Innovation Award.

STu3H • Quantum & Nonlinear
Materials & Devices—Continued

STu3H.4 • 17:15

Polymethines with Macroscopic Optical Nonlinearities Suitable for All-Optical Signal Processing, Joel M. Hales¹, Hyeongeun Kim¹, Stephen Barlow¹, Yulia Getmanenko¹, Yadong Zhang¹, Rebecca Giesking¹, Chad Risko¹, Shiva Shahin², Khanh Kieu², Robert A. Norwood², Nasser Peyghambarian², Jean-Luc Brédas¹, Seth R. Marder¹, Joseph W. Perry¹; ¹School of Chemistry and Biochemistry, Georgia Inst. of Technology, USA; ²College of Optical Sciences, Univ. of Arizona, USA. By preventing aggregation of polymethine molecules at high number density, we have developed organic materials with large third-order nonlinearities and low nonlinear absorption in the near-infrared thereby enabling demonstration of an all-optical signal processing application.

STu3H.5 • 17:30 **Invited**

Si-based Microcavity Devices with Ge Quantum Dots, Jinsong Xia¹, Cheng Zeng¹, Yong Zhang¹, Yingjie Ma², Zuimin Jiang², Jinzhong Yu^{1,3}; ¹Huazhong Univ. of Science and Technology, China; ²Fudan Univ., China; ³Inst. of Semiconductors, Chinese Academy of Science, China. Site-controlled single Ge quantum dot was grown on patterned silicon-on-insulator substrate. The single dot was then precisely embedded into a photonic crystal microcavity. Resonant photoluminescence was observed from the single Ge dot in the cavity.



For Conference News & Insights
Visit blog.cleoconference.org

CLEO: Science & Innovations

CLEO: QELS-
Fundamental ScienceCLEO: Applications
& TechnologySTu3I • Novel Applications of
Nonlinear Optics—Continued

STu3I.4 • 17:15

Experimental Demonstration of a Variable Bandwidth, Shape and Center-Frequency RF Photonics Filter using a Continuously Tunable Optical Tapped-Delay-Line and Having an Optical Output, Morteza Ziyadi¹, Amirhossein Mohajerin-Ariaei¹, Mohammed Chitgarha¹, Salman Khaleghi¹, Ahmed Al-maiman¹, Amin Abouzaid², Joseph Touch², Moshe Tur³, Loukas Paraschis⁴, Carsten Langrock⁵, Martin M. Fejer⁵, Alan Willner¹; ¹Univ. of Southern California, USA; ²Information Science Inst., Univ. of Southern California, USA; ³School of Electrical engineering, Tel Aviv Univ., Israel; ⁴Cisco Systems, USA; ⁵Edward L. Ginzton Lab, Stanford Univ., USA. We experimentally demonstrate the RF photonics filter using optical tapped delay line based on an optical frequency comb and a PPLN waveguide as the multiplexer. RF filters with variable bandwidth, shape and center-frequency are implemented.

STu3I.5 • 17:30

Coincidence Detection with Graphene Excitable Laser, Bhavin J. Shastri¹, Alexander N. Tait¹, Mitchell Nahmias¹, Ben Wu¹, Paul Prucnal¹; ¹Electrical Engineering, Princeton Univ., USA. We demonstrate a photonic coincidence detection circuit with a graphene excitable laser. This technology is a potential candidate for applications in novel all-optical devices for information processing and computing.

STu3I.6 • 17:45

Förster Resonance Energy Transfer within a Donor-Acceptor Composite Photochromic Molecule through One- and Two-Photon Absorption, Peng Zhao¹, Honghua Hu¹, Raz Gvishi², Galit Strum², Amir Tal², Shmuel Grinvald², Galit Bar², Laura Bekere³, Vladimir Lokshin³, Vladimir Khodorkovsky³, Mark Sigalov⁴, David J. Hagan¹, Eric W. Van Stryland¹; ¹CREOL, The College of Optics and Photonics, Univ. of Central Florida, USA; ²Applied Physics Division, Soreq NRC, Israel; ³Aix Marseille Université, France; ⁴Ben-Gurion Univ. of the Negev, Israel. FRET within a donor-acceptor composite photochromic molecule was investigated in a dye-doped sol-gel matrix using both 1 and 2-Photon absorption. The energy transfer efficiency was estimated from UV-excitation photokinetic measurements by applying a 2-level model.

STu3J • DSP and Coding—
Continued

STu3J.4 • 17:15

A PMD Monitoring Scheme for Direct-Detection Optical OFDM Systems Using Code-Assisted Optical Subcarriers, Tianwai Bo¹, Shuang Gao¹, Kam-Hon Tse¹, Chun-Kit Chan¹; ¹The Chinese Univ. of Hong Kong, Hong Kong. A PMD monitoring scheme is proposed for direct-detection optical OFDM systems by adding a pair of code-assisted optical subcarriers. Code correlation technique is used to retrieve DGD values over 0-25ps with <2-ps average monitoring error.

STu3J.5 • 17:30

Optimized Vector-Quantization-Based Signal Constellation Design (OVQ-SCD) for Multidimensional Optical Transport, Ivan B. Djordjevic¹, Aleksandra Jovanovic², Zoran Peric², Ting Wang³; ¹ECE Dept., Univ. of Arizona, USA; ²Faculty of Electronic Engineering, Univ. of Nis, Serbia; ³Optical Networks Dept, NEC Labs, USA. An optimized-vector-quantization-based signal-constellation-design (OVQ-SCD) suitable for beyond 1Pb/s serial multidimensional-optical-transport is proposed, in which signal-constellation-radial-transformation-function is optimized and near-uniform-distribution of points is achieved.

STu3J.6 • 17:45

Novel BCH Code Design for Mitigation of Phase Noise Induced Cycle Slips in DQPSK Systems, Miu Yoong Leong^{1,2}, Knud J. Larsen³, Gunnar Jacobsen^{1,2}, Sergei Popov², Darko Zibar³, Sergey Sergeyev⁴; ¹Acree Swedish ICT, Sweden; ²Royal Inst. of Technology (KTH), Sweden; ³Technical Univ. of Denmark (DTU), Denmark; ⁴Aston Univ., UK. We show that by proper code design, phase noise induced cycle slips causing an error floor can be mitigated for 28 Gbaud DQPSK systems. Performance of BCH codes are investigated in terms of required overhead.

FTu3K • Active Plasmonic and
Nanophotonic Modulators—
Continued

FTu3K.4 • 17:15

Dynamic Tuning of Surface Plasmon Polaritons via Thermally Controlled Liquid Crystals, Arif E. Cetin^{1,2}, Alket Mertiri³, Min Huang¹, Shyamsunder Erramilli^{3,4}, Hatice Altug^{2,1}; ¹Electrical and Computer Engineering, Boston Univ., USA; ²Bioengineering Dept, EPFL, Switzerland; ³Materials Science and Engineering, Boston Univ., USA; ⁴Physics, Boston Univ., USA. We present a thermally controlled plasmonic substrate in contact with a liquid crystal offering spectral tunings ~18.7 nm within ~180C at LC nematic phase. Nematic/isotropic transition also enables ~12 nm spectral change only within ~10C.

FTu3K.5 • 17:30

Active Plasmonics with Surface Acoustic Waves: Dynamic Electro-Mechanical Control over a Surface Plasmon Polariton Launcher, Claudia Ruppert¹, Frederike Förster¹, Artur Zrenner², Jörg B. Kinzel^{3,4}, Achim Wixforth^{3,4}, Hubert J. Krenner^{3,4}, Markus Betz¹; ¹Experimentelle Physik 2, Technische Universität Dortmund, Germany; ²Dept Physik, Universität Paderborn, Germany; ³Lehrstuhl für Experimentalphysik 1 and Augsburg Centre for Innovative Technologies (ACIT), Universität Augsburg, Germany; ⁴Nanosystems Initiative Munich (NIM), Germany. 500 MHz surface acoustic waves travel across a commensurate plasmonic grating coupler. A stroboscopic optical technique shows that the dynamic surface deformation deliberately modulates the coupler's efficiency by +/-2% during the ~2ns acoustic cycle

FTu3K.6 • 17:45


Latching Plasmonic Switch with High Extinction Ratio, Claudia Hoessbacher¹, Yuriy Fedoryshyn¹, Alexandros Emboras¹, David Hillerkuss¹, Argishti Melikyan², Manfred Kohl², Martin Sommer², Christian Hafner¹, Juerg Leuthold¹; ¹ETH Zurich, Switzerland; ²Karlsruhe Inst. of Technology, Germany. We demonstrate a plasmonic latching switch (5µm long) at 1550nm with a 6dB extinction ratio. It exploits the reversible formation of conducting nanofilaments in a plasmonic waveguide. It maintains its state without any power consumption.

ATu3L • Symposium on Laser
Processing for Consumer
Electronics II—ContinuedATu3L.3 • 17:30 **Invited**


Laser Processes for Development of Advanced Lithium-Ion Batteries - Increased Capacity and Cycle Life-Time, Wilhelm Pfleging^{1,2}; ¹Karlsruher Institut für Technologie, Germany; ²Karlsruhe Nano Micro Facility, Germany. Laser processing of electrode materials is a new technical approach in manufacturing of 3D batteries with improved electrochemical performance. Furthermore, laser-generated capillary structures transform electrodes to superwicking for liquid electrolytes leading to cost-efficient production. above

CLEO: Science & Innovations

CLEO: Applications
& TechnologySTu3M • Microresonators—
Continued

STu3M.4 • 17:15  **Controlling the Phase Front of Optical Fiber Beams using High Contrast Metastructures**, Amir Arbabi¹, Mahmood Bagheri², Alexander J. Ball¹, Yu Horie¹, David Fattal³, Andrei Faraon¹; ¹Applied Physics, California Inst. of Technology, USA; ²Jet Propulsion Lab, California Inst. of Technology, USA; ³Hewlett-Packard Labs, USA. The phase of optical beams can be modified by high contrast sub-wavelength periodic structures with gradually varying geometrical features. We present design, simulation, fabrication and characterization of planar micro-lenses shaping the beam of optical fibers.

STu3M.5 • 17:30  **Planar Retroreflector**, Amir Arbabi¹, Yu Horie¹, Andrei Faraon¹; ¹Applied Physics, California Inst. of Technology, USA. We propose a planar retroreflector composed of two cascaded high contrast periodic structures with slowly varying features. One of the high contrast structures focuses the light while the other reflects it as a concave mirror.

STu3M.6 • 17:45  **Coupled-resonator-optical-waveguide (CROW)-based On-chip Sensors with Multi-pixel Detection Using All-silicon Sub-bandgap Photodetectors**, Yu Li¹, Andrew W. Poon¹; ¹Hong Kong Univ of Science & Technology, Hong Kong. We propose a coupled-resonator-optical-waveguide-based sensor with multi-pixel detection using all-silicon sub-bandgap photodetectors at 1550 nm. Our proof-of-concept experiments of a PIN-diode-integrated three-microring CROW demonstrate sensing a minimum effective refractive index change of 2×10^{-5} .

STu3N • Fiber Measurement
and Devices—Continued

STu3N.3 • 17:15 **Near-real-time modal reconstruction using frequency-domain C² imaging**, Jeffrey Demas¹, Siddharth Ramachandran¹; ¹Dept of Electrical Engineering, Boston Univ., USA. We demonstrate frequency-domain cross-correlated (C²) imaging to reconstruct fiber modes and measure relative weights. Measurements take only 1.5 s, yield sub-ps group delay resolution and 25 dB modal discrimination, facilitating near-real-time monitoring of modal purity.

STu3N.4 • 17:30 **Effect of Dispersion Fluctuations on Longitudinal Gain Evolution in Phase-Sensitive Parametric Amplifiers**, fatemeh alishahi^{1,2}, Armand Vedadi², Mohammad Amin Shoaie², Marcelo A. Soto², Andrey Denisov², Khashayar Mehrany¹, Luc Thevenaz², Camille-Sophie Brès²; ¹sharif university of technology, Islamic Republic of Iran; ²Ecole Polytechnique Federale de Lausanne (EPFL), Switzerland. A Brillouin probing method is proposed to extract the distribution of signal power along phase-sensitive parametric amplifiers. Operation near the zero-dispersion-wavelength shows enhanced sensitivity to dispersion fluctuations, allowing effective extraction of dispersion map.

STu3N.5 • 17:45 **Oxygen sensing using hollow-core fiber based phase-shift cavity ring-down spectroscopy**, Dorit Munzke¹, Marvin Münzberg¹, Michael Böhm¹, Oliver Reich¹; ¹Univ. of Potsdam, Germany. We combine the benefits of phase-shift cavity ring-down spectroscopy and a photonic crystal fiber that acts as a sample cell. Absolute spectroscopic measurements are performed on gaseous samples (here: oxygen) of nanoliter volumes.


STu3O • Symposium on
Microcavity Exciton-Polaritons,
Devices and Applications II—
Continued

STu3O.3 • 17:15 **Ultra-fast spinor switching in polariton condensates**, Alexis Askitopoulos¹, Hamid Ohadi¹, Tim C. Liew², Zaharias Hatzopoulos^{3,4}, Pavlos Savvidis^{3,5}, Alexey Kavokin^{1,6}, Pavlos Lagoudakis¹; ¹Physics and Astronomy, Univ. of Southampton, UK; ²School of physical and mathematical sciences, Nanyang Technological Univ., Singapore; ³Microelectronics Research Group, IESL-FORTH, Greece; ⁴Dept of Physics, Univ. of Crete, Greece; ⁵Dept of Materials Science and Technology, Univ. of Crete, Greece; ⁶Spin Optics Lab, St Petersburg State Univ., Russia. We demonstrate a linear to circular polarization conversion mechanism in an optically confined polariton condensate created by an optical potential trap. Application of a non-resonant below threshold femtosecond pulse on the spinor condensate results in an ultrafast reversal of the spin state..

STu3O.4 • 17:30   **Spectroscopy of strongly-coupled organic semiconductor microcavities**, David Lidzey¹; ¹Univ. of Sheffield, UK. The strong-coupling regime allows optical and electronic states to be mixed forming cavity polaritons. I describe the basic physics of polaritons created using organic semiconductor and discuss their application in new types of device.

ATu3P • Symposium on Novel
Light Sources and Photonic
Devices in Optical Imaging II—
Continued

ATu3P.3 • 17:30  **On-Chip Supercontinuum Generation in a Dispersion-Controlled Silicon-Wire Waveguide**, Atsushi Ishizawa¹, Takahiro Goto^{1,2}, Hidetaka Nishi^{3,4}, Nobuyuki Matsuda^{1,3}, Rai Kou^{3,4}, Kenichi Hitachi¹, Tadashi Nishikawa², Koji Yamada^{3,4}, Tetsuomi Sogawa¹, Hideki Gotoh¹; ¹NTT Basic Research Labs, NTT Corporation, Japan; ²Tokyo Denki Univ., Japan; ³NTT Nanophotonics Center, NTT Corporation, Japan; ⁴NTT Microsystem Integration Labs, NTT Corporation, Japan. We demonstrate the broadest on-chip supercontinuum generation, spanning more than 2/3-octave (1300-2200 nm) bandwidth, with an 80-fs laser pulse in the 1.5-um band by controlling dispersion in a 0.9-cm-long Si-wire waveguide.

ATu3P.4 • 17:45  **Broadband, High Resolution Stimulated Raman Spectroscopy with Rapidly Wavelength Swept cw-Lasers**, Matthias Eibl¹, Sebastian Karpf¹, Wolfgang Wieser¹, Thomas Klein¹, Robert Huber^{1,2}; ¹Institut für BioMolekulare Optik, Univ. of Munich, Germany; ²Institut für Biomedizinische Optik, Univ. of Lübeck, Germany. A fast all fiber based setup for stimulated Raman spectroscopy with a rapidly wavelength swept cw-laser is presented. It enables flexible acquisition of broadband (750 cm⁻¹ to 3150 cm⁻¹) spectra with high resolution (0.5 cm⁻¹).

CLEO: QELS-Fundamental Science

FTu3A • Quantum Repeater
Technologies—Continued

FTu3A.6 • 18:00

Efficient Storage at Telecom Wavelength for Optical Quantum Memory, Julian Dajczgewand¹, Jean-Louis Le Gouët¹, Anne Louchet-Chauvet¹, Thierry Chanelière¹; ¹Laboratoire Aimé Cotton, France. We report high efficient storage at telecom wavelength using the recently proposed ROSE protocol. The bandwidth is analyzed to increase the multiplexing capacity.

FTu3A.7 • 18:15

The Quantum Memory Stick, Simon Devitt¹, Ashley Stephens², Rodney Van Meter³; ¹QIS, National Inst. of Informatics, Japan; ²National Inst. of Informatics, Japan; ³Keio Univ. Shonan Fujisawa Campu, Japan. We introduce a design a design for a quantum memory stick that uses active quantum error correction to store a qubit of encoded information for months/years.

FTu3B • Advances in High-
Harmonic Generation—
Continued

FTu3B.7 • 18:00

Theory of time-gated phase-matching for isolated attosecond soft x-ray pulse generation using mid-infrared lasers, Carlos Hernandez-Garcia^{1,2}, Ming-Chang Chen^{1,3}, Christopher Mancuso¹, Franklin Dollar¹, Benjamin Galloway¹, Dimitar Popmintchev¹, Pei-Chi Huang³, Barry C. Walker⁴, Tenio Popmintchev¹, Margaret Murnane¹, Henry Kapteyn¹, Luis Plaja², Agnieszka Jaron-Becker¹, Andreas Becker¹; ¹JILA, Univ. of Colorado, USA; ²Grupo de Investigación en Óptica Extrema, Universidad de Salamanca, Spain; ³Inst. of Photonics Technologies, National Tsing Hua Univ., Taiwan; ⁴Univ. of Delaware, USA. We model soft x-ray high harmonic generation and propagation driven by mid-infrared lasers. We find that multi-cycle laser pulses are ideal for generating shorter bright isolated attosecond pulses via time-gated phase-matching in high-density extended media.

FTu3B.8 • 18:15

Carrier-Envelope Phase Stabilization of a 10 Hz, 20 TW Laser for High-Flux Attosecond Pulse Generation, Yi Wu¹, Eric Cunningham¹, Jie Li¹, Michael Chini¹, Zenghu Chang¹; ¹CREOL and Dept of Physics, Univ. of Central Florida, USA. We developed a method to stabilize the carrier-envelope phase of a 20 TW Ti:Sapphire laser operating at 10 Hz. Phase-dependent features were observed in the high-order harmonic spectrum generated using Generalized Double Optical Gating.

FTu3C • Quantum Meta
Optics—Continued

FTu3C.6 • 18:00

Directional emission from quantum dots in a hyperbolic metamaterial, Tal Galfsky^{1,2}, Harish Krishnamoorthy^{1,2}, Ward D. Newman³, Evgenii Narimanov⁴, Zubin Jacob³, Vinod M. Menon^{1,2}; ¹Physics, Queens College of the City Univ. of New York, USA; ²Physics, Graduate Center of the City Univ. of New York, USA; ³Electrical and Computer Engineering, Univ. of Alberta, Canada; ⁴School of Computer and Electrical Engineering, Purdue Univ., USA. Directional light extraction from high-k modes in a hyperbolic metamaterial is demonstrated by direct coupling of resonance cones from quantum dots underneath a metal-dielectric composite to a high index bulls-eye grating structure.

FTu3C.7 • 18:15

Strong Light-Matter Coupling in Mid-Infrared Monolithic Metamaterial Nanocavities, Alexander Benz^{1,2}, Salvatore Campione^{1,2}, Sheng Liu^{1,2}, Ines Montano², John F. Klem², Michael B. Sinclair², Filippo Capolino³, Igal Brener^{1,2}; ¹Center for Integrated Nanotechnologies (CINT), Sandia National Labs, USA; ²Sandia National Labs, USA; ³Dept of Electrical Engineering and Computer Science, Univ. of California, Irvine, USA. We present the design and realization of strong light-matter coupling in monolithic metamaterial nanocavities. We achieve a Rabi frequency of 2.5 THz (corresponding to a polariton splitting of 20%) in a mode volume of $1.34 \times 10^{-3}(\lambda/n)^3$

FTu3D • Filamentation and the
THz Generation—Continued

FTu3D.7 • 18:00

Enhanced Spectral Broadening and Beam Collimation from Pulse-Sequence Induced Filamentation, Eric Rosenthal¹, Nihal Jhajji¹, Reuven Birnbaum¹, Howard Milchberg¹; ¹Inst. for Research in Electronics and Applied Physics, Univ. of Maryland, USA. Filaments in air, induced by pulse trains of four ultrashort pulses, each separated by the rotational revival time of nitrogen exhibit an increased degree of spectral broadening and collimation over the single pulse filament case.

FTu3D.8 • 18:15

Electronic switching mechanism in Aperiodic DFB Lasers, Thomas Folland¹, Md Khairuzzaman¹, Owen Marshall¹, Harvey E. Beere², David A. Ritchie², Subhasish Chakraborty¹; ¹Univ. of Manchester, UK; ²Univ. of Cambridge, UK. For the first time, we present direct experimental evidence of the presence of spatial hole burning within switchable aperiodic DFB terahertz quantum cascade lasers. This will lead towards the development of quasicontinuous tuneable terahertz lasers.

NOTES

CLEO: Science & Innovations

STu3E • Pulse Characterization and Ultrafast Imaging—Continued

STu3E.7 • 18:00

Single-shot ultrafast imaging using parallax-free alignment with a tilted lenslet array, Barmak Heshmat¹, Guy Satat¹, Christopher Barsi¹, Ramesh Raskar¹; ¹Media Lab, MIT, USA. We demonstrate single-shot, two-dimensional imaging of ultrafast phenomena using a streak camera and a tilted lenslet array. We derive conditions for parallax-free imaging and experimentally verify the geometry by observing scattering of femtosecond pulses.

STu3E.8 • 18:15

Time-resolved photoelectron imaging with 90-nm pump pulses, Shunsuke Adachi^{1,2}, Motoki Sato¹, Yoshi-ichi Suzuki¹, Toshinori Suzuki^{1,2}; ¹Dept of chemistry, Graduate school of Science, Kyoto Univ., Japan; ²Advanced Science Inst., RIKEN, Japan. Time-resolved photoelectron imaging was performed with 90-nm pump pulses. Quantum beat by coherent excitation of multiple Rydberg states in Kr, and photodissociation of CO₂ within a few ps from initially excited Rydberg state(s) were observed.

STu3F • Technologies for High Intensity—Continued

STu3F.6 • 18:00

Sub-fs precision measurement of relative x-ray arrival time for FELs, Nick Hartmann^{1,2}, Wolfram Helm^{1,3}, Mina R. Bionta⁴, Andreas Galler⁵, Jan Grünert⁵, Serguei Molodtsov^{5,6}, Kenneth R. Ferguson¹, Sebastian Schorb¹, Michele Swiggers¹, Sebastian Carron¹, Christoph Bostedt¹, Jean-Charles Castagna¹, John D. Bozek¹, James M. Glowia¹, Daniel J. Kane⁷, Alan Fry¹, William E. White¹, Christoph P. Hauri^{8,9}, Thomas Feurer², Ryan N. Coffee¹; ¹LCLS, SLAC National Accelerator Lab, USA; ²Inst. of Applied Physics, Univ. of Bern, Switzerland; ³Technische Universität München, Germany; ⁴LCAR-UMR, Université Paul Sabatier Toulouse III-CNRS, France; ⁵European XFEL GmbH, Germany; ⁶Inst. of Experimental Physics, Univ. of Technology Bergakademie Freiberg, Germany; ⁷Mesa Photonics, LLC, USA; ⁸Paul Scherrer Inst., Switzerland; ⁹Physics Dept, Ecole Polytechnique Fédérale de Lausanne, Switzerland. We present a spectrogram-based timing technique for x-ray free electron lasers (XFELs) that reports x-ray/optical delay below 1 fs RMS error to correct for timing jitter.

STu3F.7 • 18:15

Contrast enhancements to petawatt lasers using picosecond optical parametric amplification and frequency doubling, David I. Hillier¹, Colin Danson¹, David Egan¹, Stephern Elsmere¹, Mark Girling¹, Ewan Harvey¹, Nicholas Hopps¹, Michael Norman¹, Stefan Parker¹, Paul Treadwell¹, David Winter¹, Thomas Bett¹; ¹Atomic Weapons Establishment, UK. Nanosecond contrast of the Orion CPA beamlines is enhanced from 10⁻⁸ to 10⁻¹⁰ by inserting a picosecond OPA prior to the stretcher. In conjunction with frequency doubling post-compression this will increase the contrast to ~10⁻¹⁸.

STu3G • Photodetectors—Continued

STu3H • Quantum & Nonlinear Materials & Devices—Continued

STu3H.6 • 18:00

Controlling Quantum Dot Energies Using Submonolayer Bandstructure Engineering, Lan Yu¹, Stephanie Law¹, Daehwan Jung², Minjoo Larry Lee², Dan Wasserman¹; ¹Electrical and Computer Engineering, Univ. of Illinois, USA; ²Electrical Engineering, Yale Univ., USA. We demonstrate control of energy states in epitaxially-grown sub-monolayer quantum dots by engineering of the internal bandstructure of the dots. We show shifts of the quantum dot ground state energy from 1.38eV to 1.68eV.

STu3H.7 • 18:15

Helium ion microscope generated nitrogen-vacancy centres in type Ib diamond, David McCloskey¹, Danny Fox¹, Neal O'Hara¹, V. Usov¹, Declan Scanlan¹, Niall McEvoy¹, Georg Duesberg¹, Graham Cross¹, Hongzhou Zhang¹, John F. Donegan¹; ¹School of Physics, CRANN and AMBER, Trinity College Dublin, Ireland. We report on position and density control of nitrogen-vacancy (NV) centres created in type Ib diamond using localised exposure from a helium ion microscope and subsequent annealing. Spatial control to <380 nm has been achieved.

NOTES

CLEO: Science & Innovations

**CLEO: QELS-
Fundamental Science**

**CLEO: Applications
& Technology**

**STu3I • Novel Applications of
Nonlinear Optics—Continued**

**STu3J • DSP and Coding—
Continued**

**FTu3K • Active Plasmonic and
Nanophotonic Modulators—
Continued**

STu3I.7 • 18:00
Single-shot Coherent Raman Multiplex Planar Imaging, Alexis Bohlin¹, Christopher Kliewer¹; ¹Combustion Chemistry, Sandia National Labs, USA. We develop a coherent Raman technique for simultaneous planar imaging and multiplex spectroscopy provided in a single-laser-shot. Spatially correlated spectra from multiple species in a two-dimensional field are presented and possible gas-phase applications are discussed.

STu3J.7 • 18:00
Optimal Signal Constellation Design for Ultra-High-Speed Optical Transport in the Presence of Phase Noise, Tao Liu¹, Ivan B. Djordjevic¹, Ting Wang²; ¹Univ. of Arizona, USA; ²NEC Labs America, USA. An optimal signal constellation design algorithm suitable for the phase noise channels is proposed, in which the cumulative log-likelihood-function is used as the optimization criterion. The signal constellations obtained by this algorithm significantly outperform conventional QAM.

FTu3K.7 • 18:00
Compact multisection cavity switches in metal-dielectric-metal plasmonic waveguides, Pouya Dastmalchi¹, Georgios Veronis¹; ¹Louisiana State Univ., USA. We introduce a compact absorption switch consisting of a plasmonic metal-dielectric-metal waveguide coupled to a multisection cavity. The optimized multisection cavity switch leads to greatly enhanced modulation depth compared to an optimized Fabry-Perot cavity switch.

STu3I.8 • 18:15
Intracavity Raman lasers at 990 nm and 976 nm based on a three-level Nd:YLF fundamental laser, Dimitri Geskus¹, Jonas Jakutis Neto¹, Saara-Maarit Reijn¹, Helen M. Pask², Niklaus Wetter¹; ¹Centro de Lasers e Aplicações, IPEN/SP, Brazil; ²MQ Photonics, Dept of Physics, Macquarie Univ., Australia. This is the first time that significant Stokes output power of 0.88 W at 990 nm has been achieved using a three-level fundamental transition (quasi-cw Nd:YLF laser) with stimulated Raman scattering in a KGW crystal.

STu3J.8 • 18:15
On the Generalized LDPC Codes from Multiple Component Codes Suitable for High-Speed Optical Transport, Ivan B. Djordjevic¹, Ting Wang²; ¹ECE, Univ. of Arizona, USA; ²Optical Networks, NEC Labs, USA. A class of GLDPC-codes is proposed consisting of multiple local-codes suitable for code-rate-adaptation in high-speed optical-transport-networks, providing excellent coding-gains. GLDPC-decoder for proposed codes is more suitable for parallelization in FPGA/ASIC-hardware compared to LDPC-decoder.


FTu3K.8 • 18:15
Single-Nanoparticle Study of Switchable Exciton-Plasmon Coupling, Mingsong Wang^{1,2}, Yuebing Zheng^{1,2}; ¹Mechanical Engineering, The Univ. of Texas at Austin, USA; ²Materials Science and Engineering, The Univ. of Texas at Austin, USA. We report the single-nanoparticle study of switchable exciton-plasmon coupling. The wavelength-dependent peak shifts in localized surface plasmon resonances (LSPRs) of metal nanoparticle-spiropyran hybrids depend on the combined effects of material dispersion and sensitivity of LSPRs.


NOTES

CLEO: Science & Innovations

CLEO: Applications
& Technology

STu3M • Microresonators—
Continued

STu3M.7 • 18:00  **An On-chip All Silicon Passive Optical Diode Based on Photonic crystal L3 Cavities**, Jinsong Xia¹, Yong Zhang¹, Danping Li¹, Zengzhi Huang¹, Jinzhong Yu^{2,1}, Cheng Zeng¹; ¹Wuhan National Lab for Optoelectronics, China; ²Inst. of Semiconductors, Chinese Academy of Sciences, China. An all-silicon passive optical diode based on cascaded photonic crystal L3 cavities is demonstrated. Nonreciprocal transmission ratio of 30.8 dB and insertion loss of 8.3 dB are realized in the device.

STu3M.8 • 18:15  **Selective Mode Splitting in High-Q Microresonator for Dispersion Engineering**, Xiyuan Lu¹, Wei C. Jiang¹, Qiang Lin¹; ¹Univ. of Rochester, USA. We demonstrate selective mode splitting (SMS) in microresonators. SMS can split one selected optical mode up to 1.25 nm with other modes unperturbed. This opens a new gate for phasematching in parametric oscillations in microresonators.

STu3N • Fiber Measurement
and Devices—Continued

STu3N.6 • 18:00
Management of slow light dispersion and delay time characteristics with SNAP bottle resonators, Misha Sumetsky¹; ¹Aston Univ., UK. The nanoscale radius variation of a bottle microresonator with the required dispersion characteristics is determined theoretically. Experimentally, a microresonator with the footprint 0.08 mm² exhibiting 20 ns/nm dispersion compensation of 100 ps pulses is demonstrated.

STu3N.7 • 18:15
High-fidelity optical buffer based on temporal cavity solitons, Jae K. Jang¹, Miro J. Erkintalo¹, Jochen Schroeder², Benjamin J. Eggleton², Stuart G. Murdoch¹, Stephane Coen¹; ¹Univ. of Auckland, New Zealand; ²Univ. of Sydney, Australia. We demonstrate an all-optical data buffer implemented using temporal cavity solitons in a fiber ring. The ring can hold 4736 bits, encoded as cavity solitons, at 10 Gb/s for over one minute with 100% fidelity.

STu3O • Symposium on
Microcavity Exciton-Polaritons,
Devices and Applications II—
Continued

STu3O.5 • 18:00  **Nonlinear interactions in an organic polariton condensate**, Konstantinos Daskalakis¹, Stefan Maier¹, Ray Murray¹, Stéphane Kéna-Cohen^{1,2}; ¹Dept of Physics and Centre for Plastic Electronics, Imperial College London, UK; ²Dept of Engineering Physics, École Polytechnique de Montréal, Canada. We demonstrate an organic polariton condensate that exhibits nonlinear interactions at room-temperature. Upon reaching threshold, we observe a superlinear power dependence, a power-dependent blueshift and the emergence of long-range spatial coherence resulting from polariton interactions.

STu3O.6 • 18:15  **Room Temperature Bloch Surface Wave Polaritons**, Stefano Pirotta¹, Maddalena Patrini¹, Marco Liscidini¹, Matteo Galli¹, Giacomo Dacarro¹, Giancarlo Canazza², Giorgio Guizzetti¹, Davide Comoretto², Daniele Bajoni³; ¹Physics, Università degli Studi di Pavia, Italy; ²Chemistry, Università degli Studi di Genova, Italy; ³Engineering, Università degli Studi di Pavia, Italy. We demonstrate strong coupling between Bloch surface waves in a Ta2O5/SiO2 multilayer and J-aggregate excitons. The measured Rabi splitting is 290 meV. The mode dispersion curves are investigated by means of attenuated-total-reflection and photoluminescence experiments.

ATu3P • Symposium on Novel
Light Sources and Photonic
Devices in Optical Imaging II—
Continued

ATu3P.5 • 18:00  **Narrowband Guided Fano Resonators for Mid-Infrared Spectroscopy and Imaging**, Jui-Nung Liu¹, Matthew V. Schulmerich¹, Rohit Bhargava¹, Brian T. Cunningham¹; ¹Univ. of Illinois at Urbana-Champaign, USA. We report the demonstration of an array of high-performance one-layer narrowband mid-IR guided Fano resonators (GFRs) in the C-H stretching region (2700-3200 cm⁻¹) for high-quality microspectroscopic mid-IR imaging.

ATu3P.6 • 18:15  **Optical time-stretch microscopy using Bessel spectral shower illumination**, Yiqing Xu¹, Xiaoming Wei¹, Antony C. Chan¹, Edmund Y. Lam¹, Kenneth Wong¹, Kevin Tsia¹; ¹Dept of Electrical and Electronic Engineering, The Univ. of Hong Kong, Hong Kong. We experimentally demonstrate optical time-stretch microscopy with one dimensional Bessel spectral shower illumination for ultrafast extended depth-of-field imaging at a single-shot scan rate of 26.3 MHz.

NOTES

Large empty rectangular area for taking notes, bounded by a thin black line.

18:30–20:30
JTU4A • Poster Session 1

JTU4A.1

Studying Momentum Distributions in all Aspects Reveals Important Insight, Cornelia Hofmann¹, Alexandra S. Landsman¹, Robert Boge¹, Sebastian Heuser¹, Claudio Cirelli¹, Matthias Weger¹, André Ludwig¹, Jochen Maurer¹, Lukas Gallmann^{1,2}, Ursula Keller¹; ¹Physics Dept, ETH Zurich, Switzerland; ²Inst. of Applied Physics, Univ. of Bern, Switzerland. Strong field ionization momentum distribution contains much information. The angular distribution indicates real tunneling delay time, the center shows ellipticity dependent Coulomb effects, and the longitudinal momentum spread challenges the assumption of zero initial momentum.

JTU4A.2

An improved attosecond-pulse characterization based on the FROG-CRAB technique, Siddharth Bhardwaj¹, Phillip D. Keathley¹, Jeffrey Moses¹, Guillaume Laurent¹, Franz Kärtner^{1,2}; ¹Dept of Electrical Engineering and Computer Science, MIT, USA; ²Center for Free Electron Laser, Deutsches Elektronen-Synchrotron, Germany. The FROG-CRAB method was improved to account for the photoionization process, significantly improving its accuracy for low-photon-energy EUV pulses. A method for accounting for the photoionization step while using the conventional retrieval algorithm was also demonstrated.

JTU4A.3

Carrier-envelope phase stabilization via acoustic frequency combs, Fabian Lücking¹, Bastian Borchers², Gunter Steinmeyer²; ¹Femtolasers Produktions GmbH, Austria; ²Max Born Inst. for Nonlinear Optics, Germany. We demonstrate a novel scheme for improved feed-forward CEP stabilization of laser amplifiers. Synthesized acoustic few-cycle transients are used to stabilize the CEP of an optical pulse train at the amplifier repetition rate.

JTU4A.4

Anomalous light bending with high efficiency by plasmonic phase-discontinuous air-slit array, Cheng-Hsui Lin¹, Br-Shu Wu¹, Chen-Bin Huang¹; ¹National Tsing Hua Univ., Taiwan. V-shaped air slits inscribed in a metallic thin film is used to achieve cross-polarized anomalous refraction with high efficiency. The experimental refraction angles are in excellent agreements with theoretical values.

JTU4A.5

A Novel Hybrid Plasmonic Rod-dimer/Ring Nanostructure for Sensing and Trapping, Jia Yu Lin¹, Chia-Yang Tsai¹, Pin-Tso Lin¹, Tse-En Hsu¹, Po-Tsung Lee¹; ¹National Chiao Tung Univ., Taiwan. We propose and investigate a novel hybrid plasmonic rod-dimer/ring (RDR) nanostructure with significantly enhanced near-field at the gap region for its potential on sensing and trapping applications.

JTU4A.6

Chip-Integrated Plasmon-Induced Transparency via Plasmonic Waveguides Side-coupled of a Single Composite Nanocavity, zhen chai^{1,2}; ¹Dept of Physics, Peking Univ., China; ²State Key Lab for Mesoscopic Physics, Peking Univ., China. We experimentally reported a chip-integrated plasmon-induced transparency (PIT) by a planar plasmonic composite nanocavity. A shift of 490 nm of the transparency window and dual PIT like effect are achieved through coating the PMMA layer.

JTU4A.7

Single Nanoparticle Detection and Sizing by Using a Nanoscale Optical Fiber, Xiaochong Yu¹, Bei-Bei Li¹, Pan Wang², Limin Tong², Qihuang Gong¹, Yun-Feng Xiao¹; ¹Peking Univ., China; ²Zhejiang Univ., China. We demonstrate the detection and sizing of single nanoparticles in aqueous environment by real-time monitoring the step changes in the nanofiber transmission.

JTU4A.8

Nano-patterning based on Two-Surface-Plasmon-Polariton-Absorption using 400nm Femtosecond Laser, yunxiang Li¹, Fang Liu¹, Weisi Meng¹, Yidong Huang¹; ¹Electronic Engineering, Tsinghua Univ., China. Nano-patterning with linewidth of ~55 nm is demonstrated utilizing two-surface-plasmon-polariton-absorption (TSPPA) at the wavelength of 400 nm. The SPP field generated by plasmonic microlens is recorded by the TSPPA showing a new way for recording the SPP field in micro/nano structures.

JTU4A.9

Low-Temperature Raman G-mode of Plasmonic-Graphene Hybrid Platform, Long Xiao¹, Fang Liu¹, Yidong Huang¹; ¹Dept of Electronic Engineering, Tsinghua Univ., China. The unusual properties of Raman G-mode of plasmonic-graphene hybrid platform has been studied at varying temperatures, which provides important evidences to understand the optoelectronic characteristics of the hybrid platform.

JTU4A.10

Topological Shaping of Light using Vortex Transmutation, Nan Gao¹, Lina Shi¹, Changqing Xie¹; ¹Key Lab of Nano-Fabrication and Novel Devices Integrated Technology, Inst. of Microelectronics, Chinese Academy of Sciences, China. We show that vortex transmutation prevents the generation of high order central vortices in the topological shaping of light with nanoslits, and propose a solution to this problem utilizing the modular transmutation rule.

JTU4A.11

Super resolution phase-contrast imaging of transparent nano-objects by a plasmonic lens, Xiangang Luo¹; ¹CAS Inst. of Optics and Electronics, China. We propose a specially designed plasmonic lens for imaging transparent nano objects with small refraction index difference from surrounding medium. The spatial resolution down to 64 nm and minimum distinguishable refraction index difference down to 0.05 are numerically demonstrated.

JTU4A.12

Fabrication and Characterization of Template-Stripped Plasmonic Substrates for High-Resolution Chemical Imaging, Sarah Elliott¹, Mark Turner¹, Isabel Rich¹, Nathan Lindquist¹; ¹Physics Dept, Bethel Univ., USA. Template-stripped plasmonic nanoholes are used as high-resolution chemical imaging substrates via surface-enhanced Raman spectroscopy. Chemical patterns created with microcontact printing show these surfaces to provide large and uniform enhancements suitable for imaging.

JTU4A.13

Quantized surface-plasmon-polariton excitation and propagation on graphene, George Hanson¹, Changhyoung Lee², Dimitris Angelakis², Mark Tame³; ¹Electrical Engineering, Univ. of Wisconsin Milwaukee, USA; ²Centre for Quantum Technologies, National Univ. of Singapore, Singapore; ³School of Chemistry and Physics, Univ. of KwaZulu-Natal, South Africa. A quantum-mechanical description of the excitation of surface-plasmon polaritons (SPPs) on graphene is presented, as well as photon to quantized SPP state transfer and decoherence. The tunability of graphene allows for the control of quantized SPPs.

JTU4A.14

Experiments on Cascaded Quadratic Soliton Compression in Unpoled LN Waveguide, Hairun Guo¹, Binbin Zhou¹, Xianglong Zeng², Morten Bache¹; ¹Dept of Photonics Engineering, Technical Univ. of Denmark, Denmark; ²Key Lab of Special Fiber Optics and Optical Access Networks, Shanghai Univ., China. Experiments on cascaded quadratic soliton compression in unpoled phase-mismatched lithium niobate waveguides are presented. Pulse self-phase modulation dominated by an overall self-defocusing nonlinearity is observed, with an variation of pump wavelength and waveguide core width.

JTU4A.15

Generation and Propagation of Optical Accelerating Regular Triple-Cusp Beams, Hujun Ren^{1,2}, Ping Yu²; ¹Key Lab of Optical Information Detecting and Display Technology, Zhejiang Normal Univ., China; ²Dept of Physics and Astronomy, Univ. of Missouri, USA. Optical accelerating triple-cusp beams are generated by imposing a phase grey-scale map on a phase modulation element. We give the mechanism of controlling ballistic trajectory of main lobes of regular triple-cusp beams.

JTU4A.16

Femtosecond Supercontinuum Generation in a Silicon Wire Waveguide at Telecom Wavelengths, François Leo^{1,2}, Simon-Pierre Gorza³, Jassem Safioui³, Pascal Kockaert³, Stéphane Coen⁴, Utsav Dave^{1,2}, Bart Kuyken^{1,2}, Gunther Roelkens^{1,2}; ¹Photonics Research Group, Dept of Information Technology, Ghent Univ., Belgium; ²Center for Nano- and biophotonics (NB-photonics), Ghent Univ., Belgium; ³OPERA-Photonique, Université Libre de Bruxelles, Belgium; ⁴Physics Dept, Univ. of Auckland, New Zealand. We demonstrate femtosecond supercontinuum generation in a silicon waveguide. Despite the strong nonlinear absorption inherent to silicon at telecom wavelengths, we experimentally demonstrate that the compression and subsequent splitting of higher order solitons remains possible.

JTU4A.17

Coherent control of Snell's law, Jin-hui Shi^{1,2}, Xu Fang², Nikolay I. Zheludev^{2,3}; ¹Harbin Engineering Univ., China; ²Univ. of Southampton, UK; ³Nanyang Technological Univ., Singapore. We demonstrate coherent control of the generalized Snell's law in ultrathin gradient metasurfaces constructed by an array of V-shaped slot nanoantennas.

JTU4A.18

Measurement of Nonlinear Refraction Dynamics of CS₂, Matthew Reichert¹, Honghua Hu¹, Manuel R. Ferdinandus¹, Marcus Seidel¹, Peng Zhao¹, Jennifer M. Reed¹, Dmitry A. Fishman¹, Scott Webster¹, David J. Hagan¹, Eric W. Van Stryland¹; ¹CREOL, The College of Optics and Photonics, Univ. of Central Florida, USA. Nonlinear refractive dynamics of CS₂ are measured with the beam deflection technique. A response function model is fit, from which the pulse width dependent $n_{2,eff}$ is calculated and compared to Z-scan measurements.

JTU4A.19

Enhanced random lasing emission under plasma atmosphere in Nd³⁺ doped (Pb,Lu)(Zr,Ti)O₃ disordered ceramics, Long Xu¹, Jingwen Zhang¹, Hua Zhao¹, Yi Zhang²; ¹Dept of Physics, Harbin Inst. of Technology, China; ²Science and Technology on Special System Simulation Lab, Beijing Simulation Center, China. Great enhancement of random lasing emission in Nd³⁺ doped (Pb,Lu)(Zr,Ti)O₃ ceramics were investigated upon exposing to plasma atmosphere. The diffusion of light, optical energy storage and increased scatterers play vital roles in the experimental results.

JTU4A.20

Pump-probe study of plasma generated with linear and circularly polarized filaments in nitrogen, Amin rasoulofi¹, Brian Kamer¹, Jean-Claude M. Diels¹, Ladan Arissian¹; ¹Center for high technology materials, Univ. of New Mexico, USA. We study the dynamics of the plasma generated with 800nm filaments of 60fs in a pump-probe system in nitrogen cell. We see the effect of molecular revival and plasma dynamics on beam profile and spectrum.

JTU4A • Poster Session 1—Continued

JTU4A.21

Imaging the structure of van der Waals Complexes with Laser-driven Coulomb Explosion, Chengyin Wu¹; ¹Dept of Physics, Peking Univ., China. Geometric structures of some van der Waals Complexes were determined by precisely measuring three-dimensional momentum vectors of correlated atomic ions produced in the laser-driven Coulomb explosion of these van der Waals complexes.

JTU4A.22

Anomalous transient amplification in lossy waveguides, Konstantinos Makris¹, Li Ge^{2,1}, Hakan E. Tureci¹; ¹Princeton Univ., USA; ²College of Staten Island, CUNY, USA. In a medium that is on average lossy, we show that under appropriate initial conditions the power can be amplified by several orders of magnitude. This robust phenomenon can be quantitatively explained by pseudospectra analysis.

JTU4A.23

Interaction of Flying Electromagnetic Doughnut with Nanostructures, Tim Raybould¹, Nikitas Papisimakis¹, Vassili A. Fedotov¹, Ian J. Youngs², Nikolay I. Zheludev^{1,2}; ¹Optoelectronics Research Centre, Univ. of Southampton, UK; ²Centre for Disruptive Photonic Technologies, Nanyang Technological Univ., Singapore; ³DSTL, UK. We report on the electromagnetic properties of the single-cycle "flying doughnut" electromagnetic permutations in the context of their interactions with nanoscale objects, such as dielectric and plasmonic nanoparticles.

JTU4A.24

Octave-Spanning Mid-IR Supercontinuum Generation with Ultrafast Cascaded Nonlinearities, Binbin Zhou¹, Hairun Guo¹, Xing Liu¹, Morten Bache¹; ¹Danmarks Tekniske Universitet, Denmark. An octave-spanning mid-IR supercontinuum is observed experimentally using ultrafast cascaded nonlinearities in an LiInS₂ quadratic nonlinear crystal pumped with 70 fs energetic mid-IR pulses and cut for strongly phase-mismatched second-harmonic generation.

JTU4A.25

Relation Between Interband Dipole and Momentum Matrix Elements in Semiconductors, Baijie Gu¹, Nai H. Kwong¹, Rolf Binder¹; ¹Univ. of Arizona, USA. The relation between dipole and momentum matrix elements in crystals, treated with periodic boundary conditions, is revisited. A correction term to standard expressions is found to be large for bulk GaAs, small for THz transitions.

JTU4A.26

Quantum coherence in bulk GaAs studied by interference between electron-phonon coupled states, Kazutaka Nakamura^{1,2}, Shingo Hayashi^{1,2}, Keigo Kato^{1,2}, Katsura Norimatsu^{1,2}, Yosuke Kayanuma^{1,2}; ¹Tohoku Inst. of Technology, Japan; ²CREST-JST, Japan. Both electronic and phonon coherence in bulk GaAs is studied using an interference experiment of electron-phonon coupled states induced by two phase-locked femto-second pulses. Full coherence remains within ~ 45 fs at room temperature.

JTU4A.27

High Spatial Resolution Manipulation of the Nitrogen Vacancy Center Charge State in Diamond, Xiangdong Chen¹, Fang-Wen Sun¹, Chang-Ling Zou¹; ¹Univ. of Science and Technology of China. We showed the high resolution charge state manipulation of NV center with optical method. The result was used to detect the spin state dynamics of NV- with sub wavelength spatial resolution.

JTU4A.28

Spectral Diffusion of Excitons in Disordered GaAs Quantum Wells, Rohan Singh^{1,2}, Galan Moody³, Mark E. Siemens⁴, Hebin Li⁵, Steven T. Cundiff^{1,2}; ¹JILA, Univ. of Colorado/NIST, USA; ²Physics, Univ. of Colorado, USA; ³National Inst. of Standards and Technology, USA; ⁴Physics and Astronomy, Univ. of Denver, USA; ⁵Physics, Florida International Univ., USA. We have studied spectral diffusion of excitons in GaAs quantum wells using two-dimensional coherent spectroscopy. Localized and delocalized excitons exhibit distinct spectral diffusion characteristics. These results cannot be explained in the strong redistribution approximation.

JTU4A.29

Generic Diffusion of Phase Singularities, Xiaojun Cheng^{1,2}, Yitzchak Lockerman¹, Azriel Z. Genack^{1,2}; ¹CUNY Queens College, USA; ²Graduate Center, City Univ. of New York, USA. We find generic diffusion of phase singularities in microwave speckle patterns as the frequency is scanned and in numerical simulations in the time domain. These results give the photon diffusion coefficient through the random medium.

JTU4A.30

Ultralow-power all-optical tunable dual Fano resonances in nonlinear metamaterials, Fan Zhang^{1,2}; ¹Peking Univ., China; ²Physical college, Peking Univ., China. Dual Fano resonances are realized in a nonlinear photonic metamaterial consisting of periodic arrays of asymmetrical meta-molecules etched in a gold film coated with azobenzene polymer layer and a large tunability is maintained simultaneously.

JTU4A.31

Time-resolved Imaging of Propagation of THz Wave in SRR Metamaterials, Bin Zhang¹, Qiang Wu¹, Shibiao Wang¹, Ming Yang¹, Yiping Zuo¹, Jingjun Xu¹; ¹Nankai Univ., China. We studied the time-resolved imaging of THz wave propagating in the double-split-ring resonator (SRR) metamaterial fabricated on LiNbO₃ substrate. Distinct swerving wave-front behavior of THz wave has been observed when it interacts with SRR by phase contrast imaging method.

JTU4A.32

Ultralow-power and ultrafast all-optical tunable PIT in metamaterials at optical communication range, Zhu Yu^{1,2}; ¹School of physics, PeKing Univ., China; ²State Key Lab for Mesoscopic Physics, China. ultralow-power and ultrafast all-optical tunable plasmon-induced transparency have been realized in metamaterials coated on polycrystalline indium-tin oxide layer at the optical communication range.

JTU4A.33

Broadband Epsilon-Near-Zero Metamaterials with Step-like Metal-Dielectric Multi-layer Structures with Gain Media, Lei Sun¹, Xiaodong Yang¹, Jie Gao¹; ¹Dept of Mechanical and Aerospace Engineering, Missouri Univ. of Science and Technology, USA. The broadband epsilon-near-zero metamaterials consisting of step-like metal-dielectric multi-layer structures with gain media is proposed. Low-loss functional optical devices including prisms for broadband directional emission and S-shaped lenses for phase front shaping are demonstrated.

JTU4A.34

Metasurface-on-Fiber enabled Orbital Angular Momentum Modes in Conventional Optical Fibers, Xi Wang¹, Jinwei Zeng¹, Jingbo Sun¹, Vahid Foroughi Nezhad¹, Alexander N. Cartwright¹, Natalia M. Litchinitser¹; ¹Electrical Engineering, Univ. at Buffalo, The State Univ. of New York, USA. We demonstrate generation and propagation of an optical vortex using a metasurface fabricated directly on a cross-section of a few-mode optical fiber at visible wavelengths. The experimental results are in good agreement with numerical simulations.

JTU4A.35

Four-Photon Joint Spectral Probability Distribution of a High Spectral-Purity Photon Source, Thomas Gerrits¹, Francesco Marsili², Matthew D. Shaw², Tim J. Bartley³, Sae Woo Nam¹; ¹NIST, USA; ²Jet Propulsion Lab, USA; ³Univ. of Oxford, UK. We show that the first Schmidt mode of double pair emission equals the square of the first single pair emission Schmidt mode from a spectrally factorizable type-II parametric downconversion process.

JTU4A.36

High-Order Single-Photon W-states for Random Number Generation, Markus Graefel¹, René Heilmann¹, Armando Perez-Leija¹, Robert Keil¹, Felix Dreisow¹, Matthias Heinrich², Stefan Nolte¹, Demetrios N. Christodoulides², Alexander Szameit¹; ¹Inst. of Applied Physics, Babeş-Bolyai Univ., Romania; ²REOL, The College of Optics & Photonics, Univ. of Central Florida, USA. We experimentally realize the generation of high-order photon encoded W-states involving up to 16 optical modes. Furthermore, we exploit the inherent probabilistic properties of these multipartite entangled W-states for generating genuine random numbers.

JTU4A.37

Active Stabilization and Continuous Phase Control of Time-bin Entanglement Interferometers, Paul Toliver¹, James M. Dailey¹, Anjali Agarwal¹, Nicholas A. Peters²; ¹Applied Communication Sciences, USA; ²Applied Communication Sciences, USA. We introduce a technique for stabilizing and enabling continuous phase control of fiber-based time-bin entanglement interferometers. This technique reuses the pair creation pump, which coexists with and co-propagates with the entangled photons.

JTU4A.38

Single-photon source based on NV center in nanodiamond coupled to TiN-based hyperbolic metamaterial, Mikhail Y. Shalaginov^{1,2}, Vadim Vorobyov^{3,4}, Jing Liu^{1,2}, Marcello Ferrera^{1,7}, Alexey Akimov^{4,6}, Alexei Lagutchev², Andrey N. Smolyaninov³, Vasily V. Klimov^{3,8}, Joseph Irudayaraj⁵, Alexander Kildishev^{1,2}, Alexandra Boltasseva^{1,2}, Vladimir M. Shalaev^{1,2}; ¹School of Electrical and Computer Engineering, Purdue Univ., USA; ²Birk Nanotechnology Center, Purdue Univ., USA; ³Photonic Nano-Meta Technologies, Russia; ⁴Moscow Inst. of Physics and Technology, Russia; ⁵Agricultural and Biological Engineering, Purdue Univ., USA; ⁶Russian Quantum Center, Russia; ⁷School of Engineering and Physical Sciences, Heriot-Watt Univ., UK; ⁸Lebedev Physical Inst. RAS, Russia. We experimentally demonstrate both the lifetime reduction and the enhancement of single-photon emission from nitrogen-vacancies in nanodiamonds coupled to a TiN/Al₂O₃/6S₂ superlattice. Our results pave the way towards future CMOS-compatible integrated quantum sources.

JTU4A.39

Phase-controlled heralding of photon-number entangled states, Young-Sik Ra¹, Hyang-Tag Lim¹, JOO-EON OH¹, Yoon-Ho Kim¹; ¹Physics, Pohang Univ. of Science and Technology, Republic of Korea. We report the generation of a photon-number entangled state in which detection of ancillary photons heralds the generation of the entangled state as well as its phase. Our scheme can operate with separable input states.

JTU4A.40

Optimal Quantum Control by Composite Pulses, Elica Kyoseva^{1,2}, Nikolay Vitanov³; ¹Engineering Product Development, Singapore Univ. of Technology and Design, Singapore; ²Dept of Nuclear Science and Engineering, MIT, USA; ³Dept of Physics, Sofia Univ., Bulgaria. We present a novel design of high-fidelity composite pulse sequences for dynamical suppression of amplitude noise with applications to NMR and QIP. We derive exact analytic formulas for the composite phases.

JTU4A.41

Experimental generation of triple quantum correlated beams from cascaded four-wave mixing processes, Jietai Jing¹, Zhongzhong Qin¹, Leiming Cao¹, Hailong Wang¹, Alberto Marino², Weiping Zhang¹; ¹East China Normal Univ., China; ²The Univ. of Oklahoma, USA. We report on our recent experimental results of generating triple quantum correlated beams by using cascaded four-wave mixing processes in hot rubidium vapor. The intensity-difference noise power of the triple beams is 6.5±0.3 dB below the shot noise level (SNL).

JTU4A • Poster Session 1—Continued

JTU4A.42

Optimized Microwave Near-Field Control in a Planar Ion Trap, Martina Carsjens^{1,2}, Matthias Kohnen^{1,2}, Timko Dubielzig², Christian Ospelkaus^{2,1}; ¹Physikalisch-Technische Bundesanstalt, Germany; ²Institut für Quantenoptik, Leibniz Universität Hannover, Germany. We describe a microfabricated planar ion trap with integrated microwave conductors. Using numerical simulations, it has been optimized for multi-qubit operations driven by microwave near-fields and represents a considerable experimental simplification.

JTU4A.43

Demonstration of a Characterisation Protocol for Two-qubit Hamiltonians on a Photonic Quantum Simulator, Alex Neville¹, Simon Devitt², Alberto Peruzzo³, Jeremy L. O'Brien¹, Pete Shadbolt¹, Laura Thackeray¹; ¹Univ. of Bristol, UK; ²National Inst. of Informatics, Japan; ³Univ. of Sydney, Australia. We demonstrate an entanglement mapping based characterisation protocol for coupled-qubit Hamiltonians. This is achieved by generating and measuring time-evolved states relevant to an NV-diamond system, using a reconfigurable integrated optical device.

JTU4A.44

The Rydberg-assisted Light-shift Blockade for Ensemble Quantum Computing, May Kim¹, Yanfei Tu², Selim M. Shahriar^{2,1}; ¹Physics and Astronomy, Northwestern Univ., USA; ²Electrical Engineering and Computer Science, Northwestern Univ., USA. We show, with numerical verification, how an ensemble of Rubidium atoms can be made to behave like a single particle with only two energy levels, i.e., a quantum bit, by using Rydberg-interaction assisted light-shift blockade.

JTU4A.45

Observation of phase memory in higher-order interference in atomic vapor cells by Raman process, Liqing Chen¹, Kai Zhang¹, Zhe-Yu Jeff Ou^{1,2}, Weiping Zhang¹; ¹Quantum Inst. for Light and Atoms, Dept of Physics, East China Normal Univ., China; ²Dept of Physics, Indiana Univ.-Purdue Univ. Indianapolis, USA. We demonstrate experimentally and theoretically controlled storage and retrieval of the optical phase information. This scheme is a kind of new random phase encoding with 2nd order holographic storage.

JTU4A.46

Optical Nonlinearities Using Tapered Optical Fibers in Rubidium Vapor, Daniel E. Jones¹, James D. Franson¹, Todd B. Pittman¹; ¹Physics, Univ. of Maryland Baltimore County, USA. Sub-wavelength diameter tapered optical fibers suspended in rubidium vapor can allow ultralow-power nonlinearities that may have applications in photonic quantum information processing. Here we experimentally investigate saturation of the relevant atomic transitions with ultralow-power fields.

JTU4A.47

Phosphor-saving, Excellent Color-Rendering Index Candlelight LEDs Containing Composite Photonic Crystals, Chun-Feng Lai¹, Chia-Jung Wu¹; ¹Dept of Photonics, Feng Chia Univ., Taiwan. In this study, a technique that saved phosphor use was applied to warm white light-emitting diodes containing 3D photonic crystals to develop the candlelight that exhibits a high luminous flux and an excellent color-rendering index.

JTU4A.48

Low Efficiency Droop Green Nano-Pyramid (10 -11) InGaN/GaN Multiple Quantum Well LED, Yuh-Jen Cheng^{1,2}, Shih-Pang Chang^{2,3}, Da-Wei Lin², Hao-chung Kuo², Kang-lin Xiong³; ¹Research Center for Applied Sciences, Academia Sinica, Taiwan; ²Dept of Electro-Optical Engineering, National Chiao Tung Univ., Taiwan; ³Yale Univ., USA. We report a low efficiency droop 520 nm green nano-pyramid InGaN/GaN multiple quantum well (MQW) LED. MQWs were grown on the semipolar (10 1) nano-pyramid facets. The device physics will be discussed in details.

JTU4A.49

Third Harmonic Frequency Stabilization to Acetylene Saturated Absorption in a Hollow-core Photonic Crystal Fiber, Liang-Yu Wei¹, Che-Chung Chou¹; ¹Feng Chia Univ., Taiwan. We demonstrated a hollow-core photonic crystal fiber as an absorption cell to observe the third harmonic derivative signal for laser frequency stabilization to P(9) line of the acetylene v1+ v3 overtone band.

JTU4A.50

RLS Filter-Based Interrogation of Fiber-Optic Extrinsic Fabry-Perot Interferometry Sensors, Daniele Tosi¹, Sven Poeggel¹, Gabriel Leen¹, Elfed Lewis¹; ¹Optical Fibre Sensors Research Centre, Univ. of Limerick, Ireland. A technique for interrogation of fiber-optic extrinsic Fabry-Perot interferometry sensors, based on adaptive filtering, is reported. This approach achieves 9.6 pm accuracy on Fabry-Perot cavity length (equivalent to 0.045 mmHg pressure) and improved noise resilience.

JTU4A.51

Measurement of Sub-pulse-width Temporal Delays Via Spectral Interference Induced by Weak Value Amplification, Luis Jose Salazar Serrano^{1,2}, Davide Janner¹, Nicolas Brunner^{3,4}, Valerio Pruneri^{1,5}, Juan P. Torres^{1,6}; ¹ICFO -The Inst. of Photonic Sciences, Spain; ²Physics Dept, Universidad de los Andes, Colombia; ³Departement de Physique Theorique, Universite de Genève, Switzerland; ⁴H.H. Wills Physics Lab, Univ. of Bristol, UK; ⁵ICREA-Institució Catalana de Recerca i Estudis Avançats, Spain; ⁶Dept. of Signal Theory and Communications, Universitat Politècnica de Catalunya, Spain. We present experimental results of a scheme based on the concepts of weak measurements and weak value amplification to measure temporal delays, much smaller than the pulse width, by means of spectral interference.

JTU4A.52

Transmitter for multispecies DIAL sensing of atmospheric water vapor, methane and carbon dioxide in the 2 μm range, Jessica Barrientos Barria¹, Jean-Baptiste Dherbecourt¹, Myriam Raybaut¹, Dominique Mammiez², Antoine Godard¹, Jean-Michel Melkonian¹, Jacques Pelon³, Michel Lefebvre¹; ¹ONERA, France; ²CNES, France; ³Latmos, France. We describe a tunable transmitter - based on an amplified nanosecond single-frequency optical parametric oscillator - for multi-species monitoring of green-house gases by integrated path DIAL on the CO₂-2.05μm, H₂O-2.06μm, CH₄-2.29 μm absorption lines.

JTU4A.53

Dynamic Displacement Measurement System with Auto Calibration Using Deeply-Phase Modulated Light, Yosuke Tanaka¹, Naoyuki Miyata¹, Takamasa Ito¹, Takashi Kurokawa¹; ¹Tokyo Univ. of Agriculture and Technology, Japan. We demonstrate dynamic displacement measurement with phase-modulated light. Auto calibration using deep phase modulation makes the measurement independent of driving conditions of the modulator. Displacement of several tens nm for more-than-1-MHz vibration is successfully measured.

JTU4A.54

Mid-infrared Disordered Photonic Crystal Lasers, Houkun Liang¹, Guozhen Liang², Bo Meng², Yong Quan Zeng², Qijie Wang^{2,3}, Ying Zhang¹; ¹Singapore Inst. of Manufacturing Technology, Singapore; ²School of Electrical and Electronic Engineering, Nanyang Technological Univ., Singapore; ³CDPT, Centre for Disruptive Photonic Technology, School of Physical and Mathematical Sciences, Nanyang Technological Univ., Singapore. Electrically-pumped disordered photonic-crystal lasers in the mid-infrared regime at λ~ 10 μm have been demonstrated for the first time based on quantum cascade lasers. Both the extended and highly-localized lasing modes are generated by adjusting the degree of disorder.

JTU4A.55

Dynamic Strain Measurement at Arbitrary Multiple Points along a Fiber with 500Hz High-Speed Random Accessibility of Brillouin Optical Correlation Domain Analysis, Chunyu Zhang¹, Masato Kishi¹, Kazuo Hotate¹; ¹the Univ. of Tokyo, Japan. In this paper, we demonstrate dynamic strain measurement at arbitrary points by a basic BOCDA system with 500 points/s random access speed. This is the highest speed of the random accessibility reported so far.

JTU4A.56

Optical Quilt Packaging: A New Chip-to-Chip Optical Coupling and Alignment Process for Modular Sensors, Tahsin Ahmed¹, Aamir A. Khan¹, Genevieve Vigil¹, Jason M. Kulick², Gary H. Bernstein¹, Anthony J. Hoffman¹, Scott S. Howard¹; ¹Dept of Electrical Engineering, Univ. of Notre Dame, USA; ²Indiana Integrated Circuits, USA. A wide-bandwidth, highly efficient method of inter-chip waveguide coupling suitable for on-chip, mid-infrared sensing is discussed. Simulations and preliminary fabrication work on laser-to-waveguide coupling are presented, with losses predicted to be better than 6 dB.

JTU4A.57

A Remote-free Self-feedback Colorless FPLD with FBG Based Single-mode Filter for Multi-channel 2.5 Gbit/s DWDM-PON, Yu-Chuan Su¹, Yu-Chieh Chi¹, Gong-Ru Lin¹; ¹Graduate Inst. of Photonics and Optoelectronics, Dept of Electrical Engineering, National Taiwan Univ., Taiwan. Remote-free and low Rayleigh-backscattering OOK transmission with a colorless FPLD using FBG reflector based single-mode self-injection-locker is achieved at 2.5 Gbit/s over 25-km SMF in DWDM-PON with receiving power of -29.5 dBm at BER=10⁻⁹.

JTU4A.58

Performance Demonstration of a Burst-Mode EDFA for Packetized Radio-over-Fiber Signal Transmission, Masaki Shiraiwa¹, Atsushi Kanno¹, Yoshinari Awaji¹, Naoya Wada¹, Tetsuya Kawanishi¹; ¹National Inst. of Information and Communications Technology, Japan. We investigated the performance of a burst-mode erbium-doped fiber amplifier for packetized radio-over-fiber signals. Low error vector magnitude values were observed over a wide optical power range.

JTU4A.59

Ring-tree TWDM Optical Access Network with Dynamic Wavelength and Bandwidth Allocation, Xintian Hu¹, Xue Chen¹, Zhiguo Zhang¹, Liqian Wang¹, Chen He¹, Jinsong Bei²; ¹State Key Lab of Information Photonics and Optical Communications, Beijing Univ. of Posts and Telecommunications, China; ²ZTE Corporation, China. A novel ring-tree TWDM optical access network architecture using matrix optical switch and OEO wavelength converter is proposed. The architecture owns flexible on-demand wavelength and timeslot provision, OLT energy saving ability and backward compatibility.

JTU4A.60

100-Gb/s All-Optical Wavelength-Preserved 2R Regeneration Using Semiconductor Optical Amplifiers, Qiang Wang¹, Li Huo¹, Xin Chen¹, Caiyun Lou¹, Bingkun Zhou¹; ¹Tsinghua Univ., China. All-optical wavelength-preserved 2R regeneration with simultaneous wavelength conversion of 100-Gb/s OOK signal is experimentally demonstrated based on cross-gain compression in SOAs. Receiving sensitivity is improved by more than 1.7 dB in the regenerated signal.

JTU4A • Poster Session 1—Continued

JTU4A.61

Experimental investigation of correlation between multiple side lobes of modulation instability in dispersion oscillating fiber, Xie Wang^{1,2}, Damien Bigourd¹, Alexandre Kudlinski¹, Kenneth Wong², Marc Douay¹, Laurent Bigot¹, Antoine Lerouge¹, Yves Quiquempois¹, Arnaud Mussot¹; ¹CNRS-Université Lille 1, PhLAM/IRICA USR 3380/UMR 8523, France; ²Dept of Electrical and Electronic Engineering, Univ. of Hong Kong, Hong Kong. We experimentally investigate the spectral correlation between multiple modulation instability side lobes in dispersion oscillating fiber by leveraging the dispersive Fourier process. We found that parametric processes related to each side lobe pairs act quasi-independently.

JTU4A.62

A Fast Numerical Method to Predict Spectra of High Power CW Yb-Doped Fiber Lasers with Bidirectional Pumping, Áron Szabó¹, Zoltán Várallyay², Andrea Rosales-García³, Clifford Headley³; ¹Budapest Univ. of Technology and Economics, Hungary; ²Furukawa Electric Inst. of Technology Ltd., Hungary; ³OFS Labs, USA. A fast method is introduced to model high power, continuous wave Yb-doped fiber lasers. Excellent agreement with measurements is obtained for up to 708W output power within 5 minutes of computation on a desktop computer.

JTU4A.63

Intrinsic Temperature Compensation of Interferometric and Polarimetric Fiber-Optic Current Sensors, Klaus M. Bohnert¹, Georg M. Müller¹, Lin Yang¹, Andreas Frank¹; ¹Corporate Research, ABB Ltd, Switzerland. We theoretically and experimentally demonstrate a method to achieve insensitivity to temperature to within $\pm 0.1\%$ from -40 to 85°C for fiber-optic current sensors with dynamic and static phase biasing and different types of sensing fiber.

JTU4A.64

Control of Saturation Characteristics in a Fiber Optical Parametric Amplifier by Raman Amplification, Xiaojie Guo¹, Xuelei Fu¹, Chester Shu¹; ¹The Chinese Univ. of Hong Kong, Hong Kong. We report suppression of pump depletion and signal gain reduction in a fiber optical parametric amplifier with a backward Raman pump. The depletion and gain saturation characteristics can be controlled by tuning the Raman gain.

JTU4A.65

Highly Efficient Fast Light Generation in a Single-mode Tellurite Fiber Embedded in a Brillouin Laser Ring Cavity, Dinghuan Deng¹, Weiqing Gao¹, Tonglei Cheng¹, Edmund E. Samuel¹, Takenobu Suzuki¹, Yasutake Ohishi¹; ¹Research Center for Advanced Photon Technology, Toyota Technological Inst., Japan. Highly efficient fast light propagation at negative group velocity was demonstrated in a 6.2 m long single-mode tellurite fiber embedded in a Brillouin laser ring cavity.

JTU4A.66

Agile tunable Q-switched thulium-doped silica fiber laser, François GUTTY¹, Arnaud Grisard¹, Christian Larat¹, Dominique Papillon Ruggeri¹, Eric Lallier¹; ¹THALES R&T, France. We demonstrate a Q-switched thulium-doped fiber laser up to 20 kHz with fast tunability over 100 nm without any movable part. Emitted pulses have energies above 10 μ J and peak powers up to 400 W.

JTU4A.67

Graphene saturable absorber power scaling laser, Zhe Jiang¹, G. E. Bonacchini¹, Daniel Popa¹, Felice Torrisi¹, A. K. Ott¹, Valentin J. Wittwer¹, David Purdie¹, Andrea C. Ferrari¹; ¹Cambridge Graphene Centre, Univ. of Cambridge, UK. A solution-processed graphene-film coated on a fiber-based connector is used for stable, mode-locked femtosecond-duration pulses with 16mW average output power.

JTU4A.68

Radiation-hardened Erbium doped LMA fiber with AIP composition from solution doping process, Guillaume Canat¹, Jayanta K. Sahu², Julien Le Gouët¹, Laurent Lombard¹, Johan Nilsson², Sophie Duzellier¹, Boivin Denis¹, William Renard¹; ¹Office Natl d'Etudes Rech Aérospatiales, France; ²Optoelectronic Research Center, Univ. of Southampton, UK. We report on Erbium doped large-mode-area fibers based on the phosphoalumino-silicates. The radiation induced attenuation are reduced compared to standard highly doped fibers. We measured 22% power conversion efficiency for core pumping at 1532nm.

JTU4A.69

10 GHz Bound Soliton Mode-locking in an Environmentally Stable FM Mode-locked Er-doped Fiber Soliton Laser, Cheng-Jih Luo¹, Sheng-Min Wang¹, Yinchieh Lai¹; ¹Dept of Photonics and Inst. of Electro-Optical Engineering, National Chiao Tung Univ., Taiwan. We experimentally demonstrate an environmentally stable 10 GHz FM mode-locked Er-doped fiber soliton laser that can produce stable bound solitons even when there is no equivalent fast saturable absorption mechanism inside the cavity.

JTU4A.70

Optimizing Birefringence of Polarization-Maintaining Photonic Crystal Fiber, Zhifang Wu^{1,2}, Xuguang Shao¹, Ping Perry Shum^{1,2}, Tianye Huang^{1,2}, Wenbin Ji¹, Nan Zhang^{1,2}, Ying Cui^{1,2}, Jie Xue^{1,2}, Swee Chuan Tjin¹, Xuan Quyen Dinh^{2,3}; ¹School of EEE, Nanyang Technological Univ., Singapore; ²CINTRA, CNRS International NTU THALES Research Alliance, Singapore; ³Thales, Thales Solutions Asia Pte Ltd, R&T Dept, Singapore. We report on a theoretical and experimental investigation to demonstrate that the birefringence of a commercial polarization-maintaining photonic crystal fiber (PMPCF) can be enhanced almost one order of magnitude by scaling its diameter down to $\sim 50\mu$ m.

JTU4A.71

Low-loss, low return-loss coupling between SMF and single-mode, hollow-core fibers using connectors, Jeffrey W. Nicholson¹, Brian Mangan¹, Linli Meng¹, Anthony Desantolo¹, Robert S. Windeler¹, John M. Fini¹, Kazunori Mukasa¹, Eric M. Monberg¹, Phouangphet Vannasouk¹, Edward Warych¹, Thierry Taunay¹; ¹OFS Labs, USA. We demonstrate the first low-loss, low-return-loss FC/PC connector for a single-mode, hollow-core fiber. Connector loss of 0.3dB and return loss of -31.3dB was measured, and a 200m HCF jumper with connectors on both ends was fabricated.

JTU4A.72

Numerical Study on Pulse Energy Scaling in an All-Normal-Dispersion Fiber Laser without any Physical Spectral Filters, Yu Wang¹, Shinji Yamashita¹; ¹Research Center of Advanced Science and Technology, The Univ. of Tokyo, Japan. We investigate high-energy pulse generation in an all-fiber, all-normal-dispersion cavity without any physical spectral filters. Potential of energy scaling is verified numerically by changing the parameters of the gain fiber and the cavity design.

JTU4A.73

On-chip detection of clinical Ebola virus RNA using specific DNA binding technique, Hong CAI¹, Joshua W. Parks¹, Ricardo Carrión², Lynnell Zempoaltecatl³, Jean P. Patterson², Aaron Hawkins³, Holger Schmidt¹; ¹School of Engineering, Univ. of California, Santa Cruz, USA; ²Virology and Immunology, Texas Biomedical Research Inst., USA; ³Electrical and Computer Engineering, Brigham Young Univ., USA. Clinical Ebola RNAs are detected with virus concentration down to 6.25×10^4 pfu/ml on an optofluidic chip. Longer complementary pull-down DNA sequences provide better isolation and higher signals.

JTU4A.74

Suspended core fiber for propagating vortex LP11 modes, Hong Ji¹, Yinlan Ruan¹, Shahraam Afshar V.¹, Tanya M. Monro¹; ¹School of Chemistry and Physics, The Univ. of Adelaide, Australia. We have investigated the vortex modes in suspended core fiber with Comsol simulations. The simulation results show that this class of structured fibre is well suited to support stable propagations of the LP11 modes.

JTU4A.75

Optical Phase Imaging Using a Synthetic Aperture Phase Retrieval Technique, Dennis J. Lee¹, Andrew M. Weiner¹; ¹School of Electrical and Computer Engineering, Purdue Univ., USA. We perform quantitative phase imaging using phase retrieval to implement synthetic aperture imaging. Compared to digital holography, the developed technique is simpler, less expensive, and more stable.

JTU4A.76

Whispering Gallery Mode Biosensing Using Back-Scattered Light, Joachim Knittel¹, Jon D. Swaim¹, David L. McAuslan², Warwick P. Bowen², George Brawley²; ¹School of Mathematics and Physics, Univ. of Queensland, Australia; ²Centre for Engineered Quantum Systems, Univ. of Queensland, Australia. We present a new technique for whispering gallery mode biosensing involving direct detection of the back-scattered light. This results in suppressing laser frequency noise by 27 dB, and gives an absolute sensitivity of 76 kHz.

JTU4A.77

Patterned Optical Trapping with High Efficiency on a 2D Photonic Crystal Platform, Peifeng Jing¹, Jingda Wu¹, Lih Lin¹; ¹Electrical Engineering, Univ. of Washington, USA. We demonstrate a method to generate patterned optical trapping on a two-dimensional photonic crystal (2D PC) substrate. Enhanced trapping is achieved with a loosely focused laser beam. The pattern and scale of the optical traps is determined by the 2D PC structure.

JTU4A.78

Giant spatial phase distortion in nonspecularly reflected beams, Yuhang Wan¹, Weijing Kong¹, Zheng Zheng¹; ¹School of Electronic and Information Engineering, Beihang Univ., China. We demonstrate for the first time that nonspecular reflection could lead to strong spatial phase variation across the beam profile besides the known intensity distortion. This discovery has profound implications for phase-related applications involving sensing.

JTU4A.79

Photonic Crystal Microring Resonator based Sensors, Stanley M. Lo¹, Shuren Hu², Sharon M. Weiss^{1,2}, Philippe M. Fauchet¹; ¹Dept of Electrical Engineering and Computer Science, Vanderbilt Univ., USA; ²Dept of Physics and Astronomy, Vanderbilt Univ., USA. Experimental studies on the chemical detection sensitivity of high surface area photonic crystal microring resonators are presented. We report a detection sensitivity of ~ 170 nm/RIU for slow-light resonance modes close to the band edge.

JTU4A.80

Automated Fiber-to-Waveguide Coupling Assisted by a Non-Invasive Integrated Light Monitor, Marco Carminati¹, Stefano Grillanda¹, Francesco Morichetti¹, Pietro Ciccarella¹, Giorgio Ferrari¹, Marco Sampietro¹, Andrea Melloni¹; ¹Dipartimento di Elettronica, Informazione e Bioingegneria, Politecnico di Milano, Italy. Automated fiber-to-waveguide coupling is demonstrated in silicon photonics by a ContactLess Integrated Photonic Probe (CLIPP) not requiring an external photodetector. The CLIPP monitors the light-dependent waveguide impedance, providing a feedback signal to the alignment system.

JTU4A • Poster Session 1—Continued

JTU4A.81

Third-Order Distortion Elimination in Phase-Encoded Analog-Photonic Links using a Four-Wave Mixing Comb Source, Amit Bhatia¹, Hong-fu Ting¹, Mark A. Foster¹; ¹Electrical and Computer Engineering, Johns Hopkins Univ., USA. We present all-optical distortion cancellation in phase-modulated analog-photonic links by combining the phase-encoded signal with lines from an optical comb generated from signal. Experimentally, we fully cancel third-order distortion increasing the link SFDR by >8.3dB.

JTU4A.82

Adjustment of optical path-length difference of nested Mach-Zehnder structure utilizing optical phase shift in waveguide junction, Akito Chiba¹, Tetsuya Kawanishi², Takahide Sakamoto², Kaoru Higuma³, Kazumasa Takada¹, Masayuki Izutsu⁴; ¹Gunma Univ., Japan; ²National Institute of Information and Communications Technology, Japan; ³Sumitomo Osaka Cement Co. Ltd., Japan; ⁴Waseda Univ., Japan. Optical-path length difference of Mach-Zehnder structures embedded on an optical switch can be adjusted within less than 1.6 % of FSR of the structure, without detecting radiation mode of the structure.

JTU4A.83

Waveform-dependent laser spectral compression through pulse propagation in a dispersion-increasing fiber, Wan-Tien Chao¹, Chi-Cheng Chen¹, Jin-Long Peng², Shang-Da Yang¹, Chen-Bin Huang¹; ¹Inst. of Photonics Technologies, National Tsing Hua Univ., Taiwan; ²Center for Measurement Standards, Industrial Technology Research Inst., Taiwan. Waveform dependence of laser spectral compression in a dispersion-increasing fiber is investigated. Experimentally, record-high spectral compression ratios of 35.3 and 41.7 are respectively achieved using a stretch-pulse mode-locked fiber laser and an all-normal dispersion laser.

JTU4A.84

High-sensitivity spectral phase retrieval of 7.2 fs pulse by shaper-assisted modified interferometric field autocorrelation, Ching-Tze Weng¹, Andy Kung¹, Shang-Da Yang¹; ¹Inst. of Photonics Technologies, National Tsing Hua Univ., Taiwan. We report on spectral phase retrieval of 16 pJ, 7.2 fs pulse and tailored waveforms at 800 nm by shaper-assisted modified interferometric field autocorrelation. Experiment results confirm the high accuracy and reproducibility of this method.

JTU4A.85

Long-term Stabilization of Mode-locked Er-fiber Lasers with 1.2 fs timing jitter, Shuangyou Zhang¹, Dong Hou¹, Jiutao Wu¹, Jy Zhao¹; ¹Peking Univ., China. We demonstrate a new phase-locking technique for long-term and high-precision stabilization of mode-locked Er-fiber lasers by direct optical-microwave phase detection without high-speed photodiodes and mixers. The excellent locking performance reaches 2.1e-18 at 4000-s averaging time.

JTU4A.86

Broadband Terahertz Generation Approaching Optical Communication Frequency Using Tilted DAST Crystals, Ikufumi Katayama¹, Michitaka Bito², Eiichi Matsubara², Masaaki Ashida²; ¹Graduate School of Engineering, Yokohama National Univ., Japan; ²Graduate School of Engineering Science, Osaka Univ., Japan. To realize ultrabroadband terahertz time-domain spectroscopy reaching near-infrared spectral regions, we investigated the type-I phase matching conditions of the difference frequency generation in DAST crystals. Crystal tilting is found to be efficient for near-infrared generation.

JTU4A.87

Wide repetition rate tunable femtosecond laser with a pair of CFBGs, Young-Jin Kim¹, Jiyong Park¹, Seungman Kim¹, Seung-Woo Kim¹; ¹Korea Advanced Inst of Science & Tech, Republic of Korea. We present an Er-doped fiber femtosecond laser having a wider repetition rate tuning range by introducing a pair of CFBGs which magnifies the cavity length change by 15 times.

JTU4A.88

Ultra-Broadband Non-Collinear Quasi-Phase-Matching in a Hybrid Mid-Infrared OPCPA System, Benedikt W. Mayer¹, Christopher R. Phillips¹, Lukas Gallmann^{1,2}, Ursula Keller¹; ¹Inst. for Quantum Electronics, ETH Zurich, Switzerland; ²Inst. of Applied Physics, Univ. of Bern, Switzerland. We present a proof-of-principle of broadband, non-collinear quasi-phase-matching in a hybrid OPCPA system. It employs a combination of quasi-phase-matching and group-velocity-matching in a MgO:PPLN delivering 3.4- μ m, 17.2- μ J, 43.1-fs pulses at 50 kHz repetition-rate.

JTU4A.89

Non-invasive Beam Detection in a High Average Power Electron Accelerator, Joel Williams¹, Jorge Martinez¹, John VanKeuren¹, John Harris¹, Stephen Milton¹, Sandra Biedron¹, Stephen Benson², Pavel Evtushenko², George Neil², Yuhong Zhang²; ¹Colorado State Univ., USA; ²Jefferson National Lab, USA. Implementation of an electro-optic based beam diagnostic within the Colorado State Univ. and Jefferson Lab beamlines necessitates investigation into how high average power beams affect EO crystals.

JTU4A.90

Dual resonance approach to optical signal processing beyond the carrier relaxation rate, Mikkel Heuck¹, Philip Tröst Kristensen¹, Jesper Mørk¹; ¹Dept of Photonics Engineering, Danmarks Tekniske Universitet, Denmark. We propose using two optical cavities in a differential control scheme to increase the bandwidth of cavity-based semiconductor optical signal processing devices beyond the limit given by the slowest carrier relaxation rate of the medium.

JTU4A.91

Withdrawn

JTU4A.92

Design-specific global optimization of a variety of photonic crystal cavities, Momchil Minkov¹, Vincenzo Savona¹; ¹Ecole Polytechnique Federale de Lausanne, Switzerland. We combine the fast guided-mode expansion with a genetic algorithm to perform a global optimization of several widely used photonic crystal cavity designs. The procedure consistently improves their quality factor by more than one order of magnitude, and is in addition highly customizable.

JTU4A.93

Robustness of scalable all-optical logic gates, Akihiro Fushimi¹, Takasumi Tanabe¹; ¹Keio Univ., Japan. We designed scalable all-optical logic gates that operate at the same input and output wavelength based on microrings. We investigated the influence of input power fluctuations and fabrication errors.

JTU4A.94

Photonic Crystal (PC) Waveguide Based Optical Filters for Dense Integration of High Sensitivity PC Biosensors, Hai Yan¹, Yi Zou¹, Chun-Ju Yang¹, Zheng Wang¹, Naimei Tang², Swapnajat Chakravarty², Ray Chen^{1,2}; ¹The Univ. of Texas at Austin, USA; ²Omega Optics Inc., USA. A photonic crystal (PC) waveguide based optical filter that enables dense integration of high sensitivity L55 PC microcavities for biosensor microarrays is demonstrated.

JTU4A.95

Spatial Filtering of Light Beams by Axisymmetric Photonic Microstructures, Vytautas Purlys¹, Lina Maityte², Darius Gailevičius¹, Martynas Peckus¹, Roaldas Gadonas¹, Kestutis Staliunas^{2,3}; ¹Laser Research Center, Dept of Quantum Electronics, Vilnius University, Lithuania; ²Departament de Física i Enginyeria Nuclear, Universitat Politècnica de Catalunya, Spain; ³Institució Catalana de Recerca i Estudis Avançats (ICREA), Spain. We propose and show experimentally uniform axisymmetric spatial filtering of light beams by three-dimensional axisymmetric photonic microstructures. Such gapless structures (similar to photonic crystals) were recorded in bulk of glass. Angular filtering of 25 mrad is demonstrated experimentally.

JTU4A.96

Exploring Far-field Pattern of Asymmetric Open Microcavities for Sensitive Rotation Detection, Raktim Sarma¹, Li Ge², Jan Wiersig³, Hui Cao¹; ¹Yale Univ., USA; ²Electrical Engineering, Princeton Univ., USA; ³Universität Magdeburg, Germany. We propose a novel and ultrasensitive scheme of rotation sensing by measuring farfield intensity from an asymmetric microcavity laser. We optimize the cavity shape and show the farfield sensitivity is enhanced by introducing structural chirality.

JTU4A.97

Semiconductor Single-Photon Emitters with Tunable Polarization Output, Chu-Hsiang Teng¹, Lei Zhang², Tyler Hill², Brandon Demory¹, Hui Deng², Pei Cheng Ku¹; ¹Electrical Engineering, Univ. of Michigan, USA; ²Physics, Univ. of Michigan, USA. Semiconductor quantum dot based single photon emitters are a critical component for quantum cryptography. In this work, we show a scalable single-photon emitter structure using site-controlled elliptical quantum dots with a controllable and tunable output polarization.

JTU4A.98

Light-assisted Templated Self-Assembly of a Gold Nanoparticle Array, Ningfeng Huang¹, Luis Javier Martínez Rodríguez², Eric Jaquay¹, Camilo A. Mejía², Debarghya Sarkar³, Michelle L. Povinelli¹; ¹Ming Hsieh Dept of Electrical Engineering, Univ. of Southern California, USA; ²Dept of Physics and Astronomy, Univ. of Southern California, USA; ³Dept of Electrical Engineering, Jadavpur Univ., India. We demonstrate for the first time the assembly of an array of gold particles using a guided-resonance mode of a photonic-crystal slab. The 200nm diameter particles form a triangular lattice with spacing of 1140 nm and exhibit high stability.

JTU4A.100

Withdrawn

JTU4A.101

2.18 μ m Mid IR emission from highly transparent Er³⁺ doped tellurite glass ceramic for bio applications, Roberta Morea¹, Toney Teddy-Fernandez², Adrian Miguel², Margarita Hernandez², Jose Maria Ulloa⁴, Joaquin M. Fernandez^{2,5}, Rolindes Balda^{2,5}, Javier Solis¹, José Gonzalo¹; ¹Inst. of Optics, CSIC, Spain; ²Applied Physics, Universidad del Pais Vasco, Spain; ³Inst. for Structure of Matter, CSIC, Spain; ⁴Inst. for Systems Based on Optoelectronics and Microtechnology, Universidad Politecnica de Madrid, Spain; ⁵Materials Physics Center, CSIC-UPV/EHU and Donostia International Physics Center, Spain. Intense emission peaking at 2.18 μ m was successfully obtained from erbium upon rigorous engineering of its glass host. Highly localized crystallization of erbium sites is substantiated by micro Raman and micro-PL along with TEM.

JTU4A.102

Waveguiding in polycrystalline GaP grown on SiO₂ by molecular beam deposition, Michael Gould¹, Nicole K. Thomas¹, Russell Barbour², Yuncheng Song³, Minjoo Larry Lee³, Kai-Mei C. Fu^{1,2}; ¹Electrical Engineering, Univ. of Washington, USA; ²Physics, Univ. of Washington, USA; ³Electrical Engineering, Yale Univ., USA. Loss measurements at a wavelength of 632 nm are presented for optical waveguides fabricated in polycrystalline GaP grown directly on SiO₂. Devices fabricated in poly-GaP on diamond are also shown.

JTU4A • Poster Session 1—Continued

JTU4A.103

Electro-optic and converse piezoelectric coefficients of epitaxial thin films: GaN grown on Si, and (Sr,Ba)Nb₂O₆ (SBN) grown on Pt coated MgO, Mireille Cuniot-Ponsard¹, Irma Saraswati^{2,4}, Suk-Min Ko³, Mathieu Halbwax², Yong-Hoon Cho³, Elhadj Dogheche²; ¹Laboratoire Charles Fabry, IOGS, CNRS, France; ²Optoelectronics Dept, IEMN, France; ³Dept of Physics and Graduate School of Nanoscience and Technology, Korea Advanced Inst. of Science and Technology, Republic of Korea; ⁴Electrical Engineering, Faculty Engineering Universitas Indonesia, Indonesia. We report the first measurement of the (r₁₃, r₃₃) Pockels electro-optic coefficients in a SBN thin film and in a GaN thin film grown on silicon. The converse-piezoelectric and electro-absorptive coefficients are simultaneously determined.

JTU4A.104

Formation of Nitrogen vacancy center ensembles in Diamond Nanowires, Khadijeh Bayat¹, Won Kyu Calvin Sun², William Gilpin³, Mahdi Farrokh Baroughi⁴, Marko Loncar¹; ¹School of Engineering and Applied Science, Harvard Univ., USA; ²nanotechnology Engineering, Univ. of Waterloo, Canada; ³Physics, Princeton Univ., USA; ⁴Electrical Engineering and Computer Science, South Dakota State Univ., USA. We have demonstrated incorporation of a thin layer of nitrogen-vacancy (NV) center ensembles at the surface of diamond nanowires. The signature of NV ensembles was confirmed by photoluminescence spectroscopy and electron spin resonance measurements.

JTU4A.105

Experimental Demonstration of On-Chip Silicon Two/Three Mode (De)Multiplexer Using OFDM 64/128/256-QAM Signals, Chengcheng Gui¹, Jian Wang¹, Zhonglai Zhang¹, Dingshan Gao¹, Chao Li², Qi Yang²; ¹Wuhan National Lab for Optoelect, China; ²State Key Lab of Optical Comm. Technologies and Networks, China. We fabricate on-chip two/three mode division (de)multiplexing using a tapered asymmetrical directional coupler on SOI platform. System experiments of OFDM 64/128/256-QAM data transmission have been carried out for on-chip two/three mode (de)multiplexing application.

JTU4A.106

SiC Photoconductive Antenna for intense THz generation, xavier ropagnol¹, Marcel Bouvier³, Tsuneyuki Ozaki¹, Matt Reid²; ¹physics, INRS, Canada; ²Physics, UNBC, Canada; ³research, Axis photonique, Canada. We investigate terahertz (THz) radiation from 6H- and 4H-SiC photoconductive (PC) antennas excited at 400 and 800 nm wavelengths. We demonstrate that 6H-SiC large aperture PC antennas have the potential to generate sub-MV/cm THz fields.

JTU4A.107

A Real-Time Terahertz Beam Monitoring Application with a 1024-pixel CMOS Terahertz Camera Module, Richard Al Hadi¹, Jean-Francois Lampin², Ullrich Pfeiffer¹; ¹IHCT, Univ. of Wuppertal, Germany; ²IEMN, ISEN, France. In this paper a terahertz beam monitoring application of an optically pumped molecular terahertz laser with a 1024-pixel CMOS terahertz camera is presented. The terahertz camera has been used to detect variations in real-time of the terahertz source beam around 2.52 THz.

JTU4A.108

Active Terahertz Two-wire Waveguides, Manoj Kumar Mridha¹, Anna Mazhorova¹, Matteo Clerici^{1,2}, Ibraheem Al-Naib³, Maxime Daneau⁴, xavier ropagnol¹, Marco Peccianti⁵, Christian Reimer¹, Marcello Ferrera², Luca Razzari¹, François Vidal¹, Roberto Morandotti¹; ¹Energy Materials Telecommunications Research Centre, Institut National de la Recherche Scientifique, Canada; ²School of Engineering and Physical Sciences, Heriot-Watt Univ., UK; ³Dept of Physics, Engineering Physics and Astronomy, Queen's Univ., Canada; ⁴Univ. of Ottawa, Canada; ⁵Dept of Physics and Astronomy, Univ. of Sussex, UK. Increasing coupling of terahertz radiation into a low dispersion, broadband two-wire waveguide is an important issue to address. To resolve this, we demonstrate an active two-wire waveguide with higher performance compared to its passive counterpart.

JTU4A.109

Observation of Change of Moisture Retention of Single Human Hairs using THz Waves, Kazunori Serita¹, Hironaru Murakami¹, Iwao Kawayama¹, Yoshinori Takahashi², Masashi Yoshimura², Yusuke Mori², Masayoshi Tonouchi¹; ¹Institute of Laser Engineering, Osaka Univ., Japan; ²Graduate School of Engineering, Osaka Univ., Japan. Moisture retention of single human hairs were evaluated using localized generated THz waves. It is found that the cuticles have an important roles for the moisture retention inside the hair.

JTU4A.110

Doubly-resonant mid-infrared AgGaSe₂ optical parametric oscillator, Daniel Maser^{1,2}, Lora Nugent-Glandorf¹, Gabriel Ycas^{1,2}, Florian Adler¹, Kevin Knabe¹, Scott A. Diddams¹; ¹National Inst. of Standards and Techn, USA; ²Dept of Physics, Univ. of Colorado, USA. A doubly-resonant AgGaSe₂ mid-infrared optical parametric oscillator (OPO) is synchronously pumped by a hybrid 2 μm Er:fiber/Tm:fiber femtosecond mode-locked laser. The OPO produces spectra ranging from 3-5 μm. Numerical simulations confirm the observed behavior.

JTU4A.111

Surface-Emitting Second-Harmonic Generation: Effective Technique for Evaluating Periodically-Poled Lithium Niobate Waveguide Domains with Nanoscale Resolution, Da Li¹, Ran Wang¹, Zhaojun Liu^{1,2}, Lei Wang¹, Yujie J. Ding¹; ¹Lehigh Univ., USA; ²Shandong Univ., China. We demonstrate that surface-emitting second-harmonic generation is an effective technique for evaluating domains of periodically-poled lithium niobate waveguide: domain period, linear taper, and poling depth. Such a method reaches nanoscale spatial resolution of 0.5 nm.

JTU4A.112

Pump-to-Signal Spatial Modulation Transfer in Noncollinear Optical Parametric Amplifiers, Jake Bromage¹, Christophe Dorrer¹; ¹Lab for Laser Energetics, Univ. of Rochester, USA. Intensity modulation transfer in saturated amplifiers is simulated for different gains and spatial walk-off configurations. Pump-to-signal walk-off in high-gain amplifiers reduces modulation transfer. Increased transfer occurs at low gains, particularly with idler-only walk-off.

JTU4A.113

HgGa₂S₄-based RISTRA OPO pumped at 1064 nm, Georgi Marchev¹, Manuel Reza^{1,2}, Valeriya Badikov³, Adolfo Esteban-Martin^{1,4}, Georg Stöppler⁵, Marina Starikova^{1,4}, Dmitrii Badikov³, Vladimir Panyutin^{1,3}, Marc Eichhorn⁵, Galina Shevrydaeva³, Aleksey Tyazhev¹, Svetlana Sheina³, Antonio Agnesi², Anna Fintisoava³, Valentin Petrov¹; ¹Max Born Inst., Germany; ²Università di Pavia, Italy; ³Kuban State Univ., Russia; ⁴CFO, Spain; ⁵ISL, France; ⁶Special Technologies, Russia. Idler beam quality at 6.3 μm from HgGa₂S₄ OPO is compared for linear, planar ring and RISTRA cavities. The last one produces smooth, circular profile and much higher focal fluence.

JTU4A.114

Infrared Signal Detection by Upconversion Technique, Teh-Hwa Wong¹, Jirong Yu², Yingxin Bai¹, William Johnson³; ¹Science systems and Application Inc., USA; ²NASA Langley Research Center, USA; ³Physics, Montana State Univ., USA. We demonstrated up-conversion assisted detection of a 2.05-μm signal by using a bulk periodically poled Lithium niobate crystal. The 94% intrinsic up-conversion efficiency and 22.58% overall detection efficiency at pW level of 2.05-μm was achieved.

JTU4A.115

Mid Infrared Sources Based on Widely Tunable DFG in Monolithic Semiconductor Waveguides, Dylan Logan¹, Alain Villeneuve², Mathieu Giguere², Amr S. Helmy¹; ¹Univ. of Toronto, Canada; ²Genia Photonics Inc, Canada. Difference frequency generation in monolithic semiconductor waveguides using $\chi(2)$ nonlinearities produced mid IR radiation between 7700 - 8300 nm in a single waveguide element via 20 nm tuning of a 1550 nm fiber laser pump.

JTU4A.116

Fabrication of selective periodic electrodes in up or down domains for electro-optic control of SHG in PPLN, Adrian J. Torregrosa¹, Haroldo Maestre¹, Juan Carlos Ferrer¹, Susana Fernández de Ávila¹, Juan Capmany¹; ¹Miguel Hernandez Univ., Spain. We present a simple technique for selective deposition of a periodic electrode in one kind of up or down ferroelectric domains alone in a periodically poled lithium niobate crystal for electro-optic control of second harmonic generation.

JTU4A.117

Theoretical and experimental characterization of finite-beam Bragg diffraction in PPLN electro-optic grating, Yen-Hung Chen¹, Hung-Ping Chung¹, Jui-Wen Chang¹, Wei-Kun Chang¹; ¹Dept of Optics and Photonics, National Central Univ., Taiwan. We report, for the first time, a finite-beam diffraction model built for a PPLN electro-optic Bragg device. Via the fits to experimental results, the diffraction behavior of a finite beam in the device is modeled.

JTU4A.118

Directional-Emission III-V-on-Silicon Microspiral and Double-Notch Microdisk Lasers for Optical Interconnects, Yu ZHANG¹, Yue-De Yang², Yong-Zhen Huang², Andrew W. Poon¹; ¹Electronic and Computer Engineering, Hong Kong Univ. of Science and Technology, Hong Kong; ²State KeyLab on Integrated Optoelectronics, Inst. of Semiconductor, Chinese Academy of Science, China. We demonstrate directional-emission III-V-on-silicon microspiral and double-notch microdisk lasers with gaplessly coupled waveguides using wafer-bonding. We observe room-temperature pulsed-injection lasing with a threshold of 33 mA and a side-mode-suppression-ratio of 20 dB at 50 mA.

JTU4A.119

High Performance Excited-State Nanostructure Lasers—Modulation Response, Frequency Chirp and Linewidth Enhancement Factor, Cheng WANG^{1,2}, Benjamin Lingnau³, Eckehard Schöll³, Kathy Ludge³, Jacky Even¹, Frederic Grillo²; ¹INSA-Rennes, France; ²Telecom Paristech, France; ³Technische Universität Berlin, Germany. Excited-state lasing in quantum dot lasers is theoretically demonstrated to exhibit a broader modulation response, lower chirp-to-power ratio, and smaller linewidth enhancement factor in comparison with the conventional lasing in the ground state.

JTU4A.120

Femtosecond mode-locked VECSEL from widely cw-tunable gain chips, Christopher R. Head¹, Alexander Hein², Edward A. Shaw¹, Andrew P. Turnbull¹, Peter Unger², Anne C. Tropper¹; ¹Univ. of Southampton, UK; ²Inst. of Optoelectronics, Ulm Univ., Germany. We describe passively mode-locking of an InGaAs quantum well laser, comparing different dielectric coatings applied to the same gain wafer. A 7-fold variation in pulse duration down to 817 fs was observed.

JTU4A • Poster Session 1—Continued

JTU4A.121

Passively Harmonically Self-Mode-Locked Vertical- External-Cavity Surface-Emitting Laser (VECSEL), Mahmoud Gaafar¹, Christoph Möller¹, Matthias Wichmann¹, Bernd Heinen¹, Bernardette Kunert², Arash Rahimi-Iman¹, Wolfgang Stolz¹, Martin Koch¹; ¹Faculty of Physics and Material Sciences Center, Philipps-Universität Marburg, Germany; ²NAsP III/IV GmbH, Germany. We demonstrate a harmonically self-mode-locked optically pumped semiconductor disk laser up to the third harmonic with a central wavelength of 1014 nm. Pulse durations penetrating the femtosecond regime at 500 MHz repetition rate are achieved.

JTU4A.122

GaAsBi Laser Diodes with Low Temperature Dependence of Lasing Wavelength, Takuma Fuyuki¹, Ryo Yoshioka¹, Kenji Yoshida¹, Masahiro Yoshimoto¹; ¹Dept. Electronics, Kyoto Inst. of Technology, Japan. GaAs_xBi_{1-x} laser diodes (LDs) with low temperature dependence of the oscillation wavelength (dλ/dT) are demonstrated. The value dλ/dT for a GaAs_{0.97}Bi_{0.03} LD was as low as 0.16 nm/K. This reduction is attributed to a reduction in the temperature coefficient of the band gap.

JTU4A.123

High-Power 1230-nm Quantum-Dot Tapered External Cavity Laser, with 100 nm Tunability, Stephanie E. Hagggett¹, Michel Krakowski², Ivo Montrosset³, Maria Ana Cataluna¹; ¹Univ. of Dundee, UK; ²III-V Lab, France; ³Politecnico di Torino, Italy. A quantum-dot tapered waveguide external cavity laser is presented, with 100nm tunability. At 1230nm, a maximum power of 0.62W was achieved, representing a 16-fold increase compared with equivalent narrow-ridge lasers at the same current density.

JTU4A.124

Power Scaling a Cr:ZnSe Thin Disk Laser by Increasing Pump Diameter, Ronald Stites¹, Gary Cook¹, Patrick Berry¹, Kenneth Schepler¹; ¹Air Force Research Labs, USA. A 500 μm Cr:ZnSe thin disk gain element was pumped at five different pump diameters. Laser output versus pump power was measured. Slope efficiency, threshold, and maximum power versus pump spot size were then extracted.

JTU4A.125

Adaptive Beam Cleanup of a 1.3kW Pulsed Slab Amplifier, ping yang¹, Shuai Wang^{1,2}, Lizhi Dong¹, Wenjin Liu^{1,2}, Mingwu Ao³; ¹Lab on Adaptive Optics, Inst. of Optics and Electronics, Chinese Academy of Sciences, China; ²Univ. of Chinese Academy of Sciences, China; ³Univ. of Electronic Science and Technology of China, China. We present closed-loop adaptive phase compensation of a 1.3 kW solid-state slab laser system. Experimental results demonstrated the beam quality is greatly improved with the proposed adaptive optics system.

JTU4A.126

High Power Continuous-Wave Alexandrite Laser with Green Pump, Shirin Ghanbari¹, Arkady Major¹; ¹Univ. of Manitoba, Canada. High power operation of a continuous-wave Alexandrite laser is reported. Output power of 2.6 W at 755 nm and tunability of 85 nm were achieved using 11 W of pump at 532 nm.

JTU4A.127

Passive Mode Locking of a Diode Pumped Nd:Sc_{0.2}Y_{0.8}SiO₃ Laser, Veselin Aleksandrov¹, Hristo Iliev¹, Anton Trifonov¹, Lihe Zheng², Jun Xu², Liangbi Su², Ivan C. Buchvarov¹; ¹Sofia Univ. St. Kliment Ohridski, Bulgaria; ²Shanghai Inst. of Ceramics, Chinese Academy of Sciences, China. We demonstrate passive mode-locking of a Nd:Sc_{0.2}Y_{0.8}SiO₃ laser using a semiconductor saturable absorber mirror. The pulse train shows output power of 0.5 W and pulse duration of 3.5 ps at repetition rate of 118 MHz.

JTU4A.128

Graphene-based passive Q-switching of a Tm³⁺:ZBLAN short-infrared waveguide laser, Ju Han Lee², Simon Gross³, Ben V. Cunnings³, Chris Brown³, David Kielpinski³, Tanya M. Monro¹, David G. Lancaster¹; ¹Univ. of Adelaide, Australia; ²Univ. of Seoul, Republic of Korea; ³Griffith Univ., Australia; ⁴Macquarie Univ., Australia. We report a passively Q-switched 1.9 μm Tm:ZBLAN waveguide laser based on an extended cavity containing a flake-graphene saturable absorber film. The 790nm diode-laser-pumped laser produces up to 6 mW with ~1.4 μs pulses at ~25 kHz.

JTU4A.129

Chiral polymeric relief structures fabricated by using optical vortices, Guzhaliyi Juman¹, Mizuki Watabe¹, Katsuhiko Miyamoto¹, Takashige Omatsu^{1,2}; ¹Chiba Univ., Japan; ²CREST, Japan. We present a chiral single-arm relief on a micro-meter scale formed in an azo-polymer film by the irradiation of a green optical vortex. A 2-dimensional chiral relief array was also fabricated in the azo-polymer film.

JTU4A.130

Feasibility of Breast Surgical Margins Analysis with Fluorescence-guided Optical Coherence Tomography Imaging, Dan Savastru¹, Sorin Miclos¹, Ernest Chang², Dorin Preda², Nicusor Iftimia²; ¹National Inst. of Optoelectronics INOE 2000, Romania; ²Physical Sciences, Inc., USA. We demonstrate the feasibility of a surgery guidance approach based on fluorescence-guided optical coherence tomography (OCT) imaging. Surgical margins are assessed for cancer presence using automated analysis of OCT images, only on areas indicated by fluorescence imaging as being cancer suspicious.

JTU4A.131

Photo-addressable multi-stable optical switch, Tsung-Hsien Lin¹, Chun-Ta Wang¹, Yueh-Chi Wu¹; ¹Dept of Photonics, Taiwan. This work demonstrates an optically switchable tristable optical switch. Tristable attenuation, scattering, and transparent states can be achieved using the dichroic dye doped fingerprint, focal conic, and homeotropic textures, respectively.

JTU4A.132

Localization of Epidural Space in Piglets by Catheter-based Swept Source Optical Coherence Tomography, Kao Meng-Chun¹; ¹Inst. of Biophotonics, National Yang-Ming Univ., Taiwan. In this study, we designed and built a needle-fiber based Fourier domain swept source optical coherence tomography (SSOCT) system, that used to localize epidural space.

JTU4A.133

Functional optical imaging of neurovascular activation in the rat cerebral cortex, Kuo Yue-Ming¹; ¹National Yang-Ming Univ., Taiwan. FD-OCT system used to acquire the cross-sectional tissue structure through the cranial window at rat cortex. The intensity of cortex and flow changes during forepaw electrical stimulation. Results show that localized swelling and scattering decreases in the activation region.

JTU4A.134

Optical-Low-Coherence-Reflectometry-Assisted Non-Contact Tonometry, Tuan-Shu Ho¹, Chien-Chung Tsai¹, Kuang-Yu Hsu¹, Sheng-Lung Huang^{1,2}; ¹Graduate Inst. of Photonics and Optoelectronics, National Taiwan Univ., Taiwan; ²Dept of Electrical Engineering, National Taiwan Univ., Taiwan. A multifunctional system incorporating air-puff module and optical low-coherence reflectometry is demonstrated to measure the corneal thickness and intraocular pressure. Properties related to corneal rigidity are determined with the interferogram observed during the air-puffing process.

Technical Digest and Postdeadline Papers Available Online

- Visit www.cleoconference.org
- Select **Download Digest Paper** button
- Use your email address and CLEO Registration ID # to synchronize

Once you have synchronized your conference registration with Optics InfoBase, you can log in directly to Optics InfoBase at any point using the same email address and OSA password.

Access must be established via synchronization within 60 days of the conference start date. Access is provided only to full technical attendees.

CLEO: QELS-Fundamental Science

08:30–10:00 Plenary and Awards Session II, *Grand Ballroom*10:00–17:00 Exhibition Open, *Exhibit Halls 1 & 2*10:00–10:30 Coffee Break and Unopposed Exhibit Only Time, *Exhibit Halls 1 & 2*10:30–12:30 Market Focus Session III: Operational Strategies for the Laser and Photonics Industry, *Exhibit Hall Theater*

10:30–12:30

FW1A • Fundamental Quantum Science*Presider: Todd Pittman; Univ. of Maryland Baltimore County, USA*

FW1A.1 • 10:30

Measuring Bohm Trajectories of Entangled Photons, Dylan Mahler^{1,2}, Lee Rozema^{1,2}, Kent Fisher³, Lydia Vermeyden³, Kevin Resch³, Boris Braverman⁴, Howard Wiseman^{5,6}, Aephraim M. Steinberg^{1,2}; ¹Center for Quantum Information and Quantum Control and Inst. for Optical Sciences, Canada; ²Univ. of Toronto, Canada; ³Inst. for Quantum Computing and Dept. of Physics & Astronomy, Univ. of Waterloo, Canada; ⁴MIT-Harvard Center for Ultracold Atoms, and Research Lab of Electronics, MIT, USA; ⁵Centre for Quantum Computation and Communication Tech. (Australian Research Council), Australia; ⁶Centre for Quantum Dynamics, Griffith Univ., Australia. We measure, using weak measurement, the Bohmian trajectories of one photon that is part of an entangled pair. Our results shed light on the nonlocality of the Bohm model, as well as its so-called “surrealism.”

FW1A.2 • 10:45

Two-Photon Discrete Speckle in Anderson-Disordered Lattices, Lane Martin¹, Gianni di Giuseppe^{1,2}, Armando Perez-Leija³, Robert Keil³, Alexander Szameit³, Ayman F. Abouraddy³, Demetrios N. Christodoulides¹, Bahaa E. Saleh¹; ¹CREOL, The College of Optics and Photonics, Univ. of Central Florida, USA; ²School of Science and Technology, Physics Division, Univ. of Camerino, Italy; ³Inst. of Applied Physics, Friedrich-Schiller-Universität, Germany. Two photons in an entangled, spatially correlated (anti-correlated) state transmitted through an Anderson disordered lattice maintain their correlation (anti-correlation) but exhibit coincidence-map speckle in the Fourier plane.

10:30–12:30

FW1B • Spin Coherence in Color Centers in Diamond*Presider: Duncan England; National Research Council, Canada*

FW1B.1 • 10:30

Optical signatures of spin in silicon-vacancy centre in diamond, Benjamin Pingault¹, Tina Muller¹, Christian Hepp², Elke Neu², Christoph Becher², Mete Atature¹; ¹Univ. of Cambridge, UK; ²Universität des Saarlandes, Germany. The spin state of the silicon-vacancy centre in diamond and its optical accessibility have so far remained elusive. We here evidence spin-tagged fluorescence through resonant optical access to the electronic spin 1/2 of the centre.

FW1B.2 • 10:45

Observing bulk spin coherence in high-purity nanodiamonds, Helena S. Knowles¹, Dhiren M. Kara¹, Mete Atature¹; ¹Univ. of Cambridge, UK. Nitrogen-vacancy centres in nanodiamond allow nano-resolution magnetometry. However, their use has been limited by poor quantum state coherence times. Using high purity nanodiamonds we achieve spin coherence comparable to that in bulk.

10:30–12:30

FW1C • Symposium on Science and Applications of Structured Light in Complex Media I ▶*Presider: Natalia Litchinitser; State Univ. of New York at Buffalo, USA*FW1C.1 • 10:30 **Invited** ▶

Quantum Electromechanical Processes in Plasmonic Nanostructures, Nicholas Fang¹; ¹MIT, USA. In this invited talk I will present a quantum electromechanical analysis on enhanced angular momentum transfer observed in different metallic nanostructures. Direct applications include plasmonic angular momentum mode converters for quantum computing and optical manipulation of mechanical torque. We will also discuss our recent effort on quantum jellium model applied to the excitation of metallic interfaces that are just a few nanometer thick.

10:30–12:30

FW1D • Wavelength Conversion in Micro-Structures*Presider: J. Stewart Aitchison; Univ. of Toronto, Canada*FW1D.1 • 10:30 **Invited**

Vacuum UV to IR supercontinuum generation by impulsive Raman self-scattering in hydrogen-filled PCF, Federico Belli¹, Amir Abdolvand¹, Wonkeun Chang¹, John C. Travers¹, Philip St.J. Russell^{1,2}; ¹Max Planck Inst. for the science of light, Germany; ²Dept. of Physics, Univ. of Erlangen-Nuremberg, Germany. A supercontinuum extending from 125nm to 1200nm is generated in hydrogen-filled kagomé-PCF by means of impulsive Raman self-scattering of few- μ J ultrashort pulses at 805nm. The source shows no optical damage and is stable over time.

Visit CLEO: Exhibition

- * See the Newest Industry Products from nearly 300 Companies on the Exhibit Floor!
- * Tech Playground - Hands-On Innovation & Solutions
- * Market Focus - New Products, Emerging Technologies & Solutions

Check the Buyers' Guide and Show Floor Program Guide for more information.

CLEO: Science & Innovations

CLEO: Applications
& Technology

08:30–10:00 Plenary and Awards Session II, Grand Ballroom

10:00–17:00 Exhibition Open, Exhibit Halls 1 & 2

10:00–10:30 Coffee Break and Unopposed Exhibit Only Time, Exhibit Halls 1 & 2

10:30–12:30 Market Focus Session III: Operational Strategies for the Laser and Photonics Industry, Exhibit Hall Theater

10:30–12:30

SW1E • Pulse Compression

Presider: Gunter Steinmeyer; Max Born Inst., Germany

SW1E.1 • 10:30

CEP-stable, multi-mJ, 4.3 fs pulses from long stretched flexible hollow fibers, Frederik Böhle¹, Martin Kretschmar², Aurelie Jullien¹, Peter Simon³, Rodrigo B. Lopez-Martens¹, Tamas Nagy^{2,3}, ¹Laboratoire d'Optique Appliquée, Ecole Nationale Supérieure de Techniques Avancées-Paristech, Ecole Polytechnique, CNRS, France; ²Institut für Quantenoptik, Leibniz Universität Hannover, Germany; ³Laser-Laboratorium Göttingen e.V., Germany. CEP-stable 4.3fs pulses of 3mJ energy were generated by spectral broadening of circularly polarized 8mJ pulses in a differentially pumped 2-m-long hollow fiber. The pulses were characterized by a single-shot SHG FROG.

SW1E.2 • 10:45

Direct Measurement of Nonlinear Carrier-Envelope Phase Changes in Hollow Fiber Compression, Fabian Lücking¹, Andrea Trabattini², Sunilkumar Anumula², Giuseppe Sansone², Francesca Calegari², Mauro Nisoli², Thomas Oksenhendler³, Gabriel Tempea¹; ¹Femtolasers Produktions GmbH, Austria; ²Politecnico di Milano, Dept. of Physics, Inst. of Photonics and Nanotechnologies, CNR-IFN, Italy; ³Fastlite, France. We present a single-shot, in-situ interferometric method for measuring phase changes experienced by laser pulses upon nonlinear propagation. With this method we characterized the intensity-dependent phase fluctuations emerging in hollow fiber compressors.



10:30–12:30

SW1F • Nonlinear THz Science and Technology

Presider: Peter Jepsen; Danmarks Tekniske Universitet, Denmark

SW1F.1 • 10:30 **Invited**

Colliding Quasiparticles with Intense Terahertz Fields, Mark S. Sherwin¹; ¹Univ. of California Santa Barbara, USA. Strong quasi-cw terahertz fields accelerate and recollide electron-hole pairs injected by a near-ir laser into GaAs quantum wells. A frequency comb is emitted, with up to 18 teeth separated by twice the terahertz frequency.

10:30–12:30

SW1G • Emerging Trends in Semiconductor Lasers

Presider: Amr Helmy; Univ. of Toronto, Canada

SW1G.1 • 10:30 **Invited**

Electrically Driven Exciton-Polariton Lasers, Sven Höfling^{1,2}, Christian Schneider¹, Arash Rahimi-Iman¹, Na Young Kim^{3,4}, Matthias Amthor¹, Matthias Lerner¹, Ivan Savenko^{5,6}, Ivan Shelykh^{5,6}, Vladimir Kulakovskii⁷, Lukas Worschech¹, Martin Kamp¹, Stephan Reitzenstein⁸, Misha Durnev⁹, Alexey Kavokin^{9,10}, Alfred Forchel¹, Yoshihisa Yamamoto^{3,11}; ¹Technische Physik, Wuerzburg Univ., Germany; ²SUPA, Univ. of St Andrews, UK; ³Ginzton Lab, Stanford Univ., USA; ⁴Inst. of Industrial Science, Univ. of Tokyo, Japan; ⁵Science Inst., Univ. of Iceland, Iceland; ⁶Division of Physics and Applied Physics, Nanyang Technological Univ., Singapore; ⁷Inst. of Solid State Physics, Russian Academy of Science, Russia; ⁸Institut für Festkörperphysik, Technische Universität Berlin, Germany; ⁹Spin Optics Lab, St-Petersburg State Univ., Russia; ¹⁰Physics and Astronomy School, Univ. of Southampton, UK; ¹¹National Inst. of Informatics, Japan. We report exciton-polariton laser operation under electrical pumping. The hybrid light-matter nature of this lasing system is probed by measuring the exciton-polariton Zeeman-splitting, which clearly reveals that this laser remains in the strong coupling regime.



10:30–12:30

AW1H • Material Structuration for Next Generation Sensors and Components

Presider: Yasuhiko Shimotsuma; Kyoto Univ., Japan

AW1H.1 • 10:30

Generation of second and third order optical dispersion using nonlinearly chirped silicon waveguide gratings, George Feng Rong Chen¹, Ting Wang¹, Christine Donnelly², D. T. H. Tan¹; ¹Engineering Product Development, Singapore Univ. of Technology and Design, Singapore; ²Stanford Univ., USA. The simultaneous generation of second and third order dispersion is demonstrated using nonlinearly chirped silicon waveguide gratings. Second order dispersion of -2.3×10^6 ps/nm/km and third order dispersion of 1.2×10^5 ps/nm²/km were demonstrated at 1.55 μ m.

AW1H.2 • 10:45

Photoluminescence from GeSn/Ge Heterostructure Microdisks with 6% Sn Grown on Si via CVD, Seyed Amir Ghetmiri^{1,2}, Benjamin Conley^{1,2}, Aboozar Mosleh^{1,2}, Liang Huang^{1,2}, Wei Du², Amjad Nazzal³, Greg Sun⁴, Richard Soref⁴, John Tolle⁵, Hameed A. Naseem², Shui-Qing Yu²; ¹Microelectronics-Photonics graduate program, Univ. of Arkansas, USA; ²Electrical Engineering, Univ. of Arkansas, USA; ³Engineering and Physics, Wilkes Univ., USA; ⁴Physics, Univ. of Massachusetts, USA; ⁵ASM Company, USA. GeSn/Ge heterostructure microdisks integrated on Si were fabricated. The quality of material grown by CVD was investigated and the photoluminescence spectrum was measured using a Ti:Sapphire laser as an excitation source under variable pump powers.

Meeting Room
211 B/D

Meeting Room
212 A/C

Meeting Room
212 B/D

Marriott
Salon I & II

CLEO: Science & Innovations

CLEO: QELS-
Fundamental Science

CLEO: Applications
& Technology


08:30–10:00 Plenary and Awards Session II, *Grand Ballroom*

10:00–17:00 Exhibition Open, *Exhibit Halls 1 & 2*

10:00–10:30 Coffee Break and Unopposed Exhibit Only Time, *Exhibit Halls 1 & 2*

10:30–12:30 Market Focus Session III: Operational Strategies for the Laser and Photonics Industry, *Exhibit Hall Theater*

10:30–12:30
SW11 • Solitons and Nonlinear Propagation 
Presider: Antoine Godard, ONERA - The French Aerospace Lab, France

SW11.1 • 10:30  **Tutorial**
Supercontinuum and solitons, what's up?, Goëry Genty¹, John M. Dudley²; ¹Tampere Univ. of Technology, Finland; ²Université de Franche Comté, France. This tutorial provides an overview of the basic physical mechanisms of supercontinuum generation. Progress in the field and novel physics linked to recently discovered soliton dynamics including optical rogue waves will be reviewed.





Goëry Genty graduated from the Institute of Optics, France and obtained his PhD from the Aalto University, Finland in 2004. He is currently a Professor at the Tampere University of Technology in Finland, where he leads a research group on ultra-fast pulse propagation dynamics.

10:30–12:30
SW1J • Bandwidth Efficient Signaling
Presider: David Hillerkuss; ETH Zurich, Switzerland

SW1J.1 • 10:30
Generation of Nyquist Pulses Using a Dual Parallel Mach-Zehnder Modulator, Jizhao Zang¹, Jian Wu¹, Yan Li¹, Xinhui Nie¹, Jifang Qiu¹, Jintong Lin¹; ¹Beijing Univ. of Posts and Telecommunications, China. We demonstrated the generation of Nyquist pulses using a dual parallel Mach-Zehnder modulator. 10 GHz to 40 GHz Nyquist pulses with timing-jitter below 258 fs and signal-to-noise ratio more than 30 dB are experimentally generated.

SW1J.2 • 10:45
Experimental Investigation of Sampling Phase Sensitivity in Baud-Rate Sampled Coherent Receiver for Nyquist Pulse-Shaped High-Order QAM Signals, Guo-Wei Lu¹, Takahide Sakamoto¹, Tetsuya Kawanishi¹; ¹Natl. Inst. of Info. & Comm. Tech., Japan. We experimentally investigate the sampling phase dependence of baud-rate sampled and equalized coherent receiver for Nyquist Pulse-shaped high-order QAM signals on the modulation format and roll-off factors.


10:30–12:30
FW1K • Metasurfaces and Plasmonic Metamaterials 
Presider: Nanfang Yu; Columbia Univ., USA

FW1K.1 • 10:30  **Tutorial**
Optical Properties on Demand: Reconfigurable and Coherently Controlled Metamaterials, Nikolay I. Zheludev^{1,2}; ¹Centre for Photonic Metamaterials and Optoelectronics Research Centre, Univ. of Southampton, UK; ²Centre for Disruptive Photonic Technologies, NTU, Singapore. Transmission and reflection properties, anisotropy, chirality, optical non-linearity and luminescent of metamaterials can be controlled at will using dynamic nanostructures reconfigurable with electromagnetic forces and by exploiting structured illumination with coherent light.



Nikolay Zheludev directs the Centre for Photonics Metamaterials at the ORC, Southampton University and the Centre for Disruptive Photonic Technologies at NTU, Singapore. His awards include Senior Professorships of the UK Research Council and the Leverhulme Trust and the Royal Society Wolfson Fellowship. He was awarded PhD and DSc from Moscow State University.

10:30–12:30
AW1L • Imaging and Sensing
Presider: Hao Zhang; Northwestern Univ., USA

AW1L.1 • 10:30  **Tutorial**
Multimode Optical Bioimaging, from the Lab to the Clinic: A Translational Story, Daniel L. Farkas¹; ¹Dept. of Biomedical Engineering, Univ. of Southern California, USA. Focus will be where light and patient meet, and improvements yielding better outcomes, by detecting, characterizing and monitoring very small entities (molecules, cells) within the human body, quantitatively, dynamically, and preferably without contrast agents.



Daniel L. Farkas previously directed the National Science & Technology Center at Carnegie Mellon that won the Smithsonian Award. In addition he has been Professor of Bioengineering at the Univ. of Pittsburg and Professor of Surgery at Cedars-Sinai. He has chaired 26 international conferences, is on 10 editorial boards, and (co)founded 12 startups. His research attracted \$75M, yielding 200 publications. He was a Fulbright scholar.

Wednesday, 11 June



Join the conversation. Use #CLEO14.
Follow us @cleoconf on Twitter.

CLEO: Science & Innovations

CLEO: Applications
& Technology08:30–10:00 Plenary and Awards Session II, *Grand Ballroom*10:00–17:00 Exhibition Open, *Exhibit Halls 1 & 2*10:00–10:30 Coffee Break and Unopposed Exhibit Only Time, *Exhibit Halls 1 & 2*10:30–12:30 Market Focus Session III: Operational Strategies for the Laser and Photonics Industry, *Exhibit Hall Theater*

10:30–12:30

SW1M • Micro and Nanophotonic Devices

Presider: Douglas Gill, IBM, USA

SW1M.1 • 10:30 **Invited**

Nano-Optical Scan Probes: Opening Doors to Previously-Inaccessible Parameter Spaces, James Schuck¹; ¹Lawrence Berkeley National Lab, USA. I will discuss recent progress on new near-field probe geometries, including the “campanile” geometry, which has been used in recent hyperspectral imaging experiments, providing nanoscale spectral information distinct from what is obtained with other methods.

10:30–12:30

SW1N • Novel Fiber Laser Designs

Presider: Shenping Li; Corning Incorporated, USA

SW1N.1 • 10:30 **Invited**

Ultra-long Fibre-based Random Lasers, Sergei K. Turitsyn^{1,2}; ¹Aston Inst. of Photonic Technologies, Aston Univ., UK; ²Novosibirsk State Univ., Russia. The emerging science and applications of ultra-long random fibre lasers will be overviewed. The lasers with cavity length up to several hundred km exploit random distributed feedback provided by Rayleigh scattering amplified through Raman effect.

10:30–12:30

SW1O • Laser Frequency Combs

Presider: Axel Ruehl; Deutsches Elektronen Synchrotron, Germany

SW1O.1 • 10:30

Direct Comb Stabilization to a 12C2H₂-filled Hollow-core Fiber via Single Tooth Saturated Absorption Spectroscopy, Shun Wu¹, Chenchen Wang¹, Coralie Fourcade Dutin^{2,3}, Brian R. Washburn¹, Fetah Benabid^{2,3}, Kristan L. Corwin¹; ¹Dept. of Physics, Kansas State Univ., USA; ²GPPMM group, Xlim Research Inst., France; ³Physics Dept., Univ. of Bath, UK. Toward an all-fiber system, an erbium fiber laser-based comb is directly stabilized to a 12C₂H₂ transition at 1539.4 nm. The comb fractional instability at 1532.8 nm is 6×10⁻¹² at 100 ms gate time.

SW1O.2 • 10:45

A frequency comb that maintains optical coherence under significant vibrations, Laura C. Sinclair¹, Ian Coddington¹, William C. Swann¹, Lindsay Sonderhouse¹, Greg B. Rieker^{1,2}, Archita Hati¹, Kana Iwakuni³, Nathan R. Newbury¹; ¹NIST, USA; ²Mechanical Engineering, Univ. of Colorado, USA; ³Dept. of Physics, Keio Univ., Japan. We discuss the design and performance of an all polarization-maintaining self-referenced frequency comb that can maintain optical coherence with an optical reference laser under strong vibrations from a shaker table and a moving vehicle.

10:30–12:30

AW1P • Spectroscopy and Imaging Applications

Presider: M Krishnamurthy, Tata Inst. of Fundamental Research, India

AW1P.1 • 10:30

Rapid, wideband cavity ringdown spectroscopy for the detection of explosives, Toby K. Boyson¹, Dylan R. Rittman², Thomas G. Spence³, Paul Kirkbride⁴, David S. Moore², Charles C. Harb¹; ¹School of Engineering and Information Technology, UNSW Australia, Australia; ²Shock and Detonation Physics Group, Los Alamos National Lab, USA; ³Dept. of Chemistry, Loyola Univ. New Orleans, USA; ⁴School of Chemical and Physical Sciences, Flinders Univ., Australia. We present results from a variant of CRDS that allows large spectral bandwidths to be analysed in real time. We have applied the technique to the analysis and detection of explosives and related compounds.

AW1P.2 • 10:45

Silicon on Sapphire Chip Based Mid-Infrared Optical Spectroscopy for Detection of Chemical Warfare Simulant Triethyl phosphate, Parker Wray¹, Yi Zou¹, Swapnajt Chakravarty², Ray Chen¹; ¹Electrical Engineering, Univ. of Texas at Austin, USA; ²Omega Optics Inc., USA. Triethyl phosphate (TEP), a chemical warfare simulant, has absorption peaks in the mid-infrared. Using a single mode slot wave guide we were able to detect TEP, with a detection limit down to 75 ppm. This provides enhanced sensitivity while simultaneously achieving device miniaturization.

Download the CLEO Mobile App

Search for CLEO:2014
in the app stores or
scan the QR code



CLEO: QELS-Fundamental Science

FW1A • Fundamental Quantum Science—Continued

FW1A.3 • 11:00

Classical Realization of Dispersion Cancellation by Using Transform-limited Pulses, Kazuhisa Ogawa¹, Shuhei Tamate², Toshihiro Nakanishi¹, Hirokazu Kobayashi³, Masao Kitano¹; ¹Dept. of Electronic Science and Engineering, Kyoto Univ., Japan; ²Center for Emergent Matter Science, RIKEN, Japan; ³Dept. of Electronic and Photonic System Engineering, Kochi Univ. of Technology, Japan. We report classical optical interferometry reproducing dispersion-insensitive Hong-Ou-Mandel interferograms. Our scheme is based on the time-reversal symmetry of quantum dynamics. We achieved high-visibility Hong-Ou-Mandel interferograms owing to simplicity of our setup.

FW1A.4 • 11:15

Quantum Correlations Beyond Tsirelson's Bound, Martin Ringbauer², Alessandro Fedrizzi², Dominic W. Berry¹, Andrew G. White²; ¹Dept. of Physics and Astronomy, Macquarie Univ., Australia; ²School of Mathematics and Physics, The Univ. of Queensland, Australia. We optically demonstrate violation of the CHSH-Bell inequality and Tsirelson's bound via loss and postselection. This enables us to more easily distinguish between entangled and unentangled states, and violates information causality due to the postselected data.

FW1A.5 • 11:30

Entanglement Transmission through a Distributed Phase Sensitive Amplifier, James M. Dailey¹, Anjali Agarwal¹, Paul Toliver¹, Nicholas A. Peters²; ¹Applied Communication Sciences, USA; ²Applied Communication Sciences, USA. We demonstrate transmission of entangled photons through a $\chi(3)$ -based 5-km distributed optical amplifier operated in the low-gain limit to offset loss. No measurable degradation in entanglement quality is observed after the amplifier.

FW1A.6 • 11:45

Single-photon frequency conversion using cross-phase modulation, Nobuyuki Matsuda^{1,2}; ¹NTT Basic Research Labs, NTT Corporation, Japan; ²Nanophotonics Center, NTT Corporation, Japan. The frequency conversion of single photon wave packets was demonstrated using cross-phase modulation in a dispersion-managed photonic crystal fiber. The frequencies of single photons were successfully modulated without a significant photon loss.

FW1B • Spin Coherence in Color Centers in Diamond—Continued

FW1B.3 • 11:00

Suppression of Spin Dephasing in Diamond NV Centers with Microwave-Dressed Spin States, David Golter¹, Thomas K. Baldwin¹, Hailin Wang¹; ¹Physics, Univ. of Oregon, USA. We demonstrate a spectral domain technique for suppressing the nuclear-spin-bath induced dephasing of diamond nitrogen vacancy centers by employing microwave-dressed spin states. Reduction in spin dephasing by more than 10-fold is observed.

FW1B.4 • 11:15

High Precision Wide-Field Sensing with Individual Nitrogen-Vacancy Centers in Diamond, Matthew E. Trusheim¹, Dirk Englund¹; ¹MIT, USA. We demonstrate a microscopy technique for precision sensing across a wide field of view with high spatial precision through pulsed electron spin resonance of nitrogen vacancy centers in diamond.

FW1B.5 • 11:30 **Invited**

Quantum Information and Networks with Spins in Diamond, Tim H. Taminiau¹; ¹Technische Universiteit Delft, Netherlands. The nitrogen-vacancy center in diamond is a promising candidate to realize quantum networks. We create multi-qubit nodes of nuclear spins in the environment and couple these nodes together by entangling remote nitrogen-vacancy centers through photons.

FW1C • Symposium on Science and Applications of Structured Light in Complex Media I—Continued

FW1C.2 • 11:00 **▶**

Nanopatterned Multilayer Hyperbolic Metamaterials for Enhancing Spontaneous Light Emission, Dylan Lu¹, Lorenzo Ferrari², Jimmy J. Kan³, Eric E. Fullerton^{1,3}, Zhaowei Liu^{1,2}; ¹Electrical and Computer Engineering, Univ. of California San Diego, USA; ²Materials Science and Engineering, Univ. of California San Diego, USA; ³Center for Magnetic Recording Research, Univ. of California San Diego, USA. We show that nanopatterned hyperbolic metamaterials made of Ag-Si multilayers enhance the spontaneous emission rate of dye molecules by 76-fold at tunable frequencies and the emission intensity by ~80 fold compared to metamaterials without nanostructuring.

FW1C.3 • 11:15 **▶**

Tunable plasmonic platform for giant fluorescence enhancement, Maiken H. Mikkelsen^{1,2}, Alec Rose¹, Thang B. Hoang^{1,2}, Felicia McGuire¹, Jack J. Mock¹, Cristian Ciraci¹, David R. Smith¹; ¹Center for Metamaterials and Integrated Plasmonics, Dept. of Electrical and Computer Engineering, Duke Univ., USA; ²Dept. of Physics, Duke Univ., USA. We demonstrate a colloidal synthesized plasmonic platform for giant fluorescence enhancement and increased spontaneous emission rate of embedded fluorophores. A transition between fluorescence enhancement and quenching is revealed depending on the plasmonic resonance.

FW1C.4 • 11:30 **Invited** **▶**

Graphene Metadevices and Metamaterials for Linear and Nonlinear THz Applications, Hyeonon Kim¹, Woo Young Kim¹, Hyun Joo Choi¹, In-Hyung Baek², Bong Ju Kang², Teun-Teun Kim¹, Kanghee Lee¹, Young Uk Jeong³, Fabian Rotermund², Bumki Min¹; ¹Korea Advanced Inst of Science & Tech, Korea; ²Ajou Univ., Korea; ³Korea Atomic Energy Research Inst., Korea. Graphene metadevices and metamaterials are promising especially for the control of THz waves. Among various possible functional devices and materials, THz graphene memory metadevices and THz graphene metamaterial saturable absorbers are introduced as illustrative examples.

FW1D • Wavelength Conversion in Micro-Structures—Continued

FW1D.2 • 11:00

Investigation of Mode Interaction in Optical Microresonators for Kerr Frequency Comb Generation, Yang Liu¹, Yi Xuan^{1,2}, Xiaoxiao Xue¹, Pei-Hsun Wang¹, Andrew J. Metcalf¹, Steven Chen¹, Minghao Qi^{1,2}, Andrew M. Weiner^{1,2}; ¹School of Electrical and Computer Engineering, Purdue Univ., USA; ²Birk Nanotechnology Center, Purdue Univ., USA. Mode interaction in silicon nitride micro-resonators is investigated. We provide clear experimental evidence of mode interaction between two families of transverse modes and demonstrate a link between such interactions and initiation of comb generation in resonators with normal dispersion.

FW1D.3 • 11:15

Broadband Microresonator-Based Parametric Frequency Comb near Visible Wavelengths, Kevin Luke¹, Yoshitomo Okawachi², Daniel O. Carvalho¹, Michael R. Lamont^{1,2}, Alexander L. Gaeta^{2,3}, Michal Lipson^{1,3}; ¹School of Electrical and Computer Engineering, Cornell Univ., USA; ²School of Applied and Engineering Physics, Cornell Univ., USA; ³Kavli Inst. at Cornell for Nanoscale Science, Cornell Univ., USA. We demonstrate broadband frequency comb generation spanning over 700 nm from 830 to 1540 nm in a dispersion-engineered Si₃N₄ microresonator. To our knowledge, this is the broadest parametric comb generated near the visible wavelength range.

FW1D.4 • 11:30

Synchronization Phenomena in Mode-locked Parametric Frequency Combs, Yanan H. Wen¹, Michael R. Lamont^{1,2}, Isabel M. Kloumann⁴, Steven H. Strogatz⁴, Alexander L. Gaeta^{1,3}; ¹Applied & Engineering Physics, Cornell Univ., USA; ²Electrical & Computer Engineering, Cornell Univ., USA; ³Kavli Inst. at Cornell for Nanoscale Science, Cornell Univ., USA; ⁴Center for Applied Mathematics, Cornell Univ., USA. We show that the mode-locking dynamics in parametric frequency combs is equivalent to synchronization phenomena that occur in many physical systems as described by the Kuramoto model for coupled oscillators.

FW1D.5 • 11:45

Local fluorescent dye excitation with guided second-harmonic in lithium niobate nanowires, Anton Sergeyev¹, Reinhard Geiss¹, Alexander S. Soltsev², Ernst-Bernhard Kley¹, Thomas Pertsch¹, Rachel Grange¹; ¹Inst. of Applied Physics, Abbe Center of Photonics, Friedrich Schiller Univ., Germany; ²Nonlinear Physics Center, Research School of Physics and Engineering, Australian National Univ., Australia. We generate second-harmonic light in LiNbO₃ nanowires to excite fluorescent dye. We measure a 63pW second-harmonic threshold power to excite typical dye concentration for bioimaging. We calculate that 40x60nm² cross-sections nanowires can generate this power.

CLEO: Science & Innovations

CLEO: Applications
& TechnologySW1E • Pulse Compression—
Continued

SW1E.3 • 11:00 **Invited**
Self-Compression to Sub-Cycle Regime in Kagome Hollow-Core Photonic Crystal Fiber, Frédéric Gérôme¹, Tadas Balciunas², Coralie Fourcade-Dutin¹, Fan Guangyu², Tobias Witting³, Alexander A. Voronin⁴, Aleksei Zheltikov^{4,5}, G.g Paulus⁶, Andrius Baltuska², Fetah Benabid¹; ¹GPPMM group, Xlim Research Inst., CNRS UMR 7252, France; ²Vienna Univ. of Technology, Austria; ³Imperial College London, UK; ⁴M.V. Lomonosov Moscow State Univ., Russia; ⁵Dept. of Physics and Astronomy, Texas A&M Univ., USA; ⁶Inst. of Optics and Quantum Electronics, Germany. We demonstrate sub-cycle gigawatt peak power pulses self-compressed by optical shock waves in a simple manner based on gas-filled kagome hollow-core photonic crystal fiber.

SW1E.4 • 11:30
Low-energy Self-defocusing Soliton Compression at Optical Communication Wavelengths in Unpoled Lithium Niobate Ridge Waveguide, Hairun Guo¹, Xianglong Zeng², Binbin Zhou¹, Morten Bache¹; ¹Dept. of Photonics Engineering, Technical Univ. of Denmark, Denmark; ²Key Lab of Special Fiber Optics and Optical Access Networks, Shanghai Univ., China. Self-defocusing soliton compression supported by the cascaded phase-mismatched second-harmonic generation process is numerically demonstrated in unpoled lithium niobate ridge waveguides where nano-joule pulses are operated and quasi-phase-matching is unnecessary. The soliton range is 1100-1800 nm.

SW1E.5 • 11:45
Tunable single-cycle pulse compression at the group-velocity horizon, Ayhan Demircan¹, Shalva Amiranashvili², Carsten Bree², Uwe Morgner¹, Gunter Steinmeyer³; ¹Leibniz Univ. Hannover, Germany; ²Weierstrass Inst. for Applied Analysis and Stochastics, Germany; ³Max-Born-Institut, Germany. An adjustable adiabatic soliton compression scheme is presented, enabling pulse generation in the single-cycle regime. The compression comes without external dispersion compensation and is naturally stimulated by two-pulse collisions in an optical event horizon.

SW1F • Nonlinear THz Science
and Technology—Continued

SW1F.2 • 11:00
Extreme Terahertz Nonlinearities in Un-doped GaAs Driven by Ultrahigh Near-Fields in Metamaterials, Christoph Lange¹, Thomas Maag¹, Matthias Hohenleutner¹, Sebastian Baierl¹, Eric Edwards², Dominique Bougeard¹, Georg Woltersdorf², Rupert Huber¹; ¹Dept. of Physics, Univ. of Regensburg, Germany; ²Dept. of Physics, Univ. of Halle, Germany. Local terahertz fields of multiple 10 MV/cm tailored in gold metamaterials drive electronic interband transitions in intrinsic GaAs. The bandgap exceeds the THz photon energy 400-fold. Photoluminescence microscopy maps the THz near-field distribution.

SW1F.3 • 11:15
Nonlinear THz conductivity in graphene, Zoltan Mics¹, Soren Jensen¹, Khaled Parvez¹, Ivan Ivanov¹, Klaas-Jan Tielrooij², Frank Koppens², XinLiang Feng¹, Klaus Müllen¹, Mischa Bonn¹, Dmitry Turchinovich^{1,3}; ¹Max Planck Inst. f. Polymer Research, Germany; ²The Inst. of Photonic Sciences, Spain; ³DTU Fotonik, Technical Univ. of Denmark, Denmark. We report the nonlinear THz conductivity of graphene. The heating of charge carriers by strong THz pulses results in a reduction of the high-frequency conductivity of graphene, in spite of reduced scattering for high-energy carriers.

SW1F.4 • 11:30
Scaling up of intense terahertz pulses pumped with 800 nm light pulse, François Blanchard¹, Hadi Razavipour¹, Hassan Hafez², xavier ropagnol², Martin Bolduc³, Roberto Morandotti², Tsuneyuki Ozaki², David G. Cooke¹; ¹Physics, McGill Univ., Canada; ²Institut national de la recherche scientifique, Canada; ³Institut national d'Optique, Canada. We investigate the terahertz generation efficiency dependence as function of the pulse width durations at 800 nm. Our results confirmed conversion efficiency of 0.35% with saturation at 240 fs of pulse width duration.

SW1F.5 • 11:45
Efficient Generation of THz Pulses with 0.4 mJ Energy, József A. Fülöp^{1,3}, Zoltán Ollmann², Csaba Lombos², Christoph Skrobel^{4,5}, Sandro Klingebiel⁴, László Pálfalvi², Ferenc Krausz^{4,5}, Stefan Karsch^{4,5}, János Hebling^{1,2}; ¹MTA-PTE High-Field Terahertz Research Group, Hungary; ²Univ. of Pécs, Hungary; ³ELI-Hu Nkft., Hungary; ⁴Max-Planck-Institut für Quantenoptik, Germany; ⁵Ludwig-Maximilians-Universität, Germany. THz pulses above 0.4 mJ energy were generated with 0.77% efficiency by optical rectification of 785-fs laser pulses in LiNbO₃ using tilted-pulse-front pumping. The spectral peak is at about 0.2 THz, suitable for charged-particle manipulation.

SW1G • Emerging Trends
in Semiconductor Lasers—
Continued

SW1G.2 • 11:00 **▶**
Measurement of the Second Order Coherence of a Nanolaser Through Its Intra-cavity Second Harmonic Generation, Yasutomo Ota¹, Katsuyuki Watanabe², Satoshi Iwamoto^{1,2}, Yasuhiko Arakawa^{1,2}; ¹Nanoquine, Univ. of Tokyo, Japan; ²IIS, Univ. of Tokyo, Japan. We measured the second order coherence of a photonic crystal nanolaser through measuring frequency doubling occurring within the laser nanocavity. This method enables investigation of the intensity noise properties even far below the lasing threshold.

SW1G.3 • 11:15 **▶**
Gallium Nitride Nanotube Lasers, Changyi Li¹, Antonio Hurtado², Jeremy B. Wright^{1,3}, Huiwen Xu¹, Sheng Liu^{3,4}, Ting S. Luk^{3,4}, Igal Brener^{3,4}, Steven R. Brueck¹, George T. Wang³; ¹Center for High Technology Materials, Univ. of New Mexico, USA; ²School of Computer Science and Electronic Engineering, Univ. of Essex, UK; ³Sandia National Labs, USA; ⁴Center for Integrated Nanotechnology, Sandia National Labs, USA. Lasing is demonstrated from gallium nitride nanotubes fabricated using a two-step top-down technique. By optically pumping, we observed characteristics of lasing: a clear threshold, a narrow spectral, and guided emission from the nanotubes.

SW1G.4 • 11:30 **Tutorial** **▶**
Dealing with Loss in Plasmonics and Metamaterials, Jacob Khurgin¹; ¹Johns Hopkins Univ., USA. Loss in the metal is the main factor restricting practicality of plasmonic and metamaterial devices. In this tutorial the inevitability of the loss, its physical origins and the means to mitigate it will be considered.



Jacob B Khurgin has been a Professor of electrical and computer engineering at Johns Hopkins University for 26 years. Prior to John Hopkins Univ. he was a researcher at Philips Laboratories. His areas of interest include semiconductor devices, nonlinear optics, integrated optics, condensed matter physics and communications. He has authored of 300 journal articles and holds 30 patents.

AW1H • Material Structuration
for Next Generation Sensors—
and Components—Continued

AW1H.3 • 11:00
Femtosecond laser modification of Li(NiCoMn)O₂ electrodes for lithium-ion batteries, Peter Smyrek¹, Johannes Proell¹, Wilhelm Pflöging^{1,2}; ¹IAM-AWP, Karlsruhe Inst. of Technology, Germany; ²LMP, Karlsruhe Nano Micro Facility, Germany. Ultrafast laser micromachining processes for modification and formation of three-dimensional architectures in cathode materials were developed. The electrochemical properties were investigated applying cell test with current densities in the range of (0.05-28.79) mA/cm².

AW1H.4 • 11:30 **Invited**
Ultrafast Laser Writing of Advanced Guided Wave Communications Components, Nicholas Psaila¹; ¹Heriot-Watt Univ., UK. The use of ultrafast laser writing for fabricating advanced 3D waveguide components is presented and demonstrated. Couplers for space division multiplexing allowing beyond Shannon limit spectral efficiency, and 3D hybrid integration capabilities are discussed.

CLEO: Science & Innovations

CLEO: QELS-
Fundamental ScienceCLEO: Applications
& TechnologySW11 • Solitons and Nonlinear
Propagation—ContinuedSW1J • Bandwidth Efficient
Signaling—ContinuedFW1K • Metasurfaces and
Plasmonic Metamaterials—
ContinuedAW1L • Imaging and
Sensing—Continued

SW1J.3 • 11:00

Flexible Terabit/s Nyquist-WDM Superchannels with net SE > 7bit/s/Hz using a Gain-Switched Comb Source, Vidak Vujicic¹, Joerg Pfeifle², Regan Watts¹, Philipp C. Schindler², Claudius Weimann², Rui Zhou¹, Wolfgang Freude^{2,3}, Christian G. Koos^{2,3}, Liam Barry¹; ¹School Of Electronic Engineering, Dublin City Univ., Ireland; ²Inst. of Photonics and Quantum Electronics, Karlsruhe Inst. of Technology, Germany; ³Inst. of Microstructure Technology, Karlsruhe Inst. of Technology, Germany. We demonstrate two 1Tbit/s superchannel architectures using a compact, FSR-tunable gain-switched comb source. SSMF transmission of 18GBaud Nyquist-WDM shaped PDM-QPSK and PDM-16QAM modulation is reported, with a capacity up to 1.296Tbit/s and SE of 7.2bit/s/Hz.

SW1J.4 • 11:15

All-optical demultiplexing of Nyquist OTDM using a Nyquist gate, Jasper R. Stroud¹, Mark A. Foster¹; ¹Johns Hopkins Univ., USA. We present an approach to all-optical demultiplexing of ultrafast Nyquist OTDM signals using four-wave mixing with a Nyquist gate. Our design does not suffer from the tradeoff between SNR and ISI of existing approaches.

SW11.2 • 11:30

Spectrally resolved shot-to-shot nonlinear dynamics of a passive PCF ring cavity, Michael J. Schmidberger^{1,2}, Pooria Hosseini^{2,1}, David Novoa¹, Alessio Stefani¹, Philip St.J. Russell^{1,2}, Nicolas Joly^{2,1}; ¹Russell, Max-Planck-Inst. for the Science of Light, Germany; ²Dept. of Physics, Univ. of Erlangen-Nuremberg, Germany. The global experimental bifurcation diagram of a passively pumped PCF ring cavity is analyzed. We observe unequal shot-to-shot evolution of different spectral regions of the cavity pulse, and confirm this using two independent measurement techniques.

SW11.3 • 11:45

Experimental Measurement of Supercontinuum Second Order Coherence, Mikko Närhi¹, Minna Korhonen², Jari Turunen², Ari Friberg², Goëry Genty¹; ¹Physics, Tampere Univ. of Technology, Finland; ²Physics and Mathematics, Univ. of Eastern Finland, Finland. We report the first experimental measurements of second-order coherence functions of supercontinuum light. The method is based on measuring separately the quasi-coherent and quasi-stationary contributions using a combination of interferometric and nonlinear gating techniques.

SW1J.5 • 11:30

Transmitter Sensitivity to High PAPR in Coherent Optical OFDM Systems, Siamak Amiralizadeh¹, Leslie Rusch¹; ¹Center for Optics, Photonics and Lasers (COPL), Université Laval, Canada. We investigate degradation of QPSK CO-OFDM system due to components most susceptible to high PAPR. We vary transmitter design parameters and uncover appropriate working conditions and clipping effectiveness regions.

SW1J.6 • 11:45

Generation of SSB Optical Signals with Dual-EML Modulated with Wideband OFDM, Mohamed Essghair Chaibi¹, Didier Erasme¹, Thomas Anfray², Christelle Aupetit-Berthelemot², Christophe Kazmierski³; ¹MINES-TELECOM, TELECOM ParisTech, CNRS LTCI, France; ²XLIM-CNRS, France; ³III-V Lab-Common Lab of "Alcatel-Lucent Bell Labs France", "Thales Research and Technology" and "CEA Leti", France. The generation of optical SSB signals by a Dual-EML is generalized for wideband modulating signals. The feasibility of the proposed technique is demonstrated by transmitting 5.3 GHz baseband OFDM signal in an optical SSB context.

FW1K.2 • 11:30

Far field characterization of light propagation in hyperbolic metamaterial with multi metal-dielectric layers, Xiangang Luo¹; ¹CAS Inst. of Optics and Electronics, China. Far field characterization of light propagation in metamaterial with multi metal-dielectric layers is performed by introducing rough surface and nano grating structures. Light directional imaging and evanescent wave moiré fringes are observed in experiments.

FW1K.3 • 11:45

Angle-independent Salisbury screens based on nonlocal nanowire metamaterials, Brian Wells¹, Christopher Roberts¹, Viktor A. Podolskiy¹; ¹Physics and Applied Physics, Univ Massachusetts Lowell, USA. We demonstrate that nonlocal nanowire metamaterials can help to alleviate one of the main limitations of Salisbury screens, their dependence on the incident angle.

AW1L.2 • 11:30

Photophysical Properties of Novel Ru-complex Probes for Two-photon Dissolved Oxygen Imaging, Aamir A. Khan¹, Tahsin Ahmed¹, Genevieve Vigil¹, Susan K. Fullerton-Shirey¹, Scott S. Howard¹; ¹Dept. of Electrical Engineering, Univ. of Notre Dame, USA. Oxygen-sensitive hydrophobic indicators encapsulated in poloxamer nanomicelles are quantitatively demonstrated to preserve the oxygen-sensitivity and the two-photon induced phosphorescence in a ruthenium-complex indicator, thus providing for economical dissolved oxygen imaging probes.

AW1L.3 • 11:45

Lab-on-chip Silicon Nitride Microring Sensor at Visible Wavelength Using Glycoprotein Receptors, Farshid Ghasemi¹, Ali A. Eftekhari¹, Hamed Shams Mousavi¹, Reza Abbaspour¹, Hesam Moradinejad¹, Ali Adibi¹; ¹Electrical and Computer Engineering, Georgia Inst. of Technology, USA. A full biosensor system based on referenced and spectrally multiplexed arrays of silicon nitride microrings with glycoprotein receptors is demonstrated. Underlying system design guidelines and fundamental noise limits of the device are discussed.

CLEO: Science & Innovations

CLEO: Applications
& TechnologySW1M • Micro and Nanophotonic
Devices—Continued

SW1M.2 • 11:00

Observation of visible-wavelength electric and magnetic resonances on silicon nanorods, Wuzhou Song¹, Kenneth B. Crozier¹, ¹Harvard Univ., USA. We fabricated silicon nanorods on silica substrates, and show that they support electric and magnetic resonances by simulation and experiment. Due to these resonances, the nanorods appear vivid colors when observed by optical microscopy.

SW1M.3 • 11:15

Photonic Crystal Enhanced Photoacoustic Detection, Yunfei Zhao¹, Kaiyang Liu¹, John F. McClelland^{2,4}, Meng Lu^{1,3}, ¹Dept. of Electrical and Computer Engineering, Iowa State Univ., USA; ²Ames Lab-USDOE, USA; ³Dept. of Mechanical Engineering, Iowa State Univ., USA; ⁴Dept. of Biochemistry, Biophysics, and Molecular Biology, Iowa State Univ., USA. A photonic crystal sensor has been demonstrated to enhance photoacoustic signal from light absorbing molecules. The developed system was applied to detect an absorbing dye and gold nanoparticles and exhibited signal enhancement over 40 times.

SW1M.4 • 11:30

Narrowband Four Wave Mixing in InGaP Photonic Crystal Waveguides, Amnon Willinger¹, Gadi Eisenstein¹, Sylvain Combrie², Alfredo De Rossi², ¹Electrical Engineering, Technion - Israel Inst. of Technology, Israel; ²Thales Research and Technology, France. Abstract We demonstrate the first narrow-band parametric interaction in a semiconductor (GaInP) photonic crystal waveguide. A pulsed pump, propagating in the normal dispersion regime yields a conversion efficiency of -10dB with a moderate peak pump power of 650mW.

SW1M.5 • 11:45

Heterogeneously Integrated MIR Silicon Photonics, Yu Chen¹, Hongtao Lin², Juejun Hu², Mo Li¹, ¹Univ. of Minnesota Twin Cities, USA; ²Material Science and Engineering, Univ. of Delaware, USA. By utilizing heterogeneous integration method, integrated silicon photonics on mid-IR compatible substrate has been fabricated and on-chip cavity-enhanced mid-IR spectroscopic analysis of organic chemicals has been demonstrated.

SW1N • Novel Fiber Laser
Designs—Continued

SW1N.2 • 11:00

Ultra-short wavelength operation of a two-micron thulium fiber laser, Jae M. Daniel¹, Nikita Simakov^{1,2}, Masaki Tokurakawa^{1,3}, Morten Ibsen¹, W. A. Clarkson¹, ¹Optoelectronics Research Centre, Univ. of Southampton, UK; ²Cyber and Electronic Warfare Division, Defence Science and Technology Organisation, Australia; ³Inst. for Laser Science, Univ. of Electro-Communications, Japan. The short wavelength limit of a thulium fiber laser is investigated. Wavelength tuning from 1720nm to 1660nm was demonstrated and fixed wavelength operation up to 12.6W at 1726nm with slope efficiency of 67% was achieved.

SW1N.3 • 11:15

Watt-level fluoride fiber lasers and amplifiers in the 1.2 μm region, Xiushan Zhu^{1,2}, Jie Zong¹, Kort Wiersma¹, Robert A. Norwood², Narasimha S. Prasad³, Michael D. Omland³, Arturo Chavez-Pirson¹, Nasser Peyghambarian², ¹NP Photonics, USA; ²Univ. of Arizona, USA; ³NASA Langley Research Center, USA. Holmium-doped ZBLAN fiber has proven to be an efficient high gain material in the 1.2 μm region. In this paper, single-mode fiber lasers and amplifiers at 1178 nm, 1190 nm, and 1200 nm are reported. Over 2 watts of continuous wave output power was achieved with a 10-cm long gain fiber.

SW1N.4 • 11:30

A 160 mW Output, 5 kHz Linewidth Frequency-Stabilized Erbium Silica Fiber Laser with a Short Cavity Configuration, Keisuke Kasai¹, Akira Fujisaki¹, Masato Yoshida¹, Toshihiko Hirooka¹, Masataka Nakazawa¹, Shin Masuda², ¹Research Inst. of Electrical Communication, Tohoku Univ., Japan; ²Advantest Labs, Ltd., Japan. We demonstrate a 160mW output, ¹³C₂H₂ frequency-stabilized erbium silica fiber laser. The frequency stability reached 8.8×10⁻¹² for τ=100s. Furthermore, a linewidth of 5 kHz and a RIN of -130 dB/Hz were simultaneously achieved.

SW1N.5 • 11:45

Ultra-narrow linewidth fiber laser with self-injection feedback based on Rayleigh backscattering, leilei shi¹, Tao Zhu¹, Shihong Huang¹, ¹Chongqing Univ., China. We propose a single longitudinal mode fiber laser with ultra-narrow linewidth of ~130 Hz by combining self-injection feedback and Rayleigh backscattering, in which Rayleigh backscattering collected by self-injection feedback is utilized as linewidth compressor.

SW1O • Laser Frequency
Combs—Continued

SW1O.3 • 11:00

Carrier-Envelope-Offset Frequency Stabilization and Noise Analysis of a SESAM-Modulated Thin Disk Laser, Florian Emaury¹, Alexander Klenner¹, Andreas Diebold¹, Cinia Schriber¹, Clara J. Saraceno^{1,2}, Stephane Schilt², Ursula Keller¹, Thomas Südmeyer², ¹ETH Zurich, Switzerland; ²Université de Neuchâtel, Switzerland. We present the first phase stabilization of the carrier envelope offset frequency of a SESAM-modelocked thin disk laser (<120 mrad at 1 Hz-1 MHz) and measure the influence of different noise sources such as multi-transverse-mode high-power diode-pumping.

SW1O.4 • 11:15

Compact and ultra-high-resolution spectrograph with multi-GHz optical frequency comb, Mamoru Endo^{1,2}, Takashi Sukegawa³, Alissa Silva^{1,2}, Yohei Kobayashi^{1,2}, ¹The Inst. for Solid State Physics, The Univ. of Tokyo, Japan; ²Exploratory Research for Advanced Technology (ERATO), JST, Japan; ³Corporate R&D Headquarters, Canon Inc., Japan. A 4-GHz optical frequency comb with a laser-diode pumped Yb:Y₂O₃ ceramic oscillator is demonstrated. Each comb tooth was resolved by a home-made, sub-gigahertz frequency resolution grating spectrograph, which would be useful for many small observatories.

SW1O.5 • 11:30

500 MHz Yb: fiber laser frequency comb, Guizhong Wang¹, Fei Meng², Chen Li¹, Tongxiao Jiang¹, Yizhou Liu¹, Aimin Wang¹, Zhanjun Fang², Zhigang Zhang¹, ¹Peking Univ., China; ²National Inst. of Metrology, China. We report direct generation of 500MHz Yb: fiber laser frequency comb. The offset frequency was stabilized more than 6 hours in an open air environment. The stabilized repetition rate has an in-loop tracking stability of 4.46*10⁻¹³/s.

SW1O.6 • 11:45

Opto-Optical Modulation of an Intra-Cavity SESAM for Low-Noise CEO Stabilization of a Femtosecond Laser, Martin Hoffmann¹, Stephane Schilt¹, Thomas Südmeyer¹, ¹Université de Neuchâtel, Switzerland. We present a CEO-stabilization technique based on optical feedback to an intra-cavity SESAM with significantly improved bandwidth compared to standard pump current control, enabling a CEO-locked Er:Yb:glass laser with ten times lower residual phase noise.

AW1P • Spectroscopy and
Imaging Applications—
Continued

AW1P.3 • 11:00

Invited

Ultrafast X-ray Absorption Spectroscopy using Superconducting Microcalorimeter Sensors, Joel Ullom¹, Marla Dowell¹, Joseph Fowler¹, Luis Miaja¹, Galen O'Neil¹, Kevin Silverman¹, Daniel Swetz¹, Dodderi Sagar², Zin Yoon², Ralph Jimenez², Jens Uhlig³, Wilfred Fullagar³, Dharmalingam Kurunthu³, Ujjwal Mandal³, Villy Sundstrom³, ¹NIST, USA; ²JILA, USA; ³Dept. of Chemical Physics, Lund Univ., Sweden. We are developing a table-top system for ultrafast x-ray spectroscopy based on a sub-picosecond x-ray source. We perform high-resolution spectroscopy of the x-rays after they interact with a sample using an array of superconducting microcalorimeters.

AW1P.4 • 11:30

Single-mode, high repetition rate, compact Ho:YLF laser for space-borne lidar applications, Yingxin Bai¹, Jirong Yu², Teh-hwa Wong¹, Songsheng Chen², Mulugeta Petros², Robert Menzies³, Upendra Singh², ¹Science Systems & Applications Inc, USA; ²Active remote sensing, NASA Langley Research Center, USA; ³NASA Jet Propulsion Lab., USA. A single transverse/longitudinal mode, compact Q-switched Ho:YLF laser has been designed and demonstrated for space-borne lidar applications. The pulse energy is between 34-40 mJ for 100-200 Hz operation. The corresponding peak power is >1 MW.

AW1P.5 • 11:45

Beyond 10 Km Range wind-speed measurement with a 1.5 μm all-fiber laser source, William Renard¹, Didier Goular¹, Matthieu Valla¹, Christophe Planchat¹, Beatrice Augere¹, Agnes Dolfi-Bouteyre¹, Claudine Besson¹, Guillaume Canat¹, ¹Theoretical and Applied Optics Dept., Onera - The French Aerospace Lab., France. We report the development of a high power single-frequency all-fiber laser for long-range wind speed measurement. The laser source has been integrated in a Lidar architecture and we report wind-speed measurement beyond 10 km.

CLEO: QELS-Fundamental Science

FW1A • Fundamental Quantum Science—Continued

FW1A.7 • 12:00

Observation of Topological Structures in Photonic Quantum Walks, Graciana Puentes^{1,2}, Ilja Gerhardt², Fabian Katschmann³, Christine Silberhorn³, Jörg Wrachtrup², Maciej Lewenstein¹; ¹ICFO -The Inst. of Photonic Sciences, Spain; ²3 Physik. Insitut, Universität Stuttgart, Germany; ³Applied Physics, Universität Paderborn, Germany. We present an experimental observation of topological structure in 1D photonic discrete-time quantum walks. We probe the full topological landscape demonstrating emergence of localized bound states, and existence of extremely (de)localized non-Gaussian quantum states.

FW1A.8 • 12:15

Entanglement discloses Time as an emergent phenomenon, marco gramegna¹; ¹Quantum Optics, INRIM, Italy. Page and Wootters' mechanism of "static" time is experimentally implemented by a toy universe consisting of a polarization entangled photon pair, one of which serves as a clock to gauge the evolution of the second.

FW1B • Spin Coherence in Color Centers in Diamond—Continued

FW1B.6 • 12:00

Targeted creation and Purcell enhancement of NV centers within photonic crystal cavities in single-crystal diamond, Tim Schroeder¹, Edward Chen¹, Luozhou Li^{1,2}, Michael Walsh¹, Matthew E. Trusheim¹, Igal Bayn¹, Dirk Englund¹; ¹MIT, USA; ²Columbia Univ., USA. We demonstrate Purcell enhancement of single NV centers in L3 photonic crystal cavities made from high-purity single-crystal diamond. Furthermore, NV centers were created using an implantation mask in the cavity high field region.

FW1B.7 • 12:15

Efficient Integration of High-Purity Diamond Nanostructures into Silicon Nitride Photonic Circuits, Sara L. Mouradian¹, Tim Schroeder¹, Carl Poitras³, Luozhou Li², Jaime Cardenas³, Jordan Goldstein¹, Rishi Patel¹, Edward Chen¹, Matthew E. Trusheim¹, Igal Bayn^{1,2}, Michal Lipson³, Dirk Englund¹; ¹MIT, USA; ²Columbia Univ., USA; ³Cornell Univ., USA. A high purity diamond nanowire with implanted nitrogen-vacancy centers (NVs) is integrated into a low-loss silicon nitride photonic circuit. NV fluorescence is coupled into and collected from the waveguide system, paving the way for on-chip read out and manipulation of qubits.

FW1C • Symposium on Science and Applications of Structured Light in Complex Media I—Continued

FW1C.5 • 12:00

Switching of Mid-Infrared Light Using Plasmonic Fano-Resonant Meta-Surfaces Integrated with Graphene, Nima Dabidian¹, Iskandar Kholmanov², Alexander B. Khanikaev^{1,3}, Kaya Tatar¹, Simeon Trendafilov¹, Hossein S. Mousavi^{1,4}, Carl Magnusson², Rodney Ruoff⁵, Gennady Shvets¹; ¹physics, Univ. of Texas at Austin, USA; ²Mechanical engineering, Univ. of Texas at Austin, USA; ³physics, Queens College of The City Univ. of New York, USA; ⁴Electrical engineering, Univ. of Texas at Austin, USA. We experimentally demonstrate that graphene can strongly modulate the scattered light from Fano-resonant plasmonic metasurfaces. The Modulation depth of 1000% is achieved at around 7 μ m as the graphene carrier concentration changes.

FW1C.6 • 12:15

Scattering super-lens: subwavelength light focusing and imaging via wavefront shaping in complex media, Jung-Hoon Park¹, Chunghyun Park¹, Yong-Hoon Cho¹, YongKeun Park¹; ¹Korea Advanced Inst. of Science and Technology, Korea. We present a novel optical method exploiting multiple scattering to achieve sub-wavelength focusing and imaging using visible light. The evanescent near-field information are controlled by or transferred into far-field components by scattering from disordered nanoparticles.

FW1D • Wavelength Conversion in Micro-Structures—Continued

FW1D.6 • 12:00

Phase-Locking in Multi-Frequency Brillouin Oscillator via Four-Wave Mixing, Thomas Buettner¹, Irina V. Kabakova¹, Darren D. Hudson¹, Ravi Pant¹, Christopher G. Poulton^{2,1}, Alexander C. Judge¹, Benjamin J. Eggleton¹; ¹CUDOS, School of Physics, Univ. of Sydney, Australia; ²CUDOS, School of Mathematical Sciences, Univ. of Technology, Australia. We report the experimental demonstration and numerical modeling of phase-locking cascaded Stokes waves generated by Stimulated Brillouin Scattering via Kerr nonlinear four-wave mixing in a short, chalcogenide fiber resonator, producing phase-locked trains of picosecond pulses.

FW1D.7 • 12:15

Supercontinuum Generation in Hydrogenated Amorphous Silicon Waveguides in the Femtosecond Regime, Simon-Pierre Gorza¹, François Leo³, Bart Kuyken³, Shankar Kumar Selvaraja³, Gunther Roelkens³, Roel Baets³, Philippe Emplit¹, Serge Massar², Jassem Safioui¹; ¹Service OPERA-photonique, Université Libre de Bruxelles, Belgium; ²Laboratoire d'Information Quantique, Université libre de Bruxelles, Belgium; ³INTEC Dept., Ghent Univ.-IMEC, Belgium. Supercontinuum generation in CMOS compatible hydrogenated amorphous silicon waveguides with femtosecond pulses at telecommunication wavelengths is experimentally studied. It is shown that stable 540 nm broad supercontinua can be obtained in 1 cm-long waveguides.

12:00–13:30 VIP Industry Leaders Networking Event, Exhibit Hall 3
(lunch provided, registration required)

12:30–13:30 Lunch and Unopposed Exhibit Only Time, Exhibit Halls 1 & 2 (concessions available)

NOTES

CLEO: Science & Innovations

CLEO: Applications
& Technology

SW1E • Pulse Compression—
Continued

SW1F • Nonlinear THz Science
and Technology—Continued

SW1G • Emerging Trends
in Semiconductor Lasers—
Continued

AW1H • Material Structuration
for Next Generation Sensors
and Components—Continued

SW1E.6 • 12:00

Tilted Transmission Grisms for Pulse Compression with Dispersion Control Up to the Fourth Order, Stéphanie Grabielle¹, Nicolas Forget¹, Pierre Tournois¹; ¹FASTLITE, France. We demonstrate a grism compressor designed to compensate the second, third and fourth order dispersions of a 1.5m SF57 stretcher at 800nm.

SW1F.6 • 12:00

Terahertz Conversion Efficiency Scaling by Optical Rectification in the 800 nm Pump-Wavelength Range, Sergio Carbajo^{1,2}, Xiaojun Wu^{1,2}, Frederike Ahr¹, Franz Kärtner^{1,3}; ¹Center for Free Electron Laser Science, Germany; ²The Hamburg Center for Ultrafast Imaging, Germany; ³Research Laboratory of Electronics, MIT, USA. We report on a record 800 nm-to-terahertz energy conversion efficiency of 0.13% at room temperature in LiNbO3 by tilting the pulse intensity front and experimentally studying optimal pumping conditions.

AW1H.5 • 12:00

Monolithic Three Dimensional Dielectrophoretic Actuator for Positioning Optics Fabricated by Femtosecond Laser, Tao Yang¹, Yves Bellouard¹; ¹Eindhoven Univ. of Technology, Netherlands. We report a monolithic three dimensional dielectrophoretic micro-actuator fabricated by femtosecond laser in fused silica. Such actuators are useful for fine positioning of optical fibers and for introducing optomechanical coupling in waveguides.

SW1E.7 • 12:15

High-energy pulse compressor using self-defocusing spectral broadening in anomalously dispersive media, Morten Bache¹, Binbin Zhou¹; ¹Danmarks Tekniske Universitet, Denmark. A new high-energy pulse compressor uses self-defocusing spectral broadening in anomalously dispersive quadratic nonlinear crystals, followed by positive group-delay-dispersion compensation. Compression to sub-50 fs is possible from Joule-class 1.03 μm femtosecond amplifiers in large-aperture KDP.

SW1F.7 • 12:15

MV/cm Terahertz transients in the THz gap (1-20 THz) from organic crystals, Carlo Vicario¹, Balazs Monoszlai¹, Christoph P. Hauri^{1,2}; ¹Paul Scherrer Institut, Switzerland; ²Ecole Polytechnique Federale de Lausanne, Switzerland. We demonstrate highly efficient Terahertz production and absolute phase control in the hardly accessible THz frequency gap by optical rectification in organic crystals leading to single-cycle field oscillations beyond 150 MV/m and 0.5 Tesla.

AW1H.6 • 12:15

A monolithic micro-tensile tester for investigating silica micromechanics, fabricated and fully operated using a femtosecond laser, Christos-Edward Athanasiou¹, Ben McMillen¹, Yves Bellouard¹; ¹TU/e, Netherlands. We report on the use of femtosecond laser for fabricating, loading and in-situ measuring using third-harmonic signal generation a micro-tensile tester for characterizing silica and its polymorphic phases.

12:00–13:30 VIP Industry Leaders Networking Event, Exhibit Hall 3
(lunch provided, registration required)

12:30–13:30 Lunch and Unopposed Exhibit Only Time, Exhibit Halls 1 & 2 (concessions available)

NOTES

CLEO: Science & Innovations

CLEO: QELS-Fundamental Science

CLEO: Applications & Technology

SW11 • Solitons and Nonlinear Propagation—Continued

SW1J • Bandwidth Efficient Signaling—Continued

FW1K • Metasurfaces and Plasmonic Metamaterials—Continued


AW1L • Imaging and Sensing—Continued

SW11.4 • 12:00 

Vacuum-UV Dispersive Wave Emission Using Gas-Filled Hollow-Core PCF, Alexey Ermolov¹, Ka Fai Mak¹, Philipp Hoelzer¹, John C. Travers¹, Philip St.J. Russell^{1,2}; ¹*Max Planck Inst. for the Science, Germany*; ²*Univ. of Erlangen-Nuremberg, Germany*. Vacuum-UV radiation between 145-155 nm is generated from 40 fs, 800 nm 6.8 μ J pump pulses in a 34 μ m core-diameter kagomé-PCF filled with 20-25 bar neon. Simulations confirm the mechanism as resonant dispersive-wave emission.

SW1J.7 • 12:00

ASE Noise Suppressed Optical Multi-carrier Generation using Optical FIR Filter in Frequency Shifter Loop, Jiachuan Lin¹, Xiaoguang Zhang¹, Jianrui Li¹, Lixia Xi¹, Xia Zhang^{1,2}; ¹*State Key Lab of Information Photonics and Optical Communications, Beijing Univ. of Posts and Telecommunications, China*; ²*The Key Lab of Optical Communications Science & Technology in Shandong Province, Liaocheng Univ., China*. A low noise multi-carrier generation scheme using optical FIR filter for ASE noise suppressing is proposed. 50 and 69 low noise carriers are generated experimentally, having much higher carrier-to-noise-ratio values of 22.5dB and 19.1dB.

FW1K.4 • 12:00 

GZO/ZnO Multilayered nanodisk metasurface to engineer the plasma frequency, Jongbum Kim¹, Babak Memarzadeh², Aavek Dutta¹, Sajid M. Choudhury¹, Alexander Kildishev¹, Hossein Mosallaei², Alexandra Boltasseva¹; ¹*Purdue Univ., USA*; ²*North-eastern Univ., USA*. We demonstrate that a multilayered nanodisk metasurface based on semiconductor materials offers the design flexibility for tuning the plasmonic resonance by controlling the ratio between the metal and dielectric layers.

AW1L.4 • 12:00

Fiber-Optic EFPI/FBG Dual Sensor for Monitoring of Radiofrequency Thermal Ablation of Liver Tumors, Daniele Tosi¹, Edoardo G. Macchi², Mario Gallati², Giovanni Braschi², Alfredo Cigada³, Sandro Rossi⁴, Sven Poeggel¹, Gabriel Leen¹, Elfed Lewis¹; ¹*Optical Fibre Sensors Research Centre, Univ. of Limerick, Ireland*; ²*Dipartimento di Ingegneria Civile ed Architettura, Università, Italy*; ³*Dipartimento di Meccanica, Politecnico di Milano, Italy*; ⁴*VI Dept. of Internal Medicine, IRCCS Policlinico San Matteo Foundation, Italy*. A dual EFPI/FBG pressure and temperature sensing architecture, biocompatible and with minimum cross-sensitivity, is presented. The system performs online monitoring of radiofrequency thermal ablation in liver tumor, detecting the physical phenomena; ex-vivo experiments are reported.

SW11.5 • 12:15 

Efficiency of dispersive wave generation by cascaded four-wave mixing, Karen E. Webb¹, Miro J. Erkintalo¹, Yiqing Xu^{1,2}, Goëry Genty³, John M. Dudley⁴, Stuart G. Murdoch¹; ¹*Univ. of Auckland, New Zealand*; ²*Univ. of Hong Kong, Hong Kong*; ³*Tampere Univ. of Technology, Finland*; ⁴*Universite de Franche-Comte, France*. We experimentally show that the pump frequency detuning strongly affects the efficiency of dispersive wave generation by cascaded four-wave mixing. We explain our results in terms of higher-order soliton compression of the input beat signal.

SW1J.8 • 12:15

Improving Broad-band Mid-span Spectral Inversion Performance for Fiber Non-linearity Compensation, Mohammad M. Morshed^{1,2}, Bill Corcoran^{1,2}, Arthur Lowery^{1,2}; ¹*Electrical and Computer Systems Engineering, Monash Univ., Australia*; ²*Center for Ultrahigh bandwidth Devices for Optical Systems (CUDOS), Monash Univ., Australia*. We investigate design approaches for improving the performance of broad-band mid-span spectral inversion. Simulations show at least 0.7 dB peak Q improvement of a 160-GHz wide 16-QAM OFDM super channel after 800 km transmission.

FW1K.5 • 12:15 

Silicon on sapphire mid-IR wave-front engineering by using sub-wavelength gratings, Yuewang Huang¹, Qiancheng Zhao¹, Salih K. Kalyoncu¹, Rasul Torun¹, Yumeng Lu¹, Ozdal Boyraz¹; ¹*Univ. of California Irvine, USA*. We propose a methodology to manipulate reflected field for the design of wavefront engineered device in mid-IR range using sub-wavelength silicon gratings on sapphire substrate. High reflectivity mirror, blazed grating and focusing reflector are designed.

AW1L.5 • 12:15

High Repetition-Rate, Pulse-Burst Assisted Desorption, Electrospray Post-ionization Mass Spectrometry, Paul Flanigan¹, Fengjian Shi¹, Jieutonne Archer¹, Andrew Mills², Martin Fermann², Robert Levis¹; ¹*Chemistry, Temple Univ., USA*; ²*IMRA America, Inc, USA*. We demonstrate electrospray post-ionization mass spectrometry with an Yb fiber laser producing 500 fs, 50 μ J pulse-bursts, enabling protein, peptide and lipid identification and imaging for the pharmaceutical and biomedical realm.

12:00-13:30 VIP Industry Leaders Networking Event, Exhibit Hall 3
(lunch provided, registration required)

12:30-13:30 Lunch and Unopposed Exhibit Only Time, Exhibit Halls 1 & 2 *(concessions available)*

NOTES

CLEO: Science & Innovations

CLEO: Applications
& Technology

SW1M • Micro and Nanophotonic Devices—Continued

SW1M.6 • 12:00

Flexible Crystalline Silicon Nanomembrane Photonic Crystal Microcavity, Xiaochuan Xu^{1,2}, Harish Subbaraman², Amir Hosseini², Swapnajt Chakravarty², Ray Chen¹; ¹Univ. of Texas at Austin, USA; ²Omega Optics, Inc., USA. We for the first time demonstrated a flexible crystalline silicon nanomembrane photonic crystal microcavity, which shows a quality factor of 22000 and could be bent to a radius of 5 mm.

SW1M.7 • 12:15

Beam focalization by chirped mirrors, Yu-Chieh Cheng¹, Martynas Peckus², Simonas Kicas², Josep Trull¹, Crina Cojocaru¹, Ramon Vilaseca¹, Ramutis Drazdys², Kestutis Stalunas^{1,3}; ¹Departament de Física i Enginyeria Nuclear, Universitat Politècnica de Catalunya, Spain; ²State Research Inst. for Physical Sciences and Technology, Lithuania; ³Institució Catalana de Reserca i Estudis Avançats (ICREA), Spain. A novel application of chirped dielectric mirrors for narrow beam focalization is proposed and demonstrated numerically and experimentally. Analogy to temporal dispersion compensation by chirped dielectric mirrors is discussed.

SW1N • Novel Fiber Laser Designs—Continued

SW1N.6 • 12:00

Analysis of Dynamic Properties of Dispersion-Tuned Lasers, Yuta Hasegawa¹, Shinji Yamashita¹; ¹Univ. of Tokyo, Japan. We numerically investigate spectral changes due to sweep in dispersion-tuned lasers. We found that the sweep can be fast without spectral spread when the wavelength shifts to longer with anomalous dispersion and high modulation frequency.

SW1N.7 • 12:15

MW peak power infrared source for tunable visible light generation by Four-Wave Mixing, Romain Royon¹, Jérôme Lhermite¹, Eric Cormier¹; ¹CELIA, CNRS, France. We report on a continuously tunable fiber laser emitting between 1020 nm and 1070 nm with peak power in excess of 4 MW. This source is optimally adapted for frequency conversion in the visible by means of Four wave mixing.

SW1O • Laser Frequency Combs—Continued

SW1O.7 • 12:00

Toward an all-fiber based optically referenced frequency comb, Chenchen Wang¹, Shun Wu¹, Coralie Fourcade Dutin^{2,3}, Brian R. Washburn¹, Fetah Benabid^{2,3}, Kristan L. Corwin¹; ¹Physics, Kansas State Univ., USA; ²GPPMM group, Xlim Research Inst., France; ³Physics, Univ. of Bath, UK. A potentially portable optical metrology system is demonstrated by using an acetylene-filled optical fiber frequency reference as an optical reference to a fiber-laser based frequency comb without an intracavity EOM.

SW1O.8 • 12:15

Enhancement cavity based high harmonics generation with post-compressed 10-MHz high power fiber CPA laser system, Zhigang Zhao¹, Akira Ozawa^{1,2}, Makoto Kuwata-Gonokami^{3,4}, Yohei Kobayashi^{1,2}; ¹The Inst. for Solid State Physics, The Univ. of Tokyo, Japan; ²Core Research for Evolutional Science and Technology (CREST), JST, Japan; ³Dept. of Physics, The Univ. of Tokyo, Japan; ⁴Photon Science Center, The Univ. of Tokyo, Japan. High harmonics are generated inside an enhancement cavity with nonlinear compressed 10-MHz high power 70-fs laser as seed. Stable operation lasting over half an hour with more than 0.1 mW at 147 nm is demonstrated with low finesse cavity.

AW1P • Spectroscopy and Imaging Applications—Continued

AW1P.6 • 12:00 **Invited**

Infrared Digital Holography as New 3D Imaging Tool for First Responders and Firefighters: Recent Achievements and Perspectives, Pietro Ferraro¹; ¹Istituto Nazionale di Ottica, Italy. We demonstrate a novel concept for imaging live humans through smoke and flames. We make use of lens-less Digital Holography at far Infrared Radiation (IRDH) thus overcoming the limits of current IR sensors.

12:00–13:30 **VIP Industry Leaders Networking Event, Exhibit Hall 3**
(lunch provided, registration required)

12:30–13:30 **Lunch and Unopposed Exhibit Only Time, Exhibit Halls 1 & 2** (concessions available)

NOTES

Blank lined area for notes.

13:30–15:00
JW2A • Poster Session 2

JW2A.1

Interdigitated Back-contact Solar Cells Implemented with Foundry CMOS Processes, Yung-Jr Hung¹, Tsung-Yen Chuang², Chung-Lin Chun¹, Li-Chi Yang², San-Liang Lee²; ¹Dept. of Photonics, National Sun Yat-sen Univ., Taiwan; ²Dept. of Electronic Engineering, National Taiwan Univ. of Science & Tech, Taiwan. Interdigitated back-contact solar cells with two-dimensional doping design are realized by foundry CMOS processes. Experimental results indicate superior diode performance and a 4.6% conversion efficiency that could be further boosted by thinning down the substrate.

JW2A.2

Microsphere Based Photolithography to Make Micro-OLEDs, Getachew Tilahun Ayenew¹, Alexis P. A. Fischer^{1,2}, Chia-Hua Chan³, Chii-Chang Chen⁴, Mahmoud Chakaroun¹, Jeanne Solard^{1,2}, Azzedine Boudrioua¹; ¹Université Paris 13, Sorbonne Cité, Laboratoire de Physique de Lasers CNRS UMR 7538, France; ²Université Paris 13, Sorbonne Cité, Centrale de Proximité en nanotechnologies de Paris Nord, IUT de Villetaneuse, France; ³Graduate Inst. of Energy Engineering, National Central Univ., Taiwan; ⁴Departement of Optics and Photonics, National Central Univ., Taiwan. A simple photolithography process using monolayer of microspheres was used to pattern photoresist on ITO coated glass substrate. Organic materials and aluminum were deposited on the patterned photoresist to have completed OLED structure resulting micro-OLEDs.

JW2A.3

Colored hybrid photovoltaics with angle invariance, Kyu-Tae Lee¹, Jae Yong Lee¹, Sungyong Seo¹, L. Jay Guo¹; ¹Electrical Engineering and Computer Science, Univ. of Michigan, USA. We present hybrid photovoltaic cells with distinct and angle-insensitive colors based on efficient photon manipulation. Up to 3% of power conversion efficiency is achieved by using tens of nm thick amorphous silicon active layer.

JW2A.4

Frequency Comb Calibrated Diode Laser Interferometry for Absolute Distance Measurement, Xuejian Wu¹, Haoyun Wei¹, Honglei Yang¹, Hongyuan Zhang¹, Yan Li¹; ¹Dept. of Precision Instruments, Tsinghua Univ., China. Real-time frequency-sweeping interferometer for arbitrary distance determination is demonstrated, which is consisted by a homodyne interferometer and a diode calibrated by an optical frequency comb. For arbitrary distance of ~73 mm, the deviation is 0.91 μm .

JW2A.5

Sagnac Based Polarimetric Analysis of EBC: Experimental Relationship to Blood Glucose, Hiroshi Kajioaka¹, Tatsuya Kumagai², Yuto Yamashita³, Mikio Kataoka⁴; ¹Global Fiberoptics, Ltd., Japan; ²Optoquesto, Co., Ltd., Japan; ³Kitanihon Electric Cable, Co., Ltd., Japan; ⁴Okayama Univ., Japan. We have developed a novel polarimeter based on fiberoptic gyroscope. We have discovered that there is a good correlation between optical rotation of EBC (exhaled breath condensate) and blood glucose levels using this polarimeter.

JW2A.6

Integrated Yb: fiber laser frequency comb with three photonic crystal fibers, Tongxiao Jiang¹, Aimin Wang¹, Wei Zhang¹, Fuzeng Niu¹, Guizhong Wang¹, Chen Li¹, Zhigang Zhang¹; ¹Peking Univ., China. We demonstrated a near all-fiber femtosecond Yb: laser frequency comb incorporated with three different photonic crystal fibers. The comb removes most of free-space components so that it is more compact and stable.

JW2A.7

Simultaneous Detection of Multiple Gases by Raman Spectroscopy with Hollow-Core Fibers, David Bomse¹, Marwood N. Ediger¹; ¹Mesa Photonics, USA. Raman spectroscopy of gas flowing through a hollow-core photonic crystal fiber (HC-PCF) provides simultaneous detection of N₂, O₂, CO₂, and CH₄, with detection limits between 300 and 1000 ppm for 30 s of signal averaging.

JW2A.8

Photonic Crystal Nanobeam Air-mode Cavity for High-Q and High Sensitivity Refractive Index Sensing, Daquan Yang^{1,2}, Huiqing Tian¹, Yuefeng Ji¹; ¹State Key Lab of Information Photonics and Optical Communications, Beijing Univ. of Posts and Telecommunications, China; ²School of Engineering and Applied Sciences, Harvard Univ., USA. We demonstrate a novel photonic-crystal nanobeam air-mode cavity with high-Q and high-sensitivity for refractive-index sensing. For the air-mode, the light is strongly localized inside the air-region. The high-Q ~5.0×10⁶ and high-sensitivity of 537.8nm/RIU are achieved.

JW2A.9

Withdrawn

JW2A.10

Large-area bi-functional nano-mushroom plasmonic sensor for colorimetry and surface-enhanced Raman spectroscopy, Zhida Xu¹, Ibrahim M. Khan¹, Kevin Han¹, Jing Jiang¹, Gang L. Liu¹; ¹Dept. of Electrical and Computer Engineering, Univ. of Illinois at Urbana-Champaign, USA. Wafer-scale nano-mushroom sensor was demonstrated with the refractive index sensitivity of 373 nm/RIU, resulting in significant color shift detectable by eye. It also works for surface-enhanced Raman spectroscopy with the enhancement factor of 10^{4,7}.

JW2A.11

Sub-Rayleigh Imaging via Speckle Illumination and Correlation Measurement, JOO-EON OH¹, Young-Wook Cho¹, Giuliano Scarcellì², Yoon-Ho Kim¹; ¹Physics, POSTECH, Korea; ²Harvard Medical School and Wellman Center for Photomedicine, Massachusetts General Hospital, USA. We demonstrate a sub-Rayleigh imaging technique based on speckle illumination and the second-order correlation measurement. The image resolution is related to the speckle size or the lateral coherence length of the pseudo-thermal light.

JW2A.12

Visibility and Contrast Enhancement with Polarization Difference Ghost Imaging, Yongchao Zhu¹, Jianhong Shi¹, Hu Li¹, Guihua Zeng¹; ¹State Key Lab of Advanced Optical Communication Systems and Networks, Key Lab on Navigation and Location-based Service, Dept. of Electronic Engineering, Shanghai Jiao Tong Univ., China. We experimentally demonstrate that polarization difference ghost imaging can provide the visibility and contrast enhancement, especially when the target is under predominately reflecting objects, complex background or turbid media. It facilitates the practical applications of ghost imaging.

JW2A.13

Nonlinear-optical-loop-mirror-based, phase-preserving 2R regeneration of a high-duty-cycle RZ-DPSK signal, Lu Li¹, Michael Vasilyev², Taras I. Lakoba²; ¹Dept. of Electrical Engineering, Univ. of Texas at Arlington, USA; ²Dept. of Mathematics and Statistics, Univ. of Vermont, USA. We use a NOLM with a directional attenuator for regeneration of 50% duty-cycle RZ-DPSK signal and demonstrate eye-opening improvement of 1.5 dB for a signal degraded by a combination of ASE noise and amplitude jitter.

JW2A.14

All-Optical Phase-Preserving Amplitude Regeneration Using Coherent Nonlinear Wave Mixing, Zahra Bakhtiari¹; ¹USA. We propose and demonstrate an all-optical tunable phase-preserving scheme for amplitude regeneration of amplitude modulated signals and phase modulated signals based on coherent optical nonlinear wave mixing using HNLF.

JW2A.15

Generation of Wideband Radio Frequency Signals Carrying Orbital Angular Momentum Based on Microwave Photonics Phase Shifter, Fengkai Bian¹, Shangyuan Li¹, Yunlong Song¹, Qi Yu¹, Xinlu Gao², Xiaoping Zheng¹, Hanyi Zhang¹, Bingkun Zhou¹; ¹Dept. of Electronic Engineering, Tsinghua Univ., China; ²Dept. of Physics, Beijing Normal Univ., China. A novel way to generate the wideband radio frequency (RF) signals carrying orbital angular momentum (OAM) by phase shifting using optical spectrum processor is proposed. Stable RF-OAM signals with topological charge $l=1$ have been generated.

JW2A.16

Optical Beat Noise Suppression in OFDMA PON Uplink Transmission by Using RF Clipping Tone, Sang-Min Jung¹, Sun-Young Jung¹, Seung-Min Yang¹, Sang-Kook Han¹; ¹Yonsei Univ., Korea. A technique of suppressing optical beat interference (OBI) noise in OFDMA PON is proposed and verified experimentally by applying RF clipping tone. We achieve reliable 8Gbit/s 20km uplink transmission with spectral efficiency 2.7bit/s/Hz.

JW2A.17

High power and high efficiency Tm-doped fiber laser pumped by a 1173 nm Raman fiber laser, Xiong Wang¹, Hanwei Zhang¹, Pu Zhou¹, Xiaolin Wang¹, Hu Xiao¹, Zejin Liu¹; ¹College of Optoelectronic Science and Engineering, National Univ. of Defense Technology, China. We report a high power Tm-doped fiber laser pumped by a 1173 nm Raman fiber laser. The slope efficiency is 47%, the maximum output power is 46 W and can be scaled to higher power.

JW2A.18

Green-enhanced super-continuum generation in a tapered photonic crystal fiber for efficient fceo detection, Fuzeng Niu¹, Tongxiao Jiang¹, Guizhong Wang¹, Chen Li¹, Aimin Wang¹, Zhigang Zhang¹; ¹Inst. of Quantum Electronics, School of Electronics Engineering and Computer Science, Peking Univ., China. We report the green-enhanced (530 nm) super-continuum generation in a tapered photonic crystal fiber by 280 pJ pulses from a mode-locked Yb: fiber laser. This system offers a technique for efficient fceo beating signal detection.

JW2A.19

Divergence Angle as a Quality Parameter for Fiber Modes, Stine Møller Israelsen¹, Karsten Rottwitz¹; ¹DTU Fotonik, Technical Univ. of Denmark, Denmark. We suggest using divergence angle as a quality parameter for pure fiber modes. We demonstrate a measurement of the divergence angle of an LP₁₁-mode and obtain agreement with numerical predictions with 2-digit precision.

JW2A.20

A femtosecond thulium holmium co-doped fiber laser based on graphene oxide evanescent filed interaction, Minwan Jung^{1,2}, Joonhoi Koo¹, Jaehyun Park³, Yong Won Song³, Kwanil Lee², Sang Bae Lee², Ju Han Lee¹; ¹School of Electrical and Computer Engineering, Univ. of Seoul, Korea; ²Inst. for Multidisciplinary Convergence of Matter, Korea Inst. of Science and Technology, Korea; ³Future Convergence Research Division, Korea Inst. of Science and Technology, Korea. We demonstrate an all fiberized, passively mode-locked thulium holmium co-doped fiber laser operating at a wavelength of ~1.95 μm using the graphene-oxide evanescent field interaction.

JW2A • Poster Session 2—Continued

JW2A.21

Continuous-Wave Two-pump Fiber Optical Parametric Amplifier with 60 dB Gain, Mehdi Jamshidifar¹, Armand Vedadi¹, Michel E. Marhic¹, ¹Swansea Univ., UK. We have obtained record gain of 60 dB with a continuous-wave two-pump fiber optical parametric amplifier, over a 5.5-nm bandwidth. We used a 500-m long fiber, and 1.5 W of pump power.

JW2A.22

Direct generation of radially-polarized output from an Yb-doped fiber laser, Di Lin¹, Jae M. Daniel¹, Mindaugas Gecevicius¹, Martynas Beresna¹, Peter G. Kazansky¹, W. A. Clarkson¹, ¹Optoelectronics Research Centre, Univ. of Southampton, UK. A simple technique for directly generating a radially-polarized output beam from an ytterbium-doped fiber laser using an intracavity S-waveplate is reported. The laser yielded 7W of output with a corresponding slope efficiency of 67%.

JW2A.23

Stimulated Brillouin scattering threshold variations due to bend-induced birefringence in a non-polarization-maintaining fiber amplifier, Cyril L. Guintrand¹, ¹Nufern, USA. We report on the SBS threshold variations due to the coiling-induced birefringence in a non-polarization-maintaining fiber high power amplifier. We demonstrate that a control of the output polarization can permit higher SBS threshold operation.

JW2A.24

Radiofrequency Spectroscopy of the Active Fiber Heating under Condition of High-Power Lasing Generation, Renat Shaidulin^{1,2}, Ilya Zaytsev², Oleg A. Ryabushkin^{1,2}, ¹Moscow Inst. of Physics and Technology, Russia; ²Kotelnikov Inst. of Radio Engineering and Electronics of RAS, Russia. A novel precise method for measurement of active fiber temperature in high-power fiber lasers and amplifiers is proposed. This method allows determination of the temperature distribution along the active fiber.

JW2A.25

31 nJ sub-200 fs pulse generation from an Erbium-doped fiber amplifier similariton oscillator, Chia-lun Tsai¹, Kuan-Chen Chu¹, Shang-Da Yang¹, ¹Inst. of Photonics Technologies, National Tsing Hua Univ., Taiwan. We demonstrated the highest femtosecond pulse energy from Erbium-doped fiber similariton or dissipative soliton oscillators (to our best knowledge). The output spectrum can be manipulated by waveplates and filter to support 86 fs transform-limited pulse.

JW2A.26

Soliton trapping in a Tm fiber laser, Luming Zhao^{1,2}, Yong Wang^{1,2}, Siming Wang^{1,2}, Jiaolin Luo^{1,2}, Yanqi Ge^{1,2}, Lei Li^{1,2}, Dingyuan Tang^{1,2}, Deyuan Shen^{1,3}, Shumin Zhang⁴, Frank W. Wise⁵, ¹Jiangsu Key Lab of Advanced Laser Materials and Devices, Jiangsu Normal Univ., China; ²School of Physics and Electronic Engineering, Jiangsu Normal Univ., China, China; ³Dept. of Optical Science and Engineering, Fudan Univ., China; ⁴College of Physics Science and Information Engineering, Hebei Advanced Thin Films Lab, Hebei Normal Univ., China; ⁵Dept. of Applied Physics, Cornell Univ., USA. Soliton trapping is demonstrated in an all-fiber Tm fiber laser. The central wavelength shift between the two orthogonal polarized components of the vector soliton is determined by the cavity birefringence.

JW2A.27

Frequency-comb-referenced stable multi-channel fiber laser, Byungjae Chun¹, Sangwon Hyun¹, Seungman Kim¹, Seung-Woo Kim¹, Young-Jin Kim¹, ¹Korea Advanced Inst. of Science and Technology, Korea. We demonstrate an all-fiber-based multi-channel fiber laser referenced to the frequency comb. Three sample optical frequencies were generated within telecommunication band with a frequency stability of 2.24×10^{-12} and a linewidth less than 30 kHz.

JW2A.28

Time-to-frequency Conversion Based on Nonlinear Pulse Shaping, Dong Wang¹, Li Huo¹, Qiang Wang¹, Xin Chen¹, Caiyun Lou¹, ¹Electronic Engineering, Tsinghua Univ., China. A precise time-to-frequency conversion based on nonlinear pulse shaping is demonstrated. Simulation results also show the scheme can be applied to arbitrary waveform.

JW2A.29

Gain dynamics in Er:Yb co-doped fiber amplifiers, Michael Steinke^{1,2}, Dietmar Kracht^{1,2}, Jörg Neumann^{1,2}, Peter Wessels^{1,2}, ¹Laser Zentrum Hannover e.V., Germany; ²Centre for Quantum Engineering and Space-Time Research - QUEST, Germany. Gain dynamics of Er:Yb fiber amplifiers were studied analytically and corresponding transfer functions were measured, showing good agreement with the theoretical treatment. In addition, numerical investigations have been carried out to get deeper insight.

JW2A.30

Realization of Multiphoton Photoacoustic Microscopy via a Loss Modulation Technique, Szu-Yu Lee¹, Yu-Hung Lai^{1,2}, Kai-Chih Huang¹, Yu-Cheng Chen⁴, Chi-Kuang Sun^{1,3}, ¹Dept. of Electrical Engineering and Graduate Inst. of Photonics and Optoelectronics, National Taiwan Univ., Taiwan; ²Applied Physics Option, California Inst. of Technology, USA; ³Inst. of Physics and Research Center for Applied Sciences, Academia Sinica, Taiwan; ⁴Molecular Imaging Center, National Taiwan Univ., Taiwan. Trade-off between resolution and penetration restricts performances of microscopes. We realize a hybrid modality of multiphoton fluorescence and photoacoustic microscopy via an optical modulation technique. The new modality features both high-resolution and deep-penetration.

JW2A.31

Demonstration of Mueller polarimetry through an optical fiber for endoscopic applications, Jérémy VIZET¹, Sandeep Manhas¹, Stanislas Deby², Jean-Charles Vanel², Antonello De Martino², Dominique Pagnoux¹, ¹XLIM, Photonics Dept., Université de Limoges, CNRS, France; ²LPICM, Ecole Polytechnique, CNRS, France. Mueller polarimetry through an optical fiber is demonstrated for the first time, opening the way to endoscopic applications. Proof of principle is demonstrated by measuring with accuracy linear retardance, diattenuation and depolarization of known sample.

JW2A.32

Chalcogenide Microfiber Photonic Synapses, Behrad Gholipour¹, Paul Bastock², Khouler Khan², Chris Craig², Dan Hewak², Nikolay I. Zheludev^{1,2}, Cesare Soci¹, ¹Centre for disruptive photonic technologies (CDPT), Nanyang technological Univ., Singapore; ²Optoelectronics research centre (ORC), Univ. of Southampton, UK. Optical axons and photonic synapses implemented using chalcogenide microfibers allow the generation and propagation of photonic action potentials which give rise to the demonstration of various neuromorphic concepts.

JW2A.33

Studying Membrane Tubes with Positive and Negative Curvatures in Giant Vesicles, Raktim Dasgupta¹, Reinhard Lipowsky¹, Rumiana Dimova¹, ¹Dept. of Theory and Bio-Systems, Max Planck Inst. of Colloids and Int, Germany. Membrane tubes could be extruded both externally and internally from giant lipid vesicles using membrane-attached beads manipulated via optical trapping and controlled hydrodynamic flow. The technique has potential use for studying different membrane tubulation mechanisms.

JW2A.34

3D hollow nanostructures for multifunctional plasmonics, Mario Malerba¹, Ermanno Miele¹, Andrea Toma¹, Francesco De Angelis¹, ¹Istituto Italiano di Tecnologia, Italy. A novel top-down technique allows precise 3D nanofabrication; we exploit fully its potential by manufacturing plasmonic devices, to be employed in optoelectronics, microfluidics and advanced biosensing.

JW2A.35

Fiber torsion sensor with directional discrimination based on twist-induced circular birefringence in unbalanced Mach-Zehnder interferometer, Nan-Kuang Chen^{1,2}, Jheng-Jyun Wang¹, Gia-Ling Cheng³, Wood-Hi Cheng³, Ping Pery Shum⁴, ¹Dept. of Electro-Optical Engineering, National United Univ., Taiwan; ²Optoelectronics Research Center, National United Univ., Taiwan; ³Dept. of Photonics, National Sun Yat-sen Univ., Taiwan; ⁴Network Technology Research Centre, Nanyang Technological Univ., Singapore. We demonstrate fiber torsion sensor based on twist-induced circular birefringence in unbalanced Mach-Zehnder interferometer with two dissimilar abrupt tapers in a short (~1.4cm) highly Er/Yb co-doped fiber for simultaneous measurements of twisting angle and direction.

JW2A.36

Intermodulation distortion elimination for analog photonics link based on integrated dual-parallel Mach-Zehnder modulator, Jian Li¹, Yi-Chen Zhang¹, Song Yu¹, Tianwei Jiang¹, Xie Qian¹, Wanyi Gu¹, ¹Beijing Univ. of Posts and Telecommunications, China. We report a total third-order intermodulation distortion elimination method for analog photonics link based on integrated dual-parallel Mach-Zehnder modulator. Theoretical analysis and experiment verification of 33.57 dB suppression are both carried out.

JW2A.37

Compact Athermal Electro-optic Modulator Design Based on SOI Off-axis Microring Resonator, Raktim Haldar¹, Abhik Datta Banik¹, Sanathanan M.S¹, Shailendra K. Varshney¹, ¹Indian Inst. of Technology Kharagpur, India. In this work, we propose efficient electro-optic modulation using compact SOI off-axis microring resonator. We show that adding an extra off-axis inner-ring in conventional microring structure provides control to compensate thermal effects on electro-optic modulator.

JW2A.38

A novel InP-based 1.31/1.55- μ m wavelength demultiplexer with side-port multimode interference coupler, Shile Wei^{1,2}, Jian Wu¹, Lingjuan Zhao², Ruikang Zhang², Jifang Qiu¹, Zuoshan Yin¹, Ye Tian¹, ¹Beijing Univ of Posts & Telecom, China; ²Inst. of Semiconductors, Chinese Academy of Science, China. A novel ultrashort InP-based 1.31/1.55- μ m wavelength demultiplexer, whose MMI section is only one beat length of the two guided modes, is demonstrated. The measured extinction ratios for 1.3/1.55- μ m bands exceed 20/15 dB, respectively.

JW2A.39

Mapping molecular rotational dynamics on the time-dependent spectral minimum, meiyuan qin¹, Xiaosong Zhu¹, Peixiang Lu¹, ¹School of Physics, Huazhong Univ of Science and Technology, China. We investigate the time-dependent harmonic emissions from nonadiabatically aligned molecules. It is shown that the spectral minimum position depends linearly on $1/\langle \cos^2\theta \rangle$. This relation indicates the possibility of tracing molecular rotational dynamics by measuring the spectral minima.

JW2A.40

Ultrashort pulse generation using supercontinuum generated by Er-doped fiber laser with carbon nanotube, Atsushi Okamura¹, Youichi Sakakibara², Emiko Omoda², Hiromichi Kataura², Norihiko Nishizawa¹, ¹Nagoya Univ., Japan; ²AIST, Japan. Ultrashort pulse generation was demonstrated by dispersion compensation of coherent high quality supercontinuum generated by ultrashort pulse fiber laser with carbon nanotube and fiber amplifier system. A 22 fs ultrashort pulse was observed by X-FROG.

JW2A • Poster Session 2—Continued

JW2A.41

High-power sub-50 fs, Kerr-lens mode-locked Yb:CaF₂ oscillator pumped by high-brightness fiber-laser, pierre sevillano¹, Guillaume Machinet¹, Romain Dubrasquet^{1,2}, Patrice Camy³, Jean Louis Doualan³, Richard Moncorge³, Patrick Georges⁴, Frederic Druon⁴, Dominique Descamps¹, Eric Cormier¹; ¹CELIA, France; ²Azur light System, France; ³Centre de recherche sur les Ions, France; ⁴Laboratoire Charles Fabry, France. We investigated the influence of the spatial pump beam quality on the generation of ultra-short pulses in high-brightness Yb: fiber laser-pumped pure Kerr-lens mode-locked Yb:CaF₂ oscillators. We report pulse duration as short as 48 fs with an average output power of 2.7 W.

JW2A.42

Ultrafast Arbitrary (Non-Minimum-Phase) Optical Pulse Processors Based On Bragg Gratings in Transmission, María R. Fernández-Ruiz¹, Alejandro Carballa², José Azaña¹; ¹INRS - EMT, Canada; ²Ingeniería Electrónica, Universidad de Sevilla, Spain. A new approach to implement arbitrary (non-minimum phase) time-windowed linear optical pulse processors using minimum-phase filters is proposed and demonstrated through the design of a Terahertz-bandwidth Hilbert transformer based on a transmissive fiber Bragg grating.

JW2A.43

2.5 D photonic crystal quantum cascade detector, Peter Reiningner¹, Benedikt Schwarz², Andreas Harrer¹, Tobias Zederbauer¹, Hermann Detz¹, Aaron Maxwell Andrews¹, Roman Gansch¹, Werner Schrenk¹, Gottfried Strasser¹; ¹Inst. for Solid State Electronics and Center for Micro- and Nanostructures, Vienna Univ. of Technology, Austria. Quantum cascade detectors are intersubband photodetectors that offer a vast design freedom. By combining it with a novel photonic crystal cavity, a significant improvement of the detectors performance could be achieved.

JW2A.44

Simple Single-Shot Technique for Measuring the Complete Spatiotemporal Intensity and Phase of a Complex Ultrashort Pulse, Zhe Guang¹, Michelle Rhodes¹, Rick Trebino¹; ¹School of Physics, Georgia Inst. of Technology, USA. Our simple device measures the complete spatiotemporal field of an arbitrary ultrashort pulse complex in both space and time (x,y,t). We also demonstrate a method for displaying the resulting dual plots of complex four-dimensional data.

JW2A.45

Saturation broadening effect in an InP photonic-crystal nanocavity switch, Yi Yu¹, Evarist Palushani¹, Mikkel Heuck¹, Dragana Vukovic¹, Christophe Peucheret¹, Leif K. Oxenlow¹, Kresten Yvind¹, Jesper Mørk¹; ¹Dept. of Photonics Engineering, Danmarks Tekniske Universitet, Denmark. Pump-probe measurements on InP photonic-crystal nanocavities show large-contrast fast switching at low pulse energy. For large pulse energies, large resonance shifts passing across the probe lead to switching contrast saturation and switching time-window broadening.

JW2A.46

High Efficient Vertical Binary Blazed Grating Coupler for Chip Level Optical Interconnections, Li Yu¹, Lu Liu¹, Zhiping Zhou¹, Xingjun Wang¹; ¹Peking Univ., China. A high-efficiency vertical binary blazed grating coupler is proposed. An 83% of efficiency and 65nm 3dB bandwidth are demonstrated. The tolerance of the incident angle is 11.5°.

JW2A.47

A novel polarization and dichroic dual-functional splitter with ultra-high splitting ratios, Kun Li¹, Fan Lu¹, Dalin Liu¹, Zhijun He¹, Anshi Xu¹; ¹Peking Univ., China. A novel polarization and dichroic dual-functional splitter is proposed, with ultra-high polarization splitting ratios >33dB and >36dB for TE- and TM-polarized modes, respectively; and with high wavelength splitting ratios >26dB and >33dB for 650nm and 850nm, respectively.

JW2A.48

Effect of Quantum Confinement in Si-QD on Free-Carrier Modulation Bandwidth and Cross-Section of the SiOx:Si-QD Waveguide, Chung-Lun Wu¹, Sheng-Pin Su¹, Gong-Ru Lin¹; ¹Graduate Inst. of Photonics and Optoelectronics, Dept. of Electrical Engineering, National Taiwan Univ., Taiwan. The free-carrier cross-section of Si-QD is decreased from 5.5×10⁻¹⁷ to 9×10⁻¹⁸ cm² with shortened lifetime from 10 to 0.48 μs when shrinking Si-QD size from 4.3 to 1.7 nm due to the quantum confinement effect.

JW2A.49

A novel polarization converter and filter based on MMI couplers in silicon-on-insulator, Wei Yang¹, Tianian Li¹, Zhijuan Tu¹, Yanping Li¹, Xingjun Wang¹, Ziyu Wang¹; ¹School of Electronics Engineering and Computer Science, Peking Univ., China. A novel polarization converter and filter based on silicon multimode interference couplers (MMI) has been demonstrated. The measured transmission spectra of the proposed device for the light with arbitrary polarization exhibit a good performance.

JW2A.50

Disorder-induced resonance shifts and mode edge broadening in photonic crystal waveguides, Nishan S. Mann¹, Alisa Javadi², Pedro David Garcia², Mark Patterson¹, Peter Lodahl², Stephen Hughes¹; ¹Physics, Queen's Univ., Canada; ²Niels Bohr Inst., Denmark. We present theory and measurements for systematically disordered slow-light photonic crystal waveguides and find a pronounced disorder-induced blueshift and broadening of the photon density of states.

JW2A.51

Double Heterostructure AlGaAs/GaAs W-shaped Waveguide Mach-Zehnder Intensity Modulator for 780 nm Lasers, Bassem Arar¹, Harendra N. J. Fernando², Olaf Brox¹, Andre Maassdorf¹, Andreas Wicht¹, Achim Peters³, Markus Weyers¹, Götz Erbert¹, Günther Tränkle¹; ¹Ferdinand-Braun-Institut FBH, Germany; ²Leibniz-Institut für Astrophysik Potsdam, Germany; ³Humboldt-Universität zu Berlin, Germany. An integrated Mach-Zehnder intensity modulator for laser radiation at the wavelength 780 nm is demonstrated for the first time. The device features a double heterostructure GaAs/AlGaAs electro-optic phase modulator. The estimated insertion loss is less than 2.5 dB and the extinction ratio is 3.3 dB.

JW2A.52

Brillouin Scattering in Silicon Slot Waveguides, Yovanny A. Espinel¹, Thiago Pedro M. Alegre¹, Gustavo S. Wiederhecker¹; ¹"Gleb Wataghin" Physics Inst., Univ. of Campinas, Brazil. Here we numerically investigate Brillouin scattering (BS) in a silicon slot waveguide. We show that BS is strongly influenced by the boundary effects, instead of the photoelastic effect, leading to the interaction with novel mechanical modes.

JW2A.53

Silicon Waveguide to Hybrid Plasmonic Waveguide Polarization Rotator and Coupler, Sangsik Kim¹, Minghao Qi¹; ¹School of Electrical and Computer Engineering and Birck Nanotechnology Center, Purdue Univ., USA. We present a polarization rotator and coupler that rotates the TE₀ mode in a silicon waveguide and couples to the hybrid plasmonic (HP₀) mode. Coupling factor of ~60% and polarization conversion efficiency of ~90% is achieved.

JW2A.54

Athermal microring resonator based on the resonance splitting of dual-ring structure, Qingzhong Deng¹, Xinbai Li¹, Zhiping Zhou¹; ¹State Key Lab of Advanced Optical Communication Systems and Networks, Peking Univ., China. A novel athermal scheme based on resonance splitting of dual-ring structure is proposed and proved. An athermal resonator based on this scheme is demonstrated, achieving athermal transmission over a temperature range of at least 40K.

JW2A.55

Dynamical behave of optomechanically induced transparency in a silica micro-resonator, Chun-Hua Dong¹, Zhen Shen¹, Guang-Can Guo¹; ¹Key Lab of Quantum Information, USTC, China. We report an experimental study of transient optomechanically induced transparency (OMIT) using a silica microresonator. The transient OMIT behaviors are observed in good agreement with theoretical calculations based on the coupled-oscillator model.

JW2A.56

Optical transition between Stark levels in (ErSc)2O3 epitaxial films, Takehiko Tawara^{1,2}, Hiroo Omi^{1,2}, Adel Najar¹, Reina Kaji³, Satoru Adachi³, Hideki Gotoh¹; ¹NTT Basic Research Labs, Japan; ²NTT Nanophotonics Center, Japan; ³Hokkaido Univ., Japan. Toward quantum information applications, we control the interactions between Er ions by alloying epitaxial Er₂O₃ with scandium and suppress energy transfer and inhomogeneous broadening of Stark levels in the intra-4f band of Er ions.

JW2A.57

Investigation of Photoluminescence from Ge1-xSnx: A CMOS-Compatible Material Grown on Si via CVD, Wei Du¹, Sayed A. Ghetmiri¹, Aboozar Mosleh¹, Benjamin Conley¹, Liang Huang¹, Amjad Nazzal², Richard Soref², Greg Sun³, John Tolle⁴, Hameed A. Naseem¹, Shui-Qing Yu¹; ¹Electrical Engineering, Univ. of Arkansas, USA; ²Engineering and Physics, Wilkes Univ., USA; ³Physics, Univ. of Massachusetts Boston, USA; ⁴ASM America, USA. Photoluminescence (PL) from Ge_{1-x}Sn_x grown on Si by CVD was investigated for Sn composition of 0.9, 3.2, 6, and 7%, respectively. The direct and indirect band transitions were analyzed at different temperatures.

JW2A.58

Opto-Mechanically Tunable Polymeric Microlasers, Assegid Mengistu Flatae^{1,2}, Matteo Buresi², Hao Zeng², Sara Nocentini², Sarah Wiegele¹, Diederik Wiersma², Heinz Kalt¹; ¹Inst. of Applied Physics, Karlsruhe Inst. of Technology, Germany; ²Optics of complex system, European Lab for Nonlinear Spectroscopy, Italy. Opto-mechanically controlled liquid crystalline elastomer (LCE) integrated tunable polymeric microgoblet lasers are fabricated on a silicon chip. Symmetrical deformation of uniaxially aligned LCE microcylinders enables expansion of the microgoblet resonators for tuning the lasing modes.

JW2A.59

Intense Photoluminescence from Er Doped Chalcogenide Thin Films Fabricated by Co-thermal Evaporation, Kunlun Yan¹, Khu Vu¹, Steve Madden¹; ¹Australian National Univ., Australia. Erbium doped chalcogenide films were fabricated by cothermal evaporation and demonstrated propagation losses and lifetimes suitable for waveguide amplifiers. The 1490nm pumped photoluminescence yield is up to ~10x higher than the prior best film material, Er:TeO₂.

JW2A.60

Optical properties of Er-doped fluoride glasses for solar-pumped laser applications, Takenobu Suzuki¹, Yasuyuki Iwata¹, Yasutake Ohishi¹; ¹Toyota Technological Inst., Japan. Optical properties required for the design of a solar pumped fiber laser were evaluated for Er³⁺-fluoride glass. The quantum efficiency of the emission band at 1530nm was about 35%. The product of the stimulated emission cross-section and the emission lifetime was about 46×10⁻²⁴ cm²s.

JW2A • Poster Session 2—Continued

JW2A.61

Structural characterization and luminescence properties of ErSc₂-xSiO₇ prepared by RF sputtering, Adel Najjar¹, Takehiko Tawara^{2,1}, Hiroo Omi^{1,2}; ¹NTT Basic Research Labs, NTT Corporation, Japan; ²NTT Nanophotonics Center, NTT Corporation, Japan. Polycrystalline ErSc₂-xSiO₇ compounds were fabricated using RF-sputtering by alternating Er₂O₃, Sc₂O₃ layers separated by SiO₂ layer. This new compounds presents excitation cross section at 980nm around 1.39x10⁻²¹cm² with lifetime of 38 μs.

JW2A.62

Carrier Dynamics of a Bismuth Thin Film Accelerated via Intense Terahertz Field, Yasuo Minami¹, Kotaro Araki¹, Thang D. Dao^{2,3}, Tadaaki Nagao^{2,3}, Jun Takeda¹, Masahiro Kitajima^{4,5}, Ikufumi Katayama¹; ¹Yokohama National Univ., Japan; ²International Center for Materials Nanoarchitectonics, National Inst. for Materials Science, Japan; ³CREST, Japan Science and Technology Agency, Japan; ⁴LxRay Co. Ltd., Japan; ⁵Dept. of Applied Physics, National Defense Academy, Japan. THz pump-THz probe spectroscopy is performed to study carrier dynamics in Bi film. Transmittance of Bi film increases since effective masses of carriers increases by acceleration. After the illumination, transmittance decreases due to carrier increases.

JW2A.63

High-Power Terahertz Generation via Two-Color Laser Filamentation and Real-Time Terahertz Imaging, Taek Il Oh¹, Yung Jun Yoo¹, Yong Sing You¹, Ki-Yong Kim¹; ¹Univ. of Maryland, USA. We generate terahertz radiation via two-color laser filamentation with average output power of 1.4 mW and peak fields of 4.4 MV/cm. We also introduce a real-time, uncooled, cost-effective microbolometer camera for terahertz profiling and imaging.

JW2A.64

Narrowband Terahertz Emission from Beta-Barium Borate, David A. Valverde-Chavez¹, David G. Cooke¹; ¹Physics, McGill Univ., Canada. We observed narrowband terahertz emission from beta-barium borate crystal at a center frequency of 10.7 THz. The field emission is linear with incident pump power consistent with an optical rectification process.

JW2A.65

Mechanisms of THz trapping devices based on plasmonic grating, Baoshan Guo¹, Wei Shi¹, Jianquan Yao¹; ¹Tianjin Univ., China. The mechanisms of plasmonic THz wave trapping devices is attributed to the transformation from surface modes to cavity modes which have a saturated state. An ultraslow THz waveguide is realized by controlling the modes transformation.

JW2A.66

Terahertz surface plasmon polaritons on freestanding multi-walled carbon nanotube aerogel sheets, Shuchang Liu¹, Tho D. Nguyen², Marcio D. Lima³, Shaoli Fang³, Ray H. Baughman³, Ajay Nahata¹, Z. Vally Vardeny²; ¹Dept. of Electrical and Computer Engineering, Univ. of Utah, USA; ²Dept. of Physics and Astronomy, Univ. of Utah, USA; ³Alan G. MacDiarmid NanoTech Inst., Univ. of Texas at Dallas, USA. We demonstrate that multi-walled carbon nanotubes exhibit highly anisotropic terahertz polarization behavior. We accomplish this by measuring the complex index of refraction of planar and periodically perforated carbon nanotube sheets for two orthogonal nanotube orientations.

JW2A.67

Modeling and Design of a Soliton Mode-locked Yb:CaGdAlO₄ Laser in the Normal Dispersion Regime, Christopher R. Phillips¹, Aline Sophie Mayer¹, Alexander Klenner¹, Ursula Keller¹; ¹ETH Zurich, Switzerland. We consider SESAM soliton-modelocking via cascaded quadratic nonlinearities in the normal dispersion regime. We explain the theory, perform a design study for our experimental implementation in LiB₃O₅/Yb:CaGdAlO₄, and present detailed numerical simulations of this laser.

JW2A.68

18.7-fs DUV Pulses Generated by Using Chirped-pulse Four-wave Mixing in Bulk Material, JinPing He^{1,2}, Takayoshi Kobayashi^{1,2}; ¹Univ. of Electro-Communications, Japan; ²JST, CREST, Japan. Sub-20fs, wavelength tunable, uJ-level DUV pulses were generated by using nondegenerate, chirped-pulse four-wave mixing in CaF₂ crystal. The DUV spectrum can be tuned from 257nm to 277nm with widest spectral width of 16.8nm.

JW2A.69

Nonlinear Fourier-transform spectroscopy using ultrabroadband pulses for measurement of photobleaching spectra of fluorescent proteins, Akira Suda¹; ¹Tokyo Univ. of Science, Japan. We present the measurement of photobleaching spectra of fluorescent proteins with nonlinear Fourier-transform spectroscopy using ultrabroadband femtosecond pulses. Photobleaching of two-photon excited fluorescent molecules occurs through one-photon excited-state absorption.

JW2A.70

Frequency Doubling at 7J of a High Energy, High Repetition Rate DPSSL System, Jonathan Phillips¹, Saumyabrata Banerjee¹, Paul D. Mason¹, Jodie M. Smith¹, Magdalena Sawicka², Martin Divoky², Klaus Ertel¹, Thomas J. Butcher¹, Mariastefania de Vido¹, Tristan R. Davenne¹, Michael D. Fitton¹, Oleg Chekhlov¹, Justin Greenhalgh¹, Waseem Shaikh¹, Ophelie Wagner³, Cristina Hernandez-Gomez¹, John L. Collier¹; ¹Central Laser Facility, STFC Rutherford Appleton Lab, UK; ²HiLASE Project, Na Slovance 2, Czech Republic; ³Cristal Laser, Parc d, France. We present calculations and results for frequency doubling on DiPOLE, a 7J 10 Hz Yb:YAG DPSSL, using DKDP, YCOB and LBO. The LBO crystal achieved the highest conversion efficiency of 65%.

JW2A.71

Two new blue laser emission lines from an intracavity Raman laser, Dimitri Geskus¹, Jonas Jakutis Neto¹, Helen M. Pask², Niklaus Wetter¹; ¹Centro de Lasers e Aplicações, IPEN/SP, Brazil; ²MQ Photonics, Dept. of Physics, Macquarie Univ., Australia. Here we report quasi-CW operation of intracavity Raman laser generating three blue laser emission lines at 454 nm, 473 nm and 495 nm with a maximum output power of 230 mW.

JW2A.72

Broadband and Ultra-flat Optical Comb Generation Using an EO Comb Source and a Programmable Pulse Shaper, Hyoung-Jun Kim¹, Andrew J. Metcalfe¹, Oscar E. Sandoval¹, Daniel E. Leaird¹, Andrew M. Weiner¹; ¹School of Electrical and Computer Engineering, Purdue Univ., USA. Optical frequency comb generation using an advanced electro-optic comb source, a programmable pulse shaper, and a highly nonlinear fiber is demonstrated. The generated 18 GHz comb has 2 dB power variation within a 24 nm bandwidth.

JW2A.73

Tailoring of Saturation in Fiber Optical Parametric Amplifier by SBS-Induced Nonlinear Phase, Chaoran Huang¹, Xiaojie Guo¹, Xuelei Fu¹, Liang Wang¹, Chester Shu¹; ¹Dept. of Electronic Engineering, The Chinese Univ. of Hong Kong, Hong Kong. We use gain-transparent SBS to defer/accelerate the saturation of a fiber optical parametric amplifier by dynamically control the phase mismatch. The input signal power at saturation can be raised or reduced by ~6 dB.

JW2A.74

CW Pumped, Generation of Narrow Line-width Non-Resonant Mid-IR Radiations in Liquid Filled Single Capillary Assisted Chalcogenide Optical Fibers, Satya Pratap Singh¹, Viswatosh Mishra¹, Shailendra K. Varshney¹; ¹Indian Inst. of Technology Kharagpur, India. We report the generation of the non-resonant radiations (<100 GHz FWHM) ranging from near-IR to mid-IR in capillary-assisted chalcogenide optical fibers with three zero dispersion wavelengths owing to the temperature dependent phase-matching topologies.

JW2A.75

Defect Mode Lasing in metal-coated GaN Grating Structure at Room Temperature, Kuo-Ju Chen¹, Wan-Hai Hsu¹, Wei-Chun Liao¹, Min-Hsiung Shih^{1,2}, Hao-chung Kuo¹; ¹Dept. of Photonics, Inst. of Electro-Optical Engineering, National Chiao Tung Univ., Taiwan; ²Research Center for Applied Sciences, Academia Sinica, Taiwan. The lasing action from a metal-coated GaN with defect grating structure was observed and the wavelength is approximately 365 nm with the quality factor of 480 at room temperature.

JW2A.76

Gain compression in a quantum cascade laser: Connection between high frequency tuning and bending of LI curve, Andreas Hangauer¹, Gerard Wysocki¹; ¹Electrical Engineering Dept., Princeton Univ., USA. This paper studies relation between high-frequency chirping of a quantum-cascade laser and the curvature of its light-current characteristic. Assuming negligible thermal backfilling and a photon lifetime of 9ps, a gain-compression effect explains both experimental observations.

JW2A.77

31nm Quasi-Continuous Tuning Single Mode Laser Array Based on Slots, Qiaoyin Lu¹, Weihua Guo², Azat Abdullaev¹, Marta Nawrocka¹, James O'Callaghan³, John F. Donegan¹; ¹Univ. of Dublin Trinity College, Ireland; ²Univ. of California Santa Barbara, USA; ³Tyndall National Inst., Ireland. We present a 10-channel slotted single-mode laser array with effective-cavity-length ~300μm which exhibits quasi-continuous tuning range ~31nm over 42°C with side-mode suppression-ratio >35dB. The linewidth is about 2MHz for all channels at 150mA at 20°C.

JW2A.78

Experimental Analysis of Laterally-Coupled MQW-DFB Lasers in Optical Feedback, Ramón Maldonado-Basilio¹, Vahid Eslamdoost¹, Julie E. Nkanta¹, Trevor J. Hall¹; ¹Univ. of Ottawa, Canada. Characterization of third-order grating LC-MQW-DFB lasers in free-running and feedback is reported for various operation conditions. Relative to free-running, line-width reduction of >15 times is measured in optical feedback, obtaining a minimum of 10 kHz.

JW2A.79

High-brightness single-mode tapered laser diodes with laterally coupled high-order surface grating, Wan-hua Zheng¹, Lei Liu¹, Hongwei Qu¹, Yun Liu¹, Qi Aiji¹, Chuanlong Ma¹, Siriguleng Zhang¹, Yejin Zhang¹; ¹Chinese Acad Sci Inst of Semiconductor, China. 913 nm tapered diode lasers with 23th order laterally coupled grating is fabricated. Power of over 560 mW/facet and lateral divergence angle of 2.1° are achieved. Measured side mode suppression ratio is about 27 dB.

JW2A.80

Continuum seeded OPCPA system driven by tandem fs Yb:KGW and ps Nd:YAG lasers, Tomas Stanislavskas^{1,3}, Rimantas Budriunas¹, Roman Antipenkov¹, Audrius Zaukevicus², Jonas Adamonis², Andrejus Michailovas², Linas Giniunas³, Romualdas Danielius³, Arunas Varanavicius¹; ¹Vilnius Univ., Lithuania; ²Ekspla Ltd., Lithuania; ³Light Conversion Ltd., Lithuania. We present a compact TW-class continuum seeded multi-stage OPCPA system operated at 800 nm and pumped by femtosecond and picosecond pulses. 35 mJ pulse energies and compression to 9 fs are demonstrated.

JW2A • Poster Session 2—Continued

JW2A.81

Cryogenic laser performance of Yb:YAG diode-pumped at 940 nm and 969 nm for high power lasers, Venkatesan Jambunathan¹, Lucie Těsnohlíková¹, Taisuke Miura¹, Antonio Lucianetti¹, Tomas Mocek¹; ¹Dept. of Diode pumped lasers, Fyzikální ústav AV ČR, v.v.i., Czech Republic. We demonstrated the laser performance of Yb:YAG for different cryogenic temperatures pumped by fibre coupled diode laser emitting at 940 and 969 nm. Laser diode bandwidth, absorption bandwidth of laser material plays a crucial role.

JW2A.82

Dual-Wavelength CW Operations at 1064.1 & 1073.1 nm and 1064.1 & 1085.3 nm of Nd:YVO4 Laser, Tanant Waritanant¹, Arkady Major¹; ¹Electrical & Computer Engineering, Univ. of Manitoba, Canada. Two dual-wavelength operations of diode-pumped Nd:YVO4 laser were demonstrated at 1064.1 & 1073.1 and 1064.1 & 1085.3 nm with two intracavity birefringent plates. The output power ratio of the dual-wavelength output could be freely adjusted.

JW2A.83

Selectable dual-wavelength actively Q-switched laser by monolithic electro-optic periodically poled lithium niobate Bragg modulator, Shang-Yu Hsu¹, Yen-Yin Lin², Yuan-Yao Lin², Shou-Tai Lin¹; ¹Feng Chia Univ., Taiwan; ²National Tsing Hua Univ., Taiwan. A novel dual-wavelength actively Q-switched laser was demonstrated. When applying 20 W diode power, the output wavelength can be selected between 1063 and 1342 nm with the peak power of 27.6 and 1.6 kW, respectively.

JW2A.84

52-mJ, kHz-Nd:YAG Laser with Diffraction Limited Output, Bozhidar Oreshkov¹, Danail Chuchumishev¹, Hristo Iliev², Anton Trifonov¹, Torsten Fiebig³, Claus-Peter Richter³, Ivan Buchvarov^{1,3}; ¹Physics, Sofia Univ. St. Kliment Ohridski, Bulgaria; ²Binovation Ltd., Bulgaria; ³Otolaryngology, Northwestern Univ., USA. We present Nd:YAG, diode pumped amplifier system emitting up to 52-mJ pulse energy with 1.6-ns pulse duration and near diffraction limited beam, operating at 0.75-kHz repetition rate.

JW2A.85

Ultrahigh frequency surface acoustic wave modulation of optical resonators, Semere Tadesse¹, Mo Li²; ¹School of Physics and Astronomy, Univ. of Minnesota, USA; ²Dept. of Electrical and Computer Engineering, Univ. of Minnesota, USA. A piezoelectric aluminum nitride film on oxidized silicon wafer is used to realize high frequency surface acoustic wave devices. Optical ring resonator is integrated with the surface acoustic wave device to demonstrate a high speed acousto-optic modulation.

JW2A.86

Full determination of coupling rate of light emitter to surface plasmon polaritons in frequency- and momentum-space, Zhaolong Cao¹, H. C. Ong¹; ¹Physics, The Chinese Univ. of Hong Kong, Hong Kong. The spectrally- and momentum-resolved coupling rate between light emitters and surface plasmon polaritons has been studied. We find the coupling rate depends strongly on the interplay between the absorption and radiative decay rates of SPPs.

JW2A.87

Modulated Plasma Waveguides Generated by Intense Bessel Beams Patterned with a Spatial Light Modulator, George Hine¹, Andy Goers¹, Sung Yoon¹, Jennifer Elle¹, Howard Milchberg¹; ¹Univ. of Maryland, USA. Plasma guiding structures are generated with programmable axial density modulations using a Spatial Light Modulator (SLM). A coherent beam-combining scheme enables the sculpting of high power beams with modest energy passing through the SLM.

JW2A.88

Relevance of the transversal phase-matching in high-order harmonic generation, Carlos Hernandez-Garcia^{1,2}, Íñigo J. Sola¹, Luis Plaja¹; ¹Grupo de Investigación en Óptica Extrema, Universidad de Salamanca, Spain; ²JILA, Univ. of Colorado, USA. We demonstrate theoretically and experimentally the relevance of the transversal coherence length in high-order harmonic generation (HHG). We present results in which transversal phase matching plays the leading role in the macroscopic HHG.

JW2A.89

Exploring characteristics of strong-field ionization dynamics in the mid-infrared regime, André Ludwig¹, Jochen Maurer¹, Benedikt W. Mayer¹, Christopher R. Phillips¹, Lukas Gallmann^{1,2}, Ursula Keller¹; ¹ETH Zurich, Switzerland; ²Univ. of Bern, Switzerland. We present a study of features in photoelectron momentum distributions from strong-field ionization of noble gases for few-cycle pulses in the mid-infrared regime and assign characteristics to their classical and quantum mechanical origin.

JW2A.90

Capsule-Shaped Metallic-Cavity Laser with Reduced Plasmonic Loss, Baifu Zhang¹, Takuya Okimoto¹, Takuo Tanemura¹, Yoshiaki Nakano¹; ¹The Univ. of Tokyo, Japan. We propose novel 1.55- μm capsule-shaped metallic-cavity lasers with curved facets to reduce plasmonic losses. Significant reduction of threshold current from 291 μA to 60 μA is demonstrated with effective modal volume of 0.45 μm^3 .

JW2A.91

Graphene as a tunable reservoir for shaping the incoherent spectrum of a quantum dot via plasmonic effects, George Hanson¹, Ebrahim Forati¹, Stephen Hughes²; ¹Electrical Engineering, Univ. of Wisconsin-Milwaukee, USA; ²Physics, Engineering Physics and Astronomy, Queen, Canada. Using a realistic quantum master equation we show that the Mollow triplet of a quantum dot can be tuned by adjusting its local density of states via biasing of a graphene monolayer.

JW2A.92

Superfocusing properties of disorder-enhanced plasmonic nanolenses, Juan Sebastian Totoro Gongora¹, Maria Laura Coluccio², Remo Proietti Zaccaria², Enzo Mario Di Fabrizio^{2,3}, Andrea Fratallocchi¹; ¹PRIMALIGHT, Faculty of Electrical Engineering, Applied, Mathematics and Computational Science, King Abdullah Univ. of Science and Technology (KAUST), Saudi Arabia; ²Dept. of Nanostructures, Istituto Italiano di Tecnologia (IIT), Italy; ³PSE and BESE Divisions, King Abdullah Univ. of Science and Technology (KAUST), Saudi Arabia. We investigated a disordered plasmonic nanolens using an extensive campaign of FDTD simulations. Our results show that surface roughness plays a crucial role in the enhancement of the electromagnetic energy with respect to regular structures.

JW2A.93

Experimental observation of surface plasmon vortices with arbitrarily synthesized intensity patterns, Chen-Da Ku¹, Chen-Bin Huang¹; ¹National Tsing Hua Univ., Taiwan. Surface plasmon vortices with arbitrary pattern are synthesized via geometrical designs. The resulting vortex intensity patterns are experimentally measured using a near-field scanning optical microscope and are in good agreements as compared to numerical results.

JW2A.94

Enhancing Refractive Index Sensing Capability with Infrared Plasmonic Perfect Absorbers, Fei Cheng¹, Xiaodong Yang¹, Jie Gao¹; ¹Dept. of Mechanical and Aerospace Engineering, Missouri Univ. of Science and Technology, USA. We experimentally demonstrate an infrared refractive index sensor based on plasmonic perfect absorbers for glucose concentration sensing, with the figure of merit (FOM*) around 55 and a bulk wavelength sensitivity around 600nm/RIU.

JW2A.95

Two-photon Photoluminescence Investigation of Transverse Plasmonic Mode of Single-crystalline Gold Nanoantennas, Wei-Liang Chen¹, Yu-Yang Lee¹, Feng-Chieh Li¹, Fan-Cheng Lin², Jer-Shing Huang², Yu-Ming Chang¹; ¹Center for Condensed Matter Sciences, National Taiwan Univ., Taiwan; ²Chemistry, National Tsing Hua Univ., Taiwan. Polarization-dependent spectra of two-photon photoluminescence (TPPL) from three series of single-crystalline gold nanoantennas were studied. The peak position in transverse TPPL spectra was found to shift with the arm width, revealing the depolarization nature of nanoantenna-mediated radiation.

JW2A.96

Near-field investigation of a periodic plasmonic metasurface, Sabine Dobmann^{1,2}, Arian Kriesch^{1,2}, Daniel Ploss^{1,2}, Ulf Peschel^{1,2}; ¹Inst. of Optics, Information and Photonics, Friedrich-Alexander-Universität Erlangen-Nürnberg (FAU), Germany; ²Erlangen Graduate School in Advanced Optical Technologies (SAOT) and Cluster of Excellence, Engineering of Advanced Materials (EAM), Germany. Using a near-field scanning optical microscope we investigate the optical response of a plasmonic metasurface consisting of a sub-wavelength periodic pattern in an ultrathin (10nm) silver film, which shows extraordinarily suppressed transmission in the visible.

JW2A.97

Anisotropically Etched Silicon Surfaces for Planar Plasmonic Terahertz Guided Wave Devices, Gagan Kumar^{1,2}, Shanshan Li², Mohamad M. Jadidi³, Thomas E. Murphy⁴; ¹Dept. of Physics, Indian Inst. of Technology Guwahati, India; ²Inst. for Research in Electronics and Applied Physics, Univ. of Maryland, USA; ³Inst. for Research in Electronics and Applied Physics, Univ. of Maryland, USA; ⁴Inst. for Research in Electronics and Applied Physics, Univ. of Maryland, USA. We report a terahertz waveguide fabricated from doped crystalline silicon. Anisotropic chemically etching is used to produce a periodic array of concave pyramidal troughs in the silicon that provide confinement in both transverse directions.

JW2A.98

Dual-resonant-band enhanced optical transmission through star shape bull's eye, Tavakol Nazari¹, Woohyun Jung¹, Reza Khazaeinezhad¹, Sahar Hosseinzadeh Kassani¹, Boram Joo¹, Byung-Joo Kong¹, Kyunghwan Oh¹; ¹Yonsei Univ., Korea. Two resonant bands in enhanced optical transmission were predicted in a star shape bull's eye plasmonic structure. Fundamental and its second harmonic resonance were analyzed parametrically to find optimal conditions for linear and nonlinear responses.

JW2A.99

Hybrid Plasmonic Strip and Slot Waveguides for Deep Subwavelength Nanofocusing of TE and TM Modes, Lucas Lafone¹, Themistoklis Sidiropoulos¹, Rupert F. Oulton¹; ¹Dept. of Physics, Imperial College London, UK. We identify a hybrid plasmonic slot waveguide capable of millimetre range transport and deep subwavelength nanofocusing by varying slot width. Convenient integration with the SOI platform provides an important bridge between plasmonics and silicon photonics.

JW2A • Poster Session 2—Continued

JW2A.100

Unidirectional Scattering and Emission of Light Mediated by a Single-Element Nano-antenna, Niels Verellen^{1,2}, Dries Vercrusse^{2,1}, Yannick Sonnefraud³, Xuezhong Zheng⁴, Giuliana Di Martino³, Guy A. Vandenbosch⁴, Liesbet Lagae^{2,1}, Victor Moshchalkov¹, Stefan Maier³, Pol Van Dorpe^{2,1}; ¹Physics and Astronomy, KU Leuven, Belgium; ²imec, Belgium; ³Physics, Imperial College, UK; ⁴ESAT-TELEMIC, KU Leuven, Belgium. We experimentally and by means of FDTD simulations and eigenmode analysis demonstrate unidirectional side scattering of a plane wave and unidirectional emission from photo luminescent molecules mediated by a V-shaped single-element metallic nanoantenna.

JW2A.101

Analysis of Single Photon Micropillar Optical Switch using Semi-Analytical Model, Stewart Carswell¹, Cheyong Hu¹, Andrew Young¹, Ruth Oulton¹, Christian Schneider², Sven Höfling^{2,3}, Martin Kamp², John Rarity¹; ¹Univ. of Bristol, UK; ²Univ. of Würzburg, Germany; ³Univ. of St Andrews, UK. We have developed an optical switch with a quantum dot in a high Q-factor microcavity. Experimental reflectivity spectroscopy fitted by a semi-analytical model estimates the intracavity photon number required to switch the device as 0.13.

JW2A.102

Non-cylindrical optical vortices, Anderson M. Amaral¹, Edilson L. Falcão-Filho¹, Cid B. de Araújo¹; ¹Physics Dept., Universidade Federal de Pernambuco, Brazil. Abstract The spatial intensity profile of vortex beams may be shaped by spatially arranging topological charges on a phase mask. In our experiments, we produced and characterized vortex beams shaped as straight lines, corners and triangles.

JW2A.103

Enhanced Forward and Backward Anti-Stokes Raman Signals in Lithium Niobate Waveguides, Da Li¹, Pengda Hong¹, Zhaojun Liu^{1,2}, Yujie J. Ding¹, Lei Wang²; ¹Lehigh Univ., USA; ²Shandong Univ., China. We have observed enhancements of forward and backward anti-Stokes Raman signals generated in lithium niobate waveguides by one order of magnitude. Forward and backward exhibit different spectral features, unique for two configurations.

JW2A.104

Coherent Attosecond Beams Carrying Orbital Angular Momentum, Carlos Hernandez-Garcia^{1,2}, Antonio Picón³, Julio San Román², Luis Plaja²; ¹JILA, Univ. of Colorado, USA; ²Grupo de Investigación en Óptica Extrema, Univ. of Salamanca, Spain; ³Argonne National Lab, USA. We present a theoretical study of high-order harmonic generation and propagation driven by an infrared field carrying orbital angular momentum (OAM). We show that extreme-ultraviolet high-OAM vortices with helical attosecond pulse structure are generated.

JW2A.105

Experimental Bifurcation Diagram and Terminal Voltage Change of an External-cavity Semiconductor Laser, Byungchil Kim^{2,1}, Nianqiang Li^{3,2}, Aakash Sahai^{2,1}, Alexandre Locquet^{1,2}, David Citrin^{2,1}; ¹Electrical and Computer Engineering, Georgia Tech Lorraine, France; ²Electrical and Computer Engineering, Georgia Inst. of Technology, USA; ³Center for information photonics and communications, Southwest Jiaotong Univ., China. We present for the first time experimental bifurcation diagrams of an external-cavity semiconductor laser using the photodetected optical intensity and the laser diode terminal voltage and interpret them on the basis of the Lang and Kobayashi model.

JW2A.106

A collinear 2f-to-3f self-referencing interferometer with a dual-pitch PPLN ridge waveguide, Kenichi Hitachi¹, Atsushi Ishizawa¹, Tadashi Nishikawa², Hiroki Mashiko¹, Osamu Tadanaga³, Masaki Asobe³, Tetsuomi Sogawa¹, Hideki Gotoh¹; ¹NTT Basic Research Labs, Japan; ²Tokyo Denki Univ., Japan; ³NTT Photonics Labs, Japan. We report carrier-envelope offset beat detection (52-dB signal-to-noise ratio at 100-kHz resolution bandwidth) with a common-path 2f-to-3f self-referencing interferometer with a dual-pitch periodically poled lithium niobate ridge waveguide.

JW2A.107

Ultra-Fast Motion of Optically Driven Metallic Nanoparticles, Sergey Sukhov¹, Alexander S. Shalin², Aristide Dogariu¹; ¹Univ. of Central Florida, CREOL, USA; ²National Univ. for Information Technology, Mechanics and Optics (ITMO), Russia. The temperature of absorbing particles changes under external illumination. In turn, this temperature distribution modifies the viscosity properties of the surrounding fluid leading to nonstationary dynamics and to ultra-fast optically induced motion of particles.

JW2A.108

Accelerating beam propagation in refractive index potentials, Nikolaos K. Efremidis¹; ¹Dept. of Mathematics and Applied Mathematics, Univ. of Crete, Greece. We study the dynamics of accelerating beams impinging on different classes of index potentials. The analytic expressions for the reflected and transmitted waves show that the Airy-wave parabolic trajectory is modified with some particular exceptions.

JW2A.109

Hexagonal pattern motion induced by spin dynamics of exciton-polaritons, Oleg Egorov¹, Albrecht Werner¹, Falk Lederer¹; ¹Friedrich-Schiller-Universität Jena, Germany. We report on a spin-induced collective motion of exciton-polaritons in microresonators driven coherently by a linearly polarized pump. Hexagonal patterns start a uniform motion provided that the TE-TM mode splitting is taken into account.

JW2A.110

Biological Source of Correlated Photon Pairs, Abu Thomas¹; ¹Northwestern, USA. Photon pairs sources based on nonlinear optical techniques are essential components in modern quantum optical systems. We present here a naturally occurring biological source of photon pairs—Green Fluorescent Protein (GFP)—obtained by a non-degenerate four-wave mixing (FWM). © 2014 Optic

JW2A.111

Determination of multidimensional hyper potential surface configuration in polyacetylene derivative, Takayoshi Kobayashi^{1,3}, Tsugumasa Iiyama¹, Kotaro Okamura¹, Juan Du^{2,4}, Toshio Masuda⁵; ¹Univ. of Electro-Communications, Japan; ²JST, CREST, Japan; ³National Chiao-Tung Univ., Taiwan; ⁴Shanghai Inst. of Optics and Fine Mechanics, China; ⁵Fukui Univ. of Technology, Japan. We have for the first time obtained multi-dimensional Huang Rhys factors, which determine the potential hypersurface structures in complex polymeric system by observing the transition-energy modulations separately among many modes induced by impulsive excitation.

JW2A.112

Space Charge Effects in Strong-Field Emission From a Nanostructured Si Cathode, Phillip D. Keathley¹, Michael E. Swanwick², Arya Fallahi³, Luis F. Velasquez-Garcia¹, Franz Kärtner^{3,4}; ¹Electrical Engineering and Computer Science, MIT, USA; ²Microsystems Technology Labs, MIT, USA; ³Center for Free-Electron Laser Science, Deutsches Elektronen Synchrotron, Germany; ⁴Physics Dept. and the Hamburg Center for Ultrafast Imaging, Univ. of Hamburg, Germany. Ultrafast photoemission from a nanostructured Si-cathode array comprised of nano-sharp tips (~5 nm radius of curvature) was studied. Total current yield and electron spectra indicate a transition from multiphoton to strong-field emission followed by virtual cathode formation.

JW2A.113

Photoinduced Absorption with Ultrafast Decay Constants in a Large Single Crystal of BiFeO₃, Takeshi Mochizuki¹, Eiichi Matsubara¹, Masaya Nagai¹, Toshimitsu Ito², Masaaki Ashida¹; ¹Osaka Univ., Japan; ²National Inst. of Advanced Industrial Science and Technology (AIST), Japan. Using near-infrared pump probe technique, we demonstrate ultrafast photoinduced absorption with a decay constant as short as 100 fs in a large single crystal of bismuth ferrite with high quality grown by floating zone method.

JW2A.114

Exciton dynamics in conducting polymer polyaniline using ultrafast spin-polarized spectroscopy, Soonyoung Cha¹, Yoochan Hong², Jaemoon Yang³, Inhee Maeng¹, Seung Jae Oh³, Kiyoung Jeong³, Jin-Suck Suh³, Seungjoo Haam⁴, Yong-Min Huh³, Hyunyoung Choi¹; ¹School of Electrical and Electronic Engineering, Yonsei Univ., Korea; ²Dept. of Biomedical Engineering, Yonsei Univ., Korea; ³Dept. of Radiology, YUMS-KRIBB Medical Convergence Center, College of Medicine, Yonsei Univ., Korea; ⁴Dept. of Chemical and Biomolecular Engineering, Yonsei Univ., Korea. The non-equilibrium charge dynamics in conducting polymer polyaniline (PANI) have been barely understood. Utilizing ultrafast spin-resolved spectroscopy, we show that the charge dynamics in PANI is dominated by the excitonic photoresponse.

JW2A.115

Ring breathing mode (RBMs) coupled with exciton in semiconducting single-walled carbon nanotubes, Takayoshi Kobayashi^{1,3}, Zhaogang Nie^{1,2}, Xue Bing^{1,2}, Juan Du^{1,4}; ¹Univ. of Electro-Communications, Japan; ²JST, CREST, Japan; ³National Chiao-Tung University, Taiwan; ⁴Shanghai Inst. of Optics and Fine Mechanics, China. The probe photon energy dependent amplitude of RBMs is explained in terms of the real and imaginary parts of third-order susceptibility showing that the previous explanation by frequency modulation due to radius change is incorrect.

JW2A.116

Compact Subwavelength Cavities Using Reflecting Metasurfaces, Amr Shaltout^{1,2}, Alexander Kildishev^{1,2}, Vladimir M. Shalaev^{1,2}; ¹Electrical and Computer Engineering, Purdue Univ., USA; ²Birk Nanotechnology Center, Purdue Univ., USA. Subwavelength cavities are obtained by replacing conventional mirrors with reflecting metasurfaces that introduce arbitrary phase-shifts compensating for reduced accumulated phase through the ultra-small cavity. 100-nm cavities showed resonance in the range (0.6 - 1.1μm).

JW2A.117

Withdrawn

JW2A.118

Planar broadband terahertz metamaterial absorber using single nested resonator, Yongzheng Wen¹, Wei Ma¹, Joe Bailey^{2,3}, Guy Matmon², Xiaomei Yu¹, Gabriel Aeppli²; ¹Inst. of Microelectronics, Peking Univ., China; ²London Centre for Nanotechnology and Dept. of Physics and Astronomy, Univ. College London, UK; ³Centre for Mathematics and Physics in the Life Sciences and Experimental Biology, Univ. College London, UK. We report a broadband terahertz metamaterial absorber with two nested back-to-back split-ring resonators constituting a single planar resonator. Bandwidths of 0.66THz and 0.98THz with the absorptivity above 0.8 and 0.6 were experimentally obtained respectively.

JW2A • Poster Session 2—Continued

JW2A.119

Complex Wavefront Control for Enhancing Penetration Depth in 2-D Optical Coherence Tomography, Hyeonseung Yu¹, Jaeduck Jang², Jaegyun Lim³, Jung-Hoon Park¹, Wooyounh Jang³, Ji-Yeun Kim², Yong-Keun Park¹; ¹Physics, Korea Advanced Inst of Science & Tech, Korea; ²Samsung Advanced Inst. of Technology, Korea; ³Samsung Electronics, Korea. We report the enhancement of signal and penetration depth in 2-D imaging in optical coherence tomography by suppressing multiple scattering via complex wavefront shaping. Up to 92% enhancements of the penetration depth were observed for a highly scattering sample.

JW2A.120

Experimental Demonstration of Near-Infrared Epsilon-Near-Zero Multilayer Metamaterial Slabs, Changyu Hu¹, Huixu Deng¹, Daniel Rosenmann², David A. Czaplewski², Xiaodong Yang¹, Jie Gao¹; ¹Dept. of Mechanical and Aerospace Engineering, Missouri Univ of Science and Technology, USA; ²Center for Nanoscale Materials, Argonne National Lab, USA. Near-infrared epsilon-near-zero metamaterial slabs based on Ag-Ge multilayers are experimentally demonstrated and numerically analyzed. A post-annealing process and multilayer grating structures are introduced to reduce the optical loss and also tune the epsilon-near-zero wavelength.

JW2A.121

Unidirectional Surface Plasmon Polariton Coupler in the Visible Using Metasurfaces, FEI DING^{1,2}, Nathaniel Kinsey¹, Jingjing Liu¹, Zhuoxian Wang¹, Vladimir M. Shalaev¹, Alexander Kildishev¹; ¹Birck Nanotechnology Center, School of Electrical & Computer Engineering, Purdue Univ., USA; ²Centre for Optical and Electromagnetic Research, State Key Lab of Modern Optical Instrumentations, Zhejiang Univ., China. We have theoretically investigated a metasurface as a unidirectional surface plasmon polariton (SPP) coupler. The structure can work over a broad bandwidth in the visible region.

JW2A.122

Laser-Written Microstructures for Enhanced Single-Photon Collection Efficiency, Andreas W. Schell¹, Tanja Neumer¹, Qiang Shi², Johannes Kaschke², Joachim Fischer², Martin Wegener², Oliver Benson¹; ¹Nano-Optics, Humboldt-Universität zu Berlin, Germany; ²Inst. of Applied Physics, Karlsruhe Inst. of Technology (KIT), Germany. Highly efficient single-photon collection from solid-state single-photon emitters is an important task in quantum optics. Here, we will introduce two approaches based on three-dimensional laser-written microstructures to enhance collection efficiency as well as directivity.

JW2A.123

Nonlocal polarization interferometer for entanglement detection, Brian P. Williams¹, Warren P. Grice², Travis S. Humble²; ¹Physics and Astronomy, Univ. of Tennessee Knoxville, USA; ²Quantum Information Science, Oak Ridge National Lab, USA. We report an interferometer consisting of two spatially separated balanced Mach-Zehnder interferometers sharing a polarization entangled source. Nonlocal correlation statistics enable entanglement detection, Bell state identification, and fidelity bounding.

JW2A.124

Quantum Secret Sharing with Phase-Encoded Photons, Warren P. Grice¹, Philip Evans¹, Benjamin Lawrie¹, Matthieu Legre³, Pavel Lougovski¹, Bing Qi¹, William Ray¹, Matthew Smith²; ¹Oak Ridge National Lab, USA; ²Univ. of Tennessee, USA; ³ID Quantique, Switzerland. We demonstrate single-qubit quantum secret sharing using phase-encoded photons. The intermediate node is designed to be inserted directly between Alice and Bob, with no need for additional compensation schemes.

JW2A.125

Separable Schmidt modes of an entangled state, marco gramegna¹; ¹INRIM, Italy. Two-Photon Spectral Amplitude of entangled states is engineered to produce a losslessly decomposition in non-overlapping single Schmidt modes. The method relies on spontaneous parametric down-conversion pumped by a comb-like spectrum radiation.

JW2A.126

Broadband quasiphasematching for large-scale entanglement in quantum optical frequency combs, Wenjiang Fan¹, Pei Wang¹, Olivier Pfister¹; ¹Physics, Univ. of Virginia, USA. We observed a remarkably broad sum frequency generation quasi-phasematching bandwidth in periodically poled KTiOPO₄, consistent with theory. This is key to large-size quantum computing registers by generating continuous-variable cluster states in quantum optical frequency combs.

JW2A.127

Progress Towards On-chip Single Photon Sources Based on Colloidal Quantum Dots in Silicon Nitride Devices, Suzanne Bisschop^{1,2}, Yunpeng Zhu^{2,3}, Weiqiang Xie^{2,3}, Antoine Guille^{1,3}, Zeger Hens^{1,3}, Dries Van Thourhout^{2,3}, Edouard Brainin^{1,3}; ¹Physics and Chemistry of Nanostructures, Ghent Univ., Belgium; ²Photonics Research Group, INTEC, Ghent Univ., Belgium; ³Center for Nano and Biophotonics, Ghent Univ., Belgium. New results on integration of colloidal quantum dots (QDs) into SiN microstructures are reported, including QD positioning with nanometric accuracy and the efficient coupling of their emission to waveguides and cavities. The results are relevant to on-chip quantum optics and information processing.

JW2A.128

Adaptive Optics for Single-Photon Fiber Coupling of Ions, Alexander Hill¹, Joseph Nash¹, Martin Graham¹, David Hervas¹, Paul Kwiat¹; ¹Physics, Univ. of Illinois at Urbana-Champaign, USA. We present a new adaptive-optics technique for the optimization of photon collection from a simulated ion. Our technique uses a genetic algorithm to correct wavefront aberrations via deformable mirror before coupling into a single-mode fiber.

JW2A.129

Quantum nano optics of defect centers in diamond and h-BN with nano-cathodoluminescence, Sophie Meuret¹, Luiz H. Tizei¹, Jean-Denis Blazit¹, Romain Bourrellier¹, Marcel Tencé¹, Alberto Zobelli¹, Mathieu Kociak¹; ¹Laboratoire de Physique des Solides, France. We have developed a cathodoluminescence-based single photon emitter detection scheme with deep subwavelength resolution. Application to NV0 centers in diamond and a new type of emitter in hexagonal Boron Nitride is presented.

JW2A.130

Uniform and large volume microwave magnetic coupling to NV centers in diamond using split ring resonators, Khadijeh Bayat¹, Jennifer Choy¹, Anna V. Shneidman², Srujan Meesala¹, Mahdi Farrokh Baroughi³, Marko Loncar¹; ¹school of Engineering and Applied Science, Harvard Univ., USA; ²Dept. of Chemistry and Chemical Biology, Harvard Univ., USA; ³Electrical Engineering and Computer Science, South Dakota State Univ., USA. A microwave resonator for uniform coupling of microwave magnetic field into NV centers in diamond over a mm³ volume with an average Rabi frequency of 16 MHz with a 5% variance for 0.5 W microwave power is reported.

JW2A.131

The optimized probe light frequency detuning for Faraday-rotation cesium atomic magnetometer, Wenhao Li¹, Pingwei Lin², Xiang Peng¹, Hong Guo¹; ¹Peking Univ., China; ²National Inst. of Metrology (NIM), China. We experimentally demonstrate that the sensitivity of all-optical Faraday-rotation magnetometer can be improved by tuning probe light frequency to the edge of wings of Doppler profile with cesium atoms, which coincides with the theoretical analysis.

JW2A.132

Vacuum Rabi oscillation in coupled highly-dissipative cavity quantum electrodynamics, Yong-Chun Liu^{1,2}, Xingsheng Luan², Hao-Kun Li¹, Qihuang Gong¹, Chee Wei Wong², Yun-Feng Xiao¹; ¹Peking Univ., China; ²Columbia Univ., USA. We demonstrate strong anharmonicity of the polariton dressed states in a highly dissipative cavity quantum electrodynamics system via dark state resonances. Vacuum Rabi oscillation and photon blockade occur even for decay-to-interaction rate ratio exceeding 100.

JW2A.133

Measurement of the autocorrelation function of a cathodoluminescence signal: characteristics and applications in nanosecond time resolved and nanometer spatially resolved experiment, Sophie Meuret¹, Luiz H. Tizei¹, Jean-Denis Blazit¹, Marcel Tencé¹, Thomas Auzelle⁴, Karine Hestroffer⁴, Huan-Cheng Chang², Bruno Daudin⁴, François Treussart³, Mathieu Kociak¹; ¹Laboratoire de Physique des Solides, Université Paris-Sud, CNRS-UMR 8502, France; ²Inst. of Atomic and Molecular Sciences, Academia Sinica, Taiwan; ³Laboratoire Aimé Cotton, Université Paris Sud and ENS Cachan, France; ⁴Nanophysique et Semiconducteurs, CEA-CNRS Group, France. In this presentation we show that the autocorrelation function of the cathodoluminescence signal (CL-g(2)(t)) can be different from the photoluminescence PL-g(2)(t) showing a huge nanosecond bunching effect g(2)(0) > 1, allowing to retrieve emitters lifetime at nanometer scale.

JW2A.134

Quantum noise limit of the White-Light-Cavity assisted LIGO interferometer sensitivity, Minchuan Zhou², Selim M. Shariar^{1,2}; ¹Dept. of EECS, Northwestern Univ., USA; ²Dept. of Physics and Astronomy, Northwestern Univ., USA. We present the quantum noise limited sensitivity curves for the LIGO interferometer incorporating the white light cavity, which shows broadening effect and dips of opto-mechanical resonances for different values of reflectivities of the auxiliary mirror.

JW2A.135

Withdrawn

JW2A.136

Laser scribing of CIGS based thin films solar cells, Michele Sozzi¹, Daniele Menosini², Alessio Bosio², Annamaria Cucinotta¹, Nicola Romeo², Stefano Selleri¹; ¹Information engineering, Univ. of Parma, Italy; ²Physics and Earth Sciences, University of Parma, Italy. Laser scribing tests on CIGS based thin films solar cells have been performed. The obtained high quality incisions show that laser scribing is a valuable tool for producing low-cost photovoltaic modules.

JW2A.137

Solar tracking system for lighting fiber, Kim Sung-Hyun¹, Lee MinHwan¹, Park Jaesik¹, Lee Kyung-Goo², Hwang InKag¹; ¹Chonnam National Univ., Korea; ²Taihan Fiberoptics company, Korea. We demonstrate a simple and effective solar tracking system for collection of sunlight in an optical fiber. The system incorporates a mirror whose axes were controlled based on the known equation of solar motion.

JW2A.138

The Ability of Laser to Perforate and Analyze Rocks in Oil and Gas Wells, Mohamed Shahin¹; ¹Petroleum Engineering, Faculty of Petroleum and Mining Engineering, Suez Univ., Egypt. Lab investigations were carried out using 1 KW Nd:YAG laser to study the thermal effects on several rock samples, removal mechanisms and the feasibility of real time downhole analysis of the perforated/drilled formations.

JW2A • Poster Session 2—Continued

JW2A.139

Enhancement of Solar Energy Conversion by Internal Light Randomization in Subwavelength Active Layer, Avi Niv^{1,3}, Guy Bartal¹, Avner Rothchild²; ¹Electrical Engineering, Technion, Israel; ²Material Science and Engineering, Technion, Israel; ³Environmental Physics, Ben Gurion Univ. of the Negev, Israel. Light randomization in sub-wavelength active layers beyond the eligibility of rays is investigated. None-the-less more than 30% current enhancement in less than 50nm thick oxide layers is observed indicating a potentially game-changing approach.

JW2A.140

Dynamic Monitoring Instrument for Fluidic Water Quality, Ruey-Ching Twu¹, Guan-Min Chen¹, Hsiao-Ying Tu¹; ¹Electro-Optical Engineering, Southern Taiwan Univ. of Science and Technology, Taiwan. An optic sensing instrument is developed and demonstrated successfully for the dynamic measurements of fluidic water quality.

JW2A.141

The Coupled Electrical-Optical Simulation of Solar Cell J-V Degradation with Grating Heights, Yu Chiun Lin¹, Yan-Kai Zhong¹, Sze Ming Fu¹, Chi Wei Tseng¹, Shih-Yun Lai¹, Wei-Ming Lai¹, Sheng Lun Yan¹, Nyan-Ping Ju¹, Po-Yu Chen¹, Chi-Chung Tsai¹, Albert Lin¹; ¹National Chiao Tung Univ., Taiwan. Solar cell with grating structure is used frequently for increased optical absorption, but it can lead to electrical degradation. Here coupled simulation is conducted to clarify the physical reason causing this J-V degradation.

JW2A.142

Withdrawn

14:00–16:00 Market Focus Session IV: The Future of “Enabling” Photonics Innovation, Exhibit Hall Theater

15:00–16:30 Coffee Break (15:00-15:30) and Unopposed Exhibit Only Time, Exhibit Halls 1 & 2

NOTES

Lined area for taking notes, consisting of approximately 25 horizontal lines within a rectangular border.

CLEO: QELS-Fundamental Science

16:30–18:30

FW3A • Single Photon and Photon Pair Sources

Presider: Hiroki Takesue; NTT Basic Research Labs, Japan

FW3A.1 • 16:30

Efficient Heralding of Passively Spatial-Multiplexed O-Band Photons for Noise-Tolerant Quantum Key Distribution, Mao Tong Liu¹, Han Chuen Lim^{1,2}; ¹School of Electrical and Electronic Engineering, Nanyang Technological Univ., Singapore; ²Emerging Systems Division, DSO National Labs, Singapore. We demonstrate an O-band passively spatial-multiplexed heralded photon source with 74.5% heralding efficiency for noise-tolerant quantum key distribution. Relation between QBER and noise-degraded $g(2)(0)$ of heralded photons transmitted over a 10-km-long fiber is observed.

FW3A.2 • 16:45

Widely-Detuned All-Fiber Photon Pair Source in Standard Telecom Fiber, Shellee D. Dyer¹, Laura Wadleigh², Varun Verma¹, Sae Woo Nam¹; ¹NIST, USA; ²Physics, Carleton College, USA. We demonstrate photon pair generation in the telecom O- and L-bands thru spontaneous four-wave mixing in fiber. These wavelengths have low loss in fiber and are widely detuned from the pump, which simplifies filtering and reduces Raman.

FW3A.3 • 17:00

An integrated source of high purity single photon pairs with narrow bandwidths, Kai-Hong Luo¹, Harald Herrmann¹, Stephan Krapick¹, Raimund Ricken¹, Viktor Quiring¹, Hubertus Suche¹, Wolfgang Sohler¹, Christine Silberhorn¹; ¹Integrated Quantum Optics, Univ. of Paderborn, Germany. We implemented a compact integrated non-degenerate source which comprises a periodically poled waveguide with highly reflective dielectric mirror coatings to obtain narrowband photon pairs based on type II parametric down-conversion.

16:30–18:30

FW3B • Advances in Quantum Optics Platforms

Presider: Tim Taminiu; Technische Universiteit Delft, Netherlands

FW3B.1 • 16:30

Enhanced spin-based sensing using light trapping in a bulk diamond system, Hannah Clevenson¹, Tim Schroder¹, Matthew Trusheim¹, Dirk Englund¹, Danielle Braje²; ¹Electrical Engineering and Computer Science, Research Lab of Electronics, MIT, USA; ²MIT Lincoln Lab, USA. We introduce a room-temperature diamond magnetometer based on a multi-pass cell design. We estimate that we address $\sim 10^{10}$ nitrogen vacancy centers, achieving a sensitivity of 93 nT/Hz^{0.5} while predicting a shot-noise-limited sensitivity of 25 fT/Hz^{0.5}.

FW3B.2 • 16:45

Implantation of proximal NV clusters in diamond by lithographically defined silicon masks with 5 nm resolution, Igal Bayn^{1,2}, Edward Chen¹, Luozhou Li^{1,2}, Matthew Trusheim^{1,3}, Tim Schroeder¹, Ophir Gaathon¹, Ming Lu⁴, Aaron Stein⁴, Mingzhao Liu⁴, Kim Kisslinger⁴, Dirk Englund¹; ¹Dept. of Electrical Engineering and Computer Science, and Research Lab of Electronics, MIT, USA; ²Dept. of Electrical Engineering, Columbia Univ., USA; ³Dept. of Applied Physics and Applied Mathematics, Columbia Univ., USA; ⁴Center for Functional Nanomaterials, Brookhaven National Lab, USA. We present the fabrication of nitrogen-vacancy (NV) spin chains by implantation through a silicon mask on diamond. A minimum implantation aperture width of 5 nm is produced. Super-resolution measurements reveal NV lines 26 nm wide and minimal NV-pitch of 8 nm.

FW3B.3 • 17:00

Statistics of decay dynamics of quantum emitters in disordered photonic-crystal waveguides, Alisa Javadi¹, Pedro David Garcia¹, Luca Sapienza¹, Sebastian Maibom¹, Henri Thyrrestrup¹, Peter Lodahl¹; ¹Niels Bohr Inst., Copenhagen Univ., Denmark. We present a statistical analysis of the spontaneous emission of quantum dots coupled to Anderson-localized cavities in disordered photonic-crystal waveguides. We observe an average Purcell factor of 5 with a maximum value of 24.

16:30–18:30

FW3C • Symposium on Science and Applications of Structured Light in Complex Media II

Presider: Andrea Alu; Univ. of Texas at Austin, USA

FW3C.1 • 16:30 

Resonating Metasurface Photon and its Spin Manipulation, Xiaobo Yin^{1,2}; ¹Mechanical Engineering, Univ. of Colorado, USA; ²Mechanical Engineering, Univ. of California, USA. The ubiquitous spin-orbit interaction destroys the particles' spin rotational symmetry and introduces a universal transverse spin current. Here we show that an anomalous refracting metasurface induces a controllable spin-orbit interaction and a path-dependent polarization rotation.

16:30–18:30

FW3D • Spatio-Temporal Dynamics

Presider: Anna Peacock, Univ. of Southampton, USA

FW3D.1 • 16:30

Dark Soliton Attraction and Optical Spatial Shock Waves Observed in M-cresol/Nylon Solutions, Valtan Smith¹, Phillip Cala¹, Zhigang Chen¹, Weining Man¹; ¹San Francisco State Univ., USA. We demonstrate the strongest effect of dark-soliton attraction in a new type of nonlocal thermal self-defocusing nonlinear media (m-cresol/nylon solutions). Formation of spatial shock waves is also observed with only mW power.

FW3D.2 • 16:45

The True Nature of Spatiotemporal Light Bullets at 1.8 μm in Bulk Dielectric Media with Kerr Nonlinearity, Donatas Majus¹, Gintaras Tamošauskas¹, Ieva Grazuleviciute¹, Nail Garejev¹, Antonio Lotti², Daniele Faccio³, Audrius Dubietis¹; ¹Dept. of Quantum Electronics, Vilnius Univ., Lithuania; ²Dipartimento di Scienza e Alta Tecnologia, Università degli Studi dell'Insubria, Italy; ³School of Engineering and Physical Sciences, SUPA, Heriot-Watt Univ., UK. By three-dimensional imaging and measurements of energy density flux, we experimentally demonstrate that light bullets generated by filamentation in bulk dielectric media with anomalous group velocity dispersion are spatio-temporal, polychromatic Bessel pulses.

FW3D.3 • 17:00

Raman rogue waves in a long cavity passively mode-locked fiber laser, Antoine Runge¹, Claude Aguergaray¹, Neil Broderick¹, Miro J. Erkintalo¹; ¹Univ. of Auckland, New Zealand. Single-shot spectral measurements using the dispersive Fourier transformation reveal sporadic emission of parasitic Raman pulses at the output of an ultrafast Yb-doped, all-normal dispersion fiber laser. A statistical analysis reveals rogue-wave-like extreme energy fluctuations.



For Conference News & Insights
Visit blog.cleoconference.org

CLEO: Science & Innovations

CLEO: Applications
& Technology16:30–18:30
SW3E • Coherent Combining
and fs Fiber Lasers

Presider: Jeffrey Nicholson; OFS
Labs, USA

SW3E.1 • 16:30

464 MHz repetition rate erbium doped soliton fiber laser, Jian Zhang¹, Fuzeng Niu¹, Xing Chen¹, Xiang Gao², Yizhou Liu¹, Aimin Wang¹, Zhigang Zhang¹; ¹Institute of Quantum Electronics, School of Electronics Engineering and Computer Science, Peking Univ., China; ²School of Electronics Engineering and Computer Science, Peking Univ., China. We demonstrate an Er: fiber ring laser operated at the fundamental repetition rate of 464MHz. The output power is 115mW under the pump power of 1.65W. The pulse width is 123fs.

SW3E.2 • 16:45

1 GHz repetition rate ring cavity femto-second Yb: fiber laser, Chen Li¹, Xiang Gao¹, Guizhong Wang¹, Tongxiao Jiang¹, Aimin Wang¹, Zhigang Zhang¹; ¹Peking Univ., China. We demonstrate the first 1 GHz fundamental repetition rate ring cavity ytterbium doped fiber laser. The laser delivers 600 mW, 64fs near transform-limited pulses and supports direct octave-spanning spectrum generation.

SW3E.3 • 17:00 **Invited**

Performance Scaling of Ultrafast Laser Systems by Coherent Addition of Femtosecond Pulses, Jens Limpert¹; ¹Friedrich-Schiller-Universität Jena, Germany. The approach of coherent combination of ultrashort laser pulses will be reviewed. Concept, achievements and perspectives towards compact high peak power and high average power fiber laser systems will be discussed.

16:30–18:30
SW3F • THz Spectroscopy &
Sensing I

Presider: David Cooke; McGill
Univ., Canada

SW3F.1 • 16:30 **Tutorial**

Intense terahertz pulses: probing and controlling fundamental motions of electrons, spins and ions, Tobias Kampfrath¹; ¹Fritz Haber Inst./MPG, Germany. Terahertz radiation permits resonant and sensitive probing of electron transport, spin precession and ion vibration in solids. Recently developed sources of strong-field terahertz pulses even allow one to gain control over these fundamental modes.



Tobias Kampfrath earned his PhD in Physics in 2006 from Free University of Berlin. He was a Postdoc at AMOLF Amsterdam with K. Kuipers. Since 2010 he has been the head of the THz physics group at the Fritz Haber Institute, Berlin. His work is on THz spectroscopy of magnetically ordered solids and on ultrafast nanooptics.

16:30–18:30
SW3G • Micro-and Photonic
Crystal Lasers **▶**

Presider: Anthony Hoffman; Univ.
of Notre Dame, USA

SW3G.1 • 16:30 **Invited** **▶**

Asymmetric Heterogeneously Integrated InP Microdisk Lasers on Si for Optical Interconnect and Optical Logic, Geert I. Morthier^{1,2}, Pauline Mechet^{1,2}, Thijs Spuesens^{1,2}, Dries Van Thourhout^{1,2}, Gunther Roelkens^{1,2}; ¹Dept. of Information Technology, Ghent Univ., Belgium; ²Center for Nano- and Biophotonics, Ghent Univ., Belgium. We discuss properties and applications of heterogeneously integrated microdisk lasers coupled to an asymmetrically reflecting bus waveguide, in particular unidirectionality and sensitivity to external feedback. We also discuss the application of such lasers for low power all-optical signal regeneration.

SW3G.2 • 17:00

Electrically Driven Photonic-Crystal Lasers on Silicon Substrates Using Direct Wafer Bonding, Koji Takeda^{1,3}, Tomonari Sato^{1,3}, Takuro Fujii^{1,3}, Eiichi Kuramochi^{2,3}, Masaya Notomi^{2,3}, Koichi Hasebe^{1,3}, Takaaki Kakitsuka^{1,3}, Shinji Matsuo^{1,3}; ¹NTT Photonics Labs, NTT Corporation, Japan; ²NTT Basic Research Labs, NTT Corporation, Japan; ³Nanophotonics Center, NTT Corporation, Japan. We demonstrate the first continuous wave operation of electrically driven photonic-crystal lasers on Si at room temperature. Plasma assisted bonding integrated III-V semiconductor devices on Si. The device exhibited a 33 μ A threshold current.

16:30–17:45
AW3H • High Performance
Optical Measurement

Presider: Hugo Thienpont,
B-PHOT, Belgium

AW3H.1 • 16:30

Ultra-wideband Cueing Receiver based on Spatial-Spectral Holographic Rainbow Spectrometer, Tia Sharpe¹, Cooper McCann¹, Cal Harrington¹, Zeb W. Barber¹, R. Krishna Mohan¹, Wm. Randall Babbitt¹; ¹Montana State Univ., USA. A spatial-spectral holographic channelizer and cueing receiver capable of operating 1-110 GHz with sub-MHz resolution, high dynamic range, and 1000 variably programmable channels is presented, along with initial test results in the 10-20 GHz band.

AW3H.2 • 16:45

Method for Increasing the Operating Distance of MEMS LIDAR beyond Brownian Noise Limitation, Behnam Behroozpour¹; ¹Univ. of California, Berkeley, USA. A LIDAR based on a MEMS tunable VCSEL uses resonance tuning to increase the maximum range ten-fold. A novel demodulator reduces the peak electrical beat frequency from 52GHz to 235MHz for compatibility with standard CMOS.

AW3H.3 • 17:00

Lidar Velocity Measurement using a GHz Gated Photon Detector and Locked but Unequal Optical Pulse Rate, Gregory S. Kanter¹, Daniel Reilly¹; ¹NuCrypt, USA. A lidar system with high tolerance to background light is described. Velocity sensitivity measurements using two different signal processing methods are compared. Sensitivity of -90 dBm is realized for up to 6.9 km/s emulated speeds.



Join the conversation. Use #CLEO14.
Follow us @cleoconf on Twitter.

CLEO: Science & Innovations

CLEO: QELS-
Fundamental Science

CLEO: Applications
& Technology

16:30–18:30
SW3I • Novel Materials for Integrated Nonlinear Optics ▶
Presider: Benjamin Eggleton; Univ. of Sydney, Australia

16:30–18:30
SW3J • Subsystems for Optical Communications
Presider: Sophie LaRochelle; Universite Laval, Canada

16:30–18:30
FW3K • Devices Enabled by Nano-Optics and Plasmonics ▶
Presider: Nikolay Zheludev; Univ. of Southampton, UK

16:30–18:30
AW3L • Microscopy
Presider: Ernest Chang; Physical Sciences Inc., USA

SW3I.1 • 16:30 ▶
Mid-IR parametric frequency generation in hybrid As₂Se₃ microwires using normal dispersion modulation instability, Thomas Godin¹, Yves Combes¹, Raja Ahmad², Martin Rochette², Thibaut Sylvestre¹, John M. Dudley¹; ¹Institut FEMTO-ST, France; ²McGill Univ., Canada. We report the observation of modulation instability in the mid-infrared by pumping chalcogenide-polymer optical microwires in the normal dispersion regime. Modulation instability is allowed via negative fourth-order dispersion and leads to far-detuned parametric frequency conversion.

SW3J.1 • 16:30
Pump-Linewidth-Tolerant Wavelength Conversion with Coherent Pumps, Guo-Wei Lu¹, André Albuquerque², Benjamin J. Puttnam¹, Takahide Sakamoto¹, Miguel Drummond², Rogério Nogueira², Atsushi Kanno¹, Satoshi Shinada¹, Naoya Wada¹, Tetsuya Kawanishi¹; ¹NICT, Japan, Japan; ²Instituto de Telecomunicações (IT) - pólo de Aveiro, Portugal. We propose a pump-linewidth-tolerant wavelength conversion scheme with coherent two-tone pump, and demonstrate high quality wavelength conversion of 64QAM signals with <0.3-dB penalty at BER of 10⁻³ even using 3.5MHz-linewidth DFB pump source.

FW3K.1 • 16:30 **Invited** ▶
Transparent Displays Enabled by Resonant Nanoparticle Scattering, Chia Wei Hsu^{1,2}, Bo Zhen¹, Wenjun Qiu¹, Ofer Shapira¹, Brendan DeLacy³, John Joannopoulos¹, Marin Soljacic¹; ¹Physics, MIT, USA; ²Physics, Harvard Univ., USA; ³U.S. Army Edgewood Chemical Biological Center, USA. We create a transparent display by projecting monochromatic images onto a polymer film embedded with nanoparticles that selectively scatter light at the projected wavelength. This approach features simplicity, wide viewing angle, scalability, and low cost.

AW3L.1 • 16:30
Single Nanoparticle and Virus Detection Using a Smart Phone Based Fluorescence Microscope, Qingshan Wei^{1,2}, Hangfei Qi¹, Wei Luo¹, Derek Tseng¹, Laurent A. Bentolila^{3,5}, Ting-Ting Wu⁴, Ren Sun^{4,3}, Aydogan Ozcan^{1,2}; ¹Electrical Engineering Dept., Univ. of California Los Angeles, USA; ²Bioengineering Dept., Univ. of California Los Angeles, USA; ³California NanoSystems Inst. (CNSI), Univ. of California Los Angeles, USA; ⁴Dept. of Molecular and Medical Pharmacology, Univ. of California Los Angeles, USA; ⁵Dept. of Chemistry and Biochemistry, Univ. of California Los Angeles, USA. We demonstrate a field-portable fluorescence microscopy platform installed on a smart phone for imaging of single/isolated nanoparticles and fluorescently labeled viruses.

SW3I.2 • 16:45 ▶
Mid-infrared Supercontinuum Generation in Robust Step-Index Chalcogenide Nanotapers Pumped with a Thulium Fiber Laser, Soroush Shabahang¹, Guangming Tao¹, Kevin F. Lee², Viktor Smolski¹, Konstantin L. Vodopyanov¹, Martin Fermann², Ayman F. Abouraddy¹; ¹Univ. of Central Florida, CREOL, USA; ²IMRA, USA. We fabricate highly nonlinear and mechanically robust step-index chalcogenide nanotapers with large core-cladding index contrast. Using femtosecond pulses at 2-micron wavelength from a thulium fiber laser, mid-infrared supercontinuum spanning more than an octave was generated.

SW3J.2 • 16:45
Impact of Laser Resonance Phase Noise on the Wavelength Conversion of DQPSK Signals, Sean O Duill¹, Aravind Anthur², Tam Huynh¹, Deepa Venkitesh², Liam Barry¹; ¹The Rince Inst., Dublin City Univ., Ireland; ²Dept. of Electrical Engineering, Indian Inst. of technology, Madras, India. We show through simulations and with supporting experimental results that the performance of four-wave mixing based wavelength conversion of DQPSK signals is severely limited by resonance enhanced phase noise on the pump source.

FW3K.2 • 17:00 ▶
Aperiodic single-pixel angle-modulated plasmonic color sorter and angle sensor, Matthew S. Davis¹, Ting Xu², Christopher D. Bohn², Henri J. Lezec², Amit K. Agrawal^{1,2}; ¹Dept. of Electrical Engineering and Computer Science, Syracuse Univ., USA; ²Center for Nanoscale Science and Technology, National Inst. of Standards and Technology, USA. We demonstrate the design, simulation and experimental realization of a single aperiodic slit-groove plasmonic device that exhibits angle-selectable RGB color response at optical frequencies, as well as a high quality factor and optical contrast.

AW3L.2 • 16:45
Hyper-dimensional analysis for label-free high-throughput imaging flow cytometry, Claire Chen^{1,3}, Ata Mahjoubfar^{1,3}, Allen Huang^{1,3}, Kayvan Niaz^{3,4}, Shahrooz Rabizadeh^{3,4}, Bahram Jalali^{1,2}; ¹Dept. of Electrical Engineering, Univ. of California Los Angeles, USA; ²Dept. of Bioengineering, Univ. of California, Los Angeles, USA; ³California NanoSystems Inst., USA; ⁴NantWorks, LLC, USA. We present an imaging flow cytometer capable of capturing phase and intensity images of individual unlabeled cells at 36 million frames/second to generate multi-dimensional scatter plots, leading to a considerable enhancement in cell classification sensitivity.

SW3I.3 • 17:00 ▶
A two-octave broadband quasi-continuous mid-infrared supercontinuum generated in a chalcogenide glass waveguide, Barry Luther-Davies¹, Yi Yu¹, Pan Ma¹, Zhiyong Yang¹, Duk-Yong Choi¹, Steve Madden¹, Sukanta Dabbarma¹, Xin Gai¹, Rongping Wang¹; ¹Australian National Univ., Australia. We have produced a stable 10mW, mid-infrared supercontinuum spanning the full functional group band from 1750nm to >7000nm spanning using a 1cm long chalcogenide waveguide pumped by a 20MHz train of 320fs pulses at 4µm.

SW3J.3 • 17:00
Reconfigurable Optical Sub-harmonic Clock Recovery Based on Inverse Temporal Self-imaging, Reza Maram¹, Luis Romero Cortés¹, José Azaña¹; ¹INRS-Energie Matériaux et Telecom, Canada. We propose and experimentally demonstrate a novel, simple and efficient sub-harmonic optical clock recovery technique from RZ-OOK data based on temporal self-imaging, involving temporal phase modulation and dispersion, with a reconfigurable rate division factor.

FW3K.3 • 17:00 **Invited** ▶
Photoacoustic microscopy: current situation and new ultrasonic detectors, Biqin Dong¹, Cheng Sun¹, Hao F. Zhang¹; ¹Northwestern Univ., USA. We present the need for new ultrasonic detectors in photoacoustic microscopy and report on the development of a cover-slip type, optically transparent, all-optical ultrasonic detector based on a polymeric micro-ring resonator for various photoacoustic applications.

AW3L.3 • 17:00 **Invited** ▶
Photoacoustic microscopy: current situation and new ultrasonic detectors, Biqin Dong¹, Cheng Sun¹, Hao F. Zhang¹; ¹Northwestern Univ., USA. We present the need for new ultrasonic detectors in photoacoustic microscopy and report on the development of a cover-slip type, optically transparent, all-optical ultrasonic detector based on a polymeric micro-ring resonator for various photoacoustic applications.

CLEO: Science & Innovations

CLEO: Applications
& Technology

16:30–18:30

SW3M • Nonlinear Nanophotonics

President: Alexander Gaeta; Cornell Univ., USA

SW3M.1 • 16:30

Improved four-wave mixing with free-carrier removal in silicon coupled microring waveguides, Junrong Ong¹, Ranjeet Kumar¹, Xianshu Luo², Guo-Qiang Lo², Shayan Mookherjee¹; ¹Univ. of California San Diego, USA; ²Inst. of Microelectronics, A*STAR, Singapore. We improve CW wavelength conversion efficiency by 10 dB in an optical waveguide consisting of 51 directly-coupled silicon microrings, based on electronic free-carrier sweepout using two reverse-biased p-n junction diodes on each microring resonator.

SW3M.2 • 16:45

Wide-band On-chip Four-Wave Mixing via Coupled Cavity Dispersion Compensation, Cale M. Gentry¹, Xiaoge Zeng¹, Miloš A. Popović¹; ¹Univ. of Colorado at Boulder, USA. We demonstrate a dual-cavity resonant structure that employs frequency splitting at one of three resonances to structurally compensate dispersion. We show seeded four-wave mixing across the largest free spectral range to our knowledge of 26nm.

SW3M.3 • 17:00

Four-wave mixing in silicon “photonic molecule” resonators with port-selective, orthogonal supermode excitation, Xiaoge Zeng¹, Cale M. Gentry¹, Miloš A. Popović¹; ¹Univ. of Colorado at Boulder, USA. We propose coupled-cavity resonators for four-wave mixing (FWM) that support strong nonlinear interaction between distributed pump, signal and idler modes, yet allow independent coupling of these modes to separate ports. We demonstrate seeded FWM and discuss applications of such orthogonal coupling.

16:30–18:30

SW3N • High Power Laser

President: Michalis Zervas; Univ. of Southampton, UK

SW3N.1 • 16:30

High-power Single-frequency, Single-polarization, Thulium-doped all-fiber MOPA, Jiang Liu¹, Kun Liu¹, Hongxing Shi¹, Yubin Hou¹, Yijian Jiang¹, Pu Wang¹; ¹Beijing Univ. of Technology, China. We demonstrated a high-power single-frequency, single-polarization, thulium-doped all-fiber MOPA system. The linearly-polarized thulium-doped fiber MOPA yielded 192 W of single-frequency output at central wavelength of 2001 nm with a polarization extinction ratio of >15 dB.

SW3N.2 • 16:45

SBS Mitigation via Phase Modulation and Demodulation, Henrik Tünnemann^{1,4}, Philipp Jahn^{1,2}, Volker Quetschke³, Jörg Neumann^{1,2}, Dietmar Kracht^{1,2}, Peter Wessels^{1,2}; ¹Laser Zentrum Hannover e.V., Germany; ²Centre for Quantum Engineering and Space-Time Research - QUEST, Germany; ³Dept. of Physics and Astronomy, Univ. of Texas at Brownsville, USA; ⁴Inst. for Laser Science, Univ. of Electro-Communications, Japan. We present SBS suppression in a single frequency amplifier using frequency sidebands added by an EOM and complete recovery of the single frequency signal after amplification using a custom high power high modulation index EOM.

SW3N.3 • 17:00

High Power, Sub-GHz, Monolithic Fiber Amplifier Based on Phase Modulated Laser Gain Competition, Angel Flores¹, Iyad Dajani¹; ¹US Air Force Research Lab, USA. SBS suppression in monolithic, Yb-doped fiber amplifiers via phase modulated two-tone laser gain competition (LGC) is reported. The LGC between broad and narrow-linewidth (1036nm/1064nm) signals yielded pump-limited output powers of 600W at a 500MHz modulation-frequency.

16:30–18:30

SW3O • Optical Clocks & Dissemination

President: Zeb Barber; Montana State Univ. - Spectrum Lab, USA

SW3O.1 • 16:30 **Invited**

Optical Atomic Clocks for a Future New Definition of the Second, Fritz Riehle¹; ¹Physikalisch Technische Bundesanstalt, Germany. Optical atomic clocks outperform the best caesium atomic clocks which define the second wrt accuracy and stability. As secondary representations of the second they pave the way to a new definition of the time unit.

SW3O.2 • 17:00

650-km Fiber Link in Italy for Optical Frequency Dissemination and Remote Clocks Comparison, Cecilia Clivati¹, Claudio E. Calosso¹, Matteo Frittelli¹, Aldo Godone¹, Filippo Levi¹, Alberto Mura¹, Massimo Zucco¹, Davide Calonico¹, Denis V. Sutyurin², Guglielmo M. Tino², Nicola Poli², Giovanni A. Costanzo³; ¹Istituto Nazionale di Ricerca Metrologica, Italy; ²Politecnico di Torino, Italy. We realized a 650-km optical fiber link in Italy for frequency dissemination and remote clocks comparison. We present its implementation and characterization at the 5e-19 uncertainty level, discussing its future applications.

16:30–18:30

AW3P • Novel Optical Devices

President: Richard Sandberg; Los Alamos National Lab, USA

AW3P.1 • 16:30 **Invited**

Nanowire superconducting single photon detectors progress and promise, Sae Woo Nam¹, Varun Verma¹, Michael Allman¹, Robert Horansky¹, Richard P. Mirin¹, Adriana Lita¹, Francesco Marsili², Matthew Shaw², Andrew D. Beyer², Jeffrey A. Stern²; ¹NIST, USA; ²Jet Propulsion Lab, USA. Since the first reported detection of a single photon using a superconducting nanowire in 2001, rapid progress has been made in the development and application of superconducting nanowire single photon detectors (SNSPD or SSPD). I will briefly describe use of these detectors in new applications, progress in detector developments, and describe areas of research and their potential impact.

AW3P.2 • 17:00

Ultrafast Quantum Random Number Generation Using Off-the-shelf Components, Carlos Abellan¹, Waldimar Amaya¹, Marc Jofre¹, Marcos Curty², Antonio Acin^{1,3}, Jose Capmany⁴, Valerio Pruneri^{1,3}, Morgan W. Mitchell^{1,3}; ¹The Inst. of Photonic Sciences, Spain; ²El Telecomunicacion, Dept. of Signal Theory and Communications, Univ. of Vigo, Spain; ³ICREA, Spain; ⁴ITEAM, Universidad Politecnica de Valencia, Spain. We demonstrate a 43 Gbps quantum random number generator using DPSK demodulation of pulses from a current-modulated laser diode. The signal is random by quantum phase diffusion, macroscopic, and detectable with off-the-shelf components.

CLEO: QELS-Fundamental Science

FW3A • Single Photon
and Photon Pair Sources—
Continued

FW3A.4 • 17:15

1.5 μ m degenerate-frequency photon pair generation in silicon micro-ring cavities, Yuan Guo¹, Wei Zhang¹, Shuai Dong¹, Yidong Huang¹, Jiangde Peng¹; ¹Tsinghua Univ., China. 1.5 μ m degenerate-frequency photon pairs are generated in a silicon micro-ring cavity by reverse degenerate spontaneous four wave mixing. Their quantum interferences in Mach-Zehnder interferometers are demonstrated, showing their potential in quantum metrology and quantum information.

FW3A.5 • 17:30

Theory of scattering loss during spontaneous parametric downconversion in waveguides, Lukas G. Helt¹, John E. Sipe², Michael J. Steel¹; ¹Physics and Astronomy, Macquarie Univ., Australia; ²Physics, Univ. of Toronto, Canada. We consider simultaneous SPDC and scattering loss in waveguides by coupling waveguide modes to a reservoir. We calculate that a reduction in pair generation efficiency can be accompanied by an increase in heralded photon purity.

FW3A.6 • 17:45

Highly efficient generation of narrow-band single-mode photon pairs from a whispering gallery mode resonator, Michael J. Foertsch^{1,3}, Gerhard Schunk^{1,3}, Josef Fürst^{1,2}, Florian Sedlmeir^{1,2}, Dmitry Strekalov^{1,2}, Harald Schwefel^{1,2}, Thomas Gerrits⁴, Martin J. Stevens⁴, Sae Woo Nam⁴, Gerd Leuchs^{1,2}, Christoph Marquardt^{1,2}; ¹Max Planck Institute for the Science of Light, Germany; ²Inst. for Optics, Information, and Photonics, Germany; ³School in Advanced Optical Technologies, Germany; ⁴National Inst. of Standards and Technology, USA. We present a highly efficient narrow-band pair-photon source based on a crystalline whispering gallery mode resonator, which emits photons in exactly one spatiotemporal mode.

FW3B • Advances in Quantum
Optics Platforms—Continued

FW3B.4 • 17:15

Observation of superradiant phase transition in quantum chaos, Changxu Liu¹, Andrea Di Falco², Andrea Fratolocci¹; ¹PRIMALIGHT, Faculty of Electrical Engineering; ²Applied Mathematics and Computational Science, King Abdullah Univ of Sci & Technology, Saudi Arabia; ³SUPA; ⁴School of Physics and Astronomy, Univ. of St. Andrews, UK. We observed the phase transition of multiple superradiant states in chaotic optical cavities with multiple open decay channels base on photonic crystals.

FW3B.5 • 17:30

Quadratic Measurement and Conditional State Preparation in an Optomechanical System, George Brawley¹, Michael Vanner¹, Warwick P. Bowen¹, Silvan Schmid², Anja Boisen²; ¹School of Mathematics and Physics, The Univ. of Queensland, Australia; ²Dept. of Micro- and Nanotechnology, Technical Univ. of Denmark, Denmark. We experimentally demonstrate, for the first time, quadratic measurement of Brownian mechanical motion in an optomechanical system. We use this nonlinear measurement to conditionally prepare classical non-Gaussian states of motion of a micro-mechanical oscillator.

FW3B.6 • 17:45

Superfluid Helium Optomechanics, David L. McAuslan¹, Glen I. Harris¹, Eoin Sheridan¹, Warwick P. Bowen¹; ¹Centre for Engineered Quantum Systems, Univ. of Queensland, Australia. By evanescently coupling a helium film to a high-Q optical resonator we make the first observation of superfluid helium Brownian motion. This new system has applications in quantum optomechanics, and in understanding superfluid helium properties.

FW3C • Symposium on Science
and Applications of Structured
Light in Complex Media II—
Continued

FW3C.3 • 17:15

Bulk optical measurement of topological numbers in photonic lattices with a non-Hermitian system, Julia M. Zeuner¹, Mikael Rechtsman², Yaakov Lumer², Yonatan Plotnik², Stefan Nolte¹, Mordechai Segev², Alexander Szameit¹; ¹Inst. of Applied Physics, Friedrich-Schiller-Universität, Germany; ²Technion Israel Inst. of Technology, Israel. Topological insulators have been extended to photonics; however, the measurement of their topological invariant has been limited to probing edge states, an indirect measure. Here we optically measure a topological invariant using only bulk information.

FW3C.4 • 17:30 **Invited**

Controlling Light Propagation in Optical Waveguides Using One Dimensional Phased Antenna Arrays, Nanfang Yu¹, Myoung-Hwan Kim¹, Zhaoyi Li¹; ¹Columbia Univ., USA. We demonstrated using full-wave simulations that phased array antennas patterned on optical waveguides can strongly affect mode coupling and propagation in the waveguides. We designed broadband small-footprint integrated photonic devices based on the concept.

FW3D • Spatio-Temporal
Dynamics—Continued

FW3D.4 • 17:15

Extreme Events in Resonant Radiation from 3-dimensional light bullets, Thomas Roger¹, Donatas Majus², Gintaras Tamošauskas², Audrius Dubietis², Goëry Genty³, Miroslav Kolesik⁴, Daniele Faccio¹; ¹Inst. of Photonics and Quantum Sciences, Heriot-Watt Univ., UK; ²Dept. of Quantum Electronics, Vilnius Univ., Lithuania; ³Dept. of Physics, Tampere Univ. of Technology, Finland; ⁴College of Optical Sciences, Tucson Univ., USA. We experimentally demonstrate rogue event statistics of dispersive waves from 3-dimensional spatiotemporal light bullets. Similarities to fibre solitons, with the added complexity related to spatiotemporal dynamics render this system ideal for future rogue wave studies.

FW3D.5 • 17:30

Polarization switching in stretched pulse fiber laser, Chengbo Mou¹, Sergey Sergeev¹, Raz Arif¹, Aleksey Rozhin¹, Stanislav Kolpakov¹, Zuxing Zhang¹, Sergei K. Turitsyn¹; ¹Aston Univ., UK. We studied experimentally polarization dynamics in a carbon nanotube mode locked stretched pulse fiber laser. For the first time, polarization locked, regular and irregular polarization switching have been observed at the microsecond time scale.

FW3D.6 • 17:45

Interplay of nonlinear dynamics in silicon photonic crystal waveguides, Chad A. Husko¹, Andrea Blanco-Redondo^{1,2}, Daniel Eades¹, Juntao Li^{3,4}, Thomas F. Krauss^{5,3}, Benjamin J. Eggleton¹; ¹Univ. of Sydney, Australia; ²Tecnalia, Spain; ³Univ. of St. Andrews, UK; ⁴Sun Yat-sen Univ., China; ⁵Univ. of York, UK. We report time-domain measurements of nonlinear dynamics of picosecond pulses in silicon. The dispersion-engineered photonic crystal enables our systematic investigation of dynamic interplay between dispersion, free-carriers, and $\chi(3)$ effects for a broad parameter range.

Technical Digest and Postdeadline Papers Available Online

- Visit www.cleoconference.org
- Select **Download Digest Paper** button
- Use your email address and CLEO Registration ID # to synchronize

Once you have synchronized your conference registration with Optics InfoBase, you can log in directly to Optics InfoBase at any point using the same email address and OSA password.

Access must be established via synchronization within 60 days of the conference start date.
Access is provided only to full technical attendees.

CLEO: Science & Innovations

CLEO: Applications
& TechnologySW3E • Coherent Combining
and fs Fiber Lasers—ContinuedSW3F • THz Spectroscopy &
Sensing I—ContinuedSW3G • Micro-and Photonic
Crystal Lasers—ContinuedAW3H • High Performance
Optical Measurement—
Continued

SW3E.4 • 17:30

Soliton Wake Instability in a SESAM Modelocked Fiber Laser, Shaokang Wang¹, Curtis R. Menyuk¹, Laura Sinclair², Ian Codrington², Nathan R. Newbury²; ¹Computer Science and Electrical Engineering, Univ. of Maryland Baltimore County, USA; ²National Inst. of Standards and Technology, USA. We describe the nonlinear evolution profile of the soliton wake instability in a single-polarization SESAM modelocked fiber laser system. We show that it leads to quasi-periodicity.

SW3E.5 • 17:45

Generation of ultra-broadband pulses with axially-symmetric polarization based on coherent beam combining of optical vortices, Keisaku Yamane^{1,2}, Yasuyuki Shioda¹, Masato Suzuki^{1,2}, Yasunori Toda^{1,2}, Ryuji Morita^{1,2}; ¹Hokkaido Univ., Japan; ²JST CREST, Japan. We demonstrated the generation of ultra-broadband optical pulses with axially-symmetric polarization, on the basis of a coherent beam combining technique. The high polarization purity (~95 %) ranging from 750 to 880 nm was obtained.

SW3F.2 • 17:30

Numerical Investigation of Ultrafast interaction between THz Fields and Crystalline Materials, Pernille K. Pedersen¹, Stewart S. Clark², Peter U. Jepsen¹; ¹DTU Fotonik, Technical Univ. of Denmark, Denmark; ²Dept. of Physics, Univ. of Durham, UK. We present a quantum-mechanical molecular dynamics investigation of the interaction between strong single-cycle THz pulses and ionic crystals. We find nonlinearities in the response of the CsI crystals at field strengths higher than 10 MV/cm.

SW3F.3 • 17:45

Effects of Depolarization Fields on Transient Terahertz Spectra of Nanostructured Materials, Hynek Nemeč¹, Vit Zajac¹, Petr Kuzel¹; ¹Inst. of Physics AS CR, v.v.i, Czech Republic. Analysis of the relationship between the microscopic conductivity, morphology represented by percolation degree and terahertz transmission spectra allowed us to retrieve microscopic properties of several nanostructured materials from measurements by terahertz spectroscopy.

SW3G.3 • 17:15

Demonstration of Watt-class High-power Photonic-Crystal Lasers, Kazuyoshi Hirose^{1,2}, Yoshitaka Kurosaka^{1,2}, Akiyoshi Watanabe¹, Takahiro Sugiyama¹, Yong Liang², Susumu Noda²; ¹Hamamatsu Photonics K.K., Japan; ²Kyoto Univ., Japan. We demonstrate watt-class high output power (1.5 W) operation in single-chip photonic-crystal surface-emitting lasers under room-temperature continuous-wave condition. The beam quality factor M2 has been found to be kept at 1.0 up to 0.5 W.

SW3G.4 • 17:30

Room Temperature Operation of Optically Pumped 1.55- μ m VCSEL with Polarization-Independent HCG Mirror on SOI, Yoshihiro Tsunemi¹, Nobuhide Yokota¹, Shota Majima¹, Kazuhiro Ikeda¹, Takeo Katayama¹, Hitoshi Kawaguchi¹; ¹Graduate School of Materials Science, Nara Inst. of Science and Technology, Japan. We fabricated a VCSEL incorporating a polarization-independent HCG mirror on SOI for a novel polarization-bistable functional device. The VCSEL oscillated under an optical short pulse excitation at 300 K.

SW3G.5 • 17:45

Low-threshold photonic-band-edge laser using iron-nail-shaped rod array, Jae-Hyuck Choi¹, You-Shin No¹, Soon-Hong Kwon², Jin-Kyu Yang³, Hong-Gyu Park¹; ¹Physics, Korea Univ., Korea; ²Physics, Chung-Ang Univ., Korea; ³Optical Engineering, Kongju National Univ., Korea. We report the experimental demonstration of an optically pumped rod-type photonic-crystal band-edge laser. Lasing operation was achieved with a low threshold of ~90 μ W and a peak wavelength of 1451.5 nm at room temperature.

AW3H.4 • 17:15

Terahertz reflectometry of multi-layered paint thicknesses and estimation of particle sizes, Anis Rahman¹, Aunik Rahman¹; ¹Applied Research and Photonics Inc, USA. A terahertz reflectometer was designed and utilized for measuring paint panels comprised of layers of paint, primer and overcoat. Particle size of the paint additives were estimated by contour plot derived from 3D surface map.

AW3H.5 • 17:30

Femtosecond pulses for 3-D surface measurement of microelectronic structures, Young-Jin Kim¹, Woo-Deok Joo¹, Jiyong Park¹, Seungman Kim¹, Seung-Woo Kim¹; ¹Korea Advanced Inst of Science & Tech, Korea. We present a fast and precise 3-D measurement of microelectronic structures over a wide field-of-view by utilizing high spatial coherence, low temporal coherence and repetition rate tunability of femtosecond laser pulses.

Visit Registration to Purchase

Access your Favorite Talks or One You Missed!
On-Demand, 24/7

Over 300 high-quality, informative talks representing the full breadth of CLEO's outstanding technical program including:


Tutorials • Contributed • Postdeadline
Symposia • Plenary talks • Invited

CLEO: Science & Innovations


CLEO: QELS-
Fundamental Science

CLEO: Applications
& Technology

SW3I • Novel Materials for
Integrated Nonlinear Optics—
Continued

SW3I.4 • 17:15  **Optical Nonlinearities in High Confinement SiC Waveguides**, Jaime Cardenas¹, Mengjie Yu², Yoshitomo Okawachi², Carl Poitras¹, Ryan K. Lau², Alexander L. Gaeta^{2,3}, Michal Lipson^{1,3}; ¹School of Electrical and Computer Engineering, Cornell Univ., USA; ²School of Applied and Engineering Physics, Cornell Univ., USA; ³Kavli Inst. at Cornell for Nanoscale Science, Cornell Univ., USA. We demonstrate strong nonlinearities of $n_2 = 8 \times 10^{-15} \text{ cm}^2 \text{ W}^{-1}$ in single crystal silicon carbide at a wavelength of 2360nm. We use a high confinement SiC waveguide fabricated using a modified smart-cut process.

SW3I.5 • 17:30  **Enhanced Second-Harmonic Generation in GaP Nanopillars Arrays by Modal Engineering**, Reza Sanatinia¹, Sybren Westendorp², Srinivasan Anand¹, Marcin Swillo²; ¹KTH Royal Inst. of Technology, Sweden; ²KTH Royal Inst. of Technology, Sweden. Second harmonic generation from GaP nanopillars with optimized mode field overlap is analyzed and experimentally demonstrated. We present dispersion engineering in arrays of nanopillars to satisfy modal phase matching.

SW3I.6 • 17:45  **Third Harmonic Generation in Polycrystalline Anatase Titanium Dioxide Nanowaveguides**, Katia Shtyrkova¹, Christopher Evans², Orad Reshef², Jonathan Bradley², Michael G. Moebius², Eric Mazur², Erich Ippen¹; ¹Electrical Engineering and Computer Science, MIT, USA; ²School of Engineering and Applied Sciences, Harvard Univ., USA. We experimentally demonstrate third-harmonic generation in polycrystalline anatase titanium dioxide nano-waveguides, using ultrashort optical pulses centered around 1550 nm. Phase matching is achieved using higher order optical modes at the third harmonic wavelength.

SW3J • Subsystems for Optical
Communications—Continued


SW3J.4 • 17:15
Timing-jitter Reduction by Demultiplexed-Feedback Clock Recovery in a 160Gbaud Serial Data Transmission System, Siyuan Zhou¹, Deming Kong¹, Yan Li¹, Jizhao Zang¹, Jian Wu¹; ¹State Key Lab of Information Photonics and Optical Communications, Beijing Univ. of Posts and Telecommunications, China. Demultiplexed-feedback clock recovery for ultra-high speed serial data transmission system is proposed and analyzed through numerical simulations. A 4x40 Gbaud proof-of-concept experiment is carried out, achieving 31 fs timing-jitter of the recovered clock.


SW3J.5 • 17:30
Simple all optical modulation format conversion from 4x12.5 Gbps NRZ-OOK to 50 Gbps PDM RZ-QPSK using cross-phase modulation in a bidirectional scheme, Yu-Hsiang Wen¹, Kai-Ming Feng^{1,2}; ¹National Tsing Hua Univ., Photonics Technologies, Taiwan; ²National Tsing Hua Univ., Communications Engineering, Taiwan. We proposed and experimentally demonstrated a low-complexity and cost-effectiveness format converter using XPM in a single HNLF. Four individual 12.5 Gbps NRZ-OOK to one 50 Gbps PDM RZ-QPSK format conversion is successfully achieved.

SW3J.6 • 17:45
IQ Skew Monitoring and Alignment of Optical Quadrature Amplitude Transmitter using Reconfigurable Interference, Yang Yue¹, Bo Zhang¹, Rob Lofland¹, Jason O'Neil¹, Qiang Wang¹, Jon Anderson¹; ¹Juniper Networks, USA. IQ skew measurement of quadrature amplitude transmitter using reconfigurable interference is demonstrated with >20-dB dynamic range. The scheme is compatible with different modulation formats and patterns. Fast tracking scheme for large skew is discussed.

FW3K • Devices Enabled by
Nano-Optics and Plasmonics—
Continued

FW3K.3 • 17:15
Solid-immersion Super-oscillatory Lens for Heat Assisted Magnetic Recording Technology and Nanoscale Imaging, Tapashree Roy¹, Guanghui Yuan², Edward T. Rogers¹, Nikolay I. Zheludev^{1,2}; ¹Optoelectronics Research Centre and Centre for Photonic Metamaterials, Univ. of Southampton, UK; ²Centre for Disruptive Photonic Technologies, Nanyang Technological Univ., Singapore. We demonstrate a solid-immersion super-oscillatory planar lens for super-resolution applications with a 102 nm full-width at half maximum focal spot in a low-loss immersion medium.

FW3K.4 • 17:30  **Plasmonic Enhanced Near IR Schottky Detectors Based on Internal Photoemission in Nano Pyramids**, Boris Desiatov¹, Ilya Goykhman¹, Noa Mazurski¹, Joseph Shappir¹, Jacob Khurgin², Uriel Levy¹; ¹Hebrew Univ. of Jerusalem, Israel; ²Johns Hopkins Univ., USA. We demonstrate the detection of subband-gap light in silicon nano pyramid using the process of internal photoemission in Schottky diode. The quantum efficiency is enhanced by using metal coated silicon nano pyramids.

FW3K.5 • 17:45  **Monolithic Integration of Quantum Emitter with On-chip Beam-splitter for Quantum Information Processing**, Nikola Prtjaga¹, Rikki J. Coles¹, John O'Hara¹, Benjamin Royall¹, Anthony M. Fox¹, Edmund Clarke², Maurice S. Skolnick¹; ¹Dept. of Physics and Astronomy, Univ. of Sheffield, UK; ²Dept. of Electronic and Electrical Engineering, Univ. of Sheffield, UK. We demonstrate the monolithic integration of an on-demand quantum emitter in the form of a single self-assembled InGaAs quantum dot with an air clad, free standing directional coupler acting as a beam-splitter for anti-bunched light.

AW3L • Microscopy—Continued

AW3L.4 • 17:30
Novel wedge-based approach for simultaneous multichannel microscopy, Samuel Chung^{1,3}, Christopher V. Gabel^{1,2}; ¹Physiology and Biophysics, Boston Univ. School of Medicine, USA; ²Boston Univ. Photonics Center, USA; ³Physical Sciences Inc., USA. We demonstrate a novel device, based on wedge prisms, that enables simultaneous imaging and fluorescence microscopy of multiple color channels and is simpler, more user-friendly, and less expensive than current commercial devices.

AW3L.5 • 17:45
Temporal focusing microscopy with structured illumination for super-resolution deep imaging, Keisuke Isobe^{1,2}, Kyohei Mochizuki^{1,3}, Qiyuan Song^{1,4}, Akira Suda³, Fumihiko Kannari⁴, Hiroyuki Kawano⁵, Akiko Kumagai⁵, Atsushi Miyawaki^{5,2}, Katsumi Midorikawa^{1,2}; ¹Laser Technology Lab, RIKEN, Japan; ²RIKEN Center for Advanced Photonics, Japan; ³Tokyo Univ. of Science, Japan; ⁴Keio Univ., Japan; ⁵RIKEN Brain Science Inst., Japan. We demonstrate that temporal focusing microscopy with structured illumination provides super-resolution even if wavefront distortion within the sample results in stretching the point spread function of the microscope.



CLEO: Science & Innovations

CLEO: Applications
& TechnologySW3M • Nonlinear
Nanophotonics—Continued

SW3M.4 • 17:15

Wavelength Conversion in Low Loss Si₃N₄ Waveguides, Clemens Krücker¹, Victor Torres-Company¹, Peter Andrekson¹, Jock Bovington², Jared Bauters², Martijn Heck², John E. Bowers²; ¹Dept. of Microtechnology and Nanoscience (MC2), Chalmers Univ. of Technology, Sweden; ²Dept. of Electrical and Computer Engineering, Univ. of California, USA. We show wavelength conversion in a compact Si₃N₄ waveguide. Combining low loss, long length, relatively large nonlinear coefficient, high-power handling and absence of two-photon absorption, this platform is promising for integrated nonlinear optics applications.

SW3M.5 • 17:30

40-GHz Analog-to-Digital Converter Based on Sampling Gate of Silicon Waveguide with Ultra-Low Loss and High Conversion Efficiency, Mu-Han Yang¹, Bill P.P. Kuo¹, Stojan Radic¹, Faezeh Gholami¹, Lan Liu¹; ¹UCSD, USA. An ultra-low loss and high conversion efficiency silicon waveguide is used as sampling gate via four waves mixing, and 5.2 effective number of bits of signal at 40-GHz is achieved by 2-GHz cavity-less pulse source.

SW3M.6 • 17:45

Low-power four-channel wavelength multicasting in embedded microring resonators, Mario Souza¹, Luis A. M. Barea¹, Felipe Valini¹, Guilherme F. M. Rezende¹, Gustavo S. Wiederhecker¹, Newton C. Frateschi¹; ¹DFA - IFGW, Universidade Estadual de Campinas, Brazil. We demonstrate four-channel all-optical wavelength multicasting using only 1 mW of pump power and channel spacing of 40-60 GHz. Our device is based on a compact embedded microring design fabricated on a scalable SOI platform.

SW3N • High Power Laser—
Continued

SW3N.4 • 17:15

Yb-doped Rod-type Fiber Amplifier with 2 kW Average Power, Hans-Jürgen Otto¹, Cesar Jauregui¹, Fabian Stutzki¹, Norbert Modsching¹, Jens Limpert^{1,2}, Andreas Tünnermann^{1,3}; ¹Inst. of Applied Physics, Germany; ²Helmholtz-Inst. Jena, Germany; ³Fraunhofer Inst. for Applied Optics and Precision Engineering, Germany. The average output power of rod-type fiber-laser systems can be scaled well beyond the mode instability threshold. A record average output power of 2 kW with 83% slope-efficiency and good beam quality (M₂=3) is presented.

SW3N.5 • 17:30

High Power Single Frequency 1014.8 nm Yb-doped Fiber Amplifier and Frequency Quadrupling to 253.7 nm, Jimeng Hu^{1,2}, Lei Zhang^{1,2}, Hongli Liu^{1,3}, Kangkang Liu^{1,3}, Zhen Xu^{1,3}, Yan Feng^{1,2}; ¹Shanghai Inst. of Optics and Fine Mechanics, Chinese Academy of Sciences, China; ²Shanghai Key Lab of Solid State Laser and Application, China; ³Key Lab of Quantum Optics, and Center for Cold Atom Physics, Chinese Academy of Science, China. A 19 W linearly-polarized single-frequency 1014.8 nm fiber amplifier working at room temperature is developed. Both absorption and saturated absorption spectra of atomic mercury are measured with this radiation after frequency quadrupling to 253.7 nm.

SW3N.6 • 17:45

High power Raman fiber laser based on random Rayleigh distributed feedback, hanwei zhang¹, Pu Zhou¹, Hu Xiao¹, Xiaojun Xu¹; ¹National Univ. of Defense Technology, China. We demonstrated a high power Raman fiber laser based on randomly Rayleigh distributed feedback. A total power of 73.7W was achieved with an optical efficiency of 74.7%. The spectrums and output power characters are discussed.

SW3O • Optical Clocks &
Dissemination—Continued

SW3O.3 • 17:15

Optical Frequency Transfer via 1840 km Fiber Link with superior Stability, Stefan Droste¹, Filip Ozimek², Thomas Udem¹, Katharina Predehl¹, Theodor W. Hänsch¹, Harald Schnatz², Gesine Grosche², Ronald Holzwarth¹; ¹Max-Planck-Institut für Quantenoptik, Germany; ²Physikalisch-Technische Bundesanstalt, Germany. We transferred an optical frequency along a 1840km fiber link and achieved an instability of 3×10^{-15} at 1s with 4×10^{-19} after 100s. The transferred frequency shows no systematic offset within an uncertainty of 3×10^{-19} . Detailed analysis revealed a τ^{-2} response in the modified Allan deviation.

SW3O.4 • 17:30

One-femtosecond, long-term stable remote laser synchronization over a 3.5-km fiber link, Ming Xin¹, Kemal Safak¹, Michael Peng², Patrick Callahan², Franz Kärtner^{1,2}; ¹Center for Free-Electron Laser Science, Deutsches Elektronen-Synchrotron, Germany; ²Dept. of Electrical Engineering and Computer Science and Research Lab of Electronics, MIT, USA. Long-term stable remote laser synchronization over a 3.5 km long polarization maintaining fiber link is demonstrated. The residual rms-timing jitter and drift over 36-hour operation is 0.96 fs integrated from 100 μ Hz to 1 MHz.

SW3O.5 • 17:45

Characterization of a 450-km-baseline GPS Carrier-Phase Link using an Optical Fiber Link, Stefan Droste¹, Christian Grebing², Julia Leute², Sebastian Raupach², Andreas Bauch², Gesine Grosche², Ronald Holzwarth¹; ¹Max-Planck-Institut für Quantenoptik, Germany; ²Physikalisch-Technische Bundesanstalt, Germany. We characterize a GPS carrier-phase link with 450 km baseline, using a long-distance phase-stabilized optical fiber link. Active hydrogen masers at both ends are compared via both links simultaneously. This allows us to assess the instability and accuracy of the GPS link with sub- 10^{-15} resolution.

AW3P • Novel Optical
Devices—Continued

AW3P.3 • 17:15

Progress Towards a Near IR Single-Photon Superconducting Nanowire Camera for Free-Space Imaging of Light, Michael Allman¹, Varun B. Verma¹, Robert Horansky¹, Francesco Marsili², Jeffrey A. Stern², Matthew D. Shaw², Andrew D. Beyer², Richard P. Mirin², Sae Woo Nam²; ¹NIST, USA; ²Jet Propulsion Lab, USA. We describe our progress towards building a free-space coupled array of nanowire detectors with a multiplexed readout. The cryogenic, optical, and electronic packaging to readout the array will be discussed.

AW3P.4 • 17:30 **Invited**

Quantum Noise Reduction in the LIGO Gravitational Wave Interferometer with Squeezed States of Light, Lisa Barsotti¹; ¹MIT, USA. The quantum nature of light imposes a fundamental limit on the sensitivity of ground based gravitational wave detectors. Squeezed states of light, produced via parametric downconversion in a non linear medium, have recently been employed to beat the quantum limit and extend the astrophysical reach of the most sensitive gravitational wave detector ever built.



CLEO: QELS-Fundamental Science

FW3A • Single Photon
and Photon Pair Sources—
Continued

FW3A.7 • 18:00

Integrated Source of Multiplexed Photon Pairs, Lucia Caspani¹, Christian Reimer¹, Matteo Clerici^{1,2}, Marcello Ferrera^{1,2}, Marco Peccianti^{1,3}, Alessia Pasquazi^{1,3}, Luca Razzari¹, Brent E. Little⁴, Sai T. Chu⁵, David J. Moss^{1,6}, Roberto Morandotti¹; ¹INRS-EMT, Canada; ²School of Engineering and Physical Sciences, Heriot-Watt Univ., UK; ³Dept. of Physics and Astronomy, Univ. of Sussex, UK; ⁴HiQ Photonics, USA; ⁵Dept. of Physics and Material Science, City Univ. of Hong Kong, China; ⁶School of Electrical and Computer Engineering, RMIT Univ., Australia. We report an integrated, CMOS-compatible source of multiple and independent photon pairs at different wavelengths compatible with standard fiber communication channels and quantum memories. It operates in a self-locked mode with no external pump laser.

FW3A.8 • 18:15

Encoding and decoding of biphoton wavepackets, Joseph M. Lukens¹, Amir Dezfooliyani¹, Carsten Langrock², Martin M. Fejer², Daniel E. Leaird¹, Andrew M. Weiner¹; ¹Electrical and Computer Engineering, Purdue Univ., USA; ²Edward L. Ginzton Lab, Stanford Univ., USA. We demonstrate orthogonal spectral coding of entangled photons for the first time. Applying one code to the signal photon spreads and scrambles the biphoton; only by properly decoding the idler is the original biphoton recovered.

FW3B • Advances in Quantum
Optics Platforms—Continued

FW3B.7 • 18:00

Multimode Correlations in Chip-based Frequency Combs, Avik Dutt¹, Kevin Luke¹, Alexander L. Gaeta², Paulo A. Nussenzveig³, Michal Lipson¹; ¹School of Electrical and Computer Engineering, Cornell Univ., USA; ²School of Applied and Engineering Physics, Cornell Univ., USA; ³Instituto de Física, Universidade de São Paulo, Brazil. We demonstrate correlations between non-twin beams of a frequency comb generated from a silicon nitride ring resonator optical parametric oscillator. The normalized correlation coefficient between these two modes is 0.997, corresponding to near perfect correlations between the two beams.

FW3B.8 • 18:15

Photon lifetime and the linewidth in a superluminal laser, Jacob Scheuer¹, Selim M. Shahriar^{2,3}; ¹Tel-Aviv Univ., Israel; ²EECS, Northwestern Univ., USA; ³Physics, Northwestern Univ., USA. We present a theoretical analysis of the cavity lifetime of a superluminal laser. In contrast to the naive intuition, the lifetime is only slightly shorter than that of conventional lasers, facilitating ultra-sensitive sensors.

FW3C • Symposium on Science
and Applications of Structured
Light in Complex Media II—
Continued

FW3C.5 • 18:00

Selective Self-assembly of Symmetry-breaking Nanoplasmonic Structures, Sui Yang^{1,2}, Xiaobo Yin^{1,2}, Boubacar Kante¹, Peng Zhang¹, Jia Zhu¹, Yuan Wang¹, Xiang Zhang^{1,2}; ¹NSF Nano-scale Science and Engineering Center (NSEC), Univ. of California Berkeley, USA; ²Materials Sciences Division, Lawrence Berkeley National Lab, USA. Self-assembly approaches to construct plasmonic materials often result in high-symmetry structures within a thermodynamic limit. Here we demonstrate a novel selective self-assembly route for synthesis of a new class of nanoplasmonic structures with symmetry-breaking.

FW3C.6 • 18:15

Molding Surface Plasmons by Spinoptical Rashba Metasurfaces, Nir Shitrit¹, Igor Yulevich¹, Dekel Veksler¹, Vladimir Kleiner¹, Erez Hasman¹; ¹Technion-Israel Inst. of Technology, Israel. We report on a spin-based surface plasmon directional excitation by spinoptical Rashba metasurfaces. The light-matter interaction control via the geometric design of the metasurface symmetry ushers in a new era of light manipulation.

FW3D • Spatio-Temporal
Dynamics—Continued

FW3D.7 • 18:00

Buffering optical data with topological localized structures, Bruno Garbin¹, Julien Javaloyes², Giovanna Tissoni¹, Stephane Barland¹; ¹Institut Non Lineaire de Nice, Universite de Nice - CNRS, France; ²departamento de fisica, Universidad de la Islas Baleares, Spain. We demonstrate experimentally that a semiconductor laser based excitable system placed in a linear feedback loop can store optical bits. In the process, we show the existence of topological localized states in optics.

FW3D.8 • 18:15

Back-Action of Continuum on Solitons and the Resulting Energy Oscillations in a Mode-Locked Laser, Chien-Chung Lee¹, Thomas R. Schibli¹; ¹Dept. of Physics, Univ. of Colorado at Boulder, USA. We describe a resonant phenomenon that exists in all mode-locked lasers with non-negligible anomalous chromatic dispersion and self-phase modulation. Numerical simulation and experiment are also performed, and good agreement with the analytic results was found.

NOTES

CLEO: Science & Innovations

CLEO: Applications
& Technology

SW3M • Nonlinear
Nanophotonics—Continued

SW3M.7 • 18:00

Nonlinear optical properties of SiGe waveguides in the mid-infrared, Luca Carletti¹, Pan Ma², Barry Luther-Davies², Darren D. Hudson³, Christelle Monat¹, Steve Madden², David J. Moss⁴, Mickael Brun⁵, Sophie Ortiz², Sergio Nicoletti⁵, Christian Grillet¹; ¹Institut des Nanotechnologies de Lyon, Ecole Centrale de Lyon, France; ²CUDOS, Laser Physics Centre, Australian National Univ., Australia; ³CUDOS, School of Physics, Univ. of Sydney, Australia; ⁴School of Electrical and Computer Engineering, Royal Melbourne Inst. of Technology, Australia; ⁵CEA-Leti, MINATEC Campus, France. We measure the nonlinear response of CMOS-compatible SiGe waveguides in the mid-infrared. Comparing with numerical calculations, we extract the multi-photon absorption coefficients and the induced free-carrier absorptions for wavelengths between 3µm and 5µm.

SW3M.8 • 18:15

Below Bandgap Second Harmonic Generation in GaAs Photonic Crystal Cavities in (111) and (001) Crystal Orientations, Sonia Buckley¹, Marina Radulaski¹, Jan Petykiewicz², Konstantinos Lagoudakis¹, Klaus Biermann², Jelena Vuckovic¹; ¹Stanford Univ., USA; ²Paul-Drude-Institut für Festkörperelektronik, Germany. We demonstrate second harmonic generation in photonic crystal cavities in (001)- and (111)-oriented GaAs, with fundamental resonance at 1800nm, leading to second harmonic below the GaAs bandgap. Below bandgap operation minimizes linear and nonlinear absorption.

SW3N • High Power Laser—
Continued

SW3N.7 • 18:00

Over 50 W 589 nm single frequency laser by frequency doubling of single Raman fiber amplifier, Lei Zhang¹, Huawei Jiang¹, Shuzhen Cui¹, Jimeng Hu¹, Lingxia Chen¹, Yan Feng¹; ¹Shanghai Inst. of Optics and Fine Mechanics, China. 300W CW linearly-polarized 1120nm laser is achieved with an integrated Yb-Raman fiber amplifier. 86W 1178nm single frequency Raman fiber amplifier is generated and frequency doubled to 589nm with power up to 52.7W.

SW3N.8 • 18:15

Near Diffraction-Limited, 811W, Single-Frequency Photonic Crystal Fiber Amplifier, Benjamin Pulford¹, Iyad Dajani¹, Craig Robin¹; ¹Air Force Research Lab, USA. An acoustic and gain tailored Yb-doped polarization-maintaining photonic crystal fiber is used to demonstrate 811W single-frequency output power with near diffraction-limited beam quality; the highest power ever reported from a near diffraction-limited single-frequency fiber laser.

SW3O • Optical Clocks &
Dissemination—Continued

SW3O.6 • 18:00

A Unidirectional Scheme for High-Fidelity Optical-Carrier Dissemination Using Phase-Modulation, Homodyne Coherent-Detection, and Frequency Entrainment, Ehsan Sooudi^{1,2}, Fatima C. Garcia Gunning^{1,2}, James O’Gorman³, Stylianos Sygletos⁴, Selwan K. Ibrahim⁵, Andrew D. Ellis⁴, Robert J. Manning^{1,2}; ¹Photonic Systems Group, Tyndall National Inst., Ireland; ²Dept. of Physics, Univ. College Cork (UCC), Ireland; ³Xylophone Optics Ltd, Ireland; ⁴Aston Inst. of Photonic Technologies, Aston Univ., UK; ⁵FAZTech Research, Ireland. We report for the first time an ultra-stable optical-carrier dissemination technique for transmission over a 20km unidirectional fibre link. The optical-linewidth of the recovered carrier matches closely that of the original carrier.

SW3O.7 • 18:15

Stability Characterization of an Optical Injection Phase Locked Loop for Optical Frequency Transfer Applications, Joonyoung Kim¹, David Wu¹, Giuseppe Marra², David J. Richardson¹, Radan Slavik¹; ¹Optoelectronics Research Centre, Univ. of Southampton, UK; ²National Physics Lab, UK. We propose an optical injection phase locked loop (OIPLL) as a high-gain amplifier for precise frequency transfer via optical fibers. The suitability of this approach for international optical clock comparison is evaluated.

AW3P • Novel Optical
Devices—Continued

AW3P.5 • 18:00

Optical Encryption Based on Cancellation of Analog Noise, Ben Wu¹, Matthew Chang¹, Zhenxing Wang¹, Bhavin Shastri¹, Paul Prucnal¹; ¹Electrical Engineering, Princeton Univ., USA. We propose an optical encryption technique where the data is encrypted with wideband analog noise. Matching both the phase and amplitude of the noise is required, providing a large key space for the encryption process.

AW3P.6 • 18:15

Commercially Packaged Optical True-Time-Delay Devices With Record Delays of Wide Bandwidth Signals, Paul A. Morton¹, Jacob Khurgin², Zemer Mizrahi³, Steven Morton¹; ¹Morton Photonics, USA; ²Electrical and Computer Engineering, Johns Hopkins Univ., USA; ³Aeon Corporation, USA. Commercially packaged optical true-time-delay devices were developed utilizing ultra-low loss silicon nitride microresonators, achieving record tunable delay of 535ps for a 20GHz wide signal, 632ps for a 10GHz wide signal, with tunable loss of 3dB.

NOTES

Blank lined area for notes.

CLEO: QELS-Fundamental Science

08:00– 10:00

FTh1A • Quantum Entanglement

President: Warren Grice; Oak Ridge National Lab, USA

FTh1A.1 • 08:00

Creation and manipulation of two-dimensional photonic frequency entanglement, Laurent Olislager¹, Erik Woodhead¹, Kien Phan Huy², Jean-Marc Merolla², Philippe Emplit¹, Serge Massar¹; ¹Universite Libre de Bruxelles, Belgium; ²FEMTO-ST, France. We demonstrate, using standard telecommunication components, the creation and manipulation of frequency entangled effective qubits that exhibit nonlocal interferences in the frequency domain, violating the CHSH inequality by more than 40 standard deviations.

FTh1A.2 • 08:15

Demonstration of high-dimensional frequency-bin entanglement, Zhenda Xie¹, Tian Zhong², Xinan Xu¹, Junlin Liang¹, Yanxiao Gong³, Sajjan Shrestha¹, Jeffrey H. Shapiro², Franco Wong², Chee Wei Wong¹; ¹Columbia Univ., USA; ²MIT, USA; ³Southeast Univ., China. We exhibit high-dimensional frequency-bin entanglement from a mode-locked two-photon source via frequency-correlation measurement and Hong-Ou-Mandel interference. Generalized Bell-inequality is tested by Franson interference, showing revival interference fringes, with maximum visibility of 98.6%.

FTh1A.3 • 08:30

Emission of time-energy entangled photon pairs from an integrated silicon ring resonator, Davide Grassani¹, Stefano Azzini¹, Marco Liscidini¹, Matteo Galli¹, Michael Strain^{2,3}, Marc Sorel², John E. Sipe⁴, Daniele Bajoni⁵; ¹Physics, Universita degli Studi di Pavia, Italy; ²Univ. of Glasgow, UK; ³Univ. of Strathclyde, UK; ⁴Physics, Univ. of Toronto, Canada; ⁵Engineering, Università degli Studi di Pavia, Italy. We demonstrate an integrated silicon source of time-energy entangled photons. Entanglement is proved using a Franson type experiment, obtaining visibility exceeding 90% and a violation of the Bell's inequality by more than 10 standard deviations.

08:00– 10:00

FTh1B • Quantum Interconnects

President: Yanhong Xiao; Fudan Univ., China

FTh1B.1 • 08:00 **Tutorial**

Strong Photon-Photon Interactions, Vladan Vuletic¹, Mikhail Lukin², Kristin Beck¹, Wenlan Chen¹, Thibault Peyronel¹, Ofer Firstenberg², Qiyu Liang¹; ¹MIT, USA; ²Physics, Harvard Univ., USA. Standard nonlinear optical materials exhibit negligible nonlinearity at the level of individual photons. I will discuss two methods to generate strong photon-photon interactions using either atom-cavity coupling, or strong interactions between atoms in Rydberg states.



Vladan Vuletic received his Ph.D. from the University of Munich and has previously worked at the Max Planck Institute for Quantum Optics in Garching, Germany, and at Stanford University. He is now at the Massachusetts Institute of Technology, where his research group studies many-body entanglement, quantum measurements, cavity quantum electrodynamics, and strong photon-photon interactions.

08:00– 10:00

FTh1C • High-Field THz Physics

President: Matthias Hoffmann; SLAC National Accelerator Lab, USA

FTh1C.1 • 08:00 **Invited**

CEP Control of Dynamical Bloch Oscillations in a Bulk Semiconductor via Ultra-Intense Multi-THz Fields, Fabian Langer¹, Olaf Schubert¹, Matthias Hohenleutner¹, Benedikt Urbanek¹, Christoph Lange¹, Ulrich Huttner², Daniel Golde², Torsten Meier³, Mackillo Kira², Stephan W. Koch², Rupert Huber¹; ¹Univ. of Regensburg, Germany; ²Univ. of Marburg, Germany; ³Univ. of Paderborn, Germany. Dynamical Bloch oscillations and coherent interband polarization in bulk GaSe are controlled by CEP-stable, ultra-intense multi-THz waveforms and result in the emission of phase stable high-order harmonics covering 12.7 optical octaves from THz to VIS regimes.

FTh1C.2 • 08:30

High-field terahertz shift current in lithium niobate, Michael Woerner¹, Carmine Somma¹, Klaus Reimann¹, Thomas Elsaesser¹, Christos Flytzanis²; ¹Max Born Inst., Germany; ²Ecole Normale Supérieure, France. We study the nonlinear terahertz response of LiNbO₃ using 2D spectroscopy. Dissecting the nonlinear response into different orders in the electric field shows a strong shift current and higher harmonics of the THz fundamental.

08:00– 10:00

FTh1D • Solitons and Temporal Effects

President: Marco Peccianti; Univ. of Sussex, Italy

FTh1D.1 • 08:00

Temporal Soliton Generation in Chip-based Silicon Nitride Microresonators, Victor Brasch¹, Tobias Herr¹, Martin Pfeiffer¹, John Jost¹, Tobias Kippenberg¹; ¹EPFL, Switzerland. We demonstrate temporal dissipative soliton generation in silicon nitride microresonators for the first time. Temporal soliton states allow for low-noise RF-generation, smooth frequency comb spectra and produce ultra-short optical pulses on a chip.

FTh1D.2 • 08:15

Observation of dispersive wave emission by temporal cavity solitons, Jae K. Jang¹, Stuart G. Murdoch¹, Stephane Coen¹, Miro J. Erkintalo¹; ¹Univ. of Auckland, New Zealand. We report the first experimental observation of dispersive wave emission by temporal cavity solitons. Our results could impact on a variety of systems supporting temporal cavity solitons, such as high-Q Kerr microresonators.

FTh1D.3 • 08:30

Self-compression of Millijoule mid-IR Femtosecond Pulses in Transparent Dielectrics, Audrius Pugzlys¹, Pavel Malevich¹, Skirmantas Alisauskas¹, Alexander A. Voronin², Daniil Kartashov⁵, Andrius Baltuska¹, Aleksei Zheltikov^{2,3}, Daniele Faccio⁶; ¹Photonics Inst., vienna Univ. of technology, Austria; ²International Laser Center, M.V. Lomonosov Moscow State Univ., Russia; ³Dept. of Physics and Astronomy, Texas A&M Univ., USA; ⁴Inst. of Photonics and Quantum Sciences, Heriot-Watt Univ., UK; ⁵Inst. for Optics and Quantum Electronics, Friedrich-Schiller Univ., Germany. Self-compression of 2.2-mJ, 80-fs mid-IR pulses is achieved using a 1.5-mm-thick CaF₂ plate. Femtosecond pulses with peak powers orders of magnitude higher than the self-focusing threshold can undergo self-compression without breaking up into multiple filaments.

Join the Exhibitors for PizzaThursday, 12 June
12:30–14:00
Exhibit Hall 1 & 2

CLEO: Science & Innovations

08:00– 10:00

STH1E • Filamentation

Presider: Pavel Polynkin; Univ. of Arizona, USA

STH1E.1 • 08:00

Direct observation of pulse dynamics, influencing high-order harmonic emission along a filament, Martin Kretschmar^{1,2}, Tamas Nagy^{1,3}, Ayhan Demircan¹, Carsten Bree⁴, Michael Hofmann⁴, Heiko Kurz^{1,2}, Uwe Morgner^{1,2}, Milutin Kovacev¹; ¹Gottfried Wilhelm Leibniz Universität Hannover, Germany; ²Quest, Centre for Quantum Engineering and Space-Time Research, Germany; ³Laser-Laboratorium Goettingen e.V., Germany; ⁴Weierstrass-Institut für Angewandte Analysis und Stochastik, Germany. We present in-situ measurements of pulse dynamics along a femtosecond filament. Pulse-splitting has been observed, resulting in self-compression to 5.3 fs, influencing high-order harmonic generation along the filament.

STH1E.2 • 08:15

Direct Interferometric Measurements of the Acoustic Waves from Femtosecond Filaments, Jared K. Wahlstrand¹, Nihal Jhajj¹, Eric Rosenthal¹, Sina Zahedpour¹, Howard Milchberg¹; ¹Univ. of Maryland at College Park, USA. Interferometric measurements of submicrosecond gas density dynamics following passage of an intense ultrashort pulse are presented for single- and multi-lobed beams at 10 Hz and 1 kHz. Results are in excellent agreement with hydrodynamic simulations.

STH1E.3 • 08:30

Demonstration of long-lived high power optical waveguides in air, Nihal Jhajj¹, Eric Rosenthal¹, Reuven Birnbaum¹, Jared Wahlstrand¹, Howard Milchberg¹; ¹Univ. of Maryland, USA. We show that femtosecond filament arrays can generate robust, very long-lived optical waveguides in air. These guides have millisecond lifetime and should be suitable for the transmission of high average power beams.

08:00– 09:45

STH1F • THz Quantum Cascade Lasers

Presider: Masayoshi Tonouchi, Osaka Univ., Japan

STH1F.1 • 08:00

Widely-Tunable Monolithic Terahertz Quantum Cascade Laser Sources Based on Difference-Frequency Generation, Seungyong Jung¹, Aiting Jiang¹, Yifan Jiang¹, Karun Vijayraghavan¹, Xiaojun Wang², Mariano Troccoli², Mikhail A. Belkin¹; ¹Electrical and Computer Engineering, Univ. of Texas at Austin, USA; ²Adtech Optics, Inc., USA. We demonstrate monolithic tunable terahertz quantum cascade laser sources with a tuning range over 580 GHz at room temperature by integrating electrically separated distributed feedback section and distributed Bragg reflector section into a single device.

STH1F.2 • 08:15

In-plane surface plasmonics integrated with THz Quantum cascade lasers for high collimation, Guozhen Liang¹; ¹Nanyang Technological Univ., Singapore. We report planar integration of tapered Terahertz (THz) quantum cascade lasers (QCLs) with spoof surface plasmon (SSP) structures, which results in a surface-emitting THz beam with a beam divergence of 3.6×9.7 degree.

STH1F.3 • 08:30

Effect of Interface Roughness Scattering on performance of Indirectly Pumped Terahertz Quantum Cascade Lasers, Seyed Ghasem Razavipour¹, Emmanuel Dupont², Zbigniew Wasilewski¹, Dayan Ban¹; ¹Univ. of Waterloo, Canada; ²National Research Council Canada, Canada. The effect of interface roughness scattering on performance of indirectly-pumped terahertz quantum cascade lasers is studied and a dual-barrier structure is proposed to improve its performance in terms of threshold current density and operating temperature.

08:00– 10:00

STH1G • Semiconductor Lasers for Communication

Presider: Kent Choquette; Univ. of Illinois, USA

STH1G.1 • 08:00

50×100GHz Wavelength Tuning in Rectangular Ring-FP Semiconductor Laser, Lin Wu¹, Zhipeng Hu¹, Jian-Jun He¹; ¹Zhejiang Univ., China. We report our latest experimental results of the half-wave coupled rectangular ring-FP laser. Wavelength tuning of 50 channels covering L band at 100GHz spacing is achieved, with SMSR up to 41dB. Direct modulation at 2.5Gbps is also demonstrated.

STH1G.2 • 08:15

Error-free 25-Gbit/s direct modulation of lateral-current-injection DFB laser, Koichi Hasebe¹, Tomonari Sato¹, Koji Takeda¹, Takuro Fujii¹, Takaaki Kakitsuka¹, Shinji Matsuo¹; ¹NTT Photonics Labs, NTT Corporation, Japan. We present a lateral-current-injection InP-based DFB laser consisting of a pn junction fabricated by using Zn thermal diffusion and Si ion implantation. An error-free direct modulation with a bit rate of 25 Gbit/s is achieved.

STH1G.3 • 08:30

High Temperature Athermal Colorless Laser for Low-Cost Backhaul Networks, Jiannan Zhu¹, Adrian Wonfor¹, Rosie Cush², Michael J. Wale², Stephan Pachnicke³, Richard V. Penty¹, Ian H. White¹; ¹University of Cambridge, UK; ²Oclaro Inc., UK; ³ADVA Optical Networking SE, Germany. We describe the performance of an optimized high-temperature DS-DBR laser used as an uncooled WDM source. Constant wavelength output with less than 6GHz error without mode-hopping is shown for C-band channels from 70-90 °C.

08:00– 10:00

STH1H • Advanced Imaging Technologies

Presider: Audrey Ellerbee; Stanford Univ., USA

STH1H.1 • 08:00

Label-Free 3D Imaging for Lab-on-Chip Biomedical Applications, Lisa Miccio¹, Francesco Merola¹, Pasquale Memmolo^{1,2}, Pietro Ferraro¹; ¹CNR-INO Istituto Nazionale di Ottica, Italy; ²Istituto Italiano di Tecnologia - Center for Advanced Biomaterials for Health Care IIT@CRIB, Italy. We demonstrate through a unique and novel approach based on holographic imaging the ability to achieve full morphological 3D analysis and 3D visualization of motile cells and their accurate 3D tracking for Lab-on Chip devices.

STH1H.2 • 08:15

Two-dimensional spectral-encoding for high speed arbitrary patterned illumination, Antony C. Chan¹, Andy Lau¹, Kenneth Wong¹, Edmund Y. Lam¹, Kevin Tsia¹; ¹Dept. of Electrical & Electronic Engineering, Hong Kong. We propose a new tool for scaling the speed of arbitrary patterned illumination by two-dimensional spectral-encoding. A multi-objective optimization based on genetic algorithm is presented for its utility in different imaging modalities.

STH1H.3 • 08:30

Maximally efficient imaging through multimode fiber, Joel A. Carpenter¹, Benjamin J. Eggleton¹, Jochen Schroeder¹; ¹Univ. of Sydney, Australia. Polarization diverse images are generated at the end of a multimode fiber using spatial light modulators to completely characterize propagation through the fiber in terms of the eigenmodes.



Join the conversation. Use #CLEO14.
Follow us @cleoconf on Twitter.

CLEO: Science & Innovations

CLEO: QELS-
Fundamental Science

JOINT

08:00– 10:00
STh1I • Nonlinear Optics in Waveguides and Nanophotonic Devices
Presider: Carl Poitras; Cornell Univ., USA

STh1I.1 • 08:00
Single nanoparticle detection with mode splitting of the microcavity Raman lasers, Bei-Bei Li¹, William R. Clements¹, Xiao-Chong Yu¹, Li Wang¹, Qihuang Gong¹, Yun-Feng Xiao¹; ¹*Peking Univ., China*. We report single nanoparticle detection using mode splitting of the microcavity Raman lasers. Using this method, single polystyrene (PS) nanoparticle down to 20 nm in radius in an aqueous environment is realized.

STh1I.2 • 08:15
Demonstration of Difference Frequency Generation in a Silicon Slot Waveguide, Aleksandar Nestic¹, Robert Palmer¹, Sebastian Koeber^{1,2}, Dietmar Korn¹, Swen Koenig¹, Delwin L. Elder³, Larry R. Dalton³, Wolfgang Freude^{1,2}, Christian G. Koos^{1,2}; ¹*Inst. of Photonics and Quantum Electronics (IPQ), Karlsruhe Inst. of Technology (KIT), Germany;* ²*Inst. of Microstructure Technology, Karlsruhe Inst. of Technology, Germany;* ³*Dept. of Chemistry, Univ. of Washington, USA*. We report on the generation of microwave frequencies of up to 50 GHz by second-order nonlinear mixing of two optical carriers at 1540 nm in a silicon-organic hybrid slot waveguide.

STh1I.3 • 08:30
Supercontinuum Generation in a Silica Spiral Waveguide, Dongyoon Oh¹, David Sell¹, Hansuek Lee¹, Ki Youl Yang¹, Scott A. Diddams², Kerry J. Vahala¹; ¹*T. J. Watson Lab of Applied Physics, California Inst. of Technology, USA;* ²*Time and Frequency Division, National Inst. of Standards and Technology, USA*. A low-loss silica spiral waveguide is used for demonstrating on-chip supercontinuum generation. The broadest measured spectrum spans an octave (936 - 1888 nm) at -50 dB from peak when 2.17 nJ pulses are launched.

08:00– 10:00
STh1J • Structuring Materials with fs Lasers
Presider: Wayne Hess; Pacific Northwest National Lab, USA

STh1J.1 • 08:00 **Tutorial**
Femtosecond Laser Materials Processing, Chunlei Guo¹; ¹*The Inst. of Optics, Univ. of Rochester, USA*. In this tutorial talk, I will discuss the mechanisms and applications of femtosecond laser-material processing.



Chunlei Guo is a professor in Optics and Physics at University of Rochester. His research is in the area of femtosecond laser-matter interactions at high intensities. He is an elected Fellow for both The Optical Society and American Physical Society.

08:00– 10:00
FTh1K • Optomechanics and Optical Manipulation
Presider: Kenneth Crozier; Harvard Univ., USA

FTh1K.1 • 08:00 **Invited**
3D Optical Manipulation of a single 50 nm particle with a scanning evanescent nano-tweezers, Johann Berthelot¹, Srdjan Acimovic¹, Mathieu Juan^{2,3}, Mark Kreuzer¹, Jan Renger¹, Romain Quidant^{1,4}; ¹*ICFO, Spain;* ²*Dept. of Physics & Astronomy, Macquarie Univ., Australia;* ³*ARC Centre for Engineered Quantum Systems, Macquarie Univ., Australia;* ⁴*ICREA, Spain*. Herein, we demonstrate stable optical trapping and accurate 3D manipulation of a single dielectric nanoparticle with a scanning optical near field probe.

FTh1K.2 • 08:30
Photothermal heating enabled by plasmonic nanoantennas for electrokinetic manipulation and sorting of submicron particles, Justus C. Ndukaife^{1,2}, Avnish Mishra¹, Urcan Guler¹, Agwu A. Nnanna^{1,2}, Steven Wereley¹, Alexandra Boltasseva¹; ¹*Purdue Univ., USA;* ²*Water Inst., Purdue Univ. Calumet, USA*. The photo-induced collective heating enabled by a plasmonic nanoantenna array is for the first time harnessed for rapid concentration, manipulation and sorting of particles, with high throughput. This work could find application in biosensing, and surface enhanced spectroscopies.

08:00– 10:00
JTh1L • Symposium on Laser-Driven Sources of Particle and X-Ray Beams I
Presider: Sergei Tochitsky; Univ. of California Los Angeles, USA

JTh1L.1 • 08:00 **Invited**
Laser plasma acceleration using the PW-class BELLA laser, Wim Leemans^{1,2}, Anthony J. Gonsalves¹, Kei Nakamura¹, Hann-Shin Mao¹, Csaba Toth¹, Joost Daniels^{1,3}, Daniel Mittelberger^{1,2}, Carlo Benedetti¹, Stepan Bulanov^{2,1}, Cameron Geddes¹, Jean-Luc Vay¹, Carl B. Schroeder¹, Eric H. Esarey¹; ¹*Lawrence Berkeley National Lab, USA;* ²*UC, USA;* ³*TUE, Netherlands*. Multi-GeV electron acceleration of electrons using intense laser pulses that excite multi-gigavolt fields in plasmas will be discussed. Experimental results with the new BELLA PW-class lasers and supporting simulations will be presented as well as a path forward to apply this acceleration method towards practical machines.

JTh1L.2 • 08:30
Tunable Monoenergetic Electron Beams from Staged Ionization Assisted Laser Wakefield Accelerator, Gregory Golovin¹, Shouyuan Chen¹, Nathan Powers¹, Cheng Liu¹, Sudeep Banerjee¹, Jun Zhang¹, Ming Zeng², Zhengming Sheng², Donald Umstadter¹; ¹*Physics and Astronomy, UNL, USA;* ²*Physics and Astronomy, Shanghai Jiao Tong Univ., China*. By employing a pair of partially overlapped supersonic gas jets, we made a separation of injection and acceleration stages of laser wakefield acceleration and produced stable, quasi-monoenergetic (10-30% FWHM) and tunable (50-300 MeV) electron beams.

Marriott
Salon III

CLEO: Science &
Innovations

08:00– 10:00

STh1M • Modulators using
Novel Materials

Presider: Juerg Leuthold; ETH
Zurich, Switzerland

STh1M.1 • 08:00

Electro-optic Modulation of Small Disk Microcavity through Gated Graphene, Majid Sodagar¹, Hesam Moradinejad¹, Ali A. Eftekhar¹, Ali Adibi¹; ¹Georgia Inst. of Technology, USA. Monolayer graphene sheet has been integrated on top of small disk optical resonator in SOI platform. Electro-optic interaction between graphene and whispering gallery mode of the cavity has been demonstrated and studied for modulation application.

STh1M.2 • 08:15

Hybrid Si₃N₄-Graphene Nanophotonic Circuits for Electro-Optic Modulation, Nico Gruhler¹, Christian Benz^{1,2}, Romain Danneau^{1,2}, Wolfram Pernice¹; ¹Inst. of Nanotechnology, Karlsruhe Inst. of Technology, Germany; ²Inst. of Physics, Karlsruhe Inst. of Technology, Germany. We present graphene-based optical modulators integrated with Si₃N₄ waveguides, which allow for utilizing graphene's broad flat absorption from visible to infrared wavelengths. Tunable attenuation of 0.067 dB/μm is measured in Mach-Zehnder and microring resonators.

STh1M.3 • 08:30

Simultaneous optical modulation and detection using graphene integrated on a silicon waveguide, Nathan Youngblood¹, Yoska Anugrah¹, Rui Ma¹, Steven Koester¹, Mo Li¹; ¹Electrical and Computer Engineering, Univ. of Minnesota, USA. A dual-mode, graphene optical modulator and detector for the near-IR is demonstrated in a single device. Gate dependent photocurrent and optical transmission allow the device to operate in a highly novel mode of simultaneous optical modulation and detection.

Marriott
Salon V & VI

CLEO: Science &
Innovations

08:00– 10:00

STh1N • Comb
Spectroscopy

Presider: Brian Washburn; Kansas
State Univ., USA

STh1N.1 • 08:00

Broadband Midinfrared Comb-Resolved Fourier Transform Spectroscopy, Kevin F. Lee¹, Piotr Maslowski², Andrew Mills¹, Christian Mohr¹, Jie Jiang¹, Chien C. Lee³, Thomas R. Schibli^{3,4}, Peter G. Schunemann⁵, Martin Fermann¹; ¹IMRA America, Inc., USA; ²Inst. of Physics, Faculty of Physics, Astronomy and Informatics, Nicolaus Copernicus Univ., Poland; ³Dept. of Physics, Univ. of Colorado at Boulder, USA; ⁴JILA, National Inst. of Standards and Technology and Univ. of Colorado, USA; ⁵BAE Systems, USA. We combine a Tm-fiber frequency comb, phase-locked doubly-resonant GaAs optical parametric oscillator, multipass cell, and Fourier transform spectrometer to measure comb-resolved spectra at wavelengths of 3.1 to 5.5 micrometers for multiple gases at trace concentrations.

STh1N.2 • 08:15

Spectrally Interleaved, Comb-Mode-Resolved, Dual-Terahertz-Comb Spectroscopy, Yi-Da Hsieh¹, Yuki Iyonaga¹, Yoshiyuki Sakaguchi¹, Shuko Yokoyama², Hajime Inaba^{3,4}, Kaoru Minoshima^{4,5}, Francis Hindle⁶, Tsutomu Araki¹, Takeshi Yasui^{4,7}; ¹Osaka Univ., Japan; ²Micro Optics Co., Ltd, Japan; ³National Inst. of Advanced Industrial Science and Technology, Japan; ⁴JST-ERATO Intelligent Optical Synthesizer Project, Japan; ⁵The Univ. of Electro-Communications, Japan; ⁶Université du Littoral Côte d'Opale, Japan; ⁷The Univ. of Tokushima, Japan. We demonstrated combination of spectrally interleaved terahertz (THz) frequency comb with dual-comb spectroscopy, enabling us to achieve the spectral sampling equal to linewidth of the comb tooth in the low-pressure gas spectroscopy in THz region.

STh1N.3 • 08:30

Sub-kHz-Linewidth Mid-infrared Optical Parametric Oscillator, Maurizio De Rosa¹, Iolanda Ricciardi¹, Simona Mosca¹, Maria Parisi¹, Pasquale Maddaloni¹, Luigi Santamaria¹, Giovanni Giusfredi^{2,3}, Paolo De Natale^{2,3}; ¹Istituto Nazionale di Ottica, Consiglio Nazionale delle Ricerche, Italy; ²Istituto Nazionale di Ottica, Consiglio Nazionale delle Ricerche, Italy; ³LENS, Italy. We present a transfer oscillator scheme between the pump and signal modes of a singly resonant optical parametric oscillator, emitting in the range 2.7–4.2 μm, demonstrating sub-kHz linewidth of the idler mode.

Marriott
Willow Glen I-III

CLEO: Applications
& Technology

08:00– 10:00

ATH1O • OCT-Technology
Development & Clinical
Applications

Presider: Nicusor Iftimia; Physical
Sciences Inc., USA

ATH1O.1 • 08:00 **Invited**

Progress on Cellular Resolution Retinal Imaging: Setting the Stage for Translation between Clinical and Basic Science, Robert J. Zawadzki^{1,2}; ¹Ophthalmology & Vision Science, Univ. of California Davis, USA; ²Cell Biology and Human Anatomy, Univ. of California Davis, USA. I will review our progress on developing clinical and animal (mice) cellular resolution in vivo retinal imaging modalities. Example applications of these technologies to in vivo studies of microscopic retinal morphology will be presented.

ATH1O.2 • 08:30

Optical Coherence Imaging of Microvascular Oxygenation and Hemodynamics, Shau Poh Chong¹, Conrad Merkle¹, Harsha Radhakrishnan¹, Conor Leahy¹, Alfredo Dubra^{2,3}, Yusuf Sulai⁴, Vivek J. Srinivasan¹; ¹Biomedical Engineering, Univ. of California Davis, USA; ²Dept. of Ophthalmology, Medical College of Wisconsin, USA; ³Dept. of Biophysics, Medical College of Wisconsin, USA; ⁴The Inst. of Optics, Univ. of Rochester, USA. Here, we present high-speed spectral range using a supercontinuum source that performs angiography, oximetry, and speed assessment of red blood cells in individual vessels of the mouse pinna in vivo.

CLEO: QELS-Fundamental Science

FTh1A • Quantum
Entanglement—Continued

FTh1A.4 • 08:45

High visibility two-photon interference of entangled photons from a quasi-phase-matched AlGaAs waveguide, Peyman Sarrafi¹, Eric Y. Zhu¹, Barry Holmes², David Hutchings², J. Stewart Aitchison¹, Li Qian¹; ¹ECE, Univ. of Toronto, Canada; ²School of Engineering, Univ. of Glasgow, UK. We experimentally demonstrate time-frequency entanglement of photon pairs produced in a cw-pumped quasi-phased-matched AlGaAs superlattice waveguide, producing 8E06 pairs/s with 96.0±0.7% visibility without background subtraction, highest known visibility by far in AlGaAs waveguides.

FTh1A.5 • 09:00

Demonstration of high-visibility two-photon interference with a multimode waveguide source, Michal Jachura¹, Michal Karpinski², Czeslaw Radzewicz¹, Konrad Banaszek¹; ¹Faculty of Physics, Univ. of Warsaw, Poland; ²Clarendon Lab, Univ. of Oxford, UK. We verified interferometrically generation of spatially pure photon pairs via spontaneous parametric down-conversion in a multimode nonlinear waveguide in the 800 nm spectral region, obtaining two-photon interference visibility robustly exceeding 90% without any spatial filtering.

FTh1A.6 • 09:15

Entangling color-different photons via time-resolved measurement and active feed-forward, Tian-Ming Zhao^{1,2}, Han Zhang^{1,2}, Jian Yang^{1,2}, Zi-Ru Sang^{1,2}, Jiang Xiao^{1,2}, Xiao-Hui Bao^{1,2}, Jian-Wei Pan^{1,2}; ¹Hefei National Lab for Physical Sciences at Microscale and Dept. of Modern Physics, Univ. of Science and Technology of China, China; ²Synergetic Innovation Center of Quantum Information and Quantum Physics, Univ. of Science and Technology of China, China. We report an experiment of entangling independent color-different photons by using time-resolved measurement and active feed-forward. Our work provides an approach to solve the frequency mismatch problem for the interconnection between dissimilar quantum systems in a quantum network.

FTh1A.7 • 09:30

A Time-Bin Qubit Entangler based on Photon Switching, Hiroki Takesue¹; ¹NTT Basic Research Labs, Japan. I present a simple scheme for entangling two independent time-bin qubits using quantum interference at a high-speed 2x2 optical switch. Non-classical two photon interference fringes were observed experimentally by using the proposed scheme.

FTh1B • Quantum
Interconnects—Continued

FTh1B.2 • 09:00

Realisation of a photonic link between a trapped ion and a semiconductor quantum dot, Claire Le Gall¹, Robert Stockill¹, Matthias Steiner¹, Hendrik-Marten Meyer^{1,2}, Clemens Matthiesen¹, Jakob Reichel³, Edmund Clarke⁴, Arne Ludwig⁵, Michael Koehl^{1,2}, Mete Atatüre¹; ¹Cavendish Lab, Univ. of Cambridge, UK; ²Physikalisches Institut, Univ. of Bonn, Germany; ³Laboratoire Kastler Brossel, France; ⁴EPSRC National center for III-V nanotechnologies, Univ. of Sheffield, UK; ⁵Lehrstuhl für Festkörperphysik, Ruhr-Universität Bochum, Germany. We report on the first photonic link between a quantum dot and a single ion and show that the ion absorption probability per quantum dot photon can reach 1.2%.

FTh1B.3 • 09:15

Observation of High-Purity Single Photons Hopping between Optical Cavities, Kenzo Makino¹, Jun-ichi Yoshikawa¹, Yosuke Hashimoto¹, Peter van Loock², Akira Furusawa¹; ¹Applied Physics, Univ. of Tokyo, Japan; ²Physics, Johannes Gutenberg-Universität Mainz, Germany. We experimentally demonstrate high-purity single photons hopping coherently between coupled optical cavities. The system shows high performance also as a controllable single-photon source, which emits single photons with a negative Wigner function.

FTh1B.4 • 09:30

Certified quantum non-demolition measurement of atomic spins, Robert Sewell¹, Mario Napolitano¹, Naeimeh Behbood¹, Georgio Colangelo¹, Ferran Martin Ciarana¹, Morgan W. Mitchell^{1,2}; ¹ICFO -The Inst. of Photonic Sciences, Spain; ²CREA, Spain. We report certified quantum non-demolition measurement of atomic spins using criteria developed for continuous variable experiments in optics. We observe quantum state preparation and information–damage trade-off beyond classical limits by seven and twelve standard deviations.

FTh1C • High-Field THz
Physics—Continued

FTh1C.3 • 08:45

Selective THz excitation of collective modes in underdoped YBCO, Georgi L. Dakovski¹, Wei-Sheng Lee¹, Joshua J. Turner¹, Matthias C. Hoffmann¹; ¹SLAC National Accelerator Lab, USA. We use intense broadband THz pulses to excite underdoped YBCO exhibiting competing superconducting and charge density wave ground states. We observe pronounced coherent oscillations at 1.85 and 2.65THz, attributed to renormalized low-energy phonon modes.

FTh1C.4 • 09:00

Femtosecond Insulator-Metal Transition in VO₂ Induced by Intense Multi-THz Transients, Alexander Grupp¹, Bernhard Mayer¹, Christian Schmidt¹, Jannis Oelmann¹, Robert E. Marvel², Richard F. Haglund², Alfred Leitenstorfer¹, Alexej Pashkin¹; ¹Dept. of Physics and Center for Applied Photonics, Univ. of Konstanz, Germany; ²Dept. of Physics and Astronomy, Vanderbilt Univ., USA. A non-thermal insulator-metal transition in VO₂ has been driven by a non-resonant excitation at frequencies around 25 THz. A switching time of 80 fs is found, corresponding to approximately two cycles of the driving field.

FTh1C.5 • 09:15

High Harmonic Generation in Graphene at Terahertz Frequencies, Ibraheem Al-Naib¹, John E. Sipe², Marc M. Dignam¹; ¹Dept. of Physics, Engineering Physics and Astronomy, Queen's Univ., Canada; ²Dept. of Physics and Inst. for Optical Sciences, Univ. of Toronto, Canada. We employ a density-matrix formalism in the length gauge to simulate the nonlinear terahertz response of graphene. The generation of high harmonics is dominated by the strong interplay between intraband and interband dynamics.

FTh1C.6 • 09:30

Terahertz second-order nonlinear optics in a graphene-metamaterial device: difference-frequency generation, Chihun In¹, Hyeon-don Kim², Bumki Min², Hyunyoung Choi¹; ¹School of Electrical and Electronic Engineering, Yonsei Univ., Korea; ²Dept. of Mechanical Engineering, Korea Advanced Inst. of Science and Technology (KAIST), Korea. We show the first experimental demonstration of nonlinear second-order terahertz frequency generation in a graphene-metamaterial device. Characteristic ultrafast nature of graphene and strong metamaterials' nonlinear resonances enables to observe the nonlinear difference frequency generation.

FTh1D • Solitons and Temporal
Effects—Continued

FTh1D.4 • 08:45

Higher-Order Equilibrium States of Temporal Soliton Molecules, Alexander Hause¹, Fedor Mitschke¹; ¹Univ. of Rostock, Germany. Bound states of fiber-optic dispersion-managed solitons are investigated. When the pulse separation is increased, a sequence of alternatingly stable and unstable equilibria arises; it terminates at a point defined by the radiation background.

FTh1D.5 • 09:00

Generation of a Train of Ultrashort Pulses by Simply Inserting Transparent Plates on the Optical Path, Kazumichi Yoshii¹, Yoshitaka Nakamura¹, Kohei Hagihara¹, Masayuki Katsuragawa¹; ¹Engineering Science, Univ. of Electro-communications, Japan. We experimentally demonstrate generation of a train of ultrashort pulses with a nearly TL pulse duration of 1.78 fs by simply inserting transparent plates on the optical axis and adjusting their thicknesses precisely.

FTh1D.6 • 09:15

Dissipative Vectorial Solitons in Semiconductor Lasers, Mathias Marconi¹, Julien Javaloyes², Stephane Barland¹, Salvador Balle³, Massimo Giudici¹; ¹Institut Non Linéaire de Nice, Université de Nice Sophia Antipolis - CNRS, France; ²Departamento de Física, Universitat de les Illes Balears, Spain; ³Institut Mediterrani d'Estudis Avançats, CSIC, Spain. Nonlinear polarization dynamics of VCSELs with a long-delay external cavity lead to vectorial dissipative solitons. The large temporal aspect-ratio enables the observation of multiple -- independent and/or bound -- solitons within the same roundtrip.

FTh1D.7 • 09:30

Temporal dynamics of all-optical switching in Photonic Crystal Cavity, Pierre Colman¹, Yi Yu¹, Mikkell Heuck¹, Per Lunnemann Hansen¹, Kresten Yvind¹, Jesper Mørk¹; ¹DTU Fotonik, Denmark. The temporal dynamics of all-optical switching has been investigated in a Photonic Crystal Cavity with a 150fs-40aJ/pulse resolution. This allowed observing for the first time effects like pulse reshaping, pulse delay and intra-cavity Four-Wave-Mixing.

CLEO: Science & Innovations

STH1E • Filamentation—
Continued

STH1E.4 • 08:45

Observation of free electron density oscillation in filamentation as a function of carrier-envelope phase, Lifeng Wang¹, Hao Teng¹, Xin Lu¹, Shiyong Chen¹, Xinkui He¹, Peng He¹, Zhiyi Wei¹; ¹*Inst. of Physics, The Chinese Academ, China*. The free electron density in a 40 mm long filamentation generated by carrier-envelope stabilized few-cycle laser pulses is detected in a circular loop. The oscillation of electron density is observed as a function of CEP.

STH1E.5 • 09:00

Diagnostics of rotational wavepackets of nitrogen molecules by strong-field-ionization induced air lasers, Jielei Ni¹, Haisu Zhang¹, Wei Chu¹, Bin Zeng¹, Jinping Yao¹, Guihua Li¹, Chenrui Jing¹, Hongqiang Xie¹, Huailiang Xu², Ya Cheng¹; ¹*State Key Lab of High Field Laser Physics, Shanghai Inst. of Optics and Fine Mechanics, China*; ²*State Key Lab on Integrated Optoelectronics, College of Electronic Science and Engineering, Jilin Univ., China*. We report on diagnostics of rotational wavepackets coherently generated in strong-field-ionized nitrogen molecules with a seed-amplified air lasing scheme, and the first observation on Raman scattering of neutral nitrogen molecules with such an "air laser."

STH1E.6 • 09:15

A new and improved approach to super-continuum generation in solids, Chih-Hsuan Lu¹, Yu-Chen Cheng², Shang-Da Yang¹, Yuan-Yao Lin¹, Chia-Chen Hsu³, Andy Kung¹; ¹*National Tsing Hua Univ., Taiwan*; ²*Inst. of Atomic and Molecular Sciences, Taiwan*; ³*National Chung Cheng Univ., Taiwan*. A stable octave-spanning supercontinuum with excellent beam quality is generated by high-intensity spectral broadening in bulk fused silica plates in a cascaded arrangement.

STH1E.7 • 09:30

Study of Filamentation Threshold in Zinc Selenide, Magali M. Durand¹, Aurelien Houard², Khan Lim¹, Anne Durécu³, Olivier Vasseur³, Martin Richardson¹; ¹*Townes Laser Inst., CREOL - Univ. of Central Florida, USA*; ²*Laboratoire d'Optique Appliquée, ENSTA ParisTech - Ecole Polytechnique, CNRS, France*; ³*ONERA, France*. Filamentation in different multi-photon absorption regimes was studied using different laser wavelengths in a zinc selenide crystal. The 3-photon ionization/absorption threshold was verified, and the impact of absorption on filament formation was observed.

STH1F • THz Quantum Cascade
Lasers—ContinuedSTH1F.4 • 08:45 **Invited**

The Development and Applications of Terahertz Quantum Cascade Lasers, Edmund Linfield¹, Lianhe Li¹, P. Dean¹, A. G. Davies¹; ¹*Univ. of Leeds, UK*. This paper will review the development of terahertz frequency quantum cascade lasers, including the achievement of >1W output powers. It will also discuss self-mixing imaging, where the laser cavity is used as a coherent detector.

STH1F.5 • 09:15

THz imaging of free carrier density based on quantum cascade lasers under optical feedback, francesco P. mezzapesa^{1,2}, Lorenzo L. Colombo^{1,3}, Massimo Brambilla^{1,3}, Maurizio Dabbicco^{1,2}, Harvey E. Beere⁴, David A. Ritchie⁴, Miriam S. Vitiello⁵, Gaetano Scarmacio^{1,2}; ¹*Dip. Interuniversitario di Fisica, Università degli Studi e Politecnico di Bari, Italy*; ²*CNR-IFN, Italy*; ³*Dipartimento di Scienza ed Alta tecnologia, Università dell'Insubria, Italy*; ⁴*Cavendish Lab, Univ. of Cambridge, UK*; ⁵*NEST - CNR, Italy*. Detectorless THz imaging based on quantum cascade lasers operating under optical feedback to monitor the spatial distribution of free electron plasma induced onto a semiconductor by photo-excitation with a reconfigurable pattern of NIR laser pump.

STH1F.6 • 09:30

Towards Doppler-Free QCL-based Metrological THz Spectroscopy, Luigi Consolino¹, Saverio Bartalini^{1,2}, Annamaria Campa¹, Harvey E. Beere⁴, David A. Ritchie⁴, Miriam S. Vitiello³, Pablo Cancio Pastor¹, Davide Mazzotti¹, Paolo De Natale^{1,2}; ¹*CNR - INO, Italy*; ²*LENS, Italy*; ³*CNR - NEST, Italy*; ⁴*Cavendish Lab, UK*. New frontiers for high precision THz spectroscopy are presented. Current limits can be overcome by exploiting saturation effects on molecular transitions and coupling THz QCL radiation to an optical cavity.

STH1G • Semiconductor Lasers
for Communication—Continued

STH1G.4 • 08:45

1.55 μm DFB laser monolithically integrated with power amplifier array, Lianping Hou¹, Marc Sorel¹, John H. Marsh¹; ¹*Univ. of Glasgow, UK*. We present a highly efficient laterally-coupled 1.55 μm DFB laser monolithically integrated with multistage MMIs and SOAs, using low bias currents and providing an output power of ~100 mW with a low divergence angle.

STH1G.5 • 09:00

Optical Characteristics of 1.3- μm Dual-Mode Laser Diode with Integrated Semiconductor Optical Amplifier, Namje Kim¹, Sang-Pil Han¹, Kiwon Moon¹, Il-Min Lee¹, Eui Su Lee¹, Kyung Hyun Park¹; ¹*THz Photonics Creative Research Center, Electronics and Telecommunications Research Inst., Korea*. A 1.3- μm dual-mode laser diode with an integrated semiconductor optical amplifier with high output power of over 80 mW has been developed as an optical beat source for a continuous wave terahertz system.

STH1G.6 • 09:15

1.3 μm InAs/GaAs Quantum Dot Lasers on SOI Waveguide Structures, Katsuaki Tanabe^{1,2}, Yasuhiko Arakawa^{2,3}; ¹*Inst. for Nano Quantum Information Electronics, Univ. of Tokyo, Japan*; ²*Inst. for Photonics-Electronics Convergence System Technology, Japan*; ³*Inst. of Industrial Science, Univ. of Tokyo, Japan*. A 1.3- μm InAs/GaAs quantum dot laser on a silicon-on-insulator waveguide structure with a threshold current density of 300 A/cm² and lasing temperatures greater than 100°C is fabricated by direct wafer bonding and layer transfer.

STH1G.7 • 09:30 **Invited**

Quantum Teleportation using Entangled LEDs, Richard M. Stevenson¹, Jonas Nilsson¹, K. H. A. Chan^{1,2}, Anthony J. Bennett¹, Joanna Skiba-Szymanska¹, Marco Lucamarini¹, Martin B. Ward¹, Ian Farrer², David A. Ritchie², Andrew J. Shields¹; ¹*Toshiba Research Europe Limited, UK*; ²*Cavendish Lab, Univ. of Cambridge, UK*. Quantum teleportation can relay quantum information, and enable near-deterministic quantum circuits. Previous linear-optical implementations use optically excited, similar light sources. We show teleportation using electrically excited entangled light, even for dissimilar, laser generated input qubits.

STH1H • Advanced Imaging
Technologies—Continued

STH1H.4 • 08:45

Enhanced Spatial Resolution in Confocal Laser Microscopy by Subtractive Imaging Using Vector Beams, Susumu Segawa¹, Yuichi Kozawa¹, Shunichi Sato¹; ¹*Inst. of Multidisciplinary Research for Advanced Materials, Tohoku Univ., Japan*. The enhanced spatial resolution in confocal laser microscopy is demonstrated by subtracting two confocal images acquired by radially and azimuthally polarized beams. The effect of the side-lobe emerging in the subtraction processes is also discussed.

STH1H.5 • 09:00

Real-time Optical Diffraction Tomography for 3-D Visualization of Microscopic Particles, Kyoohyun Kim¹, Kyung Sang Kim², HyunJoo Park¹, JongChul Ye², YongKeun Park¹; ¹*Dept. of Physics, KAIST, Korea*; ²*Dept. of Bio and Brain Engineering, KAIST, Korea*. We develop a real-time reconstruction technique in optical diffraction tomography for the visualization of 3-D refractive index distribution using sparse angle illumination and graphic processing unit implementation. We apply the method to image dynamics of colloidal dimers and red blood cells.

STH1H.6 • 09:15 **Invited**

Computational Imaging and Sensing for Biophotonics Applications, Aydogan Ozcan¹; ¹*Electrical Engineering and Bio-engineering Depts., Univ. of California Los Angeles, USA*. We review our recent progress on computational imaging and sensing techniques aiming various bio-photonics applications.

CLEO: Science & Innovations

CLEO: QELS-
Fundamental Science

JOINT

STH1I • Nonlinear Optics in
Waveguides and Nanophotonics
Devices—Continued

STH1I.4 • 08:45

Effects of Multiphoton Absorption on Parametric Comb Generation in Silicon Microresonators, Ryan K. Lau¹, Yoshitomo Okawachi¹, Michael R. Lamont^{1,2}, Alexander L. Gaeta^{1,2}; ¹*School of Applied and Engineering Physics, Cornell Univ., USA*; ²*Kavli Inst. at Cornell for Nanoscale Science, Cornell Univ., USA*. We investigate theoretically parametric frequency comb generation in silicon microresonators for telecom and mid-infrared (MIR) wavelengths in the presence of multiphoton absorption. Parametric oscillation is inhibited at telecom wavelengths but can occur at MIR wavelengths.

STH1I.5 • 09:00

On-chip ultra-broad frequency conversion via simultaneous second and third-order optical nonlinearity, Steven Miller¹, Kevin Luke¹, Yoshitomo Okawachi², Jaime Cardenas¹, Alexander L. Gaeta^{2,3}, Michal Lipson^{1,3}; ¹*School of Electrical and Computer Engineering, Cornell Univ., USA*; ²*School of Applied and Engineering Physics, Cornell Univ., USA*; ³*Kavli Inst. at Cornell for Nanoscale Science, Cornell Univ., USA*. We demonstrate ultra-broad frequency conversion through simultaneous second and third-order nonlinearities. Using a high-Q resonator, we generate multiple frequency lines in both the near-IR and in the visible range using a single near-IR CW pump.

STH1I.6 • 09:15

Slow-light enhanced Brillouin frequency comb generation on a chip, Moritz Merklein¹, Irina V. Kabakova¹, Thomas Buettner¹, Steve Madden², Barry Luther-Davies², Duk-Yong Choi², Benjamin J. Eggleton¹; ¹*Univ. of Sydney, Australia*; ²*Australian National Univ., Australia*. We present the experimental observation of the slow-light enhancement effect on the generation of a frequency comb formed by stimulated Brillouin scattering (SBS) in a chip scale As_2S_3 rib waveguide.

STH1I.7 • 09:30

All chalcogenide Raman-parametric laser, wavelength converter and broadband source in a single microwire, Raja Ahmad¹, Martin Rochette¹; ¹*McGill Univ., Canada*. We present a chalcogenide microwire device that acts as a compact (~11 cm length, ~1 μ m diameter) and power efficient (sub-Watt threshold peak power, >2% slope efficiency) Raman-parametric laser, wavelength converter and ultra-broadband supercontinuum generator/amplifier.

STH1J • Structuring Materials
with fs Lasers—Continued

STH1J.2 • 09:00

Femtosecond-laser inscription via local modification of the glass composition in phosphate glasses, Jesus Hoyo¹, Belen Sotillo², Jan Siegel¹, Toney T. Fernandez¹, Paloma Fernandez², Patricia Haro³, Daniel Jaque³, Margarita Hernandez², Concepcion Domingo⁴, Javier Solis¹; ¹*Laser Processing Group, Instituto de Optica, CSIC, Spain*; ²*Depto. de Fisica de Materiales, Univ. Complutense, Spain*; ³*Fluorescence Imaging Group, Depto. de Fisica de Materiales, Univ. Autonoma de Madrid, Spain*; ⁴*Instituto de Estructura de la Materia, CSIC, Spain*. Femtosecond laser inscription of high performance active/passive waveguides is demonstrated in phosphate glass via local modification of the glass composition. La-K cross diffusion plays a key role in the performance of the generated structures.

STH1J.3 • 09:15

Polarization-Sensitive Cat's Eye Structuring of Silicon by Ultrashort Light Pulses, Jingyu Zhang¹, Rokas Drevinskas¹, Martynas Beresna¹, Mindaugas Gecevicius¹, Peter G. Kazansky¹; ¹*Optoelectronics Research Centre, Univ. of Southampton, UK*. Sub-wavelength ridge structures are observed on silicon surface after irradiation with two femtosecond pulses. Cat's-eye-shaped structures are aligned perpendicular to polarization of the second pulse and can be used for polarization-sensitive recording.

STH1J.4 • 09:30

In-Situ Measurement of the Intrinsic Polymerization Time During Three-Dimensional Direct Laser Writing, Jonathan B. Mueller¹, Joachim Fischer², Martin Wegener^{1,2}; ¹*Inst. of Applied Physics and DFG-Center for Functional Nanostructures, Karlsruhe Inst. of Technology, Germany*; ²*Inst. of Nanotechnology, Karlsruher Institut für Technologie, Germany*. We focus a short writing-pulse burst into a photo-resist, polymerizing a voxel. The time-resolved transmission of a co-focused second laser probes the voxel formation dynamics. We measure time constants as small as 400 μ s.

FTH1K • Optomechanics
and Optical Manipulation—
Continued

FTH1K.3 • 08:45

New Techniques in Optical Trapping and Sensing, Lulu Liu¹, Alexander Woolf¹, Federico Capasso¹; ¹*Harvard Univ., USA*. We demonstrate several new techniques that expand the current capabilities of optical trapping and sensing, and demonstrate the application of a combination of these techniques in the successful measurement of near-field optical and double-layer forces.

FTH1K.4 • 09:00

Optomechanics with photonic crystals slab mirrors and cavities, Isabelle Robert-Philip¹, Rémy Braive¹, Isabelle Sagnes¹, Izo Abram¹, Alexios Beveratos¹, Thomas Antoni², Kevin Makles², Aurélien Kuhn², Tristan Briant², Pierre-François Cohadon², Emanuel Gavartin³, Tobias Kippenberg³; ¹*LPN, CNRS, France*; ²*LKB, CNRS, France*; ³*EPFL, Switzerland*. We investigate optomechanical effects in photonic crystal slab membranes, either including a cavity or acting as an end-mirror in a Fabry-Perot cavity. We in particular demonstrate the non-linear behavior of the membranes fundamental mode.

FTH1K.5 • 09:15

Torsional Cavity Optomechanical Nano-Seesaw System, Huan Li¹, Mo Li¹; ¹*Electrical and Computer Engineering, Univ. of Minnesota, USA*. A novel torsional cavity optomechanical system consisting of a nano-seesaw with one photonic crystal cavity on each side has been demonstrated, which exhibits extremely high mechanical sensitivity and can potentially reveal new optomechanical phenomena.

FTH1K.6 • 09:30

Bidimensional nano-optomechanics and topological backaction in a non-conservative radiation force field, Arnaud Gloppe¹, Pierre Verlot¹, Eva Dupont-Ferrier¹, Aurélien G. Kuhn¹, Alessandro Siria², Philippe Poncharal², Guillaume Bachelier¹, Pascal Vincent², Olivier Arcizet¹; ¹*Institut Néel, Université Grenoble Alpes - CNRS UPR2940, France*; ²*Institut Lumière Matière, UMR5306, CNRS - Université Claude Bernard Lyon 1, France*. We explore the vectorial optomechanical interaction between a nanowire and a focused beam of light. The nanowire is sensitive to the topological variations of the focused laser force field which dramatically modify the phenomenology of the dynamical backaction.

JTH1L • Symposium on Laser-
Driven Sources of Particle and
X-Ray Beams I—Continued

JTH1L.3 • 08:45

High Power Guiding and Electron Acceleration in Pure N5+ Plasma Channels, Andy Goers¹, Sung Yoon¹, George Hine¹, Jennifer Elle¹, Howard Milchberg¹; ¹*Univ. of Maryland, USA*. We examine the interaction of relativistic laser pulses with plasma channels formed in a nitrogen cluster jet. We observe creation of nearly pure N5+ plasma channels and ionization injected wakefield beams with energies. >100 MeV.

JTH1L.4 • 09:00

Single-shot visualization of evolving plasma bubble accelerators by frequency-domain streak camera, Zhengyan Li¹, Hai-En Tsai¹, Chih-Hao Pai¹, Rafal Zgadzaj¹, Xiaoming Wang¹, X. Zhang¹, V. Khudik¹, Gennady Shvets¹, Michael C. Downer¹; ¹*Univ. of Texas at Austin, USA*. We visualize formation, propagation and collapse of laser-driven plasma bubbles using a single-shot frequency domain streak camera, thereby identifying bubble dynamics that optimize electron injection and acceleration.

JTH1L.5 • 09:15 **Invited**

Current Status and Future Prospects of Laser-driven Ion Sources, Marco Borghesi^{1,2}; ¹*Centre for Plasma Physics, The Queen's Univ. of Belfast, UK*; ²*ELI Beamlines project, Inst. of Physics of the ASCR, Czech Republic*. Laser-driven ion acceleration is attracting an impressive and steadily increasing research effort. The talk will review the state of the art in this field, focusing on emerging mechanisms which hold high promise for further progress.

CLEO: Science & Innovations

STh1M • Modulators using Novel Materials—Continued

STh1M.4 • 08:45 **Low Insertion Loss Graphene based Absorption Modulator on SOI Waveguide**, Muhammad Mohsin¹, Daniel Schall¹, Martin Otto¹, Daniel Neumaier¹, Heinrich Kurz¹; ¹Advanced Microelectronic Center Aachen (AMICA), AMO GmbH, Germany. We present a graphene based absorption modulator on SOI waveguide with very low insertion loss. The device showed a modulation of 16 dB and an insertion loss of only 3.3dB, surpassing GeSi based absorption modulators.

STh1M.5 • 09:00 **A silicon integrated BaTiO₃ electro-optic modulator**, Chi Xiong¹, Wolfram Pernice¹, Joseph Ngai¹, James Reiner¹, Divine Kumah¹, Fred Walker¹, Charles Ahn¹, Hong Tang¹; ¹Yale Univ., USA. A Si-integrated modulator based on epitaxial ferroelectric aTiO₃ thin films is demonstrated with gigahertz modulation bandwidth and an effective Pockels coefficient of 213 ± 49 pm/V.

STh1M.6 • 09:15 **Silicon on Lithium Niobate: A Hybrid Electro-Optical Platform for Near- and Mid-Infrared Photonics**, Jeff Chiles¹, Sasan Fathpour¹; ¹CREOL, The College of Optics and Photonics, Univ. of Central Florida, USA. A thin layer of silicon is transferred onto a lithium niobate substrate, forming a hybrid electro-optical platform, on which ring resonators are fabricated and characterized at 1550 nm, showing an optical loss of 3.0±0.5 dB/cm.

STh1M.7 • 09:30 **Large Photo-Induced Group Delay Variations in Chalcogenide-on-Silicon Mach-Zehnder Interferometers**, Ran Califa¹, Yuri Kaganovskii², Dvir Munk¹, Hadar Genish², Idan Bakish¹, Michael Rosenbluh², Avi Zadok¹; ¹Faculty of Engineering, Bar-Ilan Univ., Israel; ²Dept. of Physics, Bar-Ilan Univ., Israel. The rapid post-fabrication trimming of the group index in hybrid chalcogenide-on-silicon Mach-Zehnder interferometers is demonstrated. Index changes of 0.065 are achieved through photo-induced mass transfer in an As10Se90 layer.

CLEO: Science & Innovations

STh1N • Comb Spectroscopy—Continued

STh1N.4 • 08:45 **High-Coherence Mid-Infrared Frequency Comb Generation and Applications**, Francesco Cappelli^{1,2}, Iacopo Galli^{1,2}, Pablo Cancio Pastor^{1,2}, Giovanni Giusfredi^{1,2}, Davide Mazzotti^{1,2}, Saverio Bartalini^{1,2}, Paolo De Natale^{1,2}; ¹CNR-INO, Italy; ²LENS, Italy. We report on the generation of a highly-coherent frequency comb around 4330 nm. A quantum cascade laser has been effectively phase-locked to a comb tooth and its frequency noise has been measured.

STh1N.5 • 09:00 **Multi-octave Acousto-Optic Spectrum Analyzer for Mid-Infrared Pulsed Sources**, Grégory Gitzinger¹, Vincent Crozatier¹, Raman Maksimenka¹, Stéphanie Grabielle¹, Nicolas Forget¹, Skirmantas Alisauskas³, Audrius Puglys³, Andrius Baltuska³, Balazs Monozslai³, Carlo Vicario³, Christoph P. Hauri^{2,4}; ¹FASTLITE, France; ²Paul Scherrer Inst., Switzerland; ³Institut für Photonik, Technische Universität Wien, Austria; ⁴Ecole Polytechnique Federale de Lausanne, Switzerland. Demonstration of an acousto-optic filter based infrared spectrometer featuring a 5 cm⁻¹ resolution over more than 2 octaves (1 to 5 micron) is reported.

STh1N.6 • 09:15 **Ultra-Broadband Near-Infrared Dual-Comb Spectroscopy**, Sho Okubo¹, Kana Iwakuni^{1,2}, Hajime Inaba¹, Kazumoto Hosaka¹, Atsushi Onae¹, Hiroyuki Sasada², Feng-Lei Hong¹; ¹National Metrology Inst. of Japan, National Inst. of Advanced Industrial Science and Technology, Japan; ²Faculty of Science and Technology, Keio Univ., Japan. We extend the spectral bandwidth of dual-comb spectroscopy over a hundred THz using two optical frequency combs with relative linewidth of sub-Hz level. We record the spectrum of the entire vibration band of acetylene.

STh1N.7 • 09:30 **Ultra-Long Duration Time-Resolved Spectroscopy with Enhanced Temporal Resolution of High-Q Nano-Optomechanical Modes using Interleaved Asynchronous Optical Sampling (I-ASOPS)**, Aleem M. Siddiqui¹, Robert L. Jarecki¹, Andrew Starbuck¹, Jonathan A. Cox¹; ¹Sandia National Labs, USA. Transient responses of high-Q nano-optomechanical modes are characterized with interleaved-ASOPS, where pump-induced transients are interrogated with multiple probe pulses. Temporal resolution increases with probe-pulse-number beyond conventional ASOPS, achieving sub-ps resolution over μs durations.

CLEO: Applications & Technology

ATH1O • OCT-Technology Development & Clinical Applications—Continued

ATH1O.3 • 08:45 **Automated classification of basal cell carcinoma in mouse skin by polarization sensitive optical coherence tomography**, Lian Duan¹, Tahereh Marvdashti¹, Alex Lee², Jean Y. Tang², Audrey Ellerbee¹; ¹E.L. Gintzton Lab and Dept. of Electrical Engineering, Stanford Univ., USA; ²Dermology Dept., Stanford Univ., USA. A support-vector-machine classifier was developed to discriminate between basal cell carcinoma and healthy tissue in images of mouse skin obtained by polarization-sensitive optical coherence tomography. The achieved sensitivity and specificity were respectively 98% and 96.9%.

ATH1O.4 • 09:00
Withdrawn

ATH1PO5 • 09:15 **Spatiotemporal optical coherence (STOC) manipulation and its possible applications**, Maciej Nowakowski¹, Dawid Borycki¹, Maciej Wojtkowski¹; ¹Optical Biomedical Imaging Group, Inst. of Physics, Nicolaus Copernicus Univ., Poland. We present a novel method of spatiotemporal optical coherence (STOC) manipulation, in which the effective coherence properties of the optical field are adjusted by modulating the phase of the spectral degree of coherence.

ATH1O.6 • 09:30 **Biodynamic 3D Imaging for Personalized Cancer Care**, David D. Nolte¹, Ran An¹, Michael Childress¹, John Turek¹; ¹Purdue Univ., USA. Tumor heterogeneity and differential drug response in 3D tissue is a major obstacle for survival of cancer patients. Biodynamic 3D imaging provides personalized therapy assessment by testing heterogeneous response of tumor biopsies to anti-cancer drugs.

Technology Transfer Program

Thursday, 12 June
09:30-12:30
Exhibit Hall Theater

- Tutorial about Product Licensing and Tech Startups
- Pitch Panel
- Keynote - Becoming an Entrepreneur and Sustaining a Technology Business

CLEO: QELS-Fundamental Science

FTh1A • Quantum
Entanglement—Continued

FTh1A.8 • 09:45

Entanglement Creation by Locally Splitting a Discordant State, Callum Croal¹, Ladislav Mista², Vanessa Chille³, Christian Peuntinger³, Christoph Marquardt³, Gerd Leuchs³, Natalia V. Korolkova¹; ¹Univ. of St Andrews, UK; ²Dept. of Optics, Palacky Univ., Czech Republic; ³Max Planck Inst. for the Science of Light, Germany. We introduce and experimentally implement counter-intuitive entanglement creation by locally splitting a classical mode that is part of a larger discordant state. Possible applications are quantum advantage in information encoding and assisted dense coding.

FTh1B • Quantum
Interconnects—Continued

FTh1B.5 • 09:45

Towards Coupling Rare Earth Ions to a Y₂SiO₅ Nanophotonic Resonator, Tian Zhong¹, Alex Hartz¹, Evan Miyazono¹, Andrei Faraon¹; ¹California Inst. of Technology, USA. An yttrium orthosilicate nanophotonic resonator is fabricated with resonances near the 4I_{9/2}-4F_{3/2} hyperfine transition of Neodymium ions. Measured absorption by Neodymium embedded in a nanobeam indicates promising prospect for coupling ions to our nano-resonator.

FTh1C • High-Field THz
Physics—Continued

FTh1C.7 • 09:45

Terahertz harmonics in multi-layer graphene in the nonperturbative regime, Michael Woerner¹, Pamela Bowlan¹, Klaus Reimann¹, Thomas Elsaesser¹; ¹Max Born Inst., Germany. We report the first observation of terahertz higher harmonics in graphene by mapping the nonlinear response with broadband electrooptic sampling. The nonlinear response in the non-perturbative regime is determined by intra- and interband electron motions.

FTh1D • Solitons and Temporal
Effects—Continued

FTh1D.8 • 09:45

Mode Structure and Temporal Solitons in Optical Microresonators, Tobias Herr¹, Victor Brasch¹, John Jost¹, Ivan Mirgorodskiy¹, Martin Pfeiffer¹, Grigoriy Lihachev², Michael Gorodetsky^{2,3}, Tobias Kippenberg¹; ¹Ecole Polytechnique Federale de Lausanne, Switzerland; ²M.V. Lomonosov Moscow State Univ., Russia; ³Russian Quantum Center, Russia. Temporal dissipative solitons in microresonators constitute a novel class of ultra-short optical pulse generators. Here we study the influence of resonator mode-structure, particularly avoided mode crossings, on soliton formation and derive resonator design criteria.

09:30–12:30 Technology Transfer Program, Exhibit Hall Theater

10:00–15:00 Exhibits Open, Exhibit Halls 1 & 2

10:00–11:30 Coffee Break (10:00-10:30) and Unopposed Exhibit Only Time, Exhibit Hall 1 & 2

NOTES

CLEO: Science & Innovations

**STh1E • Filamentation—
Continued**

STh1E.8 • 09:45

Propagation of intense femtosecond laser pulse in water and acoustic waves generation, Aurelien Houard¹, Yohann Brelet¹, Amélie Jarnac¹, Jerome Carbonnel¹, André Mysyrowicz¹, Carles Milian², Arnaud Couairon², Regine Guillermin³, Jean-Pierre Sésarego³; ¹LOA, ENSTA-Ecole polytechnique-CNRS, France; ²CPHT, Ecole Polytechnique, France; ³LMA, CNRS, France. Propagation of femtosecond pulses at 800 and 400 nm is studied in water. Acoustic signals generated with MW to TW laser power are characterized, showing a directed and broadband emission in the band 0-20 MHz.

**STh1F • THz Quantum Cascade
Lasers—Continued**

**STh1G • Semiconductor Lasers
for Communication—Continued**

**STh1H • Advanced Imaging
Technologies—Continued**

STh1H.7 • 09:45

Coherent laser source for optical time-stretched microscopy, Xiaoming Wei¹, Andy Lau¹, Terence Wong², Chi Zhang¹, Kevin Tsia¹, Kenneth Wong¹; ¹Dept. of Electrical and Electronic Engineering, The Univ. of Hong Kong, Hong Kong; ²Dept. of Biomedical Engineering, Washington Univ. in St. Louis, USA. We demonstrate a coherent picosecond pulsed fiber laser for the high frame-rate optical time-stretched microscopy at 1.0 micron. Real-time flow imaging with a frame rate of 26.25 MHz is achieved based on this source.

09:30–12:30 Technology Transfer Program, Exhibit Hall Theater

10:00–15:00 Exhibits Open, Exhibit Halls 1 & 2

10:00–11:30 Coffee Break (10:00-10:30) and Unopposed Exhibit Only Time, Exhibit Hall 1 & 2

NOTES

Blank lined area for notes.

Meeting Room
211 B/D

Meeting Room
212 A/C

Meeting Room
212 B/D

Marriott
Salon I & II

CLEO: Science & Innovations

CLEO: QELS-
Fundamental Science

JOINT

STh1I • Nonlinear Optics in Waveguides and Nanophotonics Devices—Continued

STh1I.8 • 09:45
Low-loss AlGaAs waveguide performance enhancement for continuous-wave four-wave mixing, Paveen Apiratikul^{1,2}, Gyorgy Porkolab^{1,2}, Jeremiah J. Wathen^{1,2}, Bohan Wang¹, Thomas E. Murphy¹, Christopher J. K. Richardson²; ¹Univ. of Maryland at College Park, USA; ²Lab for Physical Sciences, USA. Low-loss nonlinear AlGaAs waveguides are fabricated using plasma-assisted photoresist reflow. A 6.8-dB continuous-wave four-wave mixing conversion efficiency in a 1.35- μ m-wide waveguide, and a 44-nm half-width 3-dB bandwidth in a 0.65- μ m-wide waveguide are demonstrated.


STh1J • Structuring Materials with fs Lasers—Continued

STh1J.5 • 09:45
Three-dimensional Nanostructuring in YIG Ferrite with Femtosecond Laser, Tomo Amemiya¹, Atsushi Ishikawa², Yuya Shoji³, Nam Hai Pham⁴, Masaaki Tanaka⁴, Tetsuya Mizumoto³, Takuo Tanaka², Shigehisa Arai^{1,3}; ¹Quantum Nanoelectronics Research Center, Tokyo Inst. of Technology, Japan; ²Metamaterials Lab, RIKEN, Japan; ³Dept. of Electrical and Electronic Engineering, Tokyo Inst. of Technology, Japan; ⁴Dept. of Electrical Engineering and Information Systems, The Univ. of Tokyo, Japan. We demonstrated forming nanostructures inside a substrate of cerium-substituted yttrium iron garnet by means of direct laser writing. The laser irradiation increases a refractive index by 0.7% and changes magnetic properties from hard to soft.

FTh1K • Optomechanics and Optical Manipulation—Continued

FTh1K.7 • 09:45
Shot-noise driven self-oscillations of ultra-low dissipation silicon carbide nanowires, Pierre Verlot¹, Anthony Ayari¹, Alessandro Siria¹, Sorin Perisanu¹, Pascal Vincent¹, Philippe Poncharal¹, Stephen Purcell¹; ¹Université Lyon 1, France. We report ultra-low threshold optically induced self-oscillations of a ultra-low dissipation nanowire. We interpret the asymmetrically observed responses as a signature of the laser shot noise drive, consistent with our system's parameters.

JTh1L • Symposium on Laser-Driven Sources of Particle and X-Ray Beams I—Continued

JTh1L.6 • 09:45 
A quasi-directional emission of MeV neutrals from a dense cluster nano plasma, Krishnamurthy Manchikanti¹; ¹Tata Inst. of Fundamental Research, India. Nanoclusters are strongly ionised at 10¹⁶ Wcm⁻² to generate even MeV ions. In a dense cluster ensemble a near 100% charge reduction of the ions to form fast neutrals is demonstrated. Neutrals atom emission is quasi-directional and neutralisation is more effective along the laser polarization.

09:30–12:30 Technology Transfer Program, Exhibit Hall Theater

10:00–15:00 Exhibits Open, Exhibit Halls 1 & 2

10:00–11:30 Coffee Break (10:00-10:30) and Unopposed Exhibit Only Time, Exhibit Hall 1 & 2

NOTES

Horizontal lines for taking notes.

Marriott
Salon III

CLEO: Science &
Innovations

STh1M • Modulators using
Novel Materials—Continued

STh1M.8 • 09:45 **Fast and Slow Optical Modulation of Refractive Index in a SiN Microring**, Jian Wang¹, Yi Xuan¹, Andrew M. Weiner¹, Minghao Qi¹; ¹Purdue Univ., USA. We retrieve the thermal dissipation time of $\tau\theta=0.25\mu\text{s}$ and investigate the power dependent absorption in a SiN microring resonator. We estimate $n_2=4.3\times 10^{-19}\text{m}^2/\text{W}$ based on clear 1 GHz optical modulation of the refractive index.

Marriott
Salon V & VI

CLEO: Science &
Innovations

STh1N • Comb
Spectroscopy—Continued

STh1N.8 • 09:45 **Low-Pressure Gas Spectroscopy Using Terahertz Frequency Synthesizer Traceable to Microwave Frequency Standard via Dual Optical Combs**, Yi-Da Hsieh^{1,2}, Hiroto Kimura¹, Hajime Inaba^{3,4}, Kaoru Minoshima^{4,5}, Tsutomu Araki², Takeshi Yasui^{1,4}; ¹The Univ. of Tokushima, Japan; ²Osaka Univ., Japan; ³National Inst. of Advanced Industrial Science and Technology, Japan; ⁴ERATO Intelligent Optical Synthesizer Project, Japan; ⁵The Univ. of Electro-Communications, Japan. An accurate, continuously tunable, terahertz synthesizer was proposed by photomixing of two continuous-wave lasers phase-locked to dual optical combs. This synthesizer enables us to perform the precise THz spectroscopy secured by microwave frequency standard.

Marriott
Willow Glen I-III

CLEO: Applications
& Technology

ATH1O • OCT-Technology
Development & Clinical
Applications—Continued

ATH1O.7 • 09:45 **A high power directly diode pumped Ti:sapphire laser with synchronized Yb-fiber amplifier for nonlinear optical microscopy and optical coherence tomography**, Aart J. Verhoeff¹, Alma Fernandez¹, Tschackad Kamali², Anders K. Hansen³, Ole B. Jensen³, Peter E. Andersen³, Bernd Sumpf⁴, Götz Erbert⁴, Peter M. Petersen³, Andrius Baltuska¹, Wolfgang Drexler², Angelika Unterhuber²; ¹Vienna Univ. of Technology, Austria; ²Medical Univ. Vienna, Austria; ³Technical Univ. of Denmark, Denmark; ⁴Ferdinand-Braun-Institut, Germany. A simple scheme of a compact femtosecond Ti:sapphire laser with synchronized Yb-fiber amplifier pumped by a powerful single tapered diode laser implemented in a combined coherent Anti-Stokes Raman and optical coherence tomography platform is presented.

09:30–12:30 Technology Transfer Program, Exhibit Hall Theater

10:00–15:00 Exhibits Open, Exhibit Halls 1 & 2

10:00–11:30 Coffee Break (10:00-10:30) and Unopposed Exhibit Only Time, Exhibit Hall 1 & 2

NOTES

Horizontal lines for taking notes.

JTh2A.1

Short Circuit Current Improvement of Si HIT Solar Cell by Optimal and "Chess Board" Like 1-D Light Trapping Periodical Grating Structure, Ming-Lun Lee¹, Chun Nien¹, Shih-Hung Lin², Hung-Chou Lin¹, Yao-Hong You¹, Vin-Cent Su¹, Po-Hsun Chen¹, Han-Bo Yang¹, Yen-Pu Chen¹, Shen-Han Tsai¹, Chieh-Hsiung Kuan¹; ¹Graduate Inst. of Electronics Engineering, National Taiwan Univ., Taiwan; ²Dept. of Biomedical Engineering, Hungkuang Univ., Taiwan. We experimentally report that the novel "chess board" like 1-D grating structure with optimal period of 800 nm can dramatically increase the JSC from 33.7 mA/cm² to 38.9 mA/cm² compared to the reference solar cell.

JTh2A.2

Enhancement on Photovoltaic Properties of Boron-doped Super-high Density Si Quantum Dot Thin Film, Pin-Ruei Huang¹, You-Jeng Chen¹, Jia-Ruei Chang¹, Kuang-Yang Kuo¹, Po-Tsung Lee¹; ¹Dept. of Photonics & Inst. of Electro-Optical Engineering, National Chiao Tung Univ., Taiwan. Boron-doped super-high density nano-crystalline Si quantum dot thin film is demonstrated by utilizing a gradient Si-rich oxide multilayer structure. The boron doping effect and its significant influence on photovoltaic properties are observed and discussed.

JTh2A.3

Crystal Equivalent Temperature Concept for Laser Calorimetry and Nonlinear Optics, Aleksey Konyashkin^{1,2}, Oleg A. Ryabushkin^{1,2}, Ivan S. Ulyanov^{1,2}; ¹NTO IRE-Polus, Russia; ²Moscow Inst. of Physics and Technology, Russia. Concept of equivalent temperature is proposed for temperature measurement of crystals in laser calorimetry and nonlinear optics experiments. Determination of equivalent temperature is based on frequency shift measurement of temperature calibrated acoustic resonance, excited in sample.

JTh2A.4

Dispersion Measurement and Compensation using Optical Frequency Comb, Mitsutaka Ito¹, Takayuki Miyamoto¹, Masaichi Nakamura², Toshiaki Yamazaki², Tatsutoshi Shioda¹; ¹Electrical and Electric Systems, Saitama Univ., Japan; ²Electrical Engineering, Nagaoka Univ. of Technology, Japan. A dispersion spectrum in a 3.2 Tbit/s waveform generation was controlled / compensated by a 200 GHz optical frequency comb synthesizer and optical frequency comb analyzer simultaneously.

JTh2A.5

Detecting micro-particles of explosives at ten meters using selective stimulated Raman scattering, Marshall T. Bremer¹, Marcos Dantus^{1,2}; ¹Dept. of Physics and Astronomy, Michigan State Univ., USA; ²Dept. of Chemistry, Michigan State Univ., USA. We demonstrate standoff detection using stimulated Raman scattering (SRS), simultaneously measuring stimulated Raman gain (SRG) and loss (SRL) within a single laser shot, and detect nanogram quantities of explosives using a 10mW femtosecond laser.

JTh2A.6

Rapid scanning cavity ring-down spectroscopy at the quantum noise limit, David Long¹, Adam J. Fleisher¹, Szymon Wojtcwicz¹, David F. Plusquellic², Joseph T. Hodges¹; ¹Material Measurement Lab, NIST, USA; ²Physical Measurement Lab, National Inst. of Standards and Technology, USA. We present an ultrasensitive cavity-enhanced technique for probing weak molecular absorptions. Recently, we have implemented heterodyne detection, which allowed for quantum-noise-limited detection and noise-equivalent absorption coefficients as low as 6×10^{-14} cm⁻¹Hz^{-1/2}.

JTh2A.7

Photonics-Assisted Millimeter-Wave Phase Detector for Femto-Second Fiber Delay Variation Sensing, Qizhuang Cen¹, Feifei Yin¹, Yitang Dai¹, Jianqiang Li¹, Kun Xu¹; ¹Beijing Univ. of Posts and Telecommunications, China. A novel technique to improve the fiber delay variation sensing precision by a photonics-assisted millimeter-wave phase detector is proposed and demonstrated experimentally. The capacity for sensing link delay jitter of sub-10 femtoseconds is achieved.

JTh2A.8

Fiber Strain Sensor using Spectral Line-width of FBG Reflection through Optical Filter, Shih-Hsiang Hsu¹, Yung-Chia Yang¹; ¹National Taiwan Univ. of Science & Tech, Taiwan. The FBG reflective spectrum was coupled to a optical filter for linewidth monitoring in strain sensing applications. The sensitivity was typically demonstrated as 48-MHz/ μm and the strain sensing limitation could achieve ~ 8 with kHz narrow resolution bandwidth.

JTh2A.9

Nonlinear Fluorescence Spectra Unmixing, Hayato Ikoma¹, Barmak Heshmat¹, Gordon Wetzstein¹, Ramesh Raskar¹; ¹Media Lab, MIT, USA. We have developed a nonlinear spectral unmixing algorithm that separates fluorescence excitation-emission matrix of multiple fluorophores affected by the inner filter effect. We evaluate this technique on simulated data and demonstrate its superior performance experimentally.

JTh2A.10

Open Path Chirped Laser Dispersion Spectroscopy of Methane Plume, Nart S. Daghestani¹, Richard Brownsword¹, Damien Weidmann¹; ¹Science and Technology Dept., Rutherford Appleton Lab, UK. A molecular detection method based on laser dispersion spectroscopy has been implemented to detect methane concentrations with an open-path configuration and using transitions from the ν_4 band. Preliminary results on transient seeps are presented.

JTh2A.11

Analysis of 50 Gbaud homodyne coherent receivers relying on line-coding and injection locking in lasers, Adonis Bogris¹, Constantinos Ressopoulos¹; ¹Technological Educational Inst of Athens, Greece. We present a numerical analysis of 50 Gbaud coherent detection enabled by injection locked lasers and line coding. The impact of the slave laser properties and line coding techniques on the receiver performance is highlighted.

JTh2A.12

Modified CMA Based Blind Carrier-Phase Estimation for 16-QAM Homodyne Digital Coherent Optical Receivers, Md Ibrahim Khalil¹, Arshad M. Chowdhury^{1,2}, Gee-Kung Chang²; ¹Dept. of Electrical Engineering and Computer Science, North South Univ., Bangladesh; ²School of Electrical and computer Engineering, Georgia Inst. of Technology, USA. We propose modified CMA based blind carrier-phase-estimation methods for 16-QAM homodyne digital coherent optical receivers. Through computer simulation we found proposed scheme has less hardware requirements and comparable performance to decision-directed carrier-recovery algorithms.

JTh2A.13

Passive Digital Algorithmic Stabilization of Optical Phase, Joseph Touch¹, Morteza Ziyadi², Amine Abouzaid², Mohammed Chitgarha², Salman Khaleghi², Amirhossein Mohajerin-Ariaei², Youichi Akasaka³, Jeng-yuan Yang³, Motoyoshi Sekiya³; ¹Information Sciences Inst., Univ. of Southern California, USA; ²Electrical Engineering, Univ. of Southern California, USA; ³Fujitsu Labs of America, USA. The coherent signal processing of nonlinear wave mixing often creates interferometers that require feedback stabilization. A digital electronic optical phase stabilizer is described that avoids injecting pilot control signals and supports long-duration BER measurements.

JTh2A.14

SSBI Cancellation Based on Time Diversity Reception in SSB-DD-OOFDM Transmission Systems, Hu Shi¹, Pengfei Yang¹, Cheng Ju¹, Xue Chen¹, Jinsong Bei², Rongqing Hui³; ¹Beijing Univ. of Posts and Telecommunications, China; ²ZTE Corporation, China; ³Univ. of Kansas, USA. A novel SSBI cancellation scheme based on time diversity reception is proposed. Experiment shows that the proposed scheme improves ~ 3.6 dB sensitivity compared with baseband optical OFDM scheme in a 5-Gbps SSB-DD-OOFDM system over 100-km SMF.

JTh2A.15

Real-time Demonstration of 3×10 Gb/s Uncooled MIMO DWDM System with Adaptive Laser Bias Control, Jiannan Zhu¹, Jonathan D. Ingham¹, Adrian Wonfor¹, Richard V. Pentyl¹, Ian H. White¹; ¹University of Cambridge, UK. We demonstrate a 3×10 Gb/s uncooled MIMO DWDM system using uncooled DFB lasers with real-time crosstalk cancellation, allowing separate lasers to operate on different temperatures. Adaptive laser bias control is applied to ensure adequate channel separation.

JTh2A.16

Channel-spacing tunable multiwavelength erbium-doped fiber laser based on a microfiber Fabry-Perot filter, Weihua Jia¹, Qizhen Sun¹, Zhilin Xu¹, Xiaohui Sun¹, Deming Liu¹; ¹School of Optical and Electronic Information, National Engineering Lab for Next Generation Internet Access System, Huazhong Univ. of Science and Technology, China. A tunable multiwavelength fiber laser incorporating a microfiber Fabry-Perot filter with wideband and high extinction ratio is proposed and demonstrated. By adjusting the cavity length of the filter, the channel-spacing can be continuously tuned.

JTh2A.17

Boundaries of Parametric Gain due to Four-wave Mixing in Hybrid Photonic Crystal Fibers, Sidsel R. Petersen¹, Jesper Lægsgaard¹, Thomas T. Alkeskjold²; ¹DTU Fotonik, Technical Univ. of Denmark, Denmark; ²NKT Photonics A/S, Denmark. Parametric gain by four-wave mixing is considered in photonic crystal fibers for an undepleted pump. The mode distributions are wavelength dependent, thus field overlap integrals cannot be simplified, and an extended gain region is observed.

JTh2A.18

Spectra of Raman Scattering in Micro/nano-fibers, Liang Cui¹, Cheng Guo¹, Xiaoying Li¹, Yu Hang Li², Zhong Yang Xu², Lijun Wang², Wei Fang³; ¹Tianjin Univ., China; ²Singhua Univ., China; ³Zhejiang Univ., China. We experimentally demonstrate the spectra of Raman scattering in micro/nano-fibers, which is different from that of traditional optical fibers, not only depends on their diameters, but also depends on their fabricating methods.

JTh2A.19

Coherent combining of SHG converters, Anne Durécu¹, Guillaume Canat¹, Julien Le Gouët¹, Laurent Lombard¹, Pierre Bourbon¹; ¹Onera, France. Coherent combining of frequency doubled beams at 532 nm is demonstrated. Active phase control of the 1064-nm fundamental waves enables high efficiency combining of the second harmonic beams with $\lambda/30$ residual phase error.

JTh2A.20

Polarization multiplexed, dual-frequency ultrashort pulse generation by a birefringent mode-locked fiber laser, Zheng Gong¹, Xin Zhao¹, Guoqing Hu¹, Jiansheng Liu¹, Zheng Zheng¹; ¹School of Electronic and Information Engineering, Beihang Univ., China. Two orthogonally polarized soliton pulse trains with different repetition rates are stably generated from a passively mode-locked fiber ring cavity with a section of polarization maintaining fiber. The frequency difference can be varied as well.

JTh2A • Poster Session 3—Continued

JTh2A.21

Highly-efficient Mid-IR Supercontinuum Generation in ZBLAN Fiber Pumped by Thulium-doped Fiber Amplifier, Jiang Liu¹, Kun Liu¹, Hongxing Shi¹, Fangzhou Tan¹, Yijian Jiang¹, Pu Wang¹; ¹Beijing Univ. of Technology, China. Mid-infrared supercontinuum of 8.1 W with optical-to-optical conversion efficiency of ~76% with respect to the launched pump power at 2 μm wavelength was demonstrated in a ZBLAN fiber pumped by a thulium-doped all-fiber amplifier.

JTh2A.22

Tm-doped Rod-type Photonic Crystal Fibers with Symmetry-Free Cladding, Enrico Coscelli¹, Carlo Molardi¹, Federica Poli¹, Annamaria Cucinotta¹, Stefano Selleri¹; ¹Information Engineering Dept., Università degli Studi di Parma, Italy. A new design approach for large mode area Tm-doped photonic crystal fibers, based on the reduction of cladding symmetry, is numerically analyzed to demonstrate the possibility to obtain robust single-mode guiding under severe heat load.

JTh2A.23

Efficient regenerative self-pulsating sources, Thibault North¹, Martin Rochette¹; ¹Electrical and Computer Engineering, McGill Univ., Canada. We present an improved design of regenerative self-pulsating sources including large filter bandwidths. Pico- and sub-picosecond pulses of energies 20x higher than previously reported are observed in a setup increasing the source efficiency.

JTh2A.24

Line-Plane-Switching Infrared Fiber Imaging Bundle, huan zhan^{1,2}, Xingtiao Yan^{1,2}, Zhang Aidong¹, Fu Li¹, Jianfen Yang¹, Aoxiang Lin¹; ¹State Key Lab of Transient Optics and Photonics, Xi'an Inst. of Optics and Precision Mechanics, China; ²Graduate School of Chinese Academy of Sciences, China. Using line-plane-switching infrared fiber imaging bundle made from As₂S₃ glass fibers with core of 40 μm , clad of 45 μm , and error of 1% in diameter, we demonstrated push-broom infrared sensing imaging.

JTh2A.25

Packet-Based All Optical Wavelength Conversion Using Saw-Tooth Pulse Generated by Optical Pulse Synthesizer, Ken Kashiwagi¹; ¹Tokyo Univ. of Agriculture and Technology, Japan. Packet-based wavelength conversion is demonstrated in cross phase modulation scheme using a saw-tooth pulse generated by an optical pulse synthesizer. Two different patterns of packets with 800 ps guard time were separated in small cross-talk.

JTh2A.26

Polarization Attractors in Harmonic Mode-Locked Fiber Laser With Carbon Nanotubes, Tatiana Habruseva¹, Sergey Sergeyev¹, Sergei K. Turitsyn¹; ¹Aston Univ., UK. We study polarization dynamics of a harmonic mode-locked erbium-doped fiber laser with carbon nanotubes absorber. New types of vector solitons are shown for multi-pulse and harmonic mode-locked operation with locked, switching and precessing polarization states.

JTh2A.27

Monitoring the frequency detune of harmonically mode-locked Fourier domain mode locked fiber laser using the super-mode noise peaks, Feng Li¹, Aiqin Zhang², Xinhuan Feng², Ping Kong Alexander Wai¹; ¹Dept. of Electronic and Information engineering, The Hong Kong Polytechnic Univ., Hong Kong; ²Inst. of Photonics Technology, Jinan Univ., China. The intensity of super-mode noise peaks of a harmonically mode-locked Fourier domain mode-locked fiber laser will drop significantly with the increase of frequency detune, which can be used to monitor the laser output quality.

JTh2A.28

Active mode-locking and CW regimes operating simultaneously in an Erbium doped fiber laser, Cláudia B. Santos¹, Farshad Yazdani^{2,1}, Eunézio A. Sousa¹; ¹MackGraphe, Mackenzie Presbyterian Univ., Brazil; ²Electric Engineering Dept., Universidade Federal de Sergipe, Brazil. We demonstrated an Erbium-doped fiber laser operating simultaneously in two distinct regimes, CW and active mode-locking at 1.8 GHz with pulses of 38 ps. The lasers wavelengths can be tuned in both regimes.

JTh2A.29

Effective Delivery of Analytes with Optofluidics for Ultrasensitive Biodetection, Min Huang¹, Betty C. Galarreta¹, Arif E. Cetin^{1,2}, Hatice Altug^{2,1}; ¹Electrical and Computer Engineering, Boston Univ., USA; ²Bioengineering Dept., EPFL, Switzerland. We present a plasmonic nanobiosensor offering superior analyte delivery efficiency. Our experiments with virus-like analytes show more than an order of magnitude faster response time, and seven orders-of-magnitude dynamic concentration range for 103-10⁹ particles/mL.

JTh2A.30

Group Delay Compensation of Spectrally-Filtered Picosecond Pulses for Stimulated Raman Microscopy, Yasuyuki Ozeki¹, Keisuke Nose², Kyoya Tokunaga¹; ¹The Univ. of Tokyo, Japan; ²Osaka Univ., Japan. Wavelength-tunable pulses with a constant group delay are successfully generated through spectral filtering of broadband pulses in a modified 4-f configuration. This technique effectively improves the reproducibility of spectral data in stimulated Raman spectral microscopy.

JTh2A.31

Development of a CMOS compatible biophotonics platform based on SiN nanophotonic waveguides, Pieter Neutens^{1,2}, Tom Claes¹, Roelof Jansen¹, Ananth Subramanian³, Mahmud UIHasan¹, Veronique Rochus¹, Finub James Shirley¹, Bert Du bois¹, Philippe Helin¹, Simone Severi³, Kenny Leysens³, Ashim Dhakal³, Frédéric Peyskens¹, Shankar Selvaraja³, Paru Deshpande^{1,2}, Roel Baets¹, Liesbet Lagae^{1,2}, Xavier Rottenberg¹, Pol Van Dorpe¹; ¹imec, Belgium; ²Dept. of Physics, KU Leuven, Belgium; ³Photonics Research Group, Ghent Univ., Belgium. We report on the development of low-loss photonic components fabricated in SiN for the development of a biophotonics platform. We discuss experimental demonstration of strip waveguides, MMI and evanescent couplers, fractal trees, AWGs and waveguide-integrated resonators.

JTh2A.32

Optical Tweezers with Tunable Orbital Angular Momentum, Mindaugas Gecevičius¹, Rokas Drevinskas¹, Martynas Beresna¹, Peter G. Kazansky¹; ¹Optoelectronics Research Centre, Univ. of Southampton, UK. We demonstrate a method of optical vortices generation with continuous orbital angular momentum control. The beam generated with an S-waveplate is used as an optical spanner where the rotation speed of trapped particles can be controlled.

JTh2A.33

Biological lasing in liquid microdroplets deposited on a superhydrophobic surface, Alexandr Jonas¹, Mehdi Aas², Yasin Karadag², Halil Bayraktar³, Suman Anand⁴, David McGloin⁴, Alper Kiraz²; ¹Dept. of Physics, Istanbul Technical Univ., Turkey; ²Dept. of Physics, Koç Univ., Turkey; ³Dept. of Chemistry, Koç Univ., Turkey; ⁴Electronic Engineering and Physics Division, Univ. of Dundee, UK. We demonstrate lasing in water/glycerol microdroplets which stand on a superhydrophobic surface and contain purified Venus variant of the yellow fluorescent protein or dilute suspensions of E. Coli bacterial cells expressing stably the Venus protein.

JTh2A.34

Withdrawn

JTh2A.35

Design and Fabrication of Hybrid SPP Waveguides for Ultrahigh-Bandwidth Low-Penalty 1.8-Tbit/s Data Transmission (161 WDM 11.2-Gbit/s OFDM 16-QAM), Jing Du¹, Chengcheng Gui¹, Chao Li², Qi Yang², Jian Wang¹; ¹Huazhong Univ. of Sci. and Tech., China; ²State Key Lab of Optical Comm. Technologies and Networks, China. We design and fabricate a vertical hybrid SPP waveguide. The suitability of ultrahigh-bandwidth data transmission through the proposed waveguide by transmitting 1.8-Tbit/s (161 wavelength 11.2-Gbit/s) WDM OFDM 16-QAM is studied.

JTh2A.36

High power, narrow linewidth, micro-integrated semiconductor laser modules designed for quantum sensors in space, Anja Kohfeldt¹, Ahmad Bawamia¹, Christian Kuerbis¹, Erdenetsetseg Luvsandamdin¹, Max Schiemangk^{1,2}, Andreas Wicht^{1,2}, Götz Erbert¹, Achim Peters^{1,2}, Günther Tränkle¹; ¹Ferdinand-Braun-Institut, Leibniz-Institut fuer Hoechstfrequenztechnik, Germany; ²Humboldt-Universitaet zu Berlin, Germany. We developed a very robust diode laser module platform for the deployment of cold atom based quantum sensors in space. The micro optical benches, not larger than 80 x 25 mm², host MOPA and EDCL modules.

JTh2A.37

Generation of Tunable Optical Frequency Combs with a High Side Mode Suppression Ratio, Shihu Zhang¹, Juanjuan Yan¹, Zhenya Xia¹, Xiayuan Yao¹, Ming Bai¹, Zheng Zheng¹, Zheng Zheng¹; ¹Beihang University, China. We demonstrate a new scheme of generating optical frequency combs (OFC) utilizing a single dual parallel Mach-Zehnder modulator. Gaussian-shaped OFC and flat OFC with a tunable spacing, flexible line-number and high side mode suppression ratio are generated.

JTh2A.38

Time-Bandwidth Product Expansion of Microwave Waveforms Using Anamorphic Stretch Transform, Jianping Yao¹, Jiejun Zhang¹, Mohammad H. Asghari², Bahram Jalali²; ¹Univ. of Ottawa, Canada; ²ECE, UCLA, USA. We show for the first time that a chirped fiber Bragg grating with specially engineered nonlinear group delay profile can be used to significantly increase the time-bandwidth product of a microwave waveform.

JTh2A.39

A Phase Coherent Near-Octave-Spanning Zero-Offset Composite Frequency Comb, Richard A. McCracken¹, Karolis Balskus¹, Deryck T. Reid¹; ¹Heriot Watt Univ., UK. Using a zero-offset carrier-envelope locking technique, we have demonstrated that multiple pulse sequences of different colors from a femtosecond optical parametric oscillator can be coherently combined to synthesize a near-octave-spanning composite frequency comb.

JTh2A.40

Pulse train based generation of tunable THz comb, Chao Tian¹, Tao Yang¹; ¹Stevens Inst. of Technology, USA. We present a simple and novel scheme to generate a tunable THz frequency comb using a multi pulse excitation scheme, as well as a comb-like filter in the detection process.

JTh2A.41

Generating ultra-long bound soliton sequences from a mode-locked fiber laser through intracavity spectral shaping, Ya Liu¹, Xin Zhao¹, Jiansheng Liu¹, Guoqing Hu¹, Zheng Gong¹, Zheng Zheng¹; ¹School of Electronic and Information Engineering, Beihang Univ., China. Extremely long states of bound solitons consisting of up to eleven solitons have been generated from a carbon nanotube passively mode-locked fiber laser with an intracavity pulse shaper.

JTh2A.42

Demonstration and Fabrication of Electro-Optic CaxBa_{1-x}Nb₂O₆ (CBN) Thin-Film Based Rib Waveguide Structure, Faezeh Fesharaki¹, Nadir Hossain², Sebastien Vigne², Joelle Margot³, Ke Wu¹, Mohamed Chaker²; ¹PolyGrames Research Center, Ecole Polytechnique of Montreal, Canada; ²INRS-EMT, Canada; ³Departement de Physique, Université de Montreal, Canada. We report on the design, simulation and experimental demonstration of an electro-optic SiO₂-CBN-MgO rib waveguide structure. The fabricated waveguides are characterized and results are compared with simulation, where a good agreement validates our design approach.

JTh2A.43

Locating fluorescence lifetimes behind turbid layers non-invasively using sparse, time-resolved inversion, Guy Satat¹, Christopher Barsi¹, Barmak Heshmat¹, Dan Raviv¹, Ramesh Raskar¹; ¹MIT, USA. We use time-resolved sensing and sparsity-based dictionary learning to recover the locations and lifetimes of fluorescent tags hidden behind a turbid layer. We experimentally demonstrate non-invasive target classification via fluorescence lifetimes.

JTh2A • Poster Session 3—Continued

JTh2A.44

Ultrabroadband Coherent Infrared Spectroscopy Using Air-Plasma Based Generation and Detection, Eiichi Matsubara¹, Masaya Nagai¹, Masaaki Ashida¹, ¹Osaka Univ., Japan. We generated ultrabroadband coherent infrared pulses by focusing using hollow-fiber compressed intense 10-fs pulses in air. We also coherently detected the electric-field profiles through the field induced second harmonic generation in air.

JTh2A.45

Serial time-encoded amplified microscopy (STEAM) by fully incoherent noise, Chi Zhang¹, Yiqing Xu¹, Xiaoming Wei¹, Kevin Tsia¹, Kenneth Wong¹; ¹Electrical and Electronic Engineering, Univ. of Hong Kong, Hong Kong. By introducing a time-lens in the serial time-encoded amplified microscopy (STEAM), its input temporal aperture is greatly enlarged. Therefore, the light source with arbitrary waveform can be applied, especially the amplified spontaneous emission noise.

JTh2A.46

Enhanced mid-to-near-infrared second harmonic generation in silicon-organic hybrid plasmonic microring resonators, Jihua Zhang^{1,2}, Eric Cassan², Xinliang Zhang¹; ¹Wuhan National Lab for Optoelectronics & School of Optical and Electronic Information, Huazhong Univ. of Science and Technology, China; ²Institut d'Electronique Fondamentale, Université Paris-Sud, France. We propose an enhanced mid-to-near-infrared second harmonic generation (SHG) process relying on a silicon plasmonic microring resonator. The SHG efficiency is enhanced by two orders of magnitude compared to previous results.

JTh2A.47

Optomechanical Response Spectrum of a Tapered Fiber Coupled Microsphere Pendulum, Yong Yang¹, Ramgopal Madugani¹, Jonathan Ward¹, Sile Nic Chormaic¹; ¹Light-Matter Interactions Unit, OIST Graduate Univ., Japan. We study the noise spectrum arising from absorptive and dispersive modulations to the motion of a micropendulum via transmission through the coupling tapered fiber. The observed asymmetrical line shape matches theoretical predictions.

JTh2A.48

Optimal laser cooling limits in the strong coupled cavity optomechanics, Yong-Chun Liu¹, Yu-Feng Shen¹, Qihuang Gong¹, Yun-Feng Xiao¹; ¹Physics, Peking Univ., China. In the strong coupled cavity optomechanics, we find the island structure in the temporal evolution map of mean phonon number. Analytical results are provided to obtain the optimal cooling limits with the frequency matching condition.

JTh2A.49

Fast and accurate calculation of Q factor of 2D photonic crystal cavity, Akihiro Fushimi^{1,2}, Hideaki Taniyama², Eiichi Kuramochi², Masaya Notomi², Takasumi Tanabe¹; ¹Keio Univ., Japan; ²NTT Basic Research Labs, Japan. We developed a method for calculating the Q-factor of a 2D photonic crystal nanocavity directly from the in-plane wavevector distribution of the cavity mode. A high-Q of $>10^7$ was obtained with high accuracy and speed.

JTh2A.50

Generations of vector beams in photonic crystal cavities, Xuetao Gan¹; ¹Northwestern Polytechnic Univ., China. We propose the generation of vector beams in planar photonic crystal cavities with multiple missing-hole defects. The characters of the generated vector beams are analyzed from the intensity, phase and polarization distributions.

JTh2A.51

Photothermal Tuning and Spatial Mapping of Toroidal Optical Microcavities, Kevin Heylman¹, Randall H. Goldsmith¹; ¹Univ. Wisconsin, Madison, Chemistry, USA. A new method for controlling resonance wavelengths of ultrahigh-Q toroidal optical microcavities using a focused free-space laser is presented. Tuning range, rate, and spatial dependence is investigated.

JTh2A.52

Inverted-wedge silica resonators for controlled and stable coupling, Fang Bo^{1,2}, Steven H. Huang¹, Sahin Ozdemir¹, Guoquan Zhang², Jingjun Xu², Lan Yang¹; ¹Electrical and Systems Engineering, Washington Univ. in St. Louis, USA; ²The MOE Key Lab of Weak Light Nonlinear Photonics, TEDA Applied Physics Inst. and School of Physics, Nankai Univ., China. Inverted-wedge silica resonators with $Q > 1e6$ were fabricated using conventional semiconductor methods. Robust and large-extent controllable coupling was demonstrated by horizontally moving a fiber taper on the top surface of the resonator.

JTh2A.53

Field Envelope of High Contrast Gratings with Finite Length, Hanxing Zhang¹, Chao Peng¹, Weiwei Hu¹; ¹Peking Univ., China. The complex band structure of HCG is solved with revised couple wave theory. Further, we analytically solved the field envelope for the HCG with finite length and investigate the impact on modes' Q factors.

JTh2A.54

Mid-IR flat lens based on parallelogram antennas, Xia Yu¹; ¹SIMTech, Singapore. By engineering parallelogram antenna on ZnSe substrate, we can control the wavefront of laser beam and design a flat lens at 10 μ m. The fabricated flat lens has demonstrated focusing effect matching well with simulation.

JTh2A.55

Strong Optomechanical Coupling in a Nanobeam Cavity based on Hetero Optomechanical Crystals, Zhilei Huang¹, Kaiyu Cui¹, Yongzhuo Li¹, Xue Feng¹, Yidong Huang¹, Fang Liu¹, Wei Zhang¹; ¹Electronic Engineering, Tsinghua Univ., China. A hetero optomechanical crystal nanobeam cavity with high mechanical frequency of 5.88 GHz is proposed. By enhancing the overlap between optical and strain field, an optomechanical coupling rate as high as 1.31 MHz is achieved.

JTh2A.56

Femtosecond-laser Inscribed, Tunable, Waveguide Embedded Bragg Gratings in Lithium Niobate, Sebastian Kroesen¹, Wolfgang Horn¹, Jörg Imbrock¹, Cornelia Denz¹; ¹Inst. of Applied Physics, Univ. of Muenster, Germany. We demonstrate electro-optical tunable Bragg gratings embedded into complex two-dimensional waveguides in lithium niobate by femtosecond direct laser writing. The structures support both, ordinary and extraordinary guiding and narrowband reflections around $\lambda = 1.55 \mu\text{m}$.

JTh2A.57

Single-Mode GeSn Mid-Infrared Waveguides on Group-IV Substrates, Xiaodong Yang¹, Fei Cheng¹, Richard Soref²; ¹Dept. of Mechanical and Aerospace Engineering, Missouri Univ. of Science and Technology, USA; ²The Engineering Program, Unversity of Massachusetts at Boston, USA. We design low-loss single-mode GeSn mid-infrared waveguides on group-IV substrates including Si substrates and Ge-on-SOI substrates. The waveguide geometries under single mode condition are optimized for different GeSn alloy compositions and polarizations.

JTh2A.58

Large enhancement in photoluminescence of ZnO grown on strain relaxed nanoporous GaN template by pulsed laser deposition, Jie Tang^{1,2}, Liyuan Deng¹, Jian Huang¹, Peiyuan Seetoh^{1,3}, Kwadwo Konadu Ansaah-Antwi^{1,4}, Venky Venkatesan^{1,2}, Soo Jin Chua^{1,2}; ¹National Univ. of Singapore, Singapore; ²National Univ. of Singapore, Singapore; ³Singapore-MIT Alliance, National Univ. of Singapore, Singapore; ⁴Inst. of Materials and Research Engineering, Agency for Science, Technology and Research, Singapore. ZnO thin film was grown over nanoporous GaN by PLD. Up to 8-fold PL intensity enhancement has been achieved. This is attributed to relieved misfit stress and reduced defect density.

JTh2A.59

Enhanced spontaneous emission by embedding light emitters inside hyperbolic metamaterials, Lorenzo Ferrari¹, Dylan Lu², Dominic Lepage², Zhaowei Liu^{2,1}; ¹Materials Science and Engineering, Univ. of California, San Diego, USA; ²Electrical and Computer Engineering, Univ. of California, San Diego, USA. The inclusion of an emitter inside a Ag/Si multilayer yields a 3-fold enhancement of the Purcell factor over its outer value. The radiation is outcoupled to the far-field via a triangular and a rectangular grating.

JTh2A.60

Low phonon energy fluorozirconate-based glass ceramics for efficient rare-earth luminescence, Charlotte Pfau¹, Ulrich Skrzypczak¹, Manuela Miclea¹, Gerhard Seifert^{1,2}, Bernd Ahrens^{3,4}, Stefan Schweizer^{3,4}; ¹Centre for Innovation Competence SiLi-nano, Martin Luther Univ. of Halle-Wittenberg, Germany; ²Fraunhofer Center for Silicon Photovoltaics CSP, Germany; ³Dept. of Electrical Engineering, South Westphalia Univ. of Applied Sciences, Germany; ⁴Fraunhofer Institut for Mechanics of Materials IWM, Germany. Fluorozirconate-based, highly transparent glass ceramics doped with Nd³⁺ exhibit very low multiphonon relaxation rates following an exponential energy gap dependence. The resulting high radiative quantum efficiencies show the material's potential for amplifier applications.

JTh2A.61

Rectangular-shaped sub-wavelength terahertz beam profiling via an all-optical knife-edge technique, Sze Ping Ho^{1,2}, Anna Mazhorova¹, Mostafa Shalaby¹, Marco Peccianti³, Matteo Clerici^{1,4}, Alessia Pasquazi¹, Yavuz Ozturk^{1,5}, Jalil Ali², Roberto Morandotti¹; ¹INRS-EMT, Univ. of Quebec, Canada; ²Nanophotonics Research Alliance, Universiti Teknologi Malaysia, Malaysia; ³Inst. for Complex Systems- CNR, Italy; ⁴School of Engineering and Physical Sciences, Heriot-Watt Univ., UK; ⁵Ege Univ., Turkey. An all-optical, sub-wavelength terahertz characterization technique based on an ultra-thin-knife-edge is demonstrated employing ultraviolet-pulse to project the blade image on a ZnTe crystal, where the free carriers excited on a blade-shaped area act as field-shield.

JTh2A.62

Coherent Monochromatic Terahertz-wave Pulse Detection using Nonlinear Parametric Conversion at Room, Shin'ichiro HAYASHI¹, Koji Nawata¹, Kodo Kawase^{2,1}, Hiroaki Minamide¹; ¹RIKEN, Japan; ²Nagoya Univ., Japan. We report on a coherent detection of monochromatic terahertz-wave pulses by using a frequency up-conversion in a nonlinear MgO:LiNbO₃ crystal at room temperature. We measured the intensity and the phase of the input terahertz-wave.

JTh2A.63

Modulated Beating Signal Generation via Bias Modulations of Micro-Heaters Integrated on Dual-Mode Laser, Il-Min Lee¹, Namje Kim¹, Kiwon Moon¹, Eui Su Lee¹, Gyeongho Son¹, Kyung Hyun Park¹; ¹THz Photonics Creative Research Center, ETRI, Korea. A simple and compact method of generating modulated beating signals from a dual-mode laser via bias modulation of integrated micro-heaters is proposed and successfully demonstrated. The proposed scheme will enrich the continuous-wave terahertz system applications.

JTh2A • Poster Session 3—Continued

JTh2A.64

Selective Erasure and Refilling of Liquid Metal Based Terahertz Metamaterials, Jinqi Wang¹, Shuchang Liu¹, Sivaraman Guruswamy², Ajay Nahata¹; ¹Electrical and Computer Engineering, Univ. of Utah, USA; ²Metallurgical Engineering, Univ. of Utah, USA. We demonstrate a technique to selectively erase and refill unit cells of THz metamaterials, which are formed by injecting eutectic gallium indium, a liquid metal at room temperature, into microchannels in a polydimethylsiloxane mold.

JTh2A.65

Transmission bleaching and coupling cross-over in a split tapered aperture, Shuchang Liu¹, Oleg Mitrofanov², Ajay Nahata¹; ¹Dept. of Electrical and Computer Engineering, Univ. of Utah, USA; ²Dept. of Electronic and Electrical Engineering, Univ. College London, UK. We investigate the spectral broadening of the transmitted radiation of conically tapered apertures made in a split metallic plate. We further propose a tapered shell structure to realize stronger broadband field concentration.

JTh2A.66

Two-Photon Photovoltaic Effect in Gallium Arsenide, Jichi Ma¹, Jeff Chiles¹, Yagya D. Sharma², Sanjay Krishna², Sasan Fathpour¹; ¹CREOL, The College of Optics and Photonics, Univ. of Central Florida, USA; ²Center for High Technology Material, Univ. of New Mexico, USA. The two-photon photovoltaic effect is demonstrated in gallium arsenide at 976 and 1550 nm wavelengths. A waveguide photodiode biased in its fourth quadrant is used to harvest electrical power from photons lost to two-photon absorption.

JTh2A.67

Investigation of Multiple Coupled Optical Parametric Oscillators, Ran Wang¹, Pengda Hong¹, Xingquan Zou¹, Yujie J. Ding¹, Xiaodong Mu², Huai-Chuan Lee², Stephanie Meissner², Helmut Meissner²; ¹Lehigh Univ., USA; ²Onyx Optics Inc., USA. We investigated multiple coupled optical parametric oscillators, exhibiting behaviors of strong coupling. Conversion efficiency and slope efficiency stay the same as those for conventional and two coupled optical parametric oscillators whereas linewidths are significantly reduced.

JTh2A.68

Coherence properties of optical frequency combs generated in Kerr microresonators, Miro J. Erkintalo¹, Stephane Coen¹; ¹Physics Dept., The Univ. of Auckland, New Zealand. We numerically study the stability of microresonator frequency combs in terms of the complex degree of first-order coherence. We identify different regimes of comb coherence, linked to the solutions of the Lugiato-Lefever equation.

JTh2A.69

All-fiber optical parametric amplifier for life-science application, Xiaoming Wei¹, Andy Lau¹, Yiqing Xu¹, Chi Zhang¹, Arnaud Mussot², Alexandre Kudlinski², Kevin Tsia¹, Kenneth Wong¹; ¹Dept. of Electrical and Electronic Engineering, The Univ. of Hong Kong, Hong Kong; ²PhLAM/IRCICA USR 3380/UMR 8523, 2CNRS-Université Lille 1, France. We demonstrate an all-fiber optical parametric amplifier for life-science (OPALS) application. Optical amplification of megahertz serial time-encoded amplified microscopy (STEAM) images with a resolution of less than 2 micron is achieved with a 20-dB gain.

JTh2A.70

Periodically Oriented Gallium Nitride: Materials Development, Jennifer K. Hite¹, Jaime A. Freitas¹, Ramasis Goswami¹, Michael A. Mastro¹, Igor Vurgaftman¹, Jerry R. Meyer¹, Christopher G. Brown², Francis J. Kub¹, Steven R. Bowman¹, Charles R. Eddy¹; ¹US Naval Research Lab, USA; ²Sotera Defense Solutions, USA. Methods for growing periodically alternating polarities of GaN on N-polar and Ga-polar GaN substrates have been developed. The resulting periodically oriented samples can be extended to thick growth, allowing their use in non-linear optics.

JTh2A.71

Tunable, Continuous-wave, Single-frequency Ultraviolet Source Based on BiB₃O₆, Kavita Devi¹, Suddapalli Chaitanya Kumar¹, Majid Ebrahim-Zadeh^{1,2}; ¹ICFO - The Inst. of Photonic Sciences, Spain; ²Instituto Catalana de Recerca i Estudis Avancats (ICREA), Spain. We report a single-frequency cw UV source tunable across 333-345nm using BiB₃O₆ as the nonlinear material, generating 21.6mW of UV power at 339.7nm, with >15mW over 64% of the UV tuning range in high-beam quality.

JTh2A.72

Natural Phase Matching in Microdisk Cavities, Vesselin G. Vellev¹, Prem Kumar^{1,2}, Yu-Ping Huang²; ¹Dept. of Physics and Astronomy, Center for Photonic Communication and Computing, Northwestern Univ., USA; ²Dept. of Electrical Engineering and Computer Science, Center for Photonic Communication and Computing, Northwestern Univ., USA. We identify new approaches to achieve natural phase matching in microdisk cavities for widely-spaced wavelengths across the visible and telecom bands.

JTh2A.73

Femtosecond Laser-Induced Volume Gratings in Lithium Niobate for Noncollinear Second-Harmonic Generation, Jörg Imbrock¹, Sebastian Kroesen¹, Christian Dietrich¹, Wolfgang Horn¹, Cornelia Denz¹; ¹Inst. of Applied Physics, Univ. of Muenster, Germany. Noncollinear second-harmonic generation is induced by a volume grating which is directly written into a lithium niobate wafer by femtosecond laser pulses. The efficiency can be increased by Bragg matching of the fundamental wave.

JTh2A.74

Metal-Clad Subwavelength Semiconductor Lasers with Temperature-Insensitive Spontaneous Hyper-Emission, Joseph S. Smalley¹, Qing Gu¹, Matthew W. Puckett¹, Yeshiahu Fainman¹; ¹Electrical and Computer Engineering, Univ. of California, San Diego, USA. Accounting for the temperature dependence of the cavity resonances and gain medium, we investigate a metal-clad subwavelength semiconductor laser with a spontaneous emission factor, β , approaching unity for all temperatures.

JTh2A.75

Optical trapping with Bessel beams generated from semiconductor lasers, Grigori Sokolovskii¹, Vladislav V. Dudelev¹, Sergey N. Losev¹, Ksenya Soboleva¹, Anton G. Deryagin¹, Evgeny A. Viktorov^{2,3}, Vladimir I. Kuchinskii^{1,4}, Wilson Sibbett⁵, Edik U. Rafailov⁶; ¹AF Ioffe Physical-Technical Inst., Russia; ²Univerite libre de Bruxelles, Belgium; ³National Research Univ. of Information Technologies, Mechanics and Optics, Russia; ⁴St.Petersburg State Electrotechnical Univ. "LETI", Russia; ⁵Univ. of St Andrews, UK; ⁶Ashton Univ., UK. In this paper, we demonstrate, for the first time to the best of our knowledge, utilization of Bessel beams generated from a semiconductor laser for optical trapping and manipulation of microscopic particles including living cells.

JTh2A.76

Coherent Spectral Broadening and Compression of a Mode-locked VECSEL, Adrian H. Quarterman¹, Lucy E. Hooper², Peter J. Mosley², Keith G. Wilcox¹; ¹School of Engineering, Physics and Mathematics, Univ. of Dundee, UK; ²Centre for Photonics and Photonic Materials, Univ. of Bath, UK. We report the coherent spectral broadening of a mode-locked VECSEL in normal-dispersion photonic crystal fibers. Subsequent compression produced 150 fs pulses at 270 mW average power or 220 fs pulses at 520 mW average power.

JTh2A.77

InGaAs/GaAs quantum well laser with broad spectrum of stimulated emission at 1.06 μm , Wang Huolei¹, JunPing Mi¹, Laura Meriggi², Matthew Steer², WeiXi Chen³, Jiaoqing Pan¹, Ying Ding^{2,1}; ¹Inst. of Semiconductors, CAS, China; ²School of Engineering, Univ. of Glasgow, UK; ³Peking Univ., China. We report the first demonstration to our knowledge of quantum well laser having a broadband lasing spectrum of 38 nm at a center wavelength of 1.06 μm with a pulsed output power of ~50 mW.

JTh2A.78

Impact of Absorber Bias Voltage on the Optical Feedback Sensitivity of a Passively Mode-Locked Quantum Dot Laser Operating at Elevated Temperature, Ravi Raghunathan¹, Frederic Grillot², Jesse Mee³, Luke F. Lester¹; ¹Electrical and Computer Engineering, Virginia Polytechnic Inst. and State Univ., USA; ²Telecom Paristech, Ecole Nationale Supérieure des Télécommunications, France; ³Air Force Research Lab, Kirtland AFB, USA. A feedback-sensitivity study of a two-section, passively mode-locked quantum dot laser operating at elevated temperature suggests that the absorber bias voltage is critical in determining the feedback-response of the device, even under the resonant configuration.

JTh2A.79

Phase Retrieval with an Array of Coupled Lasers, Moti Fridman¹, Oren Raz²; ¹Bar Ilan Univ., Israel; ²Physics of complex systems, Weizmann Inst. of Science, Israel. We will present how large array of coupled laser can solves complicated mathematical problems, such as phase retrieval of X-ray imaging experiments, in a microsecond instead of days or even weeks in cluster of powerful computers.

JTh2A.80

Thermal Lensing in Nd:YVO₄ Laser with In-Band Pumping at 914 nm, Tanant Waritnant¹, Arkady Major¹; ¹Electrical & Computer Engineering, Chulalongkorn Univ., Canada. Thermal lensing in Nd:YVO₄ laser with in-band pumping at 914nm was experimentally characterized. An FEA modeling showed excellent agreement. A comparison with other standard pumping wavelengths was also made, highlighting a factor of 3 difference.

JTh2A.81

Direct Manipulation of Transverse Mode of a Yb:YAG Laser by a Scanning Pump Beam, Takumi Sato¹, Yuichi Kozawa¹, Shunichi Sato¹; ¹Inst. of Multidisciplinary Research for Advanced Materials, Tohoku Univ., Japan. We demonstrate a novel method for the direct generation of single-transverse, higher-order Hermite-Gaussian and Laguerre-Gaussian mode beams from a Yb:YAG laser pumped by a high-speed scanning beam without any alignment of a laser cavity.

JTh2A.82

45W CW TEM₀₀ mode diode-side-pumped Nd:YAG rod laser with linearly polarized beam, Regiane S. Pinto¹, Dimitri Geskus¹, Niklaus Wetter¹; ¹Centro de Lasers e Aplicações, IPEN/SP, Brazil. Using a commercial, diode-side pumped Nd:YAG rod laser module, we obtain more than 53% extraction efficiency in fundamental mode with respect to multimode operation in a fully polarized beam.

JTh2A • Poster Session 3—Continued

JTh2A.83

Enhancement of Output Laser Power in High-power Nd/Cr:YAG Ceramic Amplifiers Based on Cross-relaxation Effect under Solar-Pumping, Takato Nakamachi¹, Naoki Matuoka¹, Taku Saiki¹, Kana Fuzioka², Masahiro Nakatsuka³, Yukio Iida¹; ¹kansai Univ., Japan; ²Inst. of Laser Engineering, Japan; ³Inst. for Laser Technology, Japan. Marked increase in output laser power of a high-power Nd/Cr:YAG ceramic amplifier based on the cross-relaxation effect at high temperature under quasi-solar light pumping was observed. The solar-pumped laser is applicable to renewable energy production.

JTh2A.84

Laser- and Filament-Induced Multi-scale Surface Structures on Solid Target Materials, Anthony Valenzuela¹, Kristopher Behler^{2,1}, Chase Munson¹, Andrew Porwitzky¹, Matthew Weidman³, Martin Richardson³; ¹US Army Research Lab, USA; ²Bowhead Science and Technology, USA; ³CREOL, The College of Optics & Photonics, Univ. of Central Florida, USA. Laser-induced filaments can ablate solid material at distances greater than that practically achieved through linear optics. We observed multi-scale structures on metals, polymers, and ceramics from filaments and compared to those from short-focused laser pulses.

JTh2A.85

Laser crystallization of silicon on lithium niobate, Gregorio Martinez¹, Grigoris Zisis¹, Johann Franz¹, Noel Healy¹, Anna C. Peacock¹, Harold Chong², David Grech², Sakellaris Mallis¹; ¹Optoelectronics Research Centre, Univ. of Southampton, UK; ²School of Electronics and Computer Science, Univ. of Southampton, UK. Localized laser heating of amorphous Si deposited on LiNbO₃ results in crystallization of the Si over-layer and the formation of a waveguide in the LiNbO₃ substrate that supports guided modes in the visible and IR.

JTh2A.86

Quarter-Laser-Cycle Oscillations in Attosecond Transient Absorption for Robust Delay Zero Calibration, Lukas Gallmann^{1,2}, Jens Herrmann¹, Matteo Lucchini¹, Shaohao Chen³, Mengxi Wu³, André Ludwig¹, Lamia Kasmi¹, Kenneth Schafer³, Mette Gaarde³, Ursula Keller¹; ¹Dept. of Physics, ETH Zurich, Switzerland; ²Inst. of Applied Physics, Univ. of Bern, Switzerland; ³Dept. of Physics and Astronomy, Louisiana State Univ., USA. We investigated quarter-laser-cycle oscillations in the transient absorption signal of attosecond pulse trains and infrared pulses interacting in helium. We discuss their physical origin and show their usefulness for experimental delay-zero calibration in attosecond science.

JTh2A.87

Time resolved spectroscopy of laser induced graphite plasma relevant to high-order harmonic generation, Muhammad Ashiq Fareed¹, Yoann Pertot¹, Sudipta Mondal¹, Tsuneyuki Ozaki¹; ¹Energie, Matériaux et Télécommunications, INRS-EMT, Canada. We perform spectroscopic characterization of graphite plasma to study the species responsible for high-order harmonics generation. We observed that visible region contains vibrational transitions of C₂ and C₃ molecules. Using same conditions, we found shorter delays are favorable for intense HHG.

JTh2A.88

Mapping the fragmentation of acetylene with femtosecond resolution pump probe at LCLS using 2, 3, and 4 particle coincidences, Chelsea E. Liekhus-Schmaltz¹, Ian Tenney¹, Timur Osipov², Philip H. Bucksbaum^{1,2}, Vladimir Petrovic¹; ¹Stanford Univ., USA; ²SLAC National Accelerator Lab, USA. A three-layer delay line anode detector has been used in x-ray pump x-ray probe time-resolved measurement at LCLS. We used ~10 fs long pulses to initiate and probe ultrafast dynamics in the dication of acetylene. The dynamics are discerned from the temporal evolution of multi-particle coincidences.

JTh2A.89

Accessing the optical properties of single nanoobjects at the nanometer scale through fast electron based spectroscopies, Arthur Losquin¹, Luiz F. Zagonel¹, Viktor Myroshnychenko², Benito Rodriguez-Gonzalez³, Marcel Tencé¹, Luis M. Liz-Marzan³, Javier Garcia de Abajo², Odile Stéphan¹, Mathieu Kociak¹; ¹Laboratoire de Physique des Solides, Université Paris-Sud, CNRS, France; ²IQFR, CSIC, Spain; ³Departamento de Química Física, Universidade de Vigo, Spain. Fast electron based spectroscopies are often loosely compared to light scattering. By performing Electron Energy Loss Spectroscopy and Cathodoluminescence on single metallic nanoobjects, we show that these techniques are nanometric probes of extinction and scattering.

JTh2A.90

Experimental demonstration of an efficient unidirectional coupler for surface plasmons with wide-angle efficiency, Fan Lu¹, Lin Sun², Jia Wang², Kun Li¹, Anshi Xu¹; ¹Peking Univ., China; ²Tsinghua Univ., China. We experimentally demonstrated a wide-angle unidirectional excitation of surface plasmons. Employing the plasmonic critical angle and the grating effect, a wide angular full-width-half-maximum (AFWHM = 25deg) with high unidirectionality (extinction ratio > 10dB) was realized.

JTh2A.91

Modulated spontaneous emission via the coupling between Fabry-Pérot cavity and surface plasmon polariton modes, Jianjian Jiang¹, Yubo Xie¹, Zhengyang Liu¹, Xue-jin Zhang¹, Yong-yuan Zhu¹; ¹Nanjing Univ., China. The fluorescence is experimentally controlled with bandgap engineering of structured metal surface. Grating duty ratio is optimized as 3/4 and narrow emission spectra are obtained by coupling between Fabry-Pérot cavity and surface plasmon polariton modes.

JTh2A.92

Nanocavity Enhanced Absorption of Ultrathin Films, Haomin Song¹, Luqing Guo², Zhejun Liu², Kai Liu¹, Xie Zeng¹, Dengxin Ji¹, Nan Zhang¹, Haifeng Hu³, Suhua Jiang², Qiaoqiang Gan¹; ¹Dept. of Electrical Engineering, The State Univ. of New York at Buffalo, USA; ²Dept. of Materials Science, Fudan Univ., China; ³College of Information Science and Engineering, Northeastern Univ., China. We develop a fundamental strategy to enhance the light-matter interaction of ultra-thin films based on strong interference effect in planar nanocavities, and overcome the limitation between the absorption and film thickness of energy harvesting materials.

JTh2A.93

High-Throughput Optical Biosensing Arrays Detection Using White Light Fourier Transform Method, Wan-Shao Tsai¹, Yi-Chang Lin¹; ¹Dept. of Applied Materials and Optoelectronic Engineering, Natian Chi Nan Univ., Taiwan. High-throughput detection of a large-area chip-based gold nanoslit biosensing array was detected using an imaging system based on white light Fourier transform spectrometry, with the detection sensitivity 0.02 in index change and 60nM of anti-BSA.

JTh2A.94

On-chip low-profile nano-horn metal-clad optical cavity with much improved performance, Zheng Li¹, Hyuck Choo¹; ¹Electrical Engineering, California Inst. of Technology, USA. We propose an on-chip nano-horn metal-clad optical cavity with sloped sidewalls that achieves much improved vertical mode confinement—quality factor of 1000 and effective volume of 0.31(λ/n)³—in 0.8μm height of previously reported devices.

JTh2A.95

Gold Nanorod Reshaping using a Continuous Wave Laser, David Harris-Birtill¹, Mohan Singh¹, Yu Zhou¹, Maria Elena Gallina¹, Tony Cass¹, Daniel S. Elson¹; ¹Imperial College London, UK. Gold nanorods for photothermal therapy are shown, using spectroscopy and electron microscopy, to reshape after irradiation with a 6W/cm² continuous wave laser, affecting their absorption coefficient and thus their clinical efficacy.

JTh2A.96

Reflective plasmonic imaging lithography with deep sub-wavelength resolution and high aspect ratio, Xiangang Luo¹; ¹CAS Inst. of Optics and Electronics, China. Reflective silver layer is employed to improve both resolution and fidelity of sub-diffraction lithography by amplifying evanescent waves and tailoring electric field components. Nano characters patterns with depth ~35nm and about 36nm line width are obtained.

JTh2A.97

Bowtie Plasmonic Aperture for Single Quantum Emitter Absorption Measurement, I-Chun Huang¹, Jennifer Choy¹, Russ Jensen², Mounji Bawendi², Marko Loncar¹; ¹School of Engineering and Applied Sciences, Harvard Univ., USA; ²Chemistry, MIT, USA. Bowtie apertures with gap sizes of less than 30nm are fabricated successfully by lift-off process. Simulations show that they have mode area as small as 0.011(λ/n)², which is two orders smaller than a conventional tightly focused laser spot.

JTh2A.98

Graphene-based tunable Bragg reflector with a broad bandwidth, Jin Tao^{1,3}, XueChao Yu¹, Bin Hu², Alexander Dubrovkin³, Qijie Wang^{1,3}; ¹OPTIMUS, Photonics Centre of Excellence, School of Electrical and Electronic Engineering, Nanyang Technological Univ., Singapore; ²School of Optoelectronics, Beijing Inst. of Technology, China; ³CDPT, Centre for Disruptive Photonic Technology, School of Physical and Mathematical Sciences, Nanyang Technological Univ., Singapore. We show theoretically that Bragg stopband and defect resonance mode can be achieved and dynamically tuned over a wide wavelength range by a small change in Fermi energy level of graphene in graphene plasmonic waveguide structures.

JTh2A.99

Proposal for a single-photon silicon device based on the unconventional photon blockade, Hugo Flayac¹, Dario Gerace², Vincenzo Savona¹; ¹Inst. of Theoretical Physics, EPFL, Switzerland; ²Dipartimento di Fisica, Università di Pavia, Italy. We demonstrate that the unconventional photon blockade can produce single photons under pulsed excitation at high repetition rates. Our proposal relies on two coupled photonic crystal cavities and on the Kerr nonlinearity of silicon.

JTh2A.100

Using a two-photon dressed state picture to explain Multi-frequency Raman generated spectra, Hao Yan¹, Donna T. Strickland¹; ¹Dept. of Physics and Astronomy, Univ. of Waterloo, Canada. Observations of multi-frequency Raman generated spectra indicate that at high intensities, the Raman process is better described using a dressed state picture of two-photon Stark shifted Raman levels.

JTh2A.101

Multidimensional Study of Distortions Induced by Cascaded Stimulated Raman Scattering in Potassium Titanyl Phosphate, Alexis Labruyere¹, Badr Mohamed Ibrahim Shalaby^{1,2}, Katarzyna Krupa¹, Alessandro Tonello¹, Fabio Baronio³, Vincent Couderc¹; ¹Institut XLIM, UMR 7252, Université de Limoges, France; ²Physics Dept., Faculty of Science, Tanta Univ., Egypt; ³CNISM and Dipartimento di Ingegneria dell'Informazione, Università degli Studi di Brescia, Italy. Stimulated Raman scattering was investigated in potassium titanyl phosphate. A broadband Raman cascade was generated between 1086 nm and 1250 nm. A detailed discussion is given about spatial and temporal distortions of Raman-scattered light.

JTh2A.102

Ultrafast Random Bit Generation Based on the Chaotic Dynamics of a Semiconductor Laser, Nianqiang Li^{3,1}, Byungchil Kim^{1,4}, V. n. Chizhevsky², Alexandre Locquet^{4,1}, Matthieu Bloch^{1,4}, David Citrin^{1,4}, Wei Pan³; ¹Georgia Inst. of Technology, School of Electrical and Computer Engineering, USA; ²B. I. Stepanov Inst. of Physics, National Academy of Science of Belarus, Belarus; ³Southwest Jiaotong Univ., China; ⁴UMI 2958 Georgia Tech-CNRS, Georgia Tech Lorraine, France. We achieve physical random bit generation (RBG) that does not exceed the limit set by information theory via extracting 4 bits per sample or keep 55 bits per sample, leading to faster physical-based pseudo RBG.

JTh2A • Poster Session 3—Continued

JTh2A.103

Recovery of Image after Distortion by Atmospheric Turbulence Using Phase-Conjugate Beam through Difference Frequency Generation, Xingquan Zou¹, Pengda Hong¹, Yujie J. Ding¹; ¹Lehigh Univ., USA. Using phase-conjugate beam generated by second-order nonlinear process, blurred images caused by atmospheric turbulence were fully recovered. Due to instantaneous response, it is perhaps the only scheme for efficiently recovering image distorted by atmospheric turbulence.

JTh2A.104

Generation of Coherent Ultraviolet Radiation by Efficient Frequency Conversion Based on Nitride Heterostructures, Guan Sun¹, Da Li¹, Ruolin Chen¹, Yujie J. Ding¹; ¹Lehigh Univ., USA. We show that waveguides made of GaN/AlGaN heterostructures can be used for efficient parametric up and down conversion under transverse geometry. The conversion efficiency for generation of coherent ultraviolet radiation reaches 1%.

JTh2A.105

Power Enhancement, Noise Reduction, and Linewidth Narrowing of THz Output by Mixing Beams from Coupled Oscillators, Xingquan Zou¹, Pengda Hong¹, Da Li¹, Yujie J. Ding¹; ¹Lehigh Univ., USA. THz radiation was generated by mixing idler-idler waves from coupled optical parametric oscillators based on stacked KTP plates. Power enhancement, noise reduction, and linewidth narrowing have been attributed to noise reduction between idler waves.

JTh2A.106

Third and Fifth Harmonic Generation in Transparent Solids with Few Optical Cycle Mid-infrared Pulses, Donatas Majus¹, Nail Garejev¹, Ieva Grazuleviciute¹, Gintaras Tamošauskas¹, Vytautas Jukna^{2,3}, Arnaud Couaïron², Audrius Dubietis¹; ¹Dept. of Quantum Electronics, Vilnius Univ., Lithuania; ²Centre de Physique Théorique, Ecole Polytechnique, France; ³Laboratoire Hubert Curien, Université de Lyon, Université Jean Monnet, France. We present a detailed investigation of third and fifth harmonics generation with 20 fs pulses at 2 μm in CaF₂ crystal, revealing a negligible contribution of higher-order Kerr terms up to intensities of 15 TW/cm².

JTh2A.107

Complex spatial and spectral evolutions in cascaded second order nonlinear process, Katarzyna Krupa¹, Alexis Labrùyre¹, Badr Mohamed Ibrahim Shalaby^{1,2}, Alessandro Tonello¹, Fabio Baronio³, Vincent Couderc¹; ¹Département Photonique, Institut Xlim, UMR CNRS 7252, France; ²Physics Dept., Tanta Univ., Egypt; ³Dipartimento di Ingegneria dell'Università di Brescia, Italy. We experimentally study spatio-temporal nonlinear dynamics in periodically poled lithium niobate crystal. We discuss broadband frequency conversion by modulation instability through cascading second harmonic generation under self-defocusing regime. Measurements agree well with numerical simulations.

JTh2A.108

Withdrawn

JTh2A.109

Ultrafast Resonant Optical Kerr Response due to Long-Range Coherent Coupling of Light and Multinode-Type Excitons, Masayoshi Ichimiya¹, Hiroyuki Murata¹, Takayuki Umakoshi¹, Takashi Kinoshita², Hajime Ishihara², Masaaki Ashida¹; ¹Graduate School of Engineering Science, Osaka Univ., Japan; ²Graduate School of Engineering, Osaka Prefecture Univ., Japan. Resonant optical Kerr effects have been investigated in high-quality CuCl thin films. The peculiar spectral feature and the ultrafast response below 200 fs by a remarkably strong coupling between light and multinode-type excitons are observed.

JTh2A.110

Measuring coherence dynamics of methanol using transient coherent spontaneous Raman scattering, Seth Meiselman¹, Offir Cohen², Matthew F. DeCamp¹, Virginia Lorenz¹; ¹Physics and Astronomy, Univ. of Delaware, USA; ²Joint Quantum Inst., National Inst. of Standards and Technology, USA. We demonstrate the measurement of vibrational state coherence dynamics in liquid methanol using transient coherent spontaneous Raman scattering. The resulting lifetimes and quantum beat frequency agree with frequency-domain and coherent anti-Stokes Raman scattering measurements.

JTh2A.111

Temperature Dependence of Terahertz Transmission through Photoexcited Graphene, Hassan Hafez Eid¹, Ibraheem Al-Naib², Katsuya Oguri³, Yoshiaki Sekine³, Akram Ibrahim¹, Marc Dignam², Roberto Morandotti¹, Satoru Tanaka⁴, Fumio Komori⁵, Hiroki Hibino³, Tsuneyuki Ozaki¹; ¹INRS-EMT, Canada; ²Physics, Engineering Physics and Astronomy, Queen's Univ., Canada; ³NTT Basic Research Labs, NTT Corporation, Japan; ⁴Applied Quantum Physics and Nuclear Engineering, Kyushu Univ., Japan; ⁵Inst. for Solid State Physics, Univ. of Tokyo, Japan. We report temperature dependence and thermal hysteresis behavior of terahertz transmission through photoexcited graphene. We vary the temperature between room temperature and 180° C, and use the optical-pump/terahertz-probe differential transmission technique.

JTh2A.112

Two Dimensional Coherent Spectroscopy of CdSe/ZnS Colloidal Quantum Dots, Bo Sun¹, Rohan Singh^{1,2}, Lazaro Padilha³, Wan K. Bae⁴, Jeffrey Pietryga⁵, Victor Klimov⁵, Steven T. Cundiff^{1,2}; ¹JILA/NIST and Univ. of Colorado, USA; ²Dept. of Physics, Univ. of Colorado, USA; ³Instituto de Física "Gleb Wataghin", Universidade Estadual de Campinas, Brazil; ⁴Photo-Electronic Hybrid Research Center, Korea Inst. of Science and Technology, Korea; ⁵Chemistry Division, Los Alamos National Lab, USA. We demonstrate 2D coherent spectroscopy of CdSe/ZnS nanocrystals and measure the exciton homogeneous linewidth. The 2D spectra also reveal an off-diagonal peak that oscillates as a function of the waiting time T.

JTh2A.113

Experimental Characterization of Optical Nonlocalities in Metal-Dielectric Multilayer Metamaterials, Changyu Hu¹, Jie Gao¹, Cherran J. Mathai², Shubhra Gangopadhyay², Xiaodong Yang¹; ¹Dept. of Mechanical and Aerospace Engineering, Missouri Univ. of Science and Technology, USA; ²Dept. of Electrical and Computer Engineering, Univ. of Missouri, USA. The optical nonlocalities in metal-dielectric multilayer metamaterials are characterized as functions of incident angles for different polarizations. The measured epsilon-near-zero frequency shifts due to nonlocal effects agree with the theoretical analysis developed from transfer-matrix method.

JTh2A.114

Coherent Excitation-Selective Spectroscopy in Planar Metamaterials, Xu Fang¹, Ming Lun Tseng^{2,3}, Din Ping Tsai^{3,4}, Nikolay I. Zheludev^{1,5}; ¹Optoelectronics Research Centre and Centre for Photonic Metamaterials, Univ. of Southampton, UK; ²Graduate Inst. of Applied Physics, National Taiwan Univ., Taiwan; ³Dept. of Physics, National Taiwan Univ., Taiwan; ⁴Research Center for Applied Sciences, Academia Sinica, Taiwan; ⁵Centre for Disruptive Photonic Technologies, Nanyang Technological Univ., Singapore. We demonstrated that the electric and magnetic resonances of metamaterials can be separately switches off and on by positioning the metamaterials along a standing wave, while both resonances are present in travelling-wave spectra.

JTh2A.115

Giant Optical Nonlocality near the Dirac Point in Metal-Dielectric Multilayer Metamaterials, Lei Sun¹, Jie Gao¹, Xiaodong Yang¹; ¹Dept. of Mechanical and Aerospace Engineering, Missouri Univ. of Science and Technology, USA. The giant optical nonlocality near the Dirac point in lossless metal-dielectric multilayer metamaterials is revealed and fully investigated through the band structure analysis of the multilayer stack, iso-frequency contour analysis, and numerical simulation.

JTh2A.116

An Analytical Field Density Function for All Scattering Regimes, Kevin J. Webb¹, Yulu Chen¹, Jason A. Newman¹; ¹Purdue Univ., USA. We present an analytical density function for field statistics that applies in all scattering regimes, providing a new framework for the study of Anderson localization, and facilitating imaging in random media and random laser design.

JTh2A.117

Ultrathin and smooth Aluminum-doped Silver based Meta-material with Low Loss and Homogeneous Response, Cheng Zhang¹, Long Chen¹, Xi Chen¹, Yang Yang¹, Dewei Zhao¹, L. Jay Guo¹; ¹Electrical Engineering and Computer Science, Univ. of Michigan, USA. Wetting-layer-free, ultra-thin and smooth Silver film is achieved by doping Aluminum in film deposition. Hyperbolic metamaterial using Al-doped Ag films shows high transmittance and homogeneous response.

JTh2A.118

Sub-wavelength confinement in meta-material filled-slot waveguide, Evgeny G. Mironov¹, Liming Liu¹, Haroldo T. Hattori¹, Richard M. De La Rue²; ¹School of Engineering and Information Technology, UNSW Australia, Australia; ²School of Engineering, The Univ. of Glasgow, UK. We study a meta-material-based optical waveguide formed by a silica-filled slot in a layered metal-dielectric slab. This geometry results in very strong confinement of a quasi-TE fundamental mode and gives smaller propagation losses than a purely metallic slot waveguide.

JTh2A.119

Photon-Efficient High-Dimensional Quantum Key Distribution, Tian Zhong¹, Hongchao Zhou¹, Ligong Wang¹, Gregory Wornell¹, Zheshe Zhang¹, Jeffrey H. Shapiro¹, Franco Wong¹, Robert Horansky², Varun Verma², Adriana Lita², Richard P. Mirin², Thomas Gerrits², Sae Woo Nam², Alessandro Restelli³, Joshua C. Bienfang³, Francesco Marsili⁴, Matthew D. Shaw¹; ¹MIT, USA; ²National Inst. of Standards and Technology, USA; ³Joint Quantum Inst., National Inst. of Standards and Technology and Univ. of Maryland, USA; ⁴Jet Propulsion Lab, California Inst. of Technology, USA. We demonstrate two high-dimensional QKD protocols — secure against collective Gaussian attacks — yielding up to 8.6 secure bits per photon and 6.7 Mb/s throughput, with 6.9 bits per photon after transmission through 20 km of fiber.

JTh2A.120

Adaptive Binning and On-line Certification of Quantum Random Number Generators Using Bayesian Inference, Pavel Lougovski¹; ¹Oak Ridge National Lab, USA. Quantum random number generator statistics fluctuates with time due to noise affecting quality of randomness. We use Bayesian inference to monitor the statistics after each measurement and bin data adaptively to mitigate effects of noise.

JTh2A.121

Experimental Passive Decoy-state Quantum Key Distribution, Qi-Chao Sun^{1,3}, Wei-Long Wang², Yang Liu¹, Fei Zhou⁴, Jason Pelc⁵, Martin M. Fejer⁵, Cheng-Zhi Peng¹, Xian-Feng Chen³, Xiong-feng Ma², Qiang Zhang^{1,4}, Jian-Wei Pan¹; ¹Shanghai Branch, Hefei National Lab for Physical Sciences at Microscale and Dept. of Modern Physics, Univ. of Science and Technology of China, China; ²Center for Quantum Information, Inst. for Interdisciplinary Information Sciences, Tsinghua Univ., China; ³Dept. of Physics, Shanghai Jiao Tong Univ., China; ⁴Jinan Inst. of Quantum Technology, Shandong Academy of Information and Communication Technology, China; ⁵E.-L.-Ginzton Lab, Stanford Univ., USA. By employing low dark count up-conversion single photon detectors, we have experimentally demonstrated the passive decoy-state method over a 50-km-long optical fiber and have obtained a key rate of about 100 bits/s.

JTh2A • Poster Session 3—Continued

JTh2A.122

Development of Entangled Photon Pair Sources Based on Birefringent Structures, Alex McMillan¹, Alex Clark², Giacomo Corrielli³, Bryn Bell¹, Will McCutcheon¹, Tian Wu¹, William Wadsworth⁴, Roberto Osellame³, John Rarity¹; ¹Univ. of Bristol, UK; ²Univ. of Sydney, Australia; ³Politecnico di Milano, Italy; ⁴Univ. of Bath, UK. We describe an in-line source of polarisation entangled photons, based on four-wave mixing in birefringent optical fibre. We also discuss the prospect of implementing this scheme in a birefringent, laser-written waveguide on a chip.

JTh2A.123

Quantum Random Number Generation using Spontaneous Raman Scattering, Matthew J. Collins¹, Alex Clark¹, ZhiZhong Yan², Chunle Xiong¹, Michael J. Steel², Benjamin J. Eggleton¹; ¹Centre for Ultrahigh bandwidth Devices for Optical Systems (CUDOS), Inst. of Photonics and Optical Science (IPOS), School of Physics, Univ. of Sydney, Australia; ²CUDOS, MQ Photonics Research Centre, Dept. of Physics and Astronomy, Macquarie Univ., Australia. We generate a quantum random bit-string at 650kb/s by frequency binning spontaneous Raman scattered photons from a highly-nonlinear As₂S₃ glass detected using superconducting single photon detectors. The bit-sequences pass all the NIST statistical randomness tests.

JTh2A.124

High Throughput Photon Timing Electronics For Fluorescence Lifetime And Quantum Optics Applications, Michael Wahl¹, Tino Röhlicke¹, Hans-Jürgen Rahn¹, Volker Buschmann¹, Uwe Ortmann¹, Gerald Kell²; ¹PicoQuant GmbH, Germany; ²Fachhochschule Brandenburg, Germany. New integrated photon timing electronics with three independent input channels provide very short deadtime and very high throughput. We present design features and basic tests as well as application results from fluorescence and luminescence imaging.

JTh2A.125

A delayed choice complementarity experiment using a randomly switched quantum eraser, Dirk Puhlmann¹, Axel Heuer¹, Carsten Henkel¹, Ralf Menzel¹; ¹Univ. of Potsdam, Inst. of Physics and Astronomy, Germany. Quantum correlations between photons have applications in cryptography and imaging. We present a setup where Mach-Zehnder interference of the "signal photon" is suppressed or revived depending on which measurements are made on the "idler photon".

JTh2A.126

Phase Sensitive Raman Process with Correlated Seeds, Bing Chen¹, Cheng Qiu¹, Kai Zhang¹, Jinxian Guo¹, Liqing Chen¹, Chun-Hua Yuan¹, Zhe-Yu Jeff Ou^{1,2}, Weiping Zhang¹; ¹Quantum Inst. for Light and Atoms, Dept. of Physics, East China Normal Univ., China; ²Dept. of Physics, Indiana Univ.-Purdue Univ. Indianapolis, USA. We experimentally demonstrate a phase sensitive Raman scattering by injecting a Stokes light seed into an atomic ensemble, whose internal state is initially prepared in such a way that it is coherent with the input Stokes seed.

JTh2A.127

Phonon-Mediated Spin-Photon Interface with a Diamond Nanomechanical Oscillator, Mark Kuzyk¹, Thein Oo¹, Hailin Wang¹; ¹Physics, Univ. of Oregon, USA. We propose the use of diamond nanomechanical oscillator to mediate coupling between electron spins and arbitrary optical modes in a whispering-gallery optical resonator. Fabrication and characterization of the diamond nanomechanical oscillator will also be presented.

JTh2A.128

A polarization-singularity photonic crystal waveguide design to enable quantum dot spin to photon entanglement on-chip, Andrew Young¹, Arthur Thijssen¹, Daryl Beggs¹, Kobus Kuipers², John Rarity¹, Ruth Oulton¹; ¹Bristol Univ., UK; ²FOM Inst. AMOLF, Netherlands. We show the importance of polarization and phase engineering when designing quantum information devices. Using the example of a photonic-crystal waveguide we demonstrate, for the first time, designs for an integrated quantum dot spin-photon interface.

JTh2A.129

Single-crystalline GaP cavity-waveguide structures on diamond, Nicole K. Thomas¹, Russell Barbour², Yuncheng Song³, Minjoo Larry Lee³, Kai-Mei C. Fu^{1,2}; ¹Electrical Engineering, Univ. of Washington, USA; ²Physics, Univ. of Washington, USA; ³Electrical Engineering, Yale Univ., USA. We present coupled GaP resonator-waveguide structures on diamond fabricated from single-crystalline, epitaxially grown material. This progress is critical for the integration of nitrogen-vacancy centers in diamond into optical networks with active, linear electro-optic devices.

JTh2A.130

Tunable Dual-Wavelength Ytterbium Doped Photonic Crystal Fiber Laser Based On A Mach-Zehnder Interferometer, Daniel Toral-Acosta¹, Arturo Castillo-Guzman¹, Romeo Selvas-Aguilar¹, Juan M. Sierra-Hernandez², Valentin Guzman-Ramos¹, Roberto Rojas-Laguna²; ¹UANL-FCFM, Mexico; ²UG, Mexico. A tunable dual-wavelength ytterbium doped photonic crystal fiber laser based on a Mach-Zehnder interferometer is presented. The laser tunes from 1026nm to 1034nm by controlling the birefringence with a linewidth of 0.007nm and a contrast of 40dB.

JTh2A.131

Flat-top pulse generation with pulse width continuously tunable using bandpass filter in mode locking fiber laser, Xiaohui Fang¹; ¹Guangzhou Univ., China. A 10 GHz Flat-top pulse with pulse width continuously and periodically tunable using bandpass filter is generated in active-mode-locking combined nonlinear-polarization-rotation fiber laser. The SMSR is 65 dB and the timing jitter is 92 fs.

JTh2A.132

High speed single-pixel imaging via time domain compressive sampling, Hongwei Chen^{1,2}, Zhiliang Weng^{1,2}, Yunhua Liang^{1,2}, Cheng Lei^{1,2}, Fangjian Xing^{1,2}, Minghua Chen^{1,2}, Shizhong Xie^{1,2}; ¹Tsinghua National Lab for Information Science and Technology, China; ²Dept. of Electronic Engineering, Tsinghua Univ., China. We report a high speed single-pixel microscopic imaging method by compressive sampling accomplished with time-stretch technique. By this method, we demonstrate a single-pixel imaging system with 1000 times faster than the conventional single-pixel cameras.

JTh2A.133

Withdrawn

JTh2A.134

Advanced High-Efficiency NLW Fiber Raman Lasers, Ravinder K. Jain¹, Mike Klopfer¹, Leanne Henry²; ¹Univ. of New Mexico, USA; ²AFRL, USA. We will describe key design issues and related experimental results for achieving high-efficiency high-power (~ 100 W) < 3 GHz narrow linewidth (NLW) 1178 nm fiber Raman lasers for sodium guidestar applications.

JTh2A.135

Real-time THz-wave spectroscopy via infrared lights detection interacted with evanescent THz waves, Takuya Akiba¹, Naoya Kaneko¹, Koji Sizu¹, Katsuhiko Miyamoto², Takashige Omatsu^{2,3}; ¹Chiba Inst. of Technology, Japan; ²Chiba Univ., Japan; ³CREST, Japan. We report a novel spectroscopy technique that uses an evanescent terahertz wave, without detecting the THz wave directly. It will be possible to measure various material in real-time at the terahertz frequency region.

JTh2A.136

Design of X-ray Differential Phase Contrast Imaging System for High Energy and Wide Spectrum X-ray Applications, Yuzuru Takashima¹, Jihun Kim¹, Yao-Te Cheng², Max Yuen², Jeffrey Wilde², Lambertus Hesselink²; ¹College of Optical Sciences, The Univ. of Arizona, USA; ²Stanford Univ., USA. The optimum design of a grating-based X-ray differential phase contrast imaging system is relatively insensitive to the source spectrum. High energy and wide field of view applications eventually require grating-less sources and detectors.

JTh2A.137

Ultra high sensitivity and precise solute positioning by tailoring surface wettability, Ermanno Miele¹, Mario Malerba¹, Michele Dipalo¹, Eliana Rondanina¹, Andrea Toma¹, Francesco De Angelis¹; ¹Italian Inst. of Technology, Italy. Hydrophobic and oleophobic surfaces have been used to deliver molecules and nanoparticles in given 2D arrays with spatial control. Effectiveness in sensing and assembly processes is shown, reaching ultra low sensitivity (aM) and precise positioning of colloidal nanocrystals.

JTh2A.138

Silicon Microreflector Created by Single Ultrafast Laser Pulse, Jingyu Zhang¹, Rokas Drevinskas¹, Martynas Beresna¹, Mindaugas Gecevicius¹, Peter G. Kazansky¹; ¹Optoelectronics Research Centre, Univ. of Southampton, UK. Directly written structure created on the surface of silicon by the single pulse femtosecond laser irradiation are observed to function as microreflector. The smooth surface of the structure is a result of molten material flow.

12:30–14:00 Pizza Lunch with Exhibitors, Exhibit Hall 1 & 2

CLEO: QELS-Fundamental Science

14:00– 16:00

FTh3A • Nonclassical States and Quantum Phenomena

Presider: Raphael Pooser; Oak Ridge National Lab, USA

FTh3A.1 • 14:00

Simulating Quantum Optical Networks with Ultrafast Pulse Shaping, Jonathan Roslund¹, Yin Cai¹, Claude Fabre¹, Nicolas Treps¹; ¹Laboratoire Kastler Brossel, France. Photonic cluster states are fabricated within the internal structure of a multimode frequency comb. Projective measurements combined with ultrafast pulse shaping allow the creation of arbitrary cluster states with no change in the optical footprint.

FTh3A.2 • 14:15

Weaving quantum optical frequency combs into hypercubic cluster states, Pei Wang¹, Moran Chen¹, Nicolas C. Menicucci², Olivier Pfister¹; ¹Physics, Univ. of Virginia, USA; ²School of physics, The Univ. of Sydney, Australia. We present a simple, scalable, top-down method of entangling the quantum optical frequency comb into hypercubic-lattice continuous-variable cluster states up to a maximum size of about 10000 modes using existing technology.

FTh3A.3 • 14:30

Quantum non-Gaussian and Gaussian States at Multiple Side-band Frequencies, Katanya Kuntz^{1,2}, Hongbin Song^{1,2}, James Webb¹, Trevor Wheatley^{1,2}, Akira Furusawa³, Timothy Ralph^{2,4}, Elanor Huntington^{1,2}; ¹School of Engineering and Information Technology, UNSW Canberra, Australia; ²Center for Quantum Computation and Communication Technology, Australian Research Council, Australia; ³Dept. of Applied Physics, School of Engineering, Univ. of Tokyo, Japan; ⁴School of Mathematics and Physics, Univ. of Queensland, Australia. We simultaneously generate photon-subtracted squeezed vacuum and squeezed vacuum at three frequencies from an optical parametric oscillator by utilizing its frequency nondegenerate side-bands. Quantum non-Gaussianity is demonstrated by applying a novel character witness.

14:00– 16:00

FTh3B • Quantum Optics with Atoms and Ions

Presider: Stefan Kröll, Lunds Universitet, Sweden

FTh3B.1 • 14:00

Nonlinear Optics at Ultra Low Power in a High-Finesse Optical Cavity with Metastable Xenon, Garrett Hickman¹, Todd B. Pittman¹, James D. Franson¹; ¹Physics, Univ. of Maryland, Baltimore County, USA. We propose metastable xenon gas as a medium for realizing room temperature nonlinear optics experiments in cavity QED. We demonstrate the viability of this scheme by saturating the $6s[3/2]2$ to $6p[3/2]2$ transition with nanowatt powers.

FTh3B.2 • 14:15

Measuring the Photonic Frequency Qubit Generated by an 171Yb^+ Ion in a Surface Trap, Geert Vrijsen¹, Jungsang Kim¹, Kai Hudek¹, Dan Gaultney¹, Louis Isabella¹; ¹Electrical and Computer Engineering, Duke Univ., USA. We propose a novel qubit state measurement method for photonic frequency qubits using a Mach-Zehnder interferometer with unequal path lengths. A practical implementation for photons generated by 171Yb^+ ions in a surface trap is described.

FTh3B.3 • 14:30 **Invited**

Building Quantum Networks with Ions in Optical Cavities, Tracy Northup¹, Bernardo Casabone¹, Birgit Brandstätter¹, Konstantin Friebe¹, Klemens Schuppert¹, Florian Ong¹, Rainer Blatt^{1,2}; ¹Univ. of Innsbruck, Austria; ²Inst. for Quantum Optics and Quantum Information of the Austrian Academy of Sciences, Austria. Trapped ions are a key experimental platform for quantum computing, while photons transport information over long distances. Optical cavities provide a coherent link between these two systems, as demonstrated by recent experiments with calcium ions.

14:00– 16:00

FTh3C • Low Energy Dynamics in Dirac Materials

Presider: Yun-Shik Lee, Oregon State Univ., USA

FTh3C.1 • 14:00

Effect of grain-boundary plasmon on the negative terahertz dynamics conductivity in graphene, Soonyoung Cha¹, Seong Chu Lim², Seung Jin Chae², Young Hee Lee², Hyunyoung Choi¹; ¹School of Electrical and Electronic Engineering, Yonsei Univ., Korea; ²Inst. of Basic Science, Center for Integrated Nanostructure Physics, Dept. of Physics, Sungkyunkwan Univ., Korea. We discuss the origin of negative dynamic terahertz (THz) conductivity in graphene. By performing series of fluence and photon-energy dependent studies, we show that the nonequilibrium THz dynamics is strongly affected by the polycrystalline plasmons.

FTh3C.2 • 14:15

Electronic Cooling in Epitaxial and CVD Graphene, Momchil T. Mihnev^{1,2}, Torben Winzer³, Seunghyun Lee¹, Zhaohui Zhong¹, Claire Berger⁴, Walt A. de Heer⁴, Ermin Malic³, Andreas Knorr³, Theodore B. Norris^{1,2}; ¹Dept. of Electrical Engineering and Computer Science, Univ. of Michigan, USA; ²Center for Ultrafast Optical Science, Univ. of Michigan, USA; ³Institut für Theoretische Physik, Nichtlineare Optik und Quantenelektronik, Technische Universität Berlin, Germany; ⁴School of Physics, Georgia Inst. of Technology, USA. Using ultrafast optical-pump terahertz-probe spectroscopy, we study the THz dynamics and electronic cooling in few-layer epitaxial and CVD graphene; a microscopic theory of carrier-carrier and carrier-phonon interactions accounts quantitatively for the observed dynamics.

FTh3C.3 • 14:30

Carrier dynamics in graphene studied by ultra-broadband THz time-domain spectroscopy, Masatsugu Yamashita¹, Shokkeda^{1,2}, Chiko Otani^{1,2}; ¹Center for Advanced Photonics, RIKEN, Japan; ²Graduate School of Science, Tohoku Univ., Japan. Carrier dynamics in graphene has been studied by ultrabroadband THz-TDS. We measured the optical conductivity of graphene with and without the photoexcitation. Above $I_{\text{pump}}=200\mu\text{J}/\text{cm}^2$, the negative conductivity in graphene indicating THz wave amplification are observed.

14:00– 16:00

FTh3D • Novel Optical Phenomena

Presider: Luca Razzari; INRS-Energie Materiaux et Telecom, Canada

FTh3D.1 • 14:00

Tunable Raman Soliton Self-Frequency Shift via an Asymmetric Airy Pulse, Yi Hu^{1,2}, Amirhossein Tehranchi^{1,3}, Stefan Wabnitz⁴, Zhigang Chen^{2,5}, Raman Kashyap³, Roberto Morandotti¹; ¹INRS-EMT, Canada; ²TEDA Applied Physics Inst. and School of Physics, Nankai Univ., China; ³Dept. of Electrical Engineering and Dept. of Engineering Physics, Ecole Polytechnique, Univ. of Montreal, Canada; ⁴Dipartimento di Ingegneria dell'Innovazione, Università di Brescia, Italy; ⁵Dept. of Physics & Astronomy, San Francisco State Univ., USA. We study soliton self-frequency shift initiated by an Airy pulse in an optical fiber. The asymmetric features associated with the pulse exhibiting leading or trailing oscillatory tails are revealed through the effect of Raman scattering.

FTh3D.2 • 14:15

Nonlinear optics of fiber event horizons, Karen E. Webb¹, Miro J. Erkkila¹, Yiqing Xu^{1,2}, Neil Broderick¹, John M. Dudley³, Goëry Genty⁴, Stuart G. Murdoch¹; ¹Univ. of Auckland, New Zealand; ²The Univ. of Hong Kong, Hong Kong; ³Universite de Franche-Comte, France; ⁴Tampere Univ. of Technology, Finland. We theoretically and experimentally show that fiber-optic analogues of event horizons can be explained by cascaded four-wave mixing of monochromatic continuous waves. Experiments performed with pulsed and continuous wave lasers are in excellent agreement.

FTh3D.3 • 14:30

Third-harmonic spectroscopy of all-dielectric oligomers with both electric and magnetic resonances, Maxim R. Shcherbakov¹, Dragomir N. Neshev², Alexander S. Shorokhov¹, Isabelle Staudé², Elizaveta V. Melik-Gaykazyan¹, Ben Hopkins², Jason Dominguez³, Andrey Miroshnichenko², Igal Brener³, Andrey Fedyanin¹, Yuri S. Kivshar²; ¹Faculty of Physics, Lomonosov Moscow State Univ., Russia; ²Nonlinear Physics Centre, Research School of Physics and Engineering, The Australian National Univ., Australia; ³Center for Integrated Nanotechnologies, Sandia National Lab, USA. We characterize experimentally the nonlinear optical response of silicon nanodisk oligomers using third-harmonic generation spectroscopy and reveal the contributions of magnetic and electric dipolar resonances, local field enhancement, and nonlinear interference.

CLEO: Science & Innovations

14:00– 16:00
STh3E • High Harmonics and
Field Synthesis

Presider: Tamas Nagy; Leibniz
Universität Hannover, Germany

STh3E.1 • 14:00 **Invited**
**Synthesizing Optical Fields of Arbitrary
Shape**, Andy Kung^{1,2}, Han-Sung Chan¹, Ahi-
Ming Hsieh³, Chih-Hsuan Lu², Br-Shu Wu¹,
Yu-Chen Cheng¹, Yuan-Yao Lin², Yen-Yin Lin²,
Shang-Da Yang², Chia-Chen Hsu⁴; ¹*Inst. of
Atomic and Molecular Sciences, Academia Si-
nica, Taiwan*; ²*Inst. of Photonics Technologies,
National Tsing Hua Univ., Taiwan*; ³*Physics
Dept., Fu Jen Catholic Univ., Taiwan*; ⁴*Physics
Dept., National Chung Cheng Univ., Taiwan*.
Light fields with shapes similar to those
produced from RF function generators are
realized. Such fields may be used to dictate
the microscopic motion of charged particles
in atoms and molecules and in matter.

STh3E.2 • 14:30
**Arbitrary Carrier-Envelope Phase Control
in a 10 kHz, mJ-Class Amplifier**, Fabian
Lücking¹, Vincent Crozatier², Andreas Assion¹;
¹*Femtolasers Produktions GmbH, Austria*;
²*Fastlite, France*. The carrier-envelope
phase of every single shot emitted by a 10
kHz, mJ-class amplifier is measured with
a fast spectrometer. A novel high-speed
actuator allows arbitrary phase control, with
closed-loop integrated phase noise on seed
oscillator level (98 mrad, 500000 shots, 50 s).

14:00– 16:00
STh3F • THz Waveguides and
Optics

Presider: Ajay Nahata; Univ. of
Utah, USA

STh3F.1 • 14:00
**Optically-induced mode coupling and
interference in a terahertz parallel plate
waveguide**, Lauren Gingras¹, Marcel Geor-
gin¹, David G. Cooke¹; ¹*McGill Univ., Canada*.
We demonstrate all-optical control of tera-
hertz wave mode coupling in a silicon-filled
parallel-plate waveguide. The resulting
frequency modulation is widely tunable by
moving the control beam illumination in the
propagation direction.

STh3F.2 • 14:15
**Probing Inside THz Parallel-Plate Wave-
guides with Resonant Cavities**, Kimberly
S. Reichel¹, Krzysztof Iwaszczuk², Peter U.
Jepsen², Rajind Mendis¹, Daniel M. Mittle-
man¹; ¹*Electrical and Computer Engineering,
Rice Univ., USA*; ²*DTU Fotonik, Technical Univ.
of Denmark, Denmark*. We experimentally
observe in situ the resonance due to an inte-
grated resonant cavity inside a parallel-plate
waveguide excited by the TE₁ mode. We also
observe a field enhancement associated with
this narrowband resonance.

STh3F.3 • 14:30
**Terahertz Absorption Saturation in Intrinsic
Silicon Dielectric Ridge Waveguides**,
Shanshan Li¹, Gagan Kumar², Thomas E.
Murphy¹; ¹*Inst. for Research in Electronics
& Applied Physics, Univ. of Maryland, USA*;
²*Dept. of Physics, Indian Inst. of Technology
Guwahati, India*. We measure the transmis-
sion of terahertz pulses through an intrinsic
silicon waveguide, and observe a decrease
in absorption at higher terahertz fields. The
effect is enhanced when photocarriers are in-
troduced by top-illuminating the waveguide.

14:00– 15:45
STh3G • Quantum Cascade
Lasers I

Presider: Dan Wasserman; Univ.
of Illinois, USA

STh3G.1 • 14:00
**Low-threshold InGaAs/GaAsSb 'W'-type
quantum well laser on InP substrate**, Chia-
Hao Chang¹, Zong-Lin Li¹, Hong-Ting Lu¹,
Chien-Ping Lee¹, Sheng-Di Lin¹; ¹*Electronics
Engineering, National Chiao Tung Univ.,
Taiwan*. The mid-infrared electrically-driven
laser using InGaAs/GaAsSb 'W'-type QWs
is demonstrated at room temperature. The
InP-based laser lasing at 2.35 μm with the
lowest threshold current density of 1.42 kA/
 cm^2 is presented.

STh3G.2 • 14:15
**High-Power CW Operation of 7-Stage
Interband Cascade Lasers**, Chadwick L.
Canedy¹, Joshua Abell¹, Charles D. Merritt¹,
William W. Bewley¹, Chul Soo Kim¹, Igor
Vurgafman¹, Jerry R. Meyer¹, Mijin Kim²; ¹*US
Naval Research Lab, USA*; ²*Sotera Defense
Solutions, USA*. We report a 7-stage narrow-
ridge interband-cascade laser emitting at λ
 $\approx 3.5 \mu\text{m}$ that produces up to 592 mW of cw
power, with a wallplug efficiency of 10.1%
and $M2 = 3.7$ at $T = 25^\circ\text{C}$.

STh3G.3 • 14:30
**Direct Observation of Non-uniform Electric
Field in the Active Regions of an Interband
Cascade Laser**, Rudra S. Dhar¹, Chao Xu¹,
Dayan Ban¹, Lu Li², Hao Ye², Rui Yang²,
Matthew B. Johnson³, Tetsuya D. Mishima³,
Mike Santos³; ¹*Electrical & Computer Engi-
neering, Univ. of Waterloo, Canada*; ²*School
of Electrical & Computer Engineering, Univ.
of Oklahoma, USA*; ³*Physics & Astronomy,
Univ. of Oklahoma, USA*. The non-uniform
electric field in the active regions of an in-
terband cascade laser is directly imaged and
characterized for the first time by employing
a nanoscopic voltage profiling technique.

14:00– 16:00
STh3H • Sensing with
Optofluidics

Presider: Timo Mappes;
Karlsruher Institut für
Technologie, USA

STh3H.1 • 14:00 **Tutorial**
**Optofluidics for Mobile Health, Bioenergy,
and Nanoparticle Analysis**, David Erickson¹;
¹*Sibley School of Mechanical and Aerospace
Engineering, Cornell Univ., USA*. In this talk
I will review recent progress on Optofluid-
ics at Cornell in three application spaces:
mobile and global health, bioenergy, and
nanoparticle analysis. Fundamental science
will be described as well as routes to com-
mercialization and deployment.



David Erickson is an Associate Professor in
the Sibley School of Mechanical and Aero-
space Engineering at Cornell University. Prior
to joining the faculty in 2005, he was a post-
doctoral scholar at the California Institute of
Technology and he received his Ph.D. degree
from the University of Toronto in 2004. Er-
ickson is the co-founder of Optofluidics, Inc.
which is commercializing high-throughput
nanoparticle analysis systems, and was
named Philadelphia life-sciences start-up of
the year in 2012, and VitalMe Technologies
which is developing smartphone based point-
of-care molecular diagnostics.

Meeting Room
211 B/D

CLEO: Science &
Innovations

14:00– 16:00

STh3I • Photovoltaics Sciences

President: Arthur J. Fischer; Sandia
National Labs, USA

STh3I.1 • 14:00 **Tutorial**

Flexible, Microscale Inorganic LEDs and Solar Cells, John Rogers¹; ¹Univ of Illinois at Urbana-Champaign, USA. This tutorial covers recent progress in the design of high-performance light emitting diodes with unusual sizes, shapes and forms. Applications range from large-area, flexible light sources for general illumination to cellular-scale, injectable systems for biomedicine.



John A. Rogers obtained an undergraduate degree from the University of Texas in 1989 and a Ph.D. from MIT in 1995. From 1995 to 1997, he was a Junior Fellow at Harvard University. He spent five years at Bell Labs before joining the faculty at University of Illinois in 2003.

Meeting Room
212 A/C

JOINT

14:00– 16:00

JTh3J • Symposium on High
Performance Optics I

President: Christopher J. Stolz,
Lawrence Livermore National
Lab. USA

JTh3J.1 • 14:00 **Invited**

Defect-driven laser-induced damage in optical coatings, Xinbin Cheng^{2,1}, Tao Ding^{2,1}, Bin Ma^{2,1}, Hongfei Jiao^{2,1}, Jinlong Zhang^{2,1}, Zhengxiang Shen^{2,1}, Zhanshan Wang^{2,1}; ¹Inst. of Precision Optical Engineering, School of Physics Science and Engineering, Tongji Univ., China; ²MOE Key Lab of Advanced Micro-Structured Materials, China. Defect-driven laser-induced damage in sub-surface of substrates and coatings is discussed with emphasis on the techniques for characterizing defects and the solutions to reduce defects. Consideration is also given to laser-induced damage of artificial defects.

JTh3J.2 • 14:30

Optical Damage Performance Assessment of Petawatt Final Optics for the Advanced Radiographic Capability, David A. Alessi¹, Christopher W. Carr¹, Richard P. Hackel¹, Kenneth Stanion¹, David A. Cross¹, Matthew Fischer¹, James D. Nissen¹, Ronald Luthi¹, Shawn Betts¹, William Gourdin¹, Jerry A. Britten¹, Jim Fair¹, Constantin L. Haefner¹; ¹Lawrence Livermore National Lab, USA. To predict in-vacuum optical damage performance of Advanced Radiographic Capability Petawatt final optics we have developed a ps-damage test station to measure damage density and compare results to R-on-1 tests.

Meeting Room
212 B/D

CLEO: QELS-
Fundamental Science

14:00– 16:00

FTh3K • Plasmonic Lasers and
Amplification

President: Vinod Menon, CUNY
Queens College, USA

FTh3K.1 • 14:00

Injection-Seeded Optoplasmonic Amplifier in the Visible, Manas Ranjan Gartia¹, Sujin Seo¹, JunHwan Kim¹, Te-Wei Chang¹, Gaurav Bahl¹, Meng Lu², J. Gary Eden¹, Gang L. Liu¹; ¹Electrical and Computer Engineering, Univ. of Illinois Urbana Champaign, USA; ²Electrical and Computer Engineering, Iowa State Univ., USA. An injection-seeded, WGM resonator-based amplifier has been demonstrated. Synergy between the gain medium, WGM spectrum, and the Raman modes of the amplifier constituents is fundamental. The estimated optical gain is ~ 30 dB.

FTh3K.2 • 14:15

Strong coupling of surface plasmons to dye molecules: Tailoring dispersion and beyond, Thejaswi Tumkur¹, Guohua Zhu¹, Mikhail A. Noginov¹; ¹Norfolk State Univ., USA. In the presence of dye molecules, the dispersion curve of SPPs splits into three branches and demonstrates the avoided crossing characteristic of strong coupling. It is further modified by the optical gain in the system.

FTh3K.3 • 14:30 **Invited**

Highly-directional plasmonic lasing in the visible with subwavelength hole arrays, Xiangeng Meng¹, Jingjing Liu¹, Alexander Kildishev¹, Vladimir M. Shalaev¹; ¹Purdue Univ., USA. We demonstrate directional plasmonic nanolaser emission using subwavelength hole arrays perforated in metal film as plasmonic nanocavities. The lasing exhibits a single mode in the red wavelength region.

Marriott
Salon I & II

JOINT

14:00– 16:00

JTh3L • Symposium on Laser-
Driven Sources of Particle and
X-Ray Beams II **▶**

President: Donald Umstadter; Univ.
of Nebraska Lincoln, USA

JTh3L.1 • 14:00 **Invited** **▶**

X-ray emission from laser-accelerated electrons and its use as diagnostic of laser-plasma interaction, Sebastien Corde¹, Cédric Thauray¹, Kim Ta Phuoc¹, Agustin Lifschitz¹, Rémi Lehe¹, Emillien Guillaume¹, Guillaume Lambert¹, Antoine Rousse¹, Victor Malka¹; ¹Laboratoire d'optique appliquée, France. X-ray radiation emitted by electrons during their acceleration in a laser-plasma accelerator was used to evidence two distinct self-injection mechanisms (longitudinal and transverse) and to identify one source of angular-momentum growth in laser-plasma accelerators.

JTh3L.2 • 14:30 **▶**

Angular dependence of betatron x-ray spectra in a laser-wakefield accelerator, Félicie Albert¹, Bradley Pollock¹, Jessica L. Shaw², Ken Marsh², Yu-Hsin Chen¹, David Alessi¹, Chris Clayton², Joseph Ralph¹, Arthur Pak¹, Siegfried Glenzer³, Chan Joshi²; ¹NIF and Photon Sciences, Lawrence Livermore National Lab, USA; ²Electrical Engineering, UCLA, USA; ³SLAC National Accelerator Lab, USA. Our experiments produced betatron x-rays up to 80 keV from a laser-wakefield accelerator. Measurements, performed with stacked image plates spectrometers, provide simultaneous information on the beam profile and spectrum at various angles of observation.

CLEO: Science & Innovations

CLEO: Applications
& Technology

14:00– 15:45

STh3M • Silicon Photonics

President: To be Determined

STh3M.1 • 14:00

Efficient Thermally Tunable Linear Photonic Crystal Cavities in a Zero-Change Microelectronics SOI CMOS Process, Christopher V. Poulton¹, Xiaoge Zeng¹, Mark T. Wade¹, Jeffrey M. Shainline¹, Miloš A. Popović¹; ¹Univ. of Colorado at Boulder, USA. We demonstrate directly-doped Si tunable linear photonic crystal microcavities. Also the first tunable photonic crystals realized in an advanced (45nm) SOI CMOS microelectronics process with no in-foundry process changes, they show 0.63nm/mW tuning efficiency.

STh3M.2 • 14:15

On chip wide angle beam steering Ami, Ami Yaacobi¹, Jie Sun¹, Michele Moresco¹, Gerald Leake², Douglas Coolbaugh², Michael R. Watts³; ¹MIT, USA; ²Suny College of Nanoscale Science and Engineering, USA. We demonstrate an on-chip optical phased array fabricated in a CMOS compatible process with continuous, fast (100 kHz), wide-angle (51o) beam-steering that is suitable for applications such as low-cost lidar systems.

STh3M.3 • 14:30

Non-Invasive Integrated Light Probe, Stefano Grillanda¹, Francesco Morichetti¹, Marco Carminati¹, Giorgio Ferrari¹, Michael Strain², Marc Sorel³, Marco Sampietro¹, Andrea Melloni¹; ¹Dipartimento di Elettronica, Informazione e Bioingegneria, Politecnico di Milano, Italy; ²Inst. of Photonics, Univ. of Strathclyde, UK; ³School of Engineering, Univ. of Glasgow, UK. Non-perturbative on-chip light observation is achieved in silicon photonics waveguides by a novel integrated photonic probe. Light intensity monitoring is performed over 40 dB dynamic range, -30 dBm sensitivity, and microsecond scale time response.

14:00– 16:00

STh3N • Supercontinuum Generation

President: Fetah Benabid; Univ. of Bath, UK

STh3N.1 • 14:00

Mid-infrared supercontinuum generation in concatenated fluoride and chalcogenide glass fibers covering more than three octaves, Irnis Kubat¹, Christian Rosenberg Petersen¹, Uffe Møller¹, Angela Seddon², Trevor Benson², Laurent Brilland³, David Mechin³, Peter Moselund⁴, Ole Bang¹; ¹DTU Fotonik, Dept. of Photonics Engineering, Technical Univ. of Denmark, Denmark; ²George Green Inst. for Electromagnetics Research, Faculty of Engineering, Univ. Park, Univ. of Nottingham, UK; ³Perfos, R&D Platform of Photonics Bretagne, France; ⁴NKT Photonics A/S, Denmark. Supercontinuum is generated in concatenated ZBLAN and As₂Se₃ fibers. Initially, a 0.9-4.1µm supercontinuum is obtained by pumping the ZBLAN fiber with a Tm laser, which then continues to broaden to 0.9-9µm in As₂Se₃ fiber.

STh3N.2 • 14:15

Supercontinuum Generation in As₂S₃-Silica Double-Nanospike Waveguide, Shangran Xie¹, Francesco Tani¹, John C. Travers¹, Johann Troles², Markus Schmidt^{3,1}, Philip St.J. Russell^{1,4}; ¹Russell Division, Max Planck Inst. for the Science of Light, Germany; ²Sciences Chimiques de Rennes, Université de Rennes I, France; ³Inst. of Photonic Technology, Germany; ⁴Dept. of Physics, Univ. of Erlangen-Nuremberg, Germany. A more than one-octave-wide supercontinuum (0.9 to ~2.1 µm) is generated in a double-nanospike As₂S₃-silica step-index waveguide. The average supercontinuum spectral intensity is increased by ~20 dB compared to the previously reported single-spike structure.

STh3N.3 • 14:30

Supercontinuum Generation in an As₂S₅ Chalcogenide Microstructured Optical Fiber, Weiqing Gao^{1,3}, Zhongchao Duan¹, Koji Asano¹, Tonglei Cheng¹, Dinghuan Deng¹, Morio Matsumoto², Takashi Misumi², Tak-enobu Suzuki¹, Yasutake Ohishi¹; ¹Research Center for Advanced Photon Technology, Toyota Technological Inst., Japan; ²Furukawa Denshi Co., Ltd., Japan; ³School of Electronic Science & Applied Physics, Hefei Univ. of Technology, China. We demonstrate the supercontinuum generation in an As₂S₅ microstructured optical fiber experimentally. The SC bandwidth of 4280 nm wider than two octaves covering from 1370 to 5650 nm is obtained in 4.8 cm long fiber.

14:00– 16:00

STh3O • Timing and Imaging

President: Franklyn Quinlan; NIST, USA

STh3O.1 • 14:00

High fidelity, general reflection-mode coherent diffractive imaging with a tabletop EUV source, daniel adams¹, Bosheng Zhang¹, Matthew Seaberg¹, Dennis Gardner¹, Elisabeth Shanblatt¹, Margaret Murnane¹, Henry Kapteyn¹; ¹NIST/JILA/CU, USA. We demonstrate the most general, highest fidelity, reflection mode coherent diffractive imaging to date. By combining tabletop high harmonics with ptychography and keyhole coherent diffraction techniques, images are reconstructed with < 3 nm axial resolution.

STh3O.2 • 14:15

Impact of Optical Amplification and Pulse Interleaving on Low Phase Noise Photonic Microwave Generation, Franklyn Quinlan¹, Fred N. Baynes¹, Tara M. Fortier¹, Qiugui Zhou², Allen Cross², Joe C. Campbell², Scott A. Diddams¹; ¹NIST, USA; ²Dept. of Computer and Electrical Engineering, Univ. of Virginia, USA. Using carefully constructed pulse interleavers, we demonstrate ~10 dB reduction in the quantum noise from optical amplification for short pulse detection, resulting in a phase noise floor on a 10 GHz microwave of -175 dBc/Hz.

STh3O.3 • 14:30

Optical frequency comb-based microwave distribution through a 2.3-km fiber link with 7×10⁻¹⁹ instability, Junho Shin¹, Kwangyun Jung¹, Jinho Kang¹, Stephan Hunziker², Chang-Ki Min³, Jungwon Kim¹; ¹Korea Advanced Inst. of Science and Technology (KAIST), Korea; ²Paul Scherrer Inst. (PSI), Switzerland; ³Pohang Accelerator Lab (PAL), Korea. We demonstrate a new time-of-flight stabilization technique based on all-fiber-loop optical-microwave phase detectors. The demonstrated relative frequency instability between 2.856-GHz signals separated by a 2.3-km fiber link is 6.5×10⁻¹⁹ at 82500-s averaging time.

14:00– 16:00

Ath3P • Symposium on Advanced Ultrashort Pulse Laser Technologies in Biophotonics and Nanobiophotonics I

President: Ilko Ilev; U.S. Food and Drug Administration, USA

Ath3P.1 • 14:00 **Invited**

Advances in Short-Pulse Fiber Lasers for Nonlinear Microscopy, Frank W. Wise¹; ¹Cornell Univ., USA. Recent advances in the development of fiber lasers for applications in nonlinear bioimaging will be presented.

Ath3P.2 • 14:30

Two-photon Fluorescence Resonance Energy Transfer Stoichiometry in Living Cells, Amar R. Bhagwat¹, Daniel Flynn¹, Meredith Brenner¹, Marcos Nunez¹, Jennifer Ogilvie¹, Dawen Cai², Joel Swanson²; ¹Univ. of Michigan, Ann Arbor, USA; ²Univ. of Michigan Medical School, USA. Using phase-shaped pulses, we perform, for the first time, a proof-of-principle demonstration of two-photon fluorescence resonance energy transfer (FRET) microscopy for studying the stoichiometry of intermolecular interactions within living cells.

CLEO: QELS-Fundamental Science

FTh3A • Nonclassical States and Quantum Phenomena—Continued

FTh3A.4 • 14:45

Lower Bound on the Speed of Nonlocal Correlations without Locality and Measurement Choice Loopholes, Juan Yin¹, Yuan Cao¹, Hai-Lin Yong¹, Ji-Gang Ren¹, Hao Liang¹, Sheng-Kai Liao¹, Fei Zhou¹, Chang Liu¹, Yu-Ping Wu¹, Ge-Sheng Pan¹, Li Li¹, Nai-Le Liu¹, Cheng-Zhi Peng¹, Jian-Wei Pan¹; ¹Shanghai Branch, National Lab for Physical Sciences at Microscale and Dept. of Modern Physics, Univ. of Science and Technology of China, China. Here, we strictly closed the loopholes by observing a 12 h continuous violation of the Bell inequality and concluded that the lower bound speed of spooky action was 4 orders of magnitude of the speed of light.

FTh3A.5 • 15:00

Testing randomness using multi-photon interference, Jonathan Matthews¹, Rebecca Whittaker¹, Jeremy L. O'Brien¹, Peter Turner¹; ¹Univ. of Bristol, UK. We demonstrate pseudorandom optical processes known as t-designs, showing that for $t=1(2)$ they are statistically indistinguishable from random operations for $1(2)$ -photon quantum interference, and that they fail to mimic randomness for $2(3)$ -photon interference.

FTh3A.6 • 15:15

Experimental Verification of Quantum Discord and Operational Significance of Discord Consumption, Sara Hosseini¹, Saleh Rahimi-Keshari², Jing Yan Haw¹, Assad M. Syed¹, Helen M. Chrzanowski¹, Jiri Janousek¹, Thomas Symul¹, Timothy Ralph², Ping Koy Lam¹, Mile Gu³, Kavan Modi^{4,5}, Vlatko Vedral^{4,5}; ¹Quantum Science, Australian National Univ., Australia; ²Mathematics and Physics, Univ. of Queensland, Australia; ³Quantum Technology, National Univ. of Singapore, Singapore; ⁴Atomic and Laser Physics, Univ. of Oxford, UK; ⁵Physics, National Univ. of Singapore, Singapore. We introduce a simple and efficient technique to verify quantum discord in unknown Gaussian states and certain class of non-Gaussian states. We also demonstrate that discord between bipartite systems can be consumed to encode information that can only be accessed by coherent quantum interaction.

FTh3B • Quantum Optics with Atoms and Ions—Continued

FTh3B.4 • 15:00

Frequency translation via four-wave mixing Bragg scattering in Rb filled photonic band-gap fibers, Prathamesh Donvankar¹, Vivek Venkataraman¹, Stéphane Clemmen¹, Kasturi Saha¹, Alexander L. Gaeta¹; ¹School of Applied and Engineering Physics, Cornell Univ., USA. We demonstrate frequency translation of a weak signal beam with 21% efficiency in Rb vapor confined to a hollow core photonic band-gap fiber via Bragg scattering by four-wave mixing using microwatt level pump beams.

FTh3B.5 • 15:15

Ultra-long lived atomic polarization of Rb confined in hypocycloidal Kagome HC-PCF, Ekatarina Ilinova¹, Tom Bradley^{1,2}, Meshaal Alharbi^{1,2}, John Mac Ferran¹, Benoît Debord¹, Frédéric Gérôme¹, Fetah Benabid^{1,2}; ¹GPPMM Group, Xlim Research Inst., CNRS UMR 7252, France; ²Dept. of Physics, Univ. of Bath, UK. We measure atomic polarization relaxation-time of Rb-loaded in different hypocycloidal-core Kagome HC-PCFs. The measured relaxation-time is two-orders of magnitude larger than the transit-time limit. We attribute this to slow-atom stronger contribution to the polarization build-up.

FTh3C • Low Energy Dynamics in Dirac Materials—Continued

FTh3C.4 • 14:45

Terahertz Carrier Dynamics in Graphene and Graphene Nanostructures, Soeren Jensen^{1,2}, Dmitry Turchinovich^{1,3}, Klaas-Jan Tielrooij⁴, Frank Koppens⁴, Ronald Ulbricht^{2,5}, Tobias Hertel⁶, Akimitsu Narita¹, XinLiang Feng¹, Klaus Müllen¹, Mischa Bonn¹; ¹Max Planck Inst. for Polymer Research, Germany; ²FOM Inst. for Atomic and Molecular Physics, Netherlands; ³DTU Fotonik, Technical Univ. of Denmark, Denmark; ⁴The Inst. of Photonic Sciences, Spain; ⁵Hokkaido Univ., Japan; ⁶Julius-Maximilians Univ., Germany. Photo-excited charge carriers in 2D graphene and in 1D graphene nanostructures were studied with optical pump-THz probe spectroscopy. We find efficient hot-carrier multiplication in 2D graphene, and predominantly free carrier early-time response in 1D nanostructures.

FTh3C.5 • 15:00 **Invited**

Observation of Floquet-Bloch States on the Surface of a Topological Insulator, Nuh Gedik¹; ¹MIT, USA. Using time- and angle-resolved photoemission spectroscopy, we show that an intense ultrashort mid-infrared pulse with energy below the bulk band gap hybridizes with the surface Dirac fermions of a topological insulator to form Floquet-Bloch bands.

FTh3D • Novel Optical Phenomena—Continued

FTh3D.4 • 14:45

Approaching Single-Photon Detection Level in Communication Band via Frequency Upconversion in GaP, Da Li¹, Xingquan Zou¹, Yujie J. Ding¹; ¹Lehigh Univ., USA. We have observed frequency upconversion of the incoming photons within the communication band to a visible band in a gallium phosphide crystal. Such a crystal is capable of reaching the single-photon detection level.

FTh3D.5 • 15:00

Ultralow-power nonlinear optics using tapered optical fibers in noble gases, Todd B. Pittman¹, Daniel E. Jones¹, James D. Franckson¹; ¹Univ. of Maryland Baltimore County, USA. We demonstrate ultralow-power optical nonlinearities using a sub-wavelength diameter tapered optical fiber in a gas of metastable xenon atoms. The use of inert noble gases offers advantages over reactive alkali vapors such as rubidium.

FTh3D.6 • 15:15

Investigation of Hot Photons in GaN/AlN High Electron Mobility Transistor Based on Stokes Raman Scattering, Ruolin Chen¹, Guan Sun¹, Yujie J. Ding¹, Jacob Khurgin²; ¹Lehigh Univ., USA; ²Johns Hopkins Univ., USA. We investigated hot phonons based on Stokes Raman scattering from a GaN/AlN high electron mobility transistor. Such a simple method is advantageous compared with the method based on Stokes and anti-Stokes Raman scattering.



For Conference News & Insights
Visit blog.cleoconference.org

CLEO: Science & Innovations

STh3E • High Harmonics and Field Synthesis—Continued

STh3E.3 • 14:45

CEP dependent high-order harmonic generation at 200 kHz repetition rate, Anne Harth¹, Piotr Rudawski¹, Chen Guo¹, Miguel Miranda¹, Eleonora Lorek¹, Esben Witting-Larsen¹, Christoph Heyl¹, Jan Matyschok^{2,3}, Oliver Prochnow², Thomas Binhammer², Uwe Morgner³, Anne L'Huillier¹, Cord L. Arnold¹; ¹Atomic Physics, Lund Univ., Sweden; ²VENTEON Laser Technologies GmbH, Germany; ³Institute of Quantum Optics, Leibniz Universität, Germany. We present the carrier-envelope phase dependent high-order harmonic generation in argon at 200 kHz repetition rate using ultra-short laser pulses from an optical parametric chirped pulse amplifier.

STh3E.4 • 15:00

Single Exposure Wavefront Curvature Estimation of High Harmonic Radiation by Diffraction from a Regular Array, James S. Feehan¹, Hannah M. Watts², Patrick Anderson¹, Thomas J. Butcher², Jonathan H. Price¹, Russell S. Minns², Peter Horak¹, William S. Brocklesby¹, Jeremy G. Frey²; ¹ORC, Univ. of Southampton, UK; ²School of Chemistry, Univ. of Southampton, UK; ³Rutherford Appleton Lab, UK. We present a novel technique for estimating the radius of curvature from a single exposure of EUV light from a high harmonic source diffracted by a grating of square apertures.

STh3E.5 • 15:15

Non-instantaneous polarization decay in dielectric media, Michael Hofman¹, Carsten Bree¹, Matthias Hoffmann², Ayhan Demircan², Tamas Nagy², Detelf Ristau^{2,3}, Uwe Morgner^{2,3}, Simon Birkholz⁴, Susanta Das⁴, Martin Bock⁴, Rüdiger Grunwald⁴, Janne Hytti⁵, Thomas Elsaesser⁴, Gunter Steinmeyer^{4,5}; ¹Weierstrass-Institut für Angewandte Analysis und Stochastik, Germany; ²Laser Zentrum Hannover, Germany; ³Institut für Quantenoptik, Universität Hannover, Germany; ⁴Max Born Inst., Germany; ⁵Optoelectronics Research Centre, Tampere Univ. of Technology, Finland. We demonstrate experimental evidence for non-instantaneous polarization decay in dielectrics. The few-femtosecond relaxation times agree favorable with solutions of the time-dependent Schrödinger equation and relate to resonances of the quantum mechanical dipole.

STh3F • THz Waveguides and Optics—Continued

STh3F.4 • 14:45

A Terahertz Leaky-Wave Antenna using a Parallel-Plate Waveguide, Robert W. McKinney¹, Yasuaki Monnai², Rajind Mendis¹, Daniel M. Mittleman¹; ¹Electrical and Computer Engineering, Rice Univ., USA; ²Creative Informatics, Univ. of Tokyo, Japan. A terahertz leaky-wave antenna was implemented using the TE1 mode of a parallel-plate waveguide with a plate separation of 4 mm. Peak frequencies of leaky wave radiation are shown to be consistent with predicted values.

STh3F.5 • 15:00

THz Tube Waveguides With Low Loss, Low Dispersion, and High Bandwidth, Hualong Bao¹, Kristian Nielsen¹, Ole Bang¹, Peter U. Jepsen¹; ¹DTU Fotonik - Dept. of Photonics Engineering, Technical Univ. of Denmark, Denmark. We propose, model and experimentally characterize a novel class of terahertz hollow-core tube waveguides with high-loss cladding material, resulting in propagation with low loss, low dispersion, and high useful bandwidth.

STh3F.6 • 15:15

Design and Optimization of Air-Doped 3-dB Terahertz Fiber Directional Couplers, Hualong Bao¹, Kristian Nielsen¹, Henrik K. Rasmussen², Peter U. Jepsen¹, Ole Bang¹; ¹Dept. of Photonics Engineering, Technical Univ. of Denmark, Denmark; ²Dept. of Mechanical Engineering, Technical Univ. of Denmark, Denmark. We present a thorough practical design optimization of broadband low loss, terahertz (THz) photonic crystal fiber directional couplers in which the two cores are mechanically down-doped with a triangular array of air holes.

STh3G • Quantum Cascade Lasers I—Continued

STh3G.4 • 14:45

Broadly Tunable Single-mode Slot Quantum Cascade Lasers, Bo Meng¹, Jin Tao¹, Xiao Hui Li¹, Yong Qian Zeng¹, Sheng Wu², Jie Q. Wang^{1,3}; ¹School of Electrical and Electronic Engineering, Nanyang Technological Univ., Singapore; ²Power Energy and Environmental Research Inst. Covina, USA; ³CDPT, Centre for Disruptive Photonic Technology, School of Physical and Mathematical Sciences, Nanyang Technological Univ., Singapore. Broadly tunable single-mode quantum cascade laser at ~10 μm with two-section etched slot structure is presented. The device shows 80 cm⁻¹ tuning range, ~20 dB side mode suppression ratio and ~30 to ~100 peak power.

STh3G.5 • 15:00

3 W Near-Diffraction-Limited Power from High-Index-Contrast Photonic-Crystal Quantum Cascade Lasers, Jeremy D. Kirch¹, Chun-Chieh Chang¹, Colin Boyle¹, Luke J. Mawst¹, Don Lindberg III², Thomas Earles², Dan Botez¹; ¹ECE, Univ. of Wisconsin-Madison, USA; ²Intraband, LLC, USA. Phase locking, via resonant leaky-wave coupling, of five 8.36 μm-emitting quantum cascade lasers has provided in-phase-mode operation to 3 W with 1.5 x diffraction limit lobewidth and 2.45 W emitted in the main far-field lobe.

STh3G.6 • 15:15

Surface Emission Quantum Cascade Lasers Combining First and Second Order DFB gratings, Pierre Jouy¹, Christopher Bonzon¹, Johanna Wolf¹, Mattias Beck¹, Jérôme Faist¹; ¹IQE, ETH, Switzerland. By combining first and second order DFB gratings, a new solution for surface emission QCL is presented. A QWS mode and a buried hetero-structure process allow single mode emission and low dissipation devices.

STh3H • Sensing with Optofluidics—Continued

STh3H.2 • 15:00

Mid-Infrared Opto-nanofluidics for Label-free On-Chip Sensing, Pao T. Lin¹, Sen W. Wai Kwok², Hao-Yu Greg Lin³, Vivek Singh¹, Lionel C. Kimerling¹, George Whitesides², Anu Agarwal¹; ¹Microphotonics Center, MIT, USA; ²Dept. of Chemistry and Chemical Biology, Harvard Univ., USA; ³Center for Nanoscale Systems, Harvard Univ., USA. A mid-infrared opto-nanofluidics was developed using a Si-liquid-Si slot-waveguide. Through an optical-field enhancement with a direct interaction between the probe light and analyte, the detection sensitivity is increased by 50 times compared to evanescent-wave-sensing.

STh3H.3 • 15:15

Open-access microcavities for optofluidic sensing, Aurélien Trichet¹, James Foster², Dean James², Naomi Omori¹, Philip Dolan¹, Gareth Hughes¹, Claire Vallance², Jason Smith¹; ¹Dept. of Materials, Univ. of Oxford, UK; ²Dept. of Chemistry, Univ. of Oxford, UK. Open-access microcavities are an original approach for lab-on-a-chip optofluidic sensing since they offer a direct access to the confined electromagnetic field. This work describes their basic characteristics for refractive index and nanoparticle sensing.

Technical Digest and Postdeadline Papers Available Online

- Visit www.cleoconference.org
- Select **Download Digest Paper** button
- Use your email address and CLEO Registration ID # to synchronize

Once you have synchronized your conference registration with Optics InfoBase, you can log in directly to Optics InfoBase at any point using the same email address and OSA password.

Access must be established via synchronization within 60 days of the conference start date. Access is provided only to full technical attendees.

Meeting Room
211 B/D

CLEO: Science &
Innovations

STh3I • Photovoltaics
Sciences—Continued

STh3I.2 • 15:00

Absorption enhancement and electrical transport in thin-film solar cells with randomly rough textures, Piotr Kowalczewski¹, Angelo Bozzola¹, Marco Liscidini¹, Lucio C. Andreani¹; ¹Dept. of Physics, Univ. of Pavia, Italy. With rigorous electro-optical calculations we study randomly rough silicon solar cells approaching the Lambertian Limit of absorption. We determine the efficiency dependence on the absorber thickness and discuss the role of surface recombination.

STh3I.3 • 15:15

Perfect Sunlight Absorption in Iron Oxide Photoanode, Ken Xingze Wang¹, Zongfu Yu¹, Victor Liu¹, Mark Brongersma¹, Thomas Jaramillo¹, Shanhui Fan¹; ¹Stanford Univ., USA. We design a novel core-shell nanocone structure that allows full absorption of sunlight in an iron oxide photoanode. The photocurrent approaches 12.5mA/cm² within an iron oxide thickness of 20nm, verified by full-field electromagnetic simulation.

Meeting Room
212 A/C

JOINT

JTh3J • Symposium on High
Performance Optics I—
Continued

JTh3J.3 • 14:45

Enhanced Laser Damage Behavior of Laser Mirror by Modification of the Top Layer Design, Drew Schiltz¹, Peter Langston¹, Dinesh Patel¹, Luke Emmert², Leandro Acquaroli¹, Cory Baumgarten¹, Brendan A. Reagan¹, Wolfgang Rudolph², Ashot Markosyan³, R. Route³, Martin M. Fejer³, Jorge Rocca¹, Carmen S. Menoni¹; ¹Electrical and Computer Engineering, Colorado State Univ., USA; ²Physics and Astronomy, Univ. of New Mexico, USA; ³E. L. Ginzton Lab, Stanford Univ., USA. We show the laser damage resistance of ion beam sputtered Ta₂O₅/SiO₂ for high energy lasers can be increased by 50% when the Ta₂O₅ in the top few layers of the stack is replaced by HfO₂ or Y₂O₃.

JTh3J.4 • 15:00

Increased Laser Damage Threshold in As₂S₃ Motheye Antireflective Structures, Robert J. Weilblen¹, Catalin Florea², Lynda Busse⁴, Brandon Shaw⁴, Curtis R. Menyuk¹, Ishwar Aggarwal³, Jasbinder Sanghera⁴; ¹Computer Science and Electrical Engineering, Univ. of Maryland, Baltimore County, USA; ²Avo Photonics, USA; ³Sotera Defense Solutions, USA; ⁴Naval Research Lab, USA. We computationally study the irradiance enhancement in As₂S₃ motheye structures. We show that enhancement in the glass is minimal, matching with experiments showing an increased laser damage threshold for the motheye structures versus thin-film AR coatings.

JTh3J.5 • 15:15 **Invited**

Dispersive Mirrors for Short Pulse Lasers, Vladimir Pervak^{1,2}; ¹Ludwig-Maximilians-Universität München, Germany; ²Ultrafast Innovations GmbH, Germany. A dispersive-mirror-based laser permits a dramatic simplification of high-power femto- and atto-second systems and affords promise for their further development towards shorter pulse durations, higher peak- and average powers with user-friendly systems.

Meeting Room
212 B/D

CLEO: QELS-
Fundamental Science

FTh3K • Plasmonic Lasers and
Amplification—Continued

FTh3K.4 • 15:00

Hybrid photon-plasmon nanowire lasers, Xiaoqin Wu¹, Yao Xiao¹, Cun Zheng Ning², Limin Tong¹; ¹Optical Engineering, Zhejiang Univ., China; ²Computer and Energy Engineering, Arizona State Univ., USA. By near-field coupling a high-gain CdSe nanowire (NW) and a 100-nm-diameter Ag NW, we demonstrate a hybrid photon-plasmon laser operating at 723-nm wavelength at room temperature, with a plasmon mode area of 0.008λ².

FTh3K.5 • 15:15

Ultrafast ZnO nanowire lasers: nanoplasmonic acceleration of gain dynamics at the surface plasmon polariton frequency, Theodoros Sidiropoulos¹, Sebastian Geburt², Robert Röder², Ortwin Hess¹, Stefan Maier¹, Rupert F. Oulton¹, Carsten Ronning²; ¹Physics, Imperial College London, UK; ²Univ. of Jena, Germany. We report optically pumped hybrid photonic - plasmonic ZnO nanowire lasers operating near the surface plasmon frequency. Here, we use the non-linearity of the laser process itself to reveal the internal ~1 ps dynamics of these plasmonic lasers.

Marriott
Salon I & II

JOINT

JTh3L • Symposium on Laser-
Driven Sources of Particle and
X-Ray Beams II—Continued

JTh3L.3 • 14:45 **Invited**


3rd order harmonic in inverse Compton scattering, Yusuke Sakai¹, Igor Pogorelsky², Mikhail Fedurin², Pietro Musumeci¹, Joseph Duris¹, Oliver Williams¹, James Rosenzweig¹; ¹Physics, Univ. of California Los Angeles, USA; ²ATF, BNL, USA. We report observations of strong-field effects in inverse Compton scattering via its X-ray characteristics using K-, L-edge, and attenuation filters. A CO₂ laser of a0 ≈ 0.6 is collided by a 65-MeV electron beam.


JTh3L.4 • 15:00 **Invited**


Producing Bright X-rays for Imaging Applications Using a Laser Wakefield Accelerator, Stuart Mangles¹, Michael S. Bloom¹, Jonathan Bryant¹, Jason M. Cole¹, Andreas Doeppl¹, Stefan Kneip¹, Hiroataka Nakamura¹, Kristjan Poder¹, Matthew J. Streeter¹, Jonathan Wood¹, Rodolfo Bendoyro², Jason Jiang², Nelson C. Lopes^{2,1}, Carlos Russo², Oleg Chekhlov³, Klaus Ertel³, Steven J. Hawkes³, Chris J. Hooker³, David Neely³, Peter A. Norreys³, P. P. Rajeev³, Dean R. Rusby³, Robbie Scott³, Daniel R. Symes³, James Holloway⁴, Matthew Wing⁴, John F. Seely⁵; ¹John Adams Inst. for Accelerator Science, The Blackett Lab, Imperial College London, UK; ²Grupo de Lasers e Plasmas, Instituto de Plasmas e Fusao Nuclear, Instituto Superior Tecnico, Portugal; ³Central Laser Facility, STFC Rutherford Appleton Lab, UK; ⁴Physics and Astronomy Dept., Univ. College London, UK; ⁵Artep Inc., USA. We report on the generation of bright multi-keV betatron X-ray radiation using a GeV laser wakefield accelerator and investigate the use of these X-rays for various imaging applications.

CLEO: Science & Innovations

CLEO: Applications
& TechnologySTh3M • Silicon Photonics—
Continued

STh3M.4 • 14:45  **Ultra-Efficient and Broadband Dual-Level Si3N4-on-SOI Grating Coupler**, Wesley D. Sacher¹, Ying Huang², Liang Ding², Benjamin J. Taylor¹, Hasitha Jayatilaka¹, Guo-Qiang Lo², Joyce K. Poon¹; ¹Univ. of Toronto, Canada; ²Inst. of Microelectronics, A*STAR (Agency for Science, Technology and Research), Singapore. A grating coupler with aligned Si3N4 and Si grating teeth is proposed and demonstrated. The measured coupling efficiency is -1.3 dB (competitive with the best Si-only grating couplers), and the 1-dB bandwidth is a record 80 nm.

STh3M.5 • 15:00  **Unidirectional chip-to-fiber grating couplers in unmodified 45nm CMOS Technology**, Mark T. Wade¹, Rajesh Kumar¹, Kareem Nammari¹, Cale M. Gentry¹, Jeffrey Shainline¹, Jason S. Orcutt³, Ananth Tamma⁴, Rajeev Ram³, Vladimir Stojanovic², Miloš A. Popović¹; ¹Univ. of Colorado at Boulder, USA; ²Univ. of California, USA; ³MIT, USA; ⁴UC Irvine, USA. We propose and demonstrate the first asymmetric unidirectional grating couplers fabricated in a 45nm unmodified CMOS process. Measured coupling efficiency from fiber-to-chip is ~40%. Simulations show >70% efficiency is achievable with same design.

STh3M.6 • 15:15  **Silicon Chip Based Near-Infrared and Mid-Infrared Optical Spectroscopy for Volatile Organic Compound Sensing**, Yi Zou¹, Swapnaji Chakravarty², Wei-Cheng Lai¹, Ray Chen¹; ¹Univ. of Texas at Austin, USA; ²Omega Optics Inc, USA. We compared different on-chip silicon based absorption sensors for the detection of xylene in water in both near-infrared and mid-infrared including strip waveguide, slot waveguide and PC-based chip integrated optical absorption spectroscopy devices.

STh3N • Supercontinuum
Generation—Continued

STh3N.4 • 14:45 **Visible Supercontinuum Generation by Dual-Wavelength Pumping in Multimode Rectangular Optical Fibers** Visible Supercontinuum Generation by Dual-Wavelength Pumping in Multimode Rectangular Optical Fibers, Badr M. SHALABY^{1,2}, Alexis Labrùère¹, Katarzyna Krupa¹, Denisa Subtirelu³, Nelly Rongeart³, Alessandro Tonello¹, Vincent Couderc¹; ¹Xlim-Photonics, Limoges University-CNRS, France; ²Physics-Faculty of Science, Tanat University, Egypt; ³Physics, Horiba Medical, France. We study supercontinuum generation in a multimode microstructured optical fiber by dual-wavelength pumping. We demonstrate significant blue extension of the spectrum in relatively short fiber length by exploiting cross-phase modulation between high order modes.


STh3N.5 • 15:00 **Octave spanning coherent supercontinuum generation by 46 fs pedestal free ultrashort pulse using similariton amplifier and Er-doped fiber laser with carbon nanotube**, Yoshitaka Nomura¹, Yuto Nozaki¹, Youichi Sakakibara², Emiko Omoda², Hiromichi Kataura², Norihiko Nishizawa¹; ¹Nagoya Univ., Japan; ²AIST, Japan. 46 fs, 4.0 nJ pedestal free high power ultrashort pulse was generated using Er-doped similariton amplifier seeded by nanotube fiber laser. An octave spanning coherent supercontinuum was generated in highly nonlinear normal dispersion fiber.

STh3N.6 • 15:15 **Coherent All-PM Fiber Frequency Comb Source at 2.03 μ m and 100 MHz Emitting Broadband Pulses at up to 290 mW and 128 fs Pulse Duration**, Heinar Hoogland¹, Alexandre Thai^{1,2}, Daniel Sanchez², Seth L. Cousin², Michael Hemmer², Martin Engelbrecht¹, Jens Biegert^{2,4}, Ronald Holzwarth^{1,3}; ¹Menlo Systems GmbH, Germany; ²ICFO-Institut de Ciències Fotoniques, Spain; ³Max-Planck-Inst. of Quantum Optics, Germany; ⁴ICREA - Institutio Catalana de Recerca i Estudis Avançats, Spain. We report on a compact coherent All-PM fiber laser amplifier system at around 2.03 μ m running at 100 MHz delivering broadband pulses at 290 mW average power and pulse duration down to 128 fs.


STh3O • Timing and
Imaging—Continued

STh3O.4 • 14:45  **Precise Time Recovery at Arbitrary Point in Fiber-Optic Loop Link with RF Phase Locking Assistance**, Zhongze Jiang¹, Yitang Dai¹, Feifei Yin¹, Jianqiang Li¹, Kun Xu¹; ¹BUPT, China. Precise time recovery on arbitrary point of fiber-optic link with λ -dispersion-induced RF phase locking assistance is proposed. Experiments have demonstrated the time deviation of 8.34ps@1s averaging and 0.592ps@10³s averaging within a 30-km fiber loop.


STh3O.5 • 15:00  **Long-Term Stable, Sub-Femtosecond Balanced Optical-Microwave Phase Detector**, Michael Y. Peng¹, Franz Kärtner^{1,2}; ¹Electrical Engineering and Computer Science, MIT, USA; ²Center for Free-Electron Laser Science, Deutsches Elektronen-Synchrotron, Germany. We achieved a sub-fs thermal-noise-limited noise floor in a balanced optical-microwave phase detector and demonstrated long-term stable RF extraction with <1 fs RMS drift and <7 fs pk-pk for over 10 hours of continuous operation.

STh3O.6 • 15:15  **Timing Jitter Minimization in Soliton Mode-Locked Fiber Lasers by Dispersion Engineering**, Chur Kim¹, Sangho Bae¹, Khanh Kieu², Jungwon Kim¹; ¹Korea Advanced Inst of Science & Tech, Korea; ²The Univ. of Arizona, USA. We searched for the minimal timing jitter condition in an all-fiber, soliton, CNT-mode-locked Er-laser by dispersion engineering. The measured lowest timing jitter is 490-attosecond [10-kHz to 39.4-MHz] at -0.02 ps² intra-cavity dispersion.

ATH3P • Symposium on
Advanced Ultrashort Pulse Laser
Technologies in Biophotonics
and Nanobiophotonics I—
Continued

ATH3P.3 • 14:45  **3D Visualization of Dental Anatomy in Ancient Fossil Vertebrates by Using Third Harmonic Generation Microscopy**, Yu-Cheng Chen¹, Ya-Na Wu², Dar-Bin Shieh², Chi-Kuang Sun^{1,3}, Robert R. Reisz⁴; ¹Molecular Imaging Center, National Taiwan Univ., Taiwan; ²Inst. of Oral Medicine, National Cheng Kung Univ. College of Medicine and Hospital, Taiwan; ³Inst. of Physics and Research Center for Applied Sciences, Academia Sinica, Taiwan; ⁴Dept. of Biology, Univ. of Toronto Mississauga, Canada. Clear 3D visualization in fossilized dentinal tissues was first discovered with extremely strong contrast by means of third harmonic generation microscopy, providing a novel approach to study the dental evolution of ancient vertebrates (dinosaurs) noninvasively.

ATH3P.4 • 15:00  **Measurements of Two-, Three-, and Four-Photon Excitation Action Cross Sections**, Li-Chung Cheng^{1,3}, Ke Wang², Chris Xu³; ¹Dept. of Photonics, National Cheng Kung Univ., Taiwan; ²College of Optoelectronic Engineering, Shenzhen Univ., China; ³School of Applied Engineering and Physics, Cornell Univ., USA. We report quantitative measurements of two-, three-, and four-photon excitation action cross sections of several commonly used fluorophores and fluorescent proteins at three different excitation wavelengths of 800 nm, 1300 nm, and 1680 nm.

ATH3P.5 • 15:15  **Effect of Femtosecond Laser Pulse Energy and Repetition Rate on Laser Induced Second and Third Harmonic Generation in Corneal Tissue**, William Calhoun^{1,2}, Ilko K. Ilev¹; ¹DP/OSEL/CDRH, Food and Drug Administration, USA; ²Biomedical Engineering, Virginia Commonwealth Univ., USA. We present a quantitative study on the effect of femtosecond laser pulse energy and repetition rate on the intensity and duration of the laser induced second and third harmonic generation in fresh corneal tissue.

CLEO: QELS-Fundamental Science

FTh3A • Nonclassical States and Quantum Phenomena—Continued**FTh3A.7 • 15:30**

Bi-directional Multiplexing of Heralded Single Photon Sources from a Single Silicon Photonic Chip, Chunle Xiong¹, Trung Vo^{1,2}, Matthew Collins¹, Alex Clark¹, Juntao Li³, Michael J. Steel⁴, Thomas F. Krauss^{3,4}, Benjamin J. Eggleton¹; ¹Univ. of Sydney, Australia; ²Defence Science and Technology Organisation, Australia; ³Univ. of St. Andrews, UK; ⁴Univ. of York, UK; ⁵Macquarie Univ., Australia. We demonstrate spatial multiplexing of two heralded single photon sources created by bi-directionally pumping a single 96 μm photonic crystal waveguide. This enhances the source brightness by 51.2±4.0% whilst maintaining the coincidence to accidental ratio.

FTh3A.8 • 15:45

On-Chip Heralded Single Photon Source with Demultiplexing and Pump Filtering, Nicholas C. Harris¹, Christophe Galland², Daniele Bajoni³, Mihir Pant¹, Davide Grassani³, Tom Baehr-Jones^{4,5}, Michael Hochberg^{4,5}, Dirk Englund¹; ¹RLE, MIT, USA; ²École Polytechnique Fédérale de Lausanne (EPFL), Switzerland; ³Università di Pavia, Italy; ⁴Univ. of Delaware, USA; ⁵National Univ. of Singapore, Singapore. We demonstrate an on-chip source of correlated photons with spatial demultiplexing of signal and idler photons via ring resonators and with pump suppression greater than 60 decibels.

FTh3B • Quantum Optics with Atoms and Ions—Continued**FTh3B.6 • 15:30**

Excitation of Higher-Order Modes of an Optical Nanofiber by Laser-Cooled Rb-87 Atoms, Ravi Kumar^{1,2}, Vandna Gokhroo¹, Aili Maimaiti^{1,2}, Kieran Deasy¹, Sile Nic Chormaic¹; ¹OIST Graduate Univ., Japan; ²Physics Dept., Univ. College Cork, Ireland. We demonstrate excitation of higher order modes in an optical nanofiber by resonantly-excited Rb-87 atoms. Absorption by laser-cooled atoms is enhanced when probe light propagates in higher order modes compared to the fundamental mode.

FTh3B.7 • 15:45

Spin cooling via incoherent feedback in an ensemble of cold 87Rb atoms, Naeimeh Behbood¹, Georgio Colangelo¹, Ferran Martin Ciurana¹, Mario Napolitano¹, Robert Sewell¹, Morgan W. Mitchell^{1,2}; ¹ICFO -The Inst. of Photonic Sciences, Spain; ²ICREA - Institucio Catalana de Recerca i Estudis Avancats, Spain. We report an experimental study of a new technique for spin cooling an ensemble of ultracold atoms via quantum non-demolition (QND) measurement and incoherent feedback. We have demonstrated 12db spin noise reduction.

FTh3C • Low Energy Dynamics in Dirac Materials—Continued**FTh3C.6 • 15:30**

Disorder induced Floquet topological insulators in photonic systems, Mikael Rechtsman², Netanel H. Lindner², Paraj T. Bhattacharjee¹, Gil Refael¹; ¹Physics Dept., California Inst. of Technology, USA; ²Physics Dept., Technion Israel Inst. of Technology, Israel. We propose the photonic topological Anderson insulator, the first realization of this phase in any physical context. In this phase, disorder counterintuitively induces a topological transition that breaks Anderson localization and leads to robust transport.

FTh3C.7 • 15:45

Terahertz dynamics of topological insulator Bi2Se3 : ultrafast photoexcitation suppresses hot-Dirac electron surface scattering, Sim Sangwan¹, Matthew Brahlek², Nikesh Koirala², Soonyoung Cha¹, Seongshik Oh^{2,3}, Hyunyoung Choi¹; ¹School of Electrical and Electronic Engineering, Yonsei Univ., Korea; ²Rutgers Center for Emergent Materials and Dept. of Physics and Astronomy, Rutgers the State Univ. of New Jersey, USA; ³Inst. for Advanced Materials, Devices and Nanotechnology, Rutgers the State Univ. of New Jersey, USA. We present ultrafast terahertz scattering dynamics in topological insulator Bi2Se3 thin films. Upon photoexcitation, the surface-scattering rate is increased, resulting in decrease of conductance. At high temperature, however, the photo-generated electrons suppress the surface-scattering.

FTh3D • Novel Optical Phenomena—Continued**FTh3D.7 • 15:30**

Test of Higher-Order Nonlinearity via Low-Order Harmonic Generation Revisited, Darshana L. Weerawarne¹, Xiaohui Gao², Alexander L. Gaeta², Bonggu Shim¹; ¹Physics, SUNY Binghamton, USA; ²School of Applied and Engineering Physics, Cornell Univ., USA. We measure the ratio between fifth- and third-harmonic signals from air as a function of the laser intensity determined by mode measurements. Our results do not support the presence of a higher-order Kerr nonlinearity.

FTh3D.8 • 15:45

A Quasi-Optical Tool for the Demultiplexing of Orbital Angular Momentum Carried at Millimeter-Wave Frequencies, Martin P. Lavery¹, Yan Yan², Guodong Xie², Hao Huang², Moshe Tur³, Andreas F. Molisch², Miles Padgett¹, Alan Willner²; ¹School of Physics and Astronomy, Univ. of Glasgow, UK; ²Electrical Engineering, Univ. of Southern California, USA; ³Electrical Engineering, Tel Aviv Univ., Israel. We present a quasi-optical component for the simultaneous de-multiplexing of multiple channels by the transformation of OAM into transverse momentum. A communications link comprising 4 independent channels is demonstrated achieving a data rate of 8 Gbit/s.

16:00–16:30 Coffee Break, Concourse Level

NOTES

CLEO: Science & Innovations

STh3E • High Harmonics and Field Synthesis—Continued

STh3E.6 • 15:30 **Invited**
Isolated Attosecond Continua in the Water Window via High Harmonic Generation using a Few-cycle Infrared Light Source, Nobuhisa Ishii¹, Keisuke Kaneshima¹, Henning Geiseler¹, Teruto Kanai¹, Shuntaro Watanabe², Jiro Itatani¹; ¹*Inst. for Solid State Physics, Japan*; ²*Tokyo Univ. of Science, Japan*. A few-cycle infrared light source is applied to generate isolated soft-x-ray continua in the water window via high harmonic generation. The current status of the light source and some strong-field experiments will be discussed.

STh3F • THz Waveguides and Optics—Continued

STh3F.7 • 15:30
Tunable Terahertz wave plates fabricated with a 3D printer, Stefan Busch¹, Marcel Weidenbach¹, Benedikt Scherger¹, Martin Koch¹, Maik Scheller², Christian Jansen², Enrique Castro-Camus³; ¹*Faculty of Physics and Material Sciences Center, Philipps-Universität Marburg, Germany*; ²*Lytera UG (haftungsbeschränkt), Germany*; ³*Centro de Investigaciones en Optica A.C., Mexico*. We fabricate wave plates for terahertz waves using a 3D printer. The wave plates base on the physical mechanism of form birefringence. Applying mechanical pressure to the plates allows for continuously tuning of the optical retardance.

STh3F.8 • 15:45
Extraordinary Transmission-inspired Dual-band THz Quarter-wave Plate, Víctor Torres¹, Nuria Sánchez², David Etayo¹, Rubén Ortuño¹, Alejandro Martínez², Miguel Navarro-Cia^{3,4}, Miguel Beruete¹; ¹*Universidad Pública de Navarra, Spain*; ²*Universitat Politècnica de València, Spain*; ³*Imperial College London, UK*; ⁴*Univ. College London, UK*. We propose a very compact metasurface that works as a quarter-wave plate at two different frequencies, 1 THz and 2.2 THz. The fractional bandwidth of the first band is remarkably 32.2%, beyond the state-of-the-art.

STh3G • Quantum Cascade Lasers I—Continued

STh3G.7 • 15:30
A mid-infrared Lab-on-a-Chip: Generating, Guiding and Detecting Light in a Monolithic Device, Benedikt Schwarz¹, Daniela Ristic¹, Peter Reiningner¹, Hermann Detz¹, Aaron M. Andrews¹, Werner Schrenk¹, Gottfried Strasser¹; ¹*Inst. for Solid State Electronics and Center for Micro- and Nanostructures, Vienna Univ. of Technology, Austria*. We present a fully integrated mid-infrared sensor. The laser and detector are fabricated from a bi-functional quantum cascade structure, connected through a dielectric-loaded surface plasmon waveguide, which acts as interaction zone and provides high coupling.

STh3H • Sensing with Optofluidics—Continued

STh3H.4 • 15:30
Miniature droplet-based FRET lasers stabilized by superhydrophobic surfaces, Ersan Ozelci¹, Mehdi Aas¹, Alexandr Jonas², Alper Kiraz¹; ¹*Dept. of Physics, Koc Universitesi, Turkey*; ²*Dept. of Physics, Istanbul Technical Univ., Turkey*. We demonstrate optofluidic microlasers based on liquid microdroplets stabilized by a superhydrophobic surface. Lasing is achieved using highly efficient non-radiative Förster resonance energy transfer between donor and acceptor molecules placed within the droplets.

STh3H.5 • 15:45
On-chip Opto-electrical Discrimination of Single Biological Nanoparticles, Shuo Liu¹, Yue Zhao², Joshua W. Parks¹, Aaron Hawkins², Holger Schmidt¹; ¹*School of Engineering, Univ. of California Santa Cruz, USA*; ²*Dept. of Electrical and Computer Engineering, Brigham Young Univ., USA*. Using an optofluidic chip with an integrated nanopore, a mixture of nanobeads and influenza viruses were opto-electrically detected. Different types of nanoparticles can be distinguished by different fluorescence wavelengths and fluorescence correlation functions.

16:00–16:30 Coffee Break, Concourse Level

NOTES

Blank lined area for notes.

Meeting Room
211 B/D

CLEO: Science & Innovations

STh3I • Photovoltaics Sciences—Continued

STh3I.4 • 15:30

Photocurrent enhancement in thin a-Si:H solar cells via plasmonic light trapping, Seweryn Morawiec^{1,2}, Manuel J. Mendes¹, Sergej A. Filonovich^{3,4}, Tiago Mateus^{3,4}, Salvatore Mirabella¹, Hugo Águas^{3,4}, Isabel Ferreira^{3,4}, Francesca Simone², Elvira Fortunato^{3,4}, Rodrigo Martins^{3,4}, Francesco Priolo^{1,2}, Isodiana Crupi¹; ¹MATIS IMM-CNR, Italy; ²Dipartimento di Fisica e Astronomia, Università di Catania, Italy; ³Departamento de Ciência dos Materiais, CENIMAT/13N, Portugal; ⁴Faculdade de Ciências e Tecnologia, Universidade Nova de Lisboa, CEMOP/UNINOVA, Portugal. Photocurrent enhancement in thin a-Si:H solar cells due to the plasmonic light trapping is investigated, and correlated with the morphology and the optical properties of the self-assembled silver nanoparticles incorporated in the cells' back reflector.

STh3I.5 • 15:45

Low Cost All-Dielectric Thin-Film Solar Cell Using Diffuse Medium Reflectors, Chi Wei Tseng¹, Sze Ming Fu¹, Shih-Yun Lai¹, Wei-Ming Lai¹, Sheng Lun Yan¹, Nyan-Ping Ju¹, Po-Yu Chen¹, Chi-Chung Tsai¹, Albert Lin¹; ¹National Chiao Tung Univ., Taiwan. Diffuse reflectors can be beneficial for solar cells, due to no plasmonic loss, higher reflectance, decent light scattering, and low cost. Experimental and theoretical works are presented here to demonstrate its feasibility for photovoltaics.

Meeting Room
212 A/C

JOINT

JTh3J • Symposium on High Performance Optics I—Continued

JTh3J.6 • 15:45

Temperature Dependence of Laser-Induced Damage Thresholds in Dielectric Crystals, Katsuhiko Mikami¹, Takahisa Jitsuno¹, Azumi Minako², Tsuyoshi Sugita², Azechi Hiroshi¹; ¹Inst. of Laser Engineering, Osaka Univ., Japan; ²Glass Division, NIKON Corporation, Japan. Laser-induced damage thresholds (LIDT) in dielectric crystals were evaluated at different temperature. The temperature dependence of the LIDTs could be explained with some physical models.

Meeting Room
212 B/D

CLEO: QELS-Fundamental Science

FTh3K • Plasmonic Lasers and Amplification—Continued

FTh3K.6 • 15:30

Novel physics in photonic crystal nanolasers : Dynamics and Coherence, Isabelle Robert-Philip¹, Armand Lebreton¹, Grégoire Beaudoin¹, Isabelle Sagnes¹, Rémy Braive¹, Alexios Beveratos¹, Izo Abram¹; ¹LPN, CNRS, France. Lasers of diffraction-limited volumes involve the interaction of small numbers of particles (photons and dipoles). We demonstrate that these small populations of discrete particles induce large intensity noise in the output of the laser.

FTh3K.7 • 15:45

Non-linear Fano interactions in plasmonic-vapor system, Liron Stern¹, Meir Y. Grajower¹, Uriel Levy¹; ¹Hebrew Univ. of Jerusalem, Israel. Linear and non-linear Fano interactions in a hybrid system consisting of surface plasmonic resonance and alkali vapor are presented. Using a pump probe apparatus, Doppler free lineshape and all optical modulation is experimentally demonstrated.

Marriott
Salon I & II

JOINT

JTh3L • Symposium on Laser-Driven Sources of Particle and X-Ray Beams II—Continued

JTh3L.5 • 15:30

X-ray Generation by Relativistic Laser-Accelerated Electrons, Stefan Karsch^{1,2}, Johannes Wenz¹, Konstantin Khrennikov¹, Matthias Heigoldt¹, Antonia Popp¹, Alexander Buck², Jiancai Xu², Laszlo Veisz², Shao-Wei Chou², Andreas Maier^{3,1}, Nathaniel Kajumba¹, Thorben Seggebrock¹, Florian Grüner^{3,1}, Alexander Guggenmos^{1,2}, Ulf Kleineberg^{1,2}, Simone Schlegel⁴, Martin Bech⁴, Pierre Thibault⁴, Franz Pfeiffer⁴; ¹Ludwig-Maximilians-Universität München, Germany; ²Max-Planck-Institut für Quantenoptik, Germany; ³Universität Hamburg, Germany; ⁴Technische Universität München, Germany. Laser-wakefield-accelerated electrons were used to drive an all-optical undulator source, a 5-keV betatron X-ray source and a tunable quasi-monochromatic Compton-X-ray source. Also, we present a phase-contrast tomogram of a fly obtained with the betatron beam.

JTh3L.6 • 15:45

Quasi Monoenergetic and Tunable X-rays by Laser Compton Scattering from Laser Wakefield e-beam, Nathan Powers¹, Isaac Ghebregziabher¹, Gregory Golovin¹, Cheng Liu¹, Shouyuan Chen¹, Sudeep Banerjee¹, Jun Zhang¹, Donald P. Umstadter¹; ¹Univ. of Nebraska Lincoln, USA. Quasi monoenergetic and tunable x-ray beams are reported by inverse-Compton scattering from laser wakefield accelerated electrons. The high peak brightness, ultrashort duration, and small size of the source make it uniquely suitable for many applications.


16:00–16:30 Coffee Break, Concourse Level

NOTES

CLEO: Science & Innovations

CLEO: Applications
& Technology

STh3M • Silicon Photonics—
Continued


STh3M.7 • 15:30  **Controlled Coupling of Rolled-Up Microtubes Integrated with Silicon Waveguides**, Qiuhan Zhong¹, Zhaobing Tian¹, Venkat Veerasubramanian, Mohammad Hadi Tavakoli Dastjerdi¹, David Patel¹, Zetian Mi¹, David V. Plant¹; ¹Dept. of Electrical and Computer Engineering, McGill Univ., Canada. We demonstrate, for the first time, the controlled coupling of rolled-up microtubes integrated with silicon waveguides by thermally tuning the coupling gap. Then we realize coupling modulation utilizing the dynamic tuning effect.


STh3N • Supercontinuum
Generation—Continued

STh3N.7 • 15:30 **Controlling rogue wave statistics**, Ayhan Demircan¹, Shalva Amiranashvili², Carsten Bree², Ayhan Tajalli¹, Uwe Morgner¹, Gunter Steinmeyer³; ¹Leibniz Univ. Hannover, Germany; ²Weierstrass Institute for Applied Analysis and Stochastics, Germany; ³Max-Born-Institut, Germany. We propose a radically new way of rogue wave control, modifying the statistical distribution of events via suitable injection of dispersive waves. This allows reducing the frequency of rogue events rather than only increasing it.

STh3N.8 • 15:45 **Nanotube mode-locked, low repetition rate pulse source for fiber-based supercontinuum generation at low average pump power**, Robert I. Woodward¹, Edmund J. Kelleher¹, T. H. Runcorn¹, Daniel Popa², Tawfique Hasan², Andrea C. Ferrari², Sergei V. Popov¹, James R. Taylor¹; ¹Femtosecond Optics Group, Imperial College London, UK; ²Cambridge Graphene Centre, Univ. of Cambridge, UK. We demonstrate a nanotube mode-locked fiber laser with low repetition rate (244 kHz), enabling supercontinuum generation in photonic crystal fiber spanning 600 to 2000 nm, at a low average pump power of 87 mW.


STh3O • Timing and
Imaging—Continued

STh3O.7 • 15:30  **Phase Stabilized Downlink Transmission and Optical Down-Conversion for Wideband Radio Frequency**, Anxu Zhang¹, Yitang Dai¹, Feifei Yin¹, Kun Xu¹, Jianqiang Li¹, Jintong Lin¹; ¹Beijing Univ. of Posts and Telecommunications, China. A novel wideband radio frequency phase stabilized downlink transmission and optical domain down-conversion scheme is proposed. The achieved stability of the intermediate frequency is $\sim 1.8 \times 10^{-12}$ after transferring through 30km optical fiber.

STh3O.8 • 15:45  **Spectral linewidth reduction of single-mode and mode-locked lasers using a feed-forward heterodyne detection scheme**, Regan Watts¹, Stuart G. Murdoch², Liam Barry¹; ¹School of Electronic Engineering, Dublin City Univ., Ireland; ²Dept. of Physics, Univ. of Auckland, New Zealand. We present a novel feed-forward laser linewidth reduction scheme. The linewidth of a DFB laser is reduced from 9.4MHz to 37.2kHz. Sixteen modes of a mode-locked laser are simultaneously reduced from ~ 20 MHz to below 300kHz.

ATh3P • Symposium on
Advanced Ultrashort Pulse Laser
Technologies in Biophotonics
and Nanobiophotonics I—
Continued

ATh3P.6 • 15:30  **Electrically-Tunable Multi-Color Ultrafast Cherenkov Fiber Laser**, Ask S. Svane¹, Xiaomin Liu¹, Jesper Lægsgaard¹, Haohua Tu², Stephen A. Boppart², Dmitry Turchinovich^{1,3}; ¹DTU Fotonik, Technical Univ. of Denmark, Denmark; ²Biophotonics Imaging Lab, Univ. of Illinois, USA; ³Max Planck Inst. for Polymer Research, Germany. We demonstrate the broadband electrical tunability of ultrafast fiber laser output across the visible range, from the deep blue to the infrared.

ATh3P.7 • 15:45  **Femtosecond 905nm-940nm band Nd: fiber laser**, Xiang Gao¹, Weijian Zong¹, Bingying Chen¹, Jian Zhang¹, Chen Li¹, Yizhou Liu¹, Aimin Wang¹, Yangrong Song², Zhigang Zhang¹; ¹School of Electronics Engineering and Computer Science, Peking Univ., China; ²School of Applied Science, Beijing Univ. of Technology, China. We demonstrate a passively all-normal dispersion mode-locked Nd-doped fiber laser at 905-940 nm with high optical to optical efficiency. The central wavelengths can be tunable through tuning birefringent filter.

16:00–16:30 Coffee Break, Concourse Level

NOTES

Blank lined area for notes.

CLEO: QELS-
Fundamental Science

16:30– 18:30

FTh4A • Quantum Sensing and Metrology

Presider: Yuao Chen; Univ of Science and Technology of China, China

FTh4A.1 • 16:30

High-resolution, stimulated-emission-based measurement of the joint spectral correlations of photon pairs produced in optical fiber, BIN FANG¹, Offir Cohen², Marco Liscidini³, John E. Sipe⁴, Virginia Lorenz¹; ¹Dept. of Physics and Astronomy, Univ. of Delaware, USA; ²Joint Quantum Inst., National Inst. of Standards and Technology & Univ. of Maryland, USA; ³Dept. of Physics, Univ. of Pavia, Italy; ⁴Dept. of Physics and Inst. for Optical Sciences, Univ. of Toronto, Canada. We demonstrate the measurement of photon-pair joint spectral correlations in optical fiber through stimulated four-wave mixing. This method enables us to study correlations more easily, precisely and quickly than with traditional coincidence counting measurements.

FTh4A.2 • 16:45

High-resolution measurement of the joint spectral density of quantum correlated photon pairs, Andreas Eckstein¹, Guillaume Boucher¹, A. Lemaitre², P. Filloux¹, Giuseppe Leo¹, John E. Sipe³, Marco Liscidini⁴, Sara Ducci¹; ¹Université Paris Diderot, France; ²Laboratoire de Photonique et de Nanostructures, France; ³Univ. of Toronto, Canada; ⁴Università degli Studi di Pavia, Italy. We show that the characterization of the quantum correlations generated by a photon-pair source can be directly performed via a classical measurement leading to an unprecedented spectral resolution and a shorter integration time.

FTh4A.3 • 17:00

Record-efficiency biphoton correlator and observation of high-order dispersion cancellation, Joseph M. Lukens¹, Amir Dezfouliyan¹, Carsten Langrock², Martin M. Fejer², Daniel E. Leaird¹, Andrew M. Weiner¹; ¹Electrical and Computer Engineering, Purdue Univ., USA; ²Edward L. Ginzton Lab, Stanford Univ., USA. We construct an ultrafast biphoton correlator with a record pair conversion efficiency of 1e-5 based on sum-frequency generation in a PPLN waveguide, enabling us to demonstrate high-order dispersion cancellation for the first time.

CLEO: Science &
Innovations

16:30– 18:30

STh4B • Laser-Driven Dynamics in Materials

Presider: Richard Haglund; Vanderbilt Univ., USA

STh4B.1 • 16:30 **Invited**

Ultrafast Electron Dynamics in Photo-excited Semiconductors Studied by Time and Angle-resolved Two Photon Photoelectron Spectroscopy, Junichi Kanasaki¹; ¹Osaka Univ., Japan. Ultrafast dynamics of photo-excited electrons with non-equilibrium distribution in GaAs has been studied on femtosecond time scale, by means of energy- and angle-resolved two-photon photoelectron spectroscopy. Fundamental scattering processes governing their energy relaxation are elucidated.

STh4B.2 • 17:00

Unusual phenomena with self-organized nanogratings written in silica glass with a femtosecond laser, Nathaniel Grothoff¹, Audrey Champion¹, Max-Oliver Hongler², Yves Bellouard¹; ¹Mechanical Engineering, Eindhoven Univ. of Technology, Netherlands; ²Faculty of Engineering and Technology (STI), Ecole Polytechnique Fédérale de Lausanne, Switzerland. Femtosecond laser written nanogratings show a random transition from self-organized to disordered structure and vice versa. A reason for the transition is proposed. Overlapping laser scans create nanogratings with apparent self-aligned fringes.

CLEO: QELS-Fundamental Science

16:30– 18:30

FTh4C • Carrier Dynamics in 0-D and 1-D Nanostructures

Presider: Rohit Prasankumar; Los Alamos National Lab, USA

FTh4C.1 • 16:30

Exciton-Phonon Interactions in an InAs Quantum Dot Ensemble Studied with 2D Coherent Spectroscopy, Takeshi Suzuki¹, Rohan Singh^{1,2}, Galan Moody^{1,2}, Marc Assmann^{1,3}, Ilya Akimov^{3,4}, Manfred Bayer³, Dirk Reuter⁵, Andreas Wieck⁵, Steven T. Cundiff^{1,2}; ¹JILA, Univ. of Colorado and National Inst. of Standards and Technology, USA; ²Physics, Univ. of Colorado, USA; ³Experimentelle Physik 2, Technische Universität Dortmund, Germany; ⁴A. F. Ioffe Physical-Technical Inst., Russian Academy of Sciences, Russia; ⁵Angewandte Festkörperphysik, Technische Universität Bochum, Germany. 2D coherent spectroscopy is used to study exciton-phonon interactions in an InAs quantum dot ensemble. Temperature and size dependent properties of the zero-phonon line and the phonon background in the s- and p-shells are revealed.

FTh4C.2 • 16:45

Subpicosecond adiabatic rapid passage in a single InGaAs quantum dot: Role of phonons in dephasing, Reuble Mathew¹, Eric Dilcher¹, Angela Gamouras¹, Ajan Ramachandran¹, Sabine Freisem², Dennis Deppe², Kimberley Hall¹; ¹Dalhousie Univ., Canada; ²Univ. of Central Florida, USA. Robust excitation of an exciton state via adiabatic rapid passage is demonstrated in a single InGaAs quantum dot using subpicosecond optical pulses. A chirp sign dependence of the transfer efficiency indicates dephasing tied to phonons.

FTh4C.3 • 17:00

Investigation of Quantum Dot—Quantum Dot Coupling at High Hydrostatic Pressure, Sheng Liu^{1,2}, Binsong Li¹, Hongyou Fan¹, Ting S. Luk^{1,2}, Michael B. Sinclair¹, Igal Brener^{1,2}; ¹Sandia National Labs, USA; ²Center for Integrated Nanotechnologies, USA. We performed photoluminescence and radiative lifetime measurements of quantum dots (QDs) showing different carrier dynamic mechanisms at elevated pressures that could reveal the inter-QD coupling as the QDs spacing decreases with increasing hydrostatic pressure.

16:30– 18:30

FTh4D • Nonlinear Metamaterials and Cooling

Presider: Demetrios Christodoulides; Univ. of Central Florida, USA

FTh4D.1 • 16:30 **Invited**

Inducing Giant Nonreciprocal Effects in Metamolecules, Metasurfaces and Metamaterials, Andrea Alu¹; ¹Univ. of Texas at Austin, USA. We discuss venues to realize magnetic-free nonreciprocal integrated components based on linear and/or nonlinear metamaterials. These solutions, being based on azimuthal spatio-temporal modulation or nonlinear effects, are ideally suited for newly-developed metasurfaces with giant nonlinearities.

FTh4D.2 • 17:00 **Invited**

Phase Mismatch-Free Nonlinear Propagation in Optical Zero-Index Materials, Kevin O'Brien¹, Haim Suchowski¹, Zi Jing Wong¹, Alessandro Salandrino¹, Xiaobo Yin¹, Xiang Zhang^{1,2}; ¹NSF Nano-scale Science and Engineering Center (NSEC), UC Berkeley, USA; ²Materials Sciences Division, Lawrence Berkeley National Lab, USA. Phase-matching is critical for coherent nonlinear optical processes, allowing nonlinear sources to combine constructively, resulting in more efficient emission. We experimentally demonstrate phase mismatch-free nonlinear propagation in a bulk zero index metamaterial.

CLEO: Science & Innovations

16:30– 18:30

STh4E • OPO, OPA and Regenerative Amplifiers

Presider: Takao Fujii; National Inst.s of Natural Sciences, Japan

STh4E.1 • 16:30

Regenerative Amplification of Ultrashort Pulses at 2 μm with a Thulium-doped YAP Crystal, Andreas Wienke¹, Dieter Wandt¹, Uwe Morgner^{1,2}, Jörg Neumann¹, Dietmar Kracht¹; ¹Laser Zentrum Hannover e.V., Germany; ²Institut für Quantenoptik, Leibniz Universität Hannover, Germany. Seed pulses at nJ-level of a fiber-based pre-amplified Thulium oscillator are amplified to μJ -level at 1 kHz repetition rate in a regenerative amplifier based on a Thulium-doped YAP crystal with 355 fs compressed pulse duration.

STh4E.2 • 16:45

Multi-kHz, High Energy, Femtosecond Diode-Pumped Yb:CaF₂ Regenerative Amplifier, Etienne Caracciolo^{1,2}, Matthias Kemnitzer², Annalisa Guandalini², Federico Pirzio¹, Juerg Au der Au², Antonio Agnesi¹; ¹Universita degli Studi di Pavia, Italy; ²High Q Laser GmbH, Austria. We report an efficient, high-energy, diode-pumped Yb:CaF₂ regenerative amplifier. Energies up to 1.02 mJ at 1045-nm and 5 kHz-repetition rate in 324 fs-long pulses have been obtained with a beam quality factor of $M^2 = 1.1$.

STh4E.3 • 17:00

Self-stabilization of an Intracavity Pumped fs Optical Parametric Oscillator, Xuan Luo¹, Jean-Claude M. Diels¹, Ladan Arissian¹; ¹Center for High Technology Materials, Univ. of New Mexico, USA. It is shown that auto-stabilization of an intracavity pumped Optical Parametric Oscillator can be achieved by exploiting the cascaded nonlinearities that are at the root of phase instabilities of this system.

16:30– 18:30

STh4F • THz Imaging

Presider: Hynek Nemeč; Inst. of Physics - Academy of Sciences Czech Republic, Czech Republic

STh4F.1 • 16:30 **Invited**

Sparse Imaging with Metamaterials at Terahertz Frequencies, Willie J. Padilla¹; ¹Boston College, USA. Metamaterials are composite structures which permit unprecedented control over light matter interactions. Here we show use of metamaterials as spatial light modulators permitting single pixel compressive imaging at terahertz frequencies.

STh4F.2 • 17:00

Zenneck THz Surface Waves-assisted Imaging of Subwavelength Dielectric Particles, Miguel Navarro-Cia^{1,2}, Michele Natrella², Filip Dominec³, Jean-Christophe Delagnes⁴, Petr Kuzel³, Patrick Mounaix⁴, Chris Graham², Cyril C. Renaud², Alwyn J. Seeds², Oleg Mitrofanov²; ¹Electrical and Electronic Engineering, Imperial College London, UK; ²Electronic & Electrical Engineering, Univ. College London, UK; ³Inst. of Physics, Academy of Sciences of the Czech Republic, Czech Republic; ⁴LOMA, Bordeaux 1 Univ., France. Electromagnetic Zenneck THz surface waves propagating on a bow-tie antenna are employed for time-resolved near-field imaging of subwavelength-size SrTiO₃ and TiO₂ particles. This approach provides high contrast, high-spatial resolution imaging through enhancing the field-particle interaction.

16:30– 18:30

STh4G • Quantum Cascade Lasers II

Presider: Michael Wanke; Sandia National Labs, USA

STh4G.1 • 16:30

Active Frequency-Noise Reduction of a Mid-IR Quantum Cascade Laser without Optical Frequency Reference, Lionel Tombez¹, Stephane Schilt¹, Thomas Südmeyer¹; ¹Univ. of Neuchatel, Switzerland. Frequency-noise reduction of a 4.55- μm distributed-feedback quantum cascade laser is demonstrated using the voltage fluctuations across its junction as an error signal only. A 10-fold reduction of the frequency-noise power spectral density is achieved.

STh4G.2 • 16:45

A Detailed Experimental Study of Frequency Noise in Mid-Infrared Distributed Feedback Quantum Cascade Lasers, Stephane Schilt¹, Lionel Tombez¹, Stephane Blaser², Romain Terazzi², Camille Tardy², Richard Maulini², Alfredo Bismuto², Tobias Gresch², Michel Rochat², Antoine Muller², Thomas Südmeyer¹; ¹Laboratoire Temps-Fréquence, Université de Neuchatel, Switzerland; ²Alpes Lasers SA, Switzerland. Flicker noise was studied in a set of 20 QCLs at 7-8 μm , showing significant differences among the devices and the probable existence of various noise sources. Ridge-waveguide lasers showed lower noise than buried-heterostructures.

STh4G.3 • 17:00

Electron localization in quantum cascade heterostructures due to interface roughness, Michael Harter¹, Yamac Dikmelik², Anthony J. Hoffman¹; ¹Electrical Engineering, Univ. of Notre Dame, USA; ²Electrical Engineering, Johns Hopkins Univ., USA. The localization of electron wavefunctions due to interface roughness in a quantum cascade heterostructures is investigated by observing the electroluminescence spectra. Localization is more prominent in heterostructures with designed extended states.

16:30– 18:30

STh4H • Plasmonics, Raman and Resonance Sensing

Presider: Ralph Jimenez; Univ. of Colorado at Boulder, USA

STh4H.1 • 16:30

Surface-Enhanced Raman Scattering Immuno-Assay Using Diatom Frustules, Jing Yang¹, Fanghui Ren¹, Le Zhen¹, Jeremy Campbell¹, Gregory L. Rorer¹, Alan X. Wang¹; ¹Oregon State Univ., USA. An immunoassay based on surface-enhanced Raman scattering has been developed using diatom frustules to detect antigens with high sensitivity. It was found that the diatom frustules provide 6 \times higher sensitivity than traditional glass substrates.

STh4H.2 • 16:45

Nanopore fluidic SERS, chang chen^{1,2}, Yi Li^{1,2}, Sarp Kerman^{1,2}, Pieter Neutens^{1,2}, Liesbet Lagae^{1,2}, Tim Stakenborg¹, Pol Van Dorpe^{1,2}; ¹imec, Belgium; ²KU Leuven, Belgium. We describe a technology combining nanopore fluidic with surface enhanced Raman spectroscopy (SERS) for real-time, single molecule detection at 10 ms level.

STh4H.3 • 17:00

3D plasmonic hollow nanoantennas as tools for neuroscience applications, Michele Dipalo¹, Mario Malerba¹, Gabriele C. Messina¹, Rosanna La Rocca¹, Ermanno Miele¹, Hayder Amin¹, Alessandro Maccione¹, Luca Berdoncini¹, Francesco De Angelis¹; ¹Istituto Italiano di Tecnologia, Italy. 3D plasmonic nanoantennas were fabricated on active biodevices for in-vitro neuroscience experiments. The technique consents to realize nanoantennas patterns suitable for neurons culture and that can be used concurrently as intracellular nanoelectrodes and spectroscopic probes.

Meeting Room
211 B/D

CLEO: Science &
Innovations

16:30– 18:30

STh4I • Novel Photodetectors

Presdier: Tingyi Gu, Columbia Univ., USA

STh4I.1 • 16:30

Mid-infrared graphene detectors with antenna-enhanced light absorption and photo-carrier collection, Yu Yao¹, Raji Shankar¹, Patrick Rauter¹, Yi Song², Jing Kong², Marko Loncar¹, Federico Capasso¹; ¹SEAS, Harvard Univ., USA; ²Electrical Engineering and Computer Science, MIT, USA. We demonstrated antenna-assisted mid-infrared graphene detectors at room temperature with more than 200 times enhancement of responsivity (0.4 V/W at $\lambda_0=4.45 \mu\text{m}$) compared to devices without antennas (<2 mV/W).

STh4I.2 • 16:45

Mid-Infrared GaN/AlxGa1-xN Quantum Cascade Detectors Grown by MOCVD, Yu Song¹, Rajaram Bhat², Pranav Badami¹, Tzu-Yung Huang¹, Zah Chung-En², Claire F. Gmachl¹; ¹Princeton Univ., USA; ²Corning Incorporated, USA. A III-nitride-based Quantum Cascade detector grown by MOCVD is designed, fabricated and tested. Peak responsivity of 100 $\mu\text{A/W}$ with detectivity of up to 10^8 Jones at $\sim 4 \mu\text{m}$ is measured.

STh4I.3 • 17:00

High-responsivity 1.7- μm -long InGaAs photodetectors based on photonic crystal with ultrasmall buried heterostructure, Kengo Nozaki^{1,2}, Shinji Matsuo^{1,3}, Koji Takeda^{1,3}, Tomonari Sato^{1,3}, Takuro Fujii^{1,3}, Eiichi Kuramochi^{1,2}, Masaya Notomi^{1,2}; ¹NTT Nanophotonics Center, Japan; ²NTT Basic resarch Labs, Japan; ³NTT Photonics Labs, Japan. InGaAs-embedded photonic crystal photodetectors were demonstrated towards realizing photoreceivers with small junction capacitance. A 1-A/W responsivity and a 40-Gb/s eye opening were successfully confirmed for the 1.7- μm -long device.

Meeting Room
212 A/C

JOINT

16:30– 19:00

JTh4J • Symposium on High Performance Optics II

Presider: Jeff Bude; Lawrence Livermore National Lab, USA

JTh4J.1 • 16:30

Pulse Compression of a High-Energy Thin-Disk Laser at 100 W of Average Power using an Ar-filled Kagome-Type HC-PCF, Florian Emaury¹, Clara J. Saraceno^{1,2}, Benoît Debord³, Coralie Fourcade Dutin³, Frédéric Jérôme³, Thomas Südmeyer², Fetah Benabid³, Ursula Keller¹; ¹ETH Zurich, Switzerland; ²Université de Neuchâtel, Switzerland; ³CNRS UMR 7252, Univ. of Limoges, France. We compressed a high-energy SESAM-modelocked thin-disk laser using an Ar-filled Kagome-type HC-PCF: launching 41 μJ , 1.17 ps pulses directly from a 3-MHz oscillator, we obtain 179-fs pulses at 100 W of average power, reaching 80% overall compression efficiency.

JTh4J.2 • 16:45 

James Webb Space Telescope (JWST): Optical Performance of a Large Deployable Cryogenic Telescope, Paul A. Lightsey¹; ¹Ball Aerospace & Technologies, USA. The JWST is a large deployable cryogenic telescope. The fabrication of the mirrors and the precision control for flight positioning of the mirrors using image based Wave Front Sensing and Control will be presented.

Meeting Room
212 B/D

CLEO: QELS-
Fundamental Science

16:30– 18:30

FTh4K • Nonlinear Plasmonics: From Visible to Terahertz

Presider: Gennady Shvets; Univ. of Texas at Austin, USA

FTh4K.1 • 16:30

Giant nonlinear response from plasmonic metasurfaces coupled to intersubband transitions, JONGWON LEE¹, Christos Argyropoulos¹, Pai-Yen Chen¹, Mykhailo Tymchenko¹, Feng Lu¹, Frederic Demmerle², Gerhard Boehm², Markus Amann², Andrea Alu¹, Mikhail A. Belkin¹; ¹Univ. of Texas at Austin, USA; ²Walter Schottky Institut, Germany. We report highly-nonlinear metasurfaces based on coupling of electromagnetically-engineered plasmonic nanoresonators with quantum-engineered intersubband nonlinearities. Experimentally, effective nonlinear susceptibility over 50nm/V was measured for second-harmonic generation under normal incidence.

FTh4K.2 • 16:45

7.5% Optical-to-Terahertz Conversion Efficiency through Use of Three-Dimensional Plasmonic Electrodes, Shang Hua Yang^{1,2}, Mohammed R. Hashemi^{1,2}, Christopher W. Berry¹, Mona Jarrahi^{1,2}; ¹Electrical Engineering and Computer Science Dept., Univ. of Michigan, USA; ²Electrical Engineering Dept., Univ. of California Los Angeles, USA. We present a high-efficiency photoconductive terahertz source based on high-aspect ratio plasmonic contact electrodes. At an optical pump power of 1.4 mW, a record-high optical-to-terahertz conversion efficiency of 7.5%.

FTh4K.3 • 17:00

Ultrafast Multi-Terahertz Nanoscopy with Sub-Cycle Temporal Resolution, Max Eisele¹, Tyler L. Cocker¹, Markus Huber¹, Leonardo Viti², Lucia Sorba², Miriam S. Vitiello², Rupert Huber¹; ¹Dept. of Physics, Univ. of Regensburg, Germany; ²NEST, CNR - Istituto Nanoscienze and Scuola Normale Superiore, Italy. We combine ultrafast multi-terahertz spectroscopy and near-field microscopy to achieve sub-wavelength spatial ($\sim 15 \text{ nm}$) and sub-cycle temporal ($\sim 9 \text{ fs}$) resolution. We apply our novel system to photoexcited InAs nanowires and resolve femtosecond carrier dynamics - spatially, temporally and spectrally.

Marriott
Salon I & II

JOINT


16:30– 18:30

JTh4L • Symposium on Laser-Driven Sources of Particle and X-Ray Beams III 

Presider: François Légaré; INRS-Energie Mat & Tele Site Varennes, Canada

JTh4L.1 • 16:30  

Picosecond Thin-Disk Lasers, Thomas Metzger¹, Martin Gorjan^{2,3}, Moritz Ueffing², Catherine Y. Teisset¹, Marcel Schultze¹, Robert Bessing¹, Matthias Häfner¹, Stephan Prinz¹, Dirk Sutter⁴, Knut Michel¹, Helena Barros², Zsuzsanna Major², Ferenc Krausz^{2,3}; ¹TRUMPF Scientific Lasers GmbH + Co. KG, Germany; ²Dept. für Physik, Ludwig-Maximilians-Universität München, Germany; ³Max-Planck-Institut für Quantenoptik, Germany; ⁴TRUMPF Laser GmbH + Co. KG, Germany. Short-pulse pumped optical parametric chirped pulse amplification (OPCPA) demands powerful picosecond lasers with high average powers and high pulse energies. We report on the current picosecond thin-disk amplifiers development and their applications in research.

JTh4L.2 • 17:00 

Advances in Industrial Grade TeraWatt Lasers for Accelerators, Christophe A. Simon-Boisson¹, François Lureau¹, Guillaume Matras¹, Sébastien Laux¹, Olivier Casagrande¹, Christophe Radier¹, Olivier Chalus¹, Laurent Boudjema¹; ¹Thales Optronique SAS, France. We review the recent results achieved on industrial grade Titanium Sapphire PetaWatt lasers demonstrating clear improvements. Key enabling technologies are presented. Perspectives towards higher peak power of 10 PW are discussed.

CLEO: Science & Innovations

CLEO: Applications
& Technology

16:30– 18:30

Sth4M • Silicon Modulstors ▶

Presider: Jessie Rosenberg; IBM T. J. Watson Research Center, USA

Sth4M.1 • 16:30 ▶

Hydrogenated Amorphous Silicon Microcylindrical Resonators for Ultrafast Modulation, Natasha Vukovic¹, Noel Healy¹, Fariza Suhailin¹, Priyath Mehta¹, Todd Day², John Badding², Anna C. Peacock¹; ¹Optoelectronics Research Centre, Univ. of Southampton, UK; ²Dept. of Chemistry and Materials Research Inst., Pennsylvania State Univ., USA. We report on the large Kerr induced wavelength shift observed in our hydrogenated amorphous silicon microresonators and demonstrate their use for all-optical modulation and switching on picosecond time scales with only subpicjoule pulse energies.

Sth4M.2 • 16:45 ▶

Add-drop Microring Resonator for Electro-optical Switching and Optical Power Monitoring, Anna Lena Giesecke¹, Andreas Prinzen¹, Jens Bolten¹, Caroline Porschatis¹, Bartos Chmielak¹, Christopher Matheisen¹, Thorsten Wahlbrink¹, Holger Lerch¹, Michael Waldow¹, Heinrich Kurz¹; ¹AMO GmbH, Germany. Microring based silicon depletion modulators with high extinction ratio (>25dB) are used for high frequency modulation and as resonant photodetectors at 1340nm (O-band). Photocurrent and power enhancement are investigated for modulators with different Q-factors.

Sth4M.3 • 17:00 ▶

High speed Si modulators with high modulation efficiency and low free carrier absorption by depleting carriers through fringe field junctions, Kai-Ning Ku¹, Ming-Chang M. Lee¹; ¹Inst. of Photonics Technologies and Dept. of Electrical Engineering, National Tsing Hua Univ., Taiwan. A high speed Si modulator with fringe field junctions is presented. Low carrier absorption (1.3 dB/mm) and V_{πL} (1.8 V-cm) are demonstrated. The measured modulation speed and depth are 11.8-GHz and 8-dB.

16:30– 18:30

Sth4N • Coherent Combination and Amplification

Presider: Michalis Zervas; Univ. of Southampton, UK

Sth4N.1 • 16:30 **Invited**

Phase-locked Multicore Fiber Lasers, Akira Shirakawa¹; ¹Univ. of Electro-Communications, Japan. Arraying fiber lasers is being focused for power and energy scaling and multicore fibers can be a promising format. Phase locking in evanescently-coupled multicore fiber lasers by various in-phase mode selection methods is presented.

Sth4N.2 • 17:00

4-fold Increase of the Mode-instability Threshold in an Yb-doped Multi-core Fiber Amplifier Emitting 536 W, Hans-Jürgen Otto¹, Arno Klenke^{1,2}, Cesar Jauregui¹, Fabian Stutzki¹, Jens Limpert^{1,2}, Andreas Tünnermann^{1,3}; ¹Inst. of Applied Physics, Germany; ²Helmholtz-Inst. Jena, Germany; ³Fraunhofer Inst. for Applied Optics and Precision Engineering, Germany. A compact, pulsed MOPA fiber-laser system employing a 4 core photonic-crystal fiber is presented that exhibits a 4 times increased mode-instability threshold. An average power of 536W with nearly diffraction limited beam quality was achieved.

16:30– 18:30

Sth4O • Gravity and Distance Measurements ▶

Presider: Kristan Corwin; Kansas State Univ., USA

Sth4O.1 • 16:30 **Invited** ▶

High Sensitivity Gravity Measurement with Cold Atom Interferometry, Zhongkun Hu¹, Xiao-Chun Duan¹, Min-Kang Zhou¹, Le-Le Chen¹; ¹Huazhong Univ of Science and Technology, China. We report the work of exploring atom interferometry techniques to perform precision gravity measurements in our Lab. The noise suppressions and related modulation experiments for the atom gravimeter will be presented in detail.

Sth4O.2 • 17:00 ▶

Coherent asynchronous sampling distance measurement using a single polarization-multiplexed ultrafast laser, Xin Zhao¹, Zheng Gong¹, Ya Liu¹, Jiansheng Liu¹, Zheng Zheng¹; ¹School of Electronic and Information Engineering, Beihang Univ., China. Laser ranging based on asynchronous sampling of ultrashort optical pulses is proposed and experimentally demonstrated using just one polarization-multiplexed mode-locked fiber laser, which produces two orthogonal polarized, coherent pulse trains with slightly different repetition rates.

16:30– 18:30

Ath4P • Symposium on Advanced Ultrashort Pulse Laser Technologies in Biophotonics and Nanobiophotonics II ▶

Presider: Emma Springate; STFC Rutherford Appleton Lab, UK

Ath4P.1 • 16:30 **Invited** ▶

Plasmonic Nanobubble Theranostics: Detection and Destruction of Drug-Resistant Tumors in a Single Rapid Procedure, Dmitri Lapotko¹; ¹Biochemistry and Cell Biology, Rice Univ., USA. On-demand plasmonic nanobubbles combine highly sensitive detection and guided destruction of drug-resistant tumors, minimize non-specific toxicity in a rapid theranostic procedure that converts current “macro” treatments into a cancer cell level “micro” modality.

Ath4P.2 • 17:00 ▶

Octave Spanning Mid-Infrared Frequency Comb Generation in Silicon Nanophotonic Wire Waveguides, Bart Kuyken^{1,2}, Takuro Ideguchi³, Simon Holzner³, Ming Yan³, Theodor W. Haensch³, Joris Van Campenhout⁴, Peter Verheyen⁴, Roel Baets^{1,2}, Gunther Roelkens^{1,2}, Nathalie Picqué³; ¹Photonics Research Group, Belgium; ²Center for Nano- and Biophotonics, Ghent Univ., Belgium; ³Max Planck Institut für Quantenoptik, Germany; ⁴imec, Belgium. A mid-infrared octave spanning frequency comb is generated in a silicon waveguide. By beating the generated comb on a photodetector with a narrow linewidth lightsource the linewidth of the lines is measured to be <100kHz.

CLEO: QELS-
Fundamental ScienceFTh4A • Quantum Sensing and
Metrology—Continued

FTh4A.4 • 17:15

Quantum-Enhanced Precision in Unitary Process Tomography, Rebecca Whittaker¹, Xiao-Qi Zhou¹, Jonathan Matthews¹, Jeremy L. O'Brien¹, Pete Shadbolt¹, Hugo Cable^{2,1}; ¹Centre for Quantum Photonics, Univ. of Bristol, UK; ²Centre for Quantum Technologies, National Univ. of Singapore, Singapore. A novel scheme for unitary quantum process tomography (QPT) is theoretically presented and implemented experimentally. Multi-photon input states are used to obtain quantum-enhanced precision for the unitary estimation. Our results are compared to standard QPT.

FTh4A.5 • 17:30

Sub-wavelength interfering with thermal light, Yanhua Zhai¹, Francisco. Becerra¹, Jianming Wen², Jingyun Fan¹, Alan L. Migdall¹; ¹JQI NIST and Univ. of Maryland, USA; ²Dept. of Applied Physics, USA. By using photon-number-resolving detection, high-order correlation interference with thermal light offers high spatial resolution and visibility. Experimentally, a fringe width of 15 nm is obtained for a light wavelength of 780 nm.

FTh4A.6 • 17:45

Experimental demonstration of fundamental bounds in quantum measurements for estimating quantum states, Hyang-Tag Lim¹, Young-Sik Ra¹, Kang-Hee Hong¹, Seung-Woo Lee², Yoon-Ho Kim¹; ¹Dept. of Physics, Pohang Univ. of Science and Technology (POSTECH), Korea; ²Dept. of Physics and Astronomy, Dartmouth College, USA. We investigate the conditions of an optimal measurement for estimating quantum states with minimal disturbance and maximal reversibility, and experimentally implement it in three-dimensional quantum states encoded by the single photon's polarization and path.

FTh4A.7 • 18:00

Scalable Spatial Super-Resolution using Entangled Photons, Lee Rozema¹, James D. Bateman¹, Dylan Mahler¹, Amir Feizpour¹, Ryo Okamoto², Alex Hayat^{1,3}, Aephraim M. Steinberg¹; ¹Dept. of Physics, Univ. of Toronto, Canada; ²Research Inst. for Electronic Science, Hokkaido Univ., Japan; ³Dept. of Electrical Engineering, Technion, Israel. We demonstrate spatial super-resolution, performing an optical centroid measurement on 4-photon NOON states with a scalable 11-detector measurement. Our results show spatial super-resolution with exponentially better detection efficiency than any previous NOON-state experiment.

CLEO: Science &
InnovationsSTh4B • Laser-Driven Dynamics
in Materials—Continued

STh4B.3 • 17:15

Controlling ablation mechanisms in sapphire by irradiation with temporally shaped femtosecond laser pulses, Javier Hernandez-Rueda¹, Mario Garcia-Lechuga¹, Jan Siegel¹, Javier Solis¹; ¹Instituto De Optica "Daza De Valdes", Spain. The use of temporally shaped femtosecond laser pulses is shown to enable the control of ablation mechanisms in Sapphire ranging from gentle over strong ablation to explosive boiling.

STh4B.4 • 17:30

Exciton-related electroluminescence from monolayer MoS₂, Yu Ye¹, Ziliang Ye¹, Majid Gharghi¹, Xiaobo Yin¹, Hanyu Zhu¹, Mervin Zhao¹, Xiang Zhang¹; ¹UC Berkeley, USA. We studied the microscopic origin of the electroluminescence from monolayer MoS₂ fabricated on a heavily p-type doped silicon substrate. Auger recombination of the exciton-exciton annihilation of bound exciton emission is observed.

STh4B.5 • 17:45

Double-Confinement in Plasmonic Resonators, Arthur Montazeri¹, Michael Fang¹, Nazir P. Kherani¹, Peyman Sarrafi¹; ¹Univ. of Toronto, Canada. We present a new model to investigate slow-light and light trapping with plasmonic gratings. Controlling plasmon coupling strength in narrow waveguide resonators is used as the building blocks of gratings.

STh4B.6 • 18:00

Filament Interaction with Micro-Water Droplets, Cheonha Jeon¹, Magali M. Durand¹, Matthieu Baudelet¹, Martin Richardson¹; ¹Townes Laser Inst., CREOL, UCF, USA. The interaction of a laser filament with water droplets was studied to understand the energy dissipation of filaments in aerosols. Shockwave analysis allows the quantification of the energy balance. We discuss the survival of filaments.

CLEO: QELS-Fundamental Science

FTh4C • Carrier Dynamics in
0-D and 1-D Nanostructures—
Continued

FTh4C.4 • 17:15

Thresholdless Optical Gain using Colloidal HgTe Nanocrystals, Pieter Geiregat^{1,2}, Arjan Houtepen³, Laxmi Kishore Sagar², Christophe Delerue⁴, Dries Van Thourhout¹, Zeger Hens²; ¹Information Technology, Universiteit Gent, Belgium; ²Inorganic and Physical Chemistry, Universiteit Gent, Belgium; ³Chemistry, Technische Universiteit Delft, Netherlands; ⁴IEMN, France. Thresholdless stimulated emission is observed using nanometer sized colloidal HgTe nanocrystals, in a broad spectral region covering the entire technologically relevant near-infrared spectrum.

FTh4C.5 • 17:30

Ultrafast Optical Properties of PbSe Nano-Rods: One Dimensional Excitons, Eli Kinigstein¹, Shu-Wei Huang¹, Matthew Sfeir², Weon-Kyu Koh⁴, Christopher Murray³, Tony F. Heinz¹, Chee Wei Wong²; ¹Columbia Univ., USA; ²Center For Functional Nanomaterials, Brookhaven National Laboratory, USA; ³Univ. of Pennsylvania, USA; ⁴Los Alamos National Lab, USA. Using Supercontinuum Transient Absorption Spectroscopy we observe new ultrafast exciton dynamics in PbSe Nanorods. We report distinct types of biexcitonic interactions, and propose a model to quantitatively describe the bleach using the predicted electronic structure.

FTh4C.6 • 17:45

Towards Single Molecule Infrared Vibrational Spectroscopy and Dynamics, Joanna M. Atkin¹, Paul Sass¹, Jonas Allerbeck¹, Markus B. Raschke¹; ¹Dept. of Physics, Dept. of Chemistry, and JILA, Univ. of Colorado, USA. We demonstrate ultrafast infrared vibrational free-induction decay probing in scattering-scanning near-field microscopy. We observe long-lived few picosecond vibrational coherences, far in excess of the far-field ensemble response.

FTh4C.7 • 18:00

Ultrafast non-thermal response of Plasmonic resonance in Gold Nanoantennas, Giancarlo Soavi¹, Giuseppe Della Valle¹, Paolo Biagoni¹, Andrea Cattoni², Giulio Cerullo¹, Daniele Brida³; ¹Dipartimento di Fisica, Politecnico di Milano, Italy; ²Laboratoire de Photonique et de Nanostructures, France; ³Dept. of Physics and Center for Applied Photonics, Univ. of Konstanz, Germany. Ultrafast thermalization of electrons in metal nanostructures is studied by means of pump-probe spectroscopy. We track in real-time the plasmon resonance evolution, providing a tool for understanding and controlling gold nanoantennas non-linear optical response.

FTh4D • Nonlinear
Metamaterials and Cooling—
Continued

FTh4D.3 • 17:30

Color-preserving daytime radiative cooling, Linxiao Zhu¹, Aaswath Raman², Shanhui Fan²; ¹Applied Physics, Stanford Univ., USA; ²Electrical Engineering, Stanford Univ., USA. We introduce a general approach to radiatively lower the temperature of a structure, while preserving its color under sunlight. The cooling persists in the presence of considerable non-radiative heat exchange, and for different solar absorptances.

FTh4D.4 • 17:45

Optical refrigeration cools below 100K, Seth Melgaard^{1,2}, Alexander R. Albrecht¹, Markus Hehnen³, Denis Seletskiy⁴, Mansoor Sheik-Bahae⁵; ¹Univ. of New Mexico, USA; ²Air Force Research Lab, USA; ³Los Alamos National Labs, USA; ⁴Univ. of Konstanz, Germany. We report a milestone in optical refrigeration, cooling a 10% Yb:YLF crystal to 93K ($\Delta T \sim 180K$); obtaining the coldest solid-state temperature to date. Identification of transition metal impurities via mass spectrometry allows further cooling through purification.

FTh4D.5 • 18:00

Rotation induced cooling of an optically trapped microgyroscope in vacuum, Yoshihiko Arita¹, Michael Mazilu¹, Kishan Dholakia¹; ¹School of Physics and Astronomy, Univ. of St Andrews, UK. We demonstrate optical trapping of a microgyroscope rotating at MHz rates in vacuum. The particle is cooled to 40K. This is a major step towards measuring the Casimir force resulting in rotational quantum friction.

CLEO: Science & Innovations

STh4E • OPO, OPA and
Regenerative Amplifiers—
Continued

STh4E.4 • 17:15

Burst-mode Femtosecond Non-collinear Parametric Amplifier with Arbitrary Pulse Selection, Mikhail Pergament¹, Martin Kellert¹, Kai Kruse¹, Jinxiong Wang¹, Guido Palmer¹, Laurens Wissmann¹, Ulrike Wegner¹, Max J. Lederer¹, ¹European X-Ray Free-Electron Laser-Facility GmbH, Albert-Einstein-Ring 19, Germany. We present a high power burst-mode femtosecond non-collinear parametric amplifier. High quality 15fs pulses at up to 4.5MHz intra-burst repetition rate and energies of more than 180μJ are shown. Arbitrary pulse sequences can be selected.

STh4E.5 • 17:30

Simultaneous broadening of the depleted pump and signal from an optical parametric amplifier, Derrek Wilson¹, Carlos Trallero-Herrero¹, Xiaoming Ren¹, J. R. Macdonald Lab, Kansas State Univ., USA. An optical parametric amplifier signal and its unconverted pump are studied as a method of waveform synthesis. Generating broad spectra with self phase modulation to create coherent multi-octave CEP stabilized pulses is discussed.

STh4E.6 • 17:45

Sub-4-Cycle Pulses Directly From an All-Collinear, High-Repetition-Rate, Mid-IR OPCPA, Benedikt W. Mayer¹, Christopher R. Phillips^{1,2}, Lukas Gallmann¹, Martin M. Fejer², Ursula Keller¹, ¹Inst. for Quantum Electronics, ETH Zurich, Switzerland; ²Edward L. Ginzton Lab, Stanford Univ., USA. We present an ultra-broadband OPCPA system operating at 3.4 μm delivering 41.6-fs pulses. The average output power is currently 600 mW, corresponding to 12 μJ of pulse energy at a repetition rate of 50 kHz.

STh4E.7 • 18:00

Femtosecond Optical Parametric Oscillator Frequency Combs at Harmonics of the Pump Laser Repetition Frequency, Richard A. McCracken¹, Derryck T. Reid¹, ¹Inst. of Photonics and Quantum Sciences, Heriot Watt Univ., UK. Various schemes allow femtosecond OPOs to produce pulses at harmonics of their pump laser repetition frequency, ostensibly facilitating access to widely-spaced tunable frequency combs. Here, we show not all approaches possess equivalent carrier-envelope offset characteristics.

STh4F • THz Imaging—
Continued

STh4F.3 • 17:15

Transmission of THz pulses through 3μm apertures: applications for near-field microscopy, Alexander J. Macfaden¹, John L. Reno^{2,3}, Igal Brener^{2,3}, Oleg Mitrofanov^{1,2}; ¹Univ. College London, UK; ²CINT, USA; ³Sandia National Lab, USA. We demonstrate that THz pulses transmitted through small apertures (~λ/100) exhibit strong evanescent components within 1μm of the aperture. Using this effect, we developed sub-wavelength aperture THz near-field probes that provide 3μm resolution.

STh4F.4 • 17:30

Analysis of various kinds of solar cell using Dynamic Terahertz Emission Microscope, Hidetoshi Nakanishi¹, Akira Ito¹, Kazuhisa Takayama², Iwao Kawayama², Hironaru Murakami², Masayoshi Tonouchi²; ¹Dainippon Screen Mfg. Co., Ltd, Japan; ²Osaka Univ., Japan. We developed a dynamic terahertz emission microscope to investigate dynamic response of photoexcited carriers in various kinds of solar cell, e.g. a monocrystalline silicon solar cell, a polycrystalline silicon solar cell, and a GaAs solar cell.

STh4F.5 • 17:45

Terahertz near-field phase contrast imaging, François Blanchard¹, Kenji Sumida², Christian Wolpert², Manuel Tsotsalas², Tomoko Tanaka^{2,3}, Atsushi Doi^{2,4}, Susumu Kitagawa², David G. Cooke¹, Shuhei Furukawa², Koichiro Tanaka^{2,5}; ¹Physics, McGill Univ., Canada; ²Inst. for Integrated Cell-Material Sciences, Kyoto University, Japan; ³CREST, Japan Science and Technology Agency, Japan; ⁴Olympus, Japan; ⁵Physics, Kyoto Univ., Japan. We demonstrate a method, permitting the observation of dielectric loading of hydrocarbons into a porous coordination polymer nanocrystal (PCP), by spatially resolving the phase difference between the near-field responses of two terahertz resonators.

STh4F.6 • 18:00

Real-time broadband spectroscopic terahertz imaging with diffraction grating and high-sensitivity terahertz camera, Natsuki Kanda^{1,2}, Kuniaki Konishi², Natsuki Nemoto³, Katsumi Midorikawa^{1,2}, Makoto Kuwata-Gonokami^{2,3}; ¹Laser Technology Lab., RIKEN, Japan; ²Photon Science Center, The Univ. of Tokyo, Japan; ³Dept. of Physics, The Univ. of Tokyo, Japan. We developed a broadband THz spectroscopic imaging method using intense THz pulses and a high-sensitivity THz camera. By using a diffraction grating spectrometer, real-time spectroscopic imaging, or molecular-specific imaging, is realized.

STh4G • Quantum Cascade
Lasers II—Continued

STh4G.4 • 17:15

Genetically Optimized Multi-Wavelengths QCL, Guy-Maël De Naurois¹, Stefan Kalchmair¹, Tobias Mansuripur¹, Laurent Diehl², Christian Pflügl², Marko Loncar¹, Federico Capasso¹; ¹Harvard Univ., USA; ²Eos Photonics, USA. We present a genetically optimized multi-wavelengths laser based on an aperiodic sampled grating. We show that the grating phases and amplitudes can be optimized to flatten the spectral signature allowing multi-wavelengths operation.

STh4G.5 • 17:30

High Power (>3 mW) Quantum Cascade Superluminescent Emitter, Nyan L. Aung¹, Zhouchangwan Yu², Ye Yu³, Yu Yao⁴, Peter Liu⁵, Xiaojun Wang⁶, Jen-Yu Fan⁶, Mariano Troccoli¹, Claire F. Gmachl¹; ¹Dept. of Electrical Engineering, Princeton Univ., USA; ²Dept. of Engineering, Smith College, USA; ³The Hong Kong Univ. of Science and Technology, China; ⁴School of Engineering and Applied Science, Harvard Univ., USA; ⁵Inst. of Quantum Electronics, ETH Zürich, Switzerland; ⁶AdTech Optics Inc., USA. We report high power (>3 mW) mid-infrared superluminescent emission around 2100 cm⁻¹ from Quantum Cascade devices. The superluminescent emission shows a Gaussian shape spectrum with FWHM of 80 cm⁻¹.

STh4G.6 • 17:45

Development of terahertz laser frequency combs, David P. Burghoff¹, Tsung-Yu Kao¹, Ningren Han¹, Chun Wang Ivan Chan¹, Darren J. Hayton², Jian-Rong Gao^{2,3}, John L. Reno⁴, Qing Hu¹; ¹Dept. of Electrical Engineering and Computer Science, MIT, USA; ²SRON Netherlands Inst. for Space Research, Netherlands; ³Kavli Inst. of NanoScience, Delft Univ. of Technology, Netherlands; ⁴Center for Integrated Nanotechnology, Sandia National Labs, USA. We demonstrate broadband terahertz laser frequency combs, compact semiconductor devices that combine the high power of lasers with the broad spectra of pulsed sources.

STh4G.7 • 18:00

Towards Watt-Level Performance of Terahertz Quantum Cascade Lasers, Christoph Deutsch¹, Martin Brandstetter¹, Michael Krall¹, Hermann Detz², Aaron Maxwell Andrews², Werner Schrenk², Gottfried Strasser², Karl Unterrainer¹; ¹Photonics Inst., Technische Universität Wien, Austria; ²Inst. for Solid-State Electronics, Technische Universität Wien, Austria. Terahertz quantum cascade lasers have not reached watt-level output powers yet. We present surface-plasmon devices with a peak power of 0.94 W. The device consists of two symmetric active regions combined by a wafer-bonding step.

STh4H • Plasmonics, Raman and
Resonance Sensing—Continued

STh4H.4 • 17:15

An Accurate Interferometric Referencing Method for Resonance Tracking in Lab-on-chip Applications, Farshid Ghasemi¹, Ali Adibi¹; ¹Electrical and Computer Engineering, Georgia Inst. of Technology, USA. Repeatability of resonance detection for on-chip microring resonators is systematically studied. An efficient interferometric method is presented to improve the accuracy by more than one order of magnitude in an 8 nm bandwidth, without any temperature control.

STh4H.5 • 17:30

Wide Dynamic Range Sensing in Photonic Crystal Microcavity Biosensors, Chun-Ju Yang¹, yi zou¹, Swapnait Chakravarty², Hai Yan¹, Zheng Wang¹, Ray Chen^{1,2}; ¹The Univ. of Texas at Austin, USA; ²Omega Optics Inc., USA. We experimentally demonstrated that multiplexing of PC sensors with different geometry can achieve a wide dynamic range covering 6 orders of magnitude with potential for 8 or more orders with suitable optimization.

STh4H.6 • 17:45

Plasmonic nano-optical conveyer using C-shaped engravings, Yuxin Zheng¹, Jason Ryan¹, Paul Hansen¹, Paul Hansen¹, Yao-Te Cheng¹, Tsung-Lu Lu¹, Lambertus Hesselink¹; ¹Stanford Univ., USA. We develop a near-field based optical trapping and conveyor belt system based on a novel plasmonic structure: C-shaped engraving. Using polarization rotation and wavelength switching, we demonstrate controlled transport of nanoparticles along different paths.

STh4H.7 • 18:00

Gold Nanoparticle Coated Silicon Nitride Chips For Intracellular Surface-Enhanced Raman Spectroscopy, Pieter Wuytens¹, ananth subramanian¹, Alexey Yashchenok², Andre Skirtach¹, Roel Baets¹; ¹gent Univ., Belgium; ²Max-Planck Inst. of Colloids and Interfaces, Germany. Using surface-enhanced Raman spectroscopy on gold-nanoparticle-decorated silicon nitride chips, we monitor the release of dextran-rhodamin molecules from capsules inside living cells. This demonstrates the feasibility of using photonic chips for intracellular sensing at visible wavelengths

Meeting Room
211 B/D

CLEO: Science &
Innovations

STH4I • Novel Photodetectors—
Continued

STH4I.4 • 17:15

Defect-Assisted Sub-Bandgap Avalanche Photodetection in Interleaved Carrier-Depletion Silicon Waveguide for Telecom Band, Boris Desiatov¹, Ilya Goykhman¹, Joseph Shappir¹, Uriel Levy¹; ¹Hebrew Univ. of Jerusalem, Israel. We experimentally demonstrate avalanche sub bandgap detection of light at 1550 nm wavelength via surface states using the configuration of interleaved PN junctions along a silicon waveguide. The device operates in a fully depleted mode.

STH4I.5 • 17:30

Polarization-resolved Imaging using Elliptical Silicon Nanowire Photodetectors, Hyunsung Park¹, Kenneth B. Crozier¹; ¹School of Engineering and Applied Sciences, Harvard Univ., USA. We fabricate photodetectors comprising silicon nanowires with elliptical cross sections, and show that their spectral responsivities depend on the incident light's polarization state. We perform polarization-resolved imaging using these photodetectors.

STH4I.6 • 17:45

High Power 20GHz Photodiodes with Microwave Tuning Circuits, Kejia Li¹, Qiugui Zhou¹, Xiaojun Xie¹, Andreas Beling¹, Joe C. Campbell¹; ¹Electrical and Computer Engineering, Univ. of Virginia, USA. Modified uni-travelling-carrier (MUTC) photodiodes (PDs) with microwave open and shorted stubs having RF output power (PRF_out) of 23 dBm and 21.6 dBm, respectively, at 20 GHz are demonstrated.

STH4I.7 • 18:00

Photodetectors based on Atomically Thin Transition Metal Dichalcogenides, Thomas Mueller¹, Marco M. Furchi¹, Andreas Pospischil¹; ¹Vienna Univ. of Technology, Austria. We present phototransistors based on atomically thin layers of molybdenum disulfide and van der Waals heterostructures of transition metal dichalcogenides.

Meeting Room
212 A/C

JOINT

JTh4J • Symposium on High
Performance Optics II—
Continued

JTh4J.3 • 17:15 **Invited**

Metrology and Coatings for the 40 kg LIGO Optics, Rana X. Adhikari¹; ¹California Inst. of Technology, USA. The 4 km LIGO interferometers seek to measure the gravitational fluctuations from cosmic explosions. In order to do so, their massive mirrors must meet several demanding specifications which are sometimes conflicting. I will describe why the job is so challenging and how the challenges may be met.

JTh4J.4 • 17:45

All-optical helicity dependent switching in amorphous Tb₃₀Fe₇₀ with a MHz laser oscillator, Alexander Hassdenteufel¹, Christian Schubert², Birgit Hebler², Helmut Schultheiss^{3,4}, Jürgen Fassbender^{3,4}, Manfred Albrecht², Rudolf Bratschitsch⁵; ¹Chemnitz Univ. of Technology, Germany; ²Univ. of Augsburg, Germany; ³Helmholtz Zentrum Dresden Rossendorf, Germany; ⁴Technische Universität Dresden, Germany; ⁵Univ. of Münster, Germany. All-optical magnetic switching is demonstrated in a Tb-Fe thin film with a conventional laser oscillator instead of a complex and expensive amplifier system. Overheating is prevented by a SiO₂/Si substrate as an efficient heat sink.

JTh4J.5 • 18:00 **Invited**

State of the Art Optical Materials for Lithographic Systems for Semiconductor Manufacturing, Ralf Takke¹; ¹Division Optics, Heraeus Quarzglas GmbH & Co. KG, Germany. 193nm lithography has enabled semiconductor manufacturing to achieve nm resolution. Highest quality optical materials and optics are an essential part of this. Important optical properties of and test methods for these materials will be reported.

Meeting Room
212 B/D

CLEO: QELS-
Fundamental Science

FTh4K • Nonlinear Plasmonics:
From Visible to Terahertz—
Continued

FTh4K.4 • 17:15

Control of grating-coupled ultrafast surface plasmon pulse and its nonlinear emission by shaping femtosecond laser pulse, Yuta Masaki¹, Kazunori Toma¹, Miyuki Kusaba¹, Kenichi Hirotsawa¹, Fumihiko Kannari¹; ¹Keio Univ., Japan. Spatiotemporal nanofocusing of surface plasmon polariton excited by femtosecond laser pulses on a sharp conical Au tip with a tip edge radius of few tens of nanometers is deterministically controlled.

FTh4K.5 • 17:30

Geometrical effects in second-harmonic generation from metal nanoparticles, Robert Czaplicki¹, Roope Siikanen¹, Jouni Mäkitalo¹, Hannu Husu^{1,2}, Joonas Lehtolahti³, Markku Kuittinen³, Martti Kauranen¹; ¹Dept. of Physics, Tampere Univ. of Technology, Finland; ²Centre for Metrology and Accreditation (MIKES), Finland; ³Dept. of Physics and Mathematics, Univ. of Eastern Finland, Finland. We investigate non-centrosymmetric metal nanoparticles of different geometries by second-harmonic generation. In contrast to recent emphasis on plasmonic resonances, we find that strong responses rely on the character of plasmon oscillations supported by the geometry.

FTh4K.6 • 17:45

Second Harmonic Generations from Au Nanorods Coated with Nonelectrically Poled NLO polymer, Atsushi Sugita¹, Takuma Hirabayashi¹, Atsushi Ono¹, Yoshimasa Kawata¹; ¹Shizuoka Univ., Japan. Second order nonlinear optical susceptibility of Au nanorods coated with nonelectrically poled NLO polymer will be presented. The SHG conversion efficiency at fully Surface Plasmon resonance was 70 times higher than that at off-resonance conditions.

FTh4K.7 • 18:00

Surface Nonlinearities in Plasmonics, Alexey V. Krasavin¹, Paulina Segovia¹, Pavel Ginzburg¹, Anatoly V. Zayats¹; ¹Dept. of Physics, King's College London, UK. Plasmonic nanostructures can manipulate nonlinear optical phenomena via local field enhancement, but also can serve as strong nonlinear sources themselves. Surface second-harmonic effects in nanoparticles, surfaces, and metamaterials will be analyzed via advanced hydrodynamic model.

Marriott
Salon I & II

JOINT

JTh4L • Symposium on Laser-
Driven Sources of Particle and
X-Ray Beams III—Continued

JTh4L.3 • 17:15 **Invited**

Adaptive spectral-phase control for laser wakefield electron acceleration, Cheng Liu¹, Jun Zhang¹, Gregory Golovin¹, Shouyuan Chen¹, Sudeep Banerjee¹, Baozhen Zhao¹, Nathan Powers¹, Isaac Ghebregiabher¹, Donald P. Umstadter¹; ¹Physics & Astronomy, Univ. of Nebraska, Lincoln, USA. An adaptive spectral-phase control method is demonstrated for laser wakefield acceleration of electrons. Phase control capability was implemented to experimentally study the dependence of laser wakefield acceleration on the spectral phase of intense laser light.

JTh4L.4 • 17:30 **Invited**

Status of High-Energy OPCPA at LLE and Future Prospects, Jonathan D. Zuegel¹; ¹Univ. of Rochester, USA. The scope and status of a mid-scale optical parametric amplifier line (OPAL) that will demonstrate scalable technologies will be presented along with technical challenges and prospects for an OPAL pumped by OMEGA EP.

CLEO: Science & Innovations

CLEO: Applications
& TechnologySTh4M • Silicon Modulstors—
Continued

STh4M.4 • 17:15

Adaptive Controller of Two Tuning Phases in a Microring Based Binary Phase Shift Keying (BPSK) Modulator, Jonathan Fisher¹, Moshe Nazarathy¹, Anna Kodanev¹, Nadav Shitrit¹, Meir Orenstein¹, Andrea Annoni², Francesco Morichetti², Andrea Melloni²; ¹Technion Israel Inst. of Technology, Israel; ²Elettronica e Informazione, Politecnico di Milano, Italy. The state-of-the art for control of microring based devices is tuning just resonant phase. We introduce an extremum-seeking discrete-multitone adaptive controller, concurrently tuning both resonant phase and second coupling phase parameter optimizing microring critical coupling.

STh4M.5 • 17:30

Characterization of electrically-driven silicon photonic Mach-Zehnder switches, Ryan Aguinaldo¹, George Porter¹, George Papan¹, Yeshaihua Fainman¹, Shayan Mookherjee¹; ¹Univ. of California San Diego, USA. We demonstrate a new method to extract the electronic carrier-induced loss and coupling coefficients of modern thermo-optic and electro-optic silicon Mach-Zehnder interferometer based 2x2 switches (Sandia, IBM and Kotura-Oracle) from the transmission spectra.

STh4M.6 • 17:45

Distributed Electrode Mach-Zehnder Modulator with Double-Pass Phase Shifters and Integrated Inductors, Douglas M. Gill¹, William M. Green¹, Chi Xiong¹, Jonathan E. Proesel¹, Alexander V. Rylakov¹, Clint L. Schow¹, Jessie Rosenberg¹, Tymon Barwicz¹, Marwan Khater¹, Solomon Assefa¹, Steven Shank², Carol Reinholm², Edward Kiewra², Swetha Kamlapurkar¹, Yurii Vlasov¹; ¹IBM TJ Watson Research Center, USA; ²IBM Sytems & Technology Group, USA. A novel high-speed Mach-Zehnder modulator (MZM) fully integrated into a 90 nm CMOS process is presented. The MZM features 'double-pass' optical phase shifter segments, and the first use of integrated inductors in a 'velocity-matched' distributed-electrode configuration.

STh4M.7 • 18:00

Wavelength Control of Resonant Photonic Modulators with Balanced Homodyne Locking, Jonathan A. Cox¹, Anthony L. Lentine¹, Daniel J. Savignon¹, Douglas Trotter¹, Andrew Starbuck¹; ¹Sandia National Labs, USA. We present a robust method for control of resonant modulator wavelength that is integrated with an on-chip balanced detector. Experimental results demonstrate long-term locking with low bit error rate over greater than 55 Kelvin.

STh4N • Coherent Combination
and Amplification—Continued

STh4N.3 • 17:15

Diffraction Coherent Combining of >kW Fibers, Gregory D. Goodno¹, Stuart McNaught¹, Josh Rothenberg¹, Peter Thielen¹, Marty Wacks¹; ¹Northrop Grumman Aerospace Systems, USA. Three non-PM, kW-class fiber amplifiers were coherently combined into a 2.4-kW, M²=1.2 beam with 80% efficiency. No power-limiting effects were observed, which anchored scaling predictions to higher powers and efficiencies with larger fiber count arrays.

STh4N.4 • 17:30

0.7 MW Output Power from Coherently Combined Q-switched Photonic Crystal Fiber Laser, Boris Rosenstein¹, Avry Shirakov^{1,2}, Daniel Belker¹, Amiel Ishaaya¹; ¹Dept. of Electrical and Computer Engineering, Ben-Gurion Univ. of the Negev, Israel; ²Dept. of Physics, Ben-Gurion Univ. of the Negev, Israel. We experimentally demonstrate a high peak power, Q-switched pulsed, intracavity coherently combined photonic crystal fiber laser in a power oscillator configuration. Our oscillator system provides record high peak power of ~0.7 MW.

STh4N.5 • 17:45

Divided-Pulse Lasers, Erin S. Lamb¹, Logan G. Wright¹, Frank W. Wise¹; ¹School of Applied and Engineering Physics, Cornell Univ., USA. We demonstrate coherent combining of pulses within a laser cavity and discuss applications to energy scaling and pulse-burst operation. 16-times enhancement of the pulse energy from a fiber laser is demonstrated.

STh4N.6 • 18:00

Transverse-mode Instability in High Power Fiber Amplifiers Involving Thermally-Induced Gratings Without Frequency Offset, I-Ning Hu¹, Almantas Galvanauskas¹; ¹Center for Ultrafast Optical Science, Univ. of Michigan, USA. Time-dependent coupled-mode theory predicts transverse-mode instabilities in high power fiber amplifiers originating from thermally-induced gratings possessing a spatial phase shift with respect to a beating pattern of two transversal modes of the same frequency.

STh4O • Gravity and Distance
Measurements—Continued

STh4O.3 • 17:15

Silicon Photonic Integrated Circuit for Fast Distance Measurement with Frequency Combs, Claudius Weimann^{1,2}, Matthias Lauermann¹, Thomas Fehrenbach¹, Robert Palmer¹, Frank Hoeller³, Wolfgang Freude^{1,2}, Christian G. Koos^{1,2}; ¹Inst. of Photonics and Quantumelectronics (IPO), KIT, Germany; ²Inst. of Microstructure Technology (IMT), KIT, Germany; ³Carl Zeiss AG, Germany. We demonstrate a synthetic-wavelength interferometry system on a silicon photonic chip, comprising an interferometer with tunable power splitting ratio and photodetectors. The system enables distance measurements with errors below 5µm and acquisition times of 14µs.

STh4O.4 • 17:30 Tutorial

Precision Measurement at the Quantum Limit in Gravitational Wave Detectors, Nergis Mavalvala¹; ¹MIT, USA. Interferometric gravitational wave detectors are poised to launch a new era of gravitational-wave astronomy. I will describe how we achieve sub-attometer sensitivity in kilometer-scale laser interferometers.



Nergis Mavalvala received a B.A. from Wellesley College, a Ph.D. from MIT, and was a postdoctoral fellow at Caltech. She is now Professor of Physics at the MIT and recipient of a 2010 MacArthur "genius" award. Her research spans quantum optics and optomechanics in relation to interferometric gravitational-wave detectors.

ATH4P • Symposium on
Advanced Ultrashort Pulse Laser
Technologies in Biophotonics
and Nanobiophotonics II—
Continued

ATH4P.3 • 17:15

High-speed flow imaging utilizing spectral-encoding of ultrafast pulses and compressed sensing, Bryan T. Bosworth¹, Mark A. Foster¹; ¹Johns Hopkins Univ., USA. Using chirp processing and pseudorandom bit modulation we demonstrate high-speed structured illumination for compressed sensing imaging of 1-D flows.

ATH4P.4 • 17:30 Invited

Progress in laser-driven ion acceleration towards applications in radiotherapy, Paul McKenna¹, Marco Borghesi², David Neely³, Zulfikar Najmudin⁴, Matt Zepf², Kevin Prise²; ¹Physics, Univ. of Strathclyde, UK; ²Mathematics and Physics, Queens Univ. Belfast, UK; ³CLF, Rutherford Appleton Lab, UK; ⁴Blackett Lab, Imperial College London, UK. I will outline recent progress, in the UK ASAIL laser-ion acceleration programme, which aims to advance laser-driven ion beams to the point at which they will become a serious alternative to conventional accelerators for radiotherapy.

ATH4P.5 • 18:00

Decontamination of Medical Device Surface Using Ultrashort Pulsed Laser Irradiation, Moinuddin Hassan¹, Brandon Gaiton¹, Ilko K. Ilev¹; ¹DP/OSEL/CDRH, FDA, USA. We present a novel approach for non-contact, rapid and chemical-free decontamination of medical device surfaces using near-infrared ultrashort (nano- to femtosecond) pulse lasers. A proof-of-principal experimental platform is validated through multivariable comparison studies.

Executive Ballroom
210A

CLEO: QELS-
Fundamental Science

FTh4A • Quantum Sensing and
Metrology—Continued

FTh4A.8 • 18:15

Stimulated Emission Tomography, Marco Liscidini¹, Lee A. Rozema², Chao Wang², Dylan Mahler², Alex Hayat², Aephraim M. Steinberg², John E. Sipe²; ¹Physics, Università degli Studi di Pavia, Italy; ²Physics, Univ. of Toronto, Canada. We experimentally demonstrate the reconstruction of the polarization state of entangled photon pairs by stimulated emission tomography.

Executive Ballroom
210B

CLEO: Science &
Innovations

STh4B • Laser-Driven Dynamics
in Materials—Continued

STh4B.7 • 18:15

Ablation of polymethylmethacrylate by two-color femtosecond synthesized waveform, Chih-Hsuan Lin¹, Chan Shan Yang², Alexey Zaytsev², Kuei-Chung Teng¹, Tsing-Hua Her³, Ci-Ling Pan^{1,2}; ¹Inst. of Photonics technologies, National Tsing Hua Univ., Taiwan; ²Dept. of Physics, National Tsing Hua Univ., Taiwan; ³Dept. of Physics and Optical Science, Univ. of North Carolina, USA. We demonstrated femtosecond laser ablation of PMMA using 2-color waveform synthesis. A modest and yet clear modulation in ablated area versus relative phase between the ω and 2ω beams is observed.

Executive Ballroom
210C

CLEO: QELS-Fundamental Science

FTh4C • Carrier Dynamics in
0-D and 1-D Nanostructures—
Continued

FTh4C.8 • 18:15

Charge carrier relaxation processes in TbAs nano-inclusions in GaAs measured by optical-pump THz-probe transient absorption spectroscopy, Laura Vanderhoeft², Abul K. Azad¹, Cory Bomberger², Dibakar Chowdhury¹, Bruce Chase², Antoinette Taylor¹, Joshua Zide², Matthew Doty²; ¹Los Alamos National Lab, USA; ²Univ. of Delaware, USA. By analyzing how carrier relaxation rates depend on pump fluence and sample temperature, we conclude that states of TbAs embedded in GaAs are saturable. This suggests the existence of a bandgap for TbAs nanoparticles.

Executive Ballroom
210D

FTh4D • Nonlinear
Metamaterials and Cooling—
Continued

FTh4D.6 • 18:15

Solid-state cryo-cooling using optical refrigeration, Seth Melgaard^{1,2}, Alexander R. Albrecht¹, Denis Seletskiy³, Richard Epstein^{1,4}, Jay Alden⁴, Mansoor Sheik-Bahae¹; ¹Univ. of New Mexico, USA; ²Air Force Research Lab, USA; ³Univ. of Konstanz, Germany; ⁴Thermo-Dynamic Films LLC, USA. Optical refrigeration provides the only solid-state technology capable of reaching cryogenic temperatures, currently below 100K. Novel, adaptable designs are implemented for technologies requiring vibration-free cryogenic operation.

18:30–20:00 Dinner Break (on your own)

20:00–22:00 Postdeadline Paper Sessions

The complete schedule of Postdeadline Paper Sessions can be found in the Postdeadline Digest and the CLEO Mobile App.

NOTES

CLEO: Science & Innovations

STh4E • OPO, OPA and Regenerative Amplifiers—Continued

STh4E.8 • 18:15

High Repetition Rate, mJ-Level, mid-IR OPCPA System, Michael Gerrity¹, Susanah Brown¹, Tenio Popmintchev¹, Margaret Murnane¹, Henry Kapteyn¹, Sterling Backus^{2,3}; ¹JILA - Univ. of Colorado at Boulder, USA; ²Kapteyn-Murnane Labs Inc., USA; ³Colorado State Univ., USA. We describe a kHz repetition-rate mid-IR laser system based on OPCPA, optimized for soft x-ray high harmonic generation. To date we have demonstrated 1.4mJ at 1.6 μ m, and 550 μ J at 3 μ m, each with bandwidth compressible to <100fs.

STh4F • THz Imaging—Continued

STh4F.7 • 18:15

Video Rate THz imaging based on frequency upconversion using a near-IR CMOS camera, Patrick Tekavec¹, Dylan Fast¹, Ian McNeel¹, Vladimir Kozlov¹, Yun-Shik Lee², Konstantin L. Vodopyanov²; ¹Microtech Instruments, USA; ²Physics, Oregon State Univ., USA; ³CREOL, College of Optics and Photonics, Univ. Cent. Florida, USA. We demonstrate a video-rate THz-imaging system based on upconversion of THz pulses into the infrared. Sideband generation by mixing high-power, narrowband THz pulses with picosecond pulses at 1064 nm in QPM-GaAs provide high contrast imaging.

STh4G • Quantum Cascade Lasers II—Continued

STh4G.8 • 18:15

Scaling of Micropillar Array Terahertz Lasers into the Subwavelength Regime, Michael Krall^{1,3}, Martin Brandstetter^{1,3}, Christoph Deutsch^{1,3}, Hermann Detz^{2,3}, Aaron Maxwell Andrews^{2,3}, Werner Schrenk², Gottfried Strasser^{2,3}, Karl Unterrainer^{1,3}; ¹Photonics Inst., Vienna Univ. of Technology, Austria; ²Inst. of Solid State Electronics, Vienna Univ. of Technology, Austria; ³Center for Micro- and Nanostructures, Vienna Univ. of Technology, Austria. We demonstrate terahertz quantum cascade lasers based on arrays of subwavelength micropillar structures, corresponding to scaled-down photonic crystals. Stimulated emission is measured at 4 THz for devices operating in the effective medium regime of the photonic bands.

STh4H • Plasmonics, Raman and Resonance Sensing—Continued

STh4H.8 • 18:15

Surface-Enhanced Raman Spectroscopy (SERS) using Nanopillar Arrays as Functional Substrates and an Organic Semiconductor DFB Laser as Excitation Source, Xin Liu^{1,5}, Sergei Lebedkin², Wilhelm Pfleging^{3,4}, Heino Besser^{3,4}, Markus Wissmann^{4,5}, Irina Nazarenko⁶, Timo Mappes^{5,7}, Sebastian Koeber^{5,8}, Christian G. Koos^{5,8}, Manfred Kappes², Uli Lemmer^{1,5}; ¹Light Tech. Inst., Karlsruhe Inst. of Tech., Germany; ²Inst. of Nanotechnology, Karlsruhe Inst. of Tech., Germany; ³Inst. for Applied Materials - Applied Materials Physics, Karlsruhe Inst. of Tech., Germany; ⁴Karlsruhe Nano Micro Facility, Germany; ⁵Inst. of Microstructure Tech., Karlsruhe Inst. of Tech., Germany; ⁶Inst. for Environmental Health Sciences and Hospital Infection Control, Medical Center-Univ. of Freiburg, Germany; ⁷Corporate Research and Tech., Carl Zeiss AG, Germany; ⁸Inst. of Photonics and Quantum Electronics, Karlsruhe Inst. of Tech., Germany. We demonstrate an organic semiconductor distributed feedback (DFB) laser as excitation source in surface-enhanced Raman spectroscopy (SERS). SERS-active substrates comprising nanopillar arrays were fabricated by the technique of laser-assisted nano-replication.

18:30–20:00 Dinner Break (on your own)

20:00–22:00 Postdeadline Paper Sessions

The complete schedule of Postdeadline Paper Sessions can be found in the Postdeadline Digest and the CLEO Mobile App.

NOTES

Meeting Room
211 B/D

CLEO: Science &
Innovations

STh4I • Novel Photodetectors—
Continued

STh4I.8 • 18:15

Flexible ZnO Nanocrystal Ultraviolet Photodetector on Bio-membrane, Jingda Wu¹, Lih Lin¹; ¹*Electrical Engineering, Univ. of Washington, USA*. We demonstrated an easy-to-fabricate vertical flexible UV photodetector structure with ZnO nanocrystals embedded in a thin and cellulose reed membrane sandwiched between two evaporated electrodes. The device shows photoconductive effect with good performance.

Meeting Room
212 A/C

JOINT

JTh4J • Symposium on High
Performance Optics II—
Continued

JTh4J.6 • 18:30 **Invited**

Convergent Polishing: Simple, Low Cost Finishing Method of Glass Optics, T. Suratwala¹, R. Steele¹, M. Feit¹, R. Dylla-Spears¹, R. Desjardin¹, D. Mason¹, L. Wong¹, P. Geraghty¹, P. Miller, N. Shen¹; ¹*Lawrence Livermore National Lab., USA*. A novel finishing process, called Convergent Polishing, is described where the workpiece regardless of its initial shape will converge to final surface figure under a fixed, unchanging set of polishing parameters in a single iteration.

Meeting Room
212 B/D

CLEO: QELS-
Fundamental Science

FTh4K • Nonlinear Plasmonics:
From Visible to Terahertz—
Continued

FTh4K.8 • 18:15

Plasmon-Enhanced Third-Order Harmonic Generation in Plasmonic-Organic Photonic Crystals, Fanghui Ren¹, Xiangyu Wang¹, Zhongan Li², Jongdong Luo², Sei-Hum Jang², Alex Jen², Alan X. Wang¹; ¹*Oregon State Univ., USA*; ²*Univ. of Washington, USA*. We present theoretical and experimental analysis of extraordinary third-order harmonic generation (THG) by organic materials on a plasmonic photonic crystal. The measurement shows that the hybrid nanostructure platform provides over 20 times enhancement in THG efficiency.

Marriott
Salon I & II

JOINT

JTh4L • Symposium on Laser-
Driven Sources of Particle and
X-Ray Beams III—Continued

JTh4L.6 • 18:15 

Development of high repetition rate 0.1 - 1 TW CO2 lasers, Jeremy Pigeon¹, Sergei Tochitsky¹, Chan Joshi¹; ¹*Electrical Engineering, UCLA, USA*. Amplification of 3 ps pulses to >20GW in a 1Hz CO2 laser MOPA chain is described. Several ways and experimental progress towards increase of the peak power for 10 μm pulses are discussed.

18:30–20:00 **Dinner Break** (on your own)

20:00–22:00 **Postdeadline Paper Sessions**

The complete schedule of Postdeadline Paper Sessions can be found in the Postdeadline Digest and the CLEO Mobile App.

NOTES

CLEO: Science & Innovations

CLEO: Applications & Technology

STh4M • Silicon Modulstors—Continued

STh4N • Coherent Combination and Amplification—Continued

STh4O • Gravity and Distance Measurements—Continued

ATH4P • Symposium on Advanced Ultrashort Pulse Laser Technologies in Biophotonics and Nanobiophotonics II—Continued

STh4M.8 • 18:15  **Reflective Optical Phase Modulator Based on High-Contrast Grating Mirrors**, Yu Horie¹, Amir Arbabi¹, Andrei Faraon¹; ¹T. J. Watson Lab of Applied Physics, California Inst. of Technology, USA. We propose a reflective phase-only modulator formed by two layers of high-contrast grating reflectors. By arranging such optical phase modulators in a 2D array, ultra-fast Si-based phase-only spatial light modulators can be realized.

STh4N.7 • 18:15 **3 % Thermal Load Measured in Tandem-pumped Ytterbium-doped Fiber Amplifier**, You Min Chang¹, Tianfu Yao¹, Hoon Jeong², Junhua Ji³, Seongwoo Yoo³, Timothy C. May-Smith¹, Jayanta K. Sahu¹, Johan Nilsson¹; ¹Optoelectronics Research Centre, Univ. of Southampton, UK; ²Korea Inst. of Industrial Technology, Korea; ³School of Electrical & Electronic Engineering, Nanyang Technological Univ., Singapore. A tandem-pumped Yb-doped fiber with a quantum defect of 2% generates 3% of heat. We believe this is a record-low thermal load and the first calorimetric measurement of the heat from a fiber core.

ATH4P.6 • 18:15 **2D cognitive optical data processing with phase change materials**, qian Wang^{1,2}, Jonathan Maddock¹, Edward T. Rogers¹, Tapashree Roy¹, Christopher Craig¹, Kevin F. MacDonald¹, Dan Hewak¹, Nikolay I. Zheludev^{1,3}; ¹Optoelectronics Research Centre and Centre for Photonic Metamaterials, Univ. of Southampton, UK; ²Inst. of Materials Research and Engineering, Singapore; ³Centre for Disruptive Photonic Technologies, Nanyang Technological Univ., Singapore. We demonstrate high-density, multi-level crystallization of a Ge₂Sb₂Te₅ thin film using tightly focused femtosecond laser pulses. The optical reflectivity in each distinct phase states level is characterized for applications in ultra-fast cognitive parallel data processing.

18:30–20:00 Dinner Break (on your own)

20:00–22:00 Postdeadline Paper Sessions

The complete schedule of Postdeadline Paper Sessions can be found in the Postdeadline Digest and the CLEO Mobile App.

NOTES

Horizontal lines for taking notes.

Executive Ballroom
210ACLEO: QELS-
Fundamental Science

08:00–10:00

FF1A • Coherent Effects with
Quantum Dots

President: Arka Majumdar; Intel Labs, USA

FF1A.1 • 08:00

Measuring the local environment of a quantum dot, Megan Stanley¹, Clemens Matthiesen¹, Jack Hansom¹, Claire Le Gall¹, Maxime Hugues², Edmund Clarke², Mete Atature¹; ¹Cavendish Lab, Univ. of Cambridge, UK; ²EP-SRC National center for III-V Technologies, Univ. of Sheffield, UK. We present a survey of the solid state environment of a quantum dot utilising resonance fluorescence as a sensitive probe. Nuclear field fluctuations are identified with 10 microseconds correlation times by comparison to a theoretical model.

FF1A.2 • 08:15

A comparison between experiment and theory on few-quantum-dot nanolasing in a photonic-crystal cavity, Jin Liu^{1,2}, Serkan Ates¹, Michael Lorke¹, Jesper Mørk¹, Soren Stobbe², Peter Lodahl²; ¹Danmarks Tekniske Universitet, Denmark; ²Niels Bohr Inst., Denmark. We present an experimental and theoretical study on the gain mechanism in a photonic-crystal-cavity nanolaser with embedded quantum dots and find that the gain is mainly provided by the multi-excitonic states of quantum dots.

FF1A.3 • 08:30

Ultrafast Light-Matter Interaction in a Metaphotonic Cavity Containing a Single Quantum Dot, Kevin Fischer^{1,2}, Thomas Babinec^{1,2}, Yousif Kelaita^{1,2}, Konstantinos Lagoudakis^{1,2}, Tomas Sarmiento^{1,2}, Armand Rundquist^{1,2}, Arka Majumdar^{3,4}, Jelena Vuckovic^{1,2}; ¹Ginzton Lab, Stanford Univ., USA; ²Electrical Engineering, Stanford Univ., USA; ³Electrical Engineering, Univ. of Washington, USA; ⁴Physics, Univ. of Washington, USA. Progress in cavity quantum electrodynamics (cQED) trends to decreasing mode volume and increasing light-matter interaction. We demonstrate a metal-semiconductor nanopillar cQED system that exhibits bright single-photon generation, strong Purcell enhancement, and viability as a new platform for cQED.

Executive Ballroom
210BCLEO: Applications
& Technology

08:00–10:00

AF1B • Symposium on
Advances in
Neurophotonics I

President: Jin Kang; Johns Hopkins Univ., USA

AF1B.1 • 08:00 **Invited**

Optogenetic approaches for deciphering the neural circuits of the cortex, Solange P. Brown¹; ¹Solomon H. Snyder Dept. of Neuroscience, Johns Hopkins Univ., USA. Recent developments in optogenetics have generated new opportunities for deciphering the synaptic organization of the cortex, a massively interconnected neuronal network essential for generating a rich repertoire of behavior, including perception and voluntary movement.

AF1B.2 • 08:30 **Invited**

Non-invasive 3D Optical Imaging of Tissue Microstructure and Microcirculations in Vivo, Ruikang K. Wang¹, Woo June Choi¹; ¹Univ. of Washington, USA. We present the ability of OCT microangiography to visualize tissue blood flow at capillary level for a variety of biomedical applications, some of which (along with the OCT basics and the enabling technologies) will be highlighted.

Executive Ballroom
210C

CLEO: QELS-Fundamental Science

08:00–10:00

FF1C • Metasurfaces I

President: Hui Cao; Yale Univ., USA

FF1C.1 • 08:00 **Tutorial**

Spin-Optical Metasurface Route to Spin-Controlled Photonics, Erez Hasman¹; ¹Faculty of Mechanical Engineering, Technion-Israel Inst. of Technology, Israel. We report on spinoptical metasurfaces manifested by spin-controlled optical modes - optical Rashba effect, where the inversion symmetry is violated. The design of metasurface symmetries via geometric gradients provides a route for spin-controlled nanophotonic applications.



Erez Hasman is a Professor of optical sciences, Technion - Israel Inst. of Technology. He is awarded the Fellow of OSA 2013, "for pioneering contributions in the field of nano-photonics, and specifically for developing a new branch in optics - spinoptics: the symmetry breaking in nanostructures due to spin-orbit interaction".

Executive Ballroom
210D

08:00–10:00

FF1D • Entangled Photons and
Quantum Effects

President: Yujie Ding; Lehigh Univ., USA

FF1D.1 • 08:00

Quantum Random Walks in Free Space, Toni Eichelkraut¹, Christian Vetter¹, Armando Perez-Leija¹, Demetrios N. Christodoulides², Alexander Szameit¹; ¹Inst. of Applied Physics, Friedrich-Schiller-Universität Jena, Germany; ²CREOL, Univ. of Central Florida, USA. We show that two-dimensional continuous time coherent random walks are possible in free space by properly tailoring the associated initial wave functions. Theoretical predictions along with classical experiments demonstrate the feasibility of our scheme.

FF1D.2 • 08:15

Orthogonally polarized correlated photon pair generation on a chip via self-pumped spontaneous non-degenerate FWM, Christian Reimer¹, Lucia Caspani¹, Yoann Jestin¹, Matteo Clerici^{1,2}, Marcello Ferrera^{1,2}, Marco Peccianti^{1,3}, Alessia Pasquazi^{1,3}, Brent E. Little⁴, Sai T. Chu⁵, David J. Moss^{1,6}, Roberto Morandotti¹; ¹INRS-EMT, Canada; ²School of Engineering and Physical Sciences, Heriot-Watt Univ., UK; ³Dept. of Physics and Astronomy, Univ. of Sussex, UK; ⁴HiQ Photonics, USA; ⁵Dept. of Physics and Material Science, City Univ. of Hong Kong, China; ⁶School of Electrical and Computer Engineering, RMIT Univ., Australia. We demonstrate orthogonally polarized photon pair generation via spontaneous non-degenerate four-wave-mixing (FWM) of orthogonally polarized pumps in a CMOS compatible micro-ring resonator by fully suppressing stimulated FWM. Photon coincidences and optical parametric oscillation are measured.

FF1D.3 • 08:30

Pulsed Sagnac polarization-entangled photon source with a PPKTP crystal at telecom wavelength, Rui-Bo Jin¹, Ryosuke Shimizu², Kentaro Wakui¹, Mikio Fujiwara¹, Taro Yamashita³, Shigehito Miki³, Hiroataka Terai³, Zhen Wang^{3,4}, Masahide Sasaki¹; ¹National Inst. of Information and Communications Technology, Japan; ²Univ. of Electro-Communications, Japan; ³National Inst. of Information and Communications Technology, Japan; ⁴Shanghai Inst. of Microsystem and Information Technology, China. We demonstrate pulsed polarization-entangled photons generated from a PPKTP crystal in a Sagnac interferometer configuration at telecom wavelength. We achieved fidelities of 0.981 ± 0.0002 for $|\psi^-\rangle$ and 0.980 ± 0.001 for $|\psi^+\rangle$ respectively.

CLEO: Science & Innovations

08:00–10:00

SF1E • FROG and Pulse Characterization

Presider: Rick Trebino; Georgia Inst. of Technology, USA

SF1E.1 • 08:00

Real-time lightwave measurement by using FROG capable of CEP determination with pulse-front tilt, Takao Fuji¹, Hideto Shirai¹, Yutaka Nomura¹; ¹National Inst.s of Natural Sciences, Japan. We propose frequency-resolved optical gating capable of carrier-envelope phase determination using a reference pulse with a tilted pulse front. Real-time complete waveform measurement of ultrashort pulses has been demonstrated with the method.

SF1E.2 • 08:15

Single-shot Measurement of the Complete Temporal Intensity and Phase of Supercontinuum, Tsz Chun Wong¹, Michelle Rhodes¹, Rick Trebino¹; ¹Georgia Inst. of Technology, USA. We demonstrate the first technique for the complete temporal measurement of a single supercontinuum pulse. We achieve large ranges and high resolutions using polarization gating, a tilted gate pulse, and the cancellation of geometrical smearing.

SF1E.3 • 08:30 **Invited**

Spectro-Temporal Characterization of All Channels in a Sub-Optical-Cycle Parametric Waveform Synthesizer, Giulio Maria Rossi^{1,3}, Giovanni Cirmi^{1,3}, Shaobo Fang^{1,3}, Shih-Hsuan Chia^{1,3}, Oliver D. Muecke^{1,3}, Franz Kärtner^{2,4}, Cristian Manzoni⁵, Paolo Farinello⁵, Giulio Cerullo⁵; ¹Center for Free-Electron Laser Science, Deutsches Elektronen-Synchrotron DESY, Germany; ²Physics Dept., Univ. of Hamburg, Germany; ³The Hamburg Center for Ultrafast Imaging, Germany; ⁴Dept. of Electrical Engineering and Computer Science and Research Lab of Electronics, MIT, USA; ⁵IFN-CNR, Dipartimento di Fisica, Politecnico di Milano, Italy. We present FROG characterization of all three amplification channels of a two-stage sub-optical-cycle parametric waveform synthesizer covering more than two octaves in bandwidth. A flexible dispersion compensation scheme will permit compression at the multi-mJ level.

08:00–10:00

SF1F • THz Spectroscopy & Sensing II

Presider: Peter Jepsen, Danmarks Tekniske Universitet, Denmark

SF1F.1 • 08:00

Probing Hydration Dynamics of Metal-Organic Frameworks by Broadband THz Pulses, Christian Wolpert^{1,2}, Kenji Sumida¹, François Blanchard³, Koichiro Tanaka^{1,4}; ¹Inst. for Integrated Cell-Material Sciences (WPI-iCeMS), Kyoto Univ., Japan; ²CREST, Japan Science and Technology Agency, Japan; ³Dept. of Physics, McGill Univ., Canada; ⁴Dept. of Physics, Graduate School of Science, Kyoto Univ., Japan. We probe porous metal-organic framework materials (MOFs) using broadband terahertz (THz) pulses. Water molecules that are absorbed by the pores of the material display intermolecular dynamics differing from those of free water.

SF1F.2 • 08:15

Ultra-broadband THz time-domain spectroscopy of common polymers with THz air-photonics, Francesco D'Angelo¹, Mischa Bonn¹, Ralf Gente², Martin Koch², Dmitry Turchinovich^{1,3}; ¹Molecular Spectroscopy, Max Plank Inst. for Polymer Research, Germany; ²Fachbereich Physik, Philipps-Universität Marburg, Germany; ³DTU Fotonik, Technical Univ. of Denmark, Denmark. Several common polymers are characterized in the ultra-broadband Terahertz frequency window 2-15 THz using a THz time-domain spectrometer solely based on air-photonics. The spectral features relevant for materials science and THz photonics are revealed.

SF1F.3 • 08:30

Development of a terahertz Stokes polarimeter with ultra-broadband DAST-DFG source, Takashi Notake¹, Bangdong Zhang², Yandong Gong², Hiroaki Minamide¹; ¹RIKEN RAP, Japan; ²Inst. for Infocom Research, Singapore. We have developed Stokes polarimeter which can be available over wide terahertz frequency range by using a newly developed silicon quarter-wave plate based on form birefringence. In the system, proper polarization measurements were demonstrated successfully.

08:00–10:00

SF1G • Vertical Cavity Lasers

Presider: Luke Mawst; Univ. of Wisconsin-Madison, USA

SF1G.1 • 08:00

22W Single-Frequency Vertical-External-Cavity Surface-Emitting Laser, Fan Zhang¹, Bernd Heinen¹, Christoph Möller¹, Matthias Wichmann¹, Bernardette Kunert², Arash Rahimi-Iman¹, Wolfgang Stolz¹, Martin Koch¹; ¹Dept. of Physics and Materials Sciences Center, Philipps-Universität Marburg, Germany; ²NAsP III/V GmbH, Germany. We report on a single-frequency semiconductor disk laser which generates 22.1 W output power in continuous wave operation, at a wavelength of 1030 nm. The free-running linewidth is measured to be 3.2 MHz (apparatus limited).

SF1G.2 • 08:15

50% Power Conversion Efficiency on a Non-Oxide VCSEL, Xu Yang¹, Guowei Zhao², Mingxin Li¹, Xiaohang Liu¹, Yu Zhang¹, Dennis Deppe^{1,2}; ¹CREOL, College of Optics & Photonics, Univ. of Central Florida, USA; ²sdPhotonics, LLC, USA. Over 50% power conversion efficiency (PCE) has been reached in an oxide-free VCSEL. VCSELs with very small size (2 μm) have shown high single transverse mode selectivity and good lasing characteristics.

SF1G.3 • 08:30 **Invited**

Recent progress in near-infrared vertical external cavity surface emitting laser (VECSEL) grown by metal organic vapour phase epitaxy (MOVPE), Wolfgang Stolz¹; ¹Philipps Universität Marburg, Germany. Recent developments in technology and active layer design for the realization of high-power (Galn)As-based VECSEL, applying a specific MOVPE growth process, with cw output powers in excess of 100 W will be presented and discussed.

08:00–10:00

SF1H • Optical Manipulation for Biomedical Application

Presider: Chulmin Joo; Yonsei Univ., Korea, Republic of

SF1H.1 • 08:00

Delivering Nanoparticles and Molecules to the Same Spot with a Superhydrophobic Bulls-eye for Surface-enhanced Raman Scattering, Wuzhou Song¹, Demetri Psaltis², Kenneth B. Crozier¹; ¹Harvard Univ., USA; ²École polytechnique fédérale de Lausanne, Switzerland. We present a superhydrophobic silicon bulls-eye. Water droplets remain centered as they dry, enabling delivery of nanoparticles or molecules to the center. SERS spectra of molecules (R6G) at very low concentrations (10E-15 M) are demonstrated.

SF1H.2 • 08:15

Optical manipulation of rod-shaped bacteria and adhesive cellular clusters with novel "tug-of-war" optical tweezers, Anna Bezryadina¹, John Keith¹, Joseph Chen², Zhigang Chen^{1,3}; ¹Dept. of Physics & Astronomy, San Francisco State Univ., USA; ²Dept. of Biology, San Francisco State Univ., USA; ³TEDA Applied Physical Inst. and School of Physics, Nankai Univ., China. We design a new type of "tug-of-war" optical tweezers with lateral pulling forces and demonstrate full control of rod-shaped and asymmetric bacteria, including breaking up adhesive cellular clusters inhabiting aqueous media.

SF1H.3 • 08:30

Light-driven Rotation of Helical Microstructures in a Fluidic Environment, Lindsey Anderson¹, Silke R. Kirchner¹, Debora Schamel², Peer Fischer², Theobald Lohmüller¹, Jochen Feldmann¹; ¹Ludwig Maximilians Univ., Germany; ²Max Plank Inst. for Intelligent Systems, Germany. Inspired by biological microswimmer strategies, we consider the design of helical silica particles. We characterize optically induced rotation of these "microscrews", and discuss their applications as highly controlled microswimmers in the low Reynold's number regime.

Meeting Room
211 B/D

CLEO: Science & Innovations

08:00–10:00

SF11 • Microresonator Combs

Presider: Nathan Newbury; NIST, USA

SF11.1 • 08:00

All-optical stabilization of a microresonator frequency comb, Katja Beha¹, Scott B. Papp¹, Pascal Del'Haye¹, Franklyn Quinlan¹, Hansuek Lee², Kerry Vahala², Scott A. Diddams¹; ¹Time and Frequency Division 688, National Inst. of Standards and Technology, USA; ²T. J. Watson Lab of Applied Physics, California Inst. of Technology, USA. We demonstrate an optical clock based on stabilization of a microcomb to rubidium optical transitions. The clock's output is the 33 GHz microcomb line spacing, which is a coherent, integer sub-division of the rubidium reference.

SF11.2 • 08:15

Ultrashort pulse mode-locking from a normal-dispersion on-chip Kerr frequency comb, Shu-Wei Huang¹, James F. McMillan¹, Jinghui 9. Yang¹, Andrey Matsko², Heng Zhou¹, Mingbin Yu³, Dim-Lee Kwong³, Lute Maleki², Chee Wei Wong¹; ¹Columbia Univ., USA; ²OEwaves, USA; ³Inst. of Microelectronics, Singapore. We demonstrate a broadband Kerr frequency comb and mode-locking in a globally-normal-dispersion microresonator. A record short on-chip pulse of 74-fs is directly measured. Supported by analytical theory and numerical modeling, we describe the mode-locking mechanism.

SF11.3 • 08:30

Fiber-Optic Demonstration of Optical Frequency Division for Erbium Silicon Photonics Integrated Oscillator, Duo Li¹, Michael Peng¹, Hung-Wen Chen¹, Jinkang Lim¹, Michael R. Watts¹, Franz Kärtner^{1,2}; ¹Electrical Engineering and Computer Science, MIT, USA; ²Center for Free-Electron Laser Science, Deutsches Elektronen Synchrotron, Germany. Using fiber-optic components, we demonstrate an optical frequency division scheme for a proposed erbium silicon photonics integrated oscillator. An 80-dB division ratio from 192 THz to 1 GHz is achieved without f-2f interferometer and carrier-envelope-phase locking.

Meeting Room
212 A/C

08:00–10:00

SF1J • Laser Initiated Self-organization & Patterning

Presider: Vassilia Zorba; Lawrence Berkeley National Lab, USA

SF1J.1 • 08:00

Self-Organization of Waveguides Toward Luminescent Targets in Novel Organic/Inorganic Hybrid Materials, Makoto Iida¹, Tetsuzo Yoshimura¹, Hideyuki Nawata²; ¹School of Computer Science, Tokyo Univ. of Technology, Japan; ²Nissan Chemical Industries, LTD, Japan. We demonstrate self-organization of an optical waveguide toward a luminescent target by self-focusing to enable "optical solder," namely, a self-aligned coupling of two multimode optical fiber cores in a photo-sensitive organic/inorganic hybrid material, SUNCONNECT@.

SF1J.2 • 08:15

Femtosecond Laser Nanostructuring for Polarization Sensitive Imaging, Martynas Beresna¹, Mindaugas Gecevičius¹, Peter G. Kazansky¹; ¹Optoelectronics Research Centre, Univ. of Southampton, UK. We demonstrate maskless, single-step fabrication of micro-waveplate array by femtosecond direct writing in the bulk of silica glass. The waveplate array enables instant measurement of the distribution of the Stokes vectors in the visible spectrum.

SF1J.3 • 08:30

Diffraction-assisted micropatterning of silicon surfaces by ns-laser irradiation, Giovanni Mecalco¹, Carlos Acosta-Zepeda¹, Jose Luis Hernandez-Pozos¹, Nikola Batina², Israel Morales-Reyes², Jörn Bonse³, Emmanuel Haro-Poniatowski¹; ¹Physics, Universidad Autónoma Metropolitana Iztapalapa, Mexico; ²Chemistry, Universidad Autónoma Metropolitana Iztapalapa, Mexico; ³Physics, BAM Bundesanstalt für Materialforschung und-prüfung, Germany. Single-pulse (532 nm, 10 ns) micropatterning of silicon surfaces through a pinhole is demonstrated using scanning electron and atomic force microscopy. The results are compared to the Fresnel diffraction theory and physical mechanisms are discussed.

Meeting Room
212 B/D

CLEO: QELS-Fundamental Science

08:00–10:00

FF1K • Photonic Crystals and Complex Plasmonic Nanostructures

Presider: Arif Cetin, Boston Univ., USA

FF1K.1 • 08:00

Ultrafine control of partially loaded single plasmonic nanoantennas fabricated using e-beam lithography and helium ion beam milling, Yudong Wang^{1,2}, Martina Abb², Stuart A. Boden¹, Javier Aizpurua³, Cornelis Hendrik de Groot¹, Otto L. Muskens²; ¹Nano Group, ECS, Univ. of Southampton, UK; ²Physics & Astronomy, Univ. of Southampton, UK; ³Mat Physics Ctr. CSIC-UPV/ and DIPC, Paseo Manuel Lardizabal 4, Spain. Plasmonic resonance shift between capacitive and conductive coupling of a partially loaded dimer antenna has been achieved by the ultrafine control of milling partial antenna gaps with nanometer precision using a helium ion beam microscope.

FF1K.2 • 08:15

Enhanced plasmonic performance in ultrathin silver structures using Gas Cluster Ion Beam Irradiation, Ee Jin Teo¹, Noriaki Toyoda², Chengyuan Yang³, Bing Wang¹, Nan Zhang¹, Andrew A. Bettio³, Jinghua Teng¹; ¹Inst. of Materials Research and Engineering, Singapore; ²Univ. of Hyogo, Japan; ³Physics, National Univ. of Singapore, Singapore. We demonstrate the use of Gas Cluster Ion Beam (GCIB) nanoprocessing technology for producing ultrathin silver waveguide and disk structures with smoother surfaces and wider grain sizes for enhanced surface plasmon propagation.

FF1K.3 • 08:30

Template Fabricated Plasmonic Nanoholes on Analyte-Sensitive Substrates for Vapor Sensing, Mark Turner¹, Benjamin Heppner¹, Isabel Rich¹, Nathan Lindquist¹; ¹Physics Dept., Bethel Univ., USA. Template-stripping is used to produce plasmonic nanoholes on chemically-patterned substrates for real-time, multiplex vapor sensing. The open-hole geometry allows simultaneous response from both sides of the chip during exposure to <10 ppm ethanol in nitrogen.

Marriott
Salon I & II

CLEO: Applications & Technology

08:00–10:00

AF1L • Symposium on Optofluidic Microsystems I

Presider: Andreas Vasdekis, Pacific Northwest National Labs., USA

AF1L.1 • 08:00 **Invited**

Optofluidics 10 years later, Demetri Psaltis¹; ¹EPFL, Switzerland. We will contrast the plans and expectations at the start of the optofluidics project 10 years ago with the current activities in the domain.

AF1L.2 • 08:30 **Invited**

Optofluidic Bio-Lasers: Bridging Photonics, Nanotechnology, and Biology, Xudong Fan¹; ¹Univ. of Michigan, USA. The optofluidic bio-laser integrates microfluidics, microcavity, and biochemically related gain medium. I will introduce the unique and advantageous characteristics of the optofluidic bio-laser, describe its current implementations, and discuss the future research and development.



Join the conversation. Use #CLEO14.
Follow us @cleoconf on Twitter.

Marriott
Salon IIIMarriott
Salon IVMarriott
Salon V & VIMarriott
Willow Glen I-III

CLEO: Science & Innovations

CLEO: Applications
& Technology

08:00–10:00

SF1M • Optomechanics I
President: Chee Wei Wong,
Columbia Univ., USA

SF1M.1 • 08:00

Controlling Light with Light in a Plasmonic Nanooptomechanical Metamaterial, Jun-Yu Ou¹, Eric Plum¹, Jianfa Zhang¹, Nikolay I. Zheludev^{1,2}, ¹Optoelectronics Research Centre, Univ. of Southampton, UK; ²Centre for Disruptive Photonic Technologies, Nanyang Technological Univ., Singapore. We demonstrate metamaterial with a cubic optical nonlinearity that is ten orders of magnitude greater than the reference nonlinearity of CS₂. The nonlinearity has optomechanical nature and is underpinned by light-induced electromagnetic near-field interactions.

SF1M.2 • 08:15

3C-SiC Nanobeam Optomechanical Crystals, Jonathan Yiho Lee¹, Xiyuan Lu², Philip X.-L. Feng³, Qiang Lin⁴; ¹Dept. of Electrical and Computer Engineering, Univ. of Rochester, USA; ²Dept. of Physics and Astronomy, Univ. of Rochester, USA; ³Dept. of Electrical Engineering and Computer Science, Case Western Reserve Univ., USA; ⁴Inst. of Optics, Univ. of Rochester, USA. We report the first demonstration of high-quality ($Q \sim 2.8 \cdot 3.2 \times 10^3$) 3C silicon carbide photonic crystal nanobeams. With the strong optomechanical coupling ($g_{OM}/2\pi \sim 100$ GHz/nm), we observed clear optical transduction of the thermal mechanical motion of the couple-nanobeam.

SF1M.3 • 08:30

Optomechanics in Gallium Phosphide Microdisks, Matthew Mitchell^{1,2}, Aaron C. Hryciw², Paul E. Barclay^{1,2}; ¹Inst. for Quantum Science & Tech., Univ. of Calgary, Canada; ²NRC-National Inst. for Nanotechnology, Canada. Gallium phosphide microdisk optical cavities with intrinsic quality factors $Q_i \sim 2.8 \times 10^5$ at 1.5 μm are demonstrated. No two-photon absorption is observed. Saturation of internal optical loss, and optomechanical coupling to radial breathing modes with $g_0 \sim 30$ kHz is observed.

08:00–10:00

SF1N • Next Generation Fiber Designs
President: Ayman Abouraddy;
Univ. of Central Florida, CREOL,
USASF1N.1 • 08:00 **Invited****First demonstration of single trench fiber for delocalization of higher order modes**, Deepak Jain¹, Catherine Baskiotis¹, Jaesun Kim², Jayanta K. Sahu¹; ¹Univ. of Southampton, UK; ²SPI Lasers, UK. We demonstrate an ytterbium-doped single-trench fiber ensuring a high losses ratio (~ 1000) and low power fraction (~ 0.7) between the higher-order-modes and fundamental-mode with excellent bend robustness and 85% laser efficiency at a wavelength of 1040nm.

SF1N.2 • 08:30

Yb-Doped Photonic Bandgap Fiber Lasers with Record Core Diameter, Guancheng Gu¹, Fanting Kong¹, Thomas Hawkings¹, Joshua Parsons¹, Maxwell Jones¹, Christopher Dunn¹, Monica Kalichevsky-Dong¹, Kunimasa Saitoh², Liang Dong¹; ¹ECE/COMSET, Clemson Univ., USA; ²Graduate School of Information Science and Technology, Hokkaido Univ., Japan. We have demonstrated ytterbium-doped fiber lasers in 50 μm -core photonic bandgap fibers with robust single mode output, a record core diameter for active photonic bandgap fibers, with slope efficiency exceeding 70%.

08:00–10:00

SF1O • Integrated Polarization Management
President: To be Determined

SF1O.1 • 08:00

Polarization Splitting at Infrared Wavelengths using Silicon Nanoridges, Mohammadreza Khorasaninejad¹, Kenneth B. Crozier¹; ¹Harvard Univ., USA. We propose a polarization splitting method based on near-field interference. Unlike conventional polarizers, our design does not absorb the undesired polarization but rather deflects light in a polarization-dependent manner. This could enable high efficiency polarization-resolved-imaging.

SF1O.2 • 08:15

Separating Left- from Right-Circularly Polarized Light with a Dielectric Metamaterial, Mohammadreza Khorasaninejad¹, Kenneth B. Crozier¹; ¹School of Engineering and Applied Sciences, Harvard Univ., USA. We experimentally demonstrate a dielectric metamaterial comprising silicon nanofins on a glass substrate. Left- and right-circularly polarized beams incident upon the device are deflected into different directions. Our approach avoids the efficiency issues of plasmonics.

SF1O.3 • 08:30

On-chip synthesis of circularly polarized light with a 2D grating emitter, Li He¹, Mo Li¹; ¹Univ. of Minnesota, Dept. of Electrical and Computer Engineering, USA. We demonstrate a 2D grating emitter that emits circularly polarized light beam with tunable handedness synthesized from a waveguide mode. Such a device could serve as an interface between silicon photonic waveguides and helicity-dependent optoelectronic devices.

08:00–10:00

AF1P • Photons for Environment
President: Christian Wetzel,
Rensselaer Polytechnic Institute,
USAAF1P.1 • 08:00 **Invited****Frontiers of Eco-Efficient Ultraviolet Water Treatment Technologies**, D. G. Knight¹; ¹Trojan Technologies Inc., Canada. Development of ecologically-efficient UV water treatment has resulted in lower energy consumption and compact design, as well as a reduced carbon footprint compared to alternate technologies for environmental contaminant treatment such as activated carbon.

AF1P.2 • 08:30

Solid State Mobile Lidar for Ozone Atmospheric Profiling, Russell J. De Young¹, William Carrion²; ¹Science directorate, NASA Langley Research Center, USA; ²Coherent Applications Inc., USA. A tunable Ce:LiCAF laser is pumped by a CLBO crystal pumped by a doubled Nd:YLF laser running at 1 kHz. The UV tunable Ce:LiCAF laser produces two UV pulses between 280 to 295nm. These pulses are transmitted into the atmosphere to profile the concentration of ozone as a function of altitude.For Conference News & Insights
Visit blog.cleoconference.org

Executive Ballroom
210ACLEO: QELS-
Fundamental ScienceFF1A • Coherent Effects with
Quantum Dots—Continued

FF1A.4 • 08:45

Controlled modification of the electronic wavefunction and direct observation of quantum decoherence in a room-temperature quantum-dot semiconductor optical amplifier, Amir Capua^{1,3}, Ouri Karni¹, Gadi Eisenstein¹, Vitalii Ivanov², Vitalii Sichkovskyi², Johann Peter Reithmaier²; ¹Technion Israel Inst. of Technology, Israel; ²Univ. Kassel, Germany; ³IBM Research, USA. A unique experimental setup combining short pulse pump-probe and FROG characterization, enables control by light pulses over the electronic quantum state, and a direct observation of the wavefunction decoherence in a room-temperature semiconductor laser amplifier.

FF1A.5 • 09:00

Deterministic Writing and Control of the Dark Exciton State using Short Single Optical Pulses, Ido Schwartz¹, Emma Schmidgall¹, Liron Gantz¹, Dan Cogan¹, Eli Bordo¹, David Gershoni¹; ¹Physics, Technion, Israel. We experimentally demonstrate deterministic optical writing of a quantum dot-confined dark exciton, in a pure quantum state using one optical pulse. We then control the spin state of this long-lived exciton using picosecond optical pulses.

FF1A.6 • 09:15

Fast, High Fidelity, Single-Shot Quantum Non-Demolition Measurement of a Quantum Dot Electron Spin using Cavity Exciton-Polariton Resonance, shruti puri¹, Peter L. McMahon¹, Yoshihisa Yamamoto^{1,2}; ¹Stanford Univ., USA; ²National Inst. of Informatics, Japan. We propose a novel scheme for a single-shot, fast (10's of nanoseconds), high fidelity (99.95%) quantum non-demolition (QND) readout of quantum dot (QD) electron spins based on their spin-dependent Coulomb exchange interaction with optically-excited quantum well (QW) microcavity exciton-polaritons.

Executive Ballroom
210BCLEO: Applications
& TechnologyAF1B • Symposium on
Advances in Neurophotonics I—
Continued

AF1B.3 • 09:00

Spatially Multiplexed Fiber-optic Microscopy for Simultaneous Imaging of Multiple Brain Regions, Jaepyeong Cha¹, Jin U. Kang¹; ¹Electrical and Computer Engineering, Johns Hopkins Univ., USA. Spatially multiplexed fiber-optic imager is experimentally demonstrated. Our system utilizes a trifurcated fiber bundles for real-time brain imaging in 3 different areas.

AF1B.4 • 09:15

Label Free Mid-IR Photothermal Imaging of Bird Brain With Quantum Cascade Laser, Alket Mertiri^{1,6}, Atcha Totachawattana^{2,6}, Hui Liu^{2,6}, Mi K. Hong^{3,6}, Tim Gardner⁵, Michelle Y. Sander^{2,6}, Shyamsunder Erramilli^{3,4}; ¹Materials Science and Engineering, Boston Univ., USA; ²Electrical and Computer Engineering, Boston Univ., USA; ³Physics, Boston Univ., USA; ⁴Biomedical Engineering, Boston Univ., USA; ⁵Biology, Boston Univ., USA; ⁶Photonics Center, Boston Univ., USA. Label free mid-infrared photothermal imaging on bird brain slices is presented. The Amide-I vibrational band is excited by a quantum cascade laser and an Er-doped fiber measures the photo-thermal response.

Executive Ballroom
210C

CLEO: QELS-Fundamental Science

FF1C • Metasurfaces I—
Continued

FF1C.2 • 09:00

Generation of light beams carrying orbital angular momentum using an ultrathin plasmonic metasurface, Israel De Leon¹, Ebrahim Karim¹, Sebastian A. Schulz¹, Hamam Qassim¹, Jeremy Upham¹, Robert W. Boyd^{1,2}; ¹Physics, Univ. of Ottawa, Canada; ²Inst. of Optics, Univ. of Rochester, USA. We generate optical orbital angular momentum in the visible regime via spin-to-orbital angular momentum coupling by ultrathin ($\lambda/30$), inhomogeneous, birefringent plasmonic arrays. Such metasurfaces will enable compact, efficient generation of structured light.

FF1C.3 • 09:15
WithdrawnExecutive Ballroom
210DFF1D • Entangled Photons and
Quantum Effects—Continued

FF1D.4 • 08:45

Entanglement in a Bragg Reflection Waveguide, Rolf Horn¹, Piotr Kolenderski², Dong-peng Kang³, Payam Abolghasem³, Lukas G. Helt⁴, Sergei Zhukovsky⁴, Carmelo Scarcella⁵, Adriano Della Frera⁵, Alberto Tosi⁵, John E. Sipe⁴, Gregor Wehls⁵, Amr S. Helmy³, Thomas Jennewein¹; ¹Inst. for Quantum Computing, Univ. of Waterloo, Canada; ²Inst. of Physics, Faculty of Physics, Astronomy and Informatics, Nicolaus Copernicus Univ., Poland; ³The Edward S. Rogers Sr. Dept. of Electrical and Computer Engineering, Univ. of Toronto, Canada; ⁴Dept. of Physics, Univ. of Toronto, Canada; ⁵Dipartimento di Elettronica, Informazione e Bioingegneria, Politecnico di Milano, Italy; ⁶Inst. for Experimental Physics, Univ. of Innsbruck, Austria. We demonstrate that an integrated photonic Bragg Reflection waveguide (BRW) inherently produces polarization entangled photons.


FF1D.5 • 09:00

Impact of Photon Statistics on Two-Photon Excited Fluorescence, Henning Kurzke¹, Andreas Jechow¹, Michael Seefeldt¹, Jan Kiethel¹, Axel Heuer¹, Ralf Menzel¹; ¹Univ. of Potsdam, Inst. of Physics and Astronomy, Germany. We report on utilizing the photon bunching effect in thermal light to enhance the efficiency of Two-Photon Excited Fluorescence (TPEF) under continuous wave illumination. This has potential applications in microscopy.

FF1D.6 • 09:15

Quantum Effects in Four-Wave Mixing: Collapse and Revival of Bi-Photon Interference, Rafi Z. Vered¹, Yelena Ben Or¹, Michael Rosenbluh¹, Avi Pe'er¹; ¹Physics, Bar Ilan University, Israel. We explore the classical-to-quantum transition with light produced by broadband spontaneous FWM in fibers. Observing bi-photon quantum interference and its dependence on internal loss, we demonstrate quantum collapse and revival of the interference contrast.

CLEO: Science & Innovations

SF1E • FROG and Pulse
Characterization—ContinuedSF1E.4 • 09:00 

Real-time optical time-stretch statistical characterization of supercontinuum suppression by minute continuous wave, Zhibo Ren¹, Kevin Tsia¹, Kenneth Wong¹; ¹Univ. of Hong Kong, Hong Kong. We experimentally demonstrate that a minute continuous-wave becalms Raman soliton and thus actively suppresses supercontinuum. The effects are characterized in detail by real-time spectrally-resolved statistical analysis enabled by optical time-stretch.

SF1E.5 • 09:15 

The Coherent Artifact in Interferometric Pulse-Measurement Techniques, Michelle Rhodes¹, Madhuri Mukhopadhyay², Jonathan Birge³, Gunter Steinmeyer⁴, Rick Trebino¹; ¹Georgia Inst. of Technology, USA; ²Dept. of Chemistry and Biochemistry, Univ. of Arkansas, USA; ³Lincoln Lab, USA; ⁴Max Born Inst. for Nonlinear Optics and Short Pulse Spectroscopy, Germany. We study multi-shot intensity-and-phase measurements of unstable trains of ultrashort pulses using two-dimensional spectral shearing interferometry (2DSI) and self-referenced spectral interferometry (SRSI) in order to identify warning signs of pulse-shape instability.

SF1F • THz Spectroscopy &
Sensing II—Continued

SF1F.4 • 08:45

THz spectroscopy of bovine serum albumin solution using the long-range guided mode supported by thin liquid films, Robert Szech¹, Peter Haring Bolivar¹; ¹Universität Siegen, Germany. We demonstrate THz spectroscopy of mM BSA solutions using the long-range guided mode as an alternative approach to traditional transmission and reflection concepts. The cm propagation lengths pave the way for integrating field-enhancing resonating structures.

SF1F.5 • 09:00

Measurements of Broadband THz Pulse Propagation through dense Fog, Yihong Yang¹, Mahboubeh Mandehgar¹, Daniel R. Grischkowsky¹; ¹Oklahoma State Univ., USA. We experimentally demonstrate, using a long-path THz-TDS system, non-distorted and non-attenuated broadband THz pulse propagation through a 137 m long path in dense fog with an optical visibility of only 5 m.

SF1F.6 • 09:15

Multi-Step Pattern-Recognition: A Powerful Tool for Substance Identification Based on Real-World Terahertz-Spectra, Frank Ellrich¹, Daniel Molter¹, Joachim Jonuscheit¹, Georg von Freymann¹, Rene Beigang¹, Frank Platte², Konstantinos Nalpanitidis², Thorsten Sprenger³, Daniel Hübsch³, Christoph Fredebeul²; ¹Materials Characterization and Testing, Fraunhofer Inst. for Physical Measurement Techniques IPM, Germany; ²Simulations for Fluid Flow & Optical Technologies, IANUS Simulation GmbH, Germany; ³R&D Public Security, HÜBNER GmbH & Co. KG, Germany. Combining different chemometric tools we demonstrate the reliable identification of substances out of real-world terahertz-spectra. Systematic evaluation of the spectra allows for the distinction between spectral properties arising from samples geometry versus true material absorption.

SF1G • Vertical Cavity Lasers—
Continued

SF1G.4 • 09:00

Coherently Coupled Bottom-Emitting Vertical Cavity Laser Arrays, Zihe Gao¹, Gautham Ragunathan¹, Bradley Thompson¹, Matthew Johnson^{1,2}, Bibhudutta Rout³, Kent D. Choquette¹; ¹Dept. of Electrical and Computer Engineering, Univ. of Illinois, USA; ²USA Air Force, USA; ³Dept. of Physics, Univ. of North Texas, USA. We demonstrate 2-dimensional coherently coupled bottom-emitting VCSEL arrays. In-phase operation has been obtained from 3-element triangular arrays, while out-of-phase operation has been obtained from 2x2, 3x3, and 4x4 arrays.

SF1G.5 • 09:15

Single-Mode 850 nm VCSELs Array with High-Power, Single-Lobe Pattern, and Narrow Divergence Angle, Kai-Lun Chi¹, Jia-Wei Jiang¹, Ying-Jay Yang², Jin-Wei Shi¹; ¹Electrical Engineering, National Central Univ., Taiwan; ²Electrical Engineering, National Taiwan Univ., Taiwan. A high-performance single-mode 850 nm VCSEL array is demonstrated. By using Zn-diffusion apertures with the proper array spacing, a circular-symmetric pattern with CW high-power (140 mW) and narrow divergence angle (~5°) have been simultaneously achieved.

SF1H • Optical Manipulation
for Biomedical Application—
Continued

SF1H.4 • 08:45

Microparticles Manipulation by Nonparaxial Accelerating Beams, Ran Schley¹, Ido Kaminer¹, Elad Greenfield¹, Rivka Bekenstein¹, Yaakov Lumer¹, Mordechai Segev¹; ¹Technion Israel Inst. of Technology, Israel. We introduce loss-proof shape-invariant nonparaxial accelerating beams that overcome both diffraction and absorption, and demonstrate their use in acceleration of microparticles inside liquids along curved trajectories that are significantly steeper than ever achieved.

SF1H.5 • 09:00 

Shaping the Future of Biophotonics: Imaging and Manipulation, Kishan Dholaria¹; ¹Univ. of St Andrews, UK. This talk will describe the use of the generation, use and advantages of complex light fields for applications in light sheet imaging, targeted cell transfection and manipulation.

Meeting Room
211 B/D

CLEO: Science & Innovations

SF11 • Microresonator Combs—
Continued

SF11.4 • 08:45

Phase Measurements and Phase-Locking in Microresonator-Based Optical Frequency Combs, Pascal Del'Haye¹, William Loh¹, Katja Beha¹, Scott B. Papp¹, Scott A. Diddams¹; ¹NIST, USA. We present a novel scheme for precise phase measurements of individual modes in microresonator-based optical frequency combs. We find microcomb states with characteristic phase-steps of multiples of π and $\pi/2$ in the comb spectrum.

SF11.5 • 09:00

Revealing spectral amplitude and phase correlations of an optical frequency comb with ultrafast pulse-shaping, Roman Schmeissner¹, Jonathan Roslund¹, Claude Fabre¹, Nicolas Treps¹; ¹Laboratoire Kastler Brossel, France. The spectral correlations of amplitude and phase noise in an optical frequency comb are characterized. Correlations appear at timescales $< \mu\text{s}$ and allow a generalization of comb noise from the repetition rate- and CEO-phase representation.

SF11.6 • 09:15

Quantum Limited Parameter Estimation with Pulse Shaped Frequency Combs, Valérian Thiel¹, Pu Jian¹, Jonathan Roslund¹, Nicolas Treps¹, Claude Fabre¹; ¹Quantum Optics, Laboratoire Kastler Brossel, France. Combining a multi-color homodyne detection scheme with techniques from quantum optics, we show the feasibility of shot-noise limited measurements of a medium's parameters, while also being able to compensate for their fluctuations.

Meeting Room
212 A/CSF11J • Laser Initiated Self-
organization & Patterning—
Continued

SF11J.4 • 08:45

Comparison of VO₂ thin films deposited by pulsed laser, electron-beam and sputter deposition, Robert E. Marvel¹; ¹Physics, Vanderbilt Univ., USA. The optical performance and morphology of VO₂ thin films deposited by electron beam evaporation, rf magnetron sputtering and pulsed laser deposition are compared. Laser-deposited films are strongly affected by substrate dewetting and epitaxial mismatch.

SF11J.5 • 09:00

Chiral mono-crystalline silicon nano-cone fabrication by optical vortex pumping, Fuyuto Takahashi¹, Shun Takizawa¹, Hirofumi Hidai¹, Katsuhiko Miyamoto¹, Ryuji Morita^{2,3}, Takashige Omatsu^{1,3}; ¹Chiba Univ., Japan; ²Hokkaido Univ., Japan; ³CREST, Japan. We for the first time demonstrated a chiral mono-crystalline cone-shaped silicon structure (chiral Si nano-cone). It was fabricated on a nano-scale by transferring the optical angular momentum of optical vortex to a mono-crystalline Si substrate.

SF11J.6 • 09:15

Guidelines for efficient direct ablation of dielectrics with single femtosecond pulses down to 7 fs, Marc Sentis^{1,2}, Olivier Uteza^{1,2}, Nicolas Sanner^{2,1}, Maxime Lebugle^{2,1}; ¹LP3 Lab, CNRS, France; ²LP3 Lab, Aix-Marseille Univ., France. We demonstrated that the measurement of the laser-induced ablation threshold and the fluence for maximum ablation efficiency, are only required to qualify the outcomes of laser ablation in an extended range of applied fluence.

Meeting Room
212 B/DCLEO: QELS-
Fundamental ScienceFF1K • Photonic Crystals
and Complex Plasmonic
Nanostructures—Continued

FF1K.4 • 08:45

Triangular nanobeam fabrication strategy for quantum photonic network realization in bulk diamond, Igal Bayn^{1,2}, Sara Mouradian¹, Luozhou Li^{1,2}, Tim Schroeder¹, Ophir Gaathon¹, Ming Lu³, Aaron Stein³, Dirk Englund¹; ¹Dept. of Electrical Engineering and Computer Science, and Research Lab of Electronics, MIT, USA; ²Dept. of Electrical Engineering, Columbia Univ., USA; ³Center for Functional Nanomaterials, Brookhaven National Lab, USA. A triangular nanobeam architecture for a bulk-diamond quantum photonic networks based on silicon masking and angular etching is proposed and implemented. Cavities with $Q > 3 \times 10^3$ are demonstrated. S-bent interconnects for realizing a mm-scale network are introduced.

FF1K.5 • 09:00

Photo-oxidative tuning of individual and coupled GaAs Photonic Crystal Cavities, Alexander Y. Piggott¹, Konstantinos Lagoudakis¹, Michal Bajcsy^{1,2}, Tomas Sarmiento¹, Jelena Vuckovic¹; ¹E. L. Ginzton Lab, Stanford Univ., USA; ²Inst. for Quantum Computing, Univ. of Waterloo, Canada. We demonstrate a photo-induced oxidation technique for tuning GaAs photonic crystal cavities using a 390nm laser, and show that it is applicable to cavity arrays by tuning an individual cavity in a proximity-coupled cavity pair.

FF1K.6 • 09:15

Cavity-enhanced Spontaneous Emission and Saturable Absorption of Colloidal Quantum Dots, Shilpi Gupta¹, Edo Waks¹; ¹Univ. of Maryland, USA. We demonstrate spontaneous emission enhancement (by an average factor of 4.6) and saturable absorption of cadmium selenide colloidal quantum dots coupled to a nanobeam photonic crystal cavity, at room temperature.

Marriott
Salon I & IICLEO: Applications
& TechnologyAF1L • Symposium on
Optofluidic Microsystems I—
Continued

AF1L.3 • 09:00

Liquid-Tuned Plasmonic External Cavity Laser, Meng Zhang¹, Brian T. Cunningham^{2,3}; ¹Dept. of Physics, Univ. of Illinois at Urbana-Champaign, USA; ²Dept. of Electrical and Computer Engineering, Univ. of Illinois at Urbana-Champaign, USA; ³Dept. of Bioengineering, Univ. of Illinois at Urbana-Champaign, USA. We developed a single-mode, continuous-wave and electrically pumped plasmonic external cavity laser. It offers a novel label-free biosensing approach by combining the refractive index sensitivity of surface plasmon resonance with the high spectral resolution of laser emission.

AF1L.4 • 09:15

Enabling enhanced emission and low-threshold lasing of organic molecules using special Fano resonances of macroscopic photonic crystals, Bo Zhen¹, Song-liang Chua¹, Jeongwon Lee¹, Alejandro Rodriguez¹, Xiangdong Liang¹, Steven Johnson¹, John Joannopoulos¹, Marin Soljacic¹, Ofer Shapira¹; ¹Research Lab of Electronics, MIT, USA. We present a novel optofluidic platform comprising organic molecules in solution suspended on photonic crystal slabs. Through macroscopic Fano resonances provided, enhanced spontaneous emission and low-threshold lasing of organic molecules were observed and theoretically analyzed.

Technical Digest and Postdeadline Papers Available Online

- Visit www.cleoconference.org
- Select **Download Digest Paper** button
- Use your email address and CLEO Registration ID # to synchronize

Once you have synchronized your conference registration with Optics InfoBase, you can log in directly to Optics InfoBase at any point using the same email address and OSA password.

Access must be established via synchronization within 60 days of the conference start date. Access is provided only to full technical attendees.

CLEO: Science & Innovations

CLEO: Applications
& TechnologySF1M • Optomechanics I—
Continued

SF1M.4 • 08:45

Optomechanical Nanostructures via Scalable Fabrication in Single-Crystal Diamond, Aaron C. Hryciw¹, Behzad Khanaliloo², Harishankar Jayakumar², Chris Healey², Paul E. Barclay^{1,2}, ¹National Inst. for Nanotechnology, National Research Council Canada, Canada; ²Inst. for Quantum Science and Technology, Univ. of Calgary, Canada. We demonstrate a scalable process flow to fabricate three-dimensional free-standing devices from bulk single-crystal diamond. Using a dimpled fiber taper, we couple selectively to four mechanical modes of a nanobeam to measure its optomechanical response.

SF1M.5 • 09:00

Optical Momentum Transfer to Graphene in Resonators: Generalizing Coulomb-Lorentz Force on a Conductive Single Atomic Layer, Hossein Mousavi¹, Peter Rakich², Zheng Wang¹; ¹Dept. of Electrical and Computer Engineering, UT Austin, USA; ²Dept. of Applied Physics, Yale Univ., USA. We demonstrate that judicious selection of mirrors/substrates, operational frequency, and graphene location inside a cavity yields unprecedented optical forces on graphene, while tolerably modifies Q of the cavity.

SF1M.6 • 09:15

Electromagnetically Induced Transparency in Si₃N₄ nanobeam optomechanical crystals, Marcelo I. Davanco¹, Serkan Ates², Yuxiang Liu³, Kartik Srinivasan¹; ¹NIST, USA; ²The Scientific and Technological Research Council of Turkey, Turkey; ³Mechanical Engineering, Worcester Polytechnic Inst., USA. We demonstrate electromagnetically induced transparency in sideband-resolved Si₃N₄ optomechanical crystals supporting optical modes in the 980 nm band and ≈4GHz mechanical resonances, in both ambient conditions and at cryogenic temperatures.

SF1N • Next Generation Fiber
Designs—Continued

SF1N.3 • 08:45

Highly birefringent multicore optical fibers, James M. Stone¹, Fei Yu¹, Jonathan C. Knight¹; ¹Dept. of Physics, Univ. of Bath, UK. We report on the fabrication and characterization of two polarization maintaining multicore fibres, one with three and the other with ninety eight cores. The beat length and polarization orientation are characterized.

SF1N.4 • 09:00

Plasmonic Nanowire Continuum Light Source, Behrad Gholipour¹, Nalla Venkatram¹, Paul Bastock², Khouler Khan², Chris Craig², Dan Hewak², Nikolay I. Zheludev^{1,2}, Cesare Soci¹; ¹Centre for disruptive photonic technologies (CDPT), Nanyang technological Univ., Singapore; ²Optoelectronics research centre (ORC), Univ. of Southampton, UK. Optically pumped gold nanowire, 330 nm in diameter imbedded into silicate optical fiber produces broadband, highly collimated radiation (in the range 470-900 nm) with divergence of less than 4 mrad.

SF1N.5 • 09:15

Growth of Glass-clad Cr⁴⁺:YSO Crystal Fiber for White Light Interferometry, Kuang-Yu Hsu¹, Shih-Chang Wang¹, Dong-Yo Jheng¹, Tuan-Shu Ho¹, Teng-I Yang¹, Sheng-Lung Huang¹; ¹National Taiwan Univ., Taiwan. Glass-clad Cr⁴⁺:YSO crystal fibers were grown using the laser-heated pedestal growth method. Quasi-3-level behavior of the Cr⁴⁺:YSO was observed, and the emission was red shifted to 1302 nm with a 3-dB bandwidth of 230 nm.

SF1O • Integrated Polarization
Management—Continued

SF1O.4 • 08:45

Polarization-selective Coupling to Long-Range Surface Plasmon-Polariton Waveguides, J. P. Balthasar Mueller¹, Kristján Leósson², Federico Capasso¹; ¹School of Engineering and Applied Sciences, Harvard Univ., USA; ²Science Inst., Univ. of Iceland, Iceland. We use plasmonic antenna arrays to unidirectionally couple incident light in two different polarization states to long-range surface plasmon polariton waveguide modes propagating in opposite directions. The structures enable polarization-sorting with extinction rates in excess of 30dB.

SF1O.5 • 09:00

Metal Nanorods Array Embedded Silicon Waveguide Polarization Beam Splitter, Sangsik Kim¹, Minghao Qi¹; ¹School of Electrical and Computer Engineering and Birk Nanotechnology Center, Purdue Univ., USA. We present a polarization beam splitter with a metal nanorods array embedded between two silicon waveguides. Localized surface plasmon resonance of the metal array introduces the birefringence with short coupling length and broad bandwidth.

SF1O.6 • 09:15

Polarization Cross-coupling Between Microring and Bus Waveguide in Double-layer SOI, Hesam Moradinejad¹, Amir H. Atabaki², Hossein Taheri¹, Ali A. Eftekhar¹, Ali Adibi¹; ¹Georgia Inst. of Technology, USA; ²MIT, USA. We investigate polarization cross-coupling between modes of microring resonators and waveguides due to structural asymmetries. We experimentally demonstrate the coupling between a double-layer SOI waveguide fundamental TM mode and microring higher-order radial TE modes.

AF1P • Photons for
Environment—Continued

AF1P.3 • 08:45

Noble-Metal-Free Sunlight Harvesting Meta-surface for Water Evaporation, Shinya Hakuta^{1,2}, Kevin F. MacDonald¹, Nikolay I. Zheludev^{1,3}; ¹Optoelectronics Research Centre & Centre for Photonic Metamaterials, Univ. of Southampton, UK; ²Frontier Core-Technology Labs, Fujifilm Corporation, Japan; ³Centre for Disruptive Photonic Technologies, Nanyang Technological Univ., Singapore. We present ultrathin multilayer metamaterial absorbers based on abundant, low-cost materials, to effectively harness solar energy for heating and evaporation of water.

AF1P.4 • 09:00

Multipoint Temperature and Pressure Sensing System for Monitoring CO₂ Sequestration Wells, Anas Kasten¹, Sachin N. Dekate¹, Reza Ghandi¹, William A. Challener¹, Roger Jones², Russell Craddock²; ¹GE Global Research, USA; ²GE Druck Ltd., UK. A new interrogation scheme for pressure and temperature measurement in CO₂ sequestration wells by MEMS sensors via fiber optic cable has been developed. The technique should enable sensor multiplexing for distributed downhole measurements.

AF1P.5 • 09:15

Highly Efficient InGaN-based LED with Embedded Cubic Airvoids, Da-Wei Lin¹, Jih-Kai Huang¹, Che-Yu Liu¹, Ruey-Wen Chang¹, Sheng-Wen Wang¹, Gou-Chung Chi¹, Hao-chung Kuo¹; ¹Dept. of Photonics and Inst. of Electro-Optical Engineering, National Chiao Tung Univ., Taiwan. Highly efficient InGaN-based LEDs with embedded sidewall passivation cubic airvoids made by nanoimprint lithography were demonstrated. The LEDs with embedded airvoids exhibit a 45% enhancement of light output at 20 mA compared with conventional LEDs.

Visit Registration to Purchase

Access your Favorite Talks or One You Missed!
On-Demand, 24/7

Over 300 high-quality, informative talks representing the full breadth of CLEO's outstanding technical program including:

Tutorials • Contributed • Postdeadline
Symposia • Plenary talks • Invited

Executive Ballroom
210ACLEO: QELS-
Fundamental ScienceFF1A • Coherent Effects with
Quantum Dots—Continued


FF1A.7 • 09:30

Reservoir-assisted coherent control of a quantum dot spin, Jack Hansom¹, Carsten Schulte¹, Claire Le Gall¹, Clemens Matthiesen¹, Edmund Clarke², Jacob Taylor^{3,4}, Mete Atature¹; ¹Cavendish Lab, Univ. of Cambridge, UK; ²EPSRC National Centre for III-V Technologies, Univ. of Sheffield, UK; ³Joint Quantum Inst., Univ. of Maryland, USA; ⁴National Inst. of Standards and Technology, USA. We demonstrate all-optical coherent manipulation of a quantum dot spin through coherent population trapping with a sub-linewidth spin splitting, enabled by the hyperfine interaction with a mesoscopic nuclear spin ensemble.

FF1A.8 • 09:45

Feedback-Enhanced Entanglement of Photons from a Biexciton Cascade, Sven M. Hein¹, Franz Schulze¹, Nicolas L. Naumann¹, Alexander Carmele², Andreas Knorr¹; ¹Institut für theoretische Physik, TU Berlin, Germany; ²Institut für Quantenoptik und Quanteninformation, Austrian Academy of Sciences, Austria. The entanglement of photons from a biexciton cascade is strongly diminished by exciton fine-structure splitting. We demonstrate an optical feedback mechanism to counteract this loss and to control the photon entanglement.


Executive Ballroom
210BCLEO: Applications
& TechnologyAF1B • Symposium on
Advances in Neurophotonics I—
Continued


AF1B.5 • 09:30 **Invited** 
Visible Brain-wide Networks at Single-neuron Resolution with Micro-Optical Sectioning Tomography, Qingming Luo^{1,2}; ¹Britton Chance Center for Biomedical Photonics, Wuhan National Lab for Optoelectronics-Huazhong Univ. of Science and Technology, China; ²MoE Key Lab for Biomedical Photonics, Dept. of Biomedical Engineering, Huazhong Univ. of Science and Technology, China. We report a protocol combining a novel resin-embedding method for maintaining fluorescence, an automated fluorescence MOST system for long-term stable imaging, and a digital reconstruction-registration-annotation pipeline for tracing the axonal pathways individually in the mouse brain.

Executive Ballroom
210C


CLEO: QELS-Fundamental Science


FF1C • Metasurfaces I—
Continued

FF1C.4 • 09:30 
Experimental Huygens' Surface for NIR Wavelengths, Carl Pfeiffer¹, Naresh K. Emani², Amr M. Shaltout², Alexandra Boltas-seva², Vladimir M. Shalaev², Anthony Grbic¹; ¹Electrical Engineering and Computer Science, Univ. of Michigan, USA; ²Electrical & Computer Engineering and Birk Nanotechnology Center, Purdue Univ., USA. A Huygens' surface that efficiently refracts normally incident light to an angle $\phi=35^\circ$ at telecommunication wavelengths is reported. This represents the first experimental demonstration of an isotropic metasurface that provides wavefront control for arbitrarily polarized light.

FF1C.5 • 09:45 
Twisting light using nano-waveguide arrays, Jingbo Sun¹, Xi Wang¹, Tianyou Xu¹, Alexander N. Cartwright¹, Natalia M. Litchinitser¹; ¹State Univ. of New York at Buffalo, USA. We experimentally demonstrate that an array of subwavelength channels with a spiral size distribution milled in a metal film can be used to manipulate the phase front of light beam and produce a vortex beam.

Executive Ballroom
210DFF1D • Entangled Photons and
Quantum Effects—Continued

FF1D.7 • 09:30 
Quantum Control of Molecular Gas Hydrodynamics, Sina Zahedpour Anaraki^{1,2}, Jared K. Wahlstrand^{1,3}, Howard Milchberg^{1,3}; ¹Inst. for Research in Electronics and Applied Physics, Univ. of Maryland, College Park, USA; ²Electrical and Computer Engineering, Univ. of Maryland, College Park, USA; ³Dept. of Physics, Univ. of Maryland, College Park, USA. We show that the deposition of energy in nitrogen by a train of ultrafast pulses can be greatly enhanced or diminished using multiple pulses spaced near the molecular rotational revival or half revival period.

FF1D.8 • 09:45 
Increasing Weak Measurement SNR with Recycling, Courtney Byard¹, Trent Graham¹, Andrew Jordan², Paul Kwiat¹; ¹Physics, Univ. of Illinois at UC, USA; ²Physics and Astronomy, Univ. of Rochester, USA. Recycling unmeasured photons in a system utilizing weak measurements can substantially improve the signal-to-noise ratio, even in a double-pass system. We achieve an improvement by a factor of 1.36 over a system without recycling.


10:00–10:30 Coffee Break, Concourse Level

NOTES

CLEO: Science & Innovations

SF1E • FROG and Pulse Characterization—Continued

SF1E.6 • 09:30  **Frequency-Resolved Optical Gating with Second-Harmonic and Sum-Frequency Generations**, Yuichiro Kida¹, Yuta Nakano¹, Kazuya Motoyoshi¹, Tataro Imasaka^{1,2}; ¹Dept. of Applied Chemistry, Graduate School of Engineering, Kyushu Univ., Japan; ²Division of Optoelectronics and Photonics, Center for Future Chemistry, Kyushu Univ., Japan. A frequency-resolved optical gating (FROG) that simultaneously acquires two second-harmonic-generation FROG traces and a cross-correlation FROG trace is reported. This FROG allows robust and reliable characterization of two unknown pulses.

SF1E.7 • 09:45  **Single-shot, high dynamic and long temporal range measurement of 4-fs pulses**, Thomas Oksenhendler¹, Sunilkumar Anumula², Andrea Trabattoni², Giuseppe Sansone², Gabriel Tempea³, Francesca Calegari², Mauro Nisoli²; ¹FASTLITE Ultrafast Sci Instrumentation, France; ²Dept. of Physics, Politecnico di Milano, Italy; ³Femtolasers Produktions GmbH, Austria. Single-shot Self-Referenced Spectral Interferometry method, with 40-dB dynamic range, was implemented for complete temporal characterization of 4-fs, 1.9-mJ pulses. The experimental results are in excellent agreement with pulse reconstruction from streaking with isolated attosecond pulses.

SF1F • THz Spectroscopy & Sensing II—Continued

SF1F.7 • 09:30
Hindered Molecular Reorientation of Lithium Ion Doped Succinonitrile in the Terahertz Range, Daniel Nickel¹, Hongtao Bian², Junrong Zheng², Daniel M. Mittleman¹; ¹Electrical and Computer Engineering, Rice Univ., USA; ²Chemistry, Rice Univ., USA. The THz range permittivity of succinonitrile exhibits Debye-like behavior in its plastic-crystal phase, with a characteristic Cole-Cole relaxation time of 65ps ±17ps which increases considerably in the presence of ionic dopants.

SF1F.8 • 09:45
Broadband Terahertz Spectroscopy of Electrically Gated Graphene, Sayyed Hadi Razavipour¹, Wayne Yang¹, David A. Valverde Chavez¹, Eric Whiteway¹, François Blanchard¹, Michael Hilke¹, David G. Cooke¹; ¹McGill, Canada. Broadband terahertz modulation at room temperature is realized using electrically gated graphene in the 1-10 THz range. By gate voltage modulation, the Drude conductivity of graphene varies along with the THz transmission response.

SF1G • Vertical Cavity Lasers—Continued

SF1G.6 • 09:30
Heterogeneously Integrated Long-Wavelength VCSEL using High-Contrast Grating on Silicon, James E. Ferrara¹, Weijian Yang¹, Li Zhu¹, Connie J. Chang-Hasnain¹; ¹EECS, Univ. of California Berkeley, USA. We report an electrically pumped AlGaInAs-silicon VCSEL using a high-contrast grating reflector on silicon. CW output power >1.5 mW, thermal resistance of 1.46 K/mW, and 5 Gb/s direct modulation is demonstrated.

SF1G.7 • 09:45
Control of the Emitted Polarization in a 1310 nm spin-VCSEL Subject to Circularly Polarized Optical Injection, Sami Alharthi¹, Antonio Hurtado¹, Ville-Markus Korpjärvi², Mircea Guina², Ian Hening¹, Michael Adams¹; ¹Computer Science and Electronic Engineering, Univ. of Essex, UK; ²Optoelectronics Research Centre (ORC), Tampere Univ. of Technology, Finland. We report the first optical injection experiment on a dilute nitride 1300 nm spin-VCSEL at room temperature. Effective control of the polarization of the light emitted by the spin-VCSEL is theoretically predicted and experimentally demonstrated.

SF1H • Optical Manipulation for Biomedical Application—Continued

SF1H.6 • 09:30
Optical magnetometry of single NV center scanning local magnetic field in micro fluid devices, Kangmook Lim^{1,2}, Benjamin Shapiro^{3,4}, Jacob Taylor⁵, Edo Waks^{1,5}; ¹Electrical and Computer Engineering, Univ. of Maryland, USA; ²Inst. for Research in Electronics and Applied Physics, USA; ³Fischell Dept. of Bioengineering, Univ. of Maryland, USA; ⁴Inst. for Systems Research, USA; ⁵Joint Quantum Inst., USA. By combining magnetic nanoparticle 3D positioning system and NV ESR measurements in micro-fluid device, we demonstrate sensing of magnetic fringe field of a magnetic bead repeatedly displaced and mapping field profile of the magnetic dipole.

SF1H.7 • 09:45
Power-Dependent Buffering Capacity of Silicon Nitride Microring-Resonator-Based Microparticle Buffers on an Optofluidic Chip, Jiawei Wang¹, Andrew W. Poon¹; ¹Electronic and Computer Engineering, Hong Kong Univ. of Science and Technology, Hong Kong. We demonstrate power-dependent buffering capacity of silicon nitride microring resonator-based microparticle buffers on an optofluidic chip. We observe power dependent buffering capacity of 7 to 21 particles for 2.2µm polystyrene microparticles, and buffering capacity of 14 red-blood-cells.

10:00–10:30 **Coffee Break, Concourse Level**

NOTES

Blank area for notes.

Meeting Room
211 B/D

CLEO: Science & Innovations

SF11 • Microresonator Combs—
Continued

SF11.7 • 09:30

Bandwidth Shaping of Parametric Frequency Combs via Dispersion Engineering, Yoshitomo Okawachi¹, Michael R. Lamont^{1,2}, Kevin Luke³, Daniel O. Carvalho³, Michal Lipson^{2,3}, Alexander L. Gaeta^{1,2}; ¹*School of Applied and Engineering Physics, Cornell Univ., USA*; ²*Kavli Inst. at Cornell for Nanoscale Science, Cornell Univ., USA*; ³*School of Electrical and Computer Engineering, Cornell Univ., USA*. We investigate experimentally and theoretically the role of higher-order-dispersion on the bandwidth of microresonator-based parametric frequency combs. Our results demonstrate that fourth-order dispersion plays a critical role in determining the spectral bandwidth.

SF11.8 • 09:45

Tunable Frequency Comb Generation from a Microring with a Thermal Heater, Xiaoxiao Xue¹, Yi Xuan^{1,2}, Pei-Hsun Wang¹, Jian Wang^{1,2}, Daniel E. Leaird¹, Minghao Qi^{1,2}, Andrew M. Weiner^{1,2}; ¹*School of Electrical and Computer Engineering, Purdue Univ., USA*; ²*Birk Nanotechnology Center, Purdue Univ., USA*. We demonstrate a novel comb tuning method for microresonator-based Kerr comb generators. Continuously tunable, low-noise, and coherent comb generation is achieved in a CMOS-compatible silicon nitride microring resonator.

Meeting Room
212 A/CSF1J • Laser Initiated Self-
organization & Patterning—
Continued

SF1J.7 • 09:30

Time-resolved femtosecond laser pulse absorption at the surface of transparent dielectrics, Nicolas Sanner¹, Maxime Lebugle¹, Marc Sentis¹, Olivier Uteza¹; ¹*Aix-Marseille Univ., France*. Time-resolved absorption of a 500-fs laser pulse by fused silica is measured. The results evidence a strong contribution of linear absorption for high pump fluence, during the entire pulse length.

SF1J.8 • 09:45

Femtosecond laser tuning of Si microring resonators by surface amorphization through a thick SiO₂ cladding, Daniel Bachman¹, Zhijiang Chen¹, Ying Y. Tsui¹, Robert Fedosejevs¹, Vien Van¹; ¹*Electrical and Computer Engineering, Univ. of Alberta, Canada*. Single femtosecond laser pulses are used to modify the surface of c-Si waveguides clad by SiO₂ for permanent tuning of microring resonators. Positive, controllable resonance shifts that vary with fluence are demonstrated, inducing little loss.

Meeting Room
212 B/DCLEO: QELS-
Fundamental ScienceFF1K • Photonic Crystals
and Complex Plasmonic
Nanostructures—Continued

FF1K.7 • 09:30

Strain Tuning of a Quantum Dot Strongly Coupled to a Photonic Crystal Cavity, Shuo Sun¹, Hyochul Kim¹, Glenn S. Solomon², Edo Waks¹; ¹*Electrical and Computer Engineering, Univ. of Maryland, USA*; ²*National Inst. of Standards and Technology, USA*. We experimentally demonstrate reversible strain-tuning of a quantum dot strongly coupled to a photonic crystal cavity. We observe a clear anti-crossing between the quantum dot and the cavity using the strain tuning technique.

FF1K.8 • 09:45

Four-wave Mixing in Slow-light Graphene-silicon Photonic Crystal Waveguides, Hao Zhou^{1,2}, Tingyi Gu¹, James F. McMillan¹, Nick Petrone³, Arend van der Zande³, James C. Hone³, Mingbin Yu⁴, Guo-Qiang Lo⁴, Dim-Lee Kwong⁴, Guoying Feng², Shouhuan Zhou^{2,5}, Chee Wei Wong¹; ¹*Optical Nanostructures Lab, Columbia Univ., USA*; ²*College of Electronic Information, Sichuan Univ., China*; ³*Mechanical Engineering, Columbia Univ., USA*; ⁴*The Inst. of Microelectronics, Singapore*; ⁵*North China Research Inst. of Electro-Optics, China*. We demonstrate the enhanced four-wave mixing generated in silicon photonic crystal waveguides with monolayer graphene. An enhanced high conversion efficiency and wide detuning bandwidth is observed.

Marriott
Salon I & IICLEO: Applications
& TechnologyAF1L • Symposium on
Optofluidic Microsystems I—
Continued

AF1L.5 • 09:30

Reconfigurable Plasmo-fluidic Lenses, Yongmin Liu¹, Chenglong Zhao², Yanhui Zhao², Nicholas Fang³, Tony J. Huang²; ¹*Northeastern Univ., USA*; ²*The Pennsylvania State Univ., USA*; ³*MIT, USA*. Utilizing laser-induced surface bubbles on a metal film, we demonstrate a reconfigurable plasmonic lens in a microfluidic environment to achieve divergence, collimation, and focusing of surface plasmons.

AF1L.6 • 09:45

Automated Single Molecule Nucleic Acid Detection with a Waveguide Chip, Joshua W. Parks¹, Lynnell Zempoaltecatl², Richard A. Mathies³, Aaron Hawkins², Holger Schmidt¹; ¹*Electrical Engineering, Univ. of California Santa Cruz, USA*; ²*Electrical and Computer Engineering, Brigham Young Univ., USA*; ³*Chemistry, Univ. of California Berkeley, USA*. Lambda DNA (λ -DNA) molecules were labeled with SYBR Gold nucleic acid stain using a PDMS-based programmable microfluidic chip (Automaton). Single DNA molecules were detected in a vertically integrated liquid-core waveguide chip.

10:00–10:30 Coffee Break, Concourse Level

NOTES

CLEO: Science & Innovations

CLEO: Applications
& Technology

SF1M • Optomechanics I—
Continued

SF1M.7 • 09:30

Cavity Optomechanical Magnetometry on a Chip, Eoin Sheridan¹, Stefan Forstner¹, Christopher Humphreys¹, Halina Rubinsztein-Dunlop¹, Warwick P. Bowen¹; ¹*School of Mathematics and Physics, Univ. of Queensland, Australia*. A microscale, picotesla range, silicon-chip optical magnetometer. Earth-field, fiber coupled operation, with 60 μm resolution and 40 MHz bandwidth lead to potential applications in microfluidic-MRI, spin physics in condensed matter systems and ultracold atom clouds.

SF1M.8 • 09:45

Design and Fabrication of Optomechanical Crystal Nanobeam Cavity with High Optomechanical Coupling Rate, Yongzhuo Li¹, Kaiyu Cui¹, Xue Feng¹, Yidong Huang¹, Zhilei Huang¹, Fang Liu¹, Wei Zhang¹; ¹*Tsinghua Univ., China*. An optomechanical crystal nanobeam cavity with high optomechanical coupling rate is proposed and fabricated. Only by adjusting the radius of the air holes, the cavity realizes an optomechanical coupling rate as high as 1.24 MHz.

SF1N • Next Generation Fiber
Designs—Continued

SF1N.6 • 09:30

Aperiodic all-solid VLMA-LPF strengthening the singlemode operation over the near infra-red spectral range, Aurélien Benoit^{1,3}, Romain Dauliat², Raphael Jamier¹, Stephan Grimm², Kay Schuster², François Salin³, Georges Humbert¹, Philippe Roy¹; ¹*Xlim Research Inst., France*; ²*Inst. of Photonic Technology, Germany*; ³*Eolite Systems, France*. The singlemodeness of an all-solid very large mode area fiber, based on an aperiodic cladding microstructuration, is experimentally evidenced. This outstanding ability is confirmed over a large spectral range spanning from 1 to 2 μm.

SF1N.7 • 09:45

Model for Pump Absorption in Rare-Earth Doped Double Clad Fibers, V R Supradeepa¹, John M. Fini¹; ¹*OFS Labs, USA*. We introduce and provide experimental verification for a new model and representation of pump absorption in rare-earth-doped double-clad fibers based on underlying physics. The model allows for simple evaluation of wavelength resolved, length dependent absorption.

SF1O • Integrated Polarization
Management—Continued

SF1O.7 • 09:30

Broadband mode-evolution-based four-port polarizing beam splitter, Zhan Su¹, Erman Timurdogan¹, Ehsan S. Hosseini¹, Jie Sun¹, Gerald Leake², Douglas Coolbaugh², Michael R. Watts¹; ¹*Research Lab of Electronics, MIT, USA*; ²*College of Nanoscale Science & Engineering, Univ. at Albany, USA*. The first demonstration of a four-port integrated polarizing beam splitter is reported. The device was fabricated on a silicon-on-insulator platform and exhibits crosstalk level < -10dB over a 150nm bandwidth.

SF1O.8 • 09:45

Selective excitation of guided modes in integrated aluminum nitride photonic circuits, Matthias Stegmaier¹, Wolfram Pernice¹; ¹*Inst. of Nanotechnology, Karlsruhe Inst. of Technology (KIT), Germany*. We demonstrate methods to identify the modal composition of light guided through integrated multimode waveguides and discuss a scheme how arbitrary higher-order modes can selectively be excited. Exemplary, we show efficient and broadband polarization conversion.

AF1P • Photons for
Environment—Continued

AF1P.6 • 09:30

Withdrawn

AF1P.7 • 09:45

Trace NO2 Detection Using a Multi-mode Diode Laser and Cavity Enhanced Absorption Spectroscopy, Andreas Karpf¹, Gottipaty N. Rao¹; ¹*Adelphi Univ., USA*. A simplified trace gas detector using a multi-mode Fabry-Perot diode laser and cavity enhanced absorption spectroscopy has been developed and used to detect NO2 at the 100 ppt level.

10:00–10:30 Coffee Break, Concourse Level

NOTES

Blank lined area for notes.

Executive Ballroom
210ACLEO: QELS-
Fundamental Science

10:30–12:15

FF2A • Quantum Memories

President: Irina Novikova; College of William & Mary, USA

FF2A.1 • 10:30 **Invited**

Quantum State Engineering for High Efficiency Quantum Memories and Cavity Line Narrowing, Stefan Kröll¹, Mahmood Sabooni², Qian Li¹, Diana Serrano¹, Lars Rippe¹; ¹Physics, Lund Univ., Sweden; ²Max-Planck-Institut für Quantenoptik, Germany. A 56% efficiency quantum memory is created by inserting a <1% efficiency memory in a low-finesse cavity. Changing the memory absorption profile by optical pumping decreases the cavity mode-spacing by >4 orders of magnitude.

FF2A.2 • 11:00

Progress towards the development of rare-earth doped waveguides for quantum communications applications, Sara Marzban¹, John Bartholomew¹, Matthew J. Sellars¹, Khu Vu¹; ¹Laser Physics Centre, Australian National Univ., Australia. Photon echo measurements were conducted on a slab waveguide of TeO₂ deposited on a substrate of 0.005%Pr³⁺:Y₂SiO₅. The results indicate that planar waveguide technology could be utilized for quantum communication purposes.

Executive Ballroom
210BCLEO: Applications
& Technology

10:30–12:30

AF2B • Symposium on
Advances in Neurophotonics
II

President: Nicusor Iftimia; Physical Sciences Inc., USA

AF2B.1 • 10:30 **Invited**

Serial optical coherence scanner for brain imaging and mapping, Taner Akkin¹, Hui Wang¹; ¹Dept. of Biomedical Engineering, Univ. of Minnesota, USA. The serial optical coherence scanner reconstructs macroscopic tissues at microscopic resolution using intrinsic optical contrasts. The anatomy, nerve fiber architectures and fiber orientations are shown in ex-vivo rat brains.

AF2B.2 • 11:00 **Invited**

Optical Coherence Imaging of Hemodynamics, Metabolism, and Cell Viability during Brain Injury, Vivek J. Srinivasan¹, Shau Poh Chong¹, Conrad Merkle¹, Harsha Radhakrishnan¹, Conor Leahy¹; ¹Univ. of California Davis, USA. Pre-clinical quantitative imaging endpoints have been challenging in mouse models of cerebrovascular disease. Here we present optical coherence imaging platforms that can quantify blood flow, capillary perfusion, cellular status, and oxygen extraction based on intrinsic scattering signatures.

Executive Ballroom
210C

CLEO: QELS-Fundamental Science

10:30–12:30

FF2C • Metasurfaces II

President: Erez Hasman; Technion-Israel Inst. of Technology, Israel

FF2C.1 • 10:30

Spectrally Selective Chiral Silicon Metasurfaces Based on Infrared Fano Resonances, Chih-Hui Wu¹, Nihal Arju¹, Jonathan Fan², Igal Brener², Gennady Shvets¹; ¹Univ. of Texas at Austin, USA; ²Sandia National Labs., USA; ³Univ. of Illinois at Urbana-Champaign, USA. Silicon-process compatible metasurface was designed and tested in the infrared wavelength range. These metasurfaces show very high Q (>100), extreme chirality, and polarization conversion along with very low-loss operation. They show promise for sensing applications.

FF2C.2 • 10:45

Nanostructured Transparent Conducting Oxide Films for Polarization Control with Plasmonic Metasurfaces, Jongbum Kim¹, Yang Zhao², Aweek Dutta¹, Sajid M. Choudhury¹, Alexander Kildishev¹, Andrea Alu², Alexandra Boltasseva¹; ¹Purdue Univ., USA; ²The Univ. of Texas at Austin, USA. TCOs enable the realization of practical plasmonic and metamaterial devices at the telecommunication frequency due to their low optical loss. We have fabricated GZO plasmonic waveplates, which convert linearly polarized light into circularly polarized light.

FF2C.3 • 11:00

Maximizing Strong Coupling between Metasurface Resonators and Intersubband Transitions, Salvatore Campione^{1,2}, Alexander Benz^{1,2}, John F. Klem², Michael B. Sinclair², Igal Brener^{1,2}, Filippo Capolino³; ¹Center for Integrated Nanotechnologies, Sandia National Labs, USA; ²Sandia National Labs, USA; ³Univ. of California Irvine, USA. We analyze strongly coupled systems that use metasurface resonators and provide an electrodynamic model based on the quasi-static electric near fields that can be used to predict and maximize Rabi splitting varying resonator geometry.

Executive Ballroom
210D

10:30–12:30

FF2D • Quantum Effects in
Lattices

President: Zhigang Chen; San Francisco State Univ., USA

FF2D.1 • 10:30 **Invited**

Realization of the Harper Hamiltonian with Ultracold Atoms in Optical Lattices, Hirokazu Miyake¹, Georgios A. Siviloglou¹, Colin J. Kennedy¹, William C. Burton¹, Wolfgang Ketterle¹; ¹Dept. of Physics, MIT, USA. We experimentally realized the Harper Hamiltonian with charge neutral, ultracold atoms in optical lattices using laser-assisted tunneling and a potential energy gradient. The energy spectrum of this Hamiltonian is the fractal Hofstadter butterfly.

FF2D.2 • 11:00

Rashba Effective Spin-Orbit Coupling in Photonic Lattices, Yonatan Plotnik¹, Mikael Rechtsman¹, Simon Stützer², Yaakov Lumer¹, Stefan Nolte², Alexander Szameit², Mordechai Segev¹; ¹Technion Israel Inst. of Technology, Israel; ²Friedrich Schiller Universität, Germany. We demonstrate theoretically and experimentally the Rashba effect using light in two “counterpropagating” photonic lattices. We observe breaking of inversion symmetry in the resulting band structure.

Thank you for
attending CLEO: 2014.

Look for your
post-conference survey
via email and let us
know your thoughts on
the program.

CLEO: Science & Innovations

10:30–12:30

SF2E • Frequency Combs and CEP

Presider: Simon Birkholz, Max-Born-Institut, Germany

SF2E.1 • 10:30

Self-referenced frequency comb measurement by a polarization line-by-line pulse shaper, Chi-Cheng Chen¹, Chen-Bin Huang¹, Shang-Da Yang¹; ¹Inst. of Photonics Technologies, National Tsing Hua Univ., Taiwan. A polarization line-by-line pulse shaper is used in analytically measuring optical arbitrary waveforms (OAWs) of 100% duty cycle without reference, which is essential for high repetition rate OAWs.

SF2E.2 • 10:45

Enhanced Self-frequency Shift of Cavity Soliton in Mode-locked Octave-spanning Frequency Comb Generation, Lin Zhang¹, Qiang Lin², Anu Agarwal¹, Lionel Kimerling¹, Jurgen Michel¹; ¹Dept. of Materials Science and Engineering, MIT, USA; ²Dept. of Electrical and Computer Engineering, Univ. of Rochester, USA. We show a significant self-frequency shift of ultrafast cavity solitons associated with Kerr frequency combs in a dispersion-flattened nonlinear cavity. Dispersion induces a frequency shift up to 20% of the pump frequency.

SF2E.3 • 11:00

Coherent Frequency Comb Generation in a Silicon Nitride Microresonator with Anomalous Dispersion, Pei-Hsun Wang¹, Yi Xuan^{1,2}, Jian Wang¹, Xiaoxiao Xue¹, Daniel E. Leaird¹, Minghao Qi^{1,2}, Andrew M. Weiner^{1,2}; ¹School of Electrical and Computer Engineering, Purdue Univ., USA; ²Birck Nanotechnology Center, Purdue Univ., USA. We observe a transition to a coherent-comb state in a SiN-microresonator with anomalous dispersion. Although ~300 fs pulse trains are generated after line-by-line shaping, the intensity within the microring does not appear to be pulse-like.

10:30–12:30

SF2F • Advanced THz Emission Mechanisms

Presider: François Blanchard; McGill Univ., USA

SF2F.1 • 10:30

Generation of CW Terahertz Waves in the 3 THz Range Using a MZM-Based Flat Comb Generator, Isao Morohashi¹, Yoshihisa Irimajiri¹, Motohiro Kumagai¹, Akira Kawakami¹, Takahide Sakamoto¹, Norihiko Sekine¹, Satoshi Ochiai¹, Shukichi Tanaka¹, Tetsuya Kawanishi¹, Iwao Hosako¹; ¹NICT, Japan. THz waves in the 3 THz range have been generated by photonic down-conversion using a Mach-Zehnder-modulator-based flat comb generator. THz waves were detected by a hot electron bolometer mixer with a quantum cascade laser.

SF2F.2 • 10:45

Tunable Narrowband Terahertz Generation by Optical Rectification in Single Domain Lithium Niobate Crystal, Iwao Kawayama¹, Zhang Caihong¹, Yuri Avetisyan^{1,2}, Hironaru Murakami¹, Masayoshi Tonouchi¹; ¹Inst. of Laser Engineering, Osaka Univ., Japan; ²Micro-wave Engineering Dept., Yerevan State Univ., Armenia. A simple approach to generate high energy, frequency- and bandwidth- tunable multicycle THz pulses by optical rectification of pre-shaped fs-laser pulses in the single domain lithium niobate crystal is proposed and demonstrated.

SF2F.3 • 11:00

Highly Stable Continuous Wave Terahertz Generation with Widely Tunable Dual-Mode Laser, Hiroyoshi Togo¹, Steven Jones¹, JaeYoung Kim¹, Yoshiyuki Doi², Takashi Yamada², Nobutatsu Koshoubu²; ¹NTT Microsystem Integration Labs, Japan; ²NTT Photonics Labs, Japan. Presented here is a highly stable CW THz generation utilizing a dual-mode laser capable of producing a wide range of differential frequencies. This laser employs an AOTF in a single external cavity for dual-mode selection.

10:30–12:30

SF2G • Laser Dynamics

Presider: Amr Helmy, Univ. of Toronto, Canada

SF2G.1 • 10:30

Comparison of Dynamical Properties of Ground- and Excited-State Emission in Quantum-Dot Lasers, Dejan Arsenijević¹, Holger Schmeckeber¹, Marc Spiegelberg¹, Dieter Bimberg¹, Vissarion Mikhelashvili², Gadi Eisenstein²; ¹Dept. of Solid-State Physics, Technische Universität Berlin, Germany; ²Electrical Engineering Dept. and the Russell Berrie Nanotechnology Inst., Technion, Israel. We compare dynamical properties of ground and excited state emission from 1.31 μm quantum-dot lasers. Dichroic facet mirrors ensure oscillations at either ground or excited state. Maximum bandwidths observed are 10.51 and 16.25 GHz, respectively.

SF2G.2 • 10:45

Quantum-dot-laser two-state self-mixing-velocimetry: Simulation and Experiment, Mariangela Gioannini¹, Marius Dommermuth², Lukas Drzewietzki³, Stefan Breuer³; ¹Dipartimento di Elettronica e Telecomunicazioni, Politecnico di Torino, Italy; ²Inst. of Theoretical Physics, Eberhard Karls Universität Tübingen, Germany; ³Inst. of Applied Physics, Technische Universität Darmstadt, Germany. Two-state-laser self-mixing is demonstrated. An additional Doppler-signal originating from the two-state-interaction yields the potential of high-velocity detection. Simulations verify the results and identify the relevant mechanism for the Doppler signal-generation.

SF2G.3 • 11:00

Recent advances in ultrafast MIXSELS, Mario Mangold¹, Christian A. Zaugg¹, Sandro M. Link¹, Alexander Klenner¹, Matthias Golling¹, Bauke W. Tilma¹, Ursula Keller¹; ¹Dept. of Physics, Inst. for Quantum Electronics, ETH Zurich, Switzerland. A high-power MIXSEL combining 570-fs-pulses and repetition-rate scalability from 5 GHz to record high 101.2 GHz is presented. Additionally, we achieve record low timing jitters of a free-running and piezo-stabilized picosecond MIXSEL.

Meeting Room
211 B/D

CLEO: Science & Innovations

10:30–12:30

SF21 • Combustion and Plasma Diagnostics

Presider: Thomas Reichardt;
Sandia National Labs, USA

SF21.1 • 10:30

Investigation of Fiber-Based Endoscopes for Quantitative 3D Flow and Flame Imaging, MinWook Kang¹, Xuesong Li², Lin Ma^{2,1}; ¹Mechanical Engineering, Virginia Tech, USA; ²Aerospace and Ocean Engineering, Virginia Tech, USA. This work describes instantaneous three-dimensional (3D) measurements using fiber-based endoscopes. Experimental and numerical results demonstrate their potential for kHz 3D measurements, and also for overcoming practical issues like optical access and equipment cost.

SF21.2 • 10:45

High-Temperature Flow Sensing Using Regenerated Gratings in Self-Heated High Attenuation Fibers, Rongzhang Chen¹, Aidong Yan¹, Kevin P. Chen¹; ¹Dept. of Electrical and Computer Engineering, Univ. of Pittsburgh, USA. We report a high-temperature flow sensing technique based on thermally regenerated fiber Bragg gratings in high attenuation fibers. It can provide flow rate measurements up to 800 °C with compensation for ambient temperature variations.

SF21.3 • 11:00

Detection of PbCl₂ using Collinear Photofragmentation and Atomic Absorption Spectroscopy, Tapio Sorvajärvi¹, Juha Toivonen¹; ¹Tampereen Teknillinen Yliopisto, Finland. PbCl₂ causes corrosion in waste combusting power plants and there is no method to monitor it. We demonstrate the use of collinear photofragmentation and atomic absorption spectroscopy (CPFAAS) to successfully detect PbCl₂ in-situ in a hot furnace.

Meeting Room
212 A/C

10:30–12:30

SF2J • Innovations in Laser Processing of Materials

Presider: Emmanuel Haro-Poniatowski; Physics Dept., UAM-Iztapalapa, Mexico

SF2J.1 • 10:30

Terahertz-driven non-resonant magnetization dynamics in cobalt, Carlo Vicario¹, Peter Derlet¹, Fernando Ardana-Lamas^{1,3}, Clemens Ruchert¹, Barati Tudu², Jan Luning², Christoph P. Hauri^{1,3}; ¹Paul Scherrer Institut, Switzerland; ²Univ. Pierre et Marie Curie, France; ³Ecole Polytechnique Federale de Lausanne, Switzerland. We demonstrate non-resonant magnetization dynamics in the ferromagnetic cobalt thin film induced by a high-field Terahertz pulse. The magnetization dynamics are coherent and exactly follow the THz carrier oscillations.

SF2J.2 • 10:45

Movies of filaments and plasma, Andreas U. Velten^{1,2}, Andreas Schmitt-Sody³, Adrian Lucero³, Ladan Arissian⁴, Xiaozhen Xu⁴, Chengyong Feng⁴, Shermineh Rostami⁴, Brian Kamer¹, Jean-Claude M. Diels⁴; ¹Lab for Optical and Computational Instrumentation, Univ. of Wisconsin-Madison, USA; ²Medical Engineering, Morgridge Inst. for Research, USA; ³Air Force Research Lab, USA; ⁴Dept. of Physics and Astronomy, Univ. of New Mexico, USA. Using a streak camera, and combining over 1,000 synchronized frames, 4D (2 D space, time in ps and wavelength) movies of the light and plasma emission in the wake of filaments are produced.

SF2J.3 • 11:00 **Invited**

3D chemical imaging of Li-ion batteries using femtosecond laser plasma spectroscopy, Huaming Hou¹, Vassilia Zorba¹; ¹Lawrence Berkeley National Lab, USA. We introduce the use of femtosecond laser plasma spectroscopy in chemical imaging of Li-ion battery system components. Spatially resolved mapping of major and minor elements of Li-ion batteries is presented and correlated to electrochemical performance.

Meeting Room
212 B/D

CLEO: QELS-Fundamental Science

10:30–12:15

FF2K • Nanophotonic and Plasmonic Coupling to Quantum Emitters

Presider: Vladimir Shalaev;
Purdue Univ./Birk
Nanotechnology, USA

FF2K.1 • 10:30

Spin Polarized Light Emission from Quantum Dots Coupled to Multipolar Nanoantennas, Sergey Kruk¹, Manuel Decker¹, Isabelle Staude¹, Stefan Schlecht¹, Michael Greppmair¹, Dragomir N. Neshev¹, Yuri S. Kivshar¹; ¹Australian National Univ., Australia. We experimentally demonstrate spin-polarized light emission from quantum dots coupled to a single-element nanoantenna with resonant multipolar moments. We observe spin-momentum locking resulting in photons of opposite spin emitted in opposite directions.

FF2K.2 • 10:45

Boosting the photon-extraction efficiency of nanophotonic structures by deterministic microlenses, Manuel Gschrey¹, Marc Seifried¹, Luzy Krüger¹, Ronny Schmidt¹, Jan-Hindrik Schulze¹, Tobias Heindel¹, Sven Burger², Sven Rodt¹, Frank Schmidt², Andre Strittmatter¹, Stephan Reitzenstein¹; ¹Technische Universität Berlin, Germany; ²Zuse-Institut Berlin, Germany. A novel concept for enhancing the photon-extraction efficiency of nanophotonics structures is presented. We apply in-situ electron beam lithography to enhance the single photon flux of single quantum dots by deterministically aligned microlenses.

FF2K.3 • 11:00

Highly Directional Emission of Photons from Nanocrystal Quantum Dots Positioned on Circular Plasmonic Lens Antennas, Moshe G. Harats^{1,3}, Nitzan Livneh^{2,3}, Shira Yochelis^{2,3}, Yossi Paltiel^{2,3}, Ronen Rapaport^{1,2}; ¹Racah Inst. of Physics, Hebrew Univ. of Jerusalem, Israel; ²The Dept. of Applied Physics, Selim and Rachel Benin School of Engineering and Computer Science, Hebrew Univ. of Jerusalem, Israel; ³The Center for Nanoscience and Nanotechnology, Hebrew Univ. of Jerusalem, Israel. We show enhanced directional emission from nanocrystal quantum dots positioned at the center of a circular plasmonic lens. A collimation with a divergence of only ~4 degrees FWHM is achieved, with a spectrally broad bandwidth.

Marriott
Salon I & II

CLEO: Applications & Technology

10:30–12:00

AF2L • Symposium on Optofluidic Microsystems II

Presider: To be Determined

AF2L.1 • 10:30 **Invited**

Optofluidic Manipulation and Sorting for Small Size Particle and Bio-molecule, Ai-Qun Liu¹; ¹School of Electrical & Electronic Engineering, Nanyang Technological Univ., Singapore. It is significant research approach in the field of manipulation and sorting of a small size of particle and molecule with dimensions of tens to hundreds of nanometers in a microfluidic chip.

AF2L.2 • 11:00

Freezing of microparticles in an electro-optofluidic platform, Mohammad Soltani^{1,2}, Jessica L. Killian¹, Jun Lin^{1,2}, Michal Lipson¹, Michelle D. Wang^{1,2}; ¹Cornell Univ., USA; ²Howard Hughes Medical Inst., USA. We show ability to simultaneously trap micron-size particles in an optical field and freeze their position by rapidly changing the direction of Poynting vector in an optofluidic waveguide using an electrically controlled Mach-Zehnder switch.

CLEO: Science & Innovations

CLEO: Applications
& Technology

10:30–12:30

SF2M • Optomechanics II

President: Marcelo Davanco; NIST, USA

SF2M.1 • 10:30

A fully integrated chip-scale optomechanical oscillator, Yongjun Huang^{1,2}, Xingsheng Luan¹, Ying Li¹, James F. McMillan¹, Di Wang¹, Archita Hati³, David A. Howe³, Mingbin Yu⁴, Guo-Qiang Lo⁴, Dim-Lee Kwong⁴, Chee Wei Wong¹; ¹Columbia Univ., USA; ²School of Communication and Information Engineering, Univ. of Electronic Science and Technology of China, China; ³National Inst. of Standards and Technology, USA; ⁴The Inst. of Microelectronics, Singapore. We demonstrate a chip-scale slot-type photonic crystal optomechanical oscillator fully integrated with an on-chip waveguide Ge photoreceiver, which exhibits high-harmonic tunable RF oscillations and high-quality optical resonances with controlled detuned continuous-wave laser drive.

SF2M.2 • 10:45

Coherent Regenerative Optomechanical Oscillation of a Silica Microsphere in an Aqueous Environment, Wenyan Yu¹, Wei Jiang², Qiang Lin^{2,3}, Tao Lu¹; ¹Electrical and Computer Engineering, Univ. of Victoria, Canada; ²Inst. of Optics, Univ. of Rochester, USA; ³Electrical and Computer Engineering, Univ. of Rochester, USA. We observed optomechanical oscillations at 384-kHz by immersing a silica microsphere in an aqueous environment. Despite of high dissipation, the device displays a laser threshold power of 0.98-mW and a mechanical Q of 1,648.

SF2M.3 • 11:00

Synchronization of Multiple Optomechanical Oscillators, Mian Zhang¹, Michal Lipson^{1,2}; ¹Electrical and Computer Engineering, Cornell Univ., USA; ²Kavli Inst. at Cornell, Cornell Univ., USA. We design and fabricate a 2×2 optomechanical oscillator array. We show the onset of synchronized mechanical oscillations when the array is excited by a single continuous wave laser.

10:30–12:15

SF2N • High Energy fs Fiber Laser & Applications

President: Shinji Yamashita; Univ. of Tokyo, Japan

SF2N.1 • 10:30 **Invited**

Fiber Lasers for Accelerators and Accelerator Driven Light Sources, Ingmar Hartl¹; ¹DESY, Germany. Lasers are an indispensable tool for current XUV and X-ray free electron light sources and are key to future laser driven accelerator technology. We discuss the role of fiber-laser technology in this emerging field.

SF2N.2 • 11:00

Spatially Separated Non-linear Pulse Compression, Arno Klenke^{1,2}, Steffen Hädrich^{1,2}, Jens Limpert^{1,2}, Andreas Tünnermann^{1,3}; ¹Inst. of Applied Physics, Friedrich-Schiller-Universität Jena, Germany; ²Helmholtz-Inst. Jena, Germany; ³Fraunhofer Inst. of Applied Optics and Precision Engineering, Germany. We demonstrate the coherent combination of pulses that are spectrally broadened in two spatially separated solid-core large-pitch fibers. The 320 fs input pulses could be compressed to the sub-30fs regime.

10:30–12:30

SF2O • Special and Spatial Filters

President: Mo Li, National Taiwan Univ., Taiwan

SF2O.1 • 10:30

Ultrahigh Suppression and Reconfigurable RF Photonic Notch Filter using a Silicon Nitride Ring Resonator, David Marpaung¹, Blair Morrison¹, Ravi Pant¹, Chris Roeloffzen^{2,3}, Arne Leinse⁴, Marcel Hoekman⁴, Rene Heide-man⁴, Benjamin J. Eggleton¹; ¹CUDOS Univ. of Sydney, Australia; ²Telecommunication Engineering, Univ. of Twente, Netherlands; ³Satrax BV, Netherlands; ⁴LioniX BV, Netherlands. We report a technique to simultaneously optimize the peak rejection and the resolution of a radiofrequency photonic notch filter based on a silicon nitride ring resonator.

SF2O.2 • 10:45

Supersymmetric mode converters, Matthias Heinrich¹, Simon Stützer², Mohammad-Ali Miri¹, Ramy El-Ganainy³, Stefan Nolte², Demetrios N. Christodoulides¹, Alexander Szameit²; ¹CREOL The College of Optics and Photonics, Univ. of Central Florida, USA; ²Inst. of Applied Physics, Friedrich-Schiller-Univ., Germany; ³Max-Planck Inst. for the Physics of Complex Systems, Germany. We present the first experimental realization of optical supersymmetry and demonstrate mode conversion and global phase-matching between SUSY partner structures. Our results may pave the way for compact and highly efficient integrated mode-division-multiplexing schemes.

SF2O.3 • 11:00

A High-Q Tunable Interior-Ridge Microring Filter, Erman Timurdogan¹, Zhan Su¹, Jie Sun¹, Michele Moresco¹, Gerald Leake², Douglas Coolbaugh², Michael R. Watts¹; ¹Research Lab of Electronics, MIT, USA; ²College of Nanoscale Science & Engineering, Univ. at Albany, USA. A tunable interior-ridge microring filter is demonstrated with a high quality factor of 1.5×10⁵, while achieving a thermal tuning efficiency of 5.5μW/GHz. The filter demonstrates a record low insertion-loss <0.05dB over an uncorrupted 4-THz free-spectral-range.

11:00–12:30

AF2P • Photons for Energy

President: Christian Wetzel; Rensselaer Polytechnic Inst., USA

AF2P.1 • 10:30 **Invited**

Withdrawn

AF2P.2 • 11:00

Semi-transparent and colored photovoltaic structures by using ultra-thin a-Si, Jae Yong Lee¹, Kyu-Tae Lee¹, Sungyong Seo¹, L. Jay Guo¹; ¹EECS, Univ. of Michigan, USA. We exploit optical resonance in an ultra-thin (6 to 31 nm) undoped amorphous silicon/organic hybrid photovoltaic (PV) structures that can produce semi-transparent transmissive colors insensitive to incidence angle of up to ±70° regardless of polarization.

Executive Ballroom
210ACLEO: QELS-
Fundamental ScienceFF2A • Quantum Memories—
Continued

FF2A.3 • 11:15

High-fidelity heralded polarization-state transfer of a photon onto a single atom, Christoph Kurz¹, Philipp Müller¹, Michael Schug¹, Pascal Eich¹, Jan Huwer¹, Jürgen Eschner¹; ¹Saarland Univ., Germany. We demonstrate heralded absorption of a single laser photon by a single trapped atomic ion, thereby mapping the photonic polarization state onto the atomic spin state with 97.9(1) % average fidelity.

FF2A.4 • 11:30

Raman quantum memory based on an ensemble of nitrogen-vacancy centers coupled to a microcavity, Khabat Heshami¹, Charles Santori², Behzad Khanaliloo¹, Chris Healey¹, Victor M. Acosta², Paul E. Barclay^{1,3}, Christoph Simon¹; ¹IQST, Physics and Astronomy, Univ. of Calgary, Canada; ²Hewlett Packard Labs, USA; ³NRC National Inst. for Nanotechnology, Canada. We propose a scheme to realize quantum memories based on Raman coupling for storing photons in the electronic spin of NV⁰ ensembles. We include all optical transitions in a 9-level configuration and evaluate the efficiencies.

FF2A.5 • 11:45

A THz-Bandwidth Optical Memory for Quantum Storage, Duncan England¹, Kent Fisher², Jean-Philippe MacLean², Philip J. Bustard¹, Kevin Resch¹, Benjamin J. Sussman¹; ¹National Research Council, Canada; ²Inst. for Quantum Computing, Univ. of Waterloo, Canada. We have demonstrated a THz-bandwidth quantum memory using the optical phonon modes of room-temperature diamond. A noise-floor of just 0.007 photons per pulse provides the opportunity to store photons produced by spontaneous parametric downconversion.

FF2A.6 • 12:00

Molecular Single Photons for Atomic Experiments, Wilhelm Kiefer¹, Petr Sijushchev¹, Kim Kafenda¹, Jörg Wrachtrup^{1,2}, Ilja Gerhardt^{1,2,3}; ¹Physikalisches Institut, Univ. of Stuttgart and Stuttgart Research Center of Photonic Engineering (SCoPE), Pfaffenwaldring 57, D-70569, Germany; ²Max Planck Inst. for Solid State Research, Heisenbergstrasse 1, D-70569, Germany. Single organic molecules allow for the generation of high-flux single photons. At cryogenic conditions, these photons can be as narrow as a few MHz. It is possible to find suitable molecules matching to a variety of atomic transitions, allowing for quantum hybrid systems of atoms and molecules.

Executive Ballroom
210BCLEO: Applications
& TechnologyAF2B • Symposium on
Advances in Neurophotonics
II—ContinuedAF2B.3 • 11:30 


High-Resolution Optical Microscopy Imaging of Cortical Oxygen Delivery and Consumption, Sava Sakadzic¹, Emiri T. Mandeville^{1,2}, Louis Gagnon¹, Joseph J. Musacchia¹, Mohammad A. Yaseen¹, Meryem A. Yucel¹, Joel Lefebvre³, Frederic Lesage³, Anders Dale⁴, Katharina Eikermann-Haerter¹, Cenk Ayata^{1,2}, Vivek J. Srinivasan^{1,5}, Eng Lo^{1,2}, Anna Devor^{1,4}, David A. Boas¹; ¹Dept. of Radiology, Harvard Medical School, Massachusetts General Hospital, USA; ²Dept. of Neurology, Harvard Medical School, Massachusetts General Hospital, USA; ³Département de génie électrique, École Polytechnique de Montréal, Canada; ⁴Dept. of Radiology and Neurosciences, Univ. of California, San Diego, USA; ⁵Dept. of Biomedical Engineering, Univ. of California Davis, USA. We combined Two-Photon Microscopy imaging of oxygen partial pressure (PO₂) with spectral domain OCT measurements of cerebral blood flow to quantify oxygen extraction from cerebral microvasculature during metabolic and blood flow perturbations.

AF2B.4 • 12:00 

Optical sensing and control in live animals for early detection of diseases, Daniel C. Cote^{1,2}; ¹Université Laval, Canada; ²CRI-USMQ, Canada. We show we can monitor blood vessel permeability, myelin degeneration and microglial activity with video rate microscopy. Advanced fiber optic tools are shown to permit control of activity in the spinal cord.

Executive Ballroom
210C

CLEO: QELS-Fundamental Science

FF2C • Metasurfaces II—
ContinuedFF2C.4 • 11:15 

Timing Performance Improvement of Scintillator Detectors via Inclusion of Reflection Metasurfaces, Mark S. Brown¹, Ioannis Papakonstantinou¹; ¹Electrical and Electronic Engineering, UCL, UK. A reflection metasurface is used to optimise the light transport within a scintillator detector dramatically reducing the time resolution. We present a structure design and potential improvements in Positron-Emission Tomography.

FF2C.5 • 11:30 

Large-scale Lithography-free Metasurface with Spectrally Tunable Super Absorption, Kai Liu¹, Xie Zeng¹, Suhua Jiang², Dengxin Ji¹, Haomin Song¹, Nan Zhang¹, Qiaoqiang Gan¹; ¹Dept. of Electrical Engineering, The State Univ. of New York at Buffalo, USA; ²Dept. of Materials Science, Fudan Univ., China. We demonstrate a simple, low-cost and large-area lithography-free method to fabricate three-layered metasurface structures with tunable, broadband and omnidirectional absorption properties.

FF2C.6 • 11:45 

Optical Magnetic Mirrors using All Dielectric Metasurfaces, Sheng Liu^{1,2}, Igal Brener^{1,2}, Jeremy B. Wright^{1,2}, Thomas Mahony^{1,2}, Young Chul Jun^{1,2}, Salvatore Campione^{1,2}, James Ginn^{1,2}, Daniel A. Bender¹, Joel R. Wendt¹, Jon Ihlefeld¹, Paul Clem¹, Michael B. Sinclair¹; ¹Sandia National Labs, USA; ²Center for Integrated Nanotechnologies, USA. We experimentally demonstrate the magnetic mirror behavior of all-dielectric metasurfaces at optical frequencies through phase measurements using time-domain-spectroscopy. The unique boundary conditions of magnetic mirrors can lead to advances in sensors, photodetectors and light sources.

FF2C.7 • 12:00 

Numerically Stable Reconstruction of Wavelength-Scale Objects with Sub-Wavelength Resolution, Sandeep Inampudi¹, Nicholas A. Kuhta², Viktor A. Podolskiy¹; ¹Dept. of Physics and Applied Physics, Univ. of Massachusetts, USA; ²Dept. of Physics, Oregon State Univ., USA. We present numerically stable expansion basis for diffraction-based far-field computational imaging systems and demonstrate the capabilities of reconstructing wavelength-scale objects with wavelength/20 resolution.

Executive Ballroom
210D

CLEO: QELS-Fundamental Science

FF2D • Quantum Effects in
Lattices—Continued

FF2D.3 • 11:15

Lieb Photonic Topological Insulator, Miguel A. Bandres¹, Mikael Rechtsman¹, Alexander Szameit², Mordechai Segev¹; ¹Physics Dept. and Solid State Inst., Technion, Israel; ²Inst. of Applied Physics, Friedrich-Schiller-Universität Jena, Germany. We show that a Lieb photonic lattice of helical waveguides (without any external field) have one-way edge states that are topologically protected against backscattering as they pass through defects or around corners.

FF2D.4 • 11:30 

Highly Efficient Eigenstate-Assisted Long-Distance Quantum State Transfer in Photonic Lattices, Armando P. Leija¹, Markus Graefe¹, René Heilmann¹, Robert Keil¹, Steffen Weimann¹, Demetrios N. Christodoulides², Alexander Szameit¹; ¹Inst. of Applied Physics, Friedrich-Schiller-Universität Jena, Germany; ²CREOL, UCF, USA. We introduce a new perfect state transfer protocol based on single-photon W-eigenstates of photonic lattices. Such W-eigenstates appear as impulse response of the system, e.g., when single photons are launched into single sites.

FF2D.5 • 11:45 

Simulation of two-mode squeezing in photonic waveguide lattices, Simon Stützer¹, Alexander S. Soltsev², Stefan Nolte¹, John E. Sipe³, Andrey A. Sukhorukov², Alexander Szameit¹; ¹Inst. of Applied Physics, Germany; ²Nonlinear Physics Centre, Research School of Physics and Engineering, Australia; ³Dept. of Physics and Inst. for Optical Sciences, University of Toronto, Canada. We utilized classical light simulating a nonclassical quantum process. Specially modulated waveguide arrays were utilized to emulate two-mode squeezed vacuum states as the intensity in our arrays correspond to the photon number distribution of the squeezed states.

FF2D.6 • 12:00 

Harmonic Oscillation in Coupled Waveguide Arrays, Jianxiong Wu¹, Arash Joushaghani¹, J. Stewart Aitchison¹; ¹Electrical and Computer Engineering, Univ. of Toronto, Canada. Following the idea of optical analogy to electronic systems, harmonic oscillations are spatially mimicked in waveguide arrays. We study and demonstrate the oscillations of light in AlGaAs waveguide arrays.

CLEO: Science & Innovations

SF2E • Frequency Combs and
CEP—Continued

SF2E.4 • 11:15

Direct carrier-envelope phase control of a sub-MHz Yb amplifier, Tadas Balciunas¹, Tobias Flöry¹, Tomas Stanislavskas², Roman Antipenkov², Arunas Varanavicius², Andrius Baltuska¹, Gunter Steinmeyer³; ¹Technische Universität Wien, Austria; ²Faculty of Physics, Vilnius Univ., Lithuania; ³Max Born Inst., Germany. We demonstrate direct feed-forward CEP control of a regenerative amplifier in a single stage, resulting in unprecedented sub-100 mrad phase jitters of an amplified system. Energy scalability of the approach is shown.

SF2E.5 • 11:30

1.13-GHz Repetition Rate, Sub-Femtosecond Timing Jitter, CNT-Mode-Locked Ultrafast Yb:KYW Laser, Heewon Yang¹, Hyojin Kim¹, Junho Shin¹, Chur Kim¹, Sun Young Choi², Guang-Hoon Kim³, Fabian Rothermund², Jungwon Kim¹; ¹Korea Advanced Inst. of Science and Technology, Korea; ²Ajou Univ., Korea; ³Korea Electrotechnology Research Inst., Korea. We show 1.13-GHz repetition rate, 0.70-fs timing jitter optical pulse train directly generated from diode-pumped, CNT-mode-locked Yb:KYW laser. The measured jitter is the lowest for GHz pulse trains, and is suitable for high-resolution analog-to-digital conversion.

SF2E.6 • 11:45

Jitter Reduction in Digitally Synchronized Lasers, Russell Wilcox¹, Lawrence Doolittle¹, Gang Huang¹, Alan Fry²; ¹Lawrence Berkeley National Lab, USA; ²SLAC National Accelerator Lab, USA. We synchronize a mode-locked Ti:sapphire laser to a 2.8GHz RF reference with 25fs jitter using an all-digital phase-locked loop, and a new technique for measuring the closed-loop transfer function and optimizing complex gain.

SF2E.7 • 12:00

Passive Synchronization between Two-Color Mode-Locked Lasers with Long-Term Stability and Subfemtosecond Timing Jitter, Dai Yoshitomi¹, Kenji Torizuka¹; ¹Natl Inst of Adv Industrial Sci & Tech, Japan. We demonstrate passive synchronization between Ti:sapphire and Yb-doped fiber mode-locked lasers with long-term stability for 6 h with the aid of active temperature stabilization. A timing jitter of 0.75 fs was achieved between two-color pulses.

SF2F • Advanced THz Emission
Mechanisms—Continued

SF2F.4 • 11:15

Gain Enhancement Effect of Surface Plasmon Polaritons on Terahertz Stimulated Emission in Optically Pumped Monolayer Graphene, Tetsuya Kawasaki¹, Takayuki Watanabe¹, Tetsuya Fukushima¹, Yuhei Yabe¹, Stephane A. Boubanga Tombet¹, Akira Satou¹, Alexander A. Dubinov², Vladimir Y. Aleshkin², Vladimir Mitin³, Victor Ryzhii¹, Taiichi Otsuji¹; ¹RIEC, Tohoku Univ., Japan; ²Russian Academy of Science, Russia; ³Univ. at Buffalo, USA. We experimentally observed the surface plasmon polaritons (SPPs) in photoexcited monolayer graphene. The results support the occurrence of the gain enhancement effect by the excitation of SPPs on terahertz stimulated emission in optically pumped graphene.

SF2F.5 • 11:30

Flat THz Launcher Antenna, Unai Beas-coetxea¹, Miguel Beruete¹, Mokhtar Zehar², Amit Agrawal³, Shuchang Liu⁴, Karine Blany², Abdallah Chahadih², Xiang-Lei Han², David Etayo¹, Miguel Navarro-Cia⁵, Ajay Nahata⁴, Tahsin Akalin², Mario Sorolla¹; ¹Universidad Pública de Navarra, Spain; ²Inst. of Electronics, Microelectronics and Nanotechnology (IEMN), France; ³Syracuse Univ., USA; ⁴Univ. of Utah, USA; ⁵Imperial College London, UK. 1D and 2D leaky-wave corrugated antennas working at terahertz frequencies are numerically and experimentally studied. These structures allow temporal-pulse and beam shaping by engineering the leakage rate of the surface waves induced by the corrugations.

SF2F.6 • 11:45

Frequency tunable, high dynamic range THz spectrometer using parametric processes in Lithium Niobate crystal, Kosuke Murate¹, Yuusuke Taira¹, Saroj R. Tripathi¹, Shin'ichiro Hayashi², Koji Nawata³, Hiroaki Minamide², Kodo Kawase^{1,2}; ¹Nagoya Univ., Japan; ²RIKEN, Japan. We developed spectrally flat THz wave spectrometer with the dynamic range of more than 7 orders, based on optical parametric processes in Lithium Niobate crystals for the emission and detection of THz waves.

SF2F.7 • 12:00

Improved InGaAs/InAlAs photoconductive THz receivers: 5.8 THz bandwidth and 80 dB dynamic range, Björn Globisch¹, Roman, J. B. Dietz¹, Dennis Stanze¹, Helmut Roehle¹, Thorsten Göbel¹, Martin Schell¹; ¹Fraunhofer Heinrich Hertz Inst., Germany. We investigate optimal Be-doping conditions of low-temperature-grown InGaAs/InAlAs photoconductive antennas with respect to their carrier lifetimes and carrier mobility. Employed as THz-TDS receiver bandwidths of 5.8 THz with a dynamic range of up to 80 dB is achieved.

SF2G • Laser Dynamics—
Continued

SF2G.4 • 11:15

Modulation Characteristics Enhancement by Mutual Injection Locking of Monolithically Integrated Laser Diodes, dong Liu¹, Changzheng Sun¹, Bing Xiong¹, Yi Luo¹; ¹Tsinghua Univ., China. Modulation characteristics enhancement by mutual injection locking of monolithically integrated lasers is demonstrated. Resonance frequency as high as 34.3 GHz is recorded. The nonlinearity and chirp performances are simultaneously improved compared with free running state.

SF2G.5 • 11:30

SESAM and Gain Chip Optimization Leading to a Record Performance of an Ultrafast Electrically Pumped VECSEL, Christian A. Zaugg¹, Stephan Gronenborn², Holger Moench², Mario Mangold¹, Michael Miller³, Ulrich Weichmann², Wolfgang P. Pallmann¹, Matthias Golling¹, Bauke W. Tilma¹, Ursula Keller¹; ¹Inst. for Quantum Electronics, ETH Zurich, Switzerland; ²Philips Technologie GmbH Photonics Aachen, Germany; ³Philips Technologie GmbH Photonics U-L-M Photonics, Germany. With an improved gain chip and SESAM we set new benchmarks for modelocked electrically pumped VECSELS, i.e. shortest pulses (2.47 ps), highest average power (53.2 mW), peak power (4.7 W) and repetition rate (18.2 GHz).

SF2G.6 • 11:45

Experimental study of the stability of harmonic mode-locking in quantum dot passively mode-locked lasers, Jesse Mee¹, Ravi Raghunathan², David Murrell², Alex Braga³, Yan Li⁴, Luke F. Lester²; ¹Air Force Research Labs, USA; ²Bradley Dept. of Electrical and Computer Engineering, Virginia Polytechnic Inst. and State Univ., USA; ³Center for High Technology Materials, Univ. of New Mexico, USA; ⁴APIC Corporation, USA. The stability of harmonic mode-locking in a two-section quantum dot passively mode-locked laser is examined using a Frequency Resolved Optical Gating pulse measurement system and shown for the first time to be a stable effect.

SF2G.7 • 12:00

Phase-Locked Quantum-Dot Mode-Locked Lasers For Wider Frequency Combs Generation, Tatiana Habruseva^{1,2}, Dejan Arsenijević⁴, Dieter Bimberg⁴, Guillaume Huyet^{1,3}, Stephen P. Hegarty^{1,3}; ¹CAPPA, Cork Inst. of Technology, Ireland; ²Aston Univ., UK; ³Tyndall National Inst., Ireland; ⁴Institut für Festkörperphysik, Technische Universität Berlin, Germany. We describe the technique allowing generation of wider frequency combs with low phase noise and pulses of shorter duration in quantum-dot mode-locked lasers. The devices are stabilized using coherent sidebands optical injection.

Meeting Room
211 B/D

CLEO: Science & Innovations

SF21 • Combustion and Plasma
Diagnostics—Continued

SF21.4 • 11:15

Towards Simultaneous Measurement of OH and HO₂ in Combustion Using Faraday Rotation Spectroscopy, Brian Brumfield¹, Xueliang Yang², Joseph Lefkowitz², Yiguang Ju², Gerard Wysocki¹; ¹Dept. of Electrical Engineering, Princeton Univ., USA; ²Dept. of Mechanical and Aerospace Engineering, Princeton Univ., USA. Preliminary results from the development of a dual wavelength Faraday rotation spectrometer for simultaneous quantification of HO₂ and OH in combustion research are presented.

SF21.5 • 11:30 **Invited**

Instantaneous Volumetric Combustion Diagnostics, Lin Ma¹; ¹Dept. of Aerospace and Ocean Engineering, Virginia Tech, USA. This paper reports instantaneous and volumetric flame measurements based on tomographic techniques. Experimental results at kHz temporal rate, in a volume of 16×16×16 cm³, and with a spatial resolution of 2–3 mm, are discussed.

SF21.6 • 12:00

Noninvasive Ultrafast Imaging Diagnostics in Low-Temperature Plasmas, Waruna Kulatilaka¹, Jacob Schmidt¹, Sukesh Roy¹, Kraig Frederickson², Walter Lempert², James Gord³; ¹Spectral Energies LLC, USA; ²The Ohio State Univ., USA; ³Air Force Research Lab, USA. We demonstrate femtosecond laser pulses for two-photon LIF imaging of atomic species in nonequilibrium plasmas. Femtosecond excitation enables improved signal-to-noise ratio, suppression of photolytic interferences, kilohertz-rate imaging, and potential for quenching-free measurements.

Meeting Room
212 A/CSF2J • Innovations in Laser
Processing of Materials—
Continued

SF2J.4 • 11:30

Controlled cell adhesion on microstructured Polydimethylsiloxane (PDMS) surface using femtosecond laser, Ali Alshehri^{1,3}, Z. .. Al-Rekabi^{1,4}, R. Hickey¹, A. E. Pelling^{1,2}, Ravi Bhardwaj¹; ¹physics, Univ. of Ottawa, Canada; ²biology, Univ. of Ottawa, Canada; ³physics, King Khalid Univ., Saudi Arabia; ⁴Mechanical Engineering, Univ. of Washington, USA. We demonstrate controlled cell adhesion on Polydimethylsiloxane (PDMS) substrate microstructured by a femtosecond laser. The effect of micro structures on cell attachment, alignment, patterned growth and cells proliferation were investigated over 24hrs, 48hrs and 72hrs.

SF2J.5 • 11:45

Laser-induced dispersion control, Gennady Rasskazov¹, Anton Ryabtsev¹, Vadim V. Lozovoy¹, Marcos Dantus¹; ¹Michigan State Univ., USA. We present pump-probe measurements that reveal significant changes in the group delay dispersion of a femtosecond laser pulse being controlled by the relative delay between two pulses. We suggest applications for this time-domain shaping approach.

SF2J.6 • 12:00

Locally and Reversibly Control the coupling of photonic crystal cavities using photochromic tuning, Tao Cai¹, Ranoojy Bose¹, Glenn S. Solomon², Edo Waks^{1,2}; ¹Electrical Engineering, Univ. of Maryland, USA; ²Joint Quantum Inst., Univ. of Maryland and National Inst. of Standards and Technology, USA. We demonstrate a method to control the coupling interaction in a coupled-cavity photonic crystal molecule by using a local and reversible photochromic tuning technique. This method is promising for development of integrated photonic devices with large number of cavities.

Meeting Room
212 B/DCLEO: QELS-
Fundamental ScienceFF2K • Nanophotonic and
Plasmonic Coupling to Quantum
Emitters—Continued

FF2K.4 • 11:15

Far-off-resonant coupling between a semiconductor quantum dot and an optical cavity, Anders M. Lund¹, Mikkel Setnes^{1,2}, Per Kaer¹, Jesper Mørk¹; ¹Dept. of Photonics Engineering, DTU Fotonik, Technical Univ. of Denmark, Denmark; ²Dept. of Micro- and Nanotechnology Engineering, Technical Univ. of Denmark, Denmark. We present an investigation of the far-off-resonant coupling between a semiconductor quantum dot and a cavity. We show that the enhanced coupling observed in experiments is explained by Coulomb interactions with wetting layer carriers.

FF2K.5 • 11:30

Efficient single photon sources based on nanodiamonds on a plasmonic platform, Yen-Chun Chen¹, Cheng-Yen Tsai¹, Chun-Yuan Wang², Shangir Gwo², Wen-Hao Chang¹; ¹Electrophysics, National Chiao Tung Univ., Taiwan; ²Physics, National Tsing Hua Univ., Taiwan. We report on an efficient room-temperature source of single photons based on single nitrogen-vacancy centers in nanodiamonds (NDs) placing on a large-area plasmonic platform formed by crystalline gold flakes covered with a thin dielectric layer.

FF2K.6 • 11:45

Accessing the Magnetic Dipole and Electric Quadrupole of Quantum Dots with Light, Petru Tighineanu¹, Søren Stobbe¹, Peter Lodahl¹; ¹Niels Bohr Inst., Denmark. We show that semiconductor quantum dots possess large magnetic-dipole and electric-quadrupole moments, which can be accessed with light. Moreover, quantum dots are capable of mediating multipolar interactions on dipole-allowed transitions and therefore are fundamentally different than atoms.

FF2K.7 • 12:00

Probing plasmonic electro-magnetic environment with Eu³⁺, Natalia Noginova¹, Rabia Hussain¹, Mikhail A. Noginov¹, David Keene², Maxim Durach², Sergey Kruk³, Dragomir N. Neshev³, Isabelle Staude³, Yuri S. Kivshar³; ¹Norfolk State Univ., USA; ²Georgia Southern Univ., USA; ³Research School of Physics and Engineering, Australian National Univ., Australia. We use spontaneous emission of Eu³⁺ ions as a spectroscopic tool to probe modifications of optical fields in close vicinity of metal and under the conditions of the optically-induced magnetic resonance.

Marriott
Salon I & IICLEO: Applications
& TechnologyAF2L • Symposium on
Optofluidic Microsystems II—
Continued

AF2L.3 • 11:15

Effect of Solar Thermal Energy on Photoreactions' Rate, Seyyed Mohammad Hosseini Hashemi¹, Jae-Woo Choi¹, Demetri Psaltis¹; ¹EPFL, Switzerland. The Shockley-Queisser limit predicts that at least 70% of solar energy is available to be converted into heat. In this paper, we show that this heating component can play a significant role in photocatalytic reactions.

AF2L.4 • 11:30 **Invited**

Optofluidic Integration: Past, present, and future, Holger Schmidt¹; ¹Univ. of California Santa Cruz, USA. Optofluidics promises devices and systems in which both optical and fluidic components are integrated on the same chip. We will review progress in this field to date and present an outlook on future opportunities.

CLEO: Science & Innovations

CLEO: Applications
& TechnologySF2M • Optomechanics II—
Continued

SF2M.4 • 11:15

Tuning Fork Cavity Optomechanical Transducers, Yuxiang Liu^{1,2}, Marcelo I. Davanco², Chaoyang Ti¹, Vladimir Aksyuk², Kartik Srinivasan²; ¹Mechanical Engineering, Worcester Polytechnic Inst., USA; ²Center for Nanoscale Science and Technology, National Inst. of Standards and Technology, USA. We present on-chip Si₃N₄ optomechanical transducers that integrate nanomechanical tuning forks with microdisk resonators for displacement measurements. Enhanced mechanical Q relative to single cantilevers and mechanical frequency adjustment by beam stress engineering were realized.

SF2M.5 • 11:30

Observation of Brillouin Scattering Induced Transparency in a Silica Microsphere Resonator, JunHwan Kim¹, Mark Kuzyk², Kewen Han¹, Hailin Wang², Gaurav Bahl¹; ¹Mechanical Science and Engineering, Univ. of Illinois at Urbana-Champaign, USA; ²Physics, Univ. of Oregon, USA. We experimentally demonstrate induced transparency in silica microsphere resonator using forward Brillouin scattering.

SF2M.6 • 11:45

Coherent Excitation of Multiple Nano-opto-mechanical Modes in Silicon with Ultrafast Time-domain Spectroscopy, Jonathan A. Cox¹, Aleem Siddiqui¹, Peter Rakich², Robert L. Jarecki¹, Andrew Starbuck¹; ¹Sandia National Labs, USA; ²Applied Physics, Yale Univ., USA. We present the first time-domain measurement of a guided-wave nano-opto-mechanical system, resulting in the coherent excitation of multiple mechanical modes. We deconvolved the electronic and mechanical responses to observe the evolution of the coherent superposition.

SF2M.7 • 12:00

Integrated silicon optomechanical transducers and their application in atomic force microscopy, Jie Zou^{1,2}, Houxun Miao^{1,2}, Thomas Michels^{1,2}, Vladimir Aksyuk¹; ¹Center for Nanoscale Science and Technology, NIST, USA; ²Maryland Nanocenter, Univ. of Maryland, USA. We present integrated optomechanical transducers with exposed tips and demonstrate ultrahigh force sensitivity and large bandwidth. The transducer is implemented as an atomic force microscope probe in the contact mode and nanoscale resolution is demonstrated.

SF2N • High Energy fs Fiber
Laser & Applications—
Continued

SF2N.3 • 11:15

Multi-MW Soliton Pulse Generation at 1700 nm in a Photonic Crystal Rod, Nicholas Horton¹, Kriti Charan¹, Dimitre Ouzounov¹, Chris Xu¹; ¹Cornell Univ., USA. We demonstrate tunable soliton generation in excess of 3 MW peak power in the 1,700 nm spectral region using a solid-core photonic crystal rod pumped by a compact femtosecond fiber source. This system can potentially be used for in vivo deep tissue multiphoton microscopy.

SF2N.4 • 11:30

High energy pulse compression regimes in hypocycloid-core kagome hollow-core photonic crystal fibers, Benoît Debord¹, Frédéric Gérôme^{1,2}, Meshaal Alharbi¹, Clemens Hoenninger³, Eric Mottay³, Anton Husakou⁴, Fetah Benabid^{1,2}; ¹GPPMM Group, Xlim Research Inst., CNRS UMR 7252, France; ²GLOphotonics S.A.S, France; ³Amplitude Systèmes, France; ⁴Max Born Inst., Germany. Strong self-compressions of high energy femtosecond laser pulses were experimentally obtained in several hypocycloid-core kagome fibers and under different regimes. By tailoring the fiber properties, the maximum compression-ratio was scaled over 100-600 μ J pulse energies.

SF2N.5 • 11:45

Energetic and high average power femtosecond fiber laser using chirped- and divided-pulse amplification, Yoann Zaouter², Florent Guichard^{1,2}, Robert Braunschweig², Marc Hanna¹, Franck Morin², Clemens Hoenninger², Eric Mottay², Frederic Druon¹, Patrick Georges¹; ¹Laboratoire Charles Fabry, France; ²Amplitude Systèmes, France. We implement, in the same femtosecond fiber amplifier setup, both chirped pulse amplification and divided pulse amplification. The generation of 45 W of compressed average power at 100 kHz, together with 320 fs and 450 μ J pulses, is demonstrated using a rod-type ytterbium-doped fiber.

SF2N.6 • 12:00

17.6 THz waveform synthesis by phase-locked Raman sidebands generation in HC-PCF, Meshaal Alharbi^{1,2}, Benoît Debord¹, Madhoussouhana Dontabactouny¹, Frédéric Gérôme¹, Fetah Benabid^{1,2}; ¹GPPMM group, Xlim research Inst., CNRS UMR 7252, Univ. of Limoges, France; ²Physics Dept., Univ. of Bath, UK. We report on the generation of a periodic train pulse waveform with 17.6THz repetition rate and ~26fs pulse duration. The waveform is generated by an all-fiber set-up consisting of hydrogen-filled hollow-core photonic crystal fiber.

SF2O • Special and Spatial
Filters—Continued

SF2O.4 • 11:15

An on-chip partial drop wavelength selective broadcast network, Zhan Su¹, Erman Timurdogan¹, Jie Sun¹, Michele Moresco¹, Gerald Leake², Douglas Coolbaugh², Michael R. Watts¹; ¹Research Lab of Electronics, MIT, USA; ²College of Nanoscale Science & Engineering, Univ. at Albany, USA. A wavelength selective 1-by-8-port optical broadcasting system is proposed and demonstrated utilizing partial drop adiabatic microring tunable filters, achieving a 92.7GHz filter bandwidth, 36.2nm Free-Spectral-Range, low power-variation (0.11dB), and aggregate excess loss of only 1.1dB.

SF2O.5 • 11:30

Optical and near infrared plasmonic filters integrated with terahertz metamaterials, Iain J. McCrindle¹, James Grant¹, Timothy D. Drysdale¹, David R. Cumming¹; ¹School of Engineering, Univ. of Glasgow, UK. We have designed, simulated and fabricated multi-spectral materials operating in visible, near infrared and terahertz wavebands by combining plasmonic filters with metamaterials. Multi-spectral materials offer a path to the creation of co-axial multi-spectral imagers.

SF2O.6 • 11:45

All-optical control of optofluidic ring resonator filled with magnetic fluid, Yang Liu¹, Lei Shi¹, Xinliang Zhang¹; ¹Wuhan National Lab for Optoelectronics, Huazhong Univ of Science and Technology, China. An all-optical controllable optofluidic ring resonator based on a silica microcapillary filled with magnetic fluid is proposed and demonstrated. A tuning sensitivity of 0.15nm/mW and a tuning range of up to 3 nm are achieved.

SF2O.7 • 12:00

High-Q Ring Resonators in Directly-Written Chalcogenide Glass Waveguides, Shahar Levy¹, Matvey Klebanov², Victor Lyubin², Avi Zadok¹; ¹Faculty of Engineering, Bar-Ilan Univ., Israel; ²Dept. of Physics, Ben-Gurion Univ., Israel. Planar waveguide ring resonators are directly written in thin films of As₂S₃ glass, using two-photon laser beam lithography at 810 nm. Q values of 80,000 are observed.

AF2P • Photons for Energy—
Continued

AF2P.3 • 11:15

Chaos-assisted, broadband trapping of light, Changxu Liu¹, Andrea Di Falco², Thomas F. Krauss³, Andrea Fratalocchi¹; ¹PRIMALIGHT, Electrical Engineering/Applied Mathematics and Computational Science, King Abdullah Univ. of Science and Technology (KAUST), Saudi Arabia; ²SUPA/School of Physics and Astronomy, Univ. of St. Andrews, UK; ³Dept. of Physics, Univ. of York, UK. By combining analytic theory, parallel ab-initio simulations and experiments, we demonstrate how to exploit chaos to dramatically enhance light trapping performance.

AF2P.4 • 11:30 **Invited**

High Efficiency Solar Building Envelopes for Integrated Delivery of Environmental Control Systems, Anna Dyson¹, Kenton Phillips¹, Justin Shultz¹, Jason Vollen¹, Matt Gindlesparger¹, Nick Novelli¹; ¹Center for Architecture Science and Ecology, Rensselaer Polytechnic Inst., USA. Efficacious delivery of power requirements for all environmental control systems is demonstrated through an optically transparent solar building envelope that modulates daylight, intercepts solar heat gain, while delivering electricity and high quality heat towards applications. Efficacious delivery of power requirements for all environmental control systems is demonstrated through an optically transparent solar building envelope that modulates daylight, intercepts solar heat gain, while delivering electricity and high quality heat towards applications.


AF2P.5 • 12:00

Highly Efficient Light Extraction GaN-based Light Emitting Diode with Nano-rods in Micro-holes Compound Structure, Che-Yu Liu¹, Jih-Kai Huang¹, Da-Wei Lin¹, Hung-Wen Huang¹, Po-Tsung Lee¹, Gou-Chung Chi¹, Hao-chung Kuo¹, Chun-Yen Chang²; ¹Electro-Optical Engineering, National Chiao Tung Univ., Taiwan, Taiwan; ²Electronics Engineering, National Chiao Tung Univ., Taiwan. We demonstrated a high-power GaN-based light emitting diodes (LEDs) with micro-hole array and nano-rods compound structure. The light output power of LED with micro-hole array and nanorods was as high as 1.27 times, as compared with standard LED.


Executive Ballroom
210ACLEO: QELS-
Fundamental ScienceExecutive Ballroom
210BCLEO: Applications
& TechnologyAF2B • Symposium on
Advances in Neurophotonics
II—ContinuedExecutive Ballroom
210C

CLEO: QELS-Fundamental Science

FF2C • Metasurfaces II—
Continued

FF2C.8 • 12:15 
Meta-Weaves: Nonreciprocal Sector-Way Surfaces, yarden mazor¹, Ben Z. Steinberg¹; ¹*School of EE, Tel-Aviv Univ., Israel*. Generalized 2D nonreciprocity in metasurfaces is achieved by weaving nano-scale one-way threads. The association of $t \rightarrow -t$ with $z \rightarrow -z$, commonly used in time-reversal asymmetry analysis, proves insufficient as shown by the resulting "sector-way" propagation dynamics.

Executive Ballroom
210DFF2D • Quantum Effects in
Lattices—Continued

FF2D.7 • 12:15 
Appearance of a Photonic Thermalization Gap in Symmetry-Constrained Anderson-Disordered Photonic Lattices, Hasan E. Kondakci¹, Ayman F. Abouraddy¹, Bahaa E. Saleh¹; ¹*Univ. of Central Florida, CREOL, USA*. We show that coherent light traveling through a 1-D lattice of coupled waveguides with off-diagonal disorder exhibits super-thermal statistics ($g^{(2)} > 2$) with a photonic thermalization gap at asymptotic propagation distances.

Meeting Room
211 B/D

CLEO: Science & Innovations

SF2I • Combustion and Plasma
Diagnostics—Continued

SF2I.7 • 12:15
Emission and expansion features of ns and fs laser ablation plumes in an ambient environment, Sivanandan S. Harilal¹; ¹*Purdue Univ., USA*. We investigated the role of background gas pressure on spectral emission features, absolute line intensities, signal to background ratios, plume hydrodynamics, and ablation craters for ns and fs laser ablation plumes.

Meeting Room
212 A/CSF2J • Innovations in Laser
Processing of Materials—
Continued

SF2J.7 • 12:15
Strategy in achieving almost complete polarization conversion from 2D circular nanohole arrays, Lai Yin Yiu¹, Zhaolong Cao¹, H C. Ong¹; ¹*The Chinese Univ. of Hong Kong, Hong Kong*. We study the dependence of chirality from 2D nanohole arrays on azimuthal angle and hole geometry experimentally and numerically. A strategy based on coupled mode theory is proposed to achieve almost complete polarization conversion.

Meeting Room
212 B/DCLEO: QELS-
Fundamental ScienceMarriott
Salon I & IICLEO: Applications
& Technology

Executive Ballroom
210EExecutive Ballroom
210FExecutive Ballroom
210G

CLEO: Science & Innovations

SF2E • Frequency Combs and
CEP—Continued

SF2E.8 • 12:15

Characterization of ultra-high repetition rate mode-locked lasers with an integrated all-optical RF spectrum analyzer, Marcello Ferrera^{2,1}, Christian Reimer¹, Alessia Pasquazi³, Marco Peccianti³, Matteo Clerici^{1,2}, Lucia Caspani¹, Sai T. Chu⁴, Brent E. Little⁵, Roberto Morandotti¹, David J. Moss⁶; ¹INRS-EMT, Canada; ²Heriot-Watt Univ., UK; ³Univ. of Sussex, UK; ⁴City Univ. of Hong Kong, China; ⁵HiQ Photonics, USA; ⁶MIT Univ., Australia. We report an on-chip all-optical CMOS-compatible radio frequency spectrum analyzer with a bandwidth exceeding 2.5 THz, and use it to measure the intensity power spectra of mode-locked lasers with repetition rates up to 400 GHz.

SF2F • Advanced THz Emission
Mechanisms—Continued

SF2F.8 • 12:15

Bridging the THz to RF gap by four-wave mixing in a highly nonlinear fiber. Stabilization of an opto-millimeter wave, Antoine Rolland¹, Lucien Pouget¹, Marc Brunel¹, Mehdi Alouini¹; ¹Optique et Photonique, Institut de Physique de Rennes, France. Optoelectronic down-conversion of a THz optical beatnote to a RF intermediate frequency is performed with a standard MZ modulator followed by a zero dispersion-slope fiber. This allows to detect an intermediate frequency in the MHz range in order to phase lock the THz beatnote.

SF2G • Laser Dynamics—
Continued

SF2G.8 • 12:15

Controlled Lasing from Active Optomechanical Resonators, Thomas Czerniuk¹, Christian Brüggemann¹, Jan Tepper¹, Sebastian Brodbeck², Christian Schneider², Martin Kamp², Sven Höfling², Boris A. Glavin³, Dmitri R. Yakovlev^{1,4}, Andrey V. Akimov^{4,5}, Manfred Bayer¹; ¹Experimentelle Physik 2, TU Dortmund Univ., Germany; ²Technische Physik, Univ. of Würzburg, Germany; ³V. E. Lashkaryov Inst. of Semiconductor Physics, Ukraine; ⁴A. F. Ioffe Physical-Technical Inst., Russian Academy of Sciences, Russia; ⁵School of Physics and Astronomy, Univ. of Nottingham, UK. Microcavity lasers possess mechanical resonances due to stopbands in the Bragg reflector's phonon dispersion. By injecting a picosecond strain pulse into the resonator we excite these modes, providing an ultrafast effective modulation of the emission.

Marriott
Salon IIIMarriott
Salon IVMarriott
Salon V & VIMarriott
Willow Glen I-III

CLEO: Science & Innovations

SF2M • Optomechanics II—
Continued

SF2M.8 • 12:15

Optical Trapping of 60 nm Diameter Particles in Photonic Crystal Slot-Microcavities, S. Hamed Mirsadeghi¹, Jeff F. Young¹; ¹Physics and Astronomy, Univ. Of British Columbia, Canada. We report optical trapping of 60 nm Au nanoparticles using photonic crystal slot-cavities with Qs of ~7200 and 0.3mW of guided power at 1.6 μ m. Histograms of the cavity transmission are used to quantitatively analyze the trapping dynamics by modeling the back-action of the nanoparticles in the trap.

SF2O • Special and Spatial
Filters—Continued

SF2O.8 • 12:15

Ultrathin transmission visible spectrum filters with wide viewing angle, Kyu-Tae Lee¹, Sungyong Seo¹, Jae Yong Lee¹, L. Jay Guo¹; ¹Electrical Engineering and Computer Science, Univ. of Michigan, USA. We report high angular tolerant transmission visible spectrum filters exploiting strong resonance behaviors in an ultrathin semiconductor layer between two metals. The angle robust property remains over a wide incident angular range up to $\pm 70^\circ$.

AF2P • Photons for Energy—
Continued

AF2P.6 • 12:15

Impact of Surface Recombination on the Performance of Phosphor-Free InGaN/GaN Nanowire White Light Emitting Diodes, shaofei zhang¹, Ashfiqua T. Connie¹, Hieu Pham Trung Nguyen¹, Qi Wang¹, Ishiang Shih¹, Zetian Mi¹; ¹ECE, McGill Univ., Canada. We show that the performance of InGaN/GaN axial nanowire LEDs is largely limited by the poor carrier injection efficiency. We have further demonstrated high performance phosphor-free white LEDs using InGaN/GaN/AlGaIn dot-in-a-wire core-shell heterostructures.